

STUDIES ON DISPERSION AND TURBULENCE
/ IN LIQUID FLOWS.

by

C

O. K. ELRIEDY B.Sc.(Eng.), M.Eng.

A Thesis

Submitted to the School of Graduate Studies

in Partial Fulfilment of the Requirements

for the Degree

Doctor of Philosophy

McMaster University

November 1979

STUDIES ON DISPERSION AND TURBULENCE
IN LIQUID FLOWS

TO MY PARENTS

(ii)

DOCTOR OF PHILOSOPHY (1979)
(Mechanical Engineering)

McMASTER-UNIVERSITY
Hamilton, Ontario

TITLE: Studies on Dispersion and Turbulence in
Liquid Flows

AUTHOR: O. K. El Riedy, B.Sc. (Cairo University)
M.Eng. (McMaster University)

SUPERVISOR: Dr. B. Latto

NUMBER OF PAGES: XXXV, 424

ABSTRACT

This thesis describes an experimental study of the dispersion and turbulence of Newtonian fluids and dilute aqueous solutions of a drag reducing polymer, Reten 423, when ejected from a thin wall slot or point source into either developing or fully developed turbulent internal water flow at relatively high Reynolds numbers.

Two small water tunnels with injection facilities were constructed in which concentration and energy spectra measurements were made using a spectrophotometer and a Laser Doppler Anemometer. The investigation was carried out with a maximum flow velocity of the order of 4.5 m/s. for various injection flow rates and with injection concentrations in the range 0 to 1000 w.p.p.m.

It was found that the dispersion rate for polymer solutions is reduced when compared to Newtonian diffusion. It was also observed that the velocity profiles for developing flows with polymer injection are fuller than those for water alone. Furthermore, there was no noticeable change in energy spectrum for low polymer concentration. However, for high injection concentration there was an increase of the energy within the low frequency end of the spectrum and a reduction of energy for the high frequency end of the spectrum.

Correlations for the concentration profiles, diffusion boundary layer growth, maximum concentration

and eddy diffusivity are presented. The results indicate that a universal diffusion correlation exists which represents the data for both Newtonian and polymer solutions.

A very interesting phenomenon was observed for heterogeneous polymer flow fields in which the sampling rate had an effect on the measured polymer solution concentration. The apparent concentration on the measured concentration approached the correct value when the sampling velocity approached that for the main stream, i.e. the isokinetic condition. This phenomenon is important and should be taken into consideration, for example, when using sampling techniques to obtain concentration profiles in nonhomogeneous polymer solution flow fields.

ACKNOWLEDGEMENTS

The author wishes to express his sincere gratitude to his supervisor, Dr. B. Latto, for his valuable advice, continuous encouragement and assistance throughout the duration of the present investigation.

The author also expresses his appreciation to Ms. BettyAnne Bedell for typing the manuscript.

The financial support provided by the National Research Council is also acknowledged.

TABLE OF CONTENTS

	Page
ABSTRACT	iv
ACKNOWLEDGEMENTS	vi
TABLE OF CONTENTS	vii
LIST OF FIGURES	x
NOMENCLATURE	xxxiii
CHAPTER 1 INTRODUCTION	1
CHAPTER 2 LITERATURE SURVEY	3
CHAPTER 3 EXPERIMENTAL APPARATUS	25
3.1 The Water Flow System	26
3.1.1 Fully Developed Flow Experiments	26
3.1.1.1 Test Section	27
3.1.2 Developing Turbulent Flow Experiments	28
3.1.2.1 Test Section	28
3.2 The Polymer Solution Flow System	29
3.3 Measuring Instrumentations	30
3.4 Experimental Procedure	34
3.4.1 System Preparation	34
3.4.2 Additive Solution Preparation	34
3.5 Procedures	35
CHAPTER 4 THEORY	38
4.1 Injection from Line Source on Flat Plate	38
4.1.1 Velocity Profiles	38

	Page	
4.1.2	Concentration Profiles	38
4.1.3	The Continuity Equation	40
4.1.4	The Eddy Diffusivity	41
4.2	Injection from Point Source on the Center Line	45
4.2.1	Velocity Profiles	45
4.2.2	Concentration Profiles	46
4.2.3	The Continuity Equation	46
4.2.4	The Eddy Diffusivity	48
CHAPTER 5	RESULTS	51
5.1	Injection from Line Source on Flat Plate	51
5.2	Injection from Point Source	57
5.3	Sampling Rate Effects	60
CHAPTER 6	ANALYSIS AND DISCUSSION	61
6.1	Line Source Injection	61
6.1.1	Continuity Equation	69
6.1.2	The Eddy Diffusivity	70
6.2	The Point Source Injection	70
6.2.1	Fully Developed Flow	70
6.2.2	Uniform Flow	74
6.2.3	Continuity Equation	78
6.2.4	The Eddy Diffusivity	79
6.3	Hot-Film Anemometer	79
6.4	General Observation	80
CHAPTER 7	CONCLUSIONS	82
7.1	For Line Source Injection	82

	Page
7.2 For Point Source Injection	84
REFERENCES	87
ILLUSTRATIONS	91
APPENDIX I SAMPLING RATE EFFECT	326
APPENDIX II CALIBRATION CURVES	345
APPENDIX III DATA TABLES	349
APPENDIX IV ERROR ANALYSIS	422

LIST OF FIGURES	Page
Figure 1. Experimental Apparatus (Fully Developed Flow).	92
Figure 2. Experimental Apparatus (Fully Developed Flow).	93
Figure 3. Experimental Apparatus (Developing Flow).	94
Figure 4-A. Experimental Apparatus (Developing Flow).	95
Figure 4-B. Experimental Apparatus (Developing Flow).	96
Figure 5. Flow Diagram (Fully Developed Flow).	98
Figure 6. Flow Diagram (Developing Flow).	99
Figure 7. Injection Source (Point Source).	100
Figure 8. Sectional View of Injection Plenum (Line Source).	101
Figure 9. Laser System Assembly.	102
Figure 10. Universal Velocity Profile.	103
Figure 11. Universal Velocity Profile.	104
Figure 12. Universal Velocity Profile.	105
Figure 13. Concentration Profiles (Line Source Injection-Water Injection).	106
Figure 14. Concentration Profiles (Line Source Injection- $C_i = 100$ w.p.p.m.).	107
Figure 15. Concentration Profiles (Line Source Injection- $C_i = 500$ w.p.p.m.).	108
Figure 16. Universal Concentration Profile (Line Source Injection-Water Injection-All Data).	109

Figure 17.	Universal Concentration Profile (Line Source Injection- $C_i = 100$ w.p.p.m.).	110
Figure 18.	Universal Concentration Profiles (Line Source Injection- $C_i = 500$ w.p.p.m.).	111
Figure 19.	Universal Concentration Profile (Line Source Injection- $C_i = 500$ w.p.p.m.).	112
Figure 20.	Universal Concentration Profile (Line Source Injection- $C_i = 500$ w.p.p.m.).	113
Figure 21.	Universal Concentration Profile (Line Source Injection- $C_i = 500$ w.p.p.m.).	114
Figure 22.	Universal Concentration Profile (Line Source Injection- $C_i = 500$ w.p.p.m.).	115
Figure 23.	Universal Concentration Profile (Line Source Injection- $C_i = 500$ w.p.p.m.).	116
Figure 24.	Universal Concentration Profile (Line Source Injection- $C_i = 500$ w.p.p.m.).	117
Figure 25.	Universal Concentration Profile (Line Source Injection- $C_i = 500$ w.p.p.m.).	118
Figure 26.	Universal Concentration Profile (Line Source Injection- $C_i = 500$ w.p.p.m.).	119
Figure 27.	Universal Concentration Profile (Line Source Injection- $C_i = 500$ w.p.p.m.).	120
Figure 28.	$\frac{C_m U_m}{C_i U_i}$ vs. $\frac{x}{h}$ (Line Source Injection-Water Injection).	121
Figure 29.	$\frac{C_m U_m}{C_i U_i}$ vs. $\frac{x}{h}$ (Line Source Injection- $C_i = 100$ w.p.p.m.).	122

Figure 30.	$\frac{\bar{C}_m \bar{U}_m}{\bar{C}_i \bar{U}_i}$ vs. $\frac{x}{h}$ (Line Source Injection- $C_i =$ 250 w.p.p.m.).	123
Figure 31.	$\frac{\bar{C}_m \bar{U}_m}{\bar{C}_i \bar{U}_i}$ vs. $\frac{x}{h}$ (Line Source Injection- $C_i =$ 500 w.p.p.m.).	124
Figure 32.	$\frac{\bar{C}_m \bar{U}_m}{\bar{C}_i \bar{U}_i}$ vs. $\frac{x}{h}$ (Line Source Injection- $C_i =$ 1000 w.p.p.m.).	125
Figure 33.	λ/h vs. $\frac{x}{h}$ (Line Source Injection-Water Injection).	126
Figure 34.	λ/h vs. $\frac{x}{h}$ (Line Source Injection-Water Injection).	127
Figure 35.	λ/h vs. $\frac{x}{h}$ (Line Source Injection-Water Injection).	128
Figure 36.	λ/h vs. $\frac{x}{h}$ (Line Source Injection- $C_i =$ 100 w.p.p.m.).	129
Figure 37.	λ/h vs. $\frac{x}{h}$ (Line Source Injection- $C_i =$ 100 w.p.p.m.).	130
Figure 38.	λ/h vs. $\frac{x}{h}$ (Line Source Injection- $C_i =$ 100 w.p.p.m.).	131
Figure 39.	λ/h vs. $\frac{x}{h}$ (Line Source Injection- $C_i =$ 250 w.p.p.m.).	132
Figure 40.	λ/h vs. $\frac{x}{h}$ (Line Source Injection- $C_i =$ 250 w.p.p.m.).	133
Figure 41.	λ/h vs. $\frac{x}{h}$ (Line Source Injection- $C_i =$ 250 w.p.p.m.).	134

Figure 42.	λ/h vs. $\frac{x}{h}$ (Line Source Injection- $C_i = 500$ w.p.p.m.).	135
Figure 43.	λ/h vs. $\frac{x}{h}$ (Line Source Injection- $C_i = 500$ w.p.p.m.).	136
Figure 44.	λ/h vs. $\frac{x}{h}$ (Line Source Injection- $C_i = 500$ w.p.p.m.).	137
Figure 45.	λ/h vs. $\frac{x}{h}$ (Line Source Injection- $C_i = 1000$ w.p.p.m.).	138
Figure 46.	λ/h vs. $\frac{x}{h}$ (Line Source Injection- $C_i = 1000$ w.p.p.m.).	139
Figure 47.	λ/h vs. $\frac{x}{h}$ (Line Source Injection- $C_i = 1000$ w.p.p.m.).	140
Figure 48.	Generalized Non-dimensional Diffusion Boundary Layer Thickness Profile (Line Source Injection).	141
Figure 49.	a vs. $\frac{x}{h}$ (Line Source Injection-Water Injection).	142
Figure 50.	a vs. $\frac{x}{h}$ (Line Source Injection-Water Injection).	143
Figure 51.	a vs. $\frac{x}{h}$ (Line Source Injection-Water Injection).	144
Figure 52.	a vs. $\frac{x}{h}$ (Line Source Injection- $C_i = 100$ w.p.p.m.).	145
Figure 53.	a vs. $\frac{x}{h}$ (Line Source Injection- $C_i = 100$ w.p.p.m.).	146

Figure 54.	a vs. $\frac{x}{h}$ (Line Source Injection- $C_i = 100$ w.p.p.m.).	147
Figure 55.	a vs. $\frac{x}{h}$ (Line Source Injection- $C_i = 250$ w.p.p.m.).	148
Figure 56.	a vs. $\frac{x}{h}$ (Line Source Injection- $C_i = 250$ w.p.p.m.).	149
Figure 57.	a vs. $\frac{x}{h}$ (Line Source Injection- $C_i = 250$ w.p.p.m.).	150
Figure 58.	a vs. $\frac{x}{h}$ (Line Source Injection- $C_i = 500$ w.p.p.m.).	151
Figure 59.	a vs. $\frac{x}{h}$ (Line Source Injection- $C_i = 500$ w.p.p.m.).	152
Figure 60.	a vs. $\frac{x}{h}$ (Line Source Injection- $C_i = 500$ w.p.p.m.).	153
Figure 61.	a vs. $\frac{x}{h}$ (Line Source Injection- $C_i = 1000$ w.p.p.m.).	154
Figure 62.	a vs. $\frac{x}{h}$ (Line Source Injection- $C_i = 1000$ w.p.p.m.).	155
Figure 63.	a vs. $\frac{x}{h}$ (Line Source Injection- $C_i = 1000$ w.p.p.m.).	156
Figure 64.	Generalized Exponent 'a' Profile (Line Source Injection).	157
Figure 65.	Wall Concentration Profiles (Line Source Injection).	158

Figure 66.	Velocity and Turbulence Intensity Profiles (Line Source Injection-Water Injection).	159
Figure 67.	Velocity and Turbulence Intensity Profiles (Line Source Injection- $C_i = 100$ w.p.p.m.).	160
Figure 68.	Velocity and Turbulence Intensity Profiles (Line Source Injection- $C_i = 500$ w.p.p.m.).	161
Figure 69.	Velocity and Turbulence Intensity Profiles (Line Source Injection- $C_i = 500$ w.p.p.m.).	162
Figure 70.	Velocity and Turbulence Intensity Profiles (Line Source Injection- $C_i = 1000$ w.p.p.m.).	163
Figure 71.	The Change in Velocity Profile Due to Polymer Solution Injection ($C_i = 100$ w.p.p.m.).	164
Figure 72.	The Change in Turbulence Intensity Profile Due to Polymer Solution Injection ($C_i = 100$ w.p.p.m.).	165
Figure 73.	The Change in Velocity Profile Due to Polymer Solution Injection ($C_i = 500$ w.p.p.m.).	166
Figure 74.	The Change in Velocity Profile Due to Polymer Solution Injection ($C_i = 500$ w.p.p.m.).	167
Figure 75.	The Change in Turbulence Intensity Profile Due to Polymer Solution Injection ($C_i = 500$ w.p.p.m.).	168
Figure 76.	The Change in Turbulence Intensity Profile Due to Polymer Solution Injection ($C_i = 500$ w.p.p.m.).	169

Figure 77.	The Change in Velocity Profile Due to Polymer Solution Injection ($C_i = 1000$ w.p.p.m.).	170
Figure 78.	The Change in Turbulence Intensity Profile Due to Polymer Solution Injection ($C_i = 1000$ w.p.p.m.).	171
Figure 79.	Energy Spectra Without Injection.	172
Figure 80.	Energy Spectra (Line Source Injection-Water Injection).	173
Figure 81.	Energy Spectra (Line Source Injection- $C_i = 100$ w.p.p.m.).	174
Figure 82.	Energy Spectra (Line Source Injection- $C_i = 250$ w.p.p.m.).	175
Figure 83.	Energy Spectra (Line Source Injection- $C_i = 500$ w.p.p.m.).	176
Figure 84.	Energy Spectra (Line Source Injection- $C_i = 1000$ w.p.p.m.).	177
Figure 85.	Energy Spectra (Line Source Injection- $C_i = 500$ w.p.p.m.).	178
Figure 86.	Energy Spectra (Line Source Injection- $C_i = 1000$ w.p.p.m.).	179
Figure 87.	Concentration Profiles (Point Source Injection - Fully Developed Flow - Water Injection).	180
Figure 88.	Concentration Profiles (Point Source Injection - Fully Developed Flow - $C_i = 100$ w.p.p.m.).	181
Figure 89.	Concentration Profiles (Point Source Injection - Fully Developed Flow - $C_i = 500$ w.p.p.m.).	182

Figure 90.	Concentration Profiles (Point Source Injection - Fully Developed Flow - Water Injection).	183
Figure 91.	Concentration Profiles (Point Source Injection - Fully Developed Flow - $C_i = 100$ w.p.p.m.).	184
Figure 92.	Concentration Profiles (Point Source Injection - Fully Developed Flow - $C_i = 500$ w.p.p.m.).	185
Figure 93.	Concentration Profiles (Point Source Injection - Uniform Flow - Water Injection).	186
Figure 94.	Concentration Profiles (Point Source Injection - Uniform Flow - $C_i = 100$ w.p.p.m.).	187
Figure 95.	Concentration Profiles (Point Source Injection - Uniform Flow - $C_i = 500$ w.p.p.m.).	188
Figure 96.	Universal Concentration Profile (Point Source Injection - Fully Developed Flow - Water Injection).	189
Figure 97.	Universal Concentration Profile (Point Source Injection - Fully Developed Flow - $C_i = 100$ w.p.p.m.).	190
Figure 98.	Universal Concentration Profile (Point Source Injection - Fully Developed Flow - $C_i = 500$ w.p.p.m.).	191
Figure 99.	Universal Concentration Profile (Point Source Injection - Fully Developed Flow - Water Injection).	192
Figure 100.	Universal Concentration Profile (Point Source Injection - Fully Developed Flow - $C_i = 100$ w.p.p.m.).	193

Figure 101.	Universal Concentration Profile (Point Source Injection - Fully Developed Flow - $C_i = 500$ w.p.p.m.).	194
Figure 102.	Universal Concentration Profile (Point Source Injection - Uniform Flow - Water Injection).	195
Figure 103.	Universal Concentration Profile (Point Source Injection - Uniform Flow - $C_i = 100$ w.p.p.m.).	196
Figure 104.	Universal Concentration Profile (Point Source Injection - Uniform Flow - $C_i = 500$ w.p.p.m.).	197
Figure 105.	$(C_m U_m / C_i U_i)$ vs. x/d (Point Source Injection - Fully Developed Flow - Water Injection).	198
Figure 106.	$(C_m U_m / C_i U_i)$ vs. x/d (Point Source Injection - Fully Developed Flow - Water Injection).	199
Figure 107.	$(C_m U_m / C_i U_i)$ vs. x/d (Point Source Injection - Fully Developed Flow - Water Injection).	200
Figure 108.	$(C_m U_m / C_i U_i)$ vs. x/d (Point Source Injection - Fully Developed Flow - $C_i = 50$ w.p.p.m.).	201
Figure 109.	$(C_m U_m / C_i U_i)$ vs. x/d (Point Source Injection - Fully Developed Flow - $C_i = 50$ w.p.p.m.).	202
Figure 110.	$(C_m U_m / C_i U_i)$ vs. x/d (Point Source Injection - Fully Developed Flow - $C_i = 50$ w.p.p.m.).	203

Figure 111.	$(C_m U_m / C_i U_i)$ vs. x/d (Point Source Injection - Fully Developed Flow - $C_i = 100$ w.p.p.m.).	204
Figure 112.	$(C_m U_m / C_i U_i)$ vs. x/d (Point Source Injection - Fully Developed Flow - $C_i = 100$ w.p.p.m.).	205
Figure 113.	$(C_m U_m / C_i U_i)$ vs. x/d (Point Source Injection - Fully Developed Flow - $C_i = 100$ w.p.p.m.).	206
Figure 114.	$(C_m U_m / C_i U_i)$ vs. x/d (Point Source Injection - Fully Developed Flow - $C_i = 250$ w.p.p.m.).	207
Figure 115.	$(C_m U_m / C_i U_i)$ vs. x/d (Point Source Injection - Fully Developed Flow - $C_i = 250$ w.p.p.m.).	208
Figure 116.	$(C_m U_m / C_i U_i)$ vs. x/d (Point Source Injection - Fully Developed Flow - $C_i = 250$ w.p.p.m.).	209
Figure 117.	$(C_m U_m / C_i U_i)$ vs. x/d (Point Source Injection - Fully Developed Flow - $C_i = 500$ w.p.p.m.).	210
Figure 118.	$(C_m U_m / C_i U_i)$ vs. x/d (Point Source Injection - Fully Developed Flow - $C_i = 500$ w.p.p.m.).	211
Figure 119.	$(C_m U_m / C_i U_i)$ vs. x/d (Point Source Injection - Fully Developed Flow - $C_i = 500$ w.p.p.m.).	212
Figure 120.	$(C_m U_m / C_i U_i)$ vs. x/d (point Source Injection - Fully Developed Flow - $C_i = 1000$ w.p.p.m.).	213

Figure 121.	$(C_m U_m / C_i U_i)$ vs. x/d (Point Source Injection - Fully Developed Flow - $C_i = 1000$ w.p.p.m.).	214
Figure 122.	$(C_m U_m / C_i U_i)$ vs. x/d (Point Source Injection - Fully Developed Flow - $C_i = 1000$ w.p.p.m.).	215
Figure 123.	$(C_m U_m / C_i U_i)$ vs. x/d (Point Source Injection - Fully Developed Flow - Water Injection).	216
Figure 124.	$(C_m U_m / C_i U_i)$ vs. x/d (Point Source Injection - Fully Developed Flow - Water Injection).	217
Figure 125.	$(C_m U_m / C_i U_i)$ vs. x/d (Point Source Injection - Fully Developed Flow - Water Injection).	218
Figure 126.	$(C_m U_m / C_i U_i)$ vs. x/d (Point Source Injection - Fully Developed Flow - $C_i = 50$ w.p.p.m.).	219
Figure 127.	$(C_m U_m / C_i U_i)$ vs. x/d (Point Source Injection - Fully Developed Flow - $C_i = 50$ w.p.p.m.).	220
Figure 128.	$(C_m U_m / C_i U_i)$ vs. x/d (Point Source Injection - Fully Developed Flow - $C_i = 50$ w.p.p.m.).	221
Figure 129.	$(C_m U_m / C_i U_i)$ vs. x/d (Point Source Injection - Fully Developed Flow - $C_i = 100$ w.p.p.m.).	222
Figure 130.	$(C_m U_m / C_i U_i)$ vs. x/d (Point Source Injection - Fully Developed Flow - $C_i = 100$ w.p.p.m.).	223

Figure 131.	$(C_m U_m / C_i U_i)$ vs. x/d (Point Source Injection - Fully Developed Flow - $C_i = 100$ w.p.p.m.).	224
Figure 132.	$(C_m U_m / C_i U_i)$ vs. x/d (Point Source Injection - Fully Developed Flow - $C_i = 250$ w.p.p.m.).	225
Figure 133.	$(C_m U_m / C_i U_i)$ vs. x/d (Point Source Injection - Fully Developed Flow - $C_i = 250$ w.p.p.m.).	226
Figure 134.	$(C_m U_m / C_i U_i)$ vs. x/d (Point Source Injection - Fully Developed Flow - $C_i = 250$ w.p.p.m.).	227
Figure 135.	$(C_m U_m / C_i U_i)$ vs. x/d (Point Source Injection - Fully Developed Flow - $C_i = 500$ w.p.p.m.).	228
Figure 136.	$(C_m U_m / C_i U_i)$ vs. x/d (Point Source Injection - Fully Developed Flow - $C_i = 500$ w.p.p.m.).	229
Figure 137.	$(C_m U_m / C_i U_i)$ vs. x/d (Point Source Injection - Fully Developed Flow - $C_i = 500$ w.p.p.m.).	230
Figure 138.	$(C_m U_m / C_i U_i)$ vs. x/d (Point Source Injection - Fully Developed Flow - $C_i = 1000$ w.p.p.m.).	231
Figure 139.	$(C_m U_m / C_i U_i)$ vs. x/d (Point Source Injection - Fully Developed Flow - $C_i = 1000$ w.p.p.m.).	232
Figure 140.	$(C_m U_m / C_i U_i)$ vs. x/d (Point Source Injection - Fully Developed Flow - $C_i = 1000$ w.p.p.m.).	233

Figure 141.	$(C_m U_m / C_i U_i)$ vs. x/d (Point Source Injection - Uniform Flow - Water Injection).	234
Figure 142.	$(C_m U_m / C_i U_i)$ vs. x/d (Point Source Injection - Uniform Flow - Water Injection).	235
Figure 143.	$(C_m U_m / C_i U_i)$ vs. x/d (Point Source Injection - Uniform Flow - Water Injection).	236
Figure 144.	$(C_m U_m / C_i U_i)$ vs. x/d (Point Source Injection - Uniform Flow - $C_i = 50$ w.p.p.m.).	237
Figure 145.	$(C_m U_m / C_i U_i)$ vs. \bar{x}/d (Point Source Injection - Uniform Flow - $C_i = 50$ w.p.p.m.).	238
Figure 146.	$(C_m U_m / C_i U_i)$ vs. x/d (Point Source Injection - Uniform Flow - $C_i = 50$ w.p.p.m.).	239
Figure 147.	$(C_m U_m / C_i U_i)$ vs. x/d (Point Source Injection - Uniform Flow - $C_i = 100$ w.p.p.m.).	240
Figure 148.	$(C_m U_m / C_i U_i)$ vs. x/d (Point Source Injection - Uniform Flow - $C_i = 100$ w.p.p.m.).	241
Figure 149.	$(C_m U_m / C_i U_i)$ vs. x/d (Point Source Injection - Uniform Flow - $C_i = 100$ w.p.p.m.).	242
Figure 150.	$(C_m U_m / C_i U_i)$ vs. x/d (Point Source Injection - Uniform Flow - $C_i = 250$ w.p.p.m.).	243

Figure 151.	$(C_m U_m / C_i U_i)$ vs. x/d (Point Source Injection - Uniform Flow - $C_i = .250$ w.p.p.m.).	244
Figure 152.	$(C_m U_m / C_i U_i)$ vs. x/d (Point Source Injection - Uniform Flow - $C_i = 250$ w.p.p.m.).	245
Figure 153.	$(C_m U_m / C_i U_i)$ vs. x/d (Point Source Injection - Uniform Flow - $C_i = 500$ w.p.p.m.).	246
Figure 154.	$(C_m U_m / C_i U_i)$ vs. x/d (Point Source Injection - Uniform Flow - $C_i = 500$ w.p.p.m.).	247
Figure 155.	$(C_m U_m / C_i U_i)$ vs. x/d (Point Source Injection - Uniform Flow - $C_i = 500$ w.p.p.m.).	248
Figure 156.	$(C_m U_m / C_i U_i)$ vs. x/d (Point Source Injection - Uniform Flow - $C_i = 1000$ w.p.p.m.).	249
Figure 157.	$(C_m U_m / C_i U_i)$ vs. x/d (Point Source Injection - Uniform Flow - $C_i = 1000$ w.p.p.m.).	250
Figure 158.	$(C_m U_m / C_i U_i)$ vs. x/d (Point Source Injection - Uniform Flow - $C_i = 1000$ w.p.p.m.).	251
Figure 159.	Wall Concentration Profiles (Point Source Injection - Fully Developed Flow).	252
Figure 160.	Wall Concentration Profiles (Point Source Injection - Fully Developed Flow).	253

Figure 161.	Wall Concentration Profiles (Point Source Injection - Uniform Flow).	254
Figure 162.	$(\lambda/(d/2))$ vs. x/d (Point Source Injection - Fully Developed Flow - Water Injection).	255
Figure 163.	$(\lambda/(d/2))$ vs. x/d (Point Source Injection - Fully Developed Flow - Water Injection).	256
Figure 164.	$(\lambda/(d/2))$ vs. x/d (Point Source Injection - Fully Developed Flow - Water Injection).	257
Figure 165.	$(\lambda/(d/2))$ vs. x/d (Point Source Injection - Fully Developed Flow - $C_i = 50$ w.p.p.m.).	258
Figure 166.	$(\lambda/(d/2))$ vs. x/d (Point Source Injection - Fully Developed Flow - $C_i = 50$ w.p.p.m.).	259
Figure 167.	$(\lambda/(d/2))$ vs. x/d (Point Source Injection - Fully Developed Flow - $C_i = 50$ w.p.p.m.).	260
Figure 168.	$(\lambda/(d/2))$ vs. x/d (Point Source Injection - Fully Developed Flow - $C_i = 100$ w.p.p.m.).	261
Figure 169.	$(\lambda/(d/2))$ vs. x/d (Point Source Injection - Fully Developed Flow - $C_i = 100$ w.p.p.m.).	262
Figure 170.	$(\lambda/(d/2))$ vs. x/d (Point Source Injection - Fully Developed Flow - $C_i = 100$ w.p.p.m.).	263
Figure 171.	$(\lambda/(d/2))$ vs. x/d (Point Source Injection - Fully Developed Flow - $C_i = 250$ w.p.p.m.).	264

Figure 172.	$(\lambda/(d/2))$ vs. x/d (Point Source Injection - Fully Developed Flow - $C_i = 250$ w.p.p.m.).	265
Figure 173.	$(\lambda/(d/2))$ vs. x/d (Point Source Injection - Fully Developed Flow - $C_i = 250$ w.p.p.m.).	266
Figure 174.	$(\lambda/(d/2))$ vs. x/d (Point Source Injection - Fully Developed Flow - $C_i = 500$ w.p.p.m.).	267
Figure 175.	$(\lambda/(d/2))$ vs. x/d (Point Source Injection - Fully Developed Flow - $C_i = 500$ w.p.p.m.).	268
Figure 176.	$(\lambda/(d/2))$ vs. x/d (Point Source Injection - Fully Developed Flow - $C_i = 500$ w.p.p.m.).	269
Figure 177.	$(\lambda/(d/2))$ vs. x/d (Point Source Injection - Fully Developed Flow - $C_i = 1000$ w.p.p.m.).	270
Figure 178.	$(\lambda/(d/2))$ vs. x/d (Point Source Injection - Fully Developed Flow - $C_i = 1000$ w.p.p.m.).	271
Figure 179.	$(\lambda/(d/2))$ vs. x/d (Point Source Injection - Fully Developed Flow - $C_i = 1000$ w.p.p.m.).	272
Figure 180.	$(\lambda/(d/2))$ vs. x/d (Point Source Injection - Fully Developed Flow - Water Injection).	273
Figure 181.	$(\lambda/(d/2))$ vs. x/d (Point Source Injection - Fully Developed Flow - Water Injection).	274
Figure 182.	$(\lambda/(d/2))$ vs. x/d (Point Source Injection - Fully Developed Flow - Water Injection).	275

Figure 183.	$(\lambda/(d/2))$ vs. x/d (Point Source Injection - Fully Developed Flow - $C_i = 50$ w.p.p.m.).	276
Figure 184.	$(\lambda/(d/2))$ vs. x/d (Point Source Injection - Fully Developed Flow - $C_i = 50$ w.p.p.m.).	277
Figure 185.	$(\lambda/(d/2))$ vs. x/d (Point Source Injection - Fully Developed Flow - $C_i = 50$ w.p.p.m.).	278
Figure 186.	$(\lambda/(d/2))$ vs. x/d (Point Source Injection - Fully Developed Flow - $C_i = 100$ w.p.p.m.).	279
Figure 187.	$(\lambda/(d/2))$ vs. x/d (Point Source Injection - Fully Developed Flow - $C_i = 100$ w.p.p.m.).	280
Figure 188.	$(\lambda/(d/2))$ vs. x/d (Point Source Injection - Fully Developed Flow - $C_i = 100$ w.p.p.m.).	281
Figure 189.	$(\lambda/(d/2))$ vs. x/d (Point Source Injection - Fully Developed Flow - $C_i = 250$ w.p.p.m.).	282
Figure 190.	$(\lambda/(d/2))$ vs. x/d (Point Source Injection - Fully Developed Flow - $C_i = 250$ w.p.p.m.).	283
Figure 191.	$(\lambda/(d/2))$ vs. x/d (Point Source Injection - Fully Developed Flow - $C_i = 250$ w.p.p.m.).	284
Figure 192.	$(\lambda/(d/2))$ vs. x/d (Point Source Injection - Fully Developed Flow - $C_i = 500$ w.p.p.m.).	285

Figure 193.	$(\lambda/(d/2))$ vs. x/d (Point Source Injection - Fully Developed Flow - $C_i = 500$ w.p.p.m.).	286
Figure 194.	$(\lambda/(d/2))$ vs. x/d (Point Source Injection - Fully Developed Flow - $C_i = 500$ w.p.p.m.).	287
Figure 195.	$(\lambda/(d/2))$ vs. x/d (Point Source Injection - Fully Developed Flow - $C_i = 1000$ w.p.p.m.).	288
Figure 196.	$(\lambda/(d/2))$ vs. x/d (Point Source Injection - Fully Developed Flow - $C_i = 1000$ w.p.p.m.).	289
Figure 197.	$(\lambda/(d/2))$ vs. x/d (Point Source Injection - Fully Developed Flow - $C_i = 1000$ w.p.p.m.).	290
Figure 198.	$(\lambda/(d/2))$ vs. x/d (Point Source Injection - Uniform Flow - Water Injection).	291
Figure 199.	$(\lambda/(d/2))$ vs. x/d (Point Source Injection - Uniform Flow - Water Injection).	292
Figure 200.	$(\lambda/(d/2))$ vs. x/d (Point Source Injection - Uniform Flow - Water Injection).	293
Figure 201.	$(\lambda/(d/2))$ vs. x/d (Point Source Injection - Uniform Flow - $C_i = 50$ w.p.p.m.).	294
Figure 202.	$(\lambda/(d/2))$ vs. x/d (Point Source Injection - Uniform Flow - $C_i = 50$ w.p.p.m.).	295
Figure 203.	$(\lambda/(d/2))$ vs. x/d (Point Source Injection - Uniform Flow - $C_i = 50$ w.p.p.m.).	296

Figure 204.	$(\lambda/(d/2))$ vs. x/d (Point Source Injection - Uniform Flow - $C_i = 100$ w.p.p.m.).	297
Figure 205.	$(\lambda/(d/2))$ vs. x/d (Point Source Injection - Uniform Flow - $C_i = 100$ w.p.p.m.).	298
Figure 206.	$(\lambda/(d/2))$ vs. x/d (Point Source Injection - Uniform Flow - $C_i = 100$ w.p.p.m.).	299
Figure 207.	$(\lambda/(d/2))$ vs. x/d (Point Source Injection - Uniform Flow - $C_i = 250$ w.p.p.m.).	300
Figure 208.	$(\lambda/(d/2))$ vs. x/d (Point Source Injection - Uniform Flow - $C_i = 250$ w.p.p.m.).	301
Figure 209.	$(\lambda/(d/2))$ vs. x/d (Point Source Injection - Uniform Flow - $C_i = 250$ w.p.p.m.).	302
Figure 210.	$(\lambda/(d/2))$ vs. x/d (Point Source Injection - Uniform Flow - $C_i = 500$ w.p.p.m.).	303
Figure 211.	$(\lambda/(d/2))$ vs. x/d (Point Source Injection - Uniform Flow - $C_i = 500$ w.p.p.m.).	304
Figure 212.	$(\lambda/(d/2))$ vs. x/d (Point Source Injection - Uniform Flow - $C_i = 500$ w.p.p.m.).	305
Figure 213.	$(\lambda/(d/2))$ vs. x/d (Point Source Injection - Uniform Flow - $C_i = 1000$ w.p.p.m.).	306
Figure 214.	$(\lambda/(d/2))$ vs. x/d (Point Source Injection - Uniform Flow - $C_i = 1000$ w.p.p.m.).	307

Figure 215.	($\lambda/(d/2)$) vs. x/d (Point Source Injection - Uniform Flow - $C_i = 1000$ w.p.p.m.).	308
Figure 216.	Non-dimensional Diffusion Boundary Layer Thickness Profiles (Point Source Injection - Fully Developed Flow).	309
Figure 217.	Non-dimensional Diffusion Boundary Layer Thickness Profiles (Point Source Injection - Fully Developed Flow).	310
Figure 218.	Non-dimensional Diffusion Boundary Layer Thickness Profiles (Point Source Injection - Uniform Flow).	311
Figure 219.	Energy Spectra (Point Source Injection - Fully Developed Flow - Water Injection).	312
Figure 220.	Energy Spectra (Point Source Injection - Fully Developed Flow - $C_i = 50$ w.p.p.m.).	313
Figure 221.	Energy Spectra (Point Source Injection - Fully Developed Flow - $C_i = 100$ w.p.p.m.).	314
Figure 222.	Energy Spectra (Point Source Injection - Fully Developed Flow - $C_i = 250$ w.p.p.m.).	315
Figure 223.	Energy Spectra (Point Source Injection - Fully Developed Flow - $C_i = 500$ w.p.p.m.).	316
Figure 224.	Energy Spectra (Point Source Injection - Fully Developed Flow - $C_i = 1000$ w.p.p.m.).	317

Figure 225.	Energy Spectra (Point Source Injection - Uniform Flow - Water Injection).	318
Figure 226.	Energy Spectra (Point Source Injection - Uniform Flow - $C_i = 50$ w.p.p.m.).	319
Figure 227.	Energy Spectra (Point Source Injection - Uniform Flow - $C_i = 100$ w.p.p.m.).	320
Figure 228.	Energy Spectra (Point Source Injection - Uniform Flow - $C_i = 250$ w.p.p.m.).	321
Figure 229.	Energy Spectra (Point Source Injection - Uniform Flow - $C_i = 500$ w.p.p.m.).	322
Figure 230.	Energy Spectra (Point Source Injection - Uniform Flow - $C_i = 1000$ w.p.p.m.).	323
Figure 231.	Sampling Rate Effect.	324
Figure 232.	Sampling Rate Effect.	325
Figure (A.1)	Sampling Rate Effect (Line Source Injection - $C_i = 250$ w.p.p.m.).	329
Figure (A.2)	Sampling Rate Effect (Line Source Injection - $C_i = 500$ w.p.p.m.).	330
Figure (A.3)	Sampling Rate Effect (Point Source Injection - Uniform Flow - $C_i = 50$ w.p.p.m.).	331
Figure (A.4)	Sampling Rate Effect (Point Source Injection - Uniform Flow - $C_i = 100$ w.p.p.m.).	332

Figure (A.5)	Sampling Rate Effect (Point Source Injection - Uniform Flow - $C_i = 250$ w.p.p.m.).	333
Figure (A.6)	Sampling Rate Effect (Point Source Injection - Fully Developed Flow - $C_i = 50$ w.p.p.m.).	334
Figure (A.7)	Sampling Rate Effect (Point Source Injection - Fully Developed Flow - $C_i = 50$ w.p.p.m.).	335
Figure (A.8)	Sampling Rate Effect (Point Source Injection - Fully Developed Flow - $C_i = 100$ w.p.p.m.).	336
Figure (A.9)	Sampling Rate Effect (Point Source Injection - Fully Developed Flow - $C_i = 100$ w.p.p.m.).	337
Figure (A.10)	Sampling Rate Effect (Point Source Injection - Fully Developed Flow - $C_i = 100$ w.p.p.m.).	338
Figure (A.11)	Sampling Rate Effect (Point Source Injection - Fully Developed Flow - $C_i = 250$ w.p.p.m.).	339
Figure (A.12)	Sampling Rate Effect (Point Source Injection - Fully Developed Flow - $C_i = 250$ w.p.p.m.).	340
Figure (A.13)	Sampling Rate Effect (Point Source Injection - Fully Developed Flow - $C_i = 250$ w.p.p.m.).	341
Figure (A.14)	Sampling Rate Effect (Point Source Injection - Fully Developed Flow - $C_i = 500$ w.p.p.m.).	342
Figure (A.15)	Sampling Rate Effect (Point Source Injection - Fully Developed Flow - $C_i = 500$ w.p.p.m.).	343

Figure (A.16) Sampling Rate Effect (Point Source Injection - Fully Developed Flow - $C_i = 500$ w.p.p.m.).	344
Figure (A.17) Calibration Curve for the Rotometer.	346
Figure (A.18) Optical Density (O.D.) vs. Exciting Wave Length.	347
Figure (A.19) Calibration Curve for the Spectrophotometer.	348

NOMENCLATURE

SYMBOL	DESCRIPTION	UNIT
a, a_1, a_2, \dots	Constants	
A	Constant: $\int_0^{\delta/\lambda} (\epsilon)^{1/n} f(\epsilon) \cdot d\epsilon$	
A_1	Constant $\lambda^2 C_m$	m^2
b_1, b_2, b_3, \dots	Constants	
C	Polymer concentration	
C_i	Value of C at injection source fluid	
\bar{C}	Time average value of C at a point	
\bar{C}_m	maximum concentration	
C'	Turbulent conditional average value of c at a point	
d	Injection source inner diameter	mm
D	Molecular diffusivity	m^2/s
$D(t)$	Eddy diffusivity	m^2/s
E	Energy	mv^2/H_3
G_i	Volume flux of polymer solution per unit span	m^2/s
h	Slot thickness	mm
I.D.	Pitot tube inner diameter	mm
K	Von Karman constant	
L	Injection source length	mm
n	Velocity profile power law constant	
Q_i	Volume flux of polymer solution	1/s
r	Radial location	mm

R	Radius of the test section	m
T	Turbulent intensity $((U'^2)^{1/2}/U$	
U, V, W	x, y, z-component of the velocity vector	m/s
$\bar{U}, \bar{V}, \bar{W}$	Time average value of the velocity components	m/s
U', V', W'	Turbulent conditional average value of U, V, W at a point	m/s
U_i	Injection velocity	m/s
u_τ	Local value of the friction velocity, $\sqrt{\tau_w/\rho}$	m/s
U_m	Mean free stream velocity	m/s
V_s	Sampling velocity	m/s
x, y, z	Rectangular coordinates; x measured along the flow direction from the injection source; y normal distance from the surface; z spanwise position	
δ	Boundary layer thickness	mm
θ	Boundary layer momentum thickness	mm
λ	Value of y at which $\bar{c}/\bar{c}_m = 0.5$	mm
ξ	y/λ	
η	r/λ	
ρ	Water (or polymer solution) density	kg/m ³
τ_w	Local wall shear stress	N/m ²
ω	Frequency	Hz
ν	Kinematic viscosity	m ² /s
ΔT	Change in turbulent intensity	
ΔU	Change in flow velocity	m/s

Abbreviations

w.p.p.m. Weight parts per million
O.D. Optical Density
I.O.D. Injection Optical Density

Subscripts

r Radial direction
x Longitudinal direction

CHAPTER 1
INTRODUCTION

That some additives can considerably reduce drag in turbulent flow has been well established during the past three decades, since Tom's first publication on the subject. The actual mechanism involved has not been definitely established but it certainly appears that the suppression of high frequency turbulence in the inner wall or buffer zone of the boundary layer must play an important role. However, in order to establish efficient drag reduction conditions, it is necessary to know the criteria required. Obviously if heterogeneous systems are used, the problem is to establish the mechanism and rates for diffusion of the additive and the methods for introducing it.

A number of methods may be used to get the additive into the crucial wall region of the boundary layer. For example, homogeneous dispersion, injection or additive coatings may be used. Homogeneous flows are only of practical value in internal flows such as closed loop or recirculating systems, and even then they would be inefficient since the majority of the additive has not been used and will degrade. However, some form of injection flows may be used on many practical systems, which involve external or internal flows.

Obviously it is necessary to have available methods

for determining the dispersion rate of the additive from the injection area if design calculations or feasibility studies are to be made. This thesis is concerned with the subject of the turbulent diffusion and associated phenomena of an aqueous polymer solution, when it is injected either, from a line source into a developing turbulent boundary layer, or from a point source into a fully developed flow and uniform flow.

Unfortunately, the majority of research on polymer additives has been on drag reduction efficiency and methods of getting the polymer into the boundary layer. Very little research has been reported on the prediction of turbulent diffusion rates. Furthermore, very few papers giving empirical data have been published, which are necessary if accurate methods of predicting dispersion rates and concentration levels are to be achieved.

This research was instigated to help fill the gap in the available empirical knowledge, especially regarding the near injection region, a virtually neglected area, as well as to verify existing though very sparse data for the far downstream conditions.

To this end, two small water tunnels with injector facilities were constructed, in which concentration and energy spectrum measurements were made, with a maximum flow velocity of the order of 4.5 m/s.

CHAPTER 2

LITERATURE SURVEY

That the frictional resistance of turbulent flow of liquids can be reduced by the addition of certain additives, such as polymers, is well known. The reduction of drag can be associated with polymer properties and the hydrodynamics of the flow.

Reviews by Gadd [1], Hoyt [2], Palyvos [3], Virk [4], and White and Hemmings [5] have covered the majority of publications relevant to drag reduction. However, a summary of the publications pertinent to polymer diffusion, including relevant Newtonian diffusion flows, velocity and energy spectral measurements are briefly reviewed here.

2.1 Diffusion

In an effort to better understand the drag reduction process, the diffusion or dispersion characteristics of drag reducing fluids has been the subject of several investigations. Unfortunately, very little information is available in the open literature on the diffusion of drag reducing additives.

In a study of the diffusion phenomena of drag reducing additives, it is worthwhile to compare the available data with existing theories and also data for Newtonian fluids.

Therefore, pertinent aspects on all research on the diffusion in turbulent fluid flows must be considered. The diffusion process for injected flows may be put into three categories:

- (a) Wall injection through a line slot.
- (b) Distributed or radial injection through a wall.
- (c) Point source injection.

These methods will be discussed separately below:

(a) The diffusion of wall-injected fluids

The diffusion of wall-injected polymeric solutions or any other fluids into pure water or other Newtonian fluids has been the subject of a few research papers.

With regard to Newtonian fluids, Póreh and Cermak [6] studied the two-dimensional turbulent mixing of ammonia gas injected into a turbulent boundary layer developed on the wall of a wind tunnel. The data were obtained using a 24.38 m long horizontal wind tunnel having a 1.83×1.83 m square test section with air speeds in the range 2.74 to 4.88 m/s, and a Reynolds number of up to 5×10^6 . They defined four zones in the development of the diffusion boundary layer, which were:

- (i) The initial zone, in which very large velocity and concentration gradients make it difficult to obtain reliable data. The length of the initial zone is determined by the initial conditions near the source, the physical size of the source relative to the

thickness of the sublayer, the injection velocity and the magnitude of the molecular diffusivity.

- (ii) The intermediate zone, in which longitudinal gradients are small compared to vertical gradients. Within this zone the diffusing plume is totally submerged in the boundary layer, and the rate of growth of the dimension of the plume normal to the flow is large compared to the rate of the growth of the boundary layer itself. This zone extends 20-40 hydrodynamic boundary layer thicknesses downstream from the injection slot.
- (iii) The transient zone, in which the effect of the mixing process in the ambient fluid outside the hydrodynamic boundary layer decreases the rate of growth of the diffusing plume and gradually changes the shape of concentration profile.
- (iv) The final zone, in which the diffusion of the injected matter beyond the hydrodynamic boundary layer is controlled by the molecular action and turbulent fluctuations at that location.

The major difference between the intermediate zone and the final zone is that the characteristics of the diffusion field are independent of the position of the source in the final zone.

With regard to polymer solution injection into a pure

water boundary layer, Fabula and Burns [7] studied the turbulent mixing with and without the addition of the friction reducing polymer (Polyox WSR-301) solution, in an approximately two-dimensional open channel flow. The investigation was conducted in a 2.74 m wide, by about .305 m in depth, test section and with a main stream velocity of 5.5 m/s and Reynolds number of up to 8×10^7 . Sampling stations were at locations 4.88 and 12.19 m downstream from the injection slot, with injection concentration of 500 wppm. They applied the negative roughness analogy for polymer in which the logarithmic law of the wall for the velocity distribution is,

$$u/u_{\tau} = (1/K) \ln(y u_{\tau}/\nu) + Bo + \Delta B \quad (2.1)$$

where Bo is the smooth-wall value for Newtonian fluids and ΔB is the shift of the constant Bo , which is either positive for rough surfaces or negative for polymer solutions. This analogy is useful in the case of low polymer concentration and moderate wall shear stress. Data were only taken in a region which defined the final zone. Good agreement was obtained between the calculated and experimental wall concentration. The results for both water and polymer solution injection flows were found to be quite similar.

Wetzel and Ripken [8] carried out an experimental study of the diffusion and shear in a thick boundary layer when injected with a solution of the polymer (Polyox WSR-301). Measurements were made in a plane boundary layer with lengths

of up to 12.19 m and Reynolds number varying up to 8×10^7 . Aqueous solutions of 250 to 2000 w.p.p.m. were injected tangentially into the boundary layer near its origin when the free stream velocity was 5.5 m/s. They found that complete mixing of the polymer within the boundary layer was attained when a relatively low concentration of polymer solution was injected into a thickened or partially developed turbulent boundary layer. Concentration profiles were dimensionally correlated with suitable correcting parameters for low quantities of polymer injected in the boundary layer. They also observed that the total drag reduction was a function of the distance from the injected slot and the quantity of polymer injected in the boundary layer. That is, for locations just downstream from the injection slot, greater drag reduction was attained for the lower quantities than for the higher quantities of polymer injected. However, at distances further downstream, better drag reduction was attained with larger injection quantities. This behaviour was apparently associated with more complete mixing of the injected polymer in the developing boundary layer.

In a later work, Poreh and Hsu [9] using Poreh's previous data, calculated the diffusion in the intermediate zone when a Newtonian fluid is ejected from a continuous line source. They modified a method based on Lagrangian similarity to describe the mean position of an ensemble of particle release. Furthermore, they studied the effects of roughness

and polymer additive (using negative roughness analogy) and found that the diffusion increased for the case of rough surfaces and Newtonian fluids and decreased for drag reducing additives.

In their most recent paper on the subject Poreh and Hsu [10] analyzed the diffusion of dilute drag reducing polymer solutions and the effect of the diffusing polymer on the development of the boundary layer. The results of their analysis suggest that both the diffusion rate and the drag were reduced. However, since in most practical situations the required concentration is small, the reduction in the diffusion rate would also be small. They also concluded that except for very slow moving ships, the initial stage of diffusion would be relatively short and insignificant. However, in the final zone of diffusion there would be virtually no polymer left in the viscous sublayer. Furthermore, the structure of the major portion of the turbulent boundary is not affected by the polymers because of the dilution achieved in that region. They also predicted that the distribution in the final zone can be expected to be similar to the distribution of inert tracers. Thus the main changes in the diffusion rate would occur in the intermediate zone. It was also predicted that the drag reduction per unit discharge was larger for small values of injected polymer indicating that it might be more economic to obtain only limited drag reduction. Furthermore, they estimated that the injected polymer fill the entire boundary layer within a distance smaller than 100 times

the boundary layer thickness.

Jin Wu [11] measured the concentration profile for the injection of the drag reducing polymer (Polyox WSR-301) from a thin wall slot into a developing external turbulent boundary layer, using a laser phototransistor unit. The experiments were performed in a circulating channel having a closed test section 112 cm long by 38 cm wide and 19 cm deep. Concentration measurements were made at a location 0.52 m downstream from the slot when the free stream velocity was 2.62 m/s and the Reynolds number was approximately 1.5×10^6 . The research included tests of ejecting aqueous polymer solutions of various concentrations of up to 1000 w.p.p.m. at various injection rates. It was observed that polymer thickens the viscous sublayer which appreciably increases the flow rate in the sublayer. Therefore, the dilution of polymer due to turbulent mixing outside of the sublayer takes place with a smaller fraction of the ejected solution than for water injection. There is some disagreement between Wu's concentration measurements and those reported earlier in [6] and [7]. Wu's results indicated a suppression of the diffusion of additive within a turbulent boundary layer when the concentration of the ejected solution is greater than 100 but indicated that there is very little change in turbulent diffusion with a polymer injection concentration less than 100 w.p.p.m.

Fruman and Tulin [12], studied the diffusion of a thin tangential injection of drag reducing polymer, Polyox WSR

301, into the turbulent hydrodynamic boundary layer formed on a flat plate 3.048 m long and 5.08 cm thick, with injection concentration of up to 1000 w.p.p.m. Five sampling stations were located at 0.063, 0.203, 0.508, 1.007 and 2.337 m from the injection slot. The tests were performed at a constant free stream velocity of 10.65 m/s and Reynolds number of up to 3.6×10^7 , for a variety of ratios of injection to free stream velocities. Two zones were delineated. In the first zone, the wall concentration remains almost constant, and equal to the injected one. In the second zone, the concentration varies approximately as the inverse of the distance from the injection slit. The length of the first zone is highly influenced by the additive and increases linearly with the value of the injected concentration. They concluded that the wall concentration distribution is related to the drag reduction and a simple correlation between its values and the characteristic parameters of the external flow and the drag reducing injection was established.

Collins and Gorton [13] experimentally studied the diffusion of poly(ethylene oxide) solution when injected from a line source into a two-dimensional developing turbulent boundary layer in channel flow. Concentration measurements were obtained at stations located 8, 23, 38 and 53 cm downstream from the injection source with a constant free stream velocity of 0.8 m/s and Reynolds number in the range of 1.05×10^6 to 1.44×10^6 . Runs were made with water and also

aqueous polymer solution injection with concentrations of up to 2000 w.p.p.m. The first two zones of diffusion defined by Poreh [6] were investigated. The initial zone immediately after injection grows slowly by molecular diffusion in a laminar sublayer. The growth of the initial zone is less than that of water since the molecular diffusivity is less for a polymer solution. The next zone which is the intermediate zone, grows more rapidly than the initial zone owing to the high turbulence intensity near the wall. Its concentration profile is similar to that found by [6] for a passive contaminant.

Latto and El Riedy [14] experimentally studied the diffusion of water and aqueous polymer (Reten 423), when tangentially injected from a line slot into a two-dimensional external boundary layer formed on a flat plate 1.3 m long, located in a .152 m (6 in.) I.D. pipe. Samples were taken from the flow field at locations of 0.05, 0.146, 0.304, 0.558 and 0.844 m downstream from the injection slot. Concentration profiles were obtained using a spectrophotometer. The investigation was carried out for a constant free stream velocity of 5.4 m/s and Reynolds number of up to 5.7×10^6 , for various injection flow rates and concentrations in the range 0 to 1500 w.p.p.m. Empirical equations describing the transverse and longitudinal concentration field for given injections and flow parameters were presented. The results showed that turbulent diffusion of polymer solution is suppressed compared to that of water when the concentration at the wall is higher than

0.75 w.p.p.m., but increased below this value. The data also confirmed the deduction of others that several regions can be defined, the length of which are dependent on the injection concentration and flow rate.

Recently Shulman, Z.P. et al. [15] obtained experimental data on the concentration field for polymer solutions injected from a wall slot using an electrochemical technique. The measurements were carried out in a 50 x 50 mm square duct. Concentrated Polyox WSR 301 solution was injected into the boundary layer through a wall slot at a distance of 42 diameters downstream from the duct entrance. Their results showed that the wall concentration for polymer solution injection is higher than the wall concentration obtained with water injection, indicating that the dispersion was suppressed for the polymer solution.

(b) Distributed or radial injection through a wall


Distributed polymer solution injection through the porous walls of a pipe was employed by Wells [16], who found that it substantially reduces the polymer quantity required for drag reduction when compared to injection through discrete slots.

In another such experiment, Walters and Wells [17, 18] studied the mechanism of turbulent diffusion of an aqueous solution of Polyox WSR-301 when uniformly injected through the wall of a 19 mm diameter pipe in which the flow of water was fully developed. The average velocity of the water in the

pipe was 3.66 m/s, that is a Reynolds number of 7.5×10^4 . Experimental diffusion data were obtained using very low injection rates and concentrations in the range of 0 to 1000 w.p.p.m. They observed an increase in the viscous sublayer thickness which was accompanied by an increase in the diffusion sublayer thickness. They also obtained empirically diffusion coefficient which showed that the diffusion rate of polymer in the region of the polymer deficient turbulent core is greater than that for the diffusion of a Newtonian fluid. Consequently, there is a significant reduction in the turbulent diffusion in the near wall region which leads to higher concentrations there than for the case of water injection.


Rubin [19] theoretically obtained an estimation for the reduction in the mass diffusion caused by polymeric additives. He obtained a relation between the Sherwood number which is the mass transfer coefficient and the Reynolds number. He also predicted the changes in the concentration versus the transverse height profiles due to polymeric additives.

Sidahmed and Griskey [20] used an electrochemical technique to study mass transport from liquid to the tube wall in drag reducing polymer (Polyox WSR 301). The data were obtained using a tube of 16 mm inner diameter with average fluid velocity in the range of 0.6 to 0.9 m/s which corresponds to Reynolds numbers in the range of 1.065×10^4 to 1.496×10^4 . Three concentrations of polymer solutions (10, 50,



100 w.p.p.m.) were studied. The technique used was basically to measure the limiting current of the cathodic reduction of $K_3Fe(CN)_6$. It was found that the polymeric additives retarded mass transfer in turbulent, but not in laminar, flow systems.

Walters [21] reported the effects of polymer molecular weight and injection mass flux on skin friction and turbulent diffusion when a polymer solution is injected through the hydrodynamic boundary layer formed in a pipe. He found that the optimum molecular weight for maximum drag reduction is an order of magnitude less than that normally used with homogeneous solutions or localized injection and that the turbulent diffusivity decreases exponentially with molecular weight.



In recent studies Bhowmick, S. K. et al. [22, 23] conducted experiments on the turbulent dispersion of aqueous solutions of macromolecules in hydrodynamic boundary layers, when injected annularly into circular pipe flow. Dispersion was made visible by the addition of a fluorescent dye to the injected fluid. Observations were made for Reynolds numbers of about 10,000 and with injected fluid concentrations varying from 100 to 1500 w.p.p.m. He defined a "cone of diffusion" as the cone of fluid which is not affected by the injected dye. This cone was considered the boundary layer for diffusion. It was found that for the injection of a Newtonian fluid the length of the "cone of diffusion" is practically independent

of the flow condition. Whereas for the injection of drag reducing fluids the length of the cone is primarily dependent on the Reynolds number, the injection rate and concentration of the injected fluid.

Gebel, C. et al. [24] studied the turbulent dispersion of macromolecular solutions injected annularly in a cylindrical pipe in turbulent flow. Tests were carried out at a Reynolds number of 40,000, the injection concentration varied from 200-800 w.p.p.m. They obtained the longitudinal and transverse concentration profiles and represented changes in concentrations using a mathematical model which was originally proposed by Morkovin [25].

(c) Axial Point Injection

Flint, Kada and Hanratty [26] studied the turbulent diffusion from a small source located in the center of a 76 mm diameter pipe. Hydrogen and carbon dioxide were injected into an airstream and aqueous potassium chloride solution was injected into the waterstream. The data were obtained for Reynolds numbers in the range 0.97×10^4 to 8.7×10^4 . Eddy diffusion coefficients calculated from the data were correlated as a function of Reynolds number. Their results could not be used for determining the form of the correlation coefficient because of inaccuracies in the measurements for small diffusion times.

Davar [27] studied the diffusion of anhydrous ammonia

when injected from an elevated source into a developing external air boundary layer. The data were obtained using a "low-speed wind tunnel" (1.83x1.83x8.53 m test section) which produced a constant air free stream velocity of 1.83 m/s with Reynolds numbers of up to 10^6 . The results showed that when the height of the source was less than one-third the depth of the boundary layer, the central region with the highest concentrations within the plume moved down toward the boundary immediately downstream from the source. By keeping the source elevation above the previous height, it should be possible to considerably delay the spread of the plume toward the boundary. He found that the maximum concentration in the central zone of the plume was very sensitive to the ratio of the source height to the depth of the boundary layer for downstream distances in the neighbourhood of four times the depth of the boundary layer at the source; at distances greater than thirty times the depth of the boundary layer, the variation in the maximum concentration due to changes in the source height became practically insignificant.

Koo and Wade [28] experimentally obtained concentration and velocity profiles in axisymmetric turbulent air flow using ethylene injected along the flow center line of a 0.14 m diameter pipe for Reynolds numbers from 7,300 to 58,300. The curves were analyzed to give values of the non-dimensional mass diffusivity as a function of radius ratio.

In a later work, Wade and Kumar [29] calculated the theoretical concentration curves for the injection of ethylene on the centre line of the pipe in which fully developed turbulent air flow was an entrance condition. Agreement with previous experimental results was shown to be satisfactory at stations far downstream from the injection location.

Taylor and Middleman [30] recently measured the radial dispersion of dyed water injected from an axial point source into turbulent water and also dilute Polyox WSR 301 solution of up to 50 w.p.p.m. flow in a 51 mm diameter vertical pipe. The data were obtained for a variety of Reynolds numbers in the range 18,000 to 45,000. Their results indicated that in the presence of Polyox, dispersion is due to large scale turbulent motion, while the turbulence intensity itself is reduced and the energy spectrum shifted toward that of a lower frequency.

An experimental study was carried out by Sellin [31] on the turbulent dispersion of both water and dilute aqueous polyethylene oxide solutions in water using time exposure photography of dye released from a point source. The experiments were conducted in a 44x44 mm square duct with flow Reynolds numbers of about 40,000. In the first experiment reported the polymer was added at the duct inlet to give uniform distribution along the duct length, while in the second the concentrated polymer solution was added at the duct center line at various distances upstream from the point of

the dye release. A relationship between the dispersion cone angle and the degree of drag reduction was obtained. It was shown that for the latter experiments polymer injection suppressed turbulence in the core of the duct flow before the injected polymer had dispersed to the duct walls.

2.2 Velocity and Spectral Measurements

Even though drag reduction has been reported for many polymer solutions and has been the subject of much discussion in the literature, no completely satisfactory explanation has been put forward for the mechanism by which this reduction in frictional drag occurs. Unfortunately classical experiments which have proved so successful in studying the structure of Newtonian turbulent flow, such as pitot tubes, and hot wire anemometers are being questioned, because of anomalous results, which can be attributed to the viscoelastic properties of the solutions. Therefore the more recent flow parameter measurements have been made with laser Doppler anemometers, which do not disturb the flow, and are unaffected by the fluid properties.

A summary of the publications related to the velocity and spectral measurements are briefly reviewed here.

Greated [32] used a laser velocimeter to study the effect of polymer addition on grid turbulence. The experiments were conducted in a 0.9 m long, 50 mm wide by 60 mm deep rectangular channel, and the measurements were taken along

the centre line of the channel at different distances downstream of a rectangular grid of bars. The velocity was kept constant and with a grid Reynolds number of 10^3 . The results indicated that the effect of polymer addition was both to decrease the overall turbulent intensity and to steepen the fall-off of the frequency spectrum towards higher wave numbers.

The results of experimental measurements of the spectral components of turbulent momentum transfer were presented by Bremhorst, K. and Walker, T. B. [33] for fully developed pipe flow. Hot wire anemometry for flow Reynolds numbers of about 54,000 were used. Their results indicated that near the wall two types of momentum transfer process occurred. A net positive transfer took place in the higher frequency range of the energy-containing part of the turbulence spectrum; whereas a net negative transfer returned low momentum to the wall region at the lower end of the energy spectrum. Frequency scaling spectra showed that the transition of turbulence to the universal range occurred in the same frequency band throughout the flow.

In a theoretical study which was verified experimentally, George, W. K. and Lumely, J. L. [34] deduced that the fundamental limitation of the laser Doppler anemometer, when used for the turbulent measurement, is the Doppler ambiguity introduced by the finite transit time of particles through the scattering volume, turbulent velocity fluctuations across

the scattering volume, mean velocity gradients and electronic noise. A unified account of the effect of the Doppler ambiguity on the measurement of the instantaneous velocities was presented and results were interpreted on the basis of the power spectrum. They also examined the influence of the ambiguity of the measurements of other statistical quantities.

Rudd, M. J. [35] presented results of experiments on velocity measurements using a laser Doppler anemometer on turbulent pipe flow of a dilute polymer solution. The experiments were conducted in a 12.7x12.7mm square by 2.28 m long duct with Reynolds numbers of up to 5×10^4 . The results suggested that the polymer has very little effect upon the turbulent core of the flow, but thickens and stabilizes the viscous sublayer. The turbulent intensity inside the sublayer was unchanged, but owing to its thickening, the velocity fluctuations just outside were greater. There was not a general suppression of turbulence within the sublayer, although well inside the sublayer the spanwise velocity component was found to be reduced.

A laser Doppler anemometer was used by Logan, S. E. [36] to measure the Reynolds stress and turbulence in dilute aqueous polymer solutions. The experiments were conducted in a 12.7x12.7 mm square duct with a flow Reynolds number of 25,000. His results indicated that polymer additives suppress transverse velocity fluctuations at a distance considerably beyond the viscous sublayer, although the values in the tube

center were of comparable magnitude. It was also observed that the Reynolds stress was reduced in the turbulent core by an amount proportional to the observed decrease in pressure gradient at the wall. The turbulence level measurements were in good agreement with those of Rudd [35].

Kumar, S. M. and Sylvester, N. D. [37] experimentally studied the effects of drag reducing polymer on the turbulent boundary layer using a laser Doppler anemometer. The tests were carried out on a submerged flat plate located in a 0.2x0.2 m square water tunnel with a flow Reynolds number of 2×10^5 . The results demonstrated that the polymer molecules not only affected the near wall region, as was shown by a change in the thickness and velocity gradient in the viscous sublayer, but also the turbulent core.

To study the effect of ambiguity in turbulence measurement using a laser Doppler anemometer, Berman, N. S. and Dunning, J. W. [38] conducted experiments, in pipes of 25.4 and 50.8 mm diameters with Reynolds numbers from 5000 to 15000, to measure the turbulence level at the center line and near the wall in the water flow. Their results showed that the turbulent spectra for these water flows, after accounting for the ambiguity, were equivalent to hot film measurements at similar Reynolds numbers. They also demonstrated the feasibility of laser Doppler measurements very close to the wall in shear flow.

Barker, S. J. [39] conducted experiments on a round turbulent jet to measure the mean and fluctuating flow velocities in water or dilute polymer solutions using laser Doppler anemometry. Turbulent round jets with Reynolds numbers between 5000 and 50,000 were studied. He found that for a jet issuing from a convergent nozzle the additives have no effect upon the mean axial velocity or turbulence intensity at any point in the jet. However, for a jet issuing from a long length of circular pipe, the additives reduced the center line velocity and increased the turbulence level in the early part of the jet, indicating that the principal effect of a polymer additive upon the jet appeared to result from its effect upon the initial conditions.

A technique by which the effect of the random phase fluctuations or Doppler ambiguity could be removed from the measurements of turbulence intensities was proposed by George, W. K. [40] when using a laser Doppler anemometer. He suggested that a sequence of low-pass filters at frequencies above those of the turbulence be used in the measurement of turbulence intensities.

Reischman, M. M. and Tiederman, W. G. [41] carried out experimental measurements of the mean and turbulence intensity of the streamwise velocity component in fully developed, turbulent, drag reducing flow in a two-dimensional channel using a laser Doppler anemometer. Measurements were made in a 305x28.4 mm channel with Reynolds numbers varying from 20,000

to 52,400. Their results showed that a drag reducing mean velocity profile could be divided into three zones: a viscous sublayer, a buffer or interactive region and logarithmic region. There was no evidence that the viscous sublayers of the drag reducing channel flows were thicker than those of the solvent flow. In addition, the normalized streamwise fluctuations were essentially the same in both the solvent and drag reducing sublayers. The changes caused by the polymer addition occur in the buffer region. The drag reducing buffer region was thicker and the velocity profile in the outer flow region adjusted in order to accommodate this buffer region thickening. Their results are in disagreement with those reported earlier by Rudd [35], Logan [36] and Kumar and Sylvester [37].

Bertshy, J. R. and Abernathy, F. H. [42] conducted experiments on two-dimensional boundary layer flows of dilute solutions of polyox in a free surface water table. Experiments were carried out on laminar and turbulent flows with very small Reynolds numbers. Velocity spectra were obtained using a laser Doppler anemometer. The results showed that undisturbed polymer flows at sufficient concentration exhibited velocity fluctuations distinct from turbulence which they termed as polymer induced fluctuations. They believed that they were most likely responsible for the phenomenon of so called "early turbulence". Their studies of turbulent polymer flows (disturbed artificially) indicated significant drag

reduction and were all consistent with the view that hairpin eddies are the major mixing mechanisms in a turbulent boundary layer, and that these eddies were suppressed by the addition of polymers. No distinction between artificially disturbed and undisturbed flow at the same condition could be observed.

Summary Conclusions

It is obvious from the available literature that there are only a very few publications on turbulent diffusion rates or energy spectrum analysis. To date, they may be put into the following categories:

- 1) Two on the diffusion from a point source.
- 2) Nine on injection from a line source which mainly cover the diffusion in the final zone.
- 3) Seven on uniformly distributed injection.
- 4) Eight on energy spectrum, which mainly cover the effect of polymer solution on turbulence intensity.

In all cases more data are needed to adequately present concentration fields for all the longitudinal diffusion zones. Furthermore, if there is to be a better understanding of the mechanism involved considerably more data on the effect of polymer additives on energy spectrum are needed.

The major problems being that

- i) There are several ways of introducing the polymer into the system.
- ii) There are several geometric arrangements and flow fields that have been considered.
- iii) There are numerous types of polymers that can be

24(a)

investigated.

For all the above papers it is virtually impossible /
to obtain definitive correlations for the data and
only qualitative deductions can be made. Therefore if any
realistic correlations and deductions are to be obtained
it is imperative that comprehensive data be obtained for
a particular system and polymer.

CHAPTER 3

EXPERIMENTAL APPARATUS

The research was primarily directed towards a study of turbulent dispersion and associated phenomena, for injection of Newtonian and non-Newtonian aqueous solutions from point and line source into developed and developing internal water flows at relatively high Reynolds numbers.

Schematic diagrams of the systems that were used for the research are given in Figures (5) and (6). The system was comprised of a 50 m³ capacity in-ground storage reservoir (sump tank), from which the water was pumped via a single stage centrifugal pump*, driven by a three-phase a.c. motor⁺, to a 7.5 m³ capacity constant head header tank situated above the apparatus. The water then flowed into either of two test sections, see Figures (1), (2), (3) and (4), via cylindrical brass filters and cruciforms, to reduce vorticity and air ingestion. This arrangement produced a maximum static head of 3.3 m at the test sections. It was possible to add mains water to the header tank. This made it possible to dilute the recirculating water and prolonging a

* Canada Pumps Limited, 1400 U.S. gal/min., 1150 r.p.m., 20 ft. head, 10 H.P.

+ Robbins and Meyers Company, 30, 55 V, 11 A, 1140 r.p.m., 10 H.P., continuous duty.

given experimental run by avoiding a build up of the polymer concentration in the water due to the injected solution.

The two test sections that were used were:

- (i) a 152 mm I.D. circular plexiglass pipe with central point source injection for fully developed pipe flow, and
- (ii) a 150 mm by 150 mm square section plexiglass sided duct with either central point source or wall slot injection for uniform central core flow or developing flat plate flow.

Two types of point source injection sources were used, as shown in Figure (7), which had either a 25 mm or 75 mm tube length. They had a 'T' configuration of thin walled 3.2 mm I.D. brass tubing. The cross piece supply lines were fitted with a triangular cross section tail to minimize the disturbance downstream.

The geometry of the wall slot injection orifice is shown in Figure (8). The slot was located in the bed of the duct approximately 215 mm from the parallel portion of the test section and ejected the fluid parallel to the plate surface.

3.1 The Water Flow System

3.1.1 Fully Developed Flow Experiments

The water flowed from the header tank, see Figure (5), to the test section via 152 mm I.D. by 10 m long steel pipe.

This length is equivalent to 65 pipe diameters which is greater than the normally accepted 20 to 40 diameters required for fully developed turbulent flow. A gate valve situated near the pipe entrance was used to control the water flow rate. Cruciforms located at the pipe entrance and just after the only upstream bend stopped the vorticity, and a 6.4 mm x 75 mm honeycomb prior to the test section aligned the flow and produced a homogeneous turbulence in the test section.

3.1.1.1 Test Section

The test section was comprised of a plexiglass pipe 1.3 m long and 0.152 m I.D. which permitted visual observation of the liquid flow. There were provisions for 36 total head probes, having dimensions of 0.5 mm I.D. and 1 mm O.D., for collecting samples to obtain concentration data, however only five cross sections were investigated. These cross sections were at distances of 48, 190, 403, 657 and 975 mm downstream from the 25 mm injection source, and of 57, 203, 352, 606 and 924 mm downstream from the 75 mm injection source, which could cover the zones of diffusion previously defined. The probes were attached to a crossbar which could be moved vertically. The vertical location of the bar was measured using two micrometers, having an accuracy of 0.025 mm, which were located at the end of the bar. Wall taps 0.44 m apart were used to obtain the pressure drop within the test section. In order to obtain velocity and energy spectra measurements using a

laser Doppler anemometer, the test section was equipped with three flat windows in both sides, which avoided spherical aberration.

3.1.2 Developing Turbulent Flow Experiments

Figure (6) shows a schematic of the system. In this experiment the water flowed vertically from the constant head tank through a 0.203 m diameter pipe via a plenum chamber to the test section. The plenum chamber was partly filled in the middle section with rocks to break any vorticity created by the water flow in turning. In order to obtain a uniform flow and a thin initial boundary layer in the test section a bell mouth was used at the entrance to the test section. A 6.4 mm x 75 honeycomb prior to the test section aligned the flow and produced more homogeneous turbulence in the test section.

3.1.2.1 Test Section

The test section had a 150 mm square "cross section", which was 1.5 m long, with plexiglass sides which permitted visual observation and a transparent media for the laser beam. The top and bottom were made of aluminum plate for structural strength. A 76.2 mm wide by 0.64 mm deep transverse injection slot, see Figure (8), located 70 mm downstream from the test section inlet was used to tangentially inject the solutions into the developing boundary layer. In order to obtain a uniform injection velocity profile, the injected solution was supplied to both ends of a transverse chamber situated behind the injection

slot.

The point injection sources could be located at distances 50 and 457 mm from the test section inlet for the developing flow experiments. However, only the 75 mm injection source located in the first location was used in this experiment, since in the fully developed flow experiments it was found to produce more stability of the injected fluid than the other injection source.

The concentrations at the wall were obtained at six locations 94, 170, 297, 424, 678 and 1059 mm downstream from the injection slot on the bottom plate. Total head probes were used to collect the samples and also to obtain velocity profiles, were located at distances of 102, 235, 425, 678 and 1059 mm downstream from the injection slot, and of 45, 172, 352, 606 and 997 mm downstream from the point source and could cover all zones of diffusion previously defined. Two wall taps 1.27 m apart were used to obtain the pressure drop within the test section.

3.2 The Polymer Solution Flow System

The polymer solution, see Figures (5) and (6), was supplied from a pressurized storage vessel, which was connected to a 690 kPa constant pressure air supply. The air pressure inside the vessel could be maintained at any desired value using a pressure regulator. The compressed air above the polymer solution was used to discharge the solution to the apparatus via a pipeline at the bottom of the vessel, which

was fitted with a safety valve set for 205 kPa. A rotometer type flowmeter which had been precalibrated with various polymer solution concentrations was used in the polymer solution flow line to measure the injection flow rate to the injection source.

The polymer solution which was prepared in plastic lined bins was supplied to the pressurized vessel by means of a variable speed peristaltic pump*, driven by a three-phase a.c. motor⁺.

3.3 Measuring Instrumentations

- 1) The discharge rate of the injected solution was measured using a rotameter which was calibrated prior to the experiments for various polymer concentrations.
- 2) Concentration profile measurements were made using the total head probes to obtain samples from the flow field. The flow sampling rate was done using a variable speed Peristaltic pump^x in the sampling tube lines. For given conditions the sample rate was normally kept constant, such that it was isokinetically withdrawn, see Appendix (I), so that no disturbance in the flow would occur. The samples were taken at various cross sections downstream of the injection source. The

* All Speeds Limited, type A 16FS, 1 H.P.

+ Brook Motors Limited, 3- ϕ , 865 r.p.m., 1 H.P.

x Drake-Willock Hemodialysis Systems, 100 W.

local concentration measurements of the injection fluid in the test section were based on the measurements of the concentration of a fluorescent tracer dye, Rhodamine WT, solution mixed with the injected fluid and detected in the samples. The fluorescent concentration in the samples was measured using a spectrophotometer⁺ which gives excellent sensitivity, of the order of 0.005 w.p.p.m., and specificity at very low concentrations. The level of fluorescent radiation is usually in direct proportion to the concentration of the fluorescing molecules and linear response is possible over a broad range of concentrations. Rhodamine WT has linear response in the range of 0 to 8 w.p.p.m. which covered the range used in the experiments except very close to the injection source.

- 3) The pressure drop along the test section was measured using a 'U' tube manometer filled with carbon tetrachloride dyed with iodine.
- 4) Mean velocity profiles, turbulence intensity and energy spectra were measured using a laser Doppler anemometer* in conjunction with a Fourier analyzer[†]. Comparison between velocity measurements using a laser Doppler anemometer and pitot tubes were also made. Laser anemometry is a technique which utilizes scattered

+ Gilford Instrument Laboratories Inc., Oberlin, Ohio, Automatic Recording Spectrophotometer Model 2400, For No. 04-2400-6-1-69.

* Thermo-Systems, Model No. 900.

†† Hewlett-Packard, Model No. 5460A-2100A-5475A.

light from particles in a fluid to measure the velocity of that fluid. In theory the laser anemometer needs no calibration, has a linear response, and measures a single velocity component independent of fluid properties. Forward scatter dual beam mode was used in these experiments, a schematic sketch of the laser system is shown in Figure (9), in which the laser beam is separated into two parallel beams 50 mm apart and of equal intensity. These beams, on passing through a lens, of a 243 mm focal distance and 11.52° crossing angle (included angle between the beams), cross and focus at the focal point of the lens forming the location of measuring volume, in which the wave fronts interfere to form alternate regions of high and low intensity light. As a particle passes through, these variations in incident light cause variation in the intensity of the light scattered from the particle. When this scattered light is picked up by a photodetector, it is converted to an electrical signal whose frequency is proportional to the rate at which the particle is crossing the interference fringes. It is worthwhile noting that as the crossing angle decreases then the measuring volume increases and therefore reduces the accuracy of the location and point of measurement. That is, it is desirable to have a large crossing angle.

The receiving optics were located opposite the transmitting optics and either on the same axis or, to avoid reflections, slightly off axis. This gives the maximum intensity of collected light. The mean velocity would be obtained as a voltage on the power supply of the tracker. The output from the tracker was connected to the R.M.S. meter to measure the turbulence intensity, and to the Fourier analyzer to obtain the energy spectra. The frequency range used in the experiments was from 0 to 250 Hz., with a maximum number of samples that could be taken of 1024. This gave resolution approximately 0.5 Hz. The average energy spectra was taken over 25 signals; each signal having a duration of approximately 2.05 seconds and a signal processing interval 4 seconds. Therefore the time for the processing of a particular energy spectra was always 150 seconds for the 25 signals. In order to scan the velocity distribution inside the test section. A laser table was constructed which allowed three dimensional movement. The laser table consisted of the following:

- a) Movable base, which permitted vertical movement, was equipped with dial gauge, of 0.025 mm accuracy, to determine the vertical location.
- b) Sliding table, which was used to scan the longitudinal and traversal directions, the location of

measurement was determined using two micrometers of 0.025 mm accuracy.

c) Laser bed, which was made very solid to mount the laser and receiving-optics.

3.4 Experimental Procedure

3.4.1 System Preparation

It was initially necessary before each experiment to drain off the water from the tank and the sump and then refill the system with clean untreated mains water to reduce the accumulation of the dye and polymer in the water system. This was usually done 12 hours or more before the test. The water was circulated through the system prior to the experiments to ensure thermal stability. The temperature of the water changed by about 1°C during an experiment.

3.4.2 Additive Solution Preparation

The solutions were prepared in plastic bags in large metal cans each having a capacity of 60 kg. of water and the solution was pumped via the Peristaltic pump into the storage vessel. The plastic bag was replaced prior to the preparation of each new solution.

a) Water Injection

The experimental measurements were performed by injecting an aqueous Rhodamine solution, the concentrations were within the range of 100 to 200 w.p.p.m., through the injection source into either the centerline of the test section or the

boundary layer over the flat plate. The solution was prepared 6 hours before a test run.

b) Polymer Injection

The additive used was Reten 423 (Hercules Inc.) which is an anionic acrylic polymer with an assessed molecular weight of between 10^7 to 10^8 and is known to have high resistance to shear degradation. The experimental tests were performed by injecting a mixture of aqueous polymer and Rhodamine WT dye solution. The polymer solution was prepared by carefully weighing an appropriate quantity of polymer, then dispersing it in a small quantity of alcohol and gradually adding this to the homogeneous Rhodamine-water mixture. The polymer should not be added to the water all at once since it does not disperse and flocculates. The mixture was then periodically stirred. This procedure reduced the time required to obtain a homogeneous solution and the alcohol has little effect on the solution if only small quantities were used. The solutions were prepared between one and three days before the test to ensure complete mixing.

3.5. Procedures

Initially the solutions to be injected were prepared to the required concentration and pumped into the storage vessel. For the polymer the concentrations were 50, 100, 250, 500 and 1000 w.p.p.m. The main flow was turned on and adjusted to give approximately 4.0 m/s., this was the maximum value

that could be achieved without unduly increasing the air inclusion and depleting the overhead tank. After allowing a steady state condition to be reached, the discharge valve from the polymer solution vessel was turned on and the aqueous Rhodamine or polymer-Rhodamine solution was then injected at a constant predetermined discharge rate by adjusting the vessel air pressure to a desired constant value. The ratios of U_i/U_m used in the experiments were 0.67, 1 and 1.34 for point source injection, and 0.118, 0.175 and 0.234 for wall slot injection. In order to avoid the effect of the decreasing solution level inside the polymer solution vessel on the flow rate, a fine adjustment valve was used to control the polymer solution flow rate.

To prevent the effect of eddies and disturbances created behind each probe on the dispersion data downstream, the samples were collected within the dispersion boundary layer at only one longitudinal location and after which a new longitudinal location was investigated. In addition, samples were collected upstream of the injection source to check the free stream concentration. The samples each had an approximate volume of 5 ml. and took 6 seconds to collect, and were stored in small test tubes in batches for later appraisal. Tests showed that the storage time had no apparent effect. The vertical location of the sample points was determined using the micrometers on the crossbar.

The capacity of the injection vessel was such that it

was only possible to obtain samples in five longitudinal locations before it emptied. At least two samples were taken at each point to check reproducibility of data at given flow conditions.

The mean velocity profile in the longitudinal direction was measured using the laser anemometer. The output voltage from the tracker was fed to a R.M.S. meter and a Fourier analyzer to obtain the intensity and energy spectrum respectively. The velocity components of velocity and the cross correlations were only obtained in the square test section because the cylindrical test section caused spherical aberration in areas outside the "windows".

CHAPTER 4

THEORY

4.1 Injection from Line Source
on Flat Plate4.1.1 Velocity profiles

In order to avoid the necessity of using numerical data in subsequent calculations and correlations, the velocity data were correlated. A simple power law was found suitable for the range of Reynolds numbers used in the experiments. That is, the velocity profile correlation which was found to best fit the experimental data was the well established n^{th} power law.

$$\frac{\bar{U}}{\bar{U}_m} = (y/\delta)^{1/n} \quad (4.1)$$

where in this case $n = 9$.

4.1.2 Concentration profiles

In a turbulent boundary layer over a flat plate with fluid injection from a wall slit, any quantity such as the mean local concentration of the injected solution will be a function of the location from the injection source. It can be assumed that the flow is two dimensional so that $C(x,y)$, and the concentration profiles are most probably similar.

Since the flow possesses no characteristic linear dimension;

we shall assume, therefore, that the concentration is a function of (y/λ) , where λ is a convenient dimensional characteristic of the diffusion boundary layer, defined by

$$y = \lambda \quad \text{when } \bar{C}/\bar{C}_m = 0.5$$

From dimensional analysis and similarity to the velocity profile within the boundary layer over a flat plate, we may expect that

$$\bar{C}/\bar{C}_m = f(y/\lambda) = f(\xi) \quad (4.2)$$

Morkovin [25] developed the following expression which describes the data of Poreh and Cermak [6] on the turbulent diffusion of ammonia gas into air,

$$\frac{\bar{C}}{\bar{C}_m} = \exp [-0.693 (\xi)^a] \quad (4.3)$$

where 'a' is constant, which depends on the diffusion zone, and will satisfy the intermediate, transient and final zones.

4.1.3 The continuity equation

Assuming that the flow is approximately two dimensional and that steady state conditions prevail, the continuity equation between the injection slot and any location down stream may be written as

$$G_i C_i = \int_0^{\infty} \bar{U} \bar{C} dy$$

where $U = \bar{U} + U'$

and $C = \bar{C} + C'$

assuming C' and U' tend to zero

then

$$G_i C_i = \int_0^{\infty} (\bar{U}\bar{C} + \overline{U'C'}) dy \quad (4.4)$$

However

$$\overline{U'C'} \ll \bar{U}\bar{C}$$

$$\therefore (\bar{U}\bar{C} + \overline{U'C'}) = \bar{U}\bar{C}$$

This is a reasonable assumption since even if U' and C' were "perfectly correlated", i.e., $|\overline{U'C'}| = (\overline{U'^2 C'^2})^{1/2}$, and if the relative root mean square amplitudes of U' and C' were each about 20% of the mean value, the error in neglecting $\overline{U'C'}$ compared to $\bar{U}\bar{C}$ would be only about 4% at the most. Thus neglecting $\overline{U'C'}$ is reasonable.

Therefore

$$\begin{aligned} G_i C_i &= \int_0^{\infty} \bar{U}\bar{C} dy \\ &= \int_0^{\infty} \bar{U}_m \left(\frac{y}{\delta}\right)^{1/n} \bar{C}_m f(\xi) dy + \int_{\delta}^{\infty} \bar{U}_m \bar{C}_m f(\xi) dy \end{aligned}$$

It was found that the diffusion plume will be submerged in the boundary layer,

then

$$\int_{\delta}^{\infty} \bar{U}_m \bar{C}_m f(\xi) dy = 0$$

Since λ is independent of y the following expression can be obtained

$$\frac{G_i C_i}{U_m \lambda \bar{C}_m} = \left(\frac{\lambda}{\delta}\right)^{1/n} \int_0^{\delta/\lambda} (\xi)^{1/n} f(\xi) d\xi \quad (4.5)$$

4.1.4 The Eddy diffusivity

For steady state two-dimensional flow the continuity equation of the injected fluid without chemical reaction can be written as follows:

$$U \frac{\partial \bar{C}}{\partial x} + V \frac{\partial \bar{C}}{\partial y} + \bar{C} \left(\frac{\partial U}{\partial x} + \frac{\partial V}{\partial y} \right) = \frac{\partial}{\partial x} (D \frac{\partial \bar{C}}{\partial x} - U' \bar{C}') + \frac{\partial}{\partial y} (D \frac{\partial \bar{C}}{\partial y} - V' \bar{C}') \quad (4.6)$$

The continuity equation for steady state two-dimensional incompressible mixture can be written as follows:

$$\frac{\partial U}{\partial x} + \frac{\partial V}{\partial y} = 0 \quad (4.7)$$

Treating Equations (4.6) and (4.7) simultaneously, the continuity equation for the diffusion of the injected fluid can be reduced to

$$U \frac{\partial \bar{C}}{\partial x} + V \frac{\partial \bar{C}}{\partial y} = \frac{\partial}{\partial x} (D \frac{\partial \bar{C}}{\partial x} - U' \bar{C}') + \frac{\partial}{\partial y} (D \frac{\partial \bar{C}}{\partial y} - V' \bar{C}') \quad (4.8)$$

Except near the source, a boundary layer approximation

becomes possible, in which the normal gradient is much higher than the longitudinal gradient, and gives

$$\bar{U} \frac{\partial \bar{C}}{\partial x} + \nabla \frac{\partial \bar{C}}{\partial y} = \frac{\partial}{\partial y} (D \frac{\partial \bar{C}}{\partial y} - V' \bar{C}') \quad (4.9)$$

Integration of Equation (4.9) may be achieved by using the distribution function of the concentration obtained from the experiments. Furthermore, by dividing Equation (4.2) by Equation (4.5), the following expression for the mean concentration can be obtained

$$\bar{C} = \frac{G_i C_i}{U_m \lambda A} \left(\frac{\delta}{\lambda}\right)^{1/n} f(\xi) \quad (4.10)$$

By using Equations (4.7), (4.8) and (4.10), we can obtain the values of all terms in Equation (4.9) as follows:

$$\begin{aligned} \bar{U} \frac{\partial \bar{C}}{\partial x} &= \frac{G_i C_i}{A} \frac{f(\xi) (\xi)^{1/n}}{\lambda^2} \cdot \left(\frac{d\lambda}{dx}\right) \left(\frac{1}{n} \left(\frac{\lambda}{\delta}\right) \frac{d\delta}{d\lambda} - \frac{(n+1)}{n}\right) \\ &- \frac{G_i C_i}{A} \frac{f'(\xi) (\xi)^{(1/n+1)}}{\lambda^2} \cdot \left(\frac{d\lambda}{dx}\right) \cdot \left(\frac{1}{\lambda}\right) \end{aligned} \quad (4.11)$$

From the continuity equation for the mixture

$$\begin{aligned} \nabla &= - \int_0^y \frac{\partial \bar{U}}{\partial x} dy \\ &= - \frac{1}{n} U_m \int_0^y \frac{y^{1/n}}{(\delta)^{1/n+1}} \frac{d\delta}{dx} dy \\ &= - \frac{1}{n+1} U_m (\xi)^{n+1/n} \cdot \left(\frac{\lambda}{\delta}\right)^{n+1/n} \frac{d\delta}{dx} \end{aligned} \quad (4.12)$$

From Equations (4.10) and (4.12)

$$\nabla \frac{\partial \bar{C}}{\partial y} = \frac{1}{n+1} \frac{G_i C_i}{A} \cdot \frac{f'(\xi)(\xi)^{1/n+1}}{\delta \lambda} \frac{d\delta}{dx} \quad (4.13)$$

By introducing Equations (4.11) and (4.13) into Equation (4.9)

$$\begin{aligned} \therefore \frac{\partial}{\partial y} (D \frac{\partial \bar{C}}{\partial y} - \nabla' C') &= \frac{G_i C_i}{A} \left(\frac{d\lambda}{dx} \right) \left\{ \frac{f(\xi)(\xi)^{1/n} \left[\frac{1}{n} \left(\frac{\lambda}{\delta} \right) \frac{d\delta}{d\lambda} - \left(\frac{n+1}{n} \right) \right]}{\lambda^2} \right. \\ &\quad \left. - \frac{f'(\xi)(\xi)^{1/n+1}}{\lambda^2} + \frac{1}{n+1} \frac{f'(\xi)(\xi)^{(1/n+1)}}{\delta \lambda} \frac{d\delta}{d\lambda} \right\} \end{aligned} \quad (4.14)$$

By partial integration, Equation (4.14) can be reduced to:

$$-D \frac{\partial \bar{C}}{\partial y} - \nabla' C' = - \frac{G_i C_i}{\lambda A} \left(\frac{d\lambda}{dx} \right) f(\xi)(\xi)^{1/n+1} \left[1 - \frac{1}{n+1} \left(\frac{\lambda}{\delta} \right) \frac{d\delta}{d\lambda} \right] \quad (4.15)$$

Since the molecular diffusion is very low compared to the turbulent diffusion, it is justified to neglect the molecular diffusion except near the surface. Therefore, an equation for the turbulent diffusion can be deduced as follows:

$$\nabla' C' = \frac{G_i C_i}{\lambda A} \frac{d\lambda}{dx} f(\xi)(\xi)^{(1/n+1)} \left[1 - \frac{1}{n+1} \left(\frac{\lambda}{\delta} \right) \frac{d\delta}{d\lambda} \right]$$

The order of the dimensionless factor $\left[1 - \frac{1}{n+1} \left(\frac{\lambda}{\delta} \right) \frac{d\delta}{d\lambda} \right]$ will be much smaller than unity, since

$$n = 9$$

$$0 < \frac{\lambda}{\delta} < 0.6 \quad \text{in the extreme}$$

$$\frac{d\delta}{d\lambda} \ll 1.0 \quad \text{and equal to zero in the final zone.}$$

Therefore, it is justified to reduce the equation of the turbulent diffusion to

$$\overline{V'C'} = \left(\frac{G_i C_i}{\lambda A}\right) \left(\frac{d\lambda}{dx}\right) f(\xi) (\xi)^{1/n+1} \quad (4.16)$$

By introducing the eddy diffusivity defined by

$$D(t) = - (\overline{V'C'} / (\partial C / \partial y)) \quad (4.17)$$

Treating Equations (4.10), (4.16) and (4.17) simultaneously we obtain

$$D(t) = - \lambda U_m \left(\frac{d\lambda}{dx}\right) \left(\frac{\lambda}{\delta}\right)^{1/n} (\xi)^{1/n+1} \frac{f(\xi)}{f'(\xi)} \quad (4.18)$$

Equations (4.16) and (4.18) give the turbulent diffusion and the eddy diffusivity at any location in the longitudinal or vertical directions, and is valid except near the injection slot or the surface where the molecular diffusivity will be prominent.

Treating Equations (4.3) and (4.18) simultaneously, the following general equation for the eddy diffusivity in the different zones can be obtained.

$$\frac{D(t)}{\lambda U_m} = \frac{1}{0.693 a} \left(\frac{d\lambda}{dx}\right) \left(\frac{\lambda}{\delta}\right)^{1/n} (\xi)^{(2+1/n-a)} \quad (4.19)$$

Equation (4.19) shows that the eddy diffusivity is proportional to the diffusion boundary layer growth, and it can be used for either water or diluted polymer solutions.

4.2 Injection from Point Source on the Center Line

4.2.1 Velocity profile

(a) Fully developed flows

A simple power law was found suitable for the range of the Reynolds numbers used in the experiments. That is, the velocity profile correlation which was found to best fit the experimental data was the well established power law.

$$\frac{U}{U_m} = \left(1 - \frac{r}{R}\right)^{1/n}$$

where in this case $n = 7$.

Since; the diffused matter was within the range of

$$0 \leq \frac{r}{R} \leq 0.6$$

Then for a seventh power law, the change of the velocity across the diffusion area will be within 10%. Consequently, to simplify the continuity equation for the injected solution, the flow can be assumed to have a uniform velocity.

(b) Developing flow

A uniform flow in the central core of the test section can be accurately assumed. Since, the diffused plume of the injected fluid will be within this core we can assume a uniform velocity.

4.2.2 Concentration Profile

For a turbulent flow inside a duct with fluid injection from a point source on the center line, the mean local concentration of the injected fluid will be a function of the location with respect to the injection source. It can be assumed that the flow is axisymmetric or two dimensional. So that $C(x,r)$ and the concentration profiles are similar. By introducing the characteristic linear dimension (λ), the concentration is then a function of (r,λ) where

$$r = \lambda \quad \text{when } \bar{C}/\bar{C}_m = 0.5$$

From dimensional analysis and similarity of free jet flow, we may expect

$$\bar{C}/\bar{C}_m = f(r/\lambda) = f(\eta) \quad (4.20)$$

The following expression is developed which describes the present data for (\bar{C}/\bar{C}_m) versus (r/λ) .

$$\bar{C}/\bar{C}_m = \exp[-0.693 (\eta)^a] \quad (4.21)$$

which is similar to the expression used for line source injection.

4.2.3 The Continuity Equation

Assuming steady state axisymmetric flow, the continuity equation between the injection source and any location downstream can be written as

$$Q_i C_{i_i} = \int_0^{\infty} U \bar{C} 2\pi r dr$$

where $U = \bar{U} + U'$

and $C = \bar{C} + C'$

assuming \bar{C}' and \bar{U}' tend to zero

then

$$Q_i C_{i_i} = 2\pi \int_0^{\infty} (\bar{U}\bar{C} + U'C') r dr$$

However

$$U'C' \ll \bar{U}\bar{C} \quad \therefore (\bar{U}\bar{C} + U'C') = \bar{U}\bar{C}$$

Therefore

$$Q_i C_{i_i} = 2\pi \int_0^{\infty} \bar{U}\bar{C} r dr$$

As stated before, we can assume that

$$\bar{U} = U_m$$

$$\therefore Q_i C_{i_i} = 2\pi U_m \int_0^{\infty} \bar{C} r dr$$

By substituting the value of \bar{C} from Equation (4.21) into the previous equation, we can obtain

$$Q_i C_{i_i} = 2\pi \lambda^2 U_m \bar{C}_m \int_0^{\infty} \eta [\exp(-0.693(\eta)^2)] \lambda \eta \quad (4.22)$$

if $a = 2$, which satisfied all the diffusion data, not only for fully developed and uniform flow, but also for water and polymer solution injection. Equation (4.22) can be integrated and gives:

$$\dot{Q}_i C_i = \frac{\pi}{0.693} \lambda^2 \bar{U}_m \bar{C}_m$$

or

$$\lambda^2 \bar{C}_m = A_1 \quad (4.23)$$

4.2.4 The Eddy Diffusivity

For steady state axisymmetrical flow with zero velocity in the radial direction, the continuity equation for the injected solution without chemical reaction can be written as follows:

$$\bar{U}_m \frac{\partial \bar{C}}{\partial x} = \frac{1}{r} \frac{\partial}{\partial r} (D + D_r^{(t)}) (r \frac{\partial \bar{C}}{\partial r}) + \frac{\partial}{\partial x} (D + D_x^{(t)}) \frac{\partial \bar{C}}{\partial x} \quad (4.24)$$

Except near the injection source, a boundary layer approximation becomes possible, because the normal gradient is much higher than the longitudinal gradient, and gives

$$\bar{U}_m \frac{\partial \bar{C}}{\partial x} = \frac{1}{r} \frac{\partial}{\partial r} (D + D_r^{(t)}) (r \frac{\partial \bar{C}}{\partial r}) \quad (4.25)$$

By using Equations (4.21) and (4.23), we can solve Equation (4.25) as follows:

$$\bar{C} = \frac{A_1}{\lambda^2} f(\eta)$$

$$\frac{\partial \bar{C}}{\partial x} = - \frac{A_1}{\lambda^2} [nf'(n) + 2f(n)] \frac{\partial \lambda}{\partial x} \quad (4.26)$$

and
$$\frac{\partial \bar{C}}{\partial r} = \frac{A_1}{\lambda^3} f'(\xi) \quad (4.27)$$

By substituting Equations (4.26) and (4.27) into Equation (4.25) and integrating, we can obtain

$$\begin{aligned} (D+D_r(t)) (r \frac{\partial \bar{C}}{\partial r}) &= \int_0^r U_m r \frac{\partial \bar{C}}{\partial x} dr \\ &= - \frac{U_m A_1}{\lambda} \frac{\partial \lambda}{\partial x} \int_0^n [n^2 f'(n) + 2nf(n)] dn \\ &= - \frac{U_m A_1}{\lambda} \frac{\partial \lambda}{\partial x} n^2 f(n) \end{aligned}$$

$$(D+D_r(t)) = - U_m \lambda \frac{\partial \lambda}{\partial x} n \frac{f(n)}{f'(n)} \quad (4.28)$$

Treating Equations (4.21) and (4.28) simultaneously, and assuming $a = 2$, Equation (4.28) can be reduced to:

$$\begin{aligned} (D+D_r(t)) &= \frac{U_m}{1.386} \lambda \frac{\partial \lambda}{\partial x} \\ \frac{D+D_r(t)}{U_m \lambda} &= \frac{1}{1.386} \frac{\partial \lambda}{\partial x} \quad (4.29) \end{aligned}$$

Equation (4.29) for the eddy diffusivity indicates that $D_r(t)$ will be independent of the radial location. Consequently, there is similarity between the diffusion from

a point source and free turbulence flow, where the eddy viscosity can be approximated by a constant.

CHAPTER 5

RESULTS

In excess of 4000 data were obtained which resulted in the generation of more than 1500 graphs. For obvious reasons, only the numerical data which are given in Appendix (III), and representative graphs are presented. Furthermore, for convenience, the data have been categorized as defined in the following Tables (1) and (2).

In this chapter the experimental data are presented with some explanatory comment. In all cases where curves were fitted, least square regression was used.

5.1. Injection from Line Source on Flat Plate

Figures (10, 11 and 12) show plots of non-dimensional velocity profiles, i.e., U/U_m versus y/θ at three locations inside the test section. The momentum thickness was used for the non-dimensional height instead of the boundary layer thickness, since it was virtually impossible to accurately define the boundary layer thickness in an unambiguous way. It was apparent from all the velocity profiles that a $1/9^{\text{th}}$ power law quite accurately described the experimental data.

Figures (13, 14 and 15) show plots of the non-dimensional concentration profiles C/C_1 versus y for five

CONCENTRATION MEASUREMENTS

$$U_m = 4.5 \text{ m/s}$$

	Fully Developed Flow		Developing Flow	
	25 mm Point Source	75 mm Point Source	75 mm Point Source	Line Source
	U_i/U_m	U_i/U_m	U_i/U_m	U_i/U_m
Series 1	0.67	0.67	0.67	0.118
Series 2	1.00	1.00	1.00	0.175
Series 3	1.34	1.34	1.34	0.234
	x	x	x	x
Location 1	48	57	45	102
Location 2	190	203	172	235
Location 3	403	352	352	425
Location 4	657	606	606	678
Location 5	975	924	997	1059

TABLE (1)

ENERGY SPECTRA MEASUREMENTS

$$U_m = 4.5 \text{ m/s}$$

Fully Developed Flow		Developing Flow			
25 mm Point Source		75 mm Point Source		Line Source	
x	r	x	r	x	r
190	.0	172	.0	235	0.5

TABLE (2)

longitudinal locations downstream from the injection slot, for both water and polymer solution injection at three different injection flow rates and concentrations. It is seen that for water injection all the concentration profiles have the same trend, whereas the concentration profiles for polymer solution injection can be divided into at least two groups or representative zones. The first zone is one in which the concentration gradient is very steep and the second is a zone in which the concentration gradient tends to approach that for the water injection. It would appear that the length of the first zone is a function of the polymer injection concentration and injection flow rate.

The diffusion boundary layer thicknesses were determined from the diffusion data and plots of the growth of λ for various concentrations were obtained.

Figure (16) shows a plot of non-dimensional concentration profile \bar{C}/\bar{C}_m versus the non-dimensional height y/λ at the five longitudinal locations for water injection. It is apparent that the non-dimensional concentration \bar{C}/\bar{C}_m for the water injection is only a function of non-dimensional height ξ and almost independent of the location from the injection slot. It is seen that the result can be presented by the traditionally accepted form of the concentration distribution.

$$\bar{C}/\bar{C}_m = \exp [-0.693 (y/\lambda)^a] \quad (5.1)$$

where $a = \text{constant}$.

A plot of non-dimensional concentration \bar{C}/\bar{C}_m versus a non-dimensional height y/λ for injection of polymer solution with a concentration of 100 w.p.m. for all the data is shown in Figure (17). It is apparent that the data cannot be accurately fitted with one curve. This indicates that the value of 'a' for polymer solution injection is not constant. The previous observation can be clearly seen from the plots of the non-dimensional concentration versus the non-dimensional height, for injection of polymer solution with a concentration of 500 w.p.m., as shown in Figures (18-27).

Figures (28-32) show plots of non-dimensional wall concentration $\bar{C}_m U_m / C_i U_i$ versus the non-dimensional location (x/h) for both water and polymer solution injection at different flow rates. The result can apparently be presented by an equation of the form

$$\bar{C}_m U_m / C_i U_i = a_1 (x/h)^{b_1} \quad (5.2)$$

The growth of a representative non-dimensional diffusion thickness defined by (λ/h) versus the non-dimensional location (x/h) for both water and polymer solution injection are presented in Figures (33-47). It would appear that (λ/h) is a function of (x/h) , U_m/U_i , and also a function of injection concentration.

In an attempt to generalize the results, the data are plotted on a graph of the non-dimensional function of

λ/h versus $((x/h)/(1+40(U_i/U_m) C_i^2))$ as shown in Figure (48). It is apparent that this type of plot does indeed correlate well all the data for the range of injection concentrations and flow rates that were used.

The variation of the exponent 'a' as a function of the non-dimensional locations (x/h) for both water and polymer solution injection at various concentrations and flow rates is presented in Figures (49-63). It would appear that the value of 'a' increases gradually as a function of the downstream distance from the injection slot x .

Figure (64) shows the relation between 'a' and the non-dimensional factor $((x/h)(U_m/U_i)/(1+15 C_i^2))$, for all the data. It appears that contrary to general belief the value of 'a' is not constant for boundary layer flow, and is in fact a function of the longitudinal location, injection concentration and injection flow rate.

The effect of injection flow rate and concentration on the wall concentration downstream from the injection source is shown in Figure (65). It is apparent that the wall concentration for the polymer solution is higher than for water injection. This means that the diffusion rate near the wall for polymer injection is lower than for water injection.

The velocity profile and turbulence intensity were measured at one longitudinal location 235 mm downstream from the injection slot. The velocity and turbulence intensity data for water or polymer solution injection are shown in

Figures (66-70). It is seen that the flow rate within the boundary layer for polymer solution injection increases when compared with water injection, which can also be deduced from the reduction in the momentum thickness for polymer solution. It is also apparent that the turbulence intensity for polymer injection decreased compared to the water injection, except very close to the wall. The change in the velocity profiles and turbulence intensity for polymer solutions, when using water injection as a reference are also shown in Figures (71-78).

Energy spectrum distributions for water or polymer solution injection are shown in Figures (79-84). The measurements were made at only one location 235 mm downstream from the injection source, and 0.5 mm from the wall. It can be seen that for low concentration the effect of polymer solution on the energy spectrum is negligible, while for the higher concentration the portion of the energy increases within the lower band of the frequency range and is reduced in the higher range.

Figures (85-86) show the energy spectrum distributions when the measurements were obtained at 5 mm away from the wall. The similarity between those distributions and those obtained near the wall can be seen.

5.2 Injection from Point Source

Figures (87-95) show plots of concentration profiles \bar{C}/C_i versus r , for both of the injection sources for the fully

developed flow experiments, and for the 75 mm injection source in the case of the uniform flow experiments at five locations downstream from the injection source for both water and polymer solution injection at various injection flow rates and concentrations. It is apparent that for water or dilute polymer solution injection all the concentration profiles have the same trend, while the thickness of the diffusion boundary layer is reduced as the polymer concentration is increased.

Figures (96-104) show plots of non-dimensional concentration profiles C/C_m versus the non-dimensional height r/λ for all sampling locations and injection flow rates for both water and polymer solution injection. It can be deduced that the non-dimensional concentration C/C_m is only a function of the non-dimensional radius r and almost independent of the longitudinal location and polymer concentration. It is apparent that the results can be presented by the generally accepted form for the concentration profile, that is

$$C/C_m = \exp[-0.693 (r/\lambda)^a] \quad (5.3)$$

where $a = \text{constant}$ for all data.

Plots of non-dimensional centerline concentration or maximum concentration $C_m U_m / C_i U_i$ versus the non-dimensional longitudinal location (x/d) for both water and polymer solution injection and for either fully developed flow or uniform flow are shown in Figures (105-158). The results demonstrate that the data can apparently be represented by

an equation of the form,

$$\bar{C}_m \bar{U}_m / C_i U_i = a_2 (x/d)^{b_2} \quad (5.4)$$

To study the effect of injection concentration and flow rate on the centerline concentration all the data are plotted in one graph as shown in Figures (159-161). It can be seen from these graphs that polymer solution will suppress diffusion as indicated by the higher centerline concentration than in the case of water injection.

Figures (162-215) show the growth of a representative non-dimensional diffusion thickness $(\lambda/(d/2))$ versus the non-dimensional longitudinal location (x/d) for both water and polymer solution injection. It can be seen that $(\lambda/(d/2))$ is a function of $(x/d, \bar{U}_m/U_i, C_i)$. The results demonstrate that the data can apparently be represented by an equation of the form,

$$[(\lambda/d/2) - 1] = a_3 (x/d)^{b_3} \quad (5.5)$$

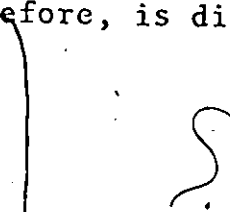
The effect of injection flow rates and concentration on the representative diffusion boundary layer thickness are shown in Figures (216-218). It is apparent that the representative diffusion boundary layer thickness is smaller for polymer solution than for water. This indicates that, for the conditions investigated, the diffusion rate for polymer solution injection is lower than that for water injection.

The effect of the water or polymer solution injection on energy spectrum for both fully developed flow and uniform

flow are shown in Figures (219-230). It can be seen that the injection of a low polymer concentration solution has no effect on energy spectrum whilst the injection of a higher polymer concentration solution reduced the turbulence intensity, and furthermore reduced the energy over the entire frequency range investigated, with the largest reductions at the higher frequency end of the spectrum.

5.3 Sampling Rate Effects

In order to assess whether the sampling rate has any effect on the accuracy of the concentration measurements, a series of tests in which the sampling rate has varied at various injection rates, probe diameters and concentration were performed. Two representative graphs are given in Figures (231, 232), see Appendix (I) for more details. It can be seen that for water injection the sampling rate has no effect on the concentration measurements, while as the injection polymer concentration increases the sample concentration becomes a function of the sampling rates and approaches the apparently correct concentration when the sampling velocity approaches the main flow velocity or isokinetic conditions. It can also be deduced that by increasing the probe's entrance diameter the effect becomes more pronounced within the range of probe diameters used. This very interesting and important phenomenon which has apparently not been specifically discussed before, is discussed in detail in the next chapter.



CHAPTER 6
ANALYSIS AND
DISCUSSION

In this section the results will be discussed in detail.

6.1 Line Source Injection

The concentration profiles, see Figure (13), for dyed water injection at various injection flow rates and at the five locations downstream from the injection slot, for the experimental data range investigated, can be transformed into a universal diagram as shown in Figure (16). It is apparent that the mean concentration distribution \bar{c}/\bar{c}_m is a function of the dimensionless height y/λ alone and is independent of the location and injection flow rate. There are no distinct zones in the longitudinal range used, which is contrary to what might be expected from [6] which indicated that there would be four zones, but is in agreement with [14]. This result could be attributed to the fact that high values of U_i/U_m were used, which affected the dispersion, and also indicates that the dispersion as a result of high values of U_i/U_m will play an active role in the diffusion in the initial zones and will considerably reduce the length of these zones. It is found that an equation similar to that obtained by Morkovin [25] (e.g., Equation (4.3)) based on the collected data of Poreh and Cermak [6] for the final zone of the

diffusion from a line slot, can be used to represent the present data. This is shown in Figure (16) where the data were best correlated by the following equation:

$$\bar{C}/\bar{C}_m = \exp [-0.693 (y/\lambda)^{1.87}] \quad (6.1)$$

Attempts to obtain a universal relationship between the concentration distribution \bar{C}/\bar{C}_m and non-dimensional height y/λ for polymer injection resulted in considerable scatter of the data, which infers that there is more than one zone and in fact the universal concentration profiles continually change within the longitudinal length. It appears that a general equation of the form

$$\bar{C}/\bar{C}_m = \exp [-0.693 (\xi)^a] \quad (6.2)$$

may be used for the experimental length investigated. However 'a' is no longer a constant, but is dependent on the location downstream from the injection slot, the non-dimensional velocity ratio (U_m/U_i), the injection concentration, and is expected to be dependent on the slot height. That is

$$a = f\left(\frac{U_m}{U_i}, \frac{x}{h}, C_i\right) \quad (6.3)$$

Furthermore, it can be deduced from all the concentration data that the value of 'a' gradually increases as U_m/U_i , C_i and x/h are increased. This is contrary to the hypothesis of Poreh [6] which suggested that there are four diffusion zones and that 'a' has a unique value depending

on the zone. However, the value of 'a' that he obtained was applicable to the intermediate and final zones. This hypothesis does not appear to be applicable for the current data. The disagreement between the current results and those of Poreh [6] could be attributed to the fact that Poreh's work within the transient and final zones, the diffusion of the injected fluid will extend beyond the hydrodynamic boundary layer. On the other hand, for the current work the liquid diffusion is within the hydrodynamic boundary layer. Consequently, it is justifiable to assume the change of 'a' is gradual. Therefore, the values of 'a' for all experimental data were plotted versus the non-dimensional factor $((x/h) (U_m/U_i)/(1+15 C_i^2))$ on Figure (64), and the following universal equation was obtained.

$$a = 0.102 \times \left(\frac{x}{h} \right) \left(\frac{U_m}{U_i} \right) / (1+15 C_i^2)^{0.51} \quad (6.4)$$

When comparing the water injection and polymer solution injection data a specific observation can be made. The value of 'a' for the case of water injection approaches a constant value, whilst for polymer solution injection it is strongly dependent on the injection concentration and injection flow rates. This is mainly due to the fact that near the injection source the polymer solution tends to cling to the wall which suppresses the mixing process.

A universal relationship between (λ/h) and the non-dimensional factor $((x/h)/(1+40 (U_i/U_m) C_i^2))$ for all experimental

data can be obtained as shown in Figure (48), and the following universal equation was found to adequately represent the data,

$$\frac{\lambda}{h} = 39.08 + 8.66 \ln \left(\left(\frac{x}{h} \right) / \left(1 + 40 \left(\frac{U_i}{U_m} \right) C_i^2 \right) \right) \quad (6.5)$$

It can also be seen that the diffusion boundary layer thickness is highly dependent on the injection concentration and injection flow rates. It can also be observed from the diffusion boundary layers, Figures (33-47), that the longitudinal range investigated on the experiments can be divided into three zones:

- i) The first zone, in which the rate of growth of the diffusion boundary layer thickness is very small, and it is believed the molecular diffusion will play an important role.
- ii) The second zone, in which the rate of growth of the diffusion boundary layer thickness increases rapidly, and then gradually approaches to steady rate of increase.
- iii) The third zone, in which the rate of growth of the diffusion boundary layer thickness increases steadily.

In spite of the apparent existence of three zones, for the sake of simplicity a single equation was used to fit the diffusion boundary layer thickness.

It was observed that the non-dimensional wall concentration $(\bar{C}_m U_m / C_i U_i)$ is a function of the non-dimensional

longitudinal location (x/h), injection concentration and injection flow rates as shown in Figures (28-32). Furthermore, as the injection concentration increases, the wall concentration approaches the injection concentration, which indicates that the polymer solution tends to cling to the solid surfaces, and consequently reduces the diffusion rate. It was also observed that for a polymer injection concentration of 1000 w.p.p.m. the wall concentration is constant and equal to the injection concentration for a distance which is dependent upon the injection flow rate. This results is in agreement with the result obtained by Furman [12].

Since values for \bar{C}_m as a function of x for the entire surface can be obtained from Equation (5.2), then, it is possible to estimate the drag reduction over the surface and an optimal design achieved. However, it should be kept in mind that increasing the polymer injection concentration or flow rate will lead to a very high \bar{C}_m in the initial zone near the injection source, which may increase the drag in that area, but nonetheless achieves the required optimum concentration at the appropriate location downstream. Furthermore, decreasing the polymer injection flow rate will reduce the value of \bar{C}_m in the initial zone but may lower \bar{C}_m downstream below that for the optimum value for drag reduction. Therefore, considerable care should be exercised in using wall injection for drag reduction.

The velocity profile measurements with or without

polymer solution injection, Figures (66-74), showed that in general the flow rate within the boundary layer increases when polymer solution is injected. Furthermore, the velocity will increase within the entire boundary layer for low polymer injection concentrations. However, for higher injection concentrations of 500 w.p.p.m. and variable flow rates, the velocity close to the wall decreased, but was greater than that for water at a distance away from the wall. This may be attributed to the fact that for low polymer solution injection concentrations the wall concentration will be within the range which gives drag reduction. But, for higher polymer solution injection concentrations, the wall concentration will be higher than that for drag reduction, which reduces the velocity in the wall region. Whilst further away from the wall, the concentration is reduced and is within the range for drag reduction, thus creating higher velocities in that region.

Turbulence intensity measurements for water and polymer solution injection, Figures (66-70) and (74-78), showed that for low injection concentrations ($0 < C_i < 100$ w.p.p.m.), when the wall concentration was about 3 w.p.p.m., the turbulence intensity is reduced. This means that the polymer solution dampens the turbulence, reducing the drag. However, for a higher injection concentration, the turbulence level near the wall increased. This is due to thickening of the viscous sublayer and the polymer solution's tendency

to cling to the wall. Furthermore, as a result of the sub-layer thickening, the turbulence level at the same vertical location compared with the case of no polymer solution injection, will increase. While further away from the wall the polymer solution concentration is drastically reduced, causing a lower turbulence level than for the case of no injection.

The velocity and turbulence intensity results showed that a very high polymer concentration causes a reduction in the velocity and an increase in the turbulence level near the wall. Whilst low concentrations, of the order of 5 w.p.p.m., increase the velocity and reduce the turbulence intensity near the wall, which reduces the drag.

On examination of the energy spectrum data using the no injection condition as a reference, see examples given in Figures (79-84), the following deductions can be made: For water injection there is no noticeable effect of the injection flow rate on the energy spectrum and most of the energy is concentrated within the frequency range of 0 to 20 Hz. Also for a polymer solution injection with a concentration of 100 w.p.p.m., there is also no noticeable effect on the energy spectrum for the various flow rates used which can be attributed to the resulting very small polymer concentration at the measurement location, which will result in flow behaviour similar to that for the injection of Newtonian fluids. As the injection concentration increases the effect of the polymer solution on the energy spectrum

becomes more apparent. When the polymer solution injection concentration reaches 250 w.p.p.m. there is no change in the energy spectrum for the low injection flow rate, whilst for medium and high injection flow rates there is an increase in the energy within the low frequency end of the energy spectrum. There is no change at the high frequency end. The effect for the high injection flow rate is more apparent, because there is a higher polymer concentration at the measurement location.

For a polymer solution injection concentration of 500 w.p.p.m. the increase of the energy within the low frequency band is predominant, while there is no change within the high frequency end. This indicates that the polymer solution thickens the viscous sublayer leading to higher energy at the measuring locations and the majority of the energy is concentrated within the low frequency end of the energy spectrum. For the highest concentrations used in these experiments (i.e., 1000 w.p.p.m.) the polymer solution affected the entire frequency range of the energy spectrum. Such that in the low frequency end the energy increases by increasing the injection flow rate, while within the high frequency end the energy is slightly reduced. This indicates that the polymer solution reduces the high frequency turbulence, and that the increase in the energy within the low frequency end may be attributed to a thickening of the viscous sublayer, creating higher energy at the measuring location.

In order to study the effect of polymer solution on

energy spectrum further away from the wall, measurements were taken at a distance of 5 mm from the wall for injection concentrations of 500 and 1000 w.p.p.m. at variable injection flow rates. The measurements indicated a reduction in the turbulence intensity when polymer injection is used whilst the injection flow rate had a negligible effect on the turbulence intensity. There was also a reduction in the energy spectrum over the entire frequency range with polymer solution injection. However, the injection flow rate has no effect on the energy spectrum.

6.1.1 Continuity Equation

The continuity equation for two-dimensional flow, Equation (4.5), for an approximately constant value of 'a' can be reduced to

$$\lambda \bar{C}_m = \text{constant} \quad (6.6)$$

By substituting the value of λ and \bar{C}_m from Equations (6.5) and (5.2), it was found that the value of $(\lambda \bar{C}_m)$ is a function of the location downstream from the injection slot, that is

$$\lambda \bar{C}_m = a'_4 (x)^{b_4} \quad (6.7)$$

This result implies that the fitted equations for λ and \bar{C}_m do not accurately represent the data. However, any curve fitting errors are magnified when the functions for λ and \bar{C}_m are multiplied and therefore this conclusion is not

accurately justified. Moreover, when the calculated values for \bar{C}_m and λ , obtained directly from the experimental data, are used, the continuity equation is satisfied within experimental error.

6.1.2 The Eddy Diffusivity

From Equation (4.21), the eddy diffusivity can be written as follows:

$$D(t) = \frac{1}{0.693 \cdot a} \lambda U_m \frac{d\lambda}{dx} \left(\frac{\lambda}{\delta}\right)^{1/n} (\xi)^{2+1/n-a} \quad (6.8)$$

Therefore, within the boundary layer, it is apparent from the above equation that the eddy diffusivity is approximately independent of the height above the flat plate, but is only a function of λ , when $a = 2.1$.

6.2 The Point Source Injection

6.2.1 Fully Developed Flow

The concentration profiles, see Figures (87,90), for dyed water injection for both injection sources at various injection flow rates and for the five locations downstream from the point source, can be transformed into a universal diagram, for the experimental data range used in these experiments, as shown in Figures (96 and 99). It is apparent that the mean concentration distribution \bar{C}/\bar{C}_m is only a function of the dimensionless height r/λ alone and is independent of the location and the injection flow rate. There is similarity

between the concentration profile obtained and the velocity distribution in a circular turbulent free jet. Furthermore, there are no distinct zones in the longitudinal distance range used. It can also be deduced from the experimental results that using an injection velocity of less or higher than the main stream velocity will not affect the mixing process within the longitudinal distance range used. It is found that an equation similar to that obtained for ejection from a line source can be used to represent the present data as shown in Figures (96, 99) by the following equations:

$$\bar{C}/\bar{C}_m = \exp [-0.693 (r/\lambda)^2] \quad (6.9)$$

It is worthwhile pointing out that within the length of the test section the diffused plume will be within the central core of the main flow, where the velocity is approximately constant and the plume can be assumed to be in an infinite media.

The concentration profiles, see Figures (87, 88, 91, 92) for polymer solution injection indicated that the diffusion boundary layer thickness is reduced by increasing the injection concentration, while there is no change in the diffusion boundary layer thickness by changing the injection flow rate.

Attempts to obtain a universal relationship between the concentration distribution \bar{C}/\bar{C}_m as a function of r/λ for polymer injection, see Figures (97, 98, 100, 101), gave

similar results to that for water injection. This means that the polymer solution has no effect on the mixing process. It was found that an equation similar to the equation obtained for water diffusion can represent all polymer diffusion data for various injection concentrations and flow rates.

The non-dimensional center line or maximum concentration ($C_m U_m / C_i U_i$) was found to be a function of the non-dimensional longitudinal location (x/d), injection concentration and injection flow rate. As the injection concentration or flow rate increases the maximum concentration increases indicating that the polymer solution suppresses the diffusion rate. It was also apparent that the 75 mm injection source produced higher center line concentration than that for the 25 mm source. This could be attributed to the disturbance created behind the injection source, causing higher dispersion for the 25 mm injection source. As previously mentioned in the results, it was observed that the oscillation of the injected fluid were much smaller when the 75 mm source was used when compared with the 25 mm source. This is mainly due to longer source length which permitted the flow to stabilize.

It was found that the non-dimensional diffusion boundary layer thickness ($2 \lambda/d$) is a function of the non-dimensional longitudinal location (x/d), injection concentration and injection flow rates. The effect of the injection flow rate is negligible on the diffusion boundary layer

thickness. While the injection concentration has a significant effect on the diffusion boundary layer thickness, however, increasing the injection will greatly reduce the diffusion boundary layer thickness indicating that the polymer solution suppresses the diffusion. Furthermore, increasing the polymer solution concentration will also affect the shape of the diffusion boundary layer thickness versus longitudinal location curve, and in actual fact increasing the injection concentration will gradually change the curve from convex to concave. In other words, increasing the injection concentration will reduce the rate of increase of the diffusion boundary layer thickness, especially close to the injection source where the polymer concentration is higher than that further downstream. The general shape of the diffusion boundary layer curve could be assumed to change gradually from concave to a straight line thence to convex. However, a simple power law curve fit was used to represent the data.

The energy spectrum measurements for water injection, for various injection flow rates, showed no apparent effect on the energy distribution. While the energy spectrum measurements for polymer injection solution indicated that for an injection concentration of 50 w.p.p.m., there is no apparent effect on the energy spectrum. Increasing the injection concentration to 100 and 250 w.p.p.m., there was no noticeable change on the energy spectra for $U_i/U_m = 0.67$ and 1.0. However for the highest injection flow rate the energy within

the high frequency band is reduced compared to that for water, but there is no change within the low frequency band. For injection concentrations of 500 and 1000 w.p.p.m. there is no change in the energy spectrum for the smallest injection flow rate, while on increasing the injection flow rate ($U_i/U_m = 1.0$) there is a reduction in the energy over the entire frequency range, with maximum reduction over the higher frequency end of the spectrum. The energy reduction is increased for the highest injection flow rate, with maximum reduction within the high frequency end. This result indicates that the polymer solution tends to dampen the high frequency turbulence and in general suppresses the turbulence level.

6.2.2 Uniform Flow

There is a similarity between the concentration profiles obtained in these experiments and those for the fully developed flow. It was also found that the equation used to represent water injection diffusion from point source can also represent all the data in these experiments, as shown in Figures (102-104). There is some scatter of the data which is mainly due to the oscillation of the injected fluid and some instability in the flow due to the fact that the test section was very close to the duct inlet which was originally done to reduce the boundary layer thickness in the test section. These results indicate that the dispersion process or mechanism is not affected by the flow conditions,

i.e., whether it is fully developed or uniform flow.

The non-dimensional centerline or maximum concentration ($\bar{C}_m U_m / C_i U_i$) was found to be a function of the non-dimensional longitudinal location (x/d), injection concentration and injection flow rate. There is also no apparent difference between the maximum concentration levels obtained in these experiments and those obtained for the fully developed flow, as shown in Figures (159-161).

The non-dimensional diffusion boundary layer thickness ($\lambda/d/2$) is also a function of (x/d), C_i and the injection flow rate. A comparison between Figures (206-208), for the diffusion boundary layer thickness for all the data, shows that λ is reduced for the uniform flow, which may be attributed to a smaller traverse turbulent velocity component. However, there is similarity in the general trend of the growth of the diffusion boundary layer thickness for both uniform flow and fully developed flow.

It can be concluded from the results that the mixing or the dispersion phenomena is independent of the injection flow rate, injection concentration, the length of the injection source and the type of the flow, i.e., whether fully developed or uniform turbulent flow. However, the centerline concentration and the diffusion boundary layer thickness are affected by these factors. The dispersion rate for uniform flow is lower than that for fully developed flow, which was deduced from the diffusion boundary layer thickness and the centerline concentration profiles. Also the polymer

solution tends to reduce the rate of dispersion.

The energy spectrum measurements for water injection indicated that there was no apparent effect on the energy distribution when $U_i/U_m \leq 1.0$, while for the highest injection flow rate there is a reduction of the energy over the entire frequency range. This may be related to the fact that higher injection flow rates reduce the oscillation and therefore leads to more stable flow conditions. The energy spectrum measurements for polymer solution injection indicated that for injection concentrations of 50 and 100 w.p.p.m., there was no apparent effect on the energy spectrum for $U_i/U_m < 1.0$, but there was an energy reduction over the entire frequency range for $U_i/U_m \geq 1.0$. On comparing the 50 and 100 w.p.p.m. polymer injection concentration with water injection, it is apparent that the difference in the energy spectrum only occurs when $U_i/U_m = 1.0$, while there is no noticeable change when the injection velocity is higher or lower than the main stream velocity.

For a polymer injection concentration of 250 w.p.p.m. there was a slight reduction of the energy over the high frequency end of the energy spectrum for $U_i/U_m < 1$, while for the higher injection flow rates when $U_i/U_m \geq 1$ there is energy suppression over the entire frequency range. However, the energy suppression within the high frequency end is greater than within the low frequency end. There is also an apparent change in the energy spectrum when compared with that

for water injection. In general the energy was suppressed for all injection flow rates with higher suppression within the high frequency end.

For polymer injection concentrations of 500 and 1000 w.p.p.m. with $U_i/U_m < 1$ there is a slight reduction of energy within the high frequency end of the energy spectrum, while there is an increase of the energy in the low end of the energy spectrum. Also, when $U_i/U_m = 1.0$ there is energy suppression over the entire frequency range. While for $U_i/U_m > 1.0$ the reduction of energy is mainly within the high frequency end.

From the energy spectra results for fully developed and uniform flow, the following comparison can be considered: the frequency range in the case of uniform flow is about twice that for fully developed flow, which is mainly due to the fact that for the fully developed flow an entrance honeycomb was used, which may change the turbulence spectrum. Furthermore, the test section was further downstream from the inlet than was the case on uniform flow which would allow enough length to stabilize the flow.

The effect of low polymer injection concentration (50 and 100 w.p.p.m.) on the energy spectrum is negligible for the fully developed flow experiments, but it will reduce the energy, especially when $U_i/U_m = 1.0$, for the uniform flow experiment.

For the higher injection concentration of 250 w.p.p.m., for fully developed flow, there was only a reduction of

energy within the high frequency end for the highest injection flow rate, there being no noticeable change for the other injection flow rates. However, for uniform flow there was energy suppression for all flow rates used. On comparing the highest concentration used (500 and 1000 w.p.p.m.), it can be deduced that, for fully developed flow, the energy is reduced for the medium and highest injection flow rates, however, there was no change for the smallest flow rate. In the case of uniform flow there was a slight reduction of energy within the high frequency band with an increase in the energy within the low frequency end. While there was a reduction of energy for $U_i/U_m \geq 1.0$.

6.2.3 Continuity Equation

Since the dispersion in both the fully developed flow and uniform flow is within the central core, in which the velocity can be assumed to be uniform and equal to the maximum velocity, the continuity equation, Equation (4.22), can be reduced to

$$\lambda^2 \bar{C}_m = \text{constant} \quad (6.10)$$

By substituting the values obtained from the experiments for λ and \bar{C}_m , Equation (6.10) will be satisfied. However, when using the values obtained from the fitted equations for λ and \bar{C}_m , the product $\lambda^2 \bar{C}_m$ is a function of the location downstream from the injection source which obviously disagrees with Equation (6.10). However this discrepancy can

be anticipated because the individual curve fitting errors are magnified by squaring the value of λ and then multiplying it by \bar{C}_m .

6.2.4 The Eddy Diffusivity

From Equation (4.29), the eddy diffusivity can be written as follows:

$$D^{(t)} = \frac{1}{0.693x^2} \lambda \bar{U}_m \frac{d\lambda}{dx} \quad (6.11)$$

Therefore, it is apparent from the above equation that the eddy diffusivity is independent of the radial location, but is a function of λ or the longitudinal location. By introducing the values of λ and $\frac{d\lambda}{dx}$ into Equation (6.11) for both water and polymer solution injection, it can be concluded that the polymer solution will suppress the dispersion process, where the value of the eddy diffusivity is reduced.

6.3 Hot-Film Anemometer

An attempt to obtain velocity, turbulence intensity and energy spectra data using a hot film anemometer was made. But no reliable results were obtained because of the following reasons:

- Most of the available hot film sensors are not very sensitive to signal change for the velocity range used in the experiments.
- It is very difficult and tedious to obtain calibration curves for the sensor as a function of both velocity and

polymer concentration especially for non-homogeneous flow.

- The phenomena of rod climbing of the polymer solution on the sensor support, which was actually observed, would cause errors in the measurement of the velocity, turbulence intensity and energy spectra.

6.4 General Observations

- It was observed that, for the uniformly injected polymer solution from the line slot over the flat plate, that shortly after injection the flow organized into a pattern of large wavering parallel streaks. This phenomena was not noticed for water injection.
- It was also noticed that, for the sampling stations close to the injection source, there was rod climbing by the polymer solution on the sampling probe. This phenomena was also noticed further downstream when the injection concentration or flow rate was increased. However this would not affect the accuracy of the results because the effects would be exhibited downstream of the particular problem.
- There was oscillation of the injected fluid, when injected from the point source. This oscillation was minimised in the case of a 75 mm source, which can be attributed to the longer length of the source, allowing more distance for stability, and also

avoiding the disturbance created behind the injection source.

- The effect of sampling rate on the concentration measurements indicated that, for polymer solution injection, the measured concentration is a function of the sampling rate, see Appendix (I) for more details. This can be attributed to the fact that the solution was sucked from the low concentration solution from radial directions rather than the high concentration solution at the probe centerline.

CHAPTER 7
CONCLUSIONS

As a summary to the previous discussion, the following conclusions can be drawn:

7.1 For Line Source Injection

- 1) A general equation for the concentration distribution for water or polymer solution injection from a line slot into a two-dimensional flow can be approximated by the following equation:

$$\bar{C}/\bar{C}_m = \exp [-0.693 (\frac{y}{\lambda})^2] \quad (7.1)$$

with an assessed accuracy of better than $\pm 8\%$.

with the following universal equation for 'a'

$$a = 0.102 ((x/h)(U_m/U_i)/(1+15 C_1^2))^{0.51} \quad (7.2)$$

with an assessed accuracy of better than $\pm 3.0\%$.

- 2) The values of the representative diffusion boundary layer thickness and the wall concentration for both water and polymer solution injection can be approximated by the following equations:

$$\lambda/h = -39.08 + 8.66 \ln((x/h)/(1+40(U_i/U_m)C_i^2)) \quad (7.3)$$

with an assessed accuracy of better than $\pm 6\%$.

$$\bar{C}_m U_m / C_i U_i = a_1 (\frac{x}{h})^{b_1} \quad (7.4)$$

with an assessed accuracy of better than $\pm 2\%$.

where the value of a_1 and b_1 are a function of the injection concentration and flow rate.

- 3) A comparison between water and polymer solution injection shows that the polymer solution will suppress the turbulent diffusion process, which is attributed to the tendency of the polymer solution to cling to the wall.
- 4) The velocity profiles for flows with polymer injection are fuller than those for water alone, and the displacement thickness was reduced.
- 5) Turbulence intensity measurements near the wall indicated an increase of turbulence level for high injection concentrations. Whilst low concentration, of the order of 5 w.p.p.m., reduced the turbulence and consequently reduced the drag.
- 6) There was no noticeable effect on the energy spectra with low polymer concentration injection. However, for high injection concentration there was an increase of the energy within the low frequency end of the spectra and a reduction of energy for the high frequency end of the spectra. This can be attributed to a thickening of the viscous sublayer and a damping of the high frequency turbulence.
- 7) The value of the eddy diffusivity can be obtained from Equation (6.8).

7.2 For Point Source Injection

- 1) A general equation for the concentration distribution for water and polymer solution, both, for fully developed flow and uniform flow can be approximated by the following equation:

$$\bar{C}/\bar{C}_m = \exp [-0.693 (r/\lambda)^2] \quad (7.5)$$

with an assessed accuracy of better than $\pm 8\%$.

This equation, which is independent of the injection flow rate and the type of the injection, is similar to the equation used for the velocity distribution in a turbulent free jet.

- 2) The values of the representative diffusion boundary layer thickness and the maximum or center line concentration can be approximated by the following equations:

$$[(\lambda/d/2)-1] = a_3 (x/d)^{b_3} \quad (7.6)$$

$$C_m U_m / C_i U_i = a_2 (x/d)^{b_2} \quad (7.7)$$

with an assessed accuracy of better than $\pm 2\%$ for equations (7.6) and (7.7).

where the values of a_2 , b_2 , a_3 and b_3 are a function of the injection concentration and flow rate.

- 3) The polymer solution will suppress the turbulent diffusion process when compared with water injection.
- 4) There was almost no change of the velocity profile with polymer solution injection.

5) The energy spectra analysis showed that:

a) For fully developed flow -

There was no apparent effect of polymer addition on the energy spectra for low injection concentration. However, for high injection concentration, the energy was reduced over the entire frequency range.

b) For uniform flow -

There was generally a reduction of energy over the entire frequency range, except for very high injection concentration when there was an increase of the energy within the low frequency end with a reduction of energy over the high frequency end. Consequently, it can be concluded that in general that polymer solution tends to damp out the high frequency turbulence.

6) The value of the eddy diffusivity can be obtained from Equation (6.11).

7.3 Sampling Rate Effect

It was found that the sampling rate has an effect on the measured polymer solution concentration, and the apparent concentration or the measured concentration will approach the correct concentration when the sampling velocity approaches the main stream velocity or isokinetic condition. However, the measured concentration for water injection is independent

of the sampling rate. This indicates that the sampling rate effect is only associated with a non uniform concentration of the polymer solution in the flow field.

REFERENCES

1. Gadd, G. E., "Friction Reduction", Encyclopedia of Polymer Science and Technology. New York: Interscience, Wiley, Vol. 15, 1971, pp. 224-253.
2. Hoyt, J. W., "The Effect of Additives on Fluid Friction", Transactions of the American Society of Mechanical Engineers, Vol. 94, (June 1972), pp. 258-285.
3. Palyvos, J. A., "Drag Reduction and Associated Phenomena in Internal and External Liquid Flows", Report No. 741, 1974, National Technical University, Transport Phenomena Laboratory, Athens, Greece.
4. Virk, P. S., "Drag Reduction Fundamentals", A.I.Ch.E. Journal, Vol. 21, No. 4, (July 1975), pp. 625-656.
5. White, A. and Hemmings, J. A. G., "Drag Reduction by Additives Review and Bibliography", 1976, BHRA Fluid Engineering.
6. Poreh, M. and Cermak, J. E., "Study of Diffusion from a Line Source in a Turbulent Boundary Layer", International Journal of Heat and Mass Transfer, Vol. 7, (1964), pp. 1083-1095.
7. Fabula, A. G. and Burns, T. J., "Dilution in a Turbulent Boundary Layer with Polymeric Drag Reduction", TP171 (April 1970), Naval Under Sea Research and Development Center, Pasadena, CA.
8. Wetzel, J. M. and Ripken, J. F., "Shear and Diffusion in a Large Boundary Layer Injected with Polymer Solution", Report 114, (February 1970), St. Anthony Falls Hydraulic Lab., University of Minnesota, Minneapolis, Minn.
9. Poreh, M. and Hsu, K. S., "Diffusion from a Line Source in a Turbulent Boundary Layer", International Journal of Heat and Mass Transfer, Vol. 14 (1971), pp. 1473-1483.
10. Poreh, M. and Hsu, K. S., "Diffusion of Drag Reducing Polymers in a Turbulent Boundary Layer", Journal of Hydronautics, Vol. 6, (January 1972), pp. 27-33.
11. Wu, J., "Suppressed Diffusion of Drag-Reducing Polymer in a Turbulent Boundary Layer", Journal of Hydronautics, Vol. 6 (January 1972), pp. 46-50.

12. Fruman, D. H. and Tulin, M. P., "Drag Reduction and Diffusion Accompanying Thin Slit Injections of a Drag Reducing Polymer on a Flat Plate at Big Reynolds Numbers", Report No. 7101-3, (June 1972), Hydronautics, Incorporated Research in Hydrodynamics.
13. Collins, D. J. and Gorton, C. W., "An Experimental Study of Diffusion from a Line Source in a Turbulent Boundary Layer, A.I.Ch.E. Journal, Vol. 22, No. 3, (May 1976), pp. 610-612.
14. Latto, B. and El Riedy, O. K., "Diffusion of Polymer Additives in a Developing Turbulent Boundary Layer", Journal of Hydronautics, Vol. 10, No. 4 (October 1976), pp. 135-139.
15. Shulman, Z. P., Pokryvailo, N. A., Prokopchuk, D. A., and Nesterov, A. K., "Specific Properties of Turbulent Mass Transfer at the Wall in Dilute Polymer Solutions", Proceedings 2nd International Conference on Drag Reduction, (1977), BHRA Fluid Engineering.
16. Wells, C. S., "An Analysis of Uniform Injection of a Drag Reducing Fluid into a Turbulent Boundary Layer", Viscous Drag Reduction, Proceedings of the Symposium in Dallas, Texas, (September 1968), Plenum Press, New York, 1969, pp. 361-382.
17. Walters, R. R. and Wells, C. S., "An Experimental Study of Turbulent Diffusion of Drag Reducing Additives", Journal of Hydronautics, Vol. 5, No. 2, (April 1971), pp. 65-77.
18. Walters, R. R. and Wells, C. S., "Effects of Distributed Injection of Polymer Solutions on Turbulent Diffusion", Journal of Hydronautics, Vol. 6, No. 2, (July 1972), pp. 69-76.
19. Rubin, H., "Estimation of Mass Diffusion Reduction by Drag Reducing Polymeric Additives", Journal of Hydronautics, Vol. 5, No. 2, (April 1971), pp. 73-75.
20. Sidahmed, G. H. and Giskey, R. G., "Mass Transfer in Drag Reducing Fluid Systems", A.I.Ch.E. Journal, Vol. 18, No. 1, (January 1972), pp. 138-141.
21. Walters, R. R., "Drag Reducing Polymer Molecular Weight Effects on Turbulent Diffusion for Uniformly Distributed Polymer Injection", Advanced Technology Center, Inc., Report B/94300/4CR/11, (March 1974).

22. Bhowmick, S. K., "Contribution to the Study of Turbulent Diffusion in Non-Newtonian Fluid", (Contribution à l'Etude de la Diffusion Turbulente de Fluides Non-Newtoniens en Ecoulement Interne - Etude de la Correlation entre la Diffusion Turbulente et la Reduction du Frottement), Doctoral Thesis, Universite Louis Pasteur, Strasbourg, France (1975). (In French).
23. Bhowmick, S. K., C. Gebel and H. Reitzer, "Turbulent Diffusion and Drag Reduction of Drag-Reducing Fluids", *Rheol. Acta.*, 14, (1975), p. 1026.
24. Gebel, C., Reitzer, H., and Bues, M., "Diffusion of Macromolecular Solutions in the Boundary Layer", *Rheol. Acta.*, 17, (1978), pp. 172-175.
25. Morkovin, M. W., "On Eddy Diffusivity, Quasi-similarity and Diffusion Experiments in Turbulent Boundary Layers", *International Journal of Heat and Mass Transfer*, Vol. 8, (1965), pp. 129-145.
26. Flint, D. L., Kada, H., and Hanratty, T. J., "Point Source Turbulent Diffusion in a Pipe", *A.I.Ch.E. Journal*, Vol. 6, No. 2, (June 1960), pp. 325-331.
27. Davar, K., "Diffusion from a Point Source Within a Turbulent Boundary Layer", Ph.D. Dissertation, Colorado State University, Fort Collins, Colorado (1961).
28. Koo, J. K. and Wade, J. H. T., "The Measurement of Diffusivity in Fully Developed Turbulent Pipe Flow", *C.A.S.I. Transactions*, Vol. 2, No. 2, (September 1969), pp. 58-66.
29. Wade, J. H. T. and Kumar, P., "Effects of Injected Gas Diffusion and of Swirl on Fully Developed Turbulent Pipe Flow", *C.A.S.I. Transactions*, Vol. 4, No. 2, (September 1971), pp. 121-125.
30. Taylor, A. R. and Middleman, S., "Turbulent Dispersion in Drag-Reducing Fluids", *A.I.Ch.E. Journal*, Vol. 20, No. 3, (May 1974), pp. 454-461.
31. Sellin, R. H. J., "The Suppression of Turbulent Diffusion by Drag Reducing Polymer Additives", in *Colloques Internationaux du C.N.R.S. No. 233-Polymeres et Lubrification*, Paris, (1975), pp. 331-340.
32. Greated, C. A., "Effect of Polymer Additive on Grid Turbulence", *Nature*, Vol. 224, (December 1969), pp. 1196-1197.

33. Bremhorst, K. and Walker, T. B., "Spectral Measurements of Turbulent Momentum Transfer in Fully Developed Pipe Flow", *Journal of Fluid Mechanics*, Vol. 61, Part 1, (1973), pp. 1973-186.
34. George, W. K. and Lumely, J. L., "The Laser-Doppler Velocimeter and Its Application to the Measurement of Turbulence", *Journal of Fluid Mechanics*, Vol. 60, Part 2, (1973), pp. 321-362.
35. Rudd, M. J., "Velocity Measurements Made with a Laser-Doppler Meter on the Turbulent Pipe Flow of a Dilute Polymer Solution", *Journal of Fluid Mechanics*, Vol. 51, Part 4, (1972), pp. 673-685.
36. Logan, S. E., "Laser Velocimeter Measurement of Reynolds Stress and Turbulence in Dilute Polymer Solutions", *AIAA Journal*, Vol. 10, No. 7, (July 1972), pp. 962-964.
37. Kumar, S. M. and Sylvester, N. D., "Effects of a Drag-Reducing Polymer on the Turbulent Boundary Layer", *A.I.Ch.E. Symposium Series*, Vol. 69, No. 130, (1973), pp. 1-13.
38. Berman, N. S. and Dunning, J. W., "Pipe Flow Measurements of Turbulence and Ambiguity Using Laser-Doppler Velocimetry", *Journal of Fluid Mechanics*, Vol. 61, Part 2, (1973), pp. 289-299.
39. Barker, S. J., "Laser-Doppler Measurements on a Round Turbulent Jet in Dilute Polymer Solutions", *Journal of Fluid Mechanics*, Vol. 60, Part 4, pp. 721-731.
40. George, W. K., "The Measurements of Turbulence Intensities Using Real-Time Laser-Doppler Velocimetry", *Journal of Fluid Mechanics*, Vol. 66, Part 1, pp. 11-16.
41. Reischman, M. M. and Tiederman, W. G., "Laser-Doppler Anemometer Measurements in Drag-Reducing Channel Flows", *Journal of Fluid Mechanics*, Vol. 70, Part 2, pp. 369-392.
42. Bertshy, J. R. and Abernathy, F. H., "Modifications to Laminar and Turbulent Boundary Layers Due to the Addition of Dilute Polymer Solutions", *BHRA Fluid Engineering*, Paper G1, (September 1977).

43. Balakrishnan, C. and Gordon, R. J., "Extensional Flow of Dilute Polymer Solutions", Proceedings, VIIth International Congress on Rheology (1976).
44. Bird, R. B., Armstrong, R. C. and Hassager, O., "Dynamics of Polymeric Liquids", John Wiley & Sons, New York, (1977), pp. 109-112.



Figure 1. Experimental Apparatus (Fully Developed Flow).



Figure 2. Experimental Apparatus (Fully Developed Flow).

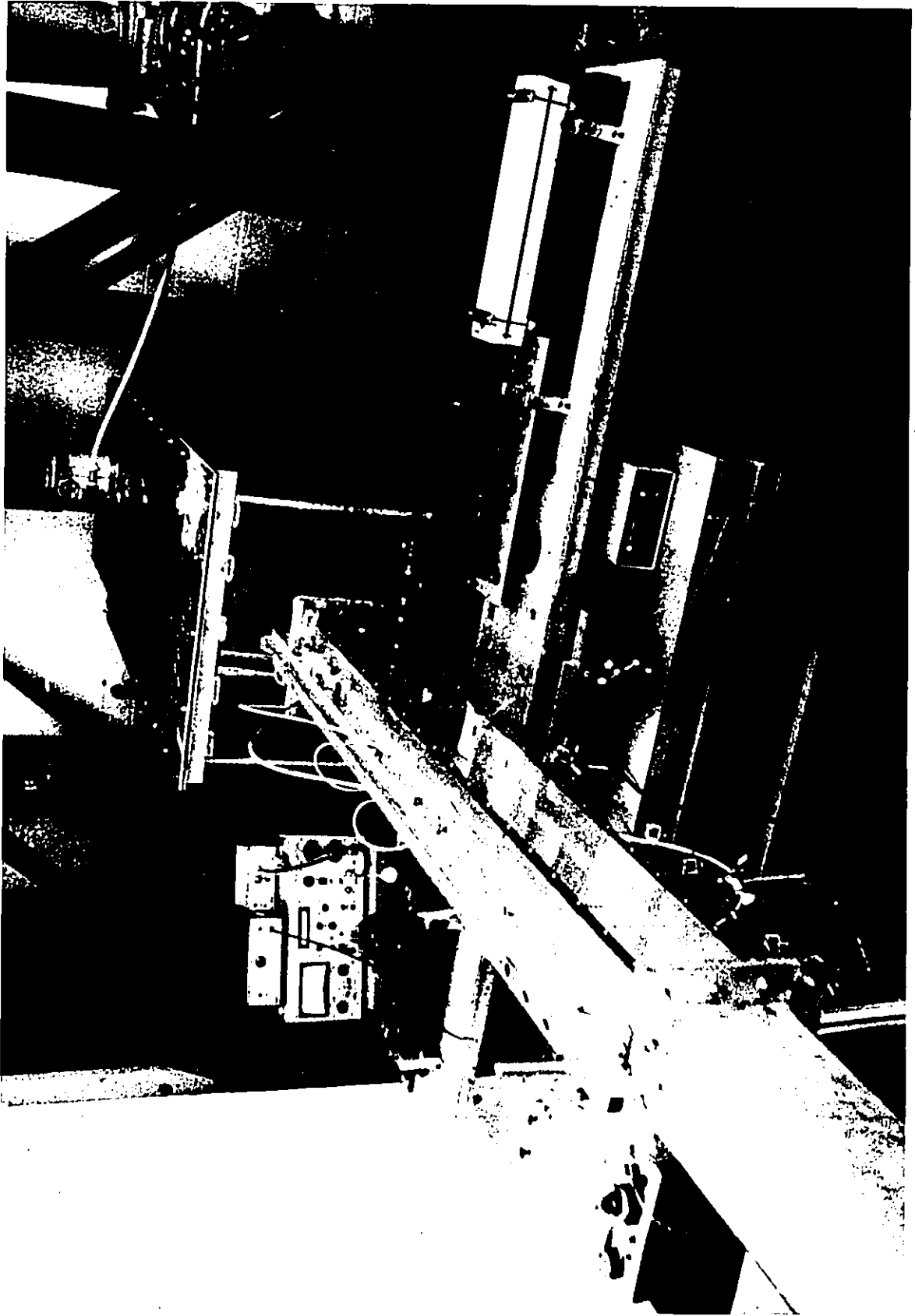


Figure 3. Experimental Apparatus (Developing Flow).

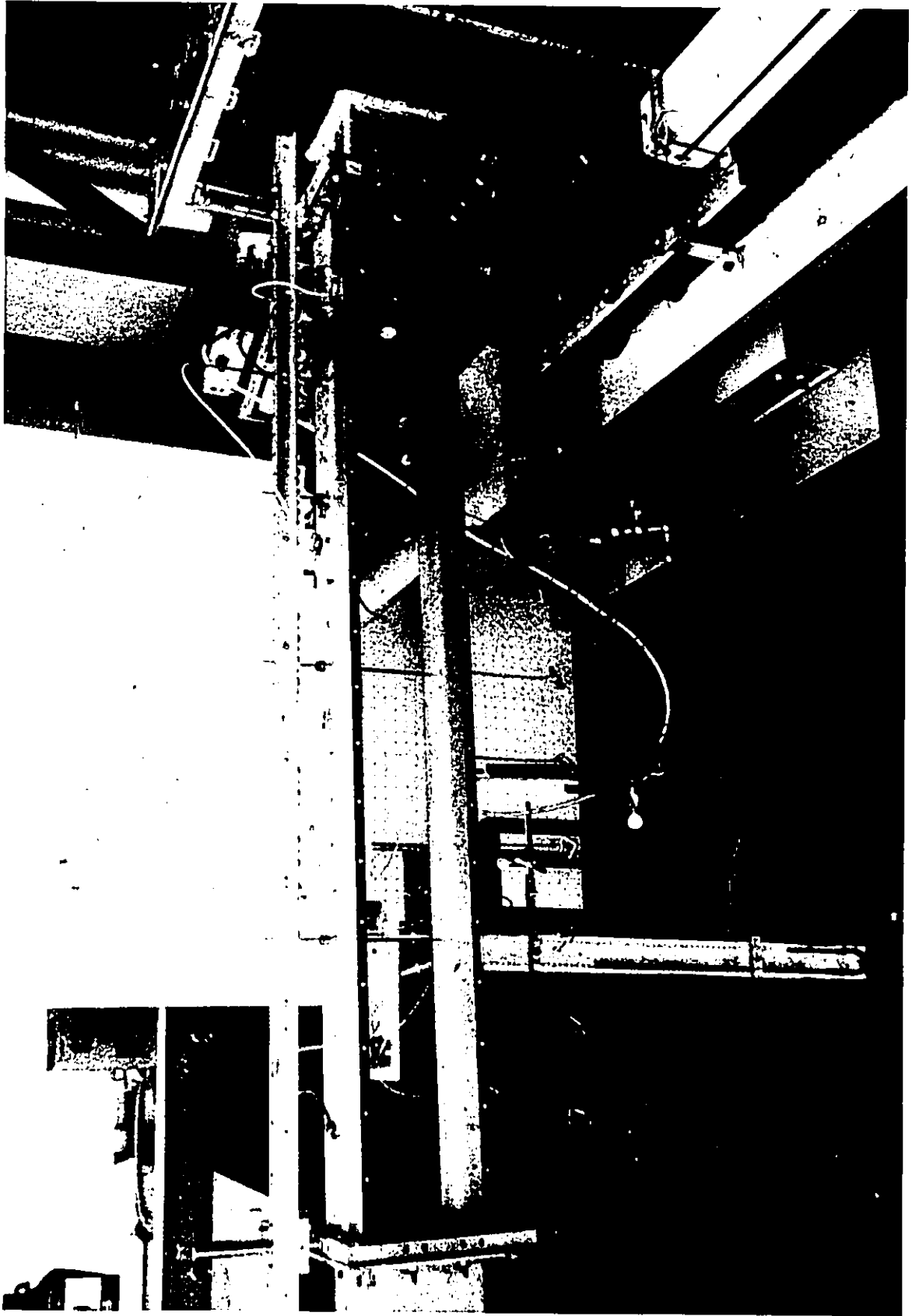


Figure 4-A. Experimental Apparatus (Developing Flow).

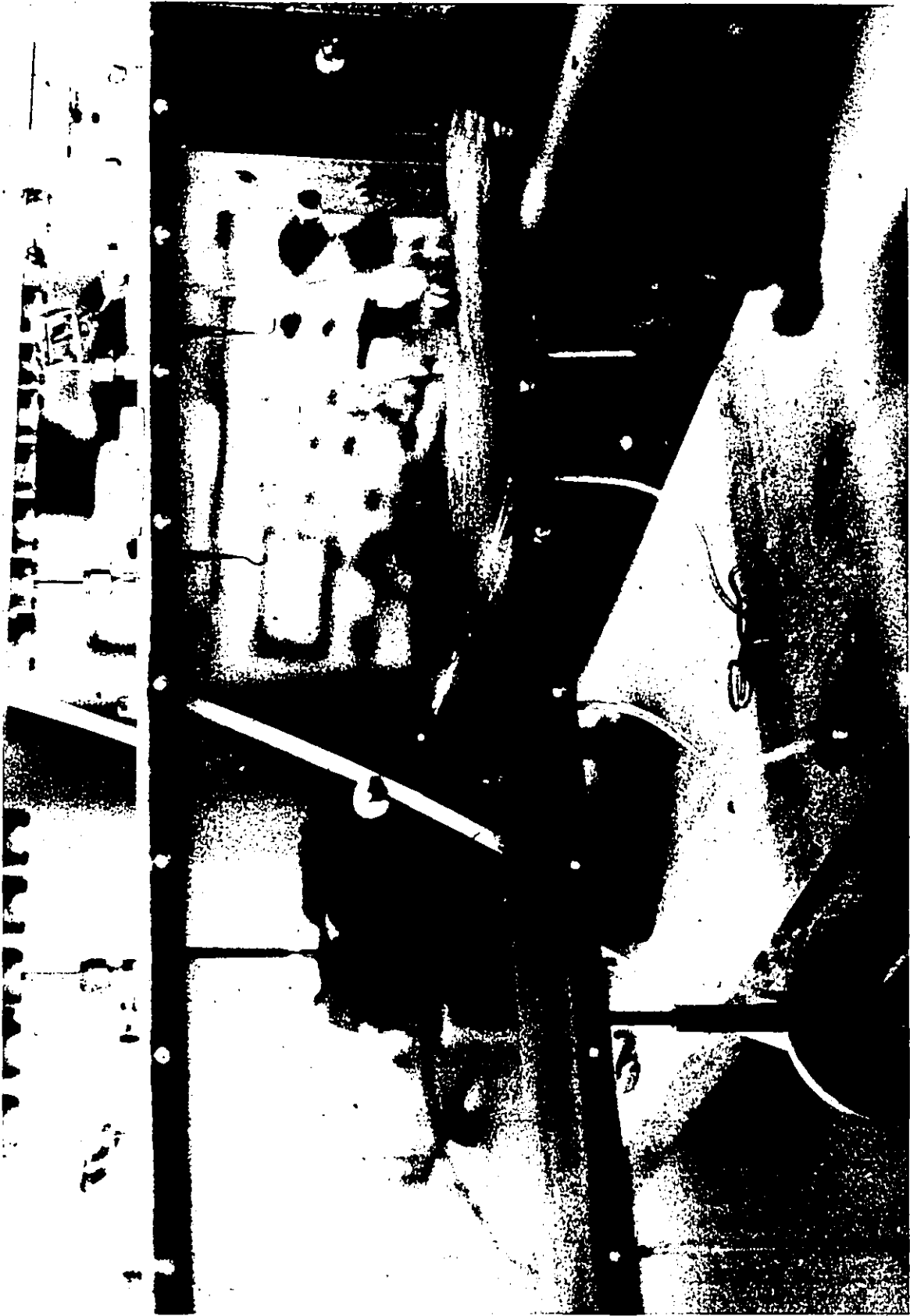


Figure 4-B. Experimental Apparatus (Developing Flow).

LEGEND

Figures 5 and 6

a	Regulator
b	Safety valve
c	Polymer solution vessel
d	relief valve
e	Rotometer
f	Sump tank
g	Injection source
h	Test section
i	Sampling probes
K	Centrifugal pump
l	Constant head tank
m	Screen and cruciform
n	Over flow
P	Sectional view in the test section
r	Honeycomb
s	Bell mouth
t	Plenum chamber

2

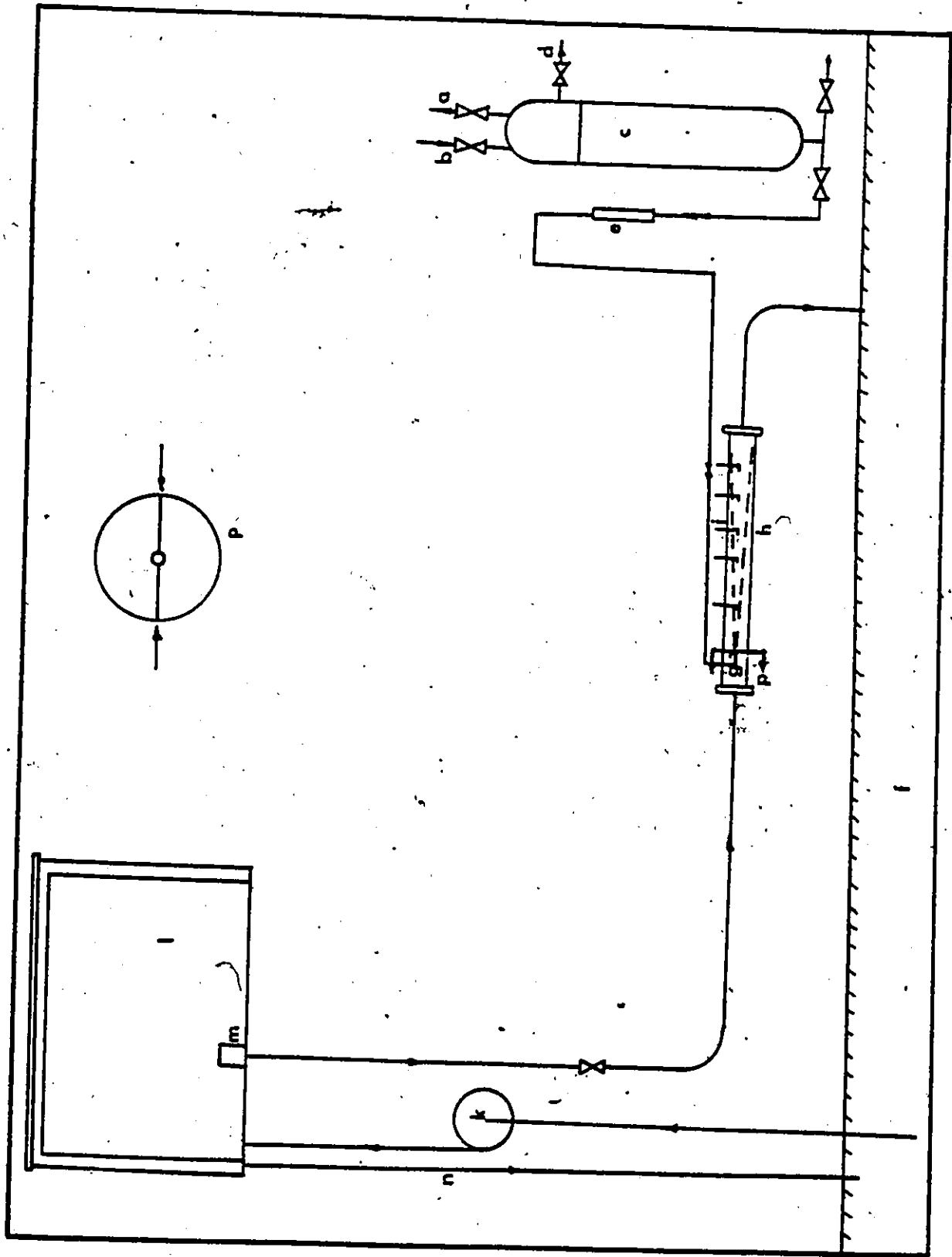


Figure 5. Flow Diagram (Fully Developed Flow).

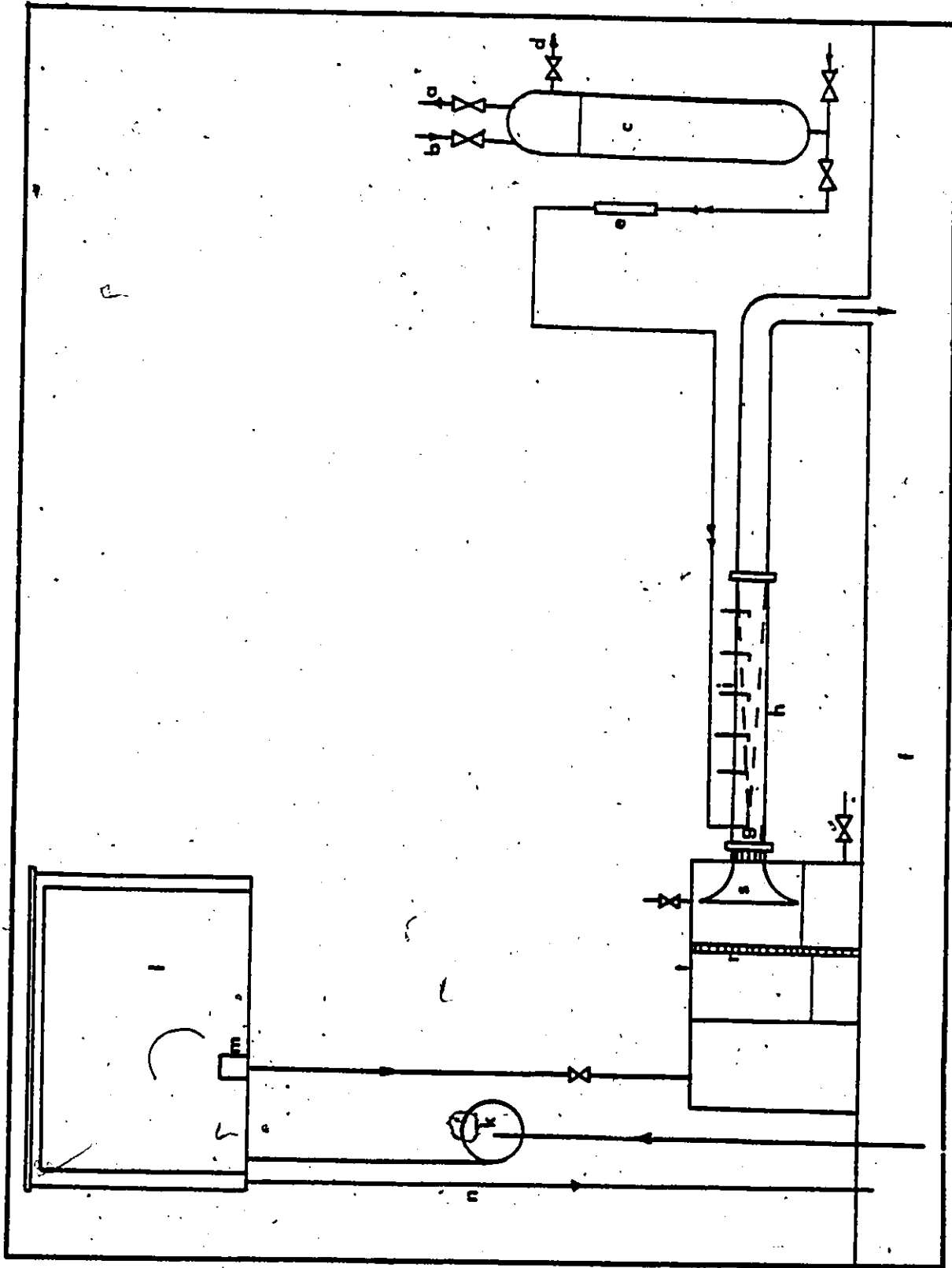


Figure 6. Flow Diagram (Developing Flow).

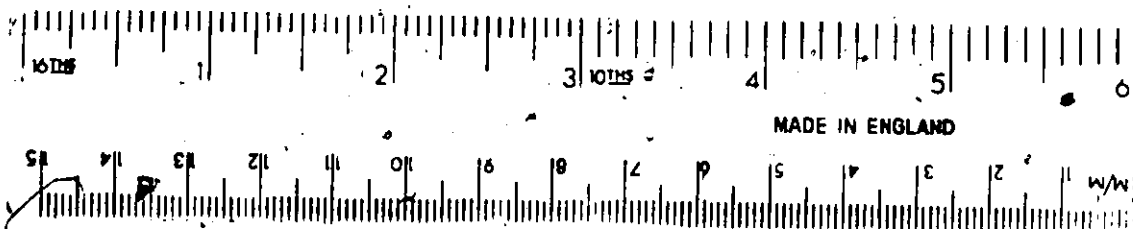
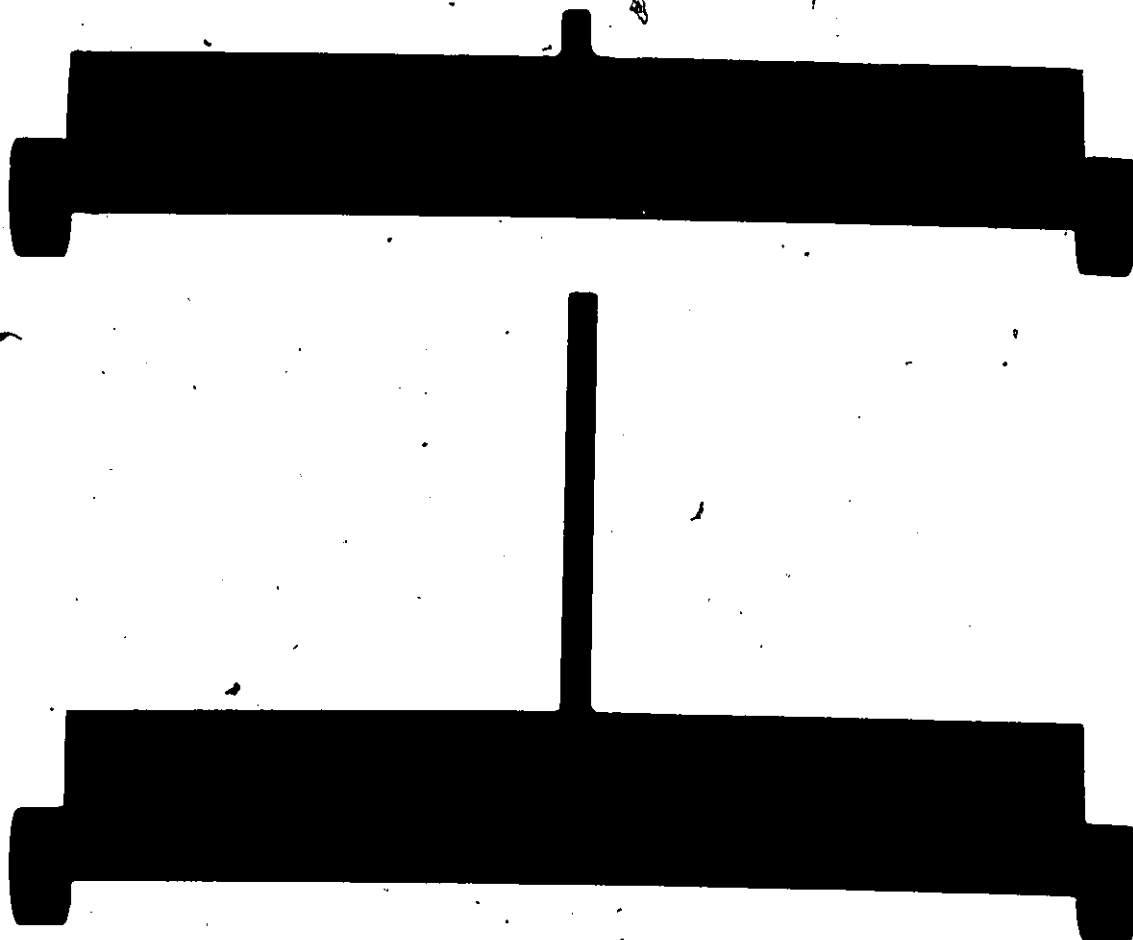


Figure 7. Injection Source (Point Source).

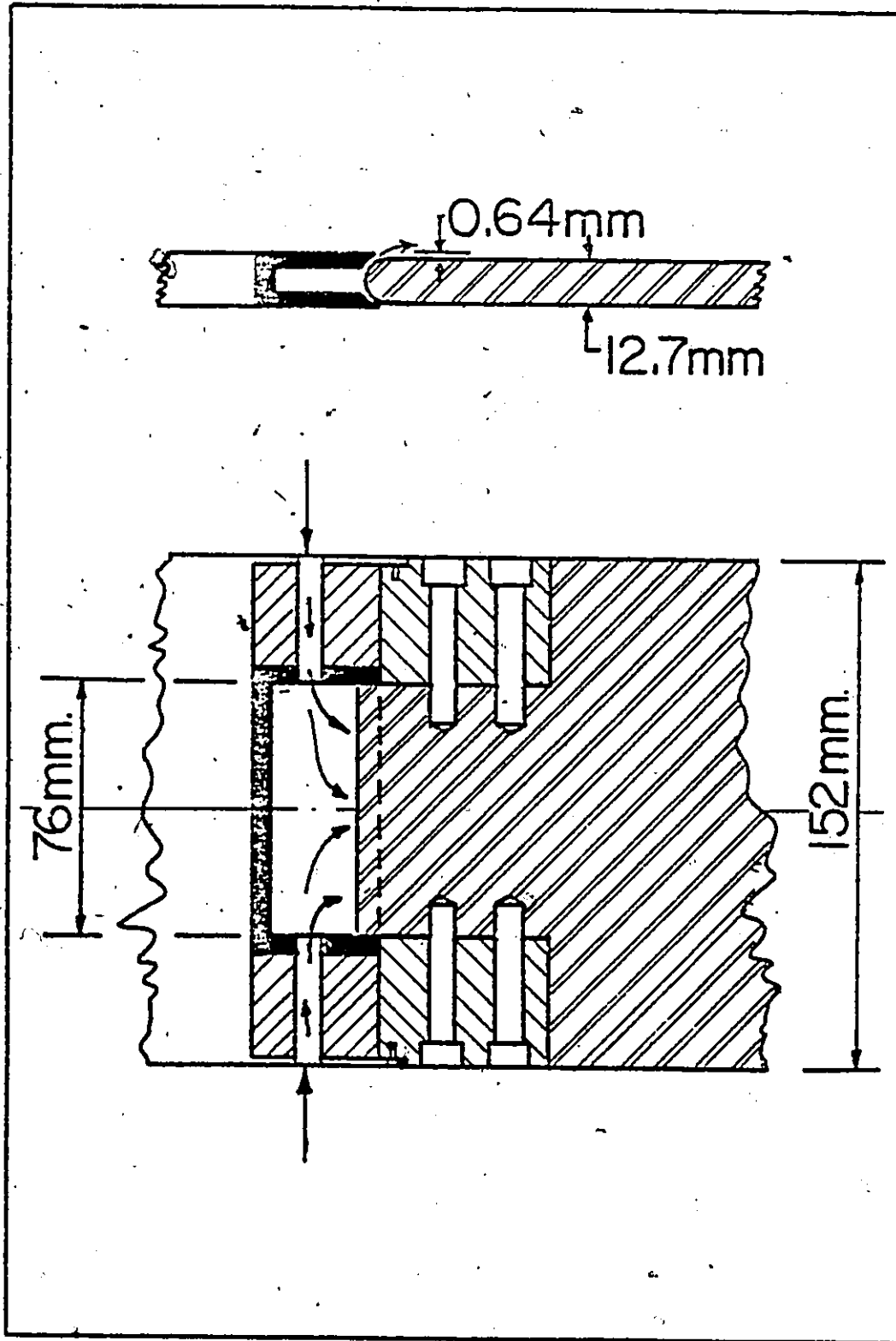


Figure 8. Sectional View of Injection Plenum (Line Source).

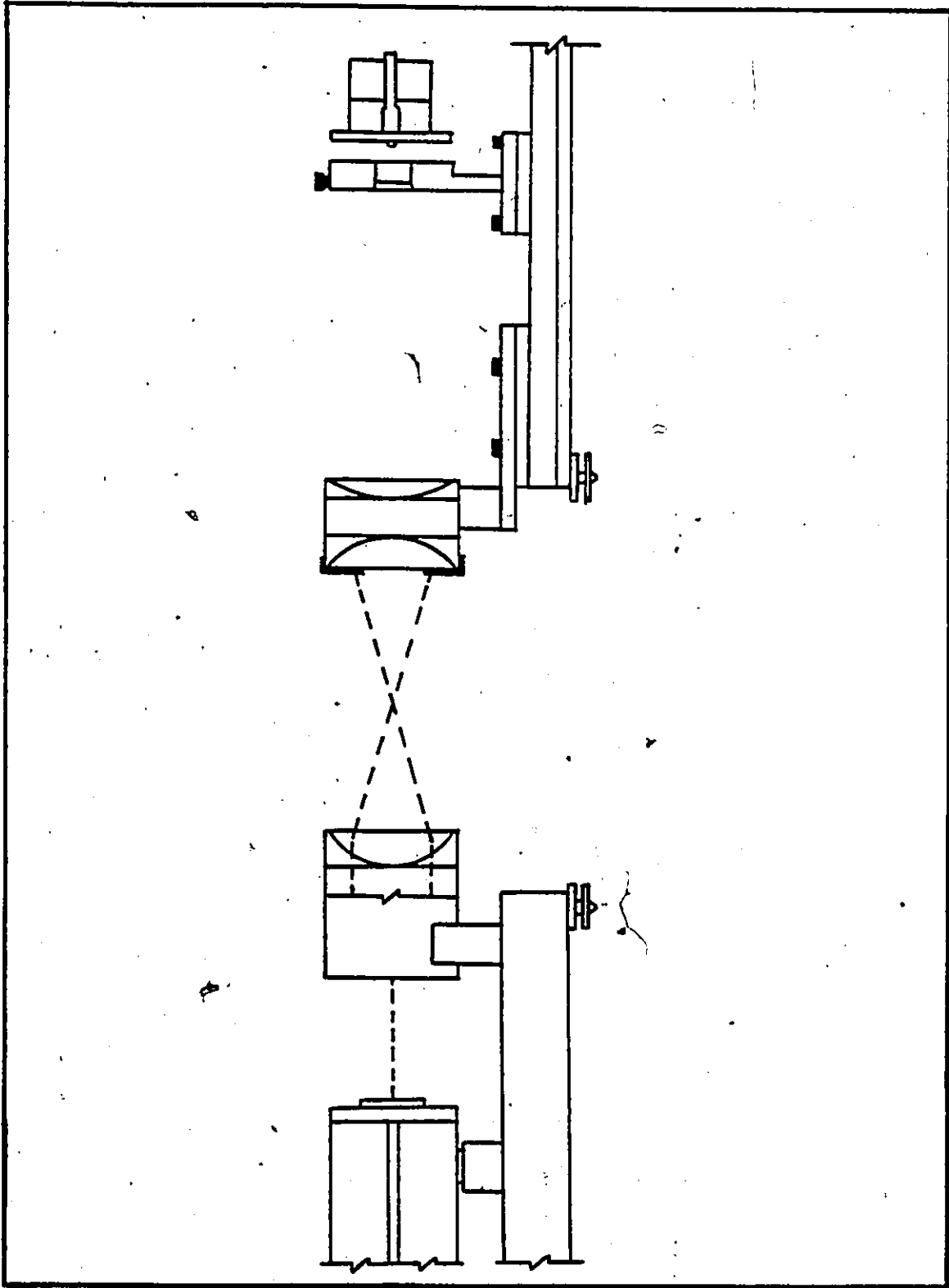


Figure 9. Laser System Assembly.

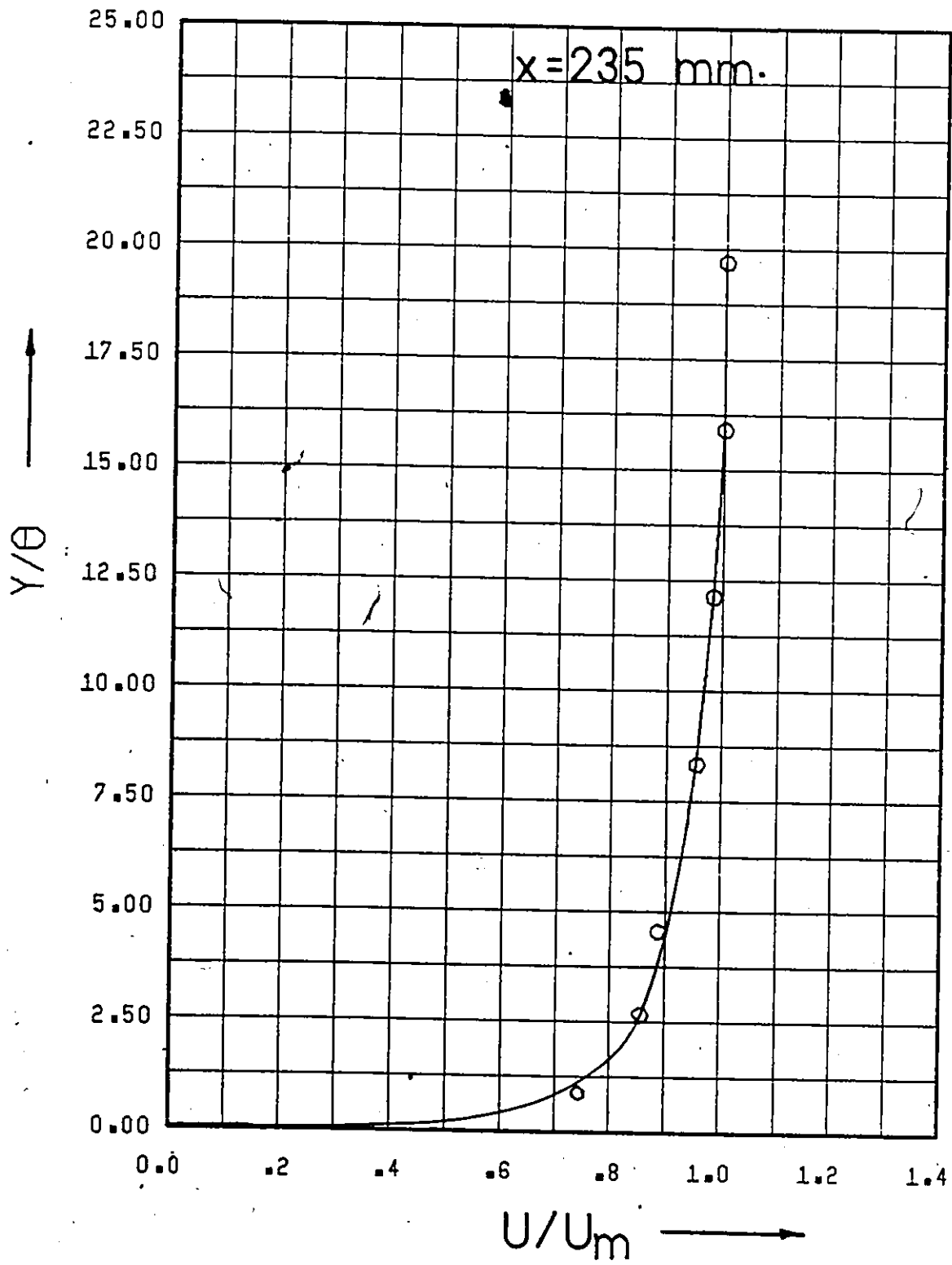


Figure 10. Universal Velocity Profile.

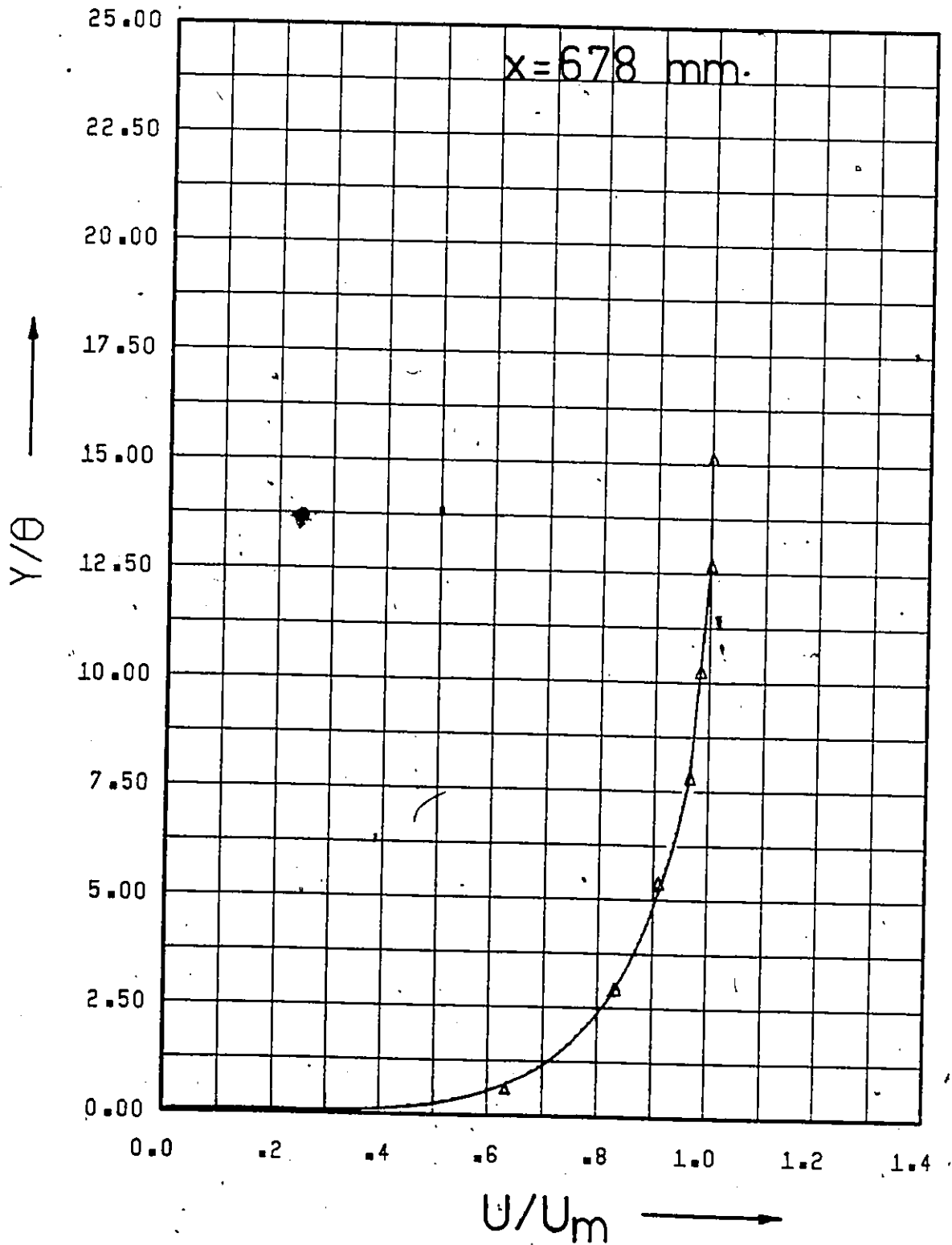


Figure 11. Universal Velocity Profile.

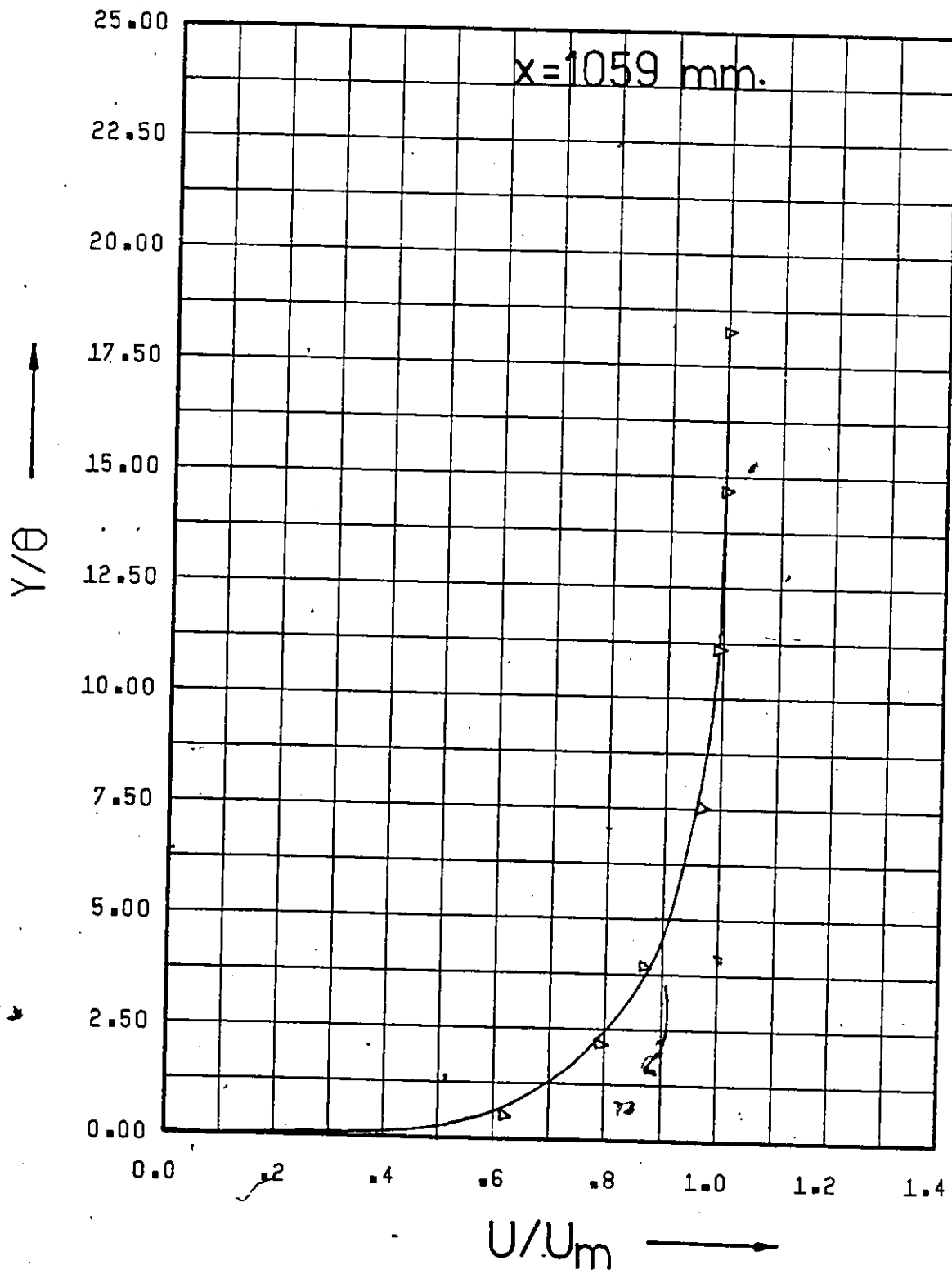


Figure 12. Universal Velocity Profile.

Symbols Used for Concentration Curves

	<u>Series</u>	<u>Location</u>
◇	1	1
*	2	1
◆	3	1
▽	1	2
+	2	2
▼	3	2
△	1	3
x	2	3
▲	3	3
□	1	4
◁	2	4
■	3	4
○	1	5
▷	2	5
○	3	5

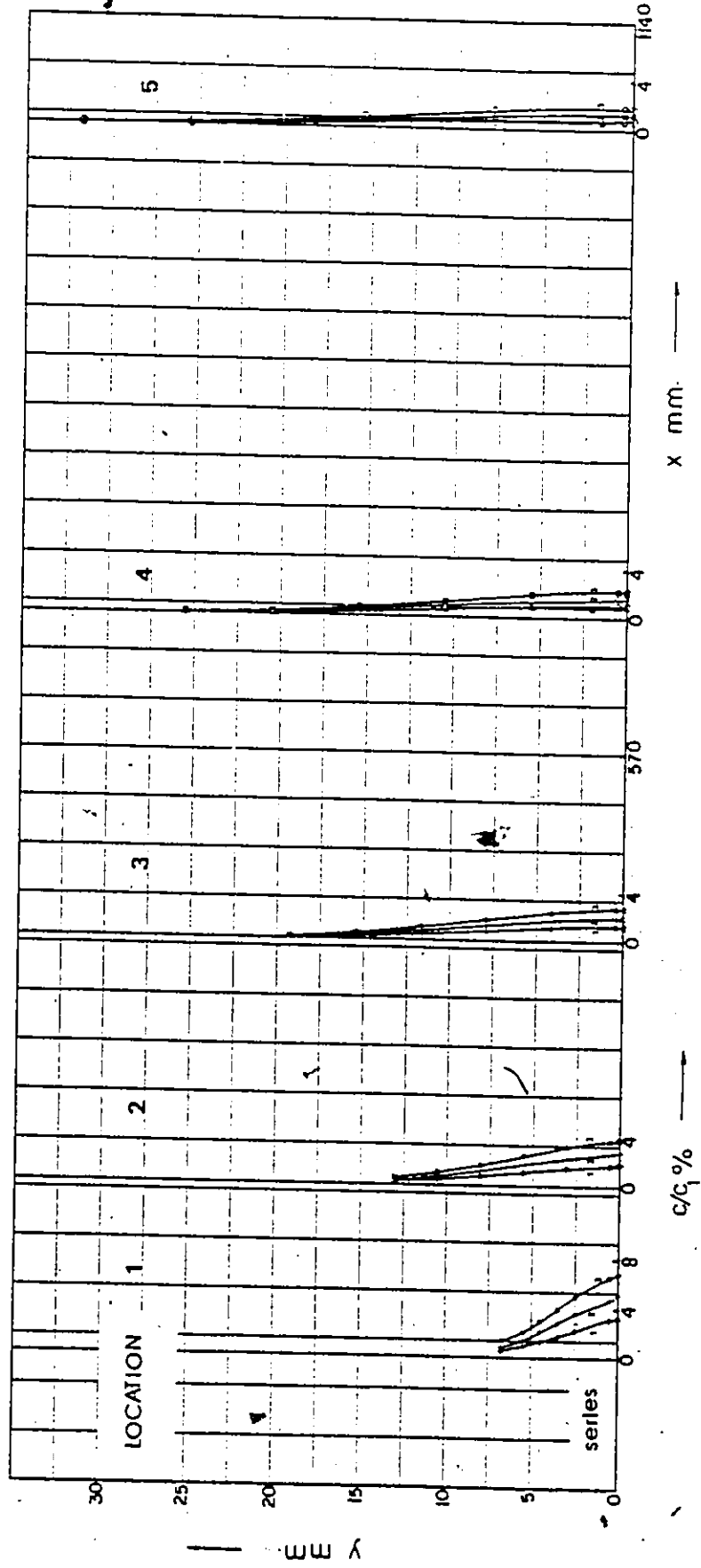


Figure 13. Concentration Profiles (Line Source Injection-Water Injection).

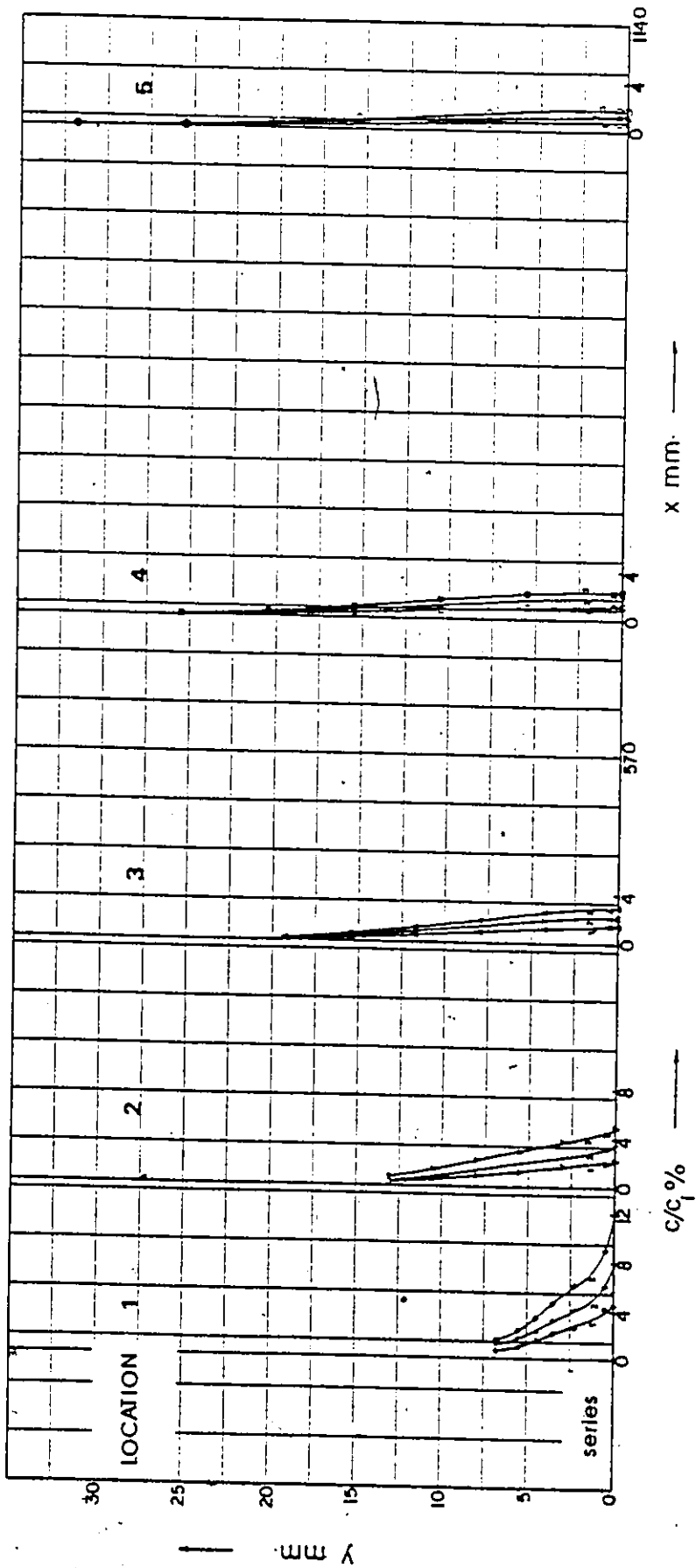


Figure 14. Concentration Profiles (Line Source Injection- $C_i = 100$.w.p.p.m.).

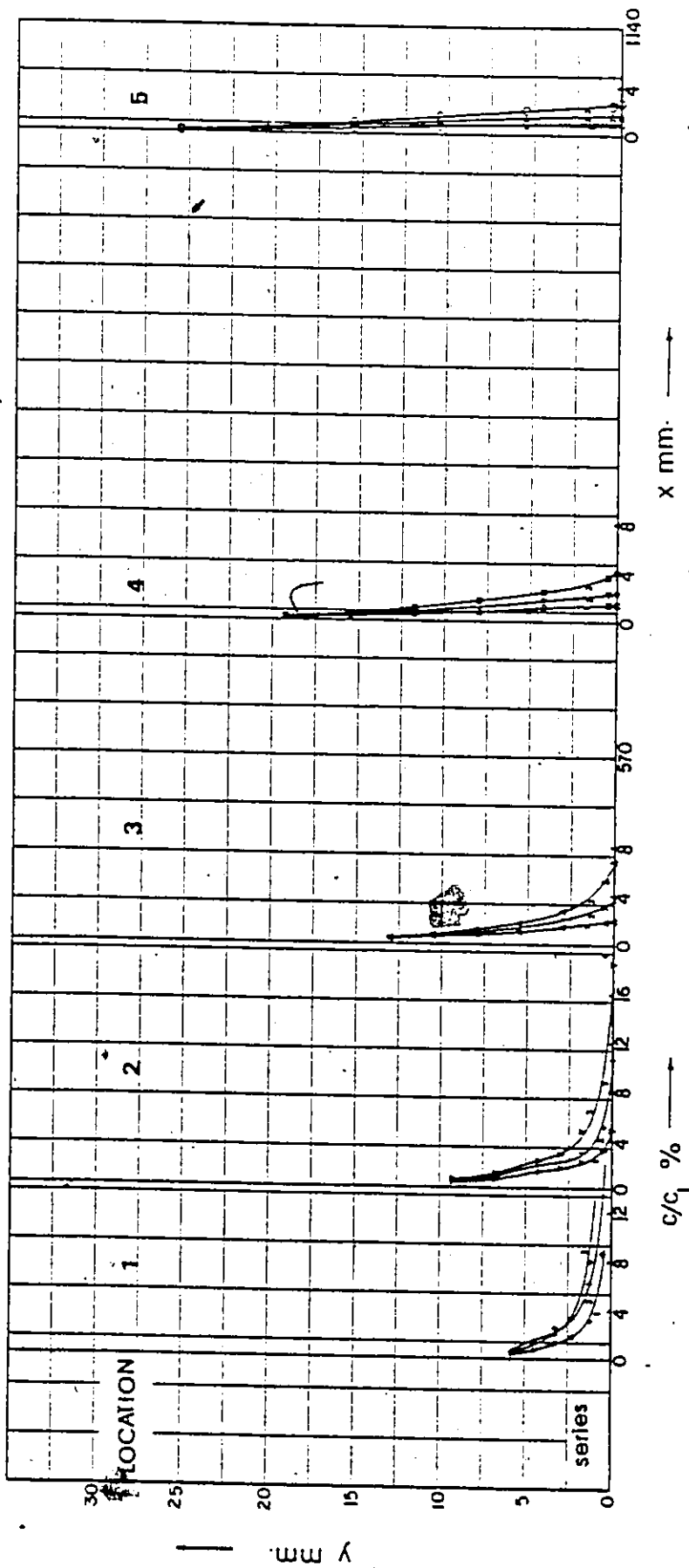


Figure 15. Concentration Profiles (Line Source Injection- $C_1 = 500$ w.p.p.m.).

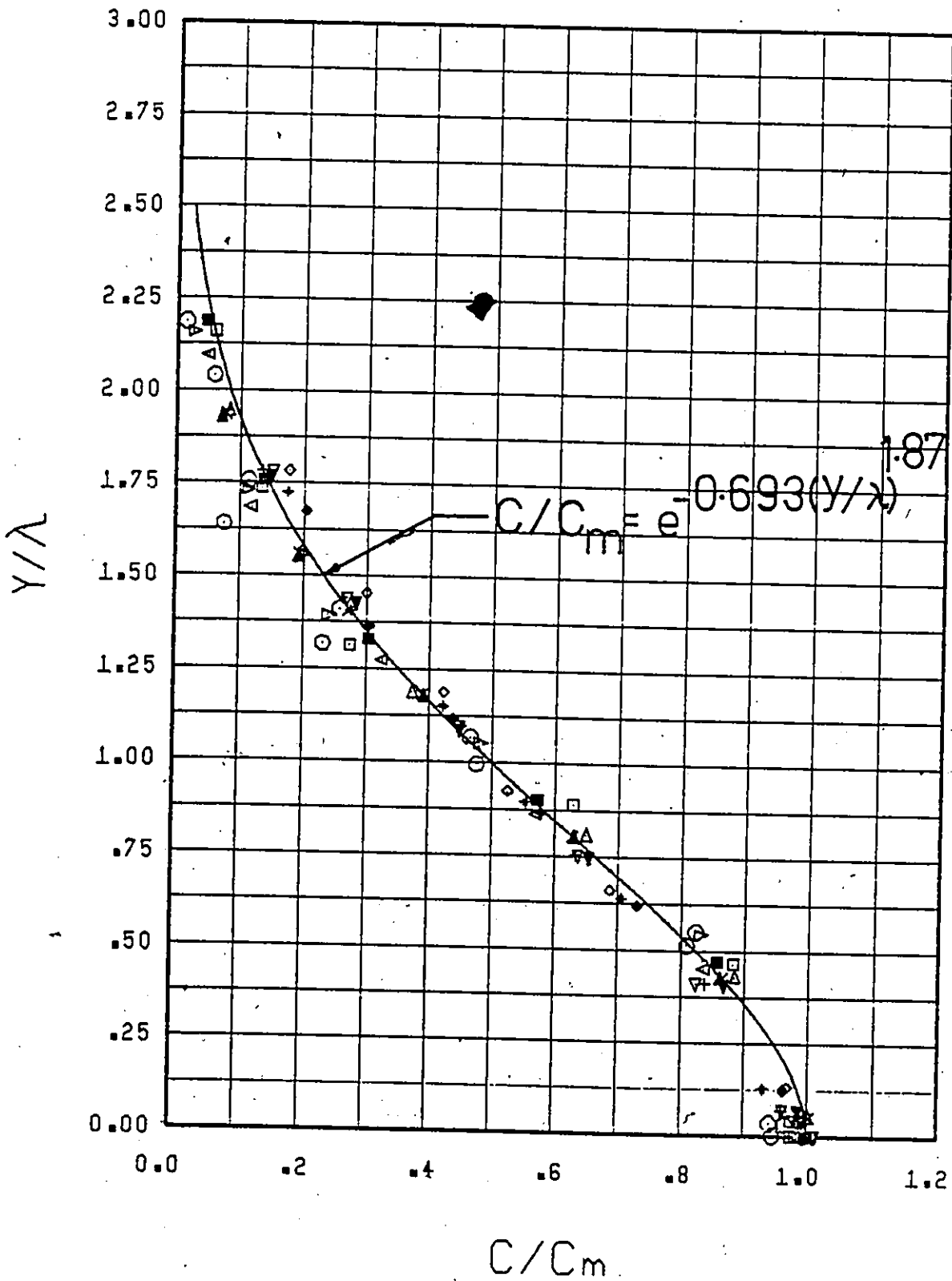


Figure 16. Universal Concentration Profile (Line Source Injection-Water Injection-All Data).

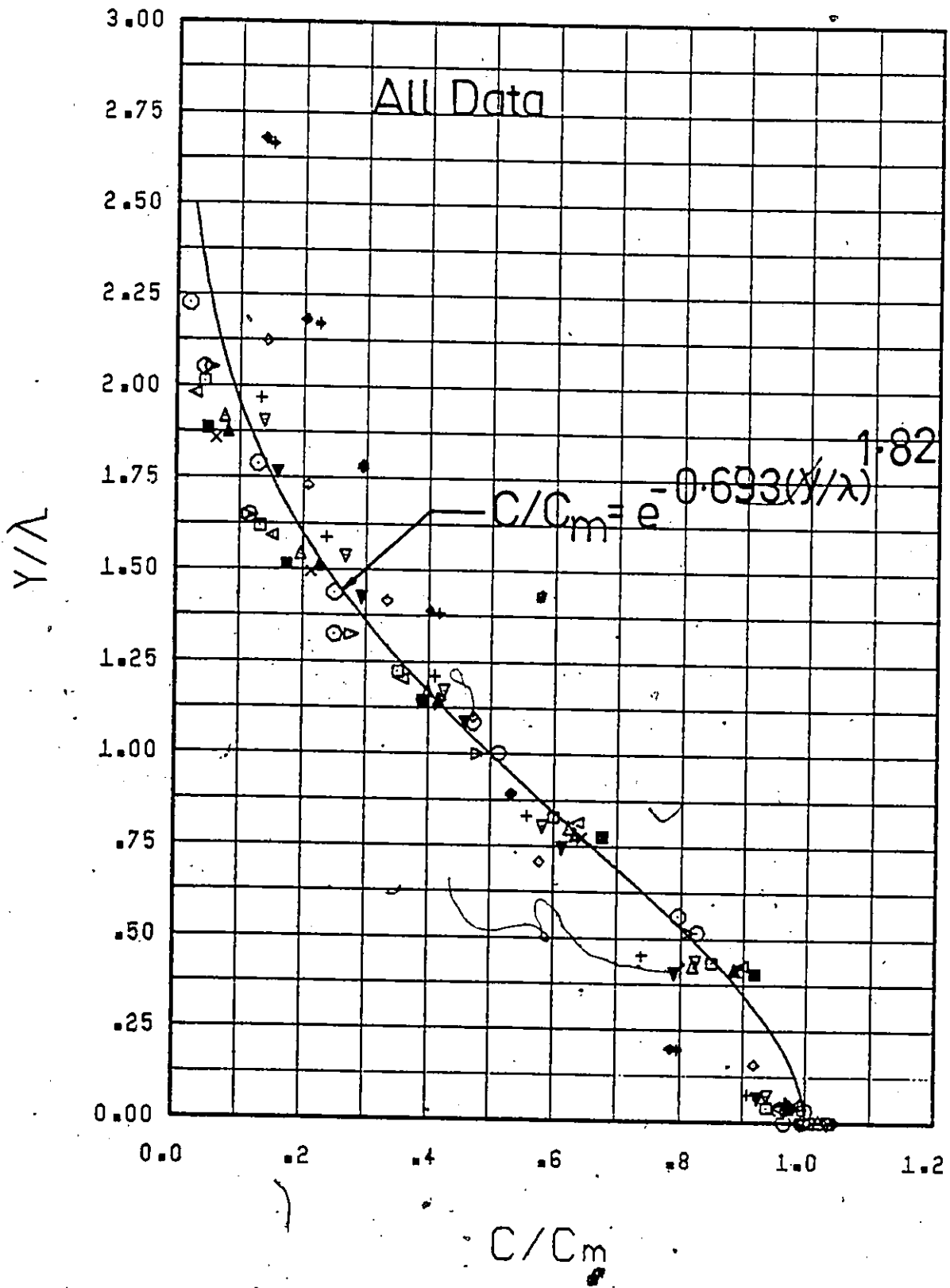


Figure 17. Universal Concentration Profile (Line Source Injection- $C_i = 100$ w.p.p.m.).

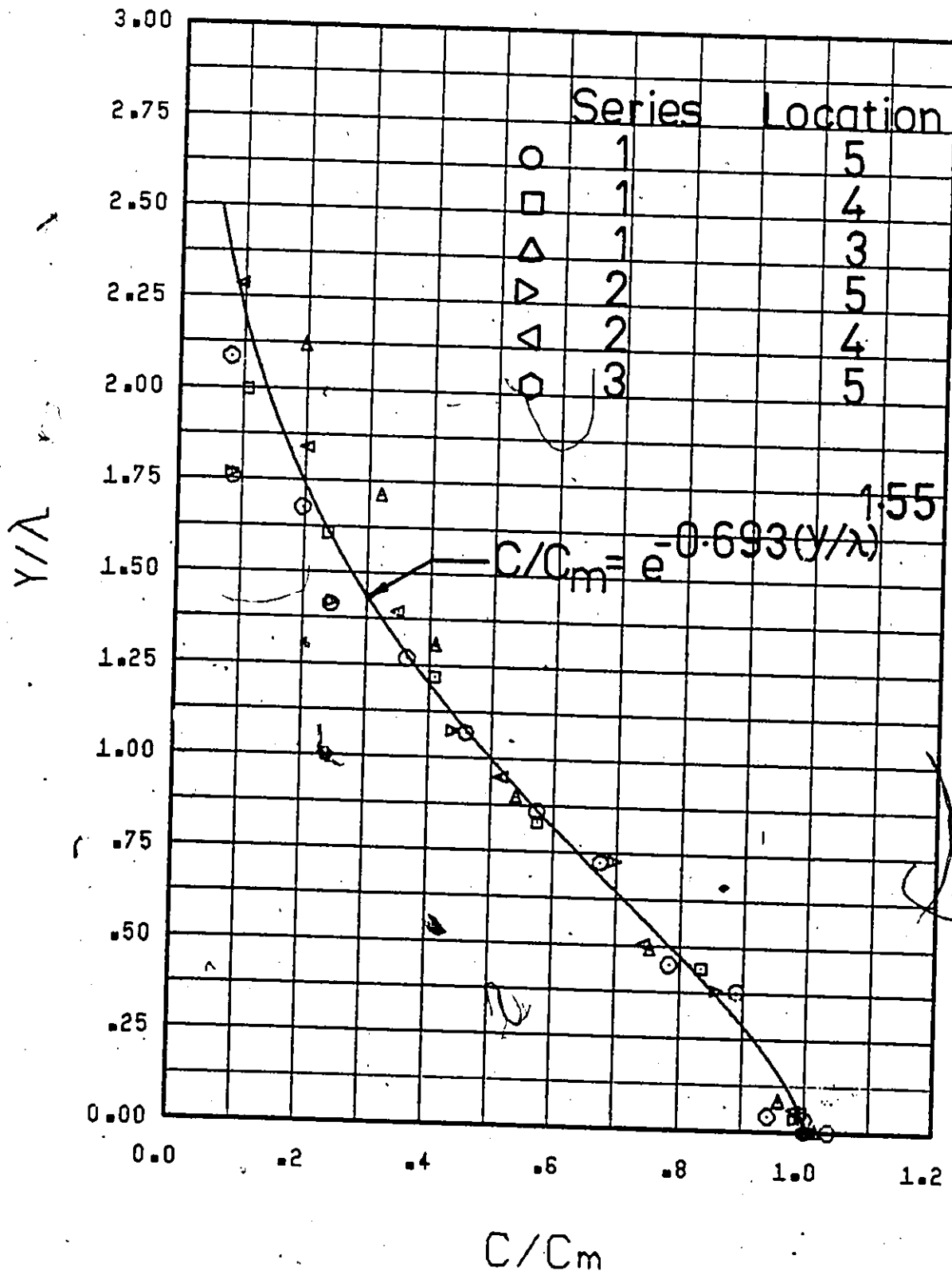


Figure 18. Universal Concentration Profiles (Line Source Injection- $C_i = 500$ w.p.p.m.).

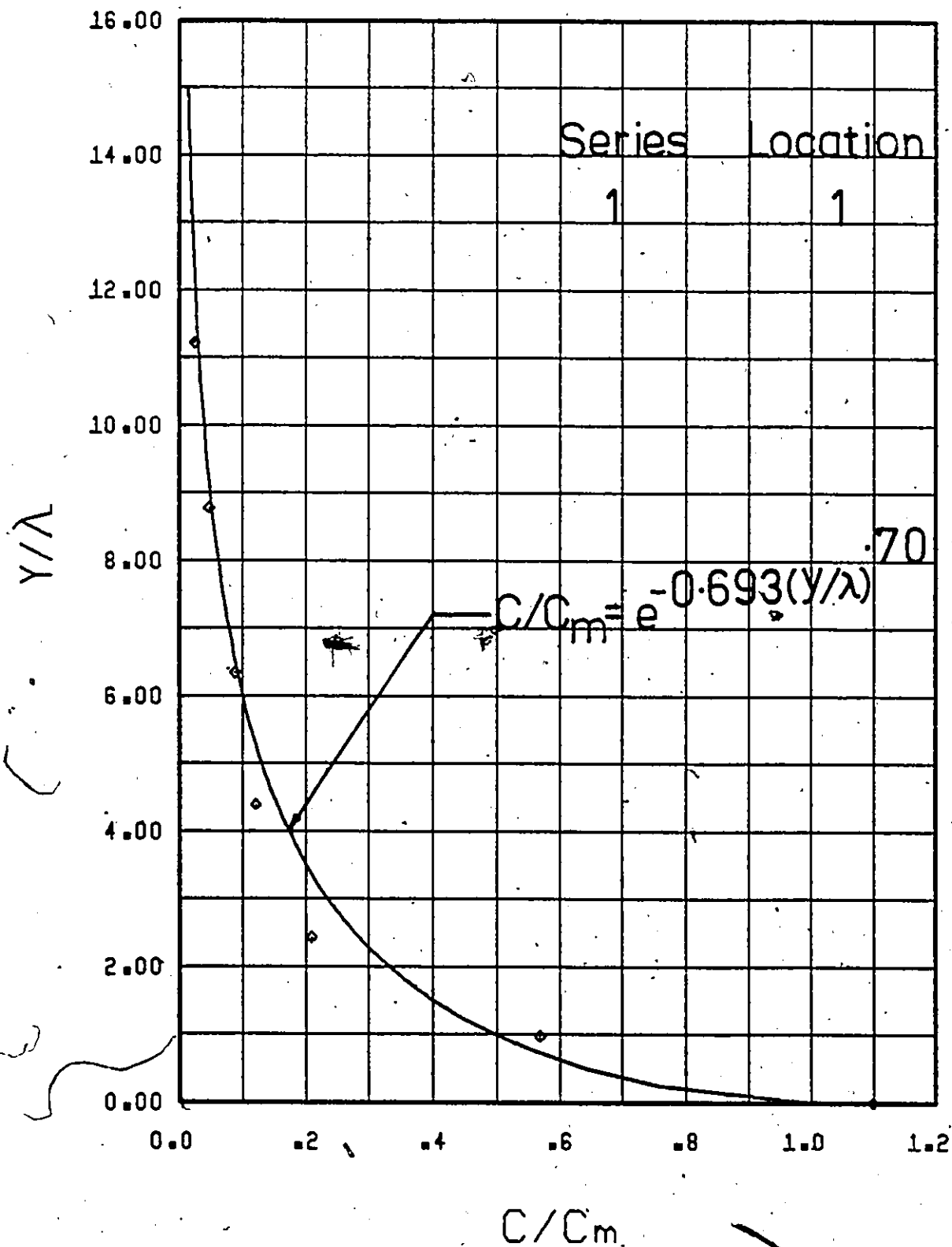


Figure 19. Universal Concentration Profile (Line Source Injection- $C_i = 500$ w.p.p.m.).

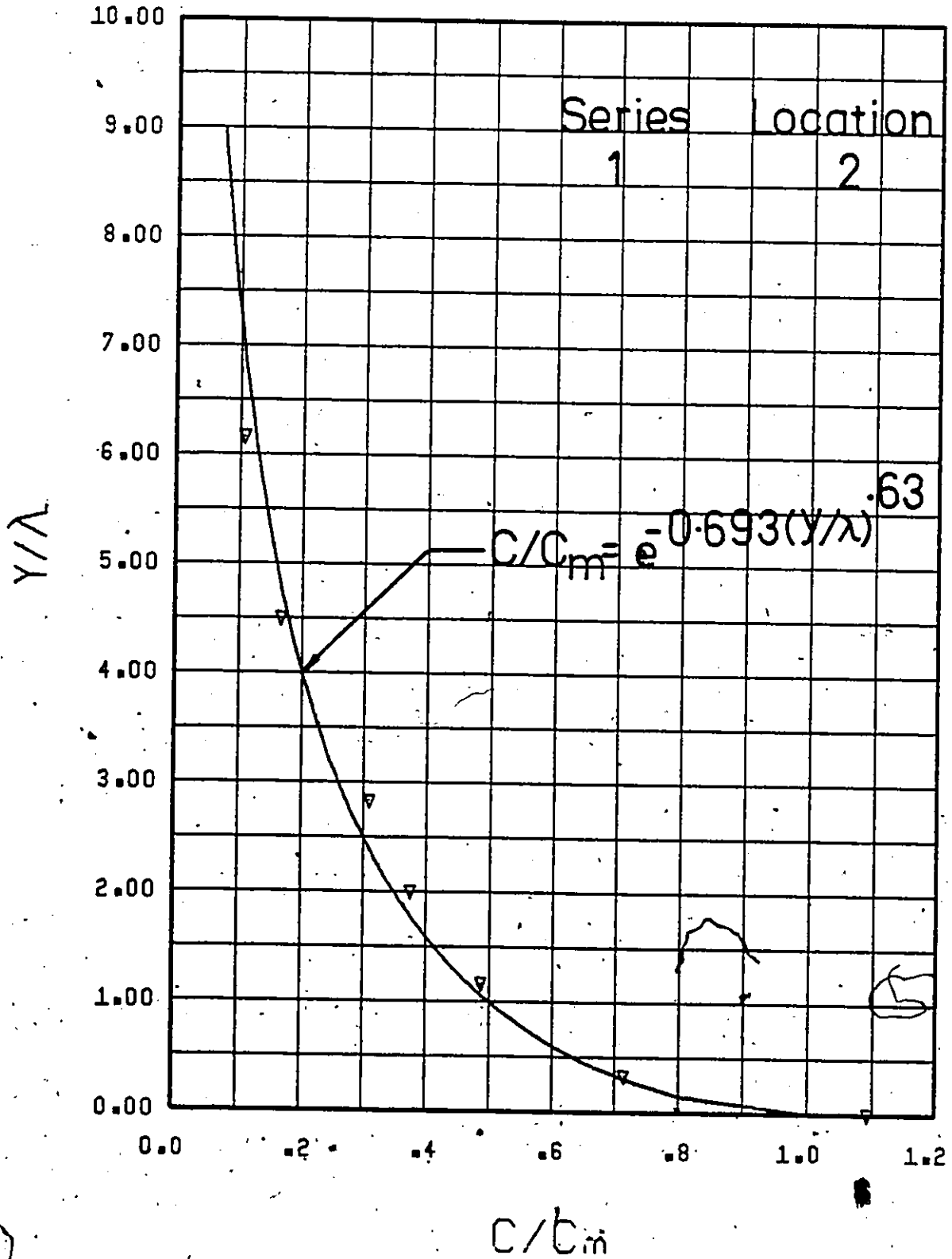


Figure 20. Universal Concentration Profile (Line Source Injection- $C_i = 500$ w.p.p.m.).

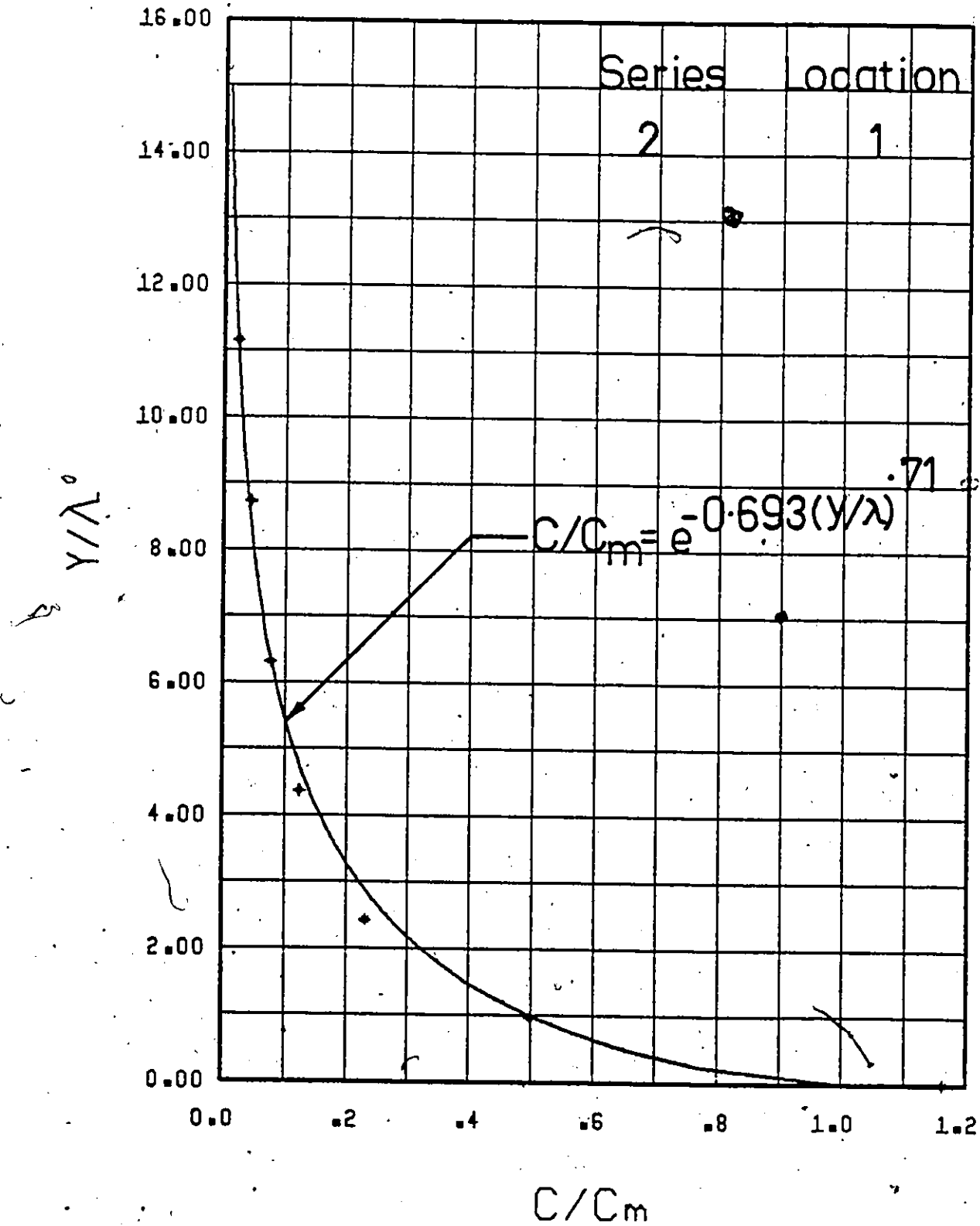


Figure 21. Universal Concentration Profile (Line Source Injection- $C_i = 500$ w.p.p.m.).

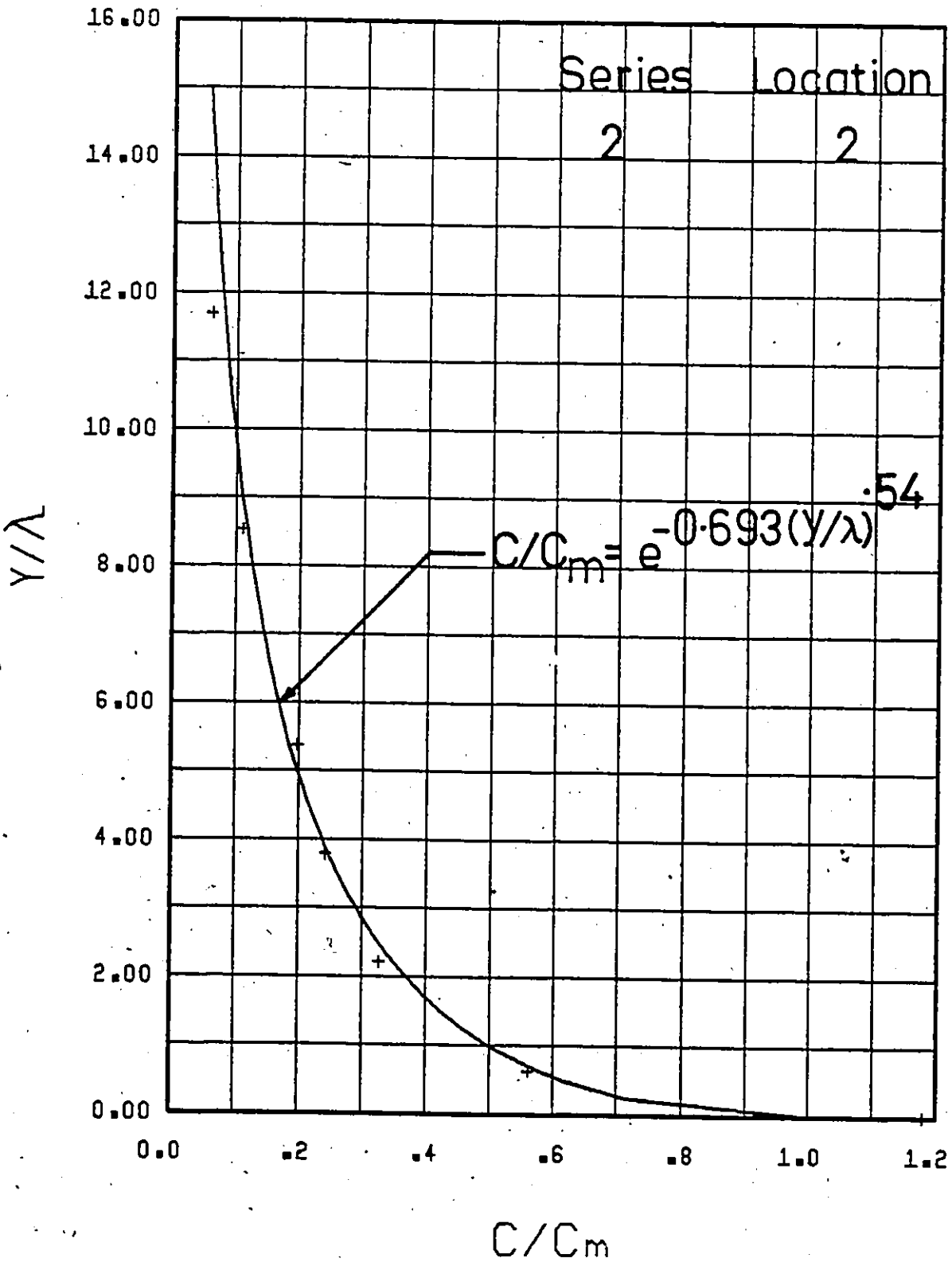


Figure 22. Universal Concentration Profile (Line Source Injection- $C_i = 500$ w.p.p.m.).

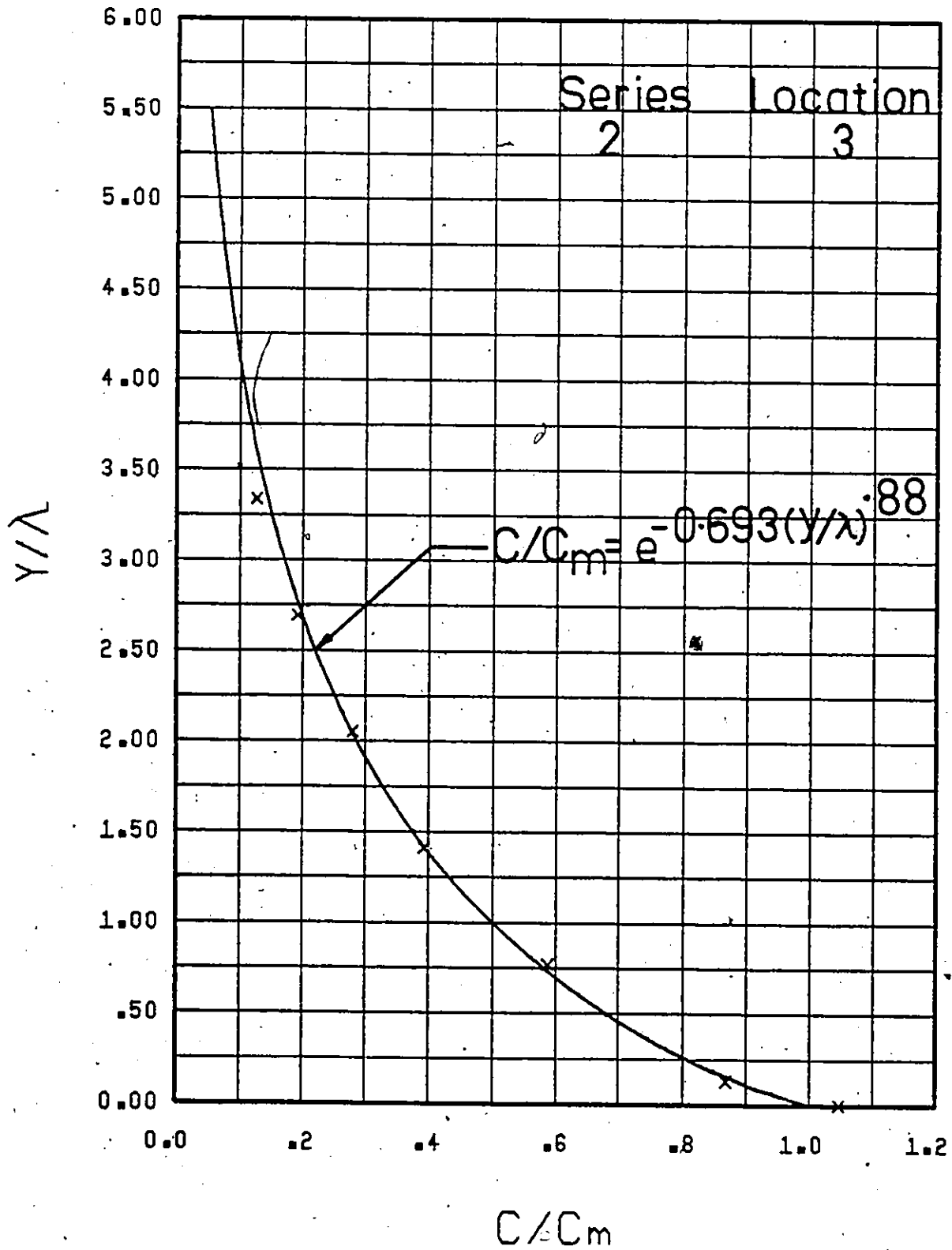


Figure 23. Universal Concentration Profile (line Source Injection- $C_i = 500$ w.p.p.m.).

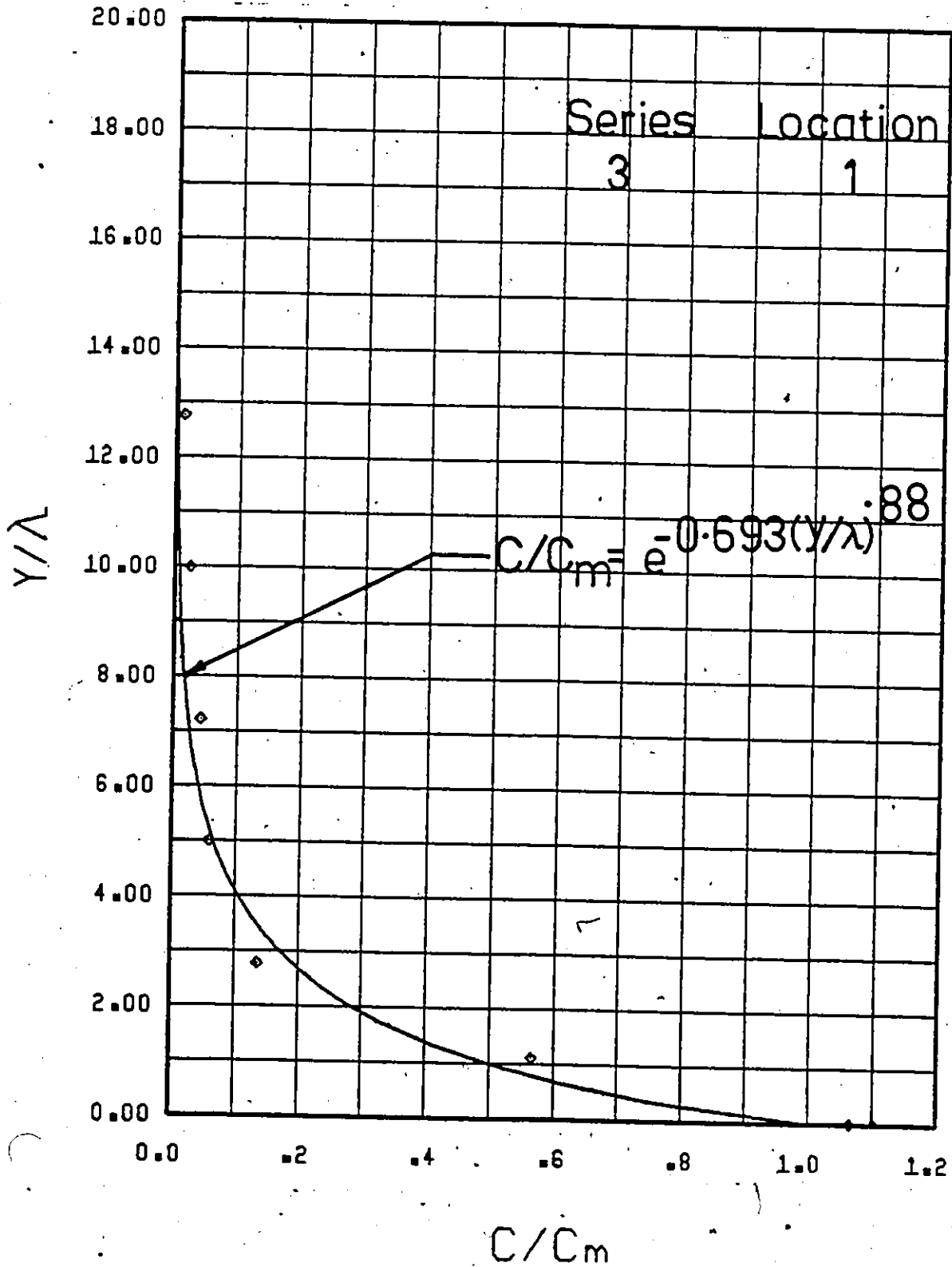


Figure 24. Universal Concentration Profile (Line Source Injection- $C_i = 500$ w.p.p.m.).

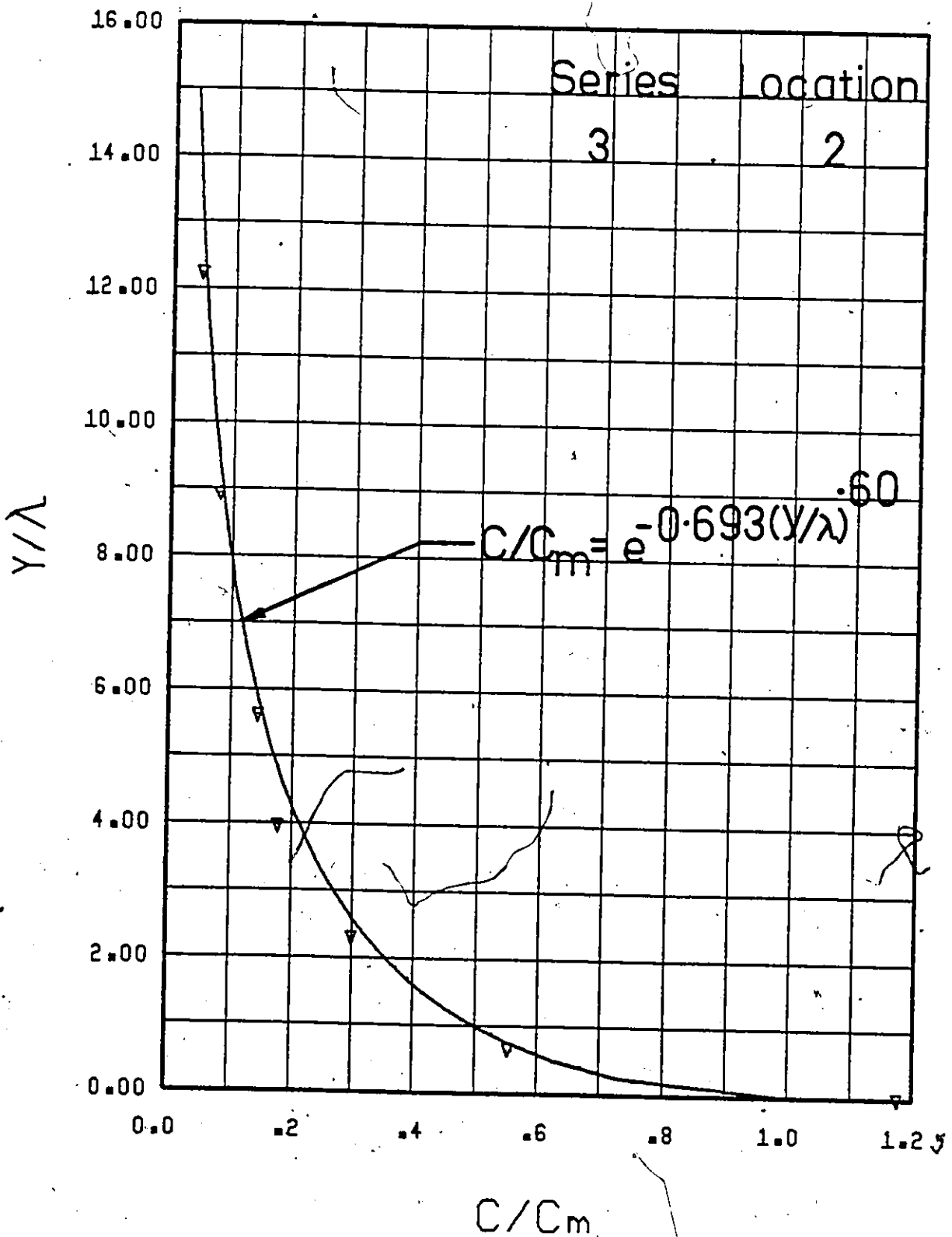


Figure 25. Universal Concentration Profile (Line Source Injection- $C_i = 500$ w.p.p.m.).

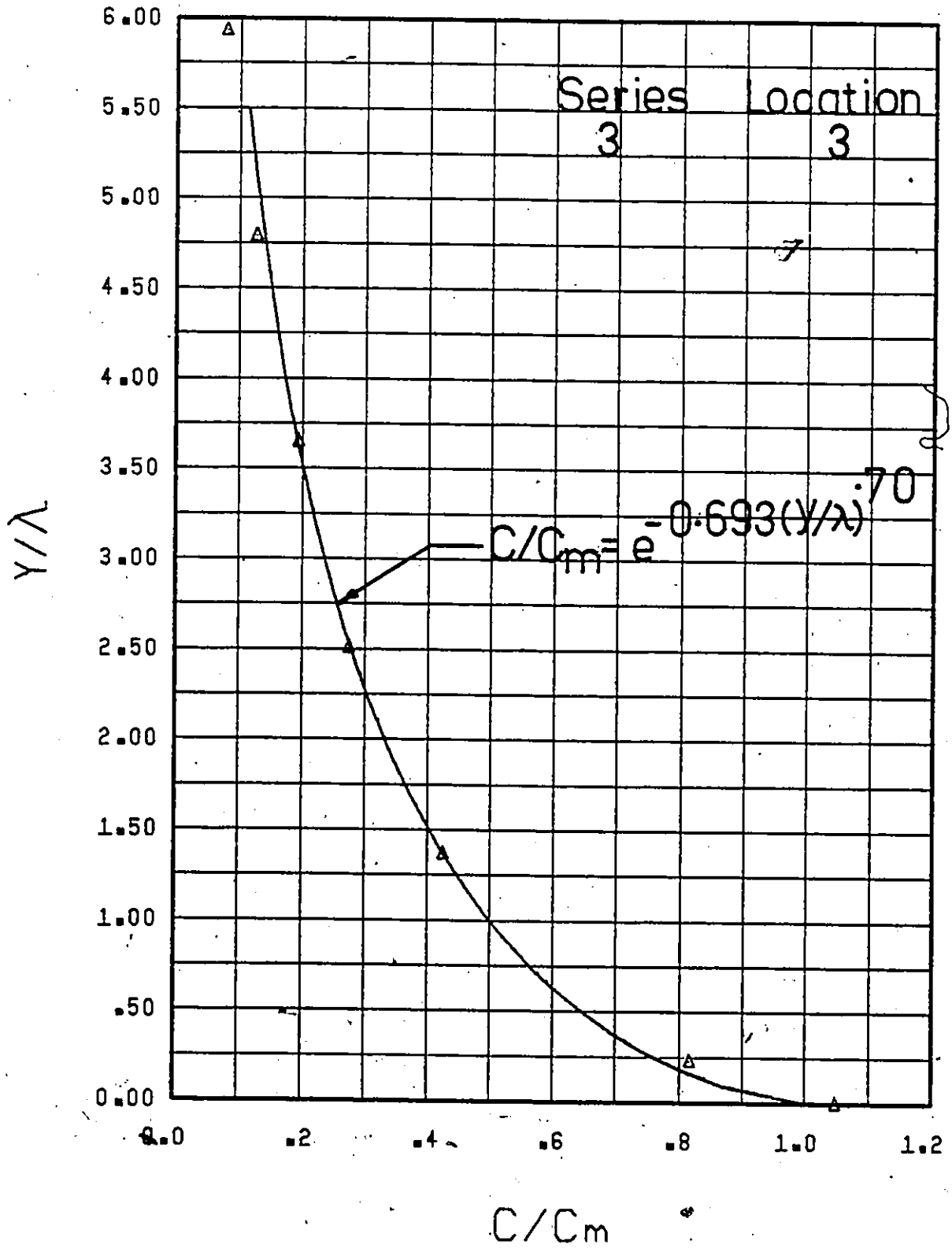


Figure 26. Universal Concentration Profile (Line Source Injection- $C_i = 500$ w.p.p.m.).

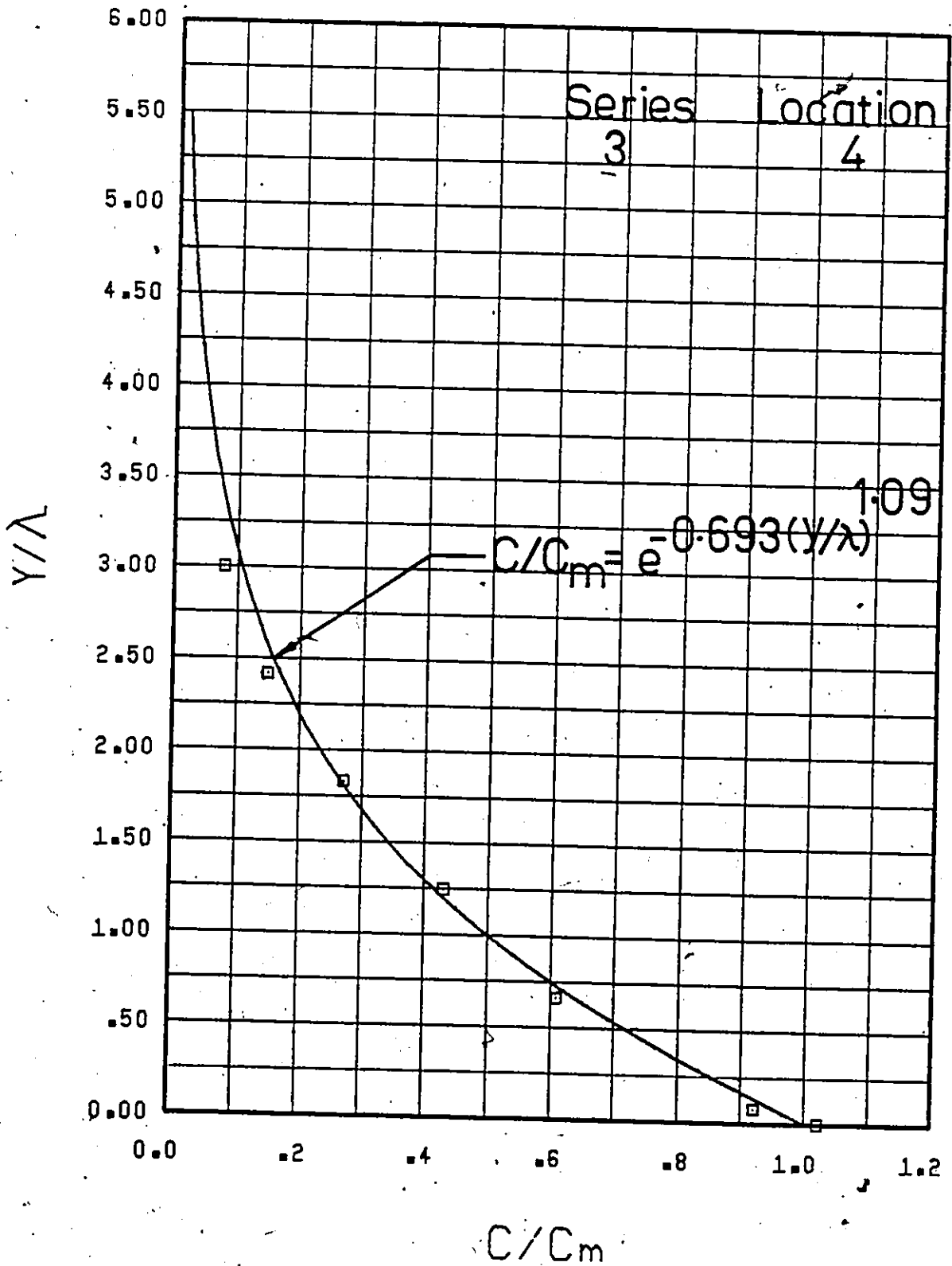


Figure 27. Universal Concentration Profile (Line Source Injection- $C_i = 500$ w.p.p.m.).

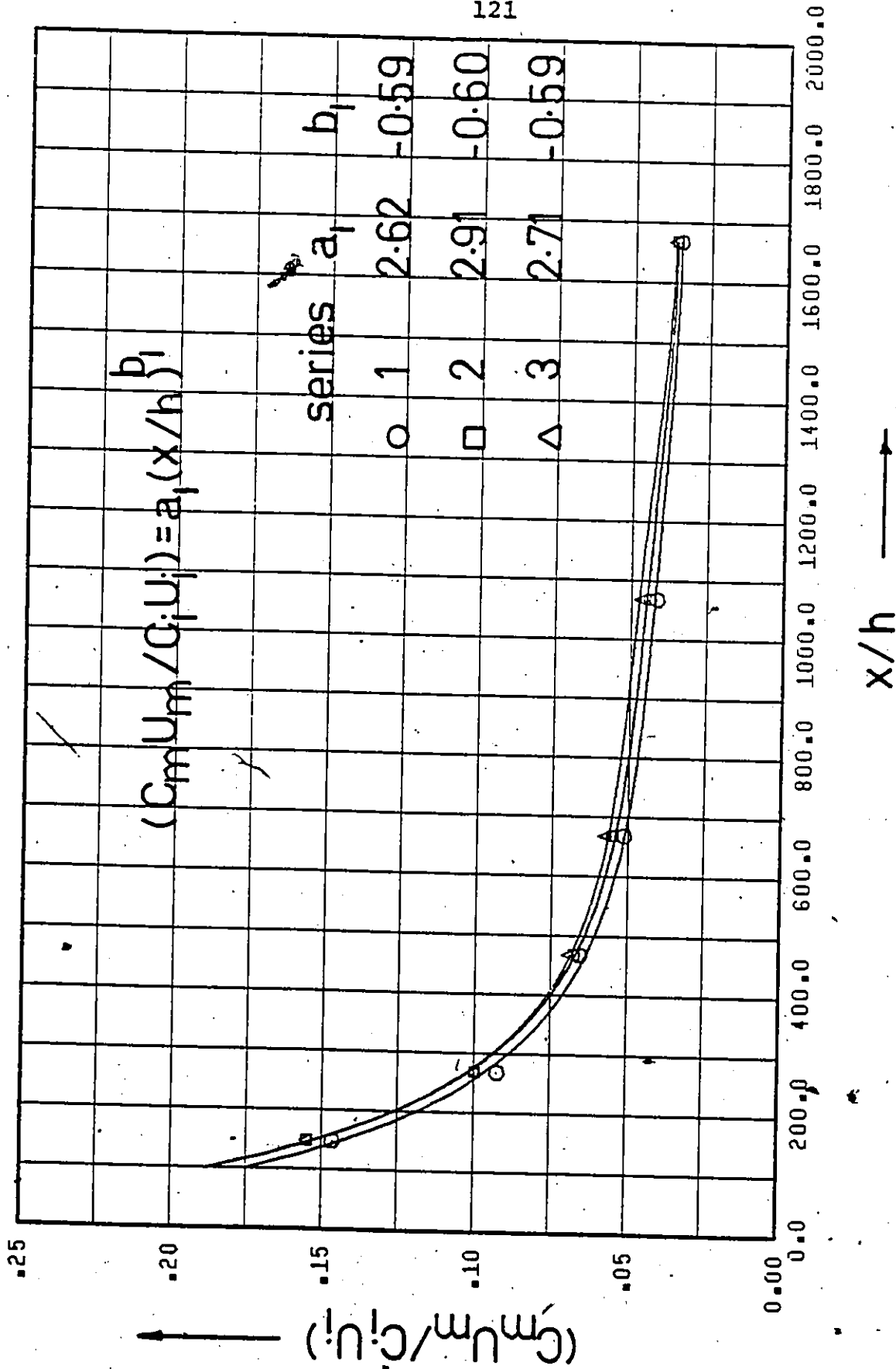


Figure 28. $\frac{C_m U_m}{C_i U_i}$ vs. $\frac{x}{h}$ (Line Source Injection-Water Injection).

100
1,293

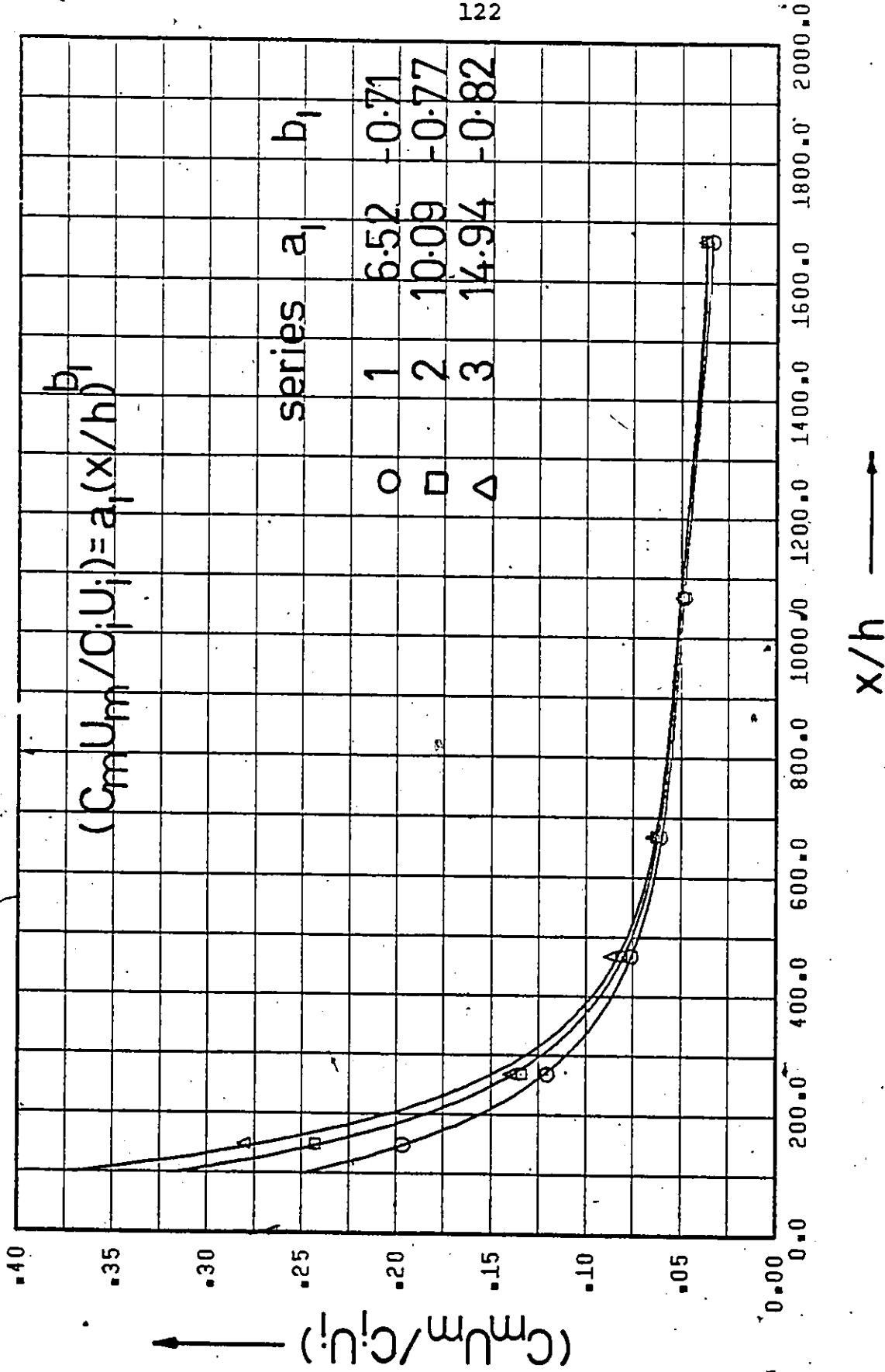


Figure 29. $\frac{C_m U_m}{C_i U_i}$ vs. $\frac{x}{h}$ (Line Source Injection- $C_i = 100$ w.p.p.m.).

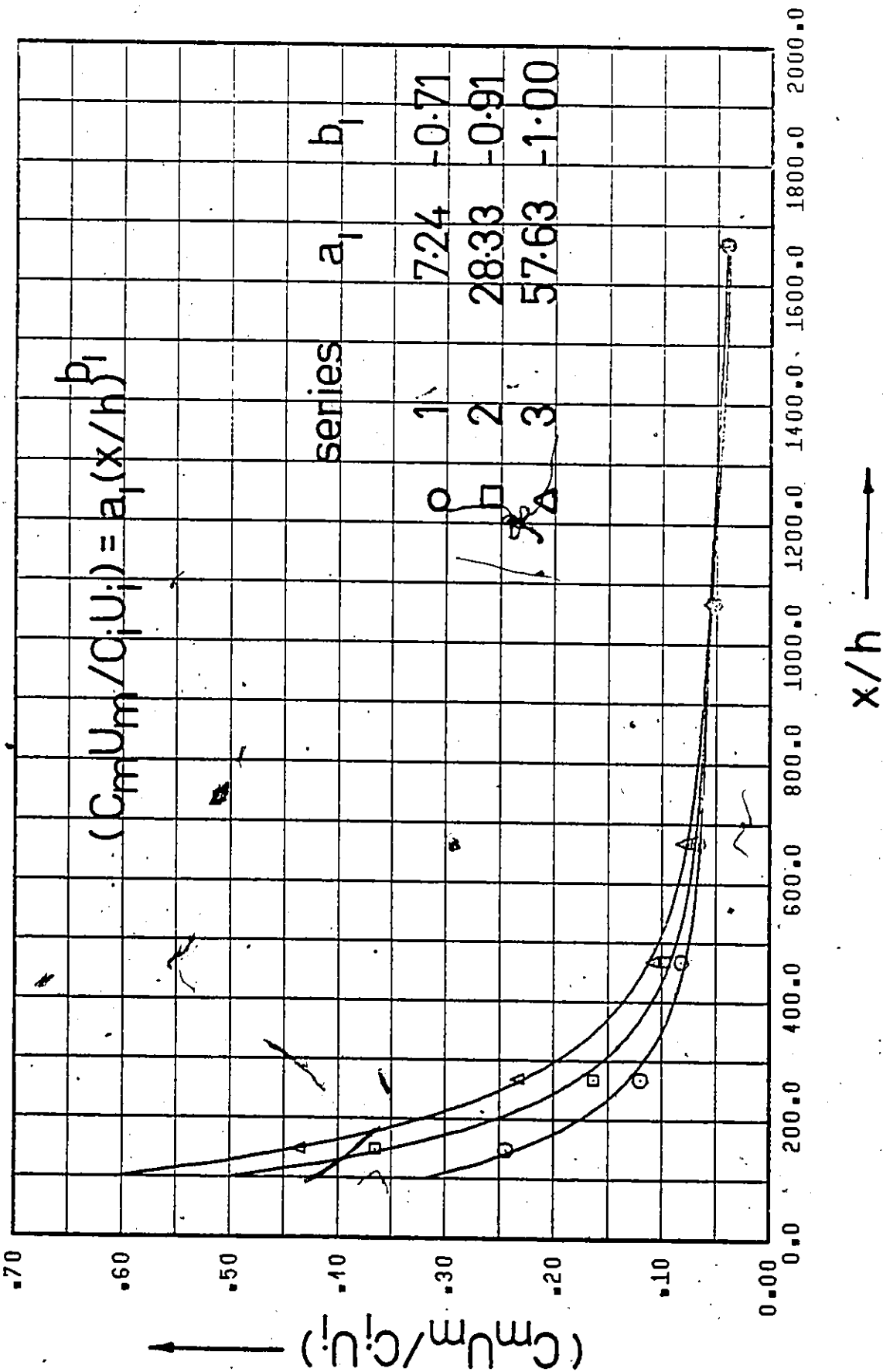


Figure 30. $\frac{C_m U_m}{C_i U_i}$ vs. $\frac{x}{h}$ (Line Source Injection - $C_i = 250$ w.p.p.m.).

2,3

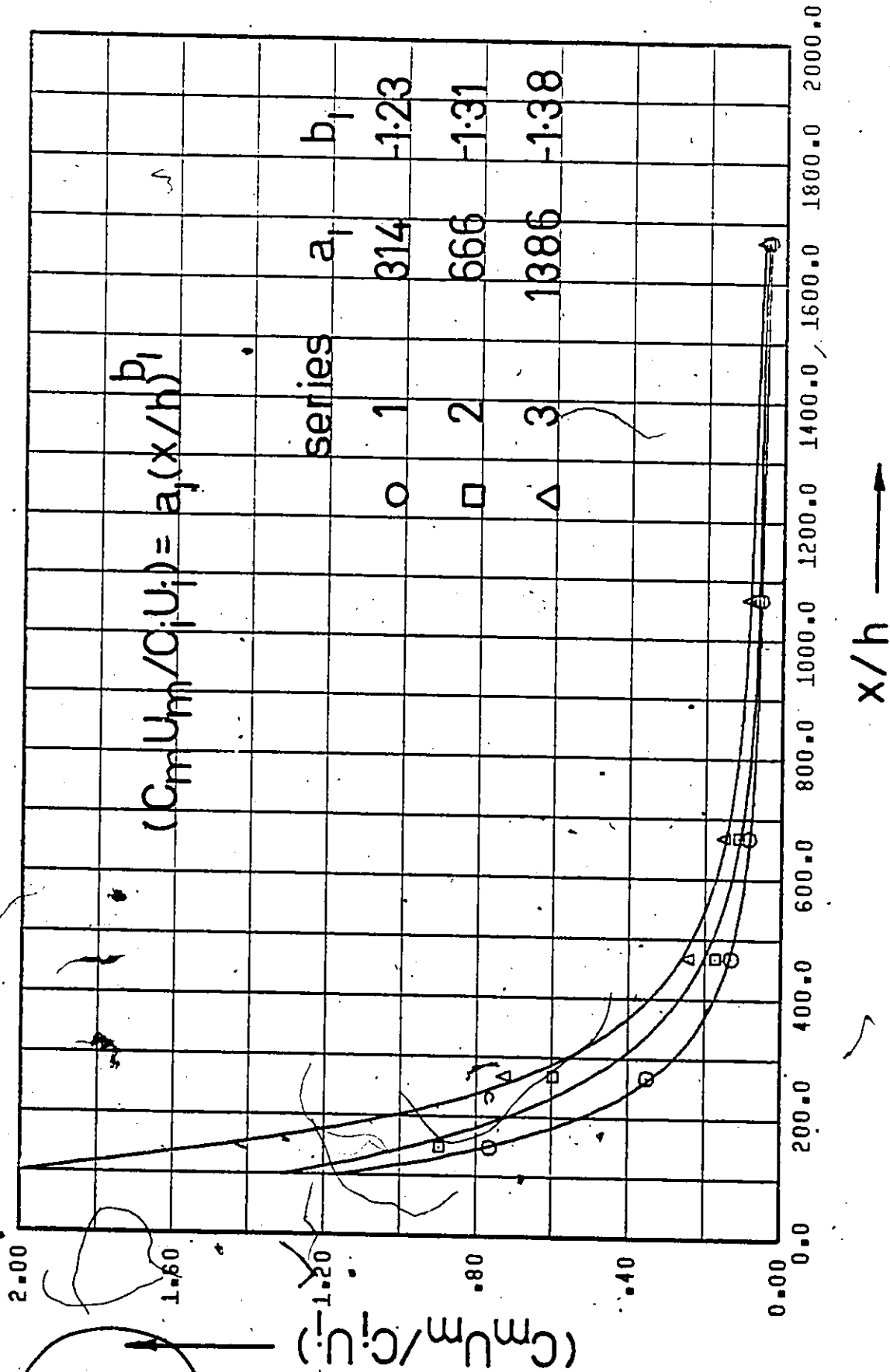


Figure 31. $\frac{C_m U_m}{C_i U_i}$ vs. $\frac{x}{h}$ (Line Source Injection - $C_i = 500$ w.p.p.m.).

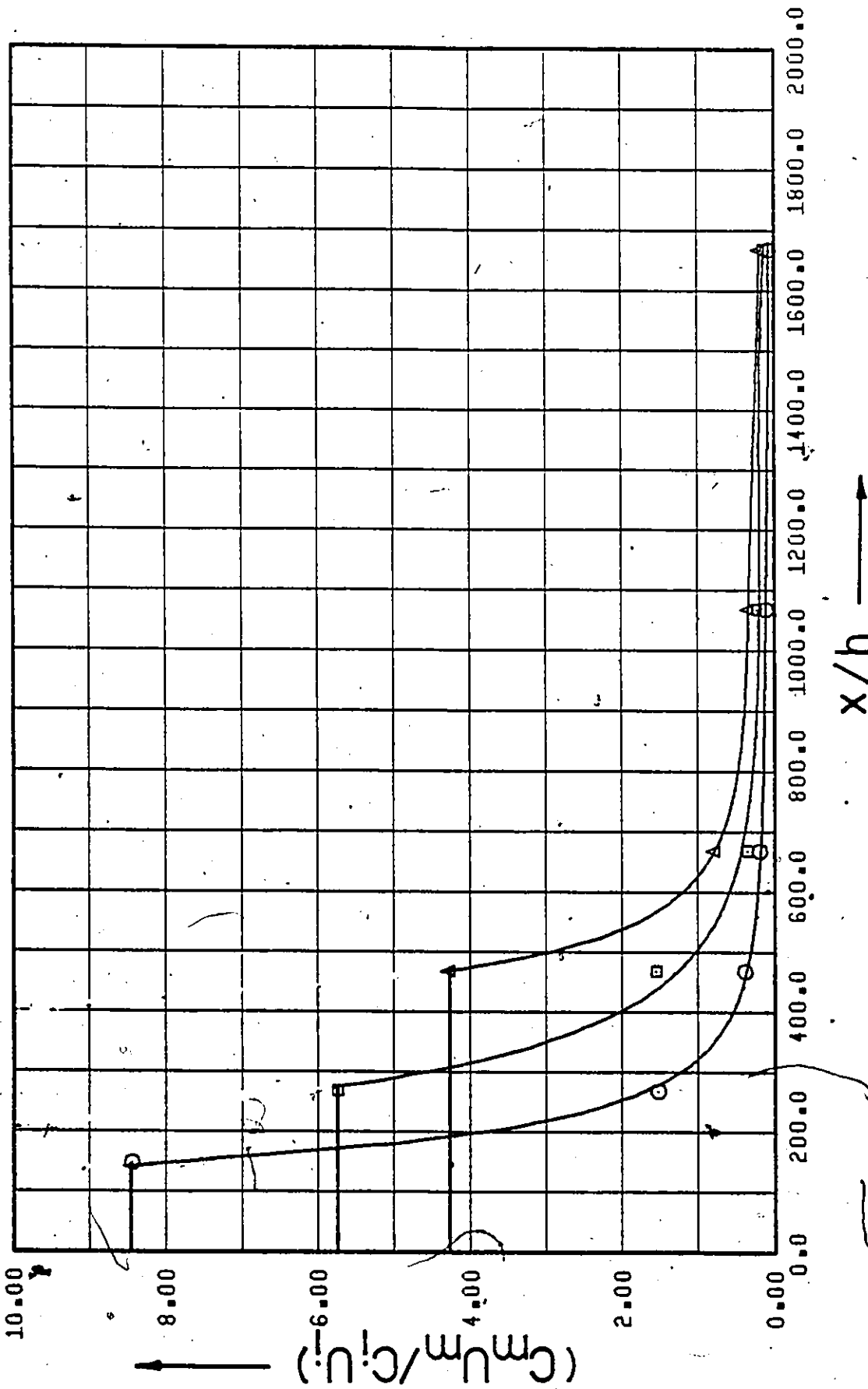
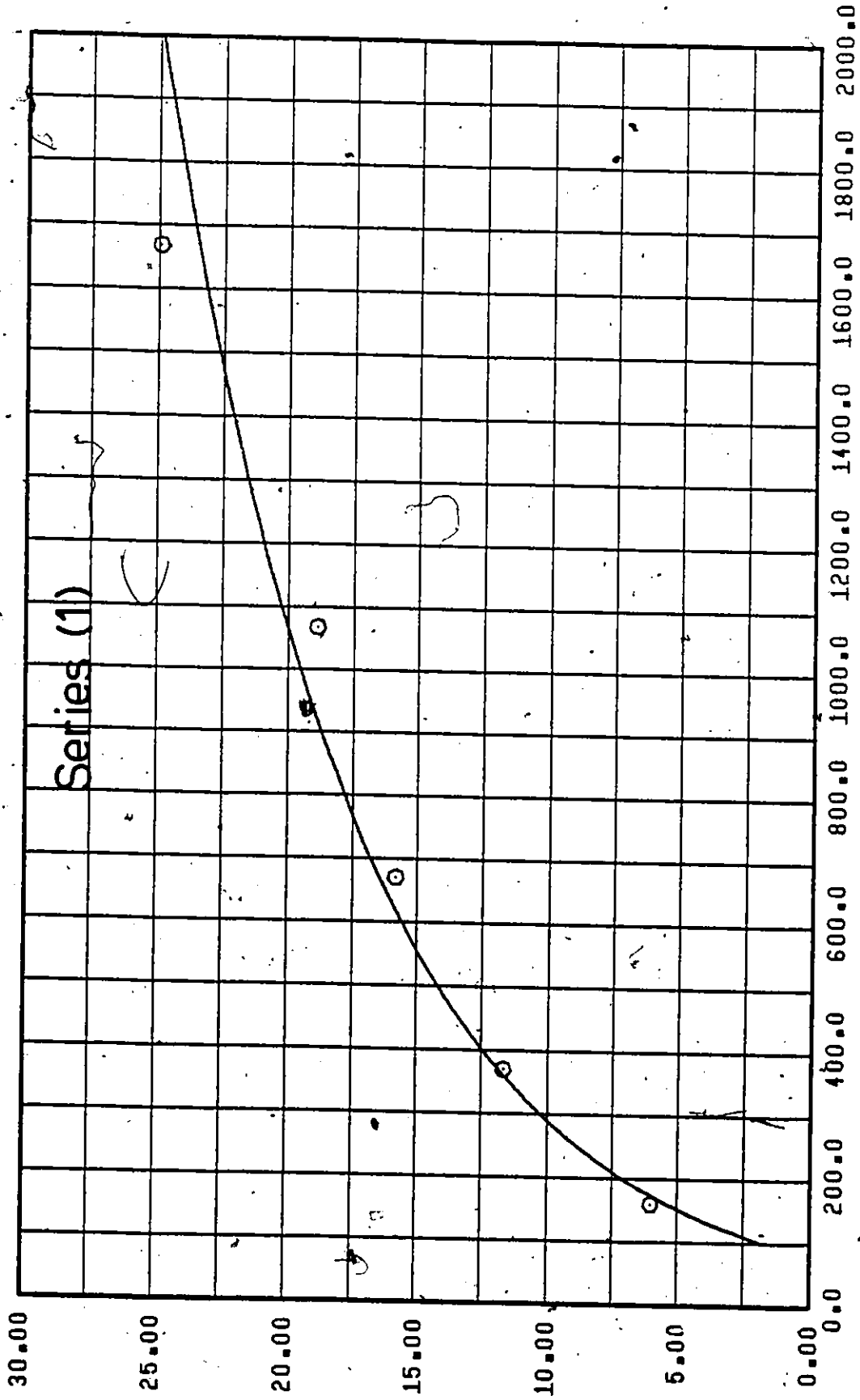


Figure 32. $\frac{C_m U_m}{C_i U_i}$ vs. $\frac{x}{h}$ (Line Source Injection- $C_i = 1000$ w.p.p.m.).



x/h

Figure 33. λ/h vs. $\frac{x}{h}$ (Line Source Injection-Water Injection),

4/h

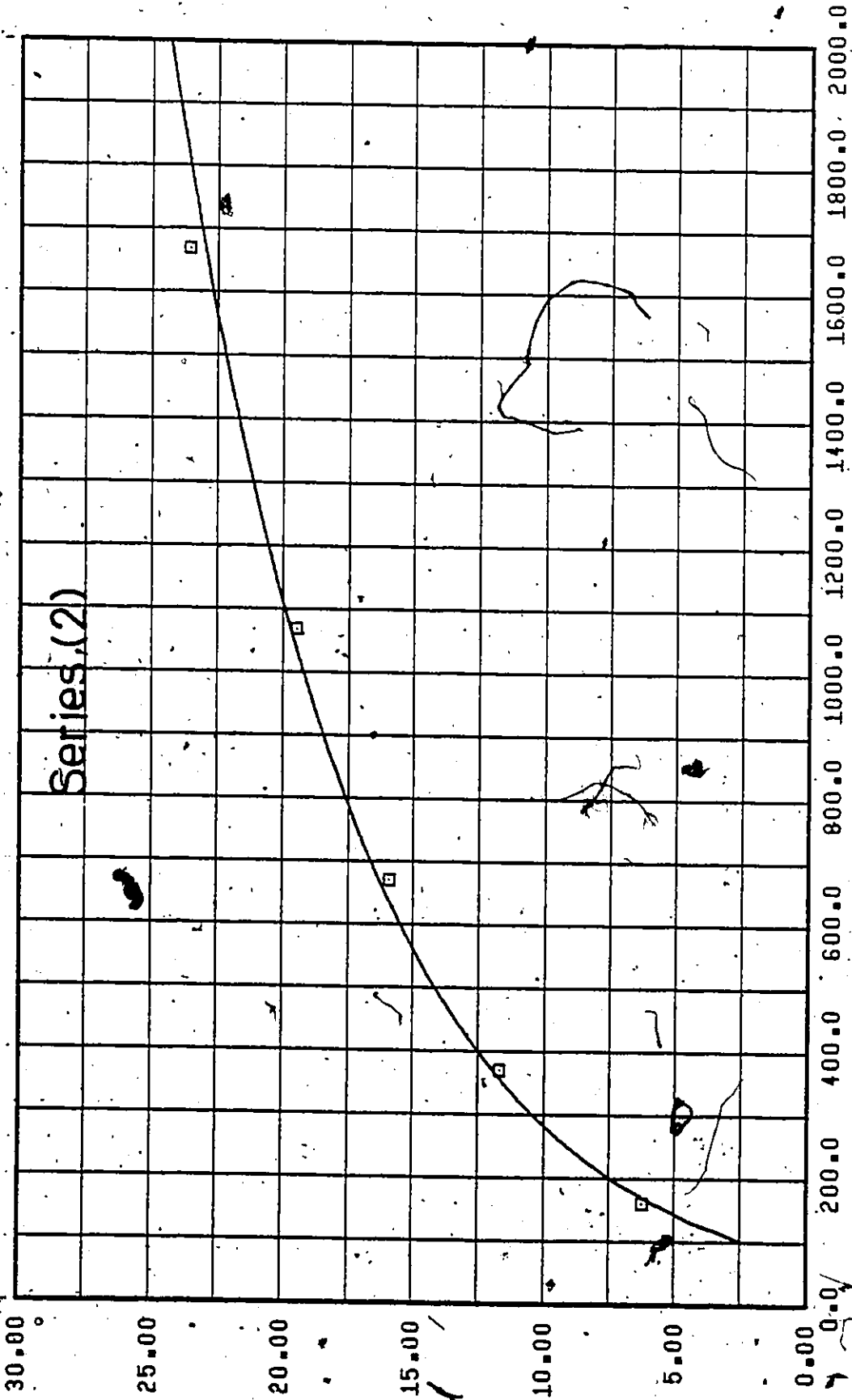
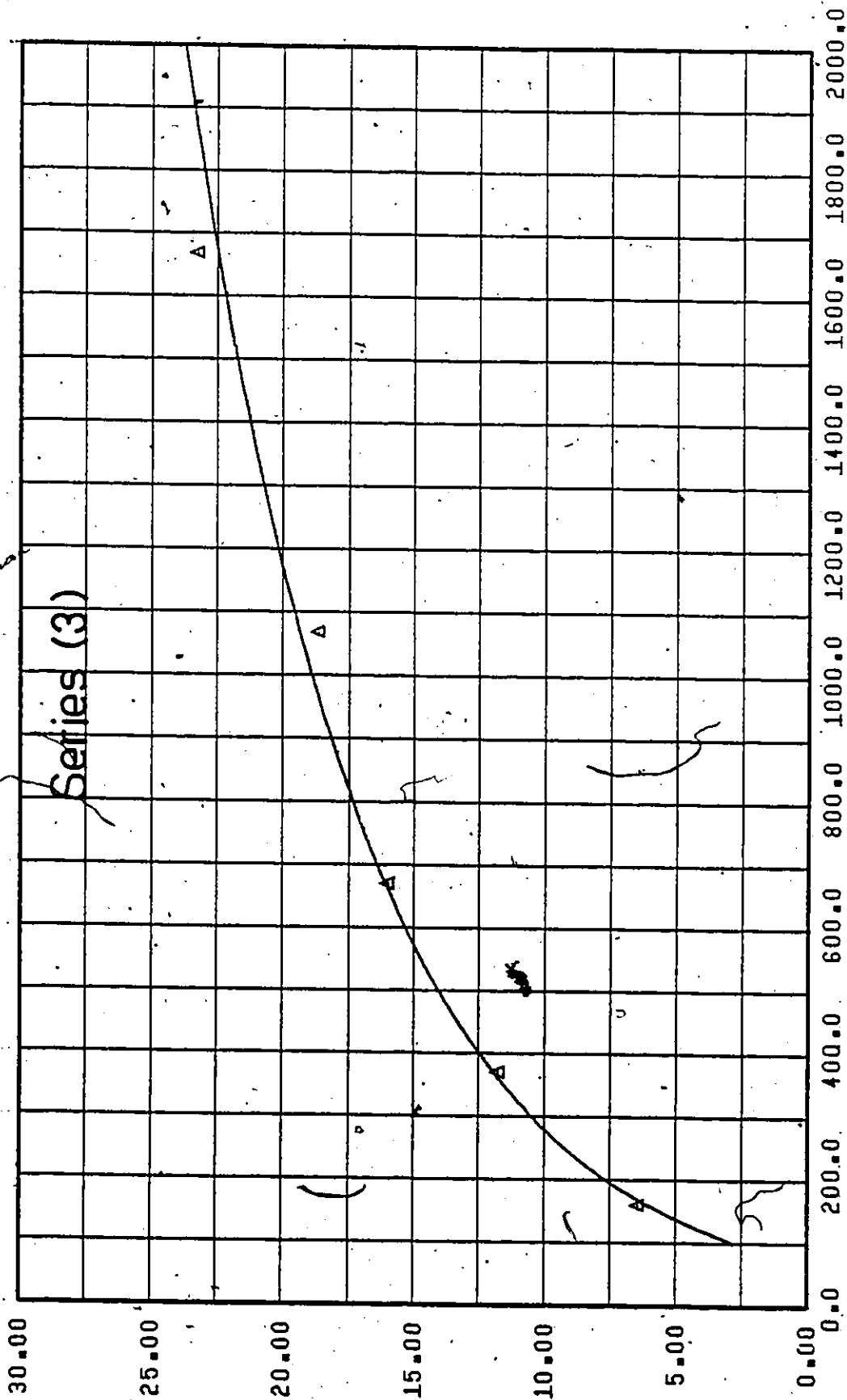


Figure 34. λ/h vs. $\frac{x}{h}$ (Line Source Injection-Water Injection).

x/h

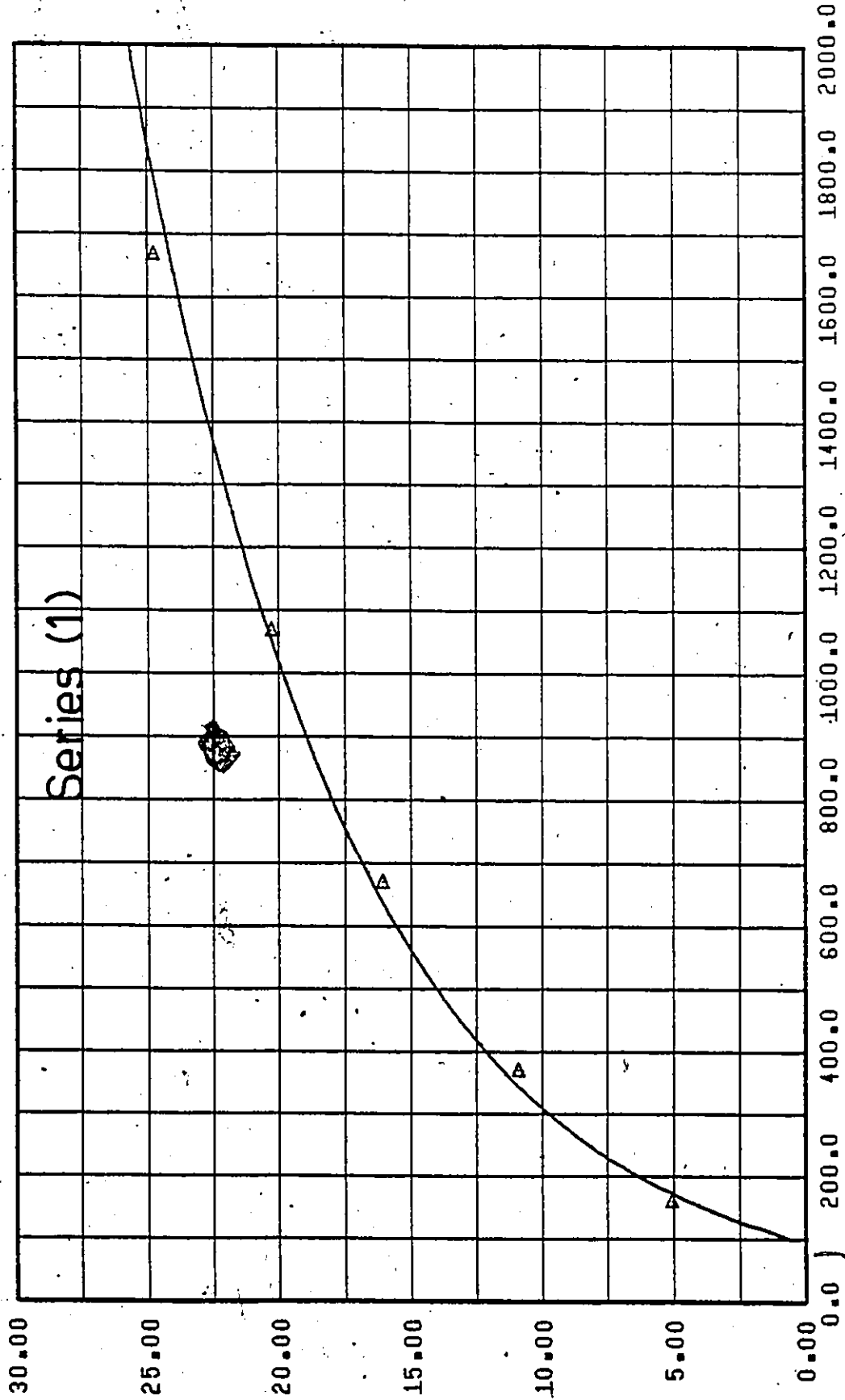
λ/h



x/h

Figure 35. λ/h vs. $\frac{x}{h}$ (Line Source Injection-Water Injection).

λ/h



λ/h

x/h

Figure 36. λ/h vs. $\frac{x}{h}$ (Line Source Injection- $C_i = 100$ w.p.p.m.).

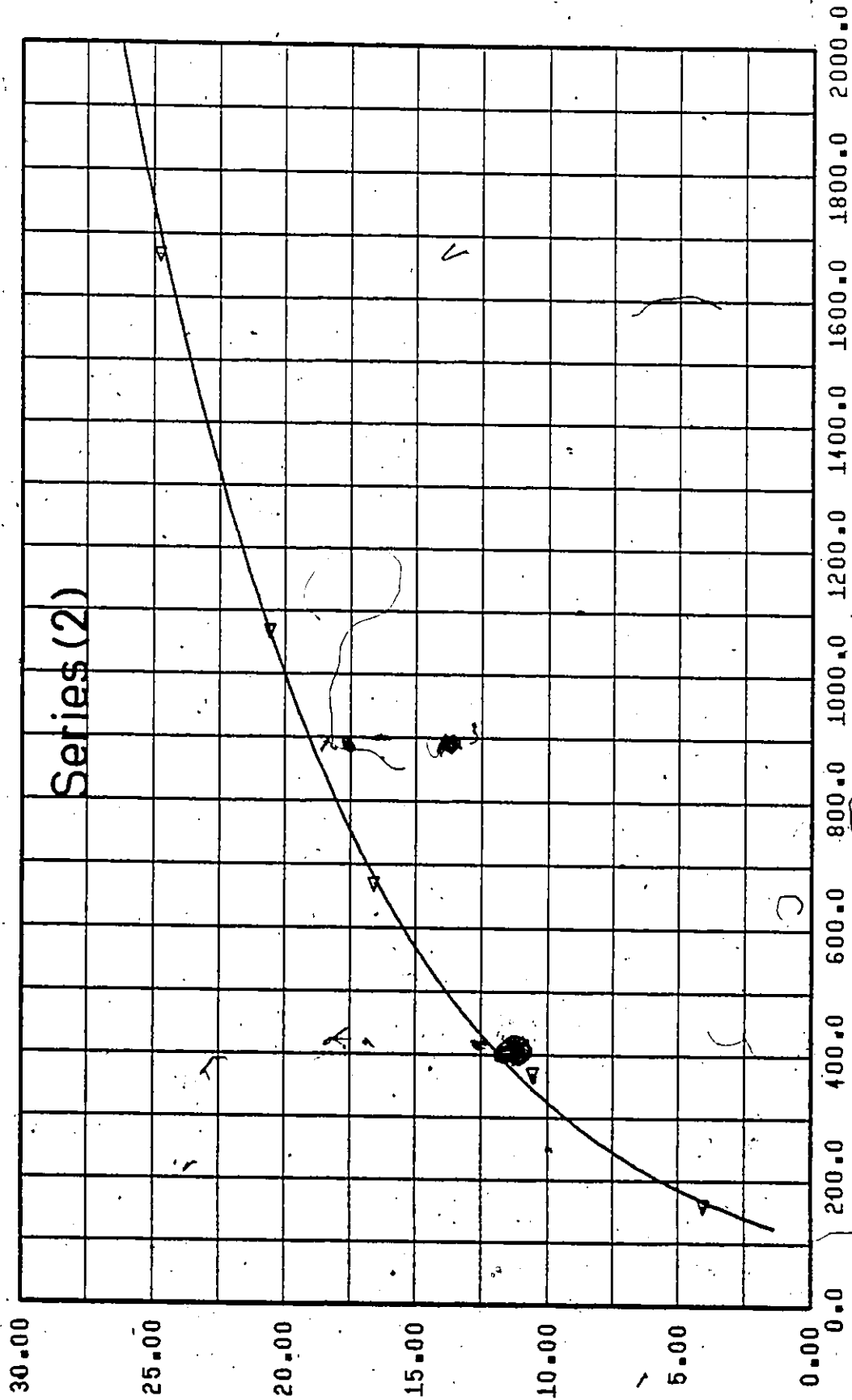


Figure 37. λ/h vs. $\frac{x}{h}$ (Line Source Injection- $C_i = 100$ w.p.p.m.).

x/h

λ/h

2

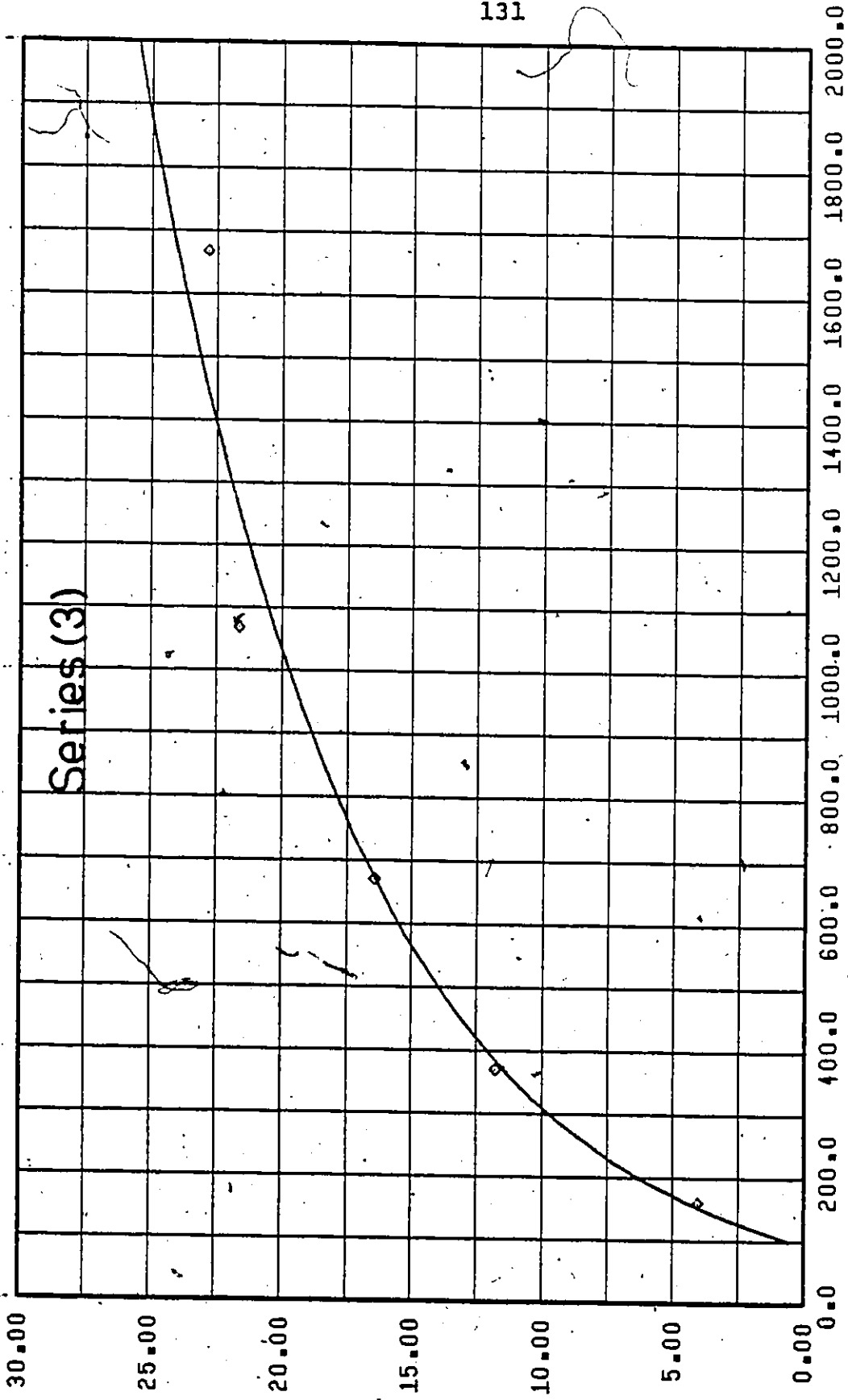


Figure 38. λ/h vs. $\frac{x}{h}$ (Line Source Injection- $C_i = 100$ w.p.f.m.).

λ/h

x/h

3

A

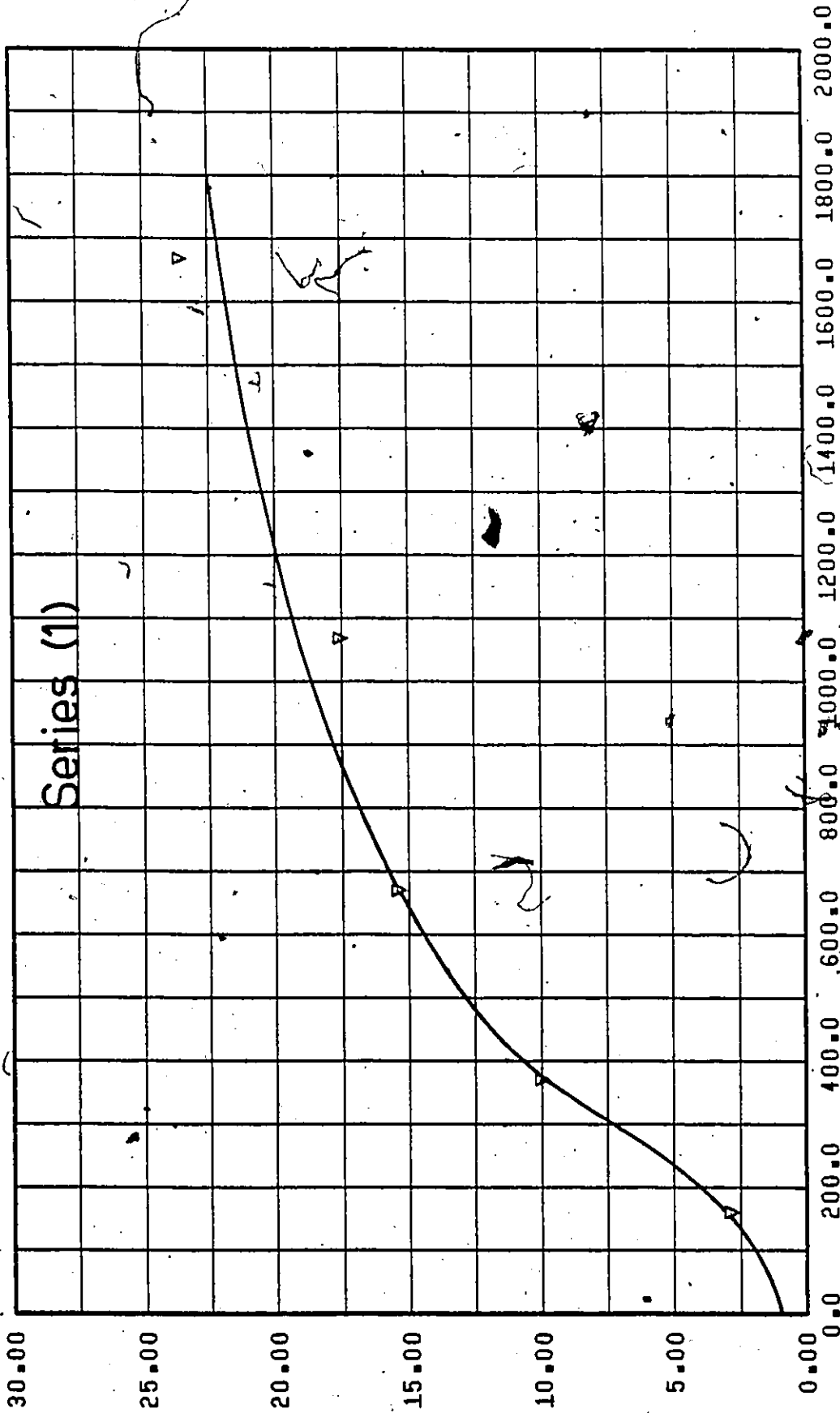


Figure 39. λ/h vs. $\frac{x}{h}$ (Line Source Injection- $C_i = 250$ w.p.p.m.).

x/h

λ/h

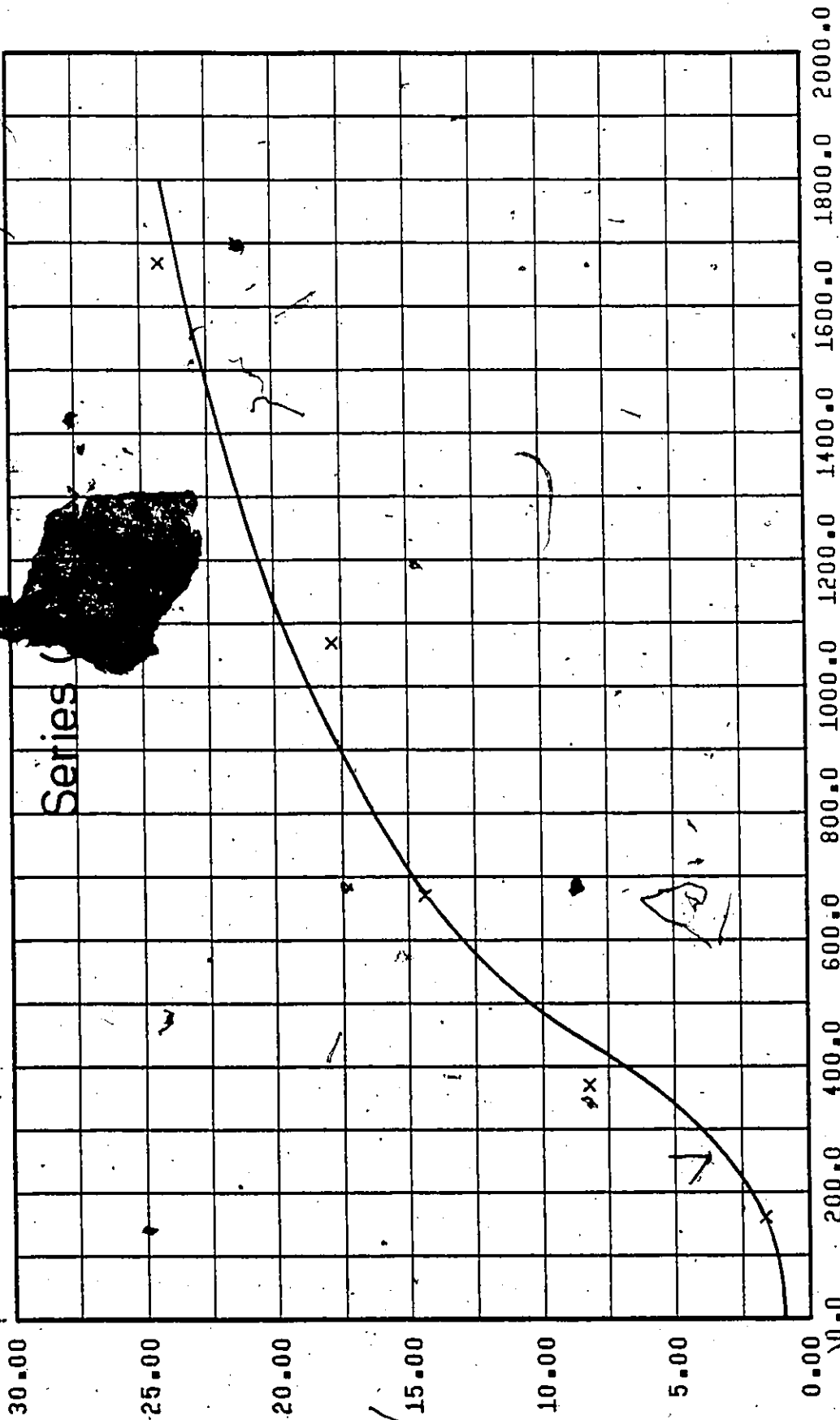


Figure 40. λ/h vs. $\frac{x}{h}$ (Line Source Injection- $C_i = 250$ w.p.p.m.).

x/h

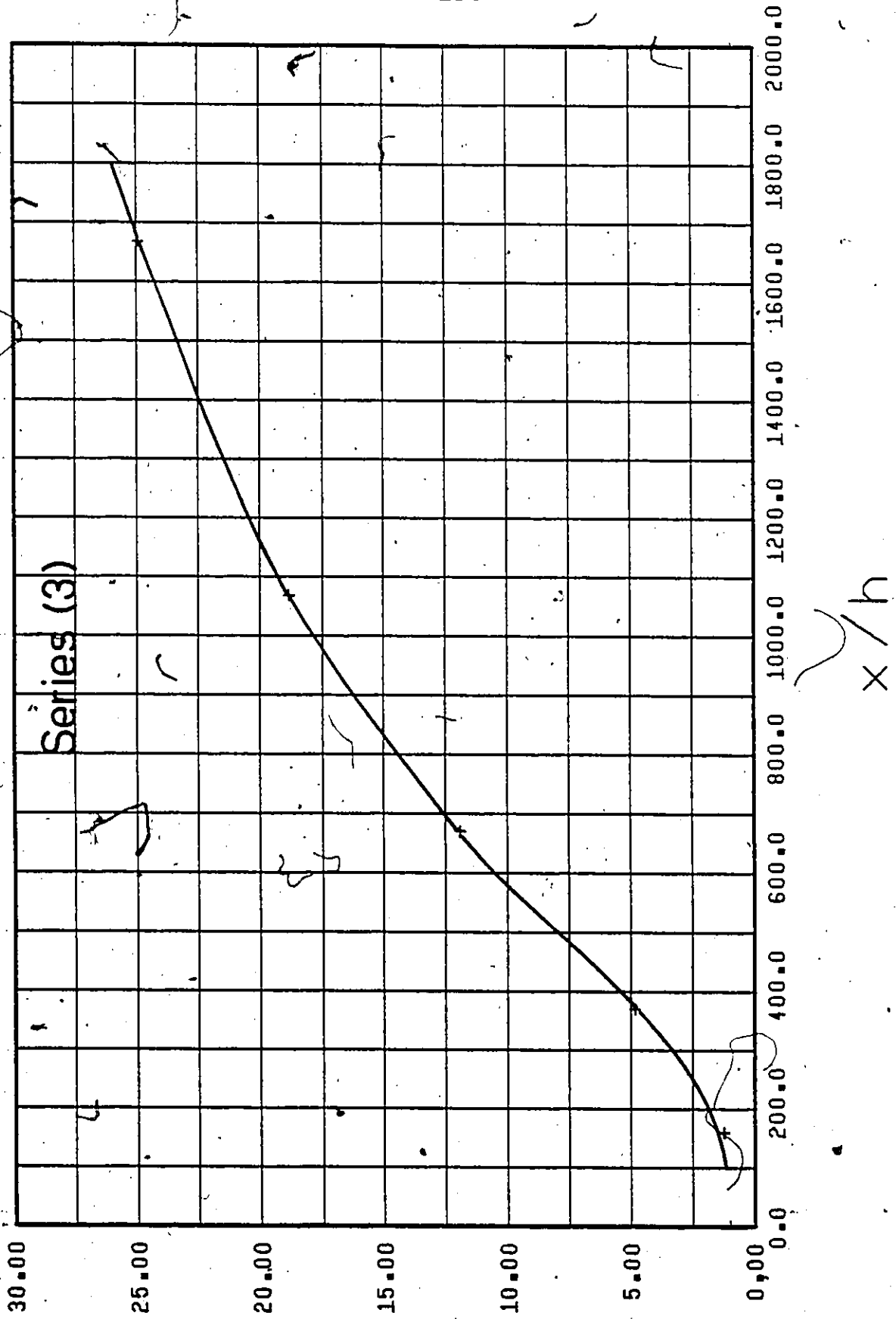


Figure 41. λ/h vs. $\frac{x}{h}$ (Line Source Injection- $C_i = 250$ w.p.p.m.).

λ/h

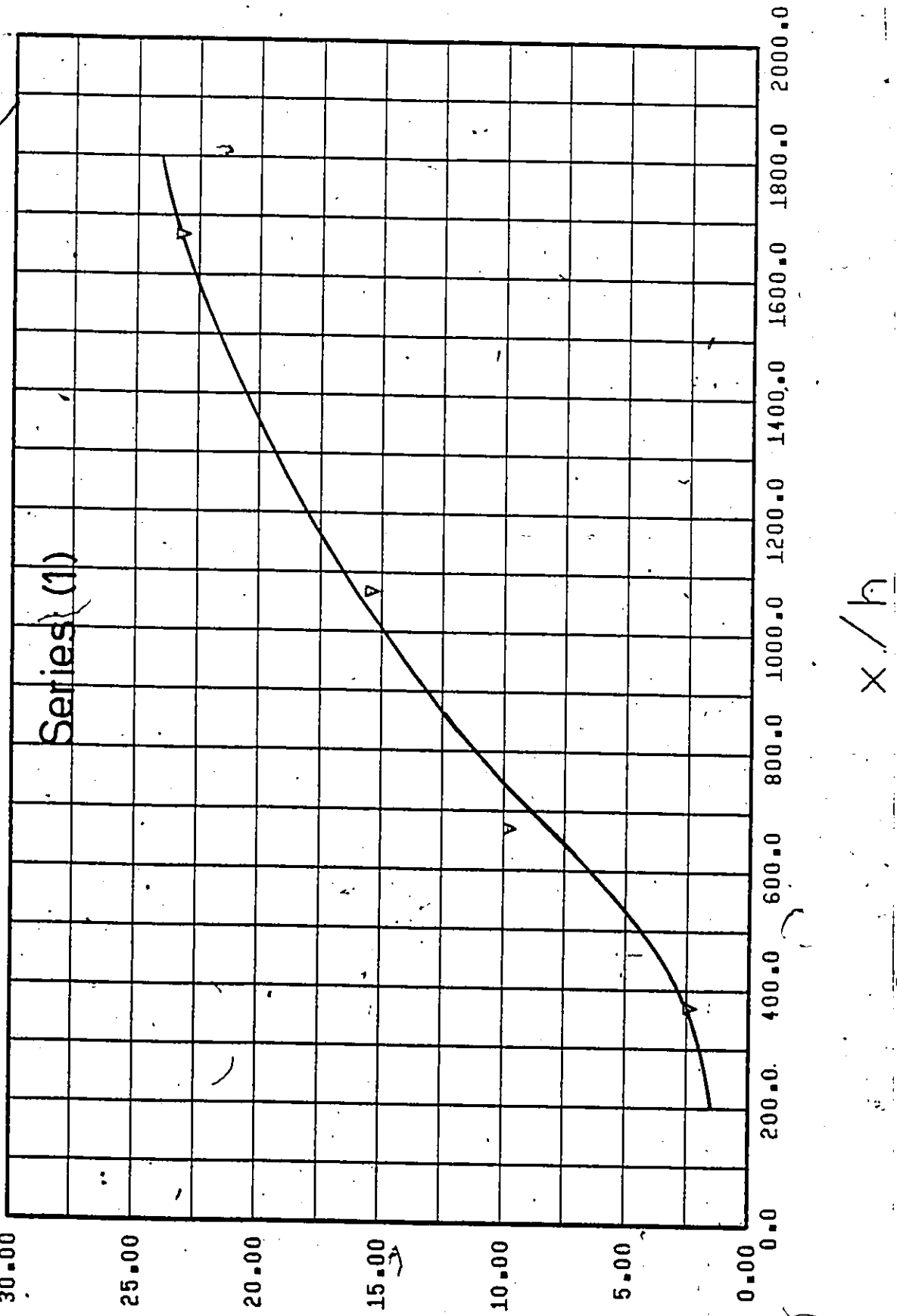
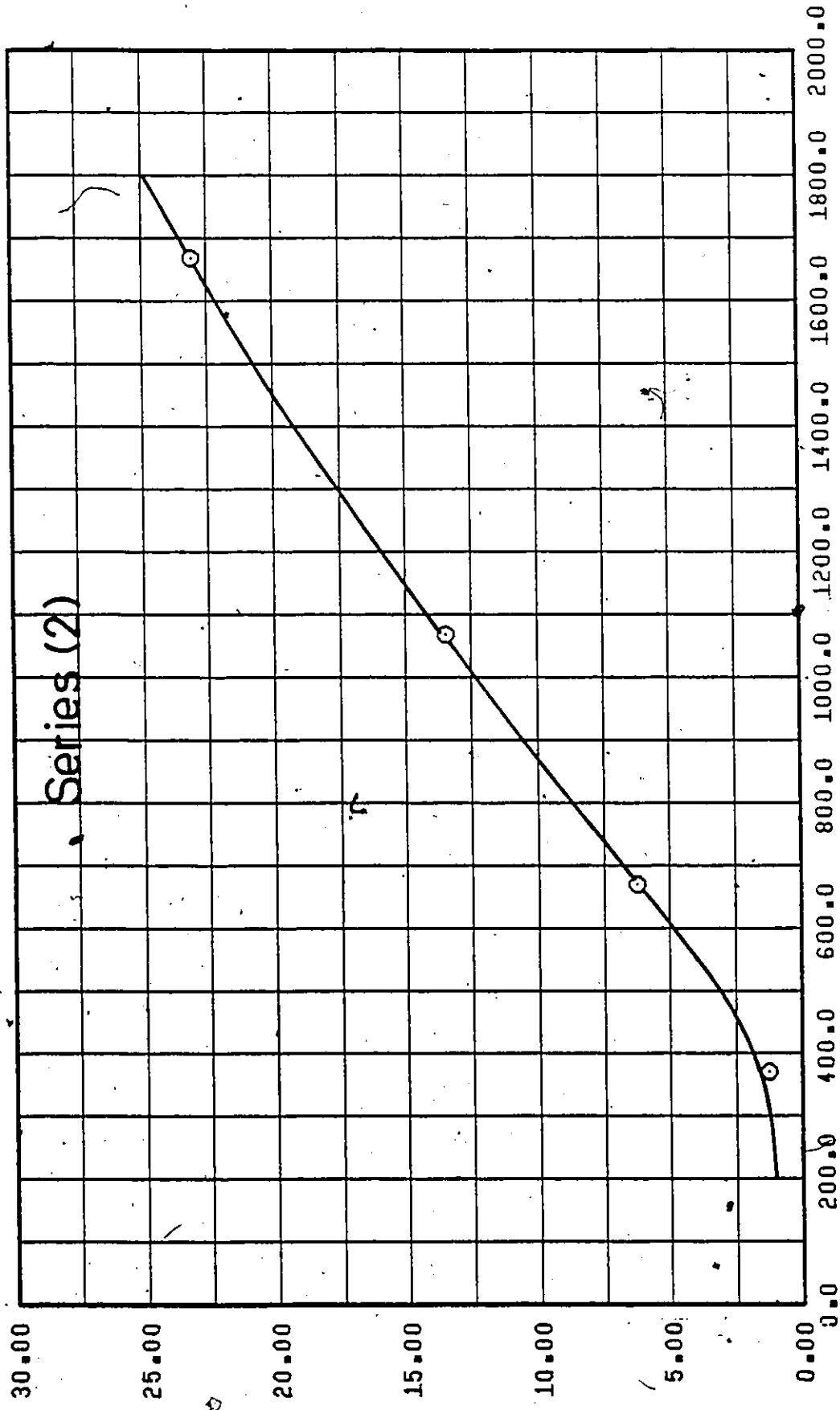


Figure 42. λ/h vs. $\frac{x}{h}$ (Line Source Injection- $C_i = 500$ w.p.p.m.).

14/12



Series (2)

x/h

Figure 43. λ/h vs. x/h (Line Source Injection- $C_i = 500$ p.p.m.).

lambda/h

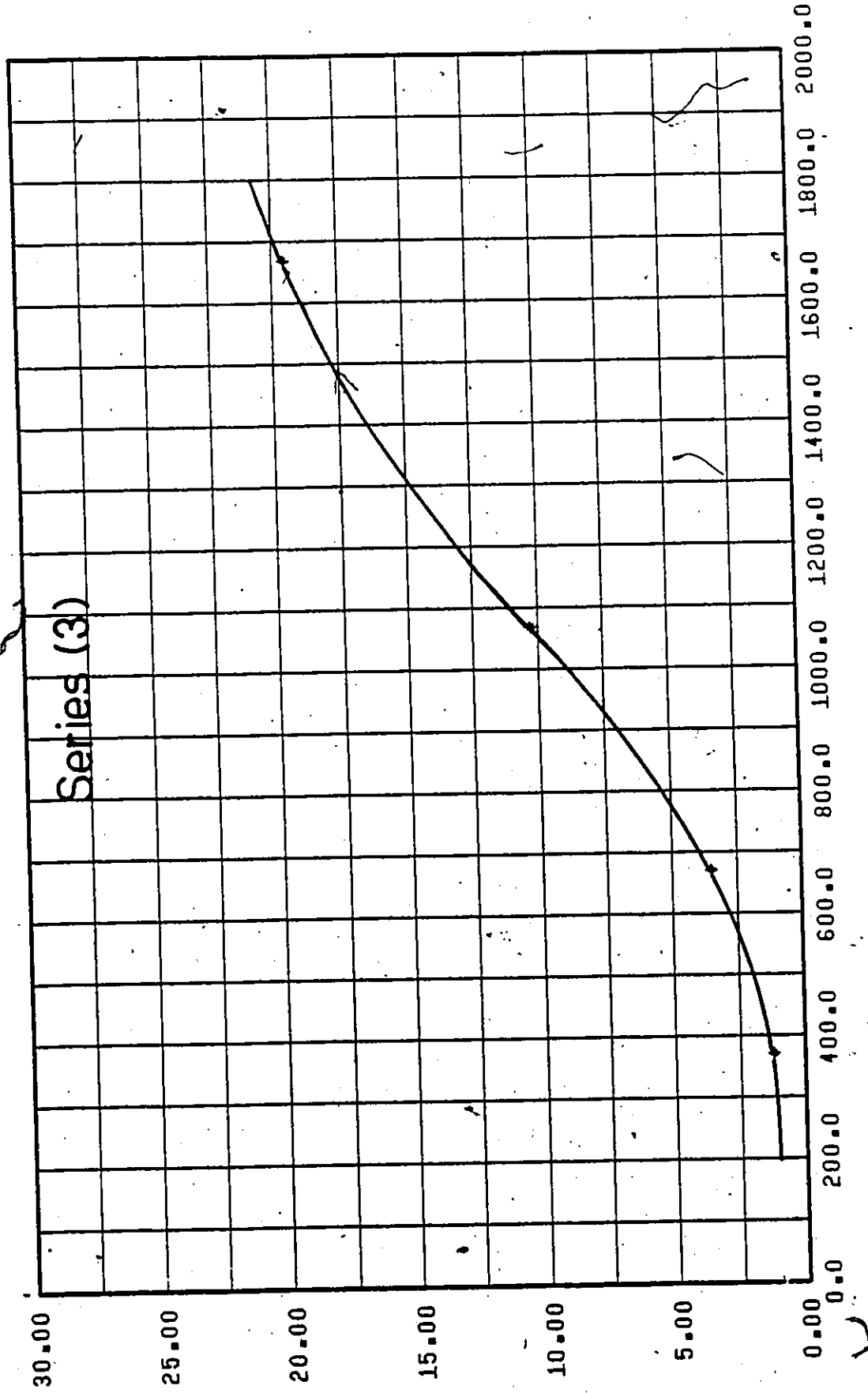


Figure 44. λ/h vs. $\frac{x}{h}$ (Line Source Injection- $C_i = 500$ w.p.p.m.).

λ/h

x/h

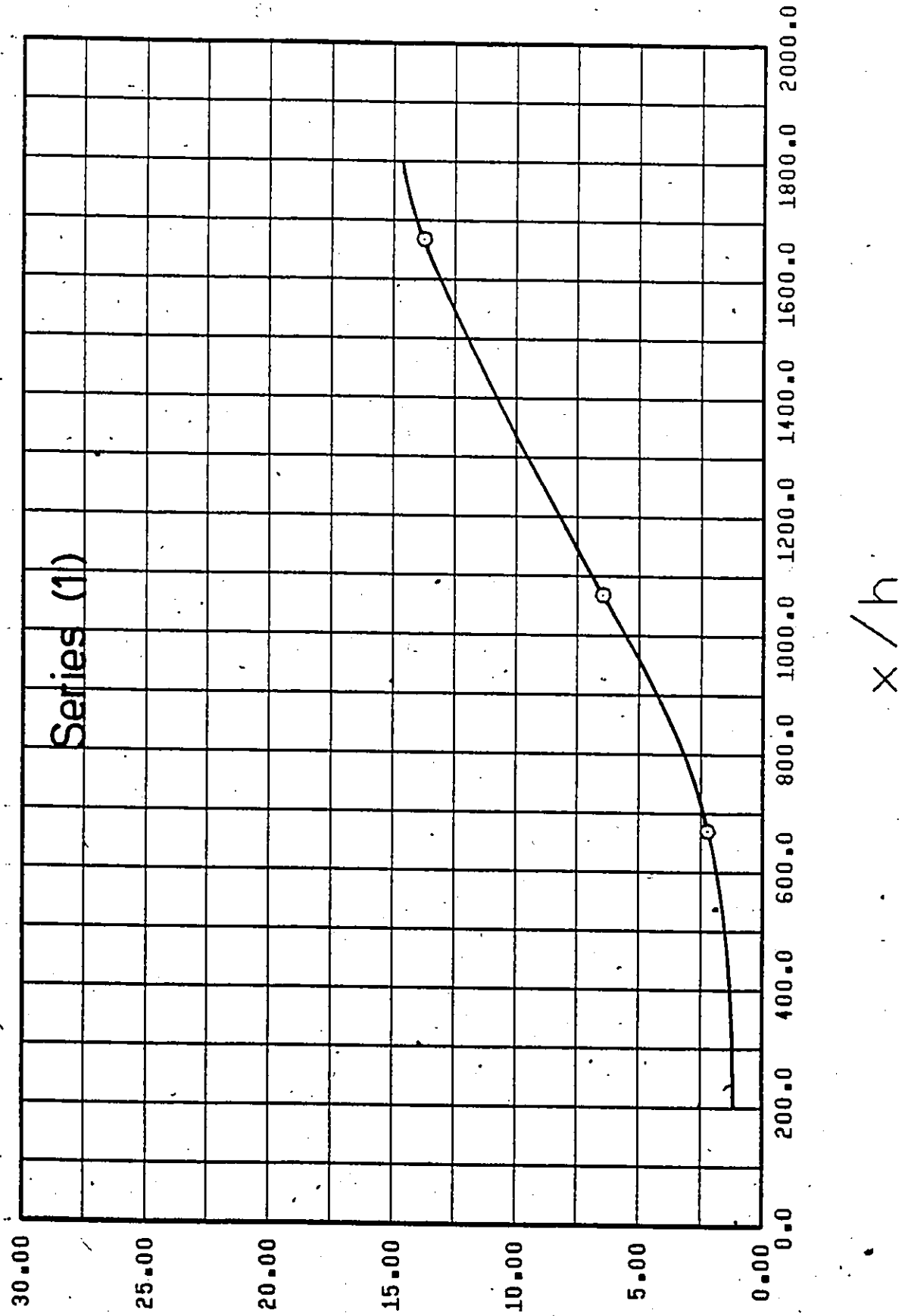
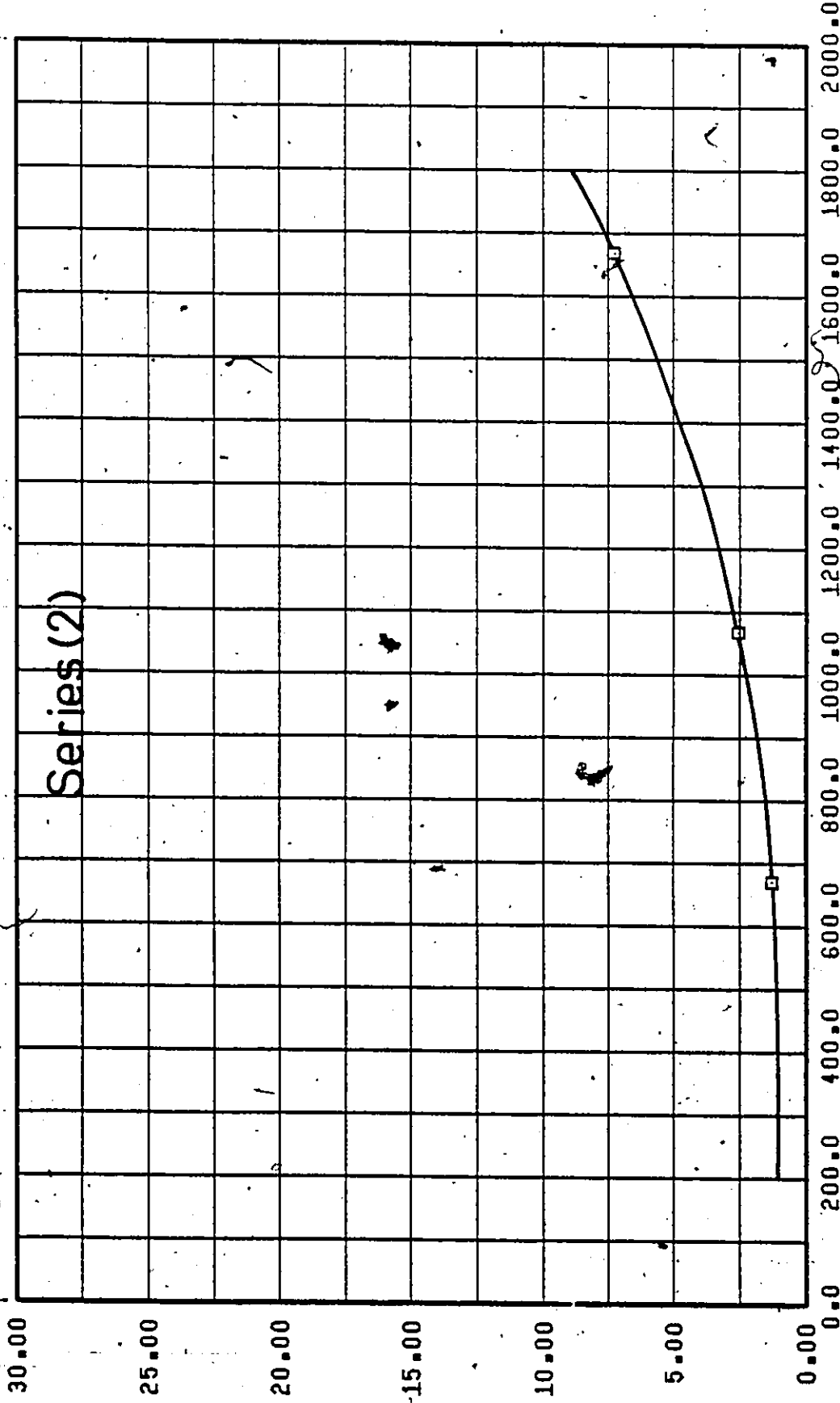


Figure 45. λ/h vs. $\frac{x}{h}$ (Line Source Injection- $C_i = 1000$ w.p.p.m.).

λ/h

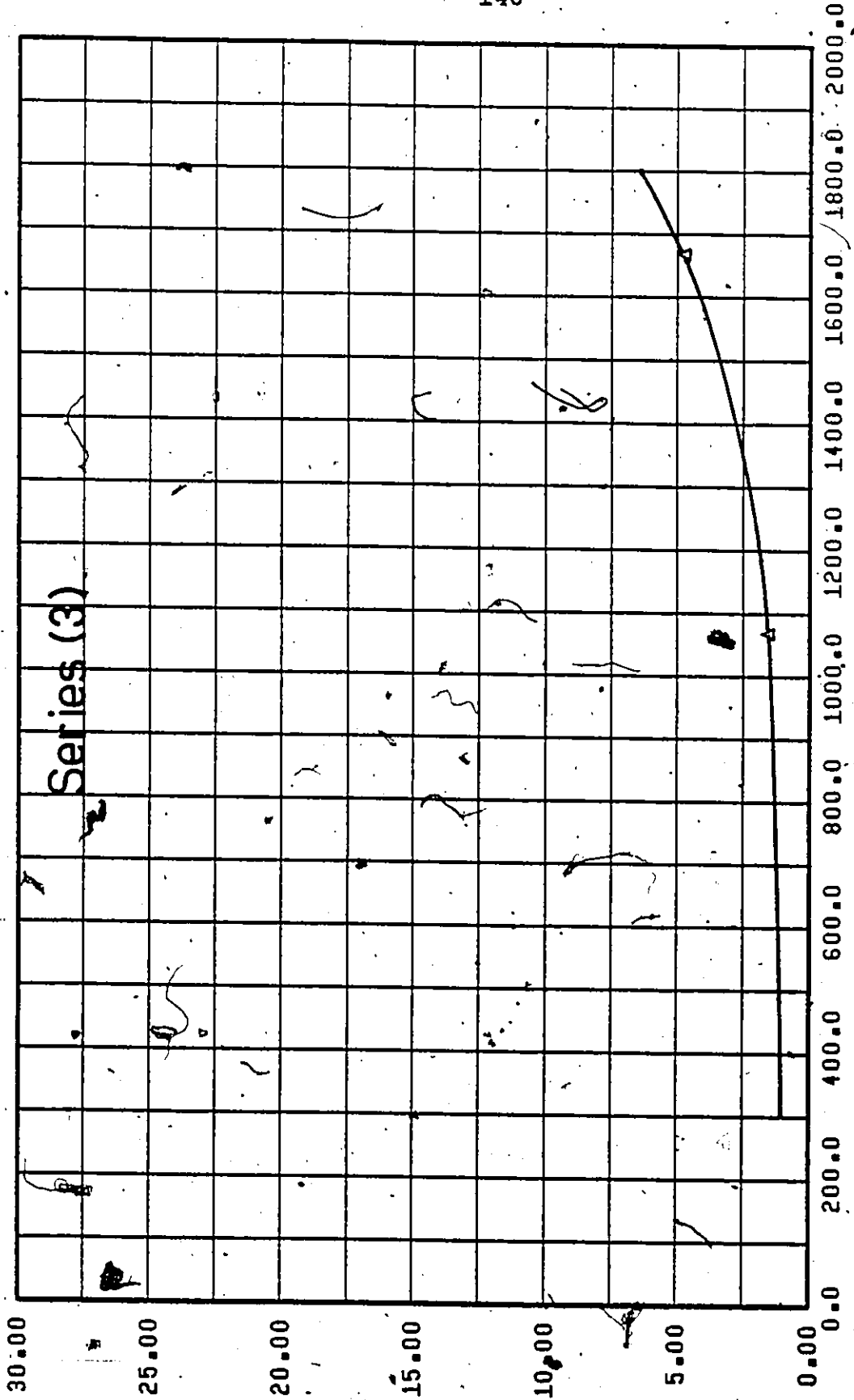
x/h



λ/h

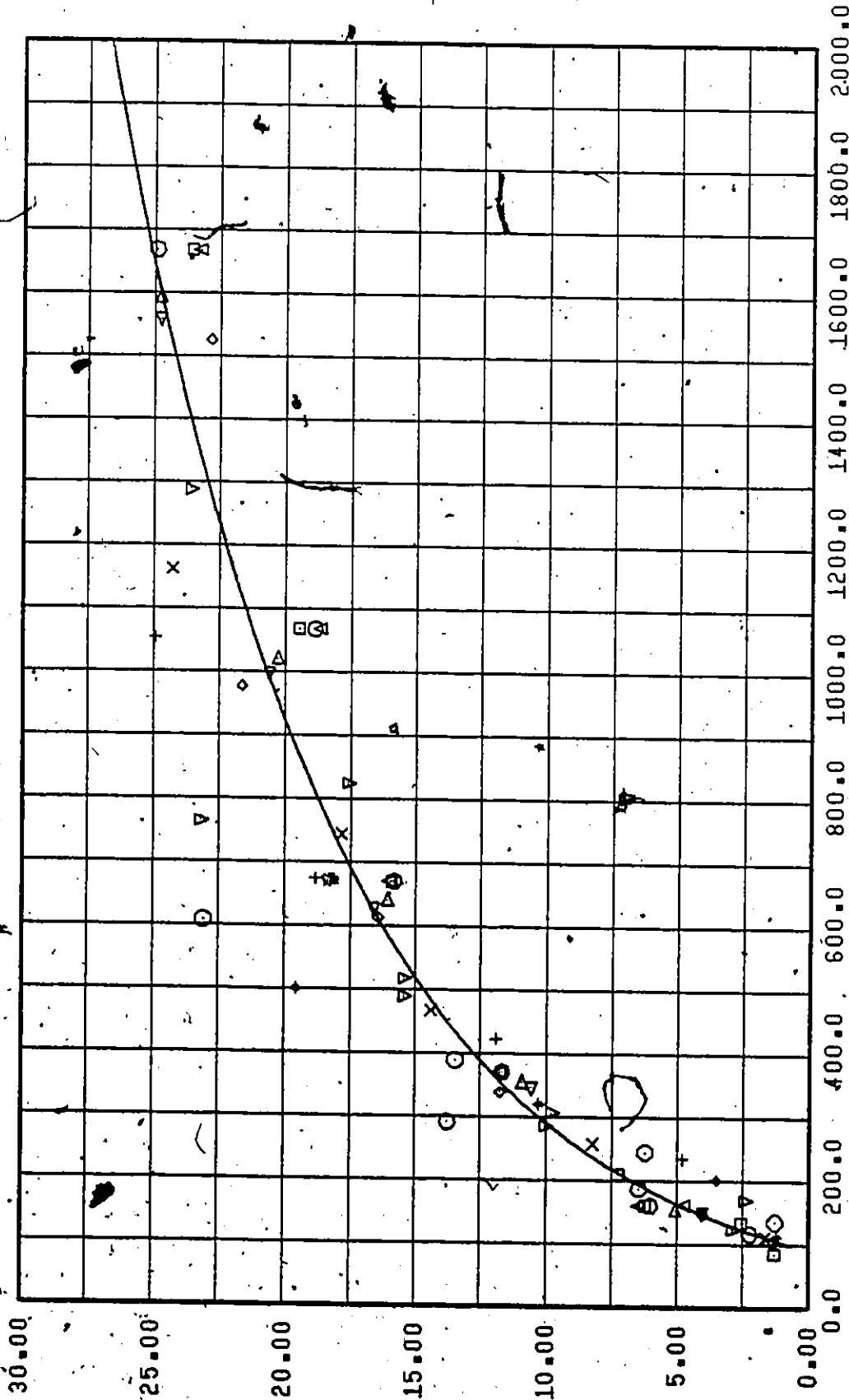
Figure 46. λ/h vs. $\frac{x}{h}$ (Line Source Injection- $C_i = 1000$ w.p.p.m.).

λ/h



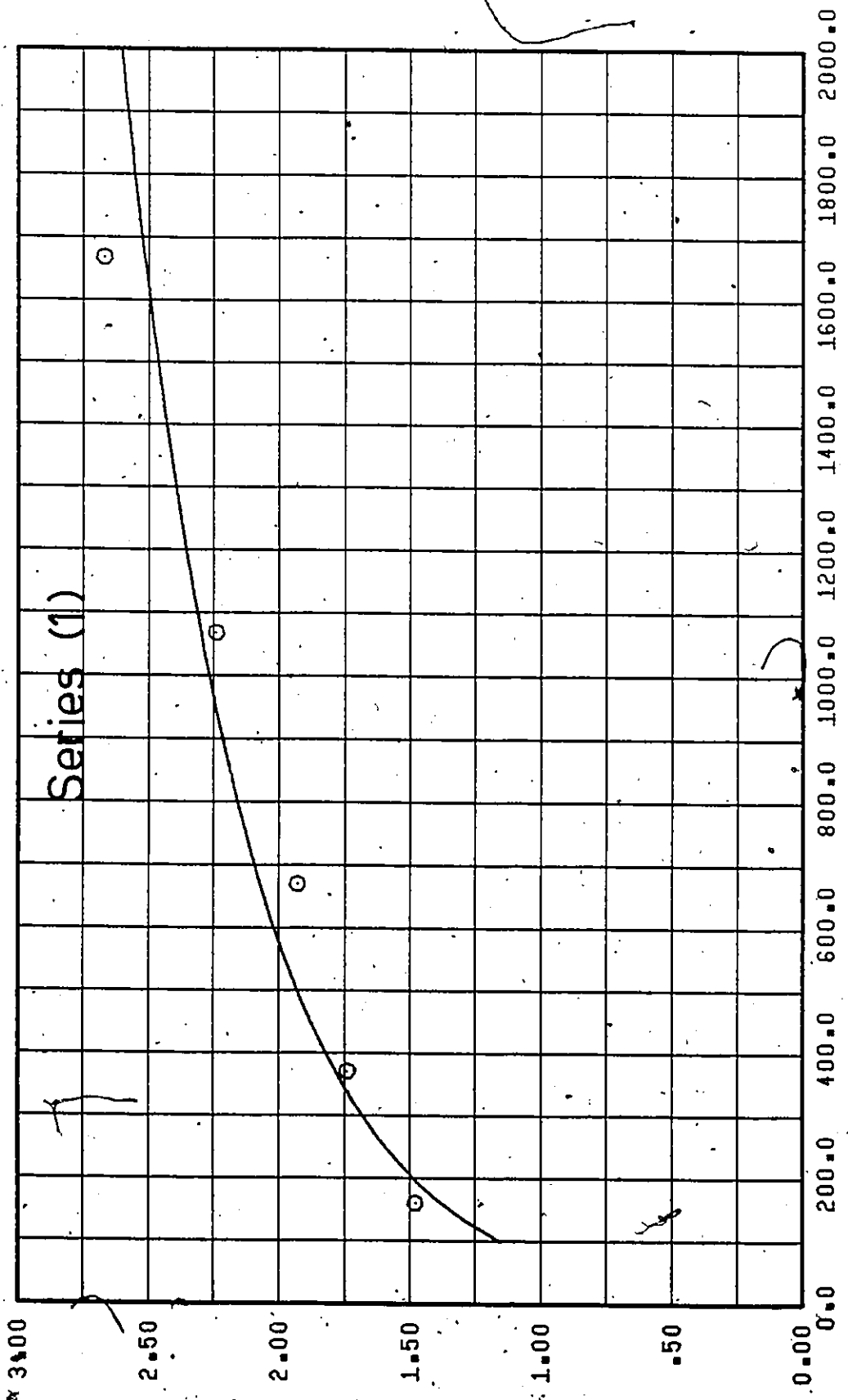
x/h

Figure 47. λ/h vs. $\frac{x}{h}$ (Line Source Injection- $C_i = 1000$ w.p.p.m.).



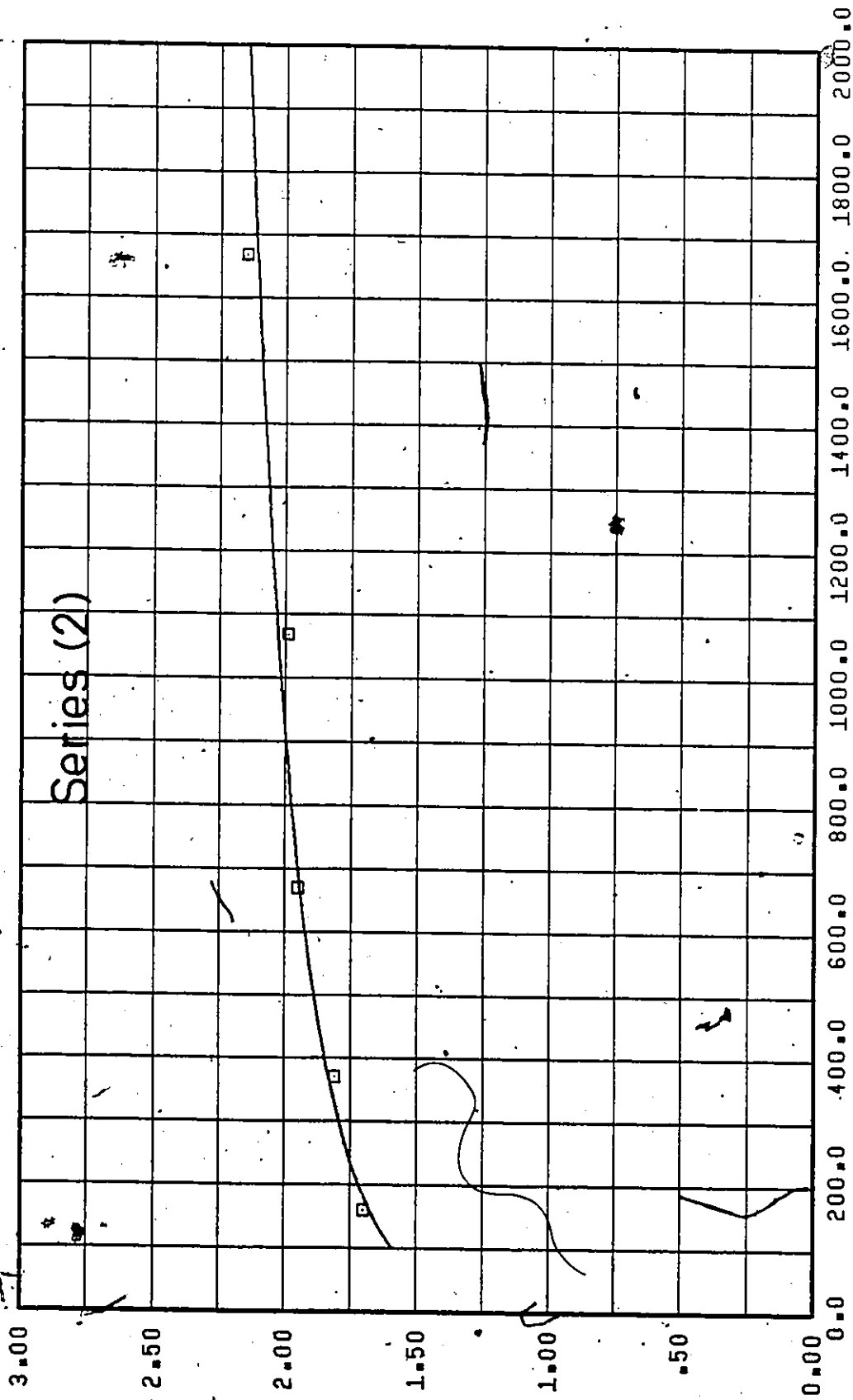
$$((x/h)/(1 + 40(U_p/U_m)C_i))$$

Figure 48. Generalized Non-dimensional Diffusion Boundary Layer Thickness Profile (Line Source Injection).



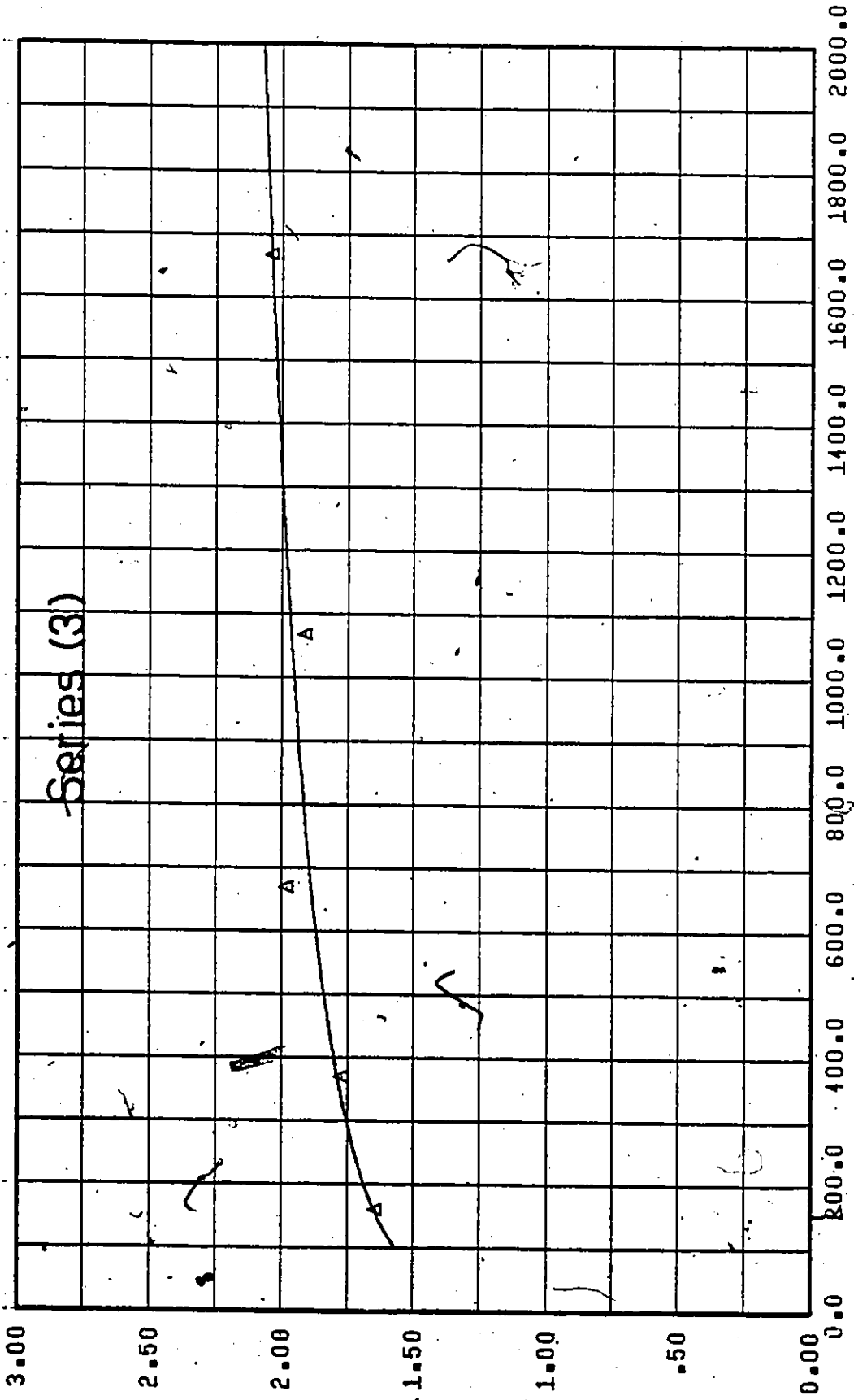
x/h

Figure 49. a vs. $\frac{x}{h}$ (Line Source Injection-Water Injection).



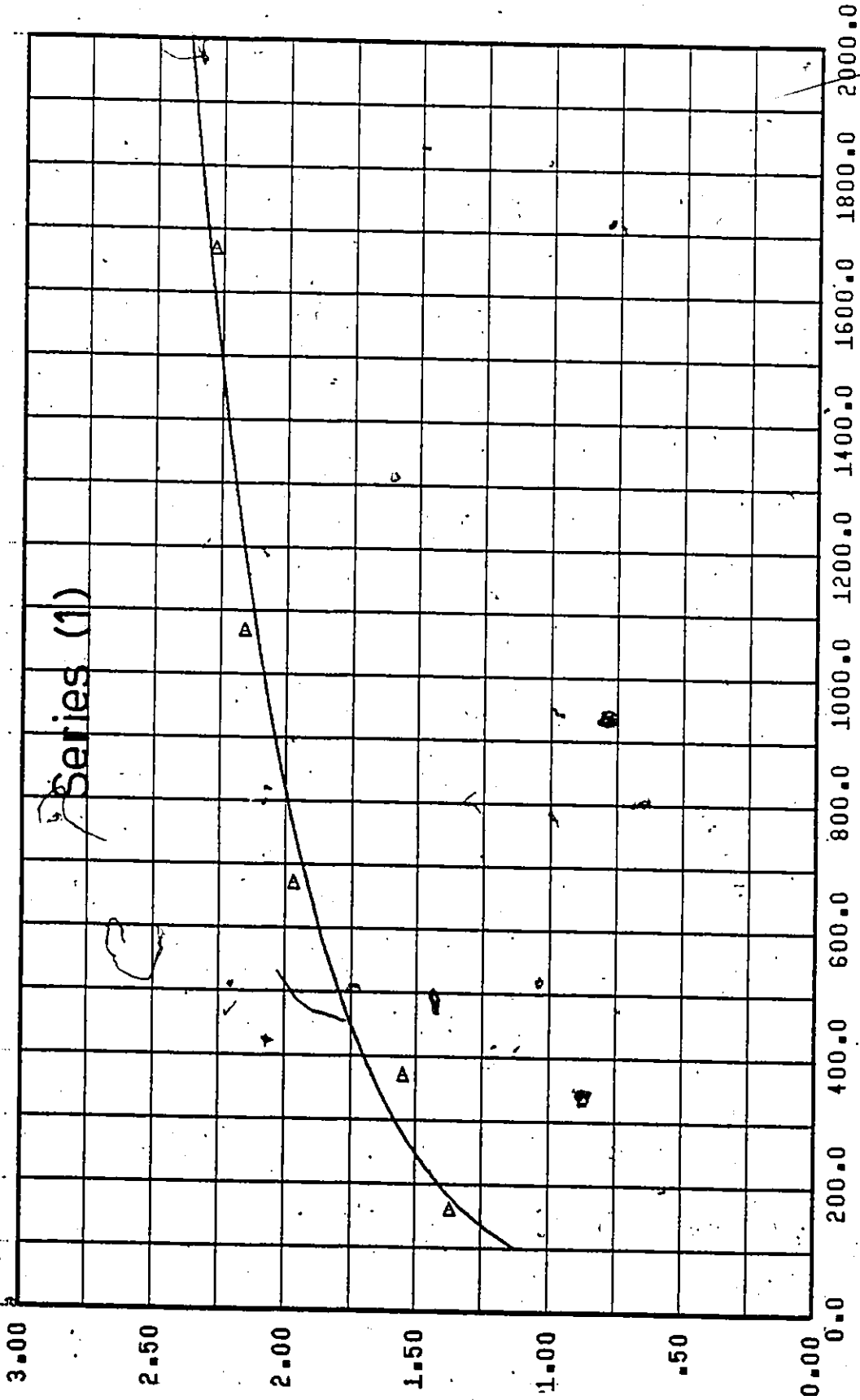
x/h

Figure 50. a vs. $\frac{x}{h}$ (Line Source Injection-Water Injection).



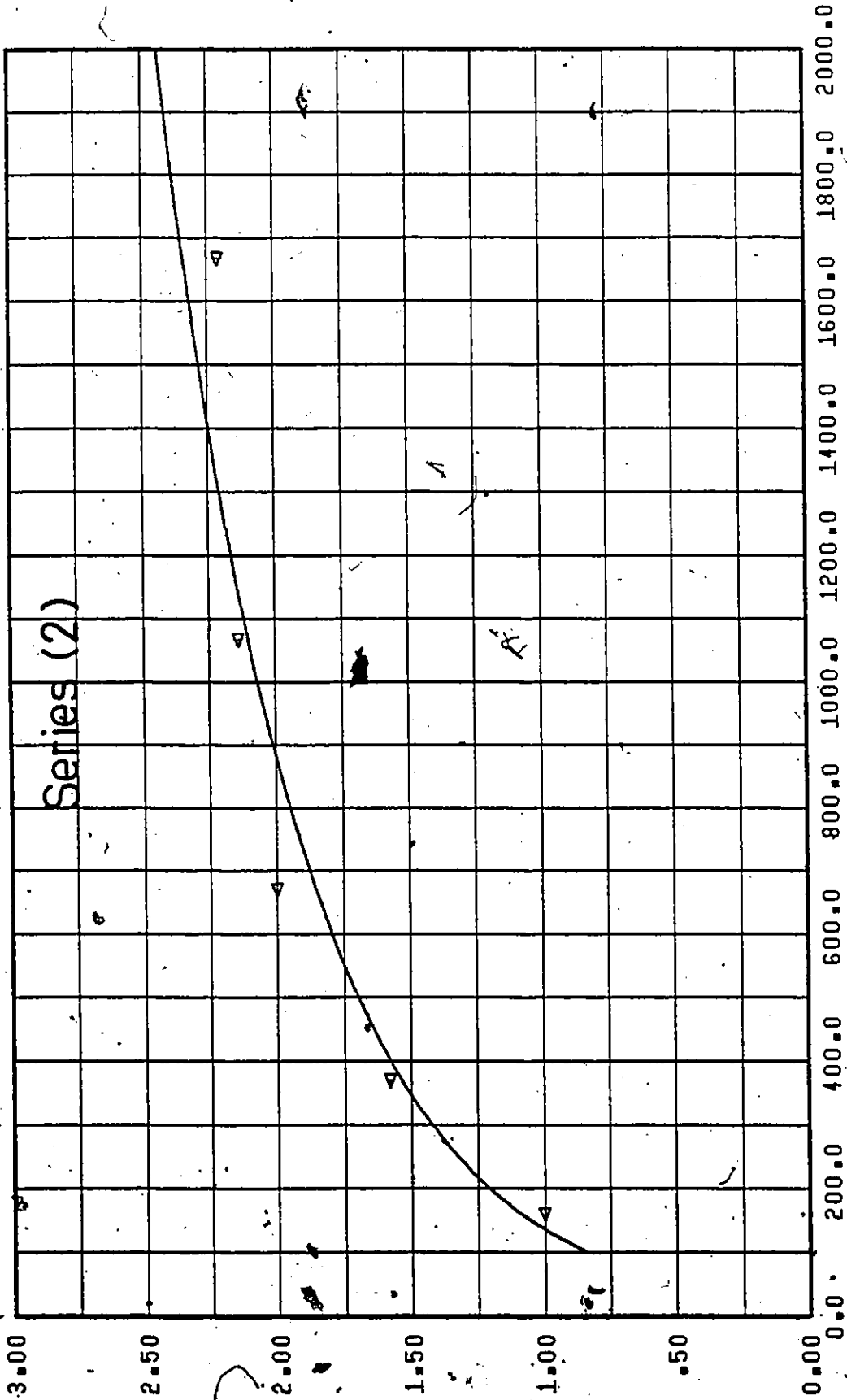
x/h

Figure 51. α vs. $\frac{x}{h}$ (Line Source Injection-Water Injection).



x/h

Figure 52. \bar{x} vs. $\frac{x}{h}$ (Line Source Injection- $C_1 = 100$ w.p.p.m.).



x/h

Figure 53. a vs. $\frac{x}{h}$ (Line Source Injection- $C_i = 100$ w.p.p.m.).

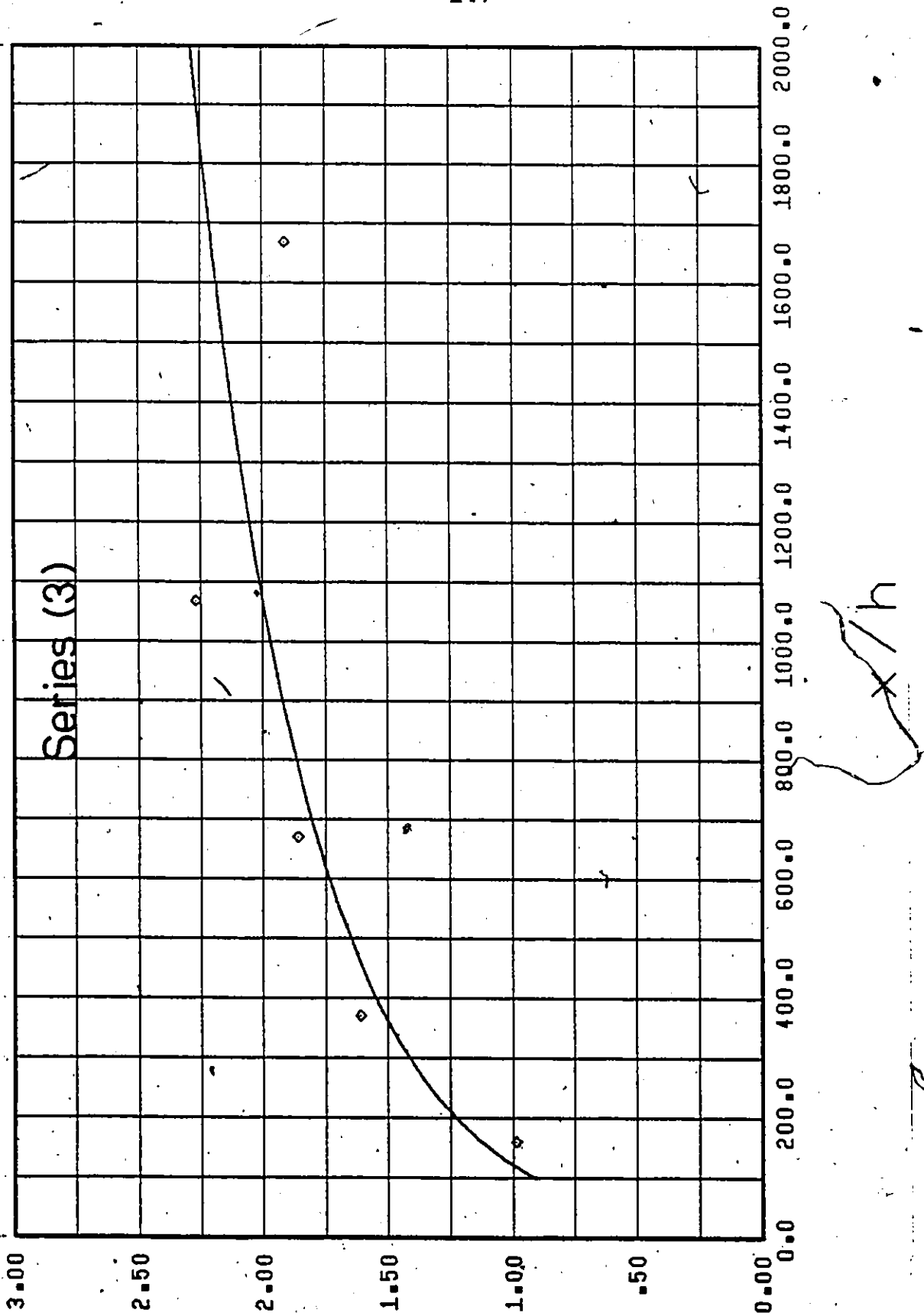


Figure 54. a vs. $\frac{x}{h}$ (Line Source Injection- $C_i = 100$ w.p.p.m.).

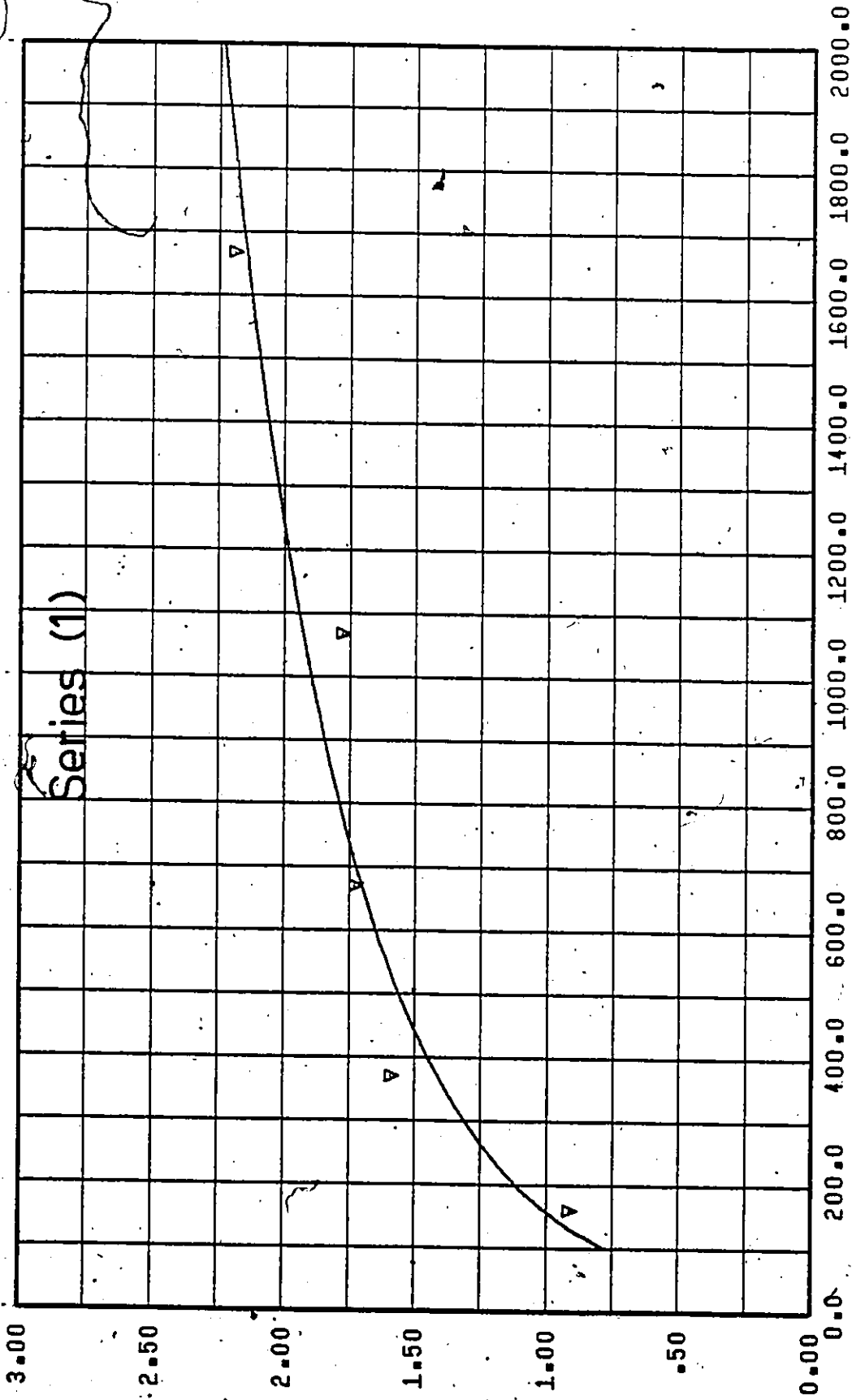

 x/h

Figure 55. a vs. $\frac{x}{h}$ (Line Source Injection- $C_i = 250$ w.p.p.m.).

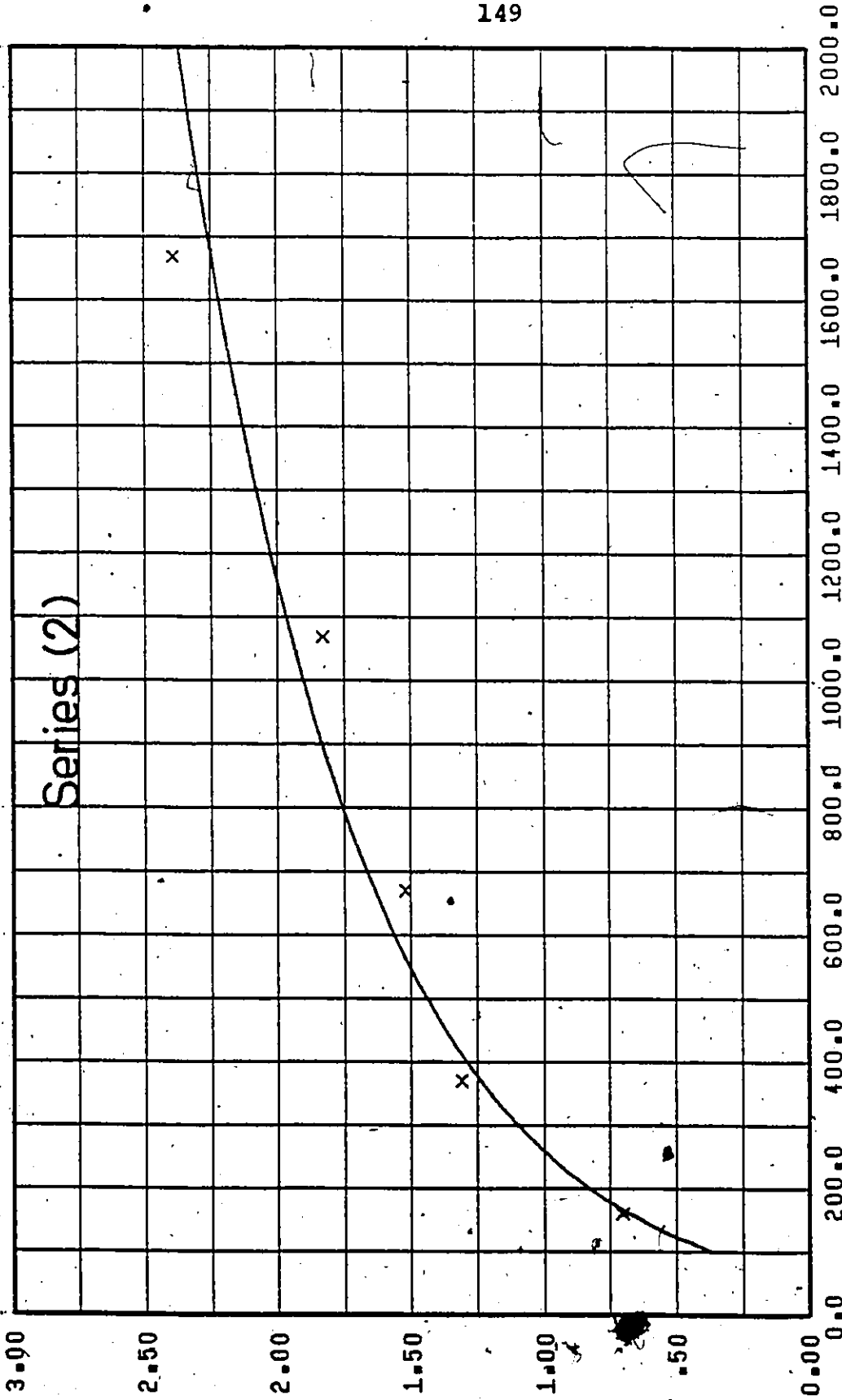


Figure 56. a vs. $\frac{x}{h}$ (Line Source Injection- $C_i = 250$ w.p.p.m.).

x/h

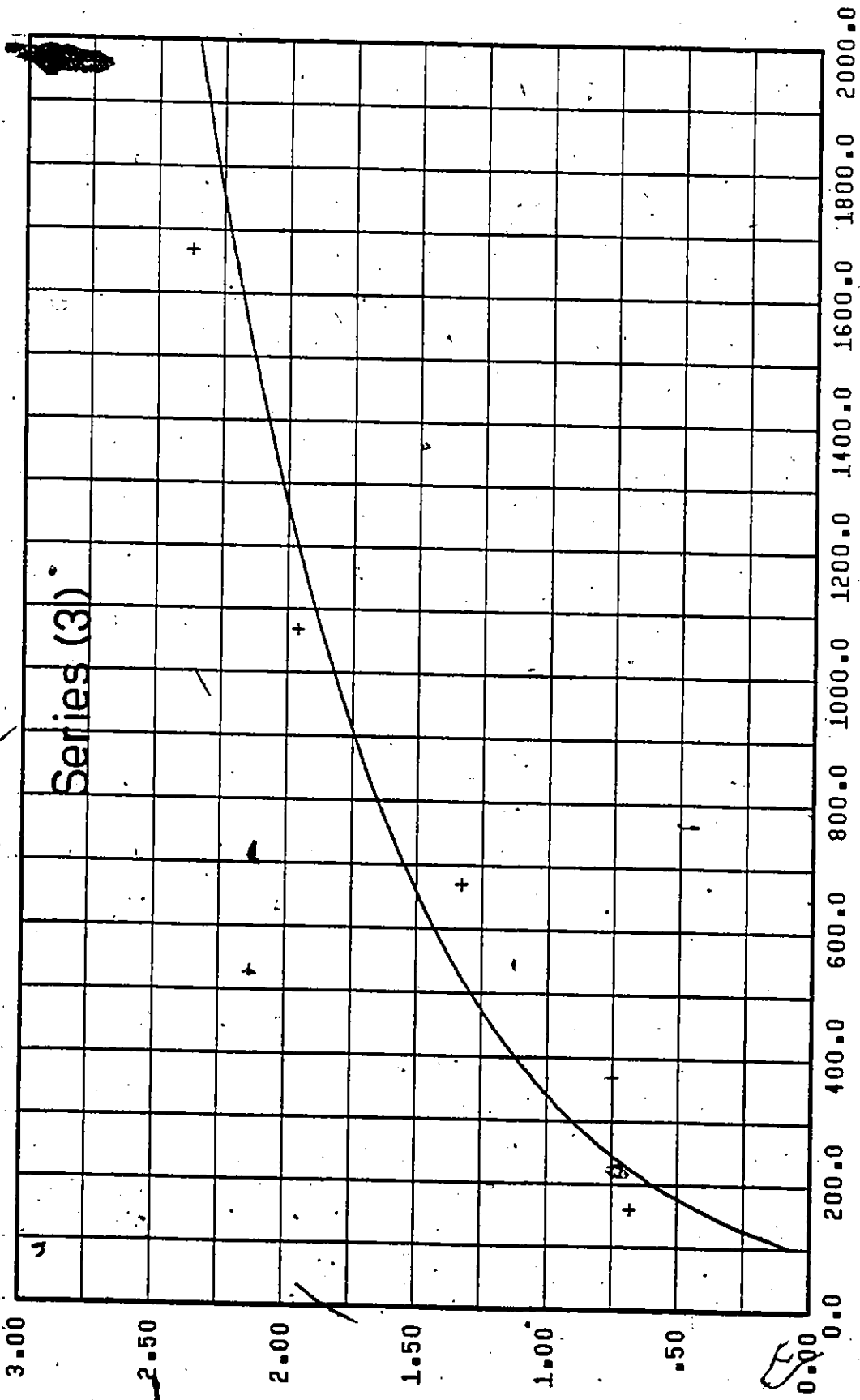


Figure 37. \bar{x} vs. \bar{h} (Line Source Injection- $C_i = 250$ w.p.p.m.).

x/h

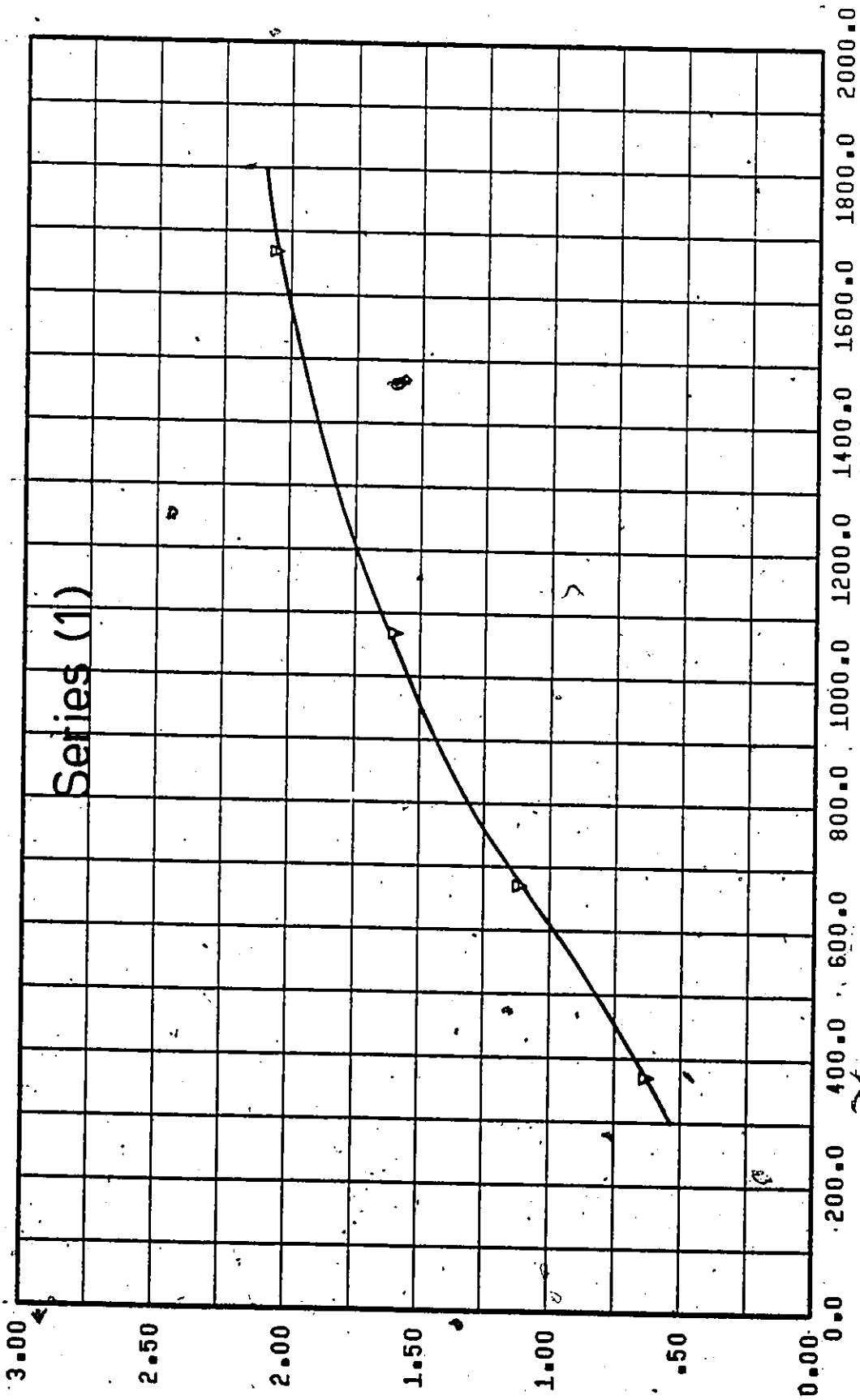
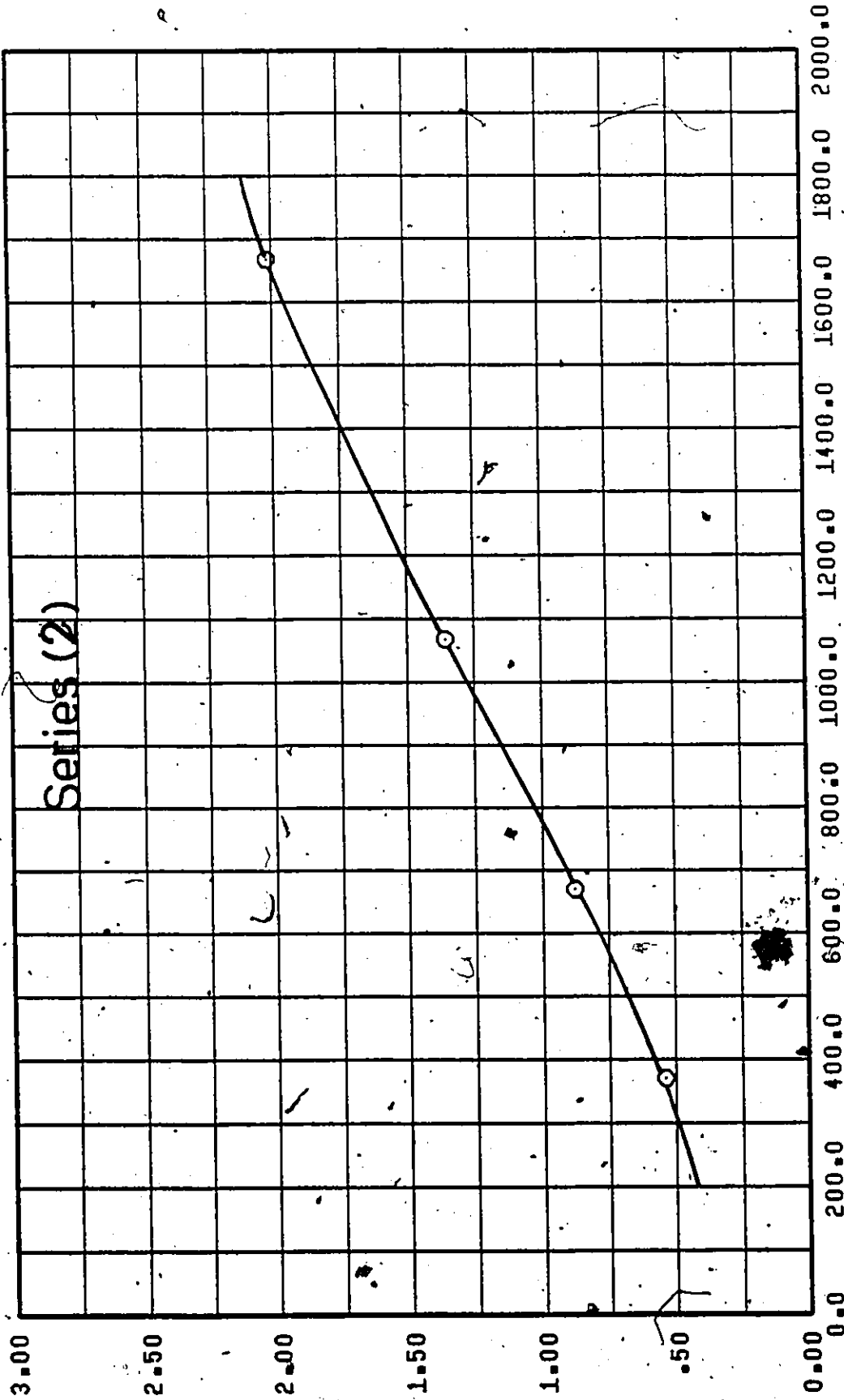
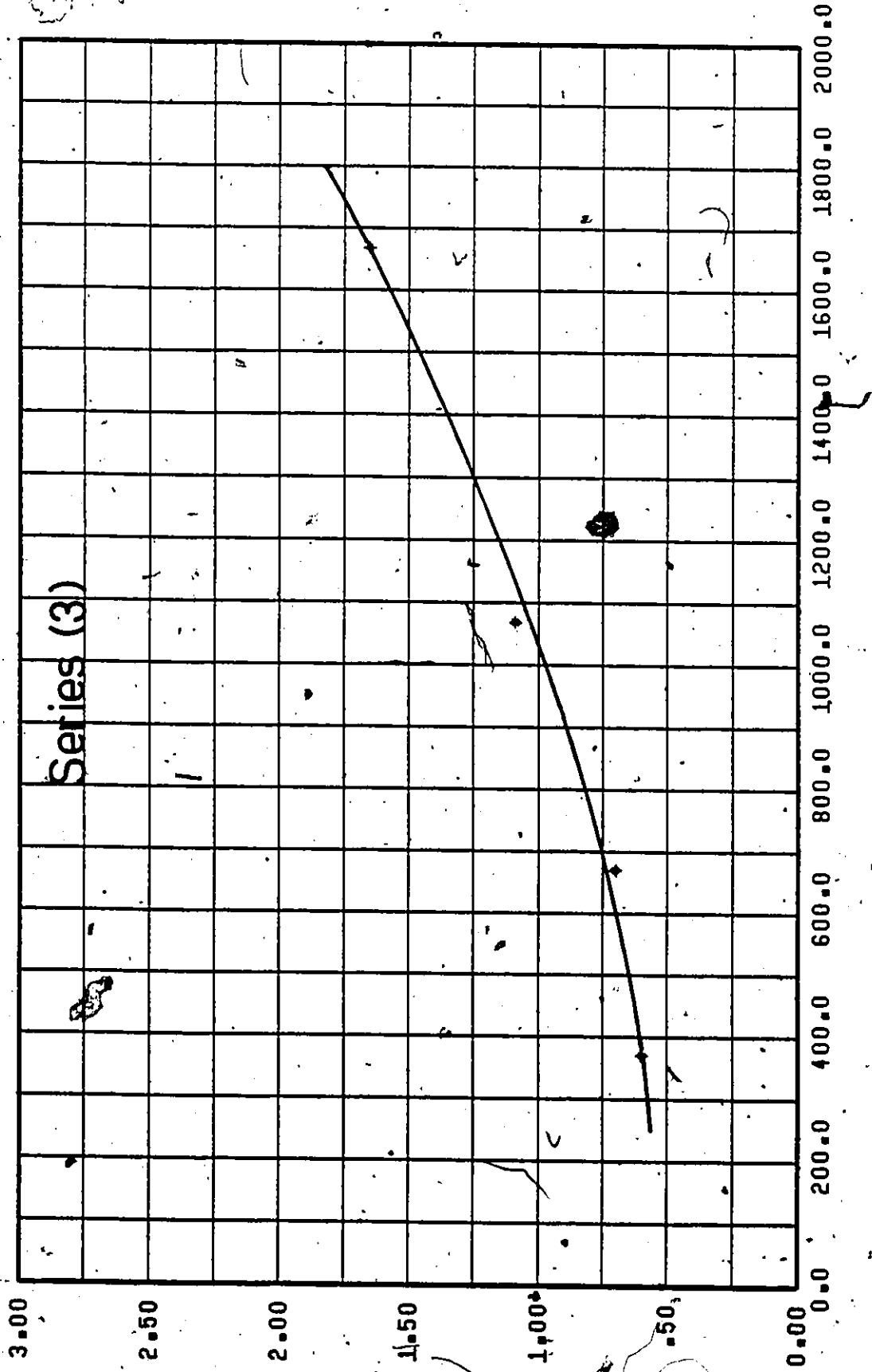


Figure 58. q vs. $\frac{x}{h}$ (Lime Source Injection- $C_i = 500$, w.p.p.m.).



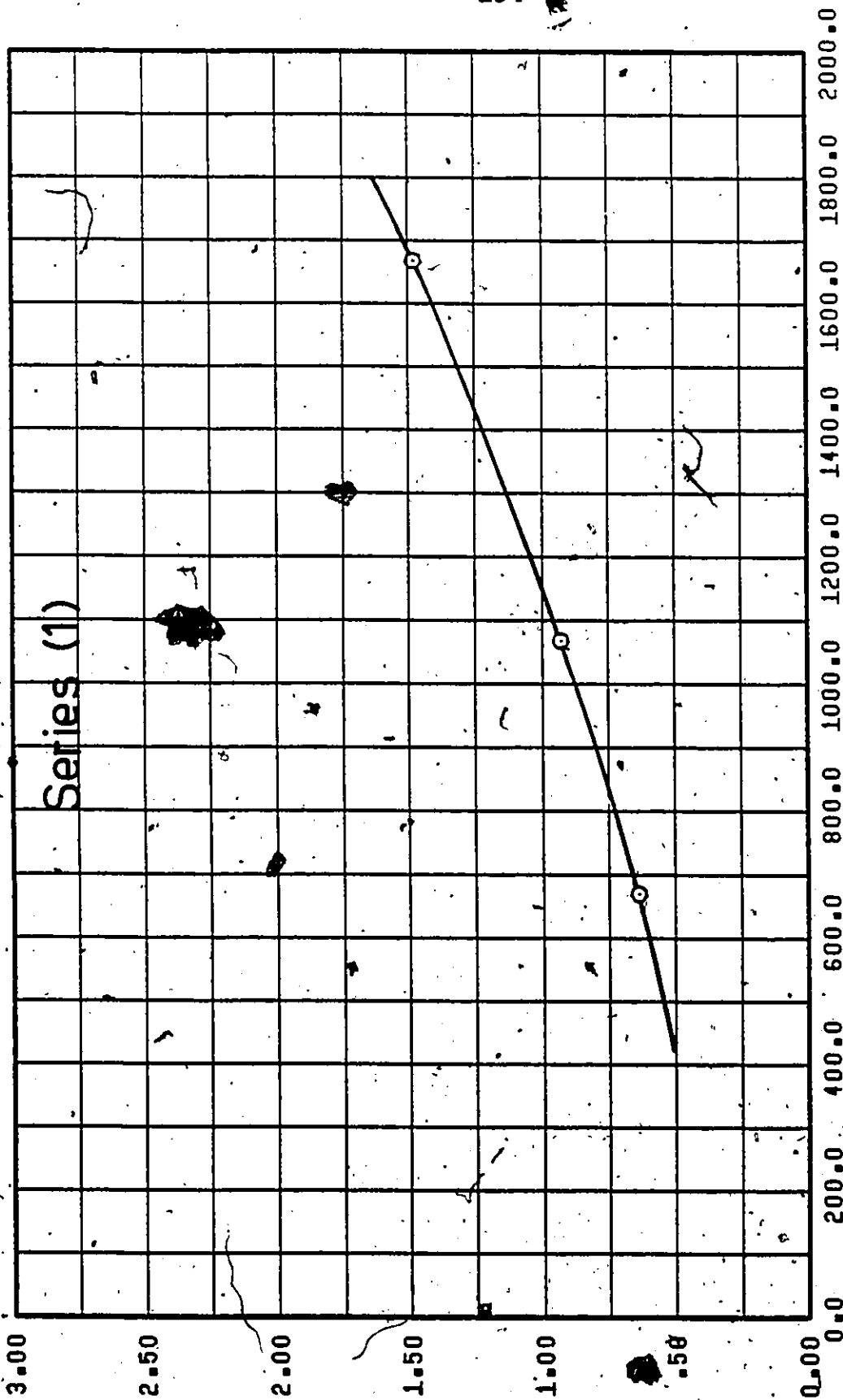
x/h

Figure 59. \bar{x} vs. $\frac{x}{h}$ (Line Source Injection-C_i = 500 w.p.p.m.).



x/h

Figure 60. a vs. $\frac{x}{h}$ (Line Source Injection- $C_i = 500$ w.p.p.m.)



x/h

Figure 61. a vs. $\frac{x}{h}$ (Line Source Injection- $C_i = 1000$ w.p.p.m.).

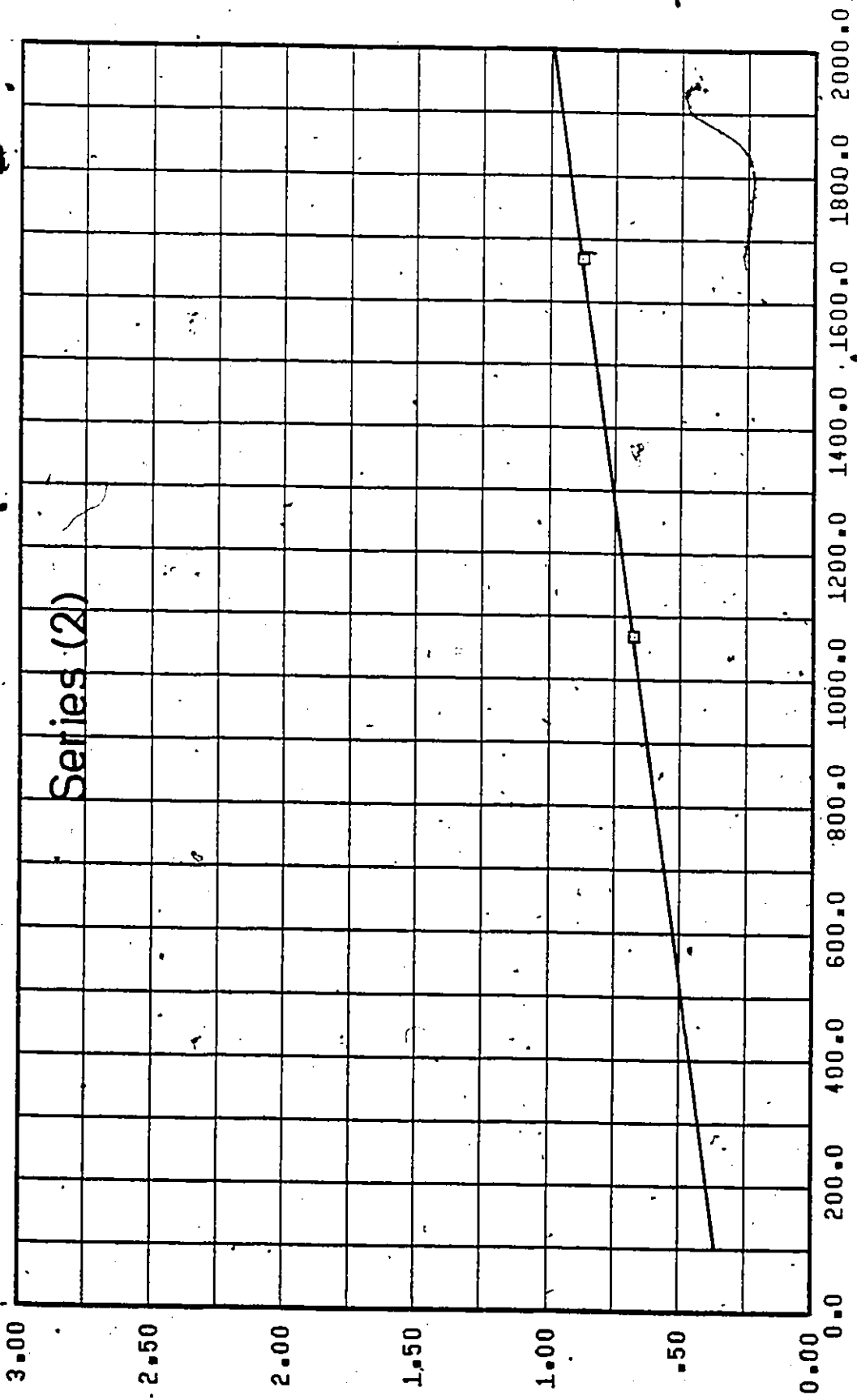
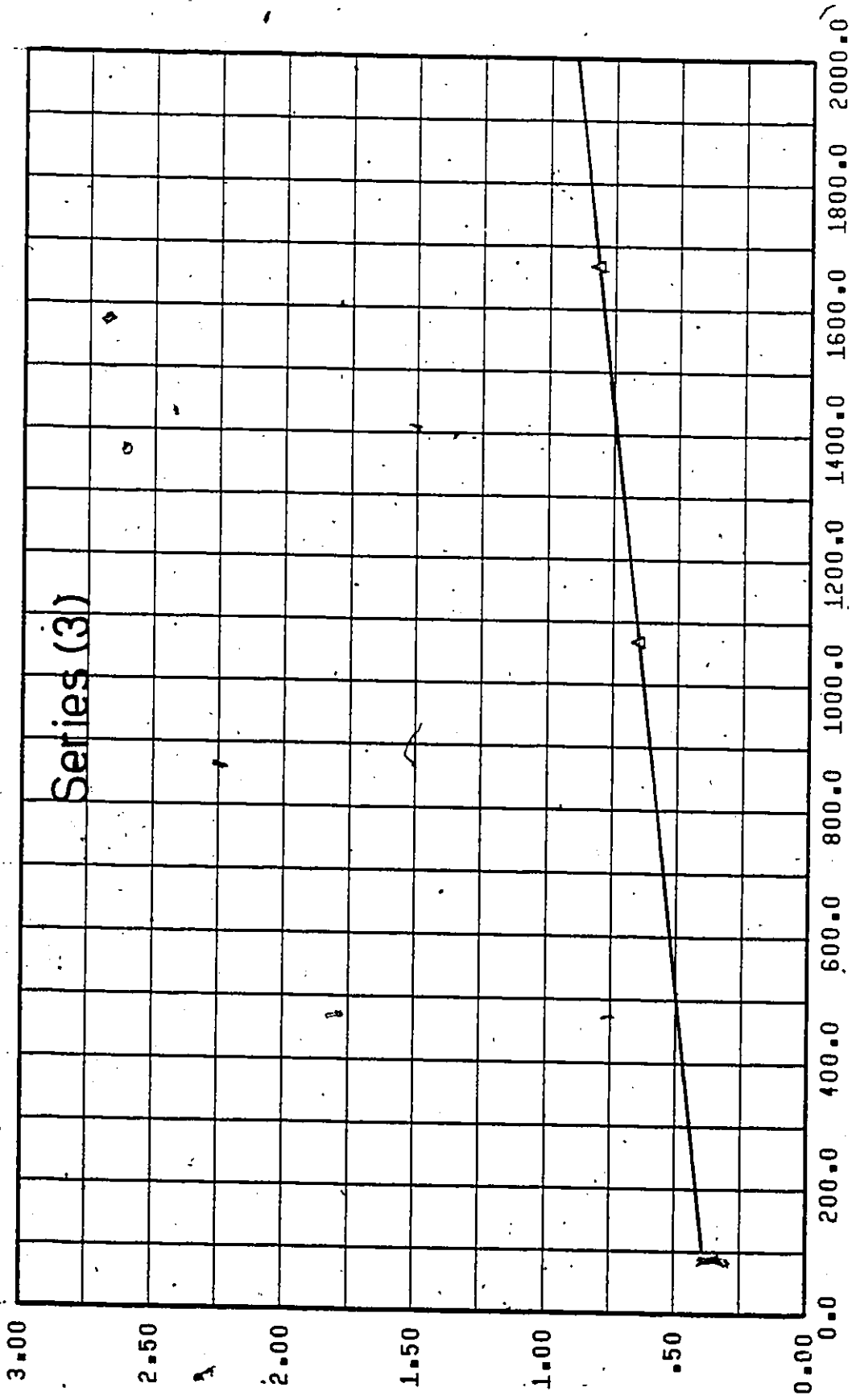


Figure 62. α vs. $\frac{x}{h}$ (Line Source Injection- $C_i = 1000$ w.p.p.m.).



x/h

Figure 63. a vs. $\frac{x}{h}$ (Line Source Injection- $C_1 = 1000$ w.p.p.m.).

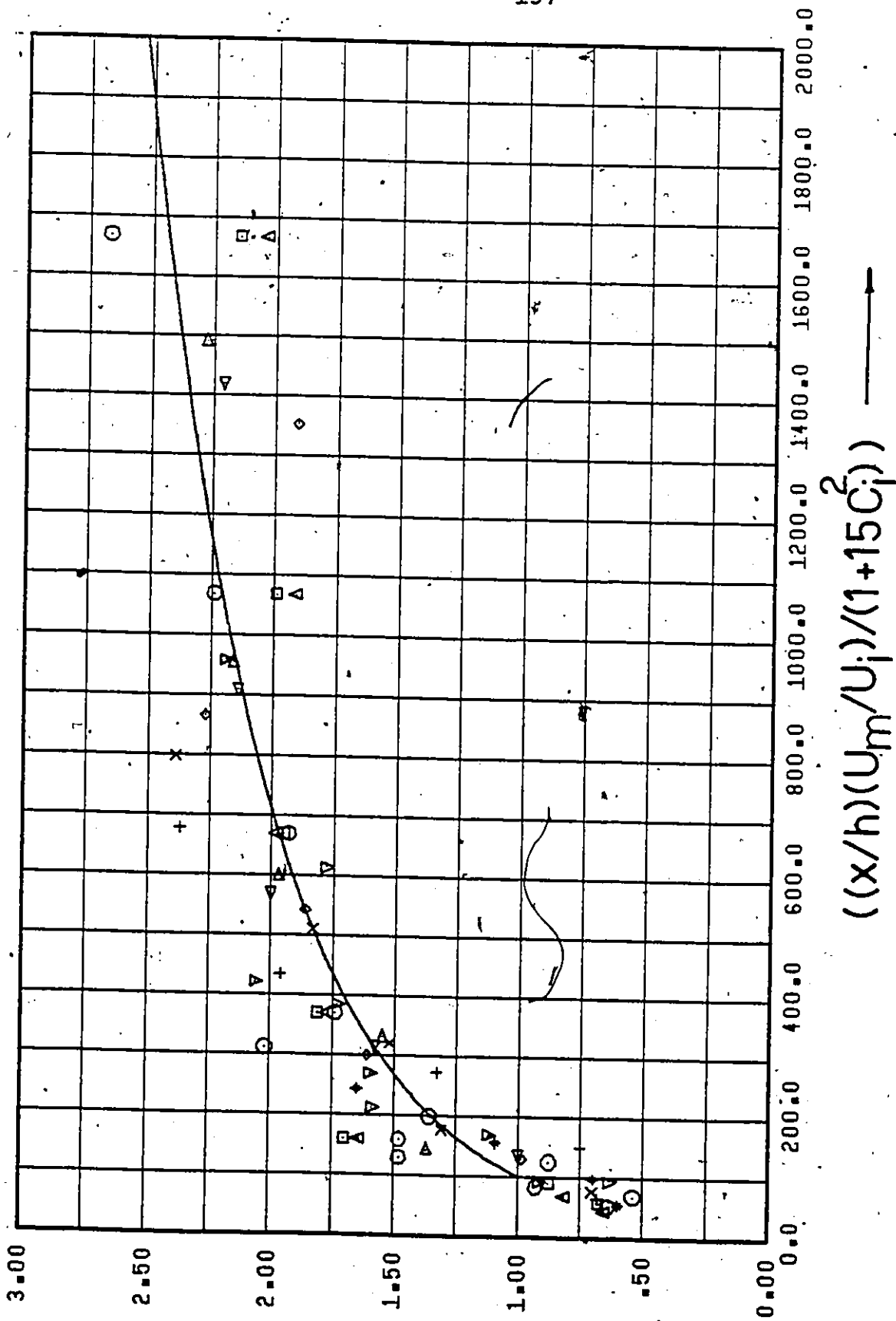


Figure 64. Generalized Exponent 'a' Profile (Line Source Injection).

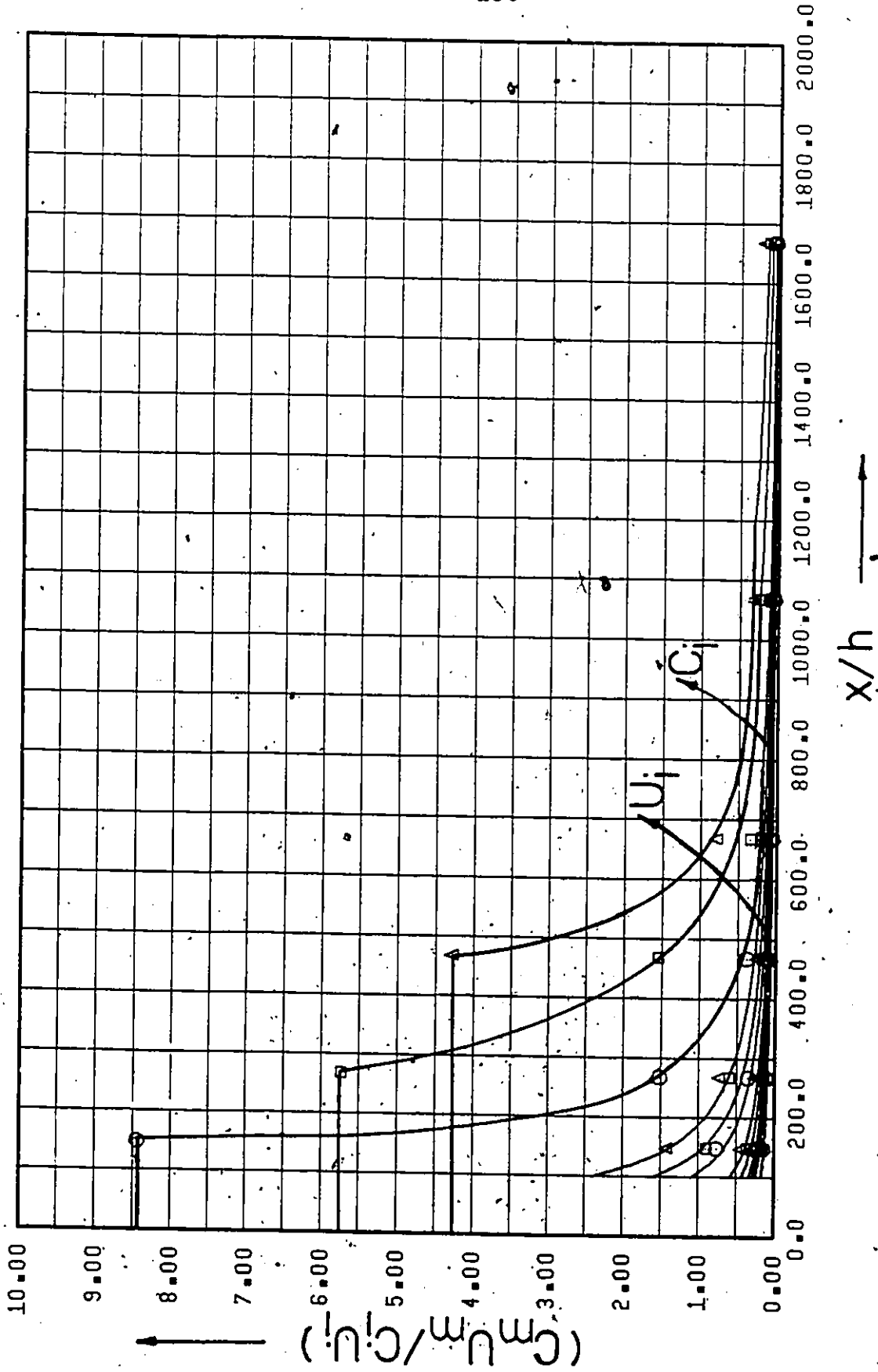


Figure 65. Wall Concentration Profiles (Line Source Injection).

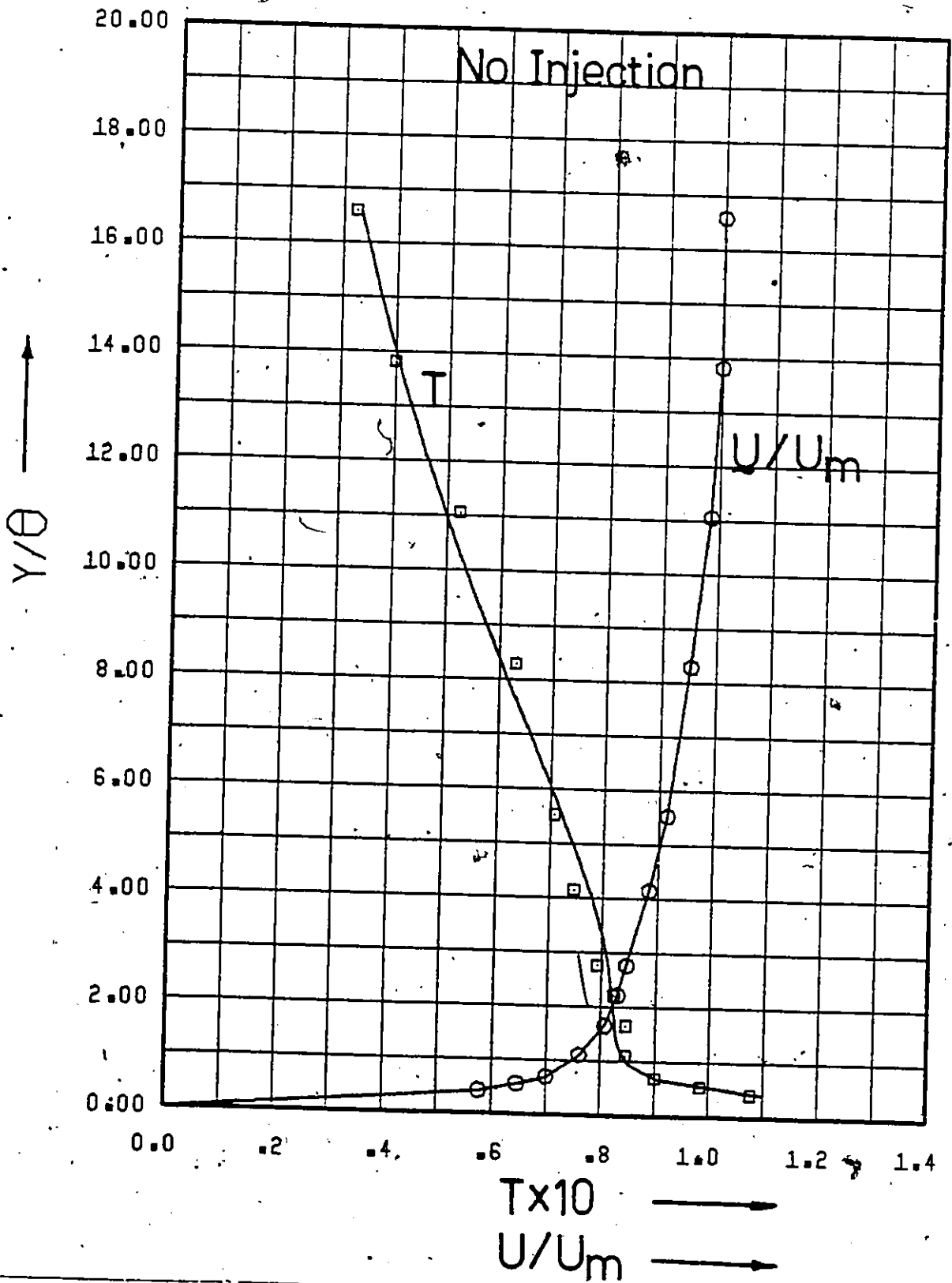


Figure 65. Velocity and Turbulence Intensity Profiles (Line Source Injection-Water Injection).

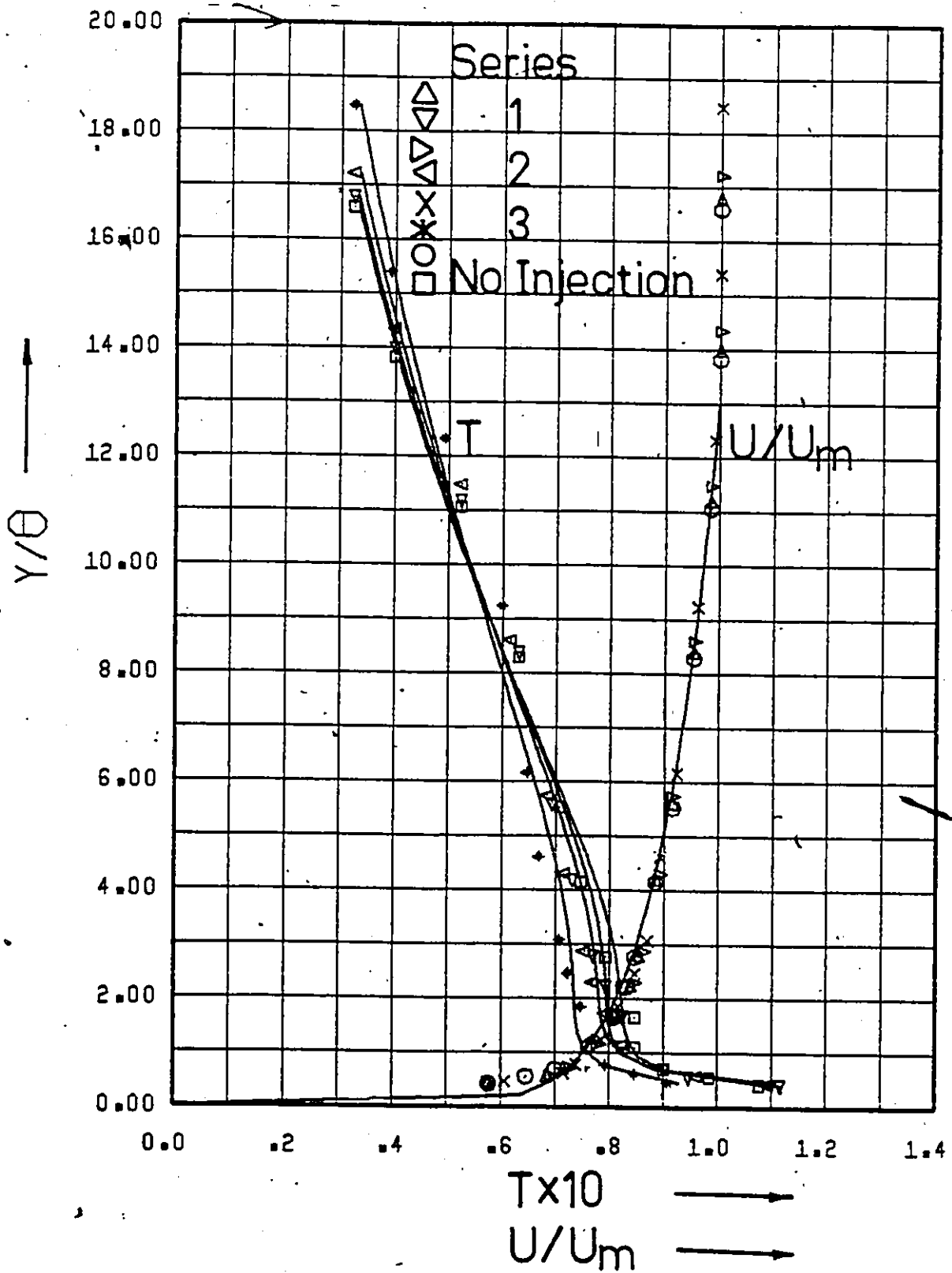


Figure 67. Velocity and Turbulence Intensity Profiles (Line Source Injection- $C_i = 100$ w.p.p.m.).

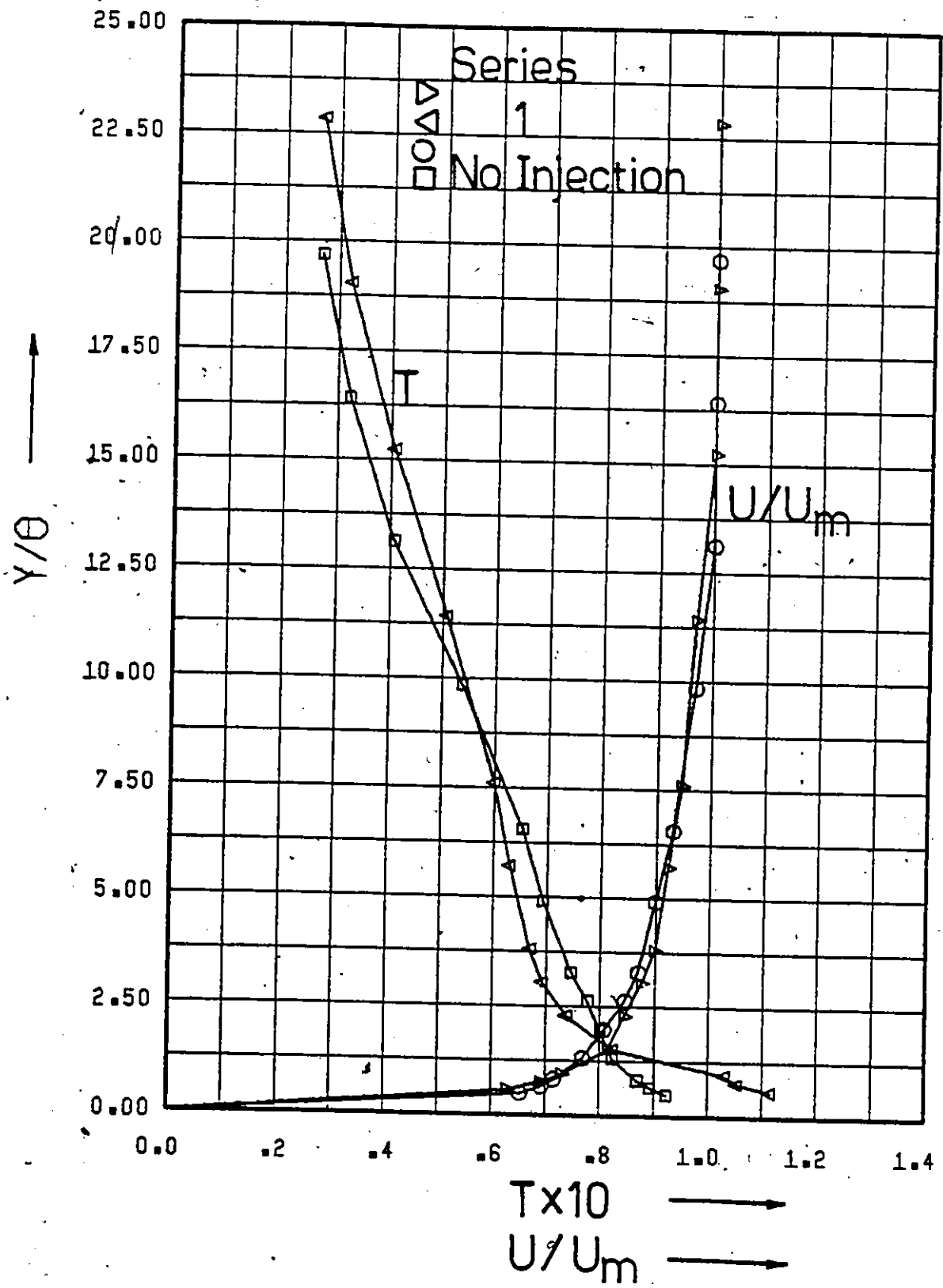


Figure 68. Velocity and Turbulence Intensity Profiles (Line Source Injection- $C_i = 500$ w.p.p.m.).

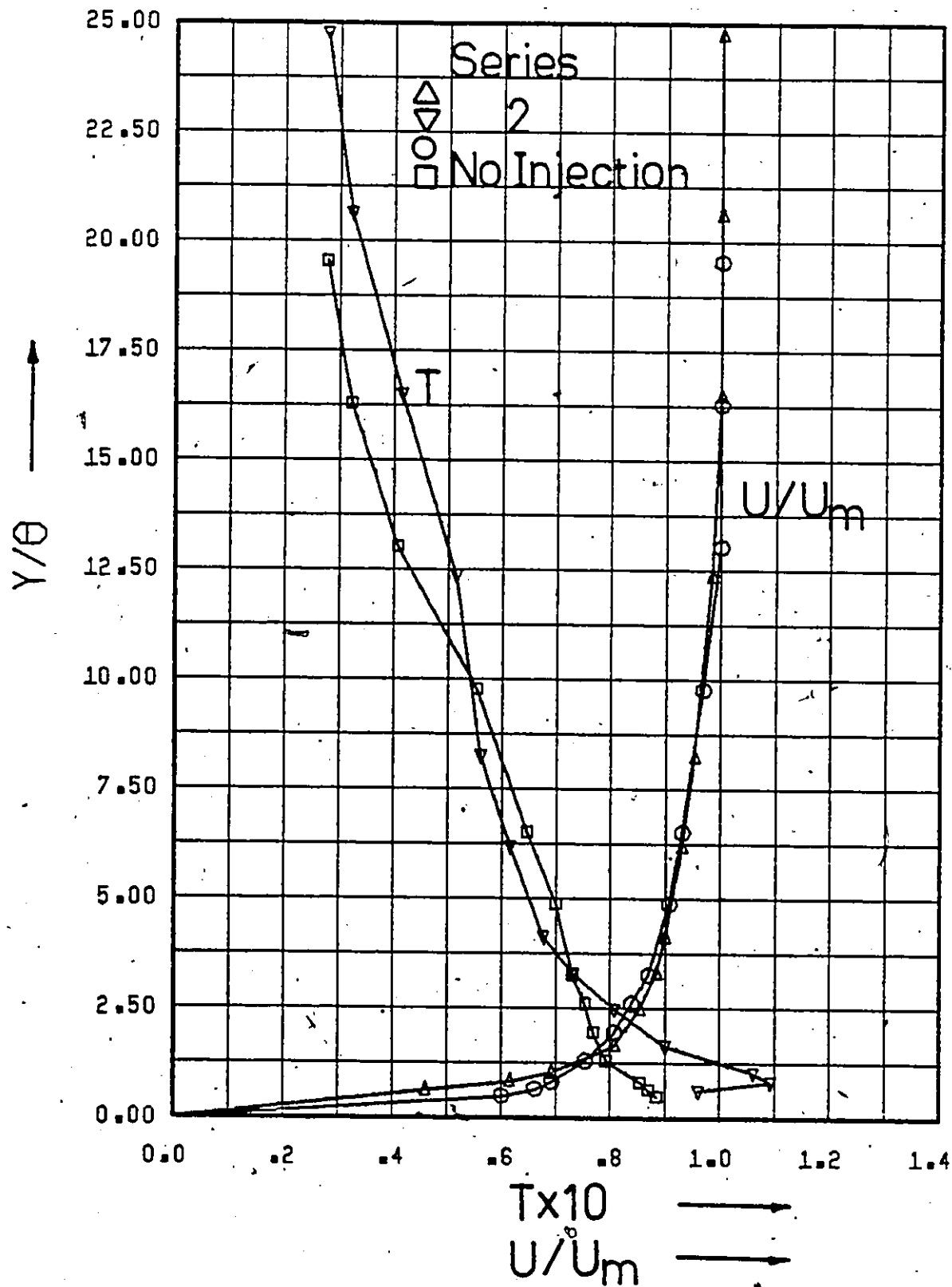


Figure 69. Velocity and Turbulence Intensity Profiles (Line Source Injection- $C_i = 500$ w.p.p.m.).

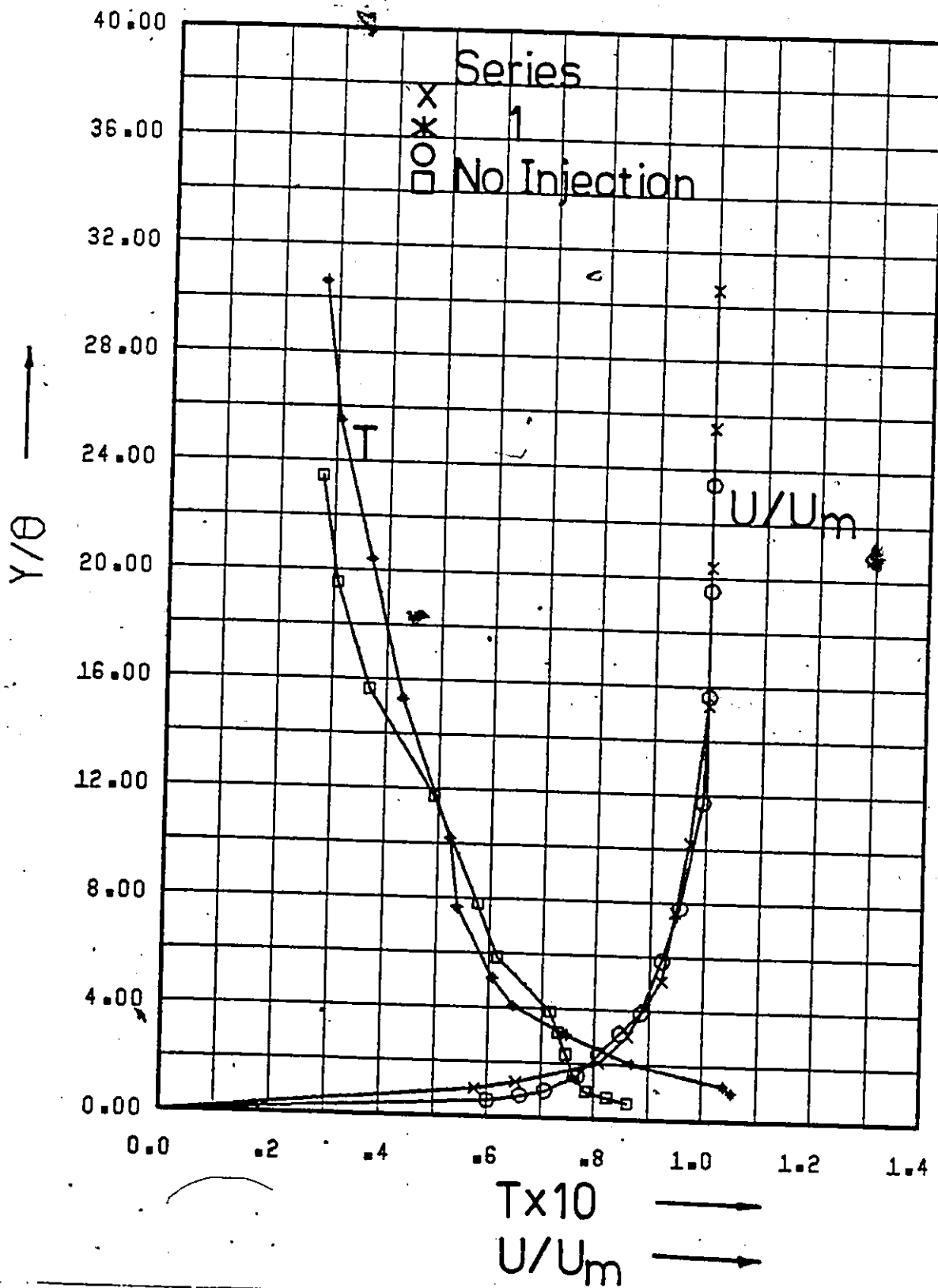


Figure 70. Velocity and Turbulence Intensity Profiles (Line Source Injection- $C_i = 1000$ w.p.p.m.).

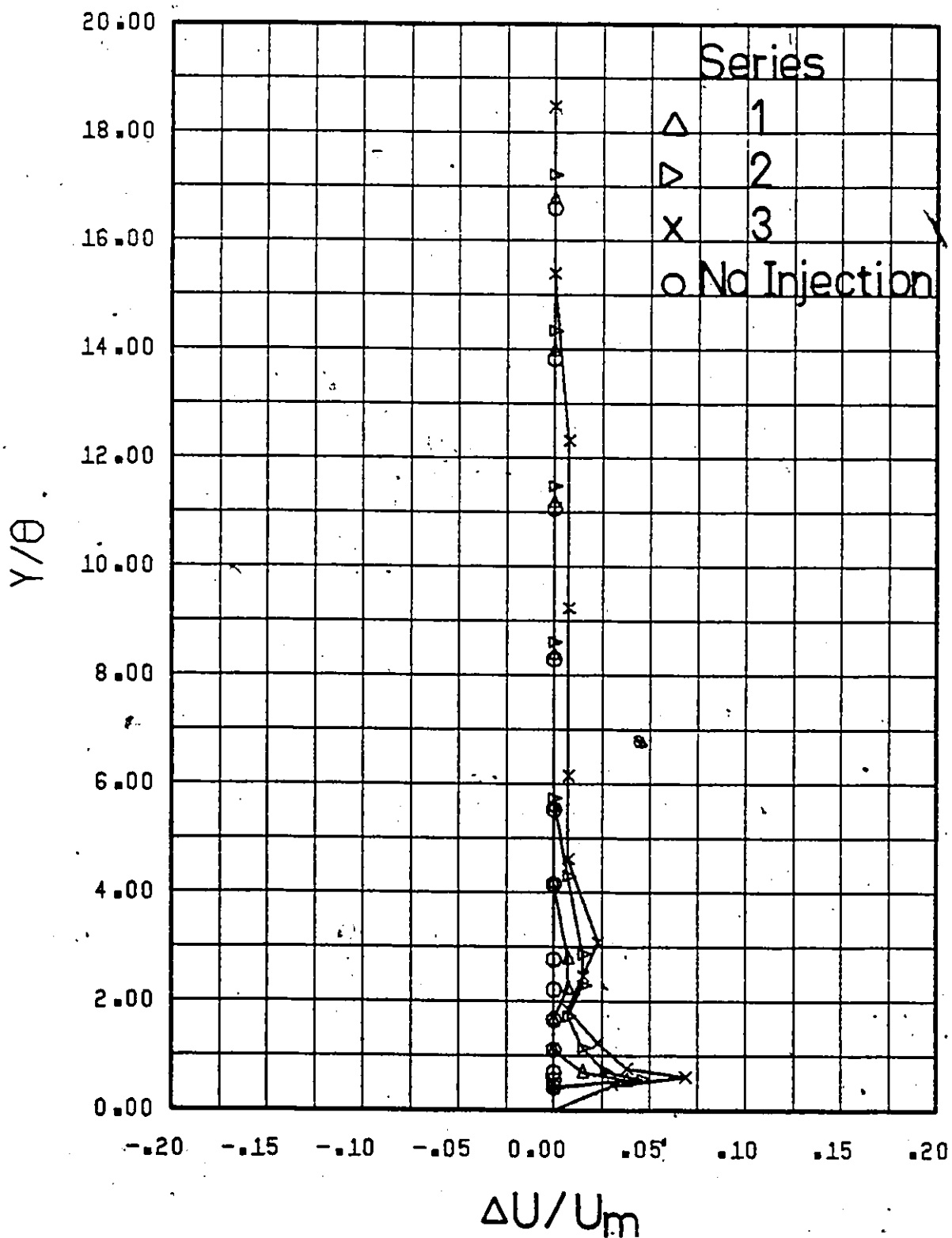


Figure 71. The Change in Velocity Profile Due to Polymer Solution Injection ($C_i = 100$ w.p.p.m.).

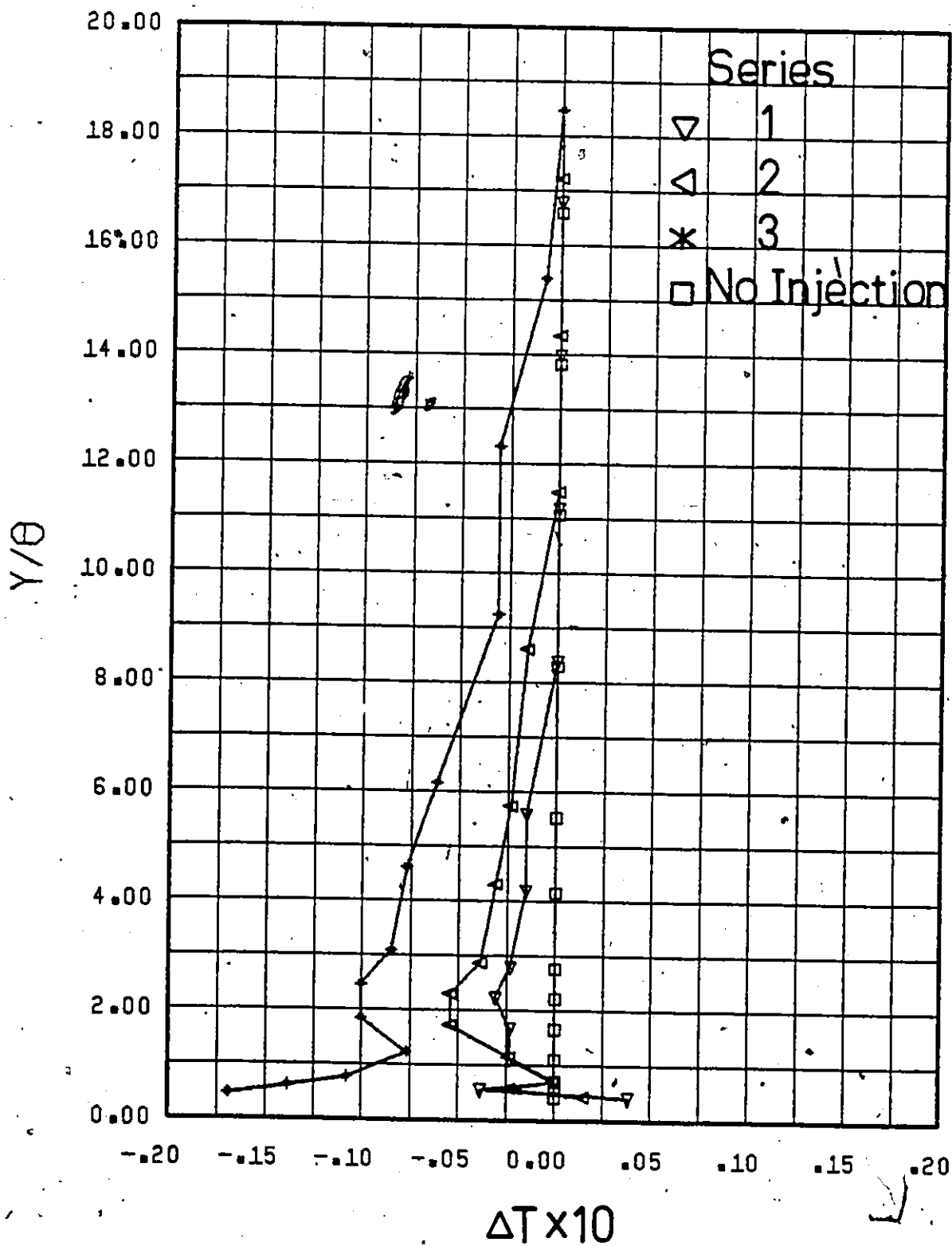


Figure 72. The Change in Turbulence Intensity Profile Due to Polymer Solution Injection ($C_i = .100$ w.p.p.m.).

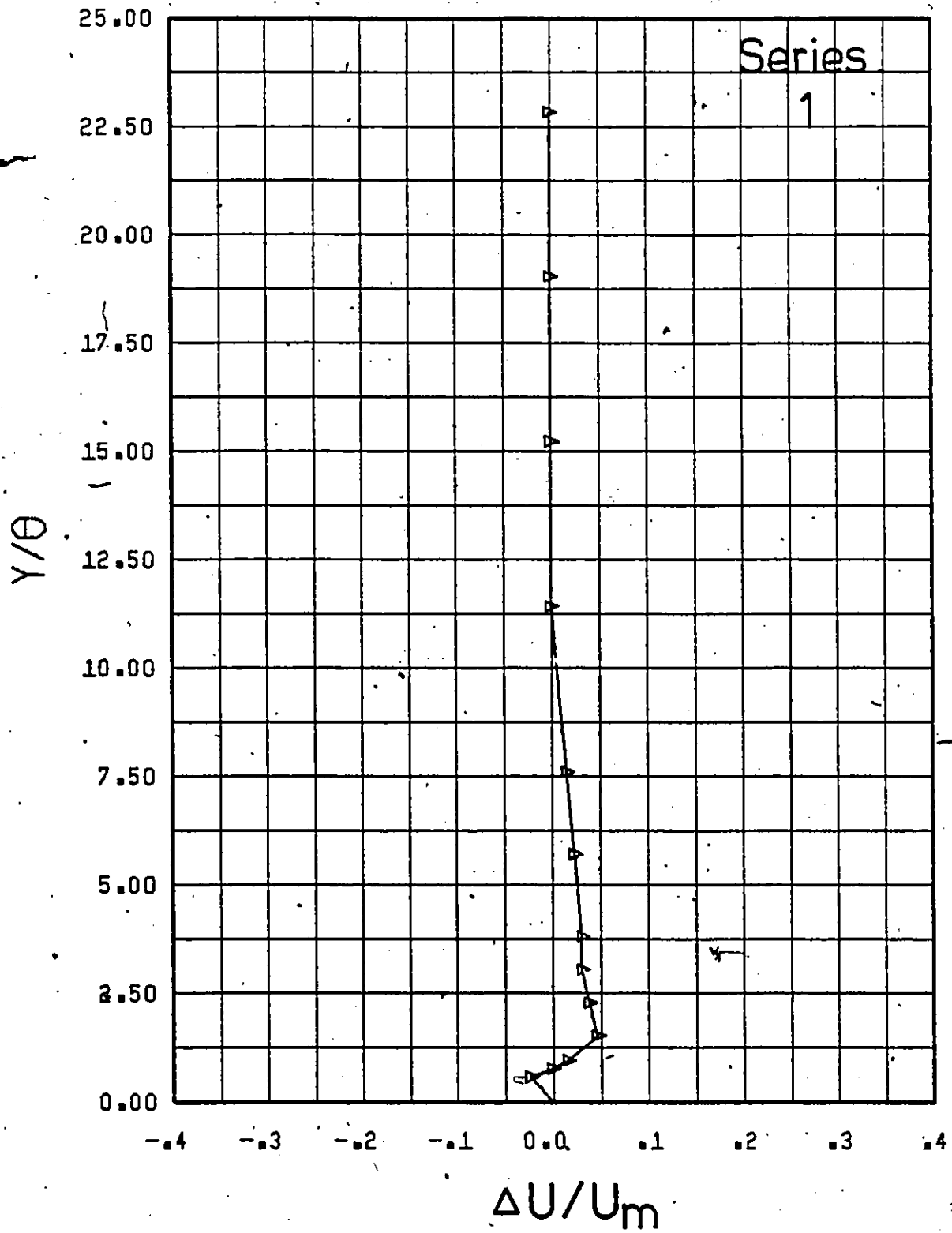


Figure 73. The Change in Velocity Profile Due to Polymer Solution Injection ($C_i = 500$ w.p.p.m.).

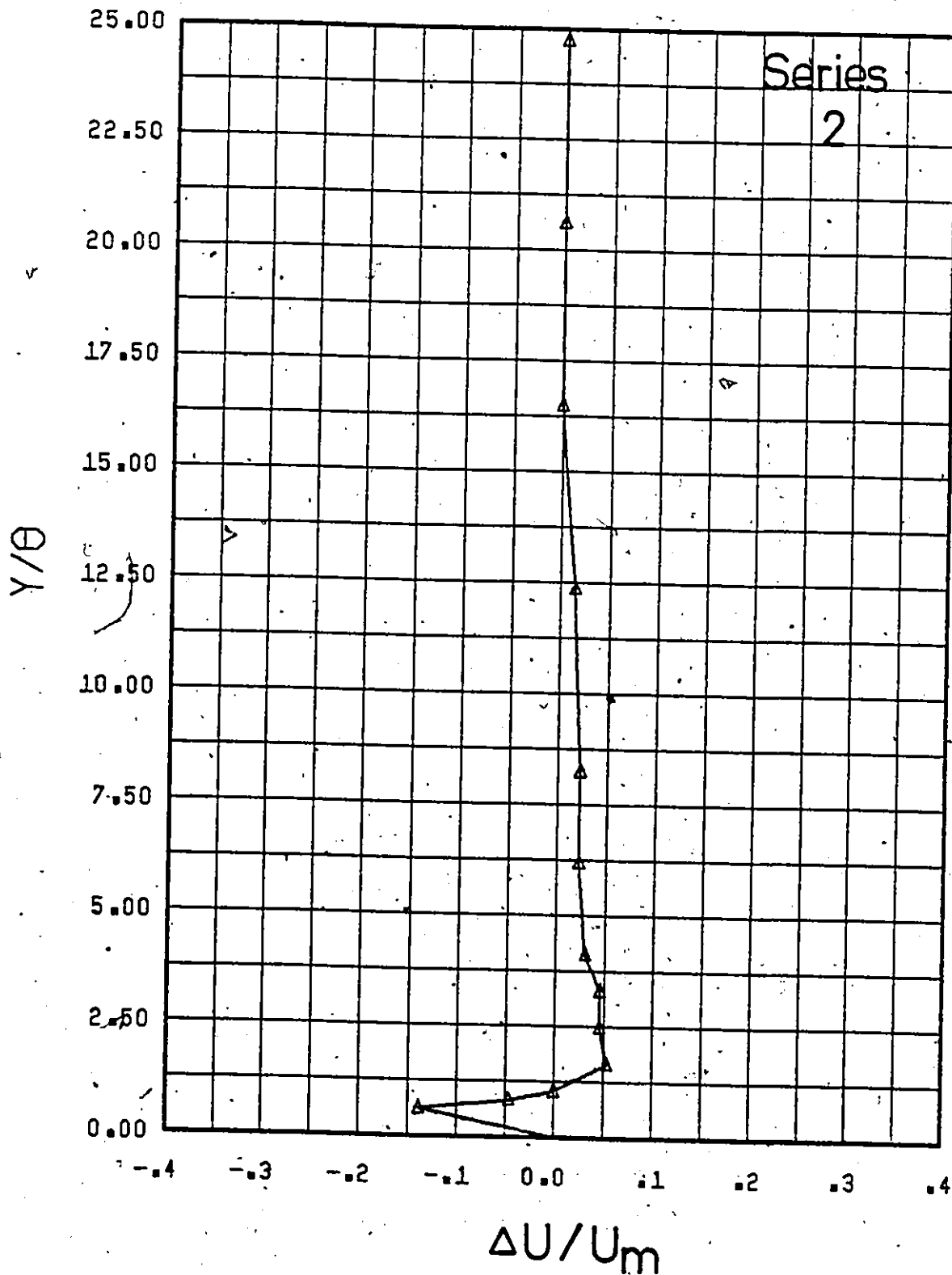


Figure 74. The Change in Velocity Profile Due to Polymer Solution Injection ($C_i = 500$ w.p.p.m.).

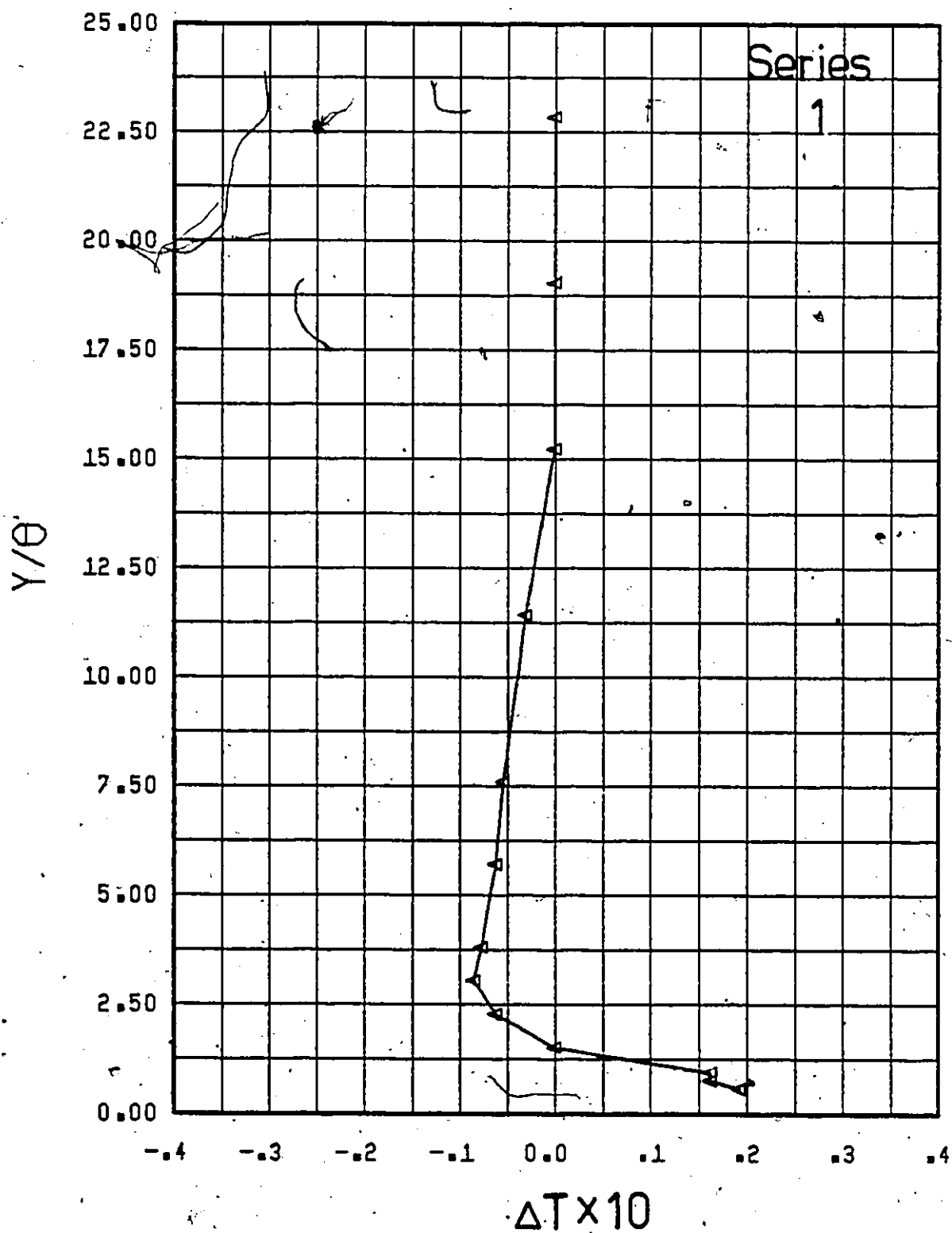


Figure 75. The Change in Turbulence Intensity Profile Due to Polymer Solution Injection ($C_i = 500$ w.p.p.m.).

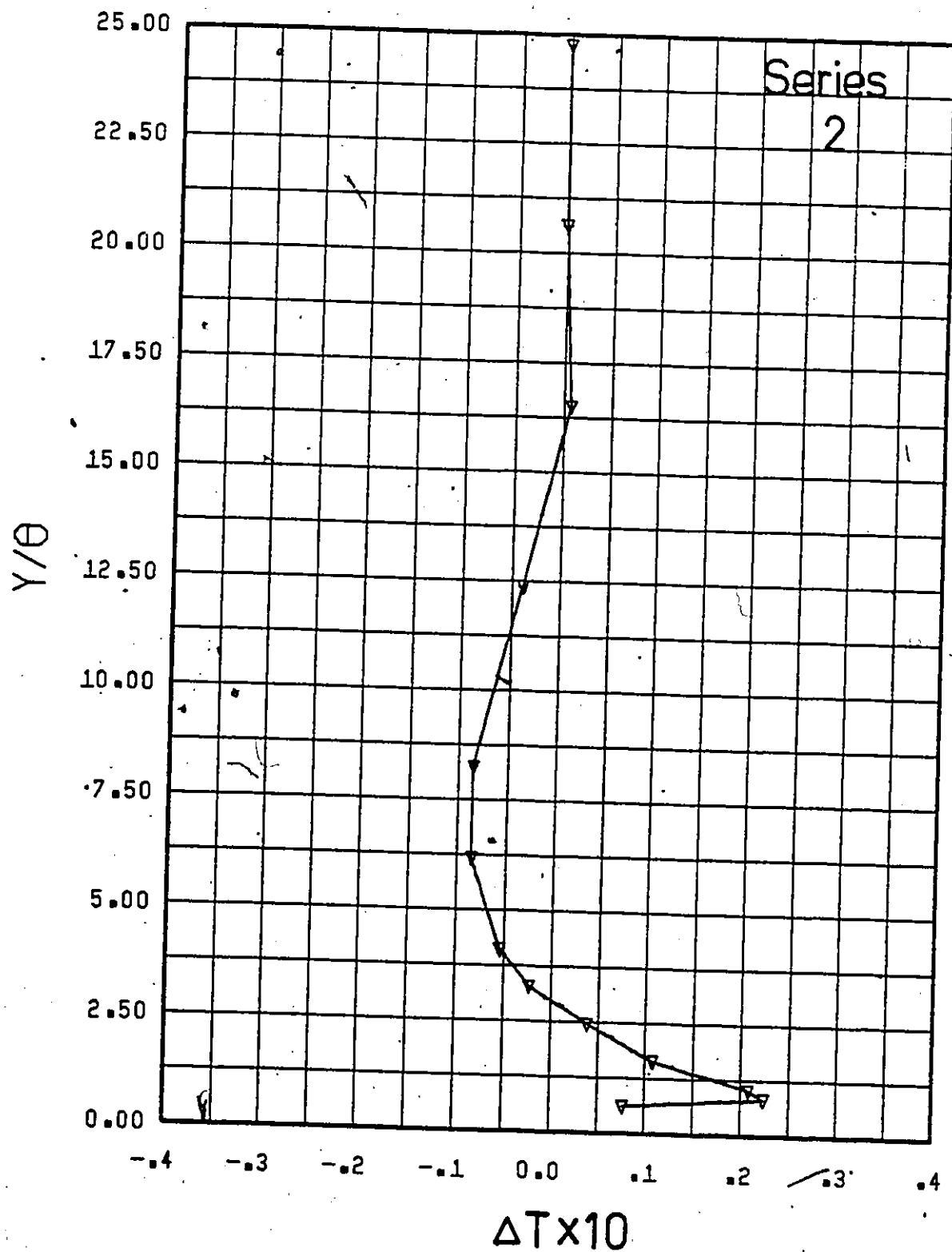


Figure 76. The Change in Turbulence Intensity Profile Due to Polymer Solution Injection ($C_i = 500$ w.p.p.m.).

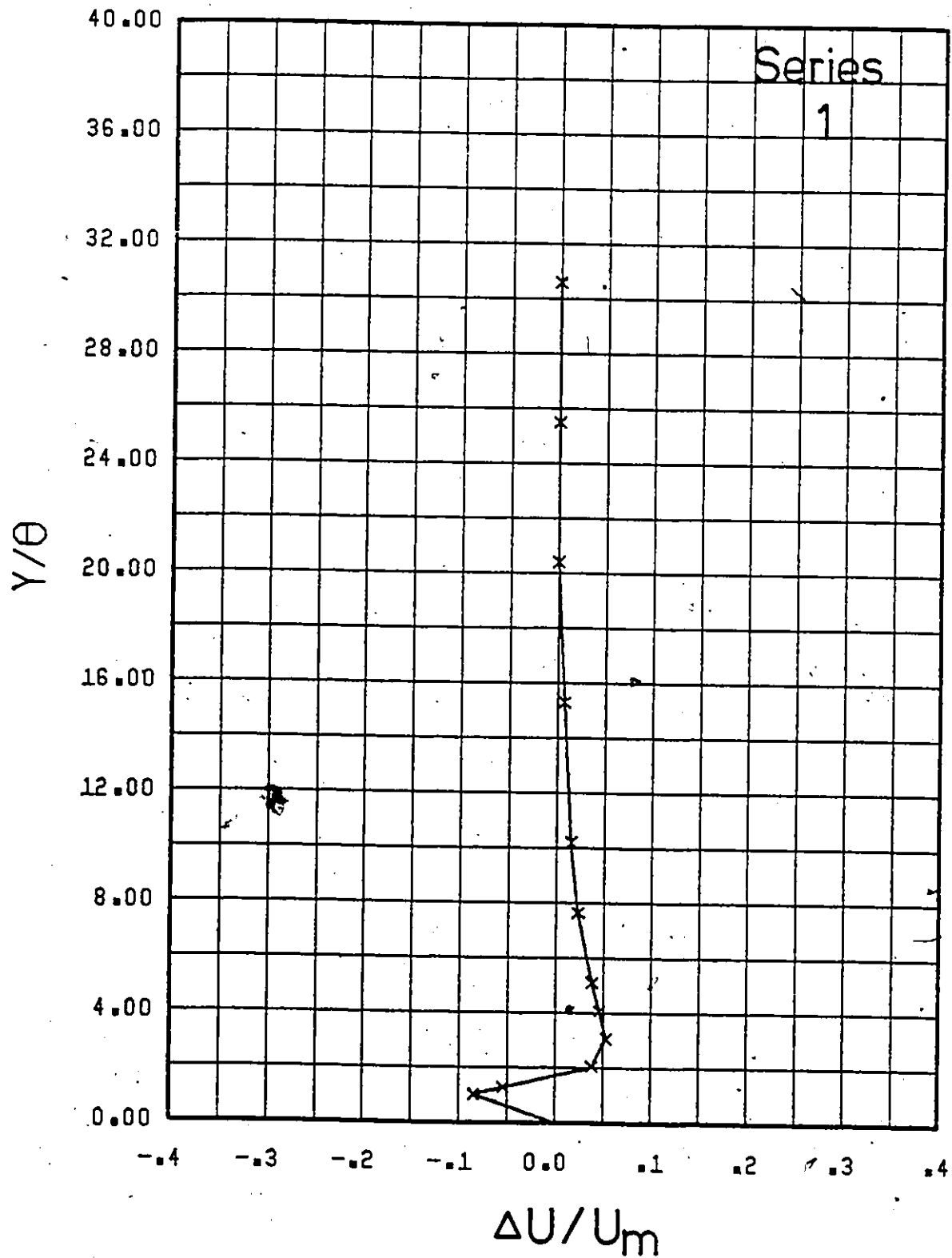


Figure 77. The Change in Velocity Profile Due to Polymer Solution Injection ($C_i = 1000$ w.p.p.m.).

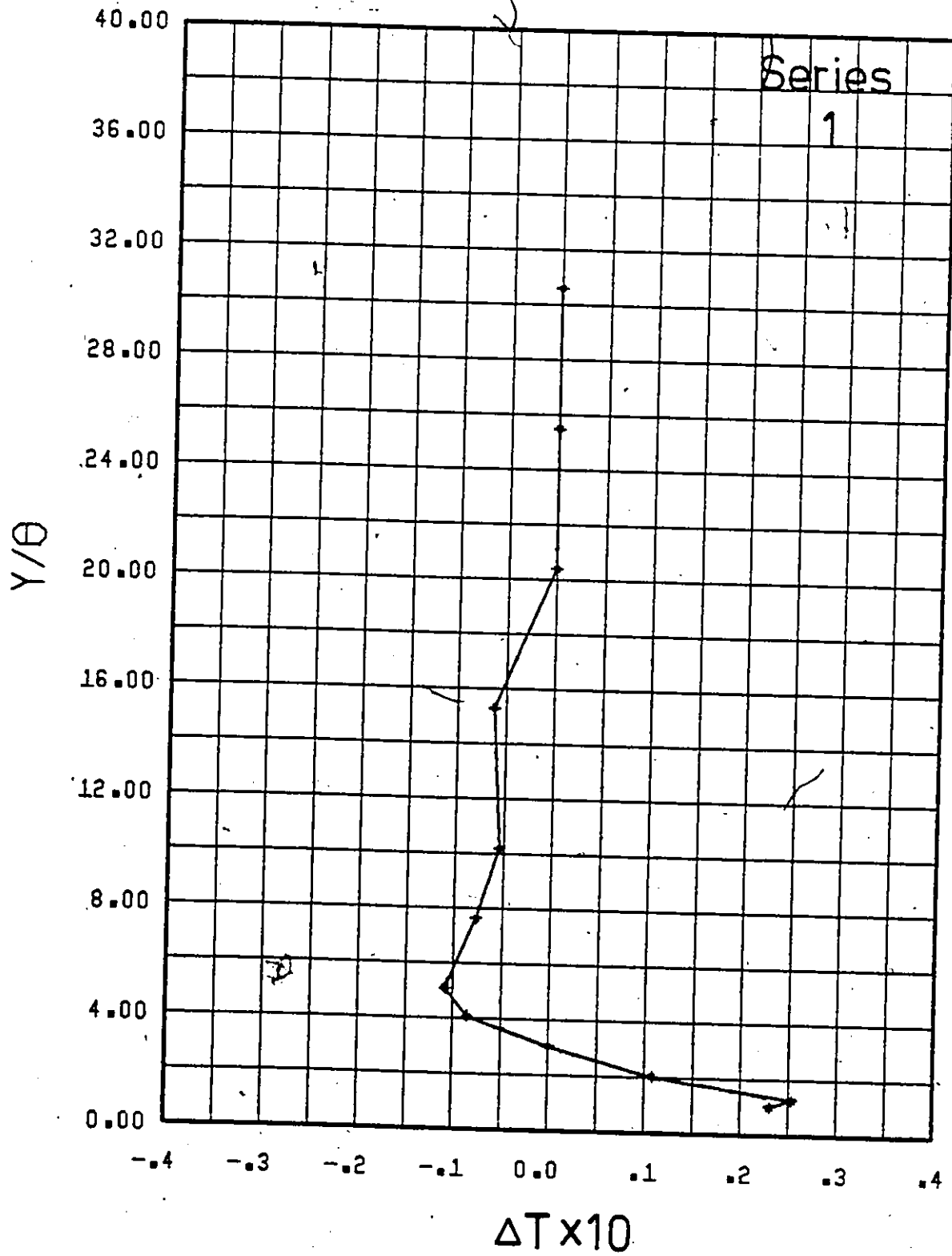


Figure 78. The Change in Turbulence Intensity Profile Due to Polymer Solution Injection ($C_i = 1000$ w.p.p.m.).

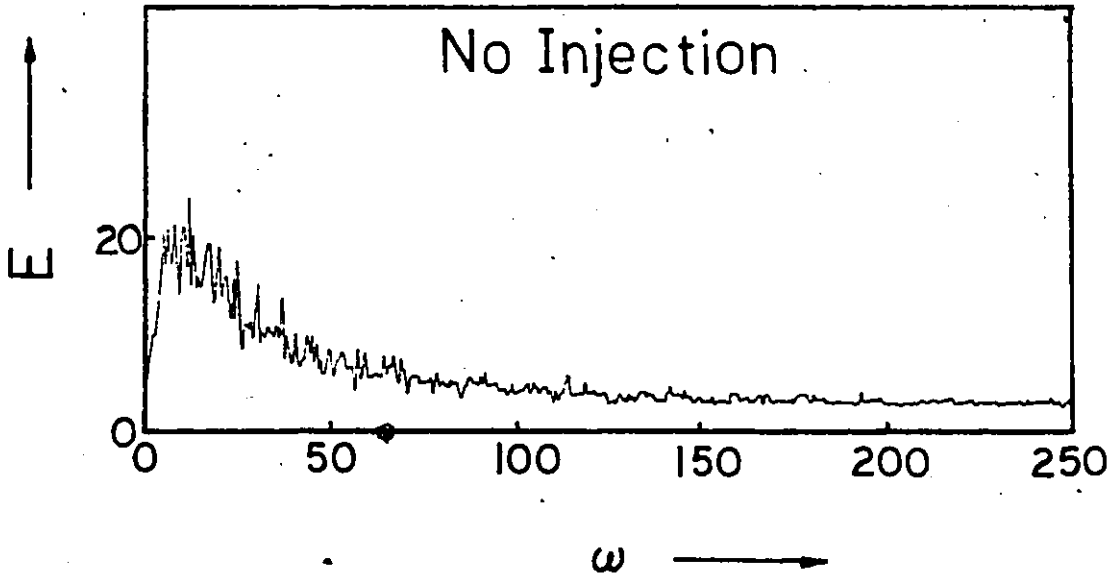


Figure 79. Energy Spectra Without Injection.

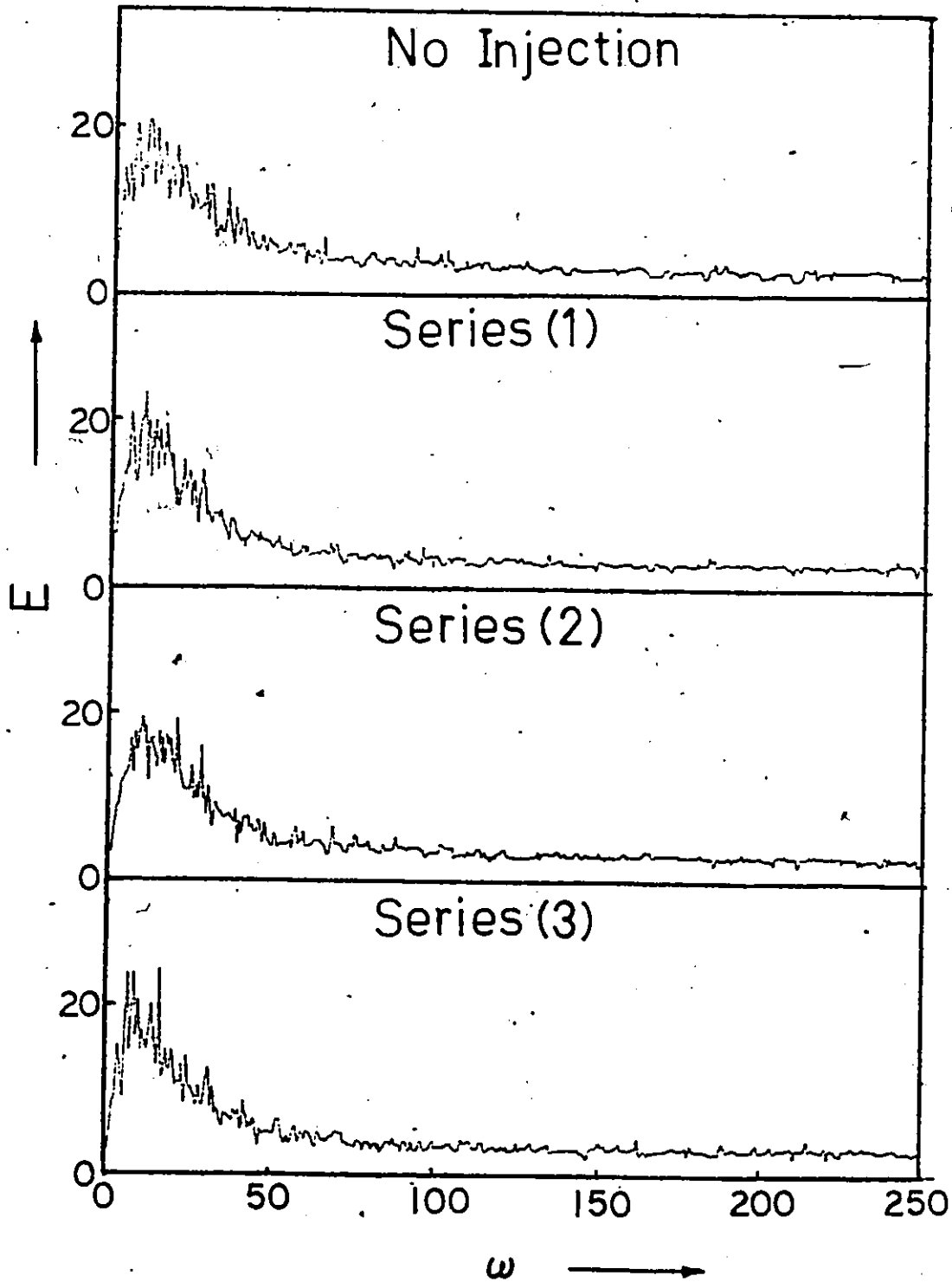


Figure 80. Energy Spectra (Line Source Injection-Water Injection).

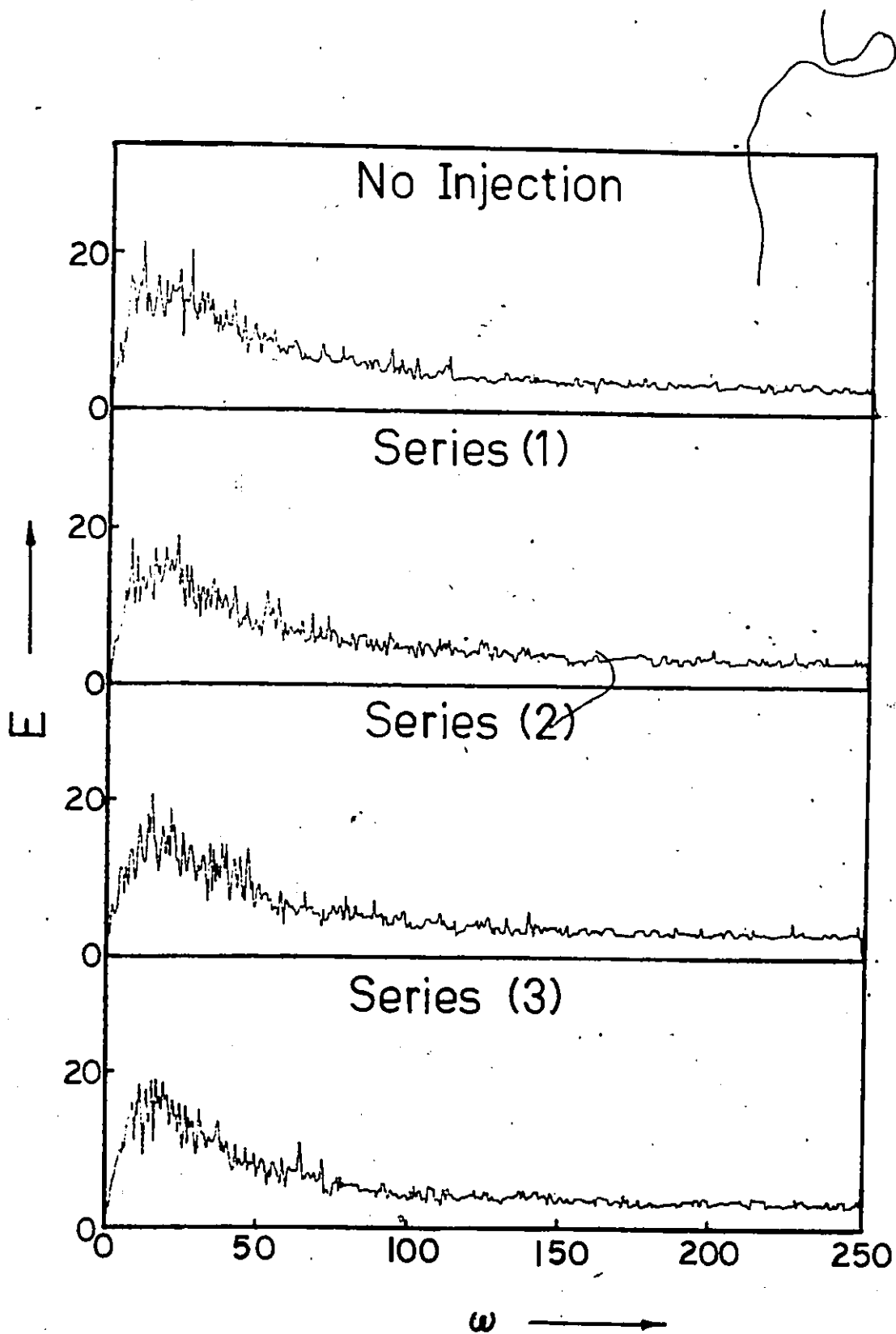


Figure 81. Energy Spectra (Line Source Injection- $C_i = 100$ w.p.p.m.).

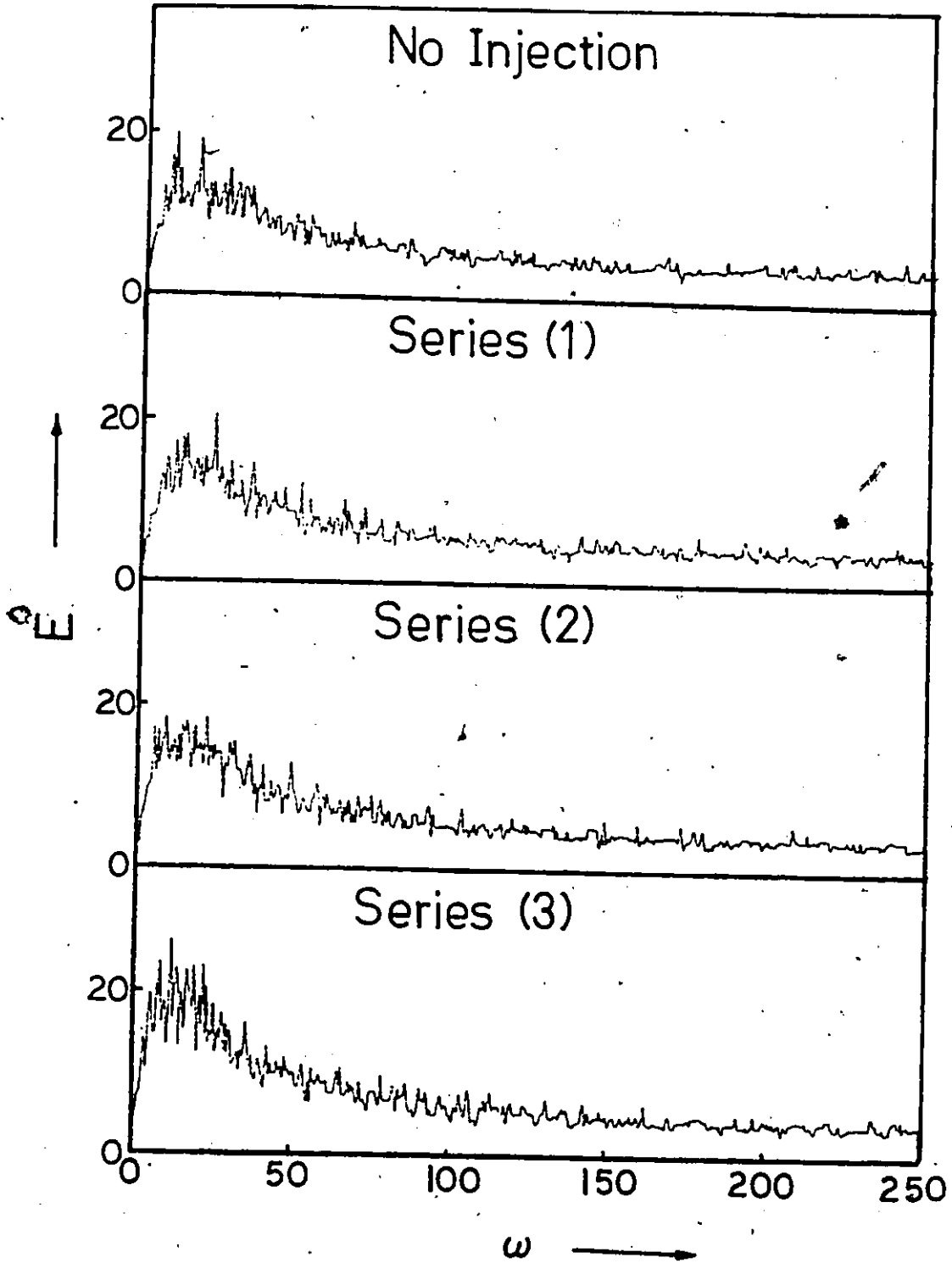


Figure 82. Energy Spectra (Line Source Injection-
 $C_i = 250$ w.p.p.m.).

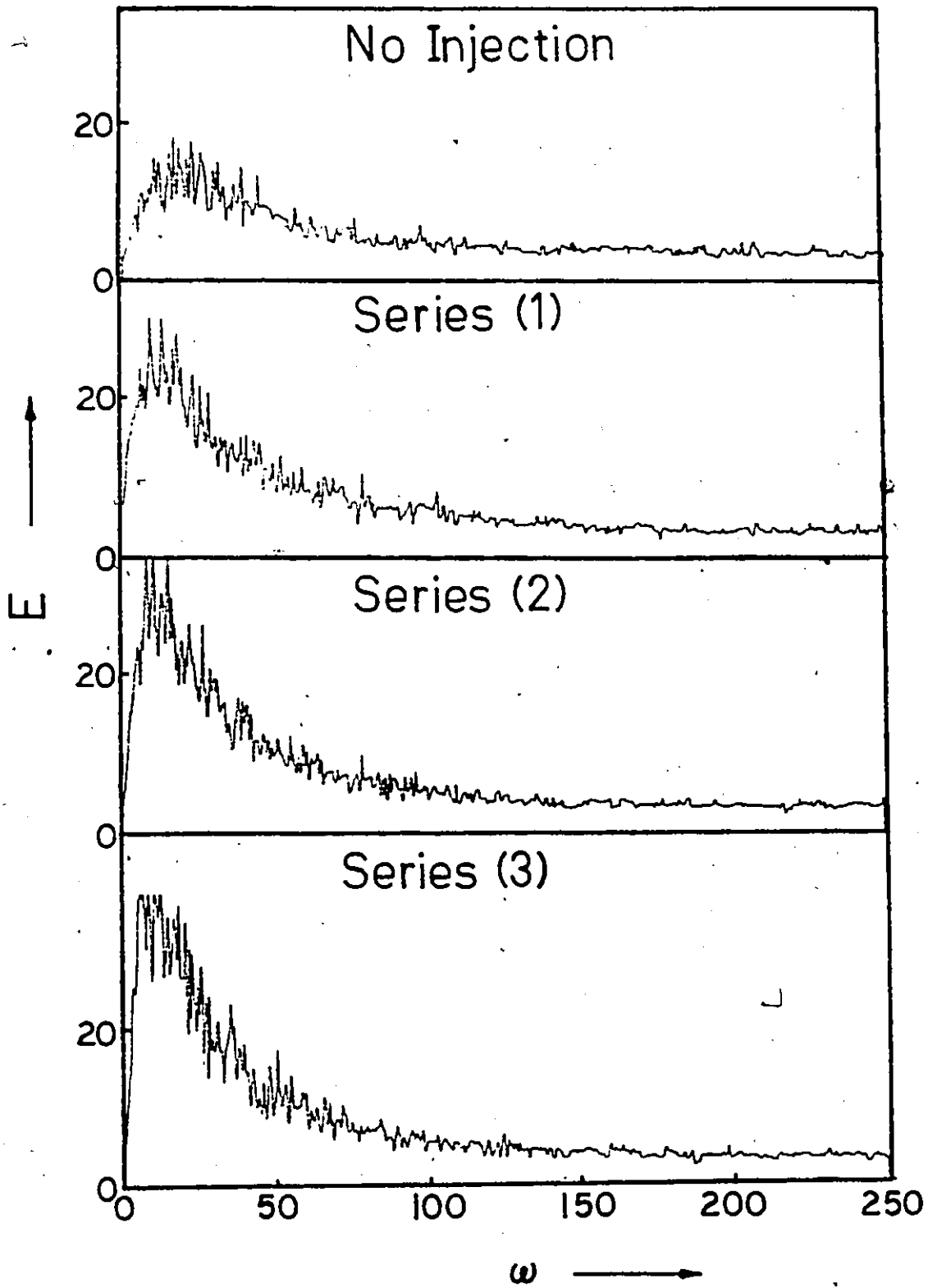


Figure 83. Energy Spectra (Line Source Injection- $C_i = 500$ w.p.p.m.).

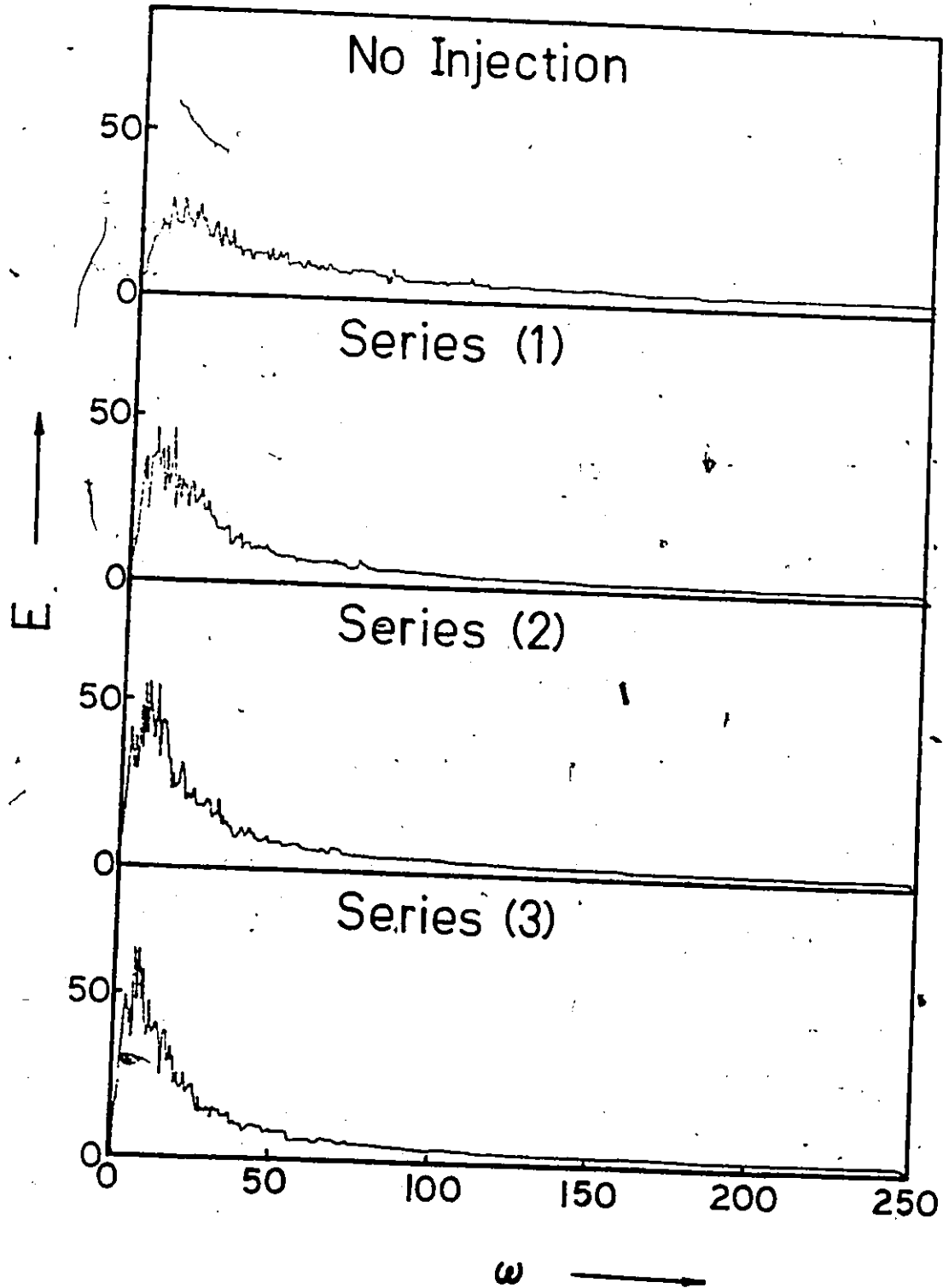


Figure 84. Energy Spectra (Line Source Injection-
 $C_i = 1000$ w.p.p.m.).

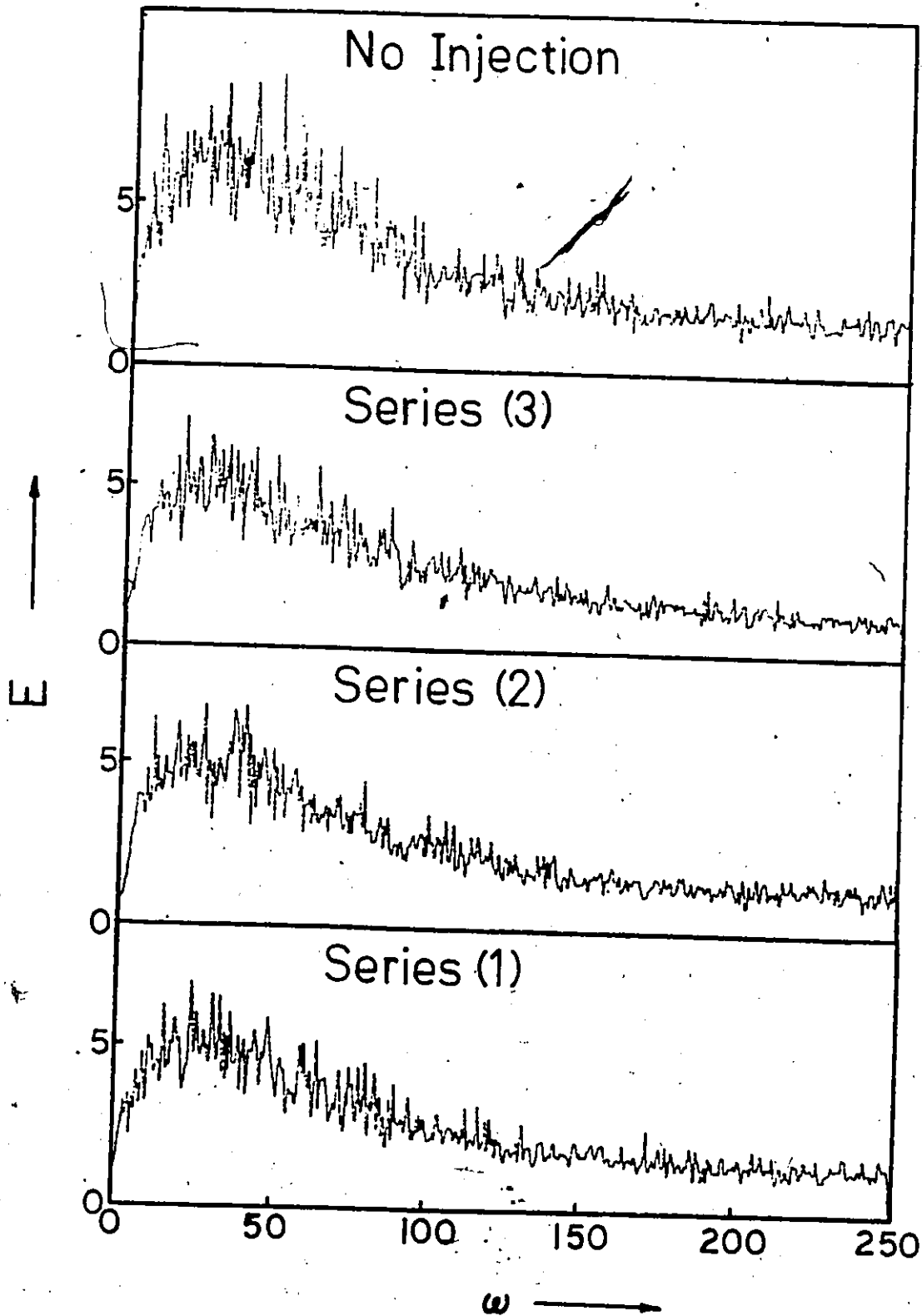


Figure 85. Energy Spectra (Line Source Injection-
 $C_i = 500$ w.p.p.m.).

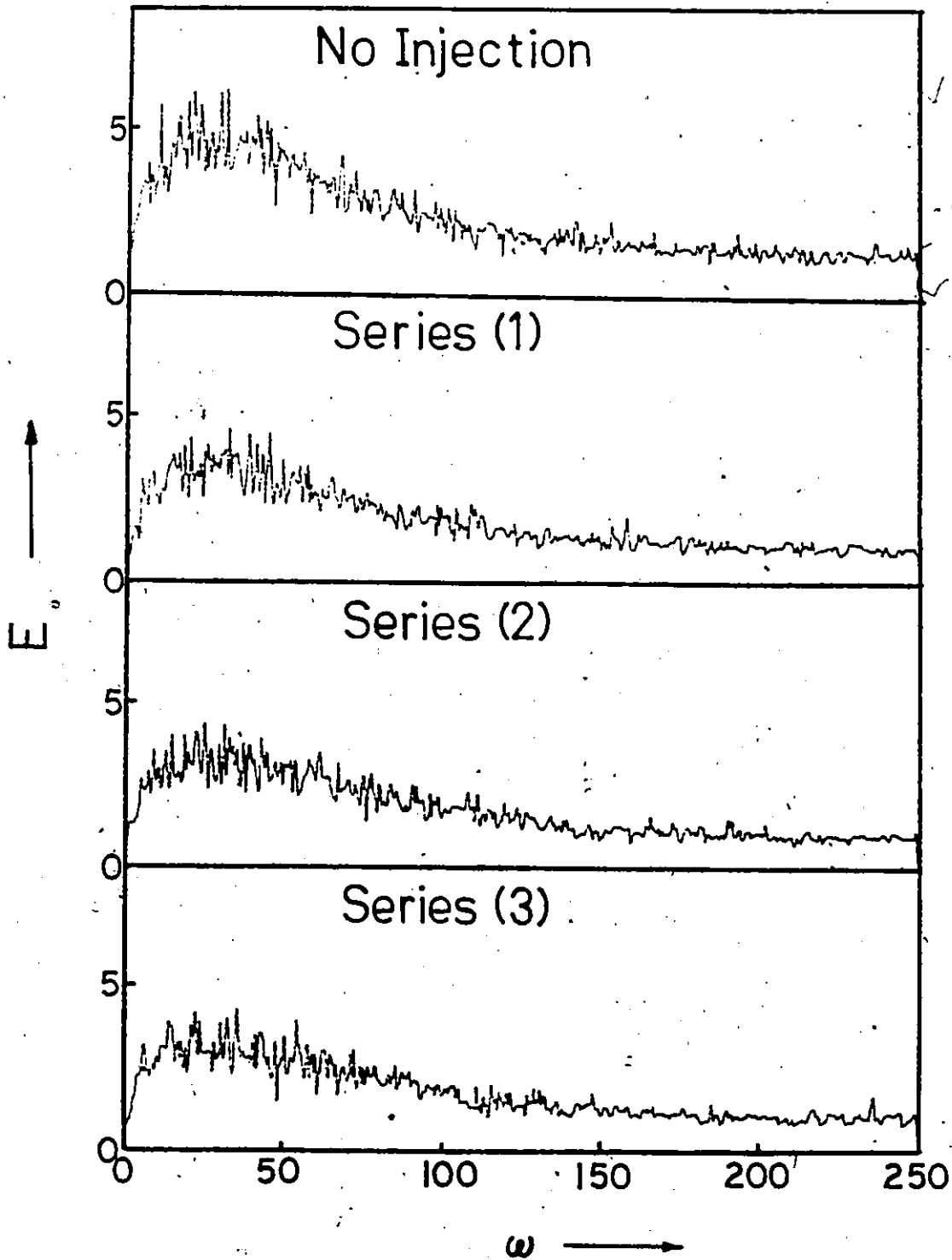


Figure 86. Energy Spectra (Line Source Injection-
 $C_i = 1000$ w.p.p.m.).

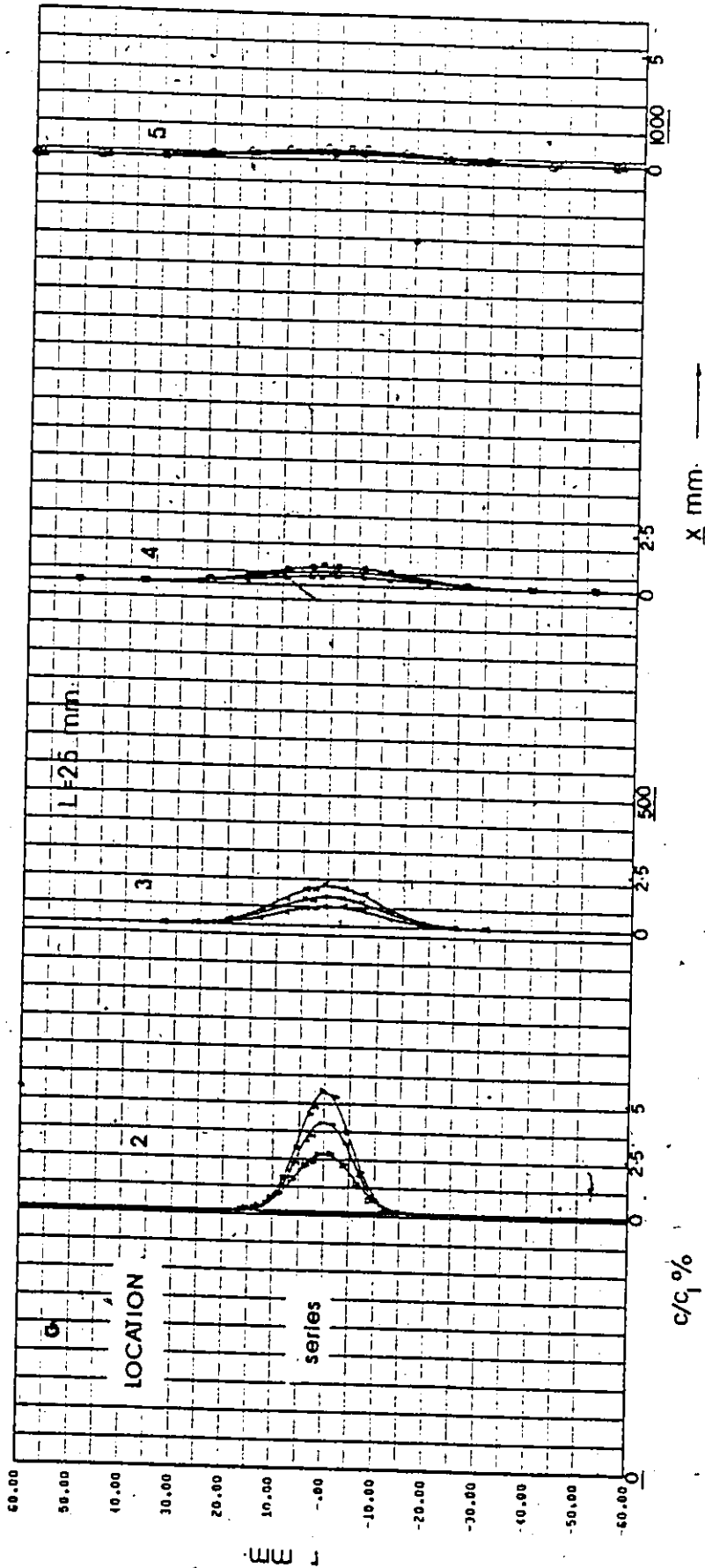


Figure 87. Concentration Profiles (Point Source Injection - Fully Developed Flow - Water Injection).

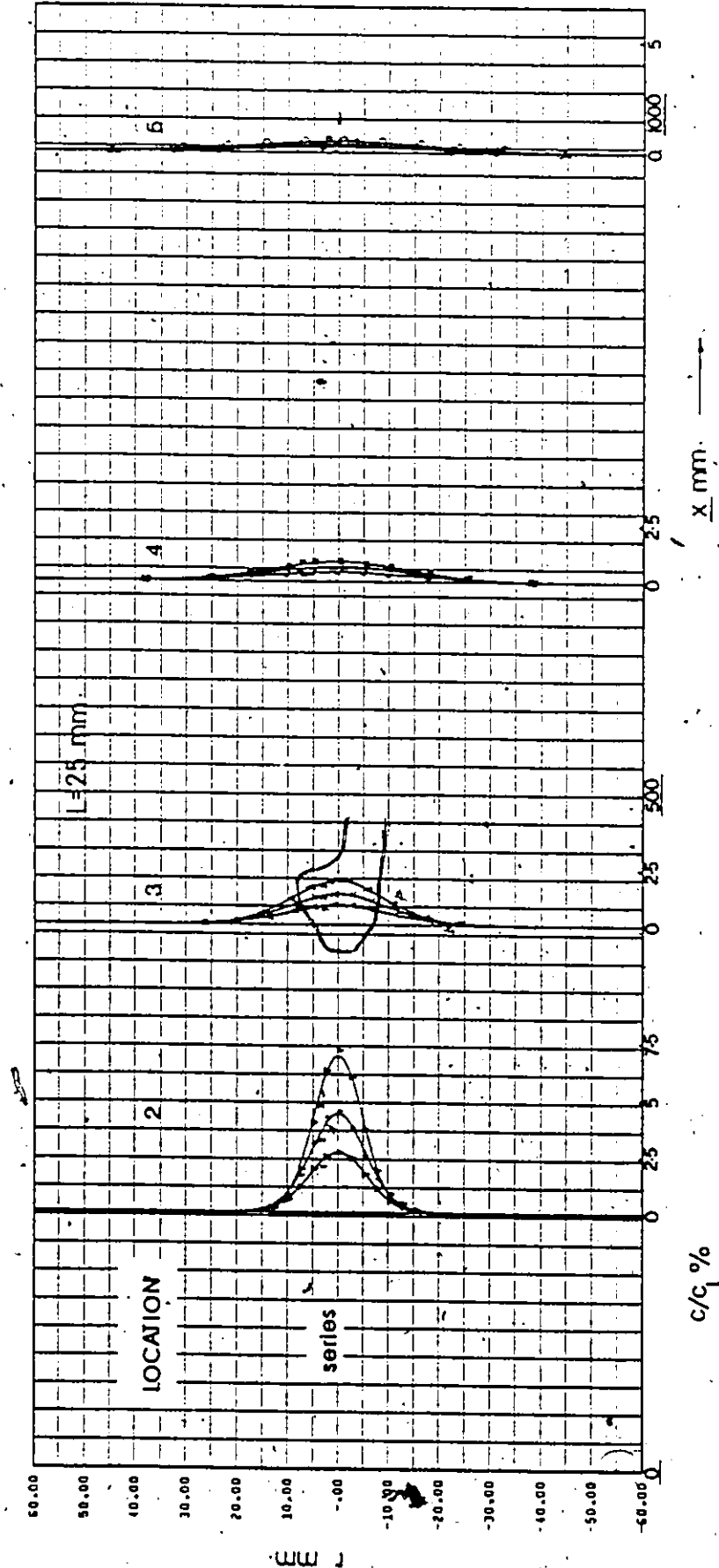


Figure 88. Concentration Profiles (Point Source Injection - Fully Developed Flow - $C_i = 100$ w.p.p.m.).

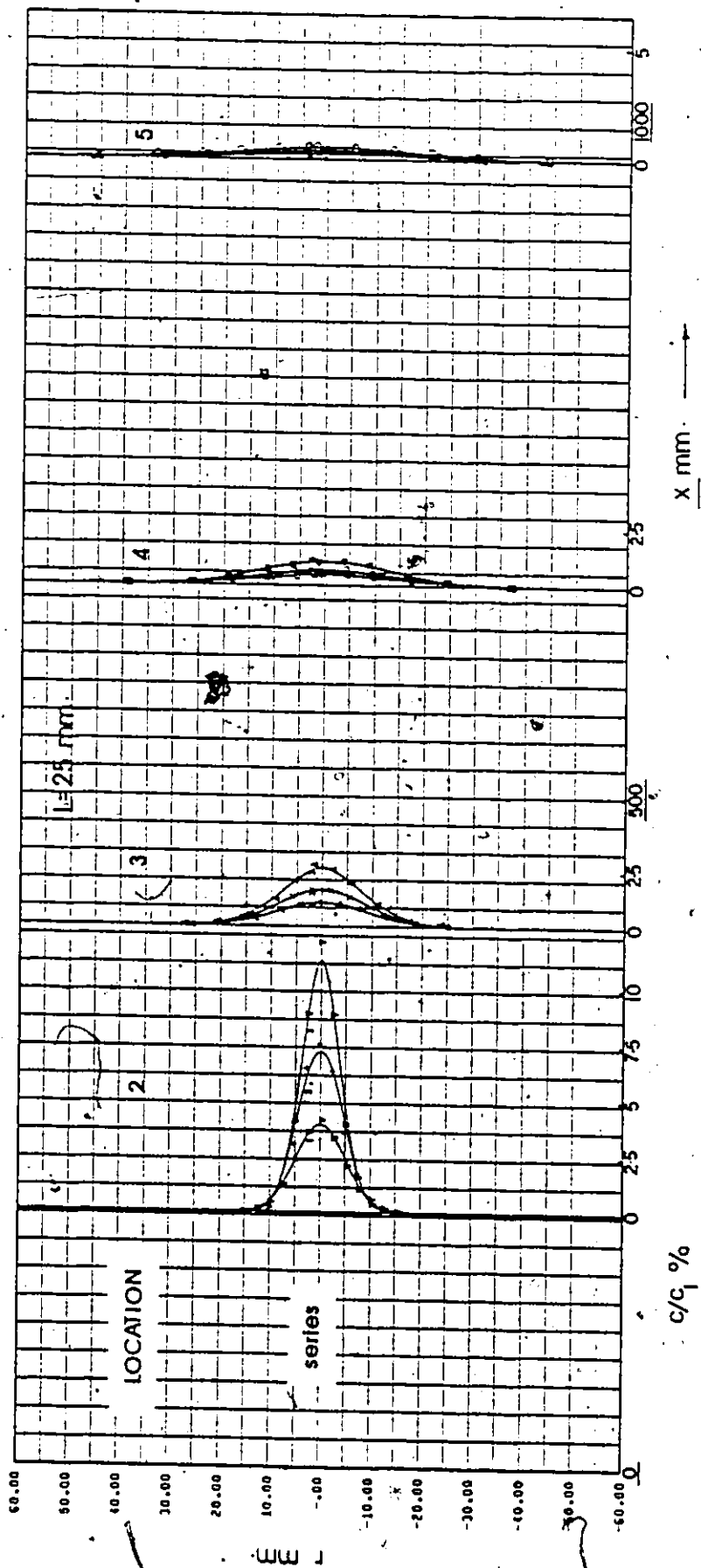


Figure 89. Concentration Profiles (Point Source Injection - Fully Developed Flow - $C_i = 500$ w.p.p.m.).

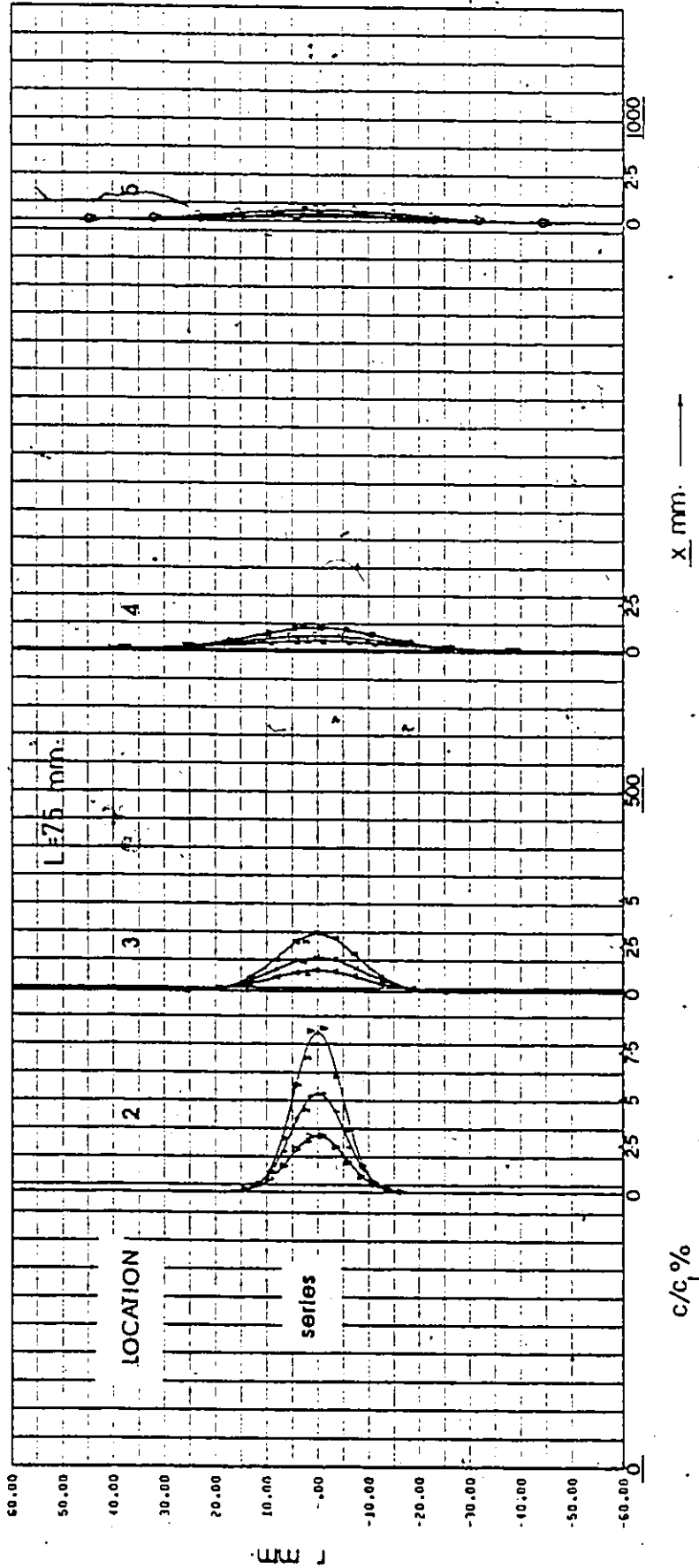


Figure 90. Concentration Profiles (Point Source Injection / Fully Developed Flow - Water Injection).

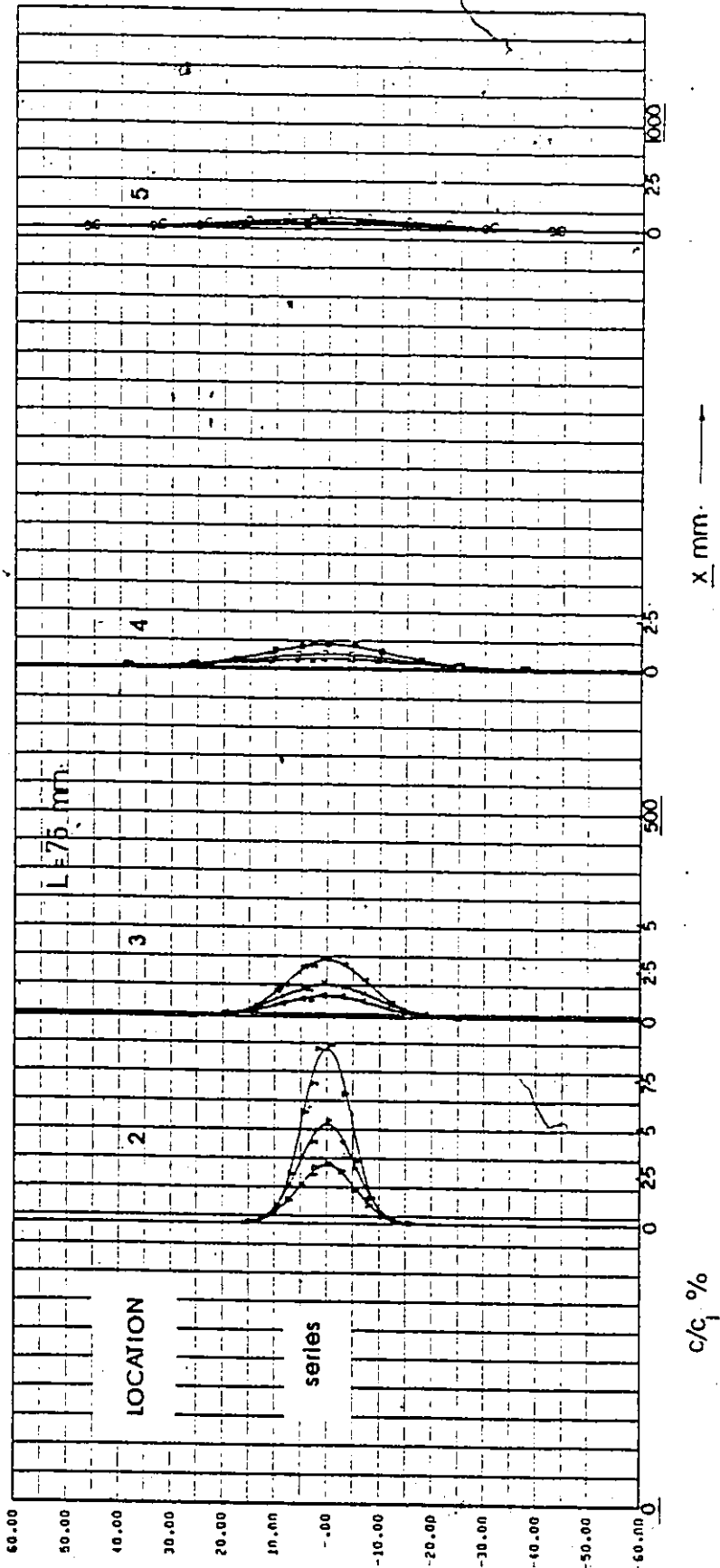


Figure 91. Concentration Profiles (Point Source Injection - Fully Developed Flow - $C_i = 100$ w.p.p.m.).

Handwritten signature or initials.

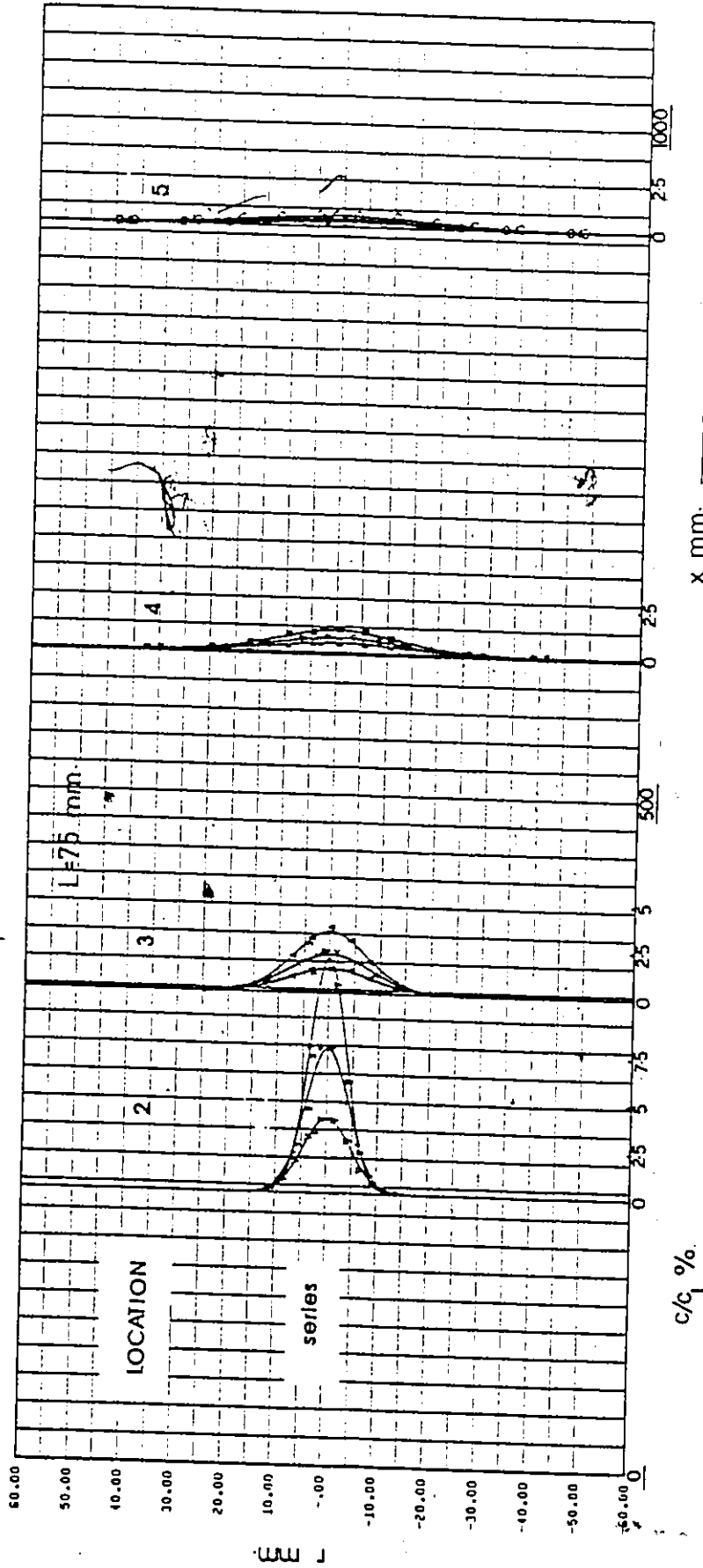


Figure 92. Concentration Profiles (Point Source Injection - Fully Developed Flow - $C_i = 500$ w.p.p.m.).

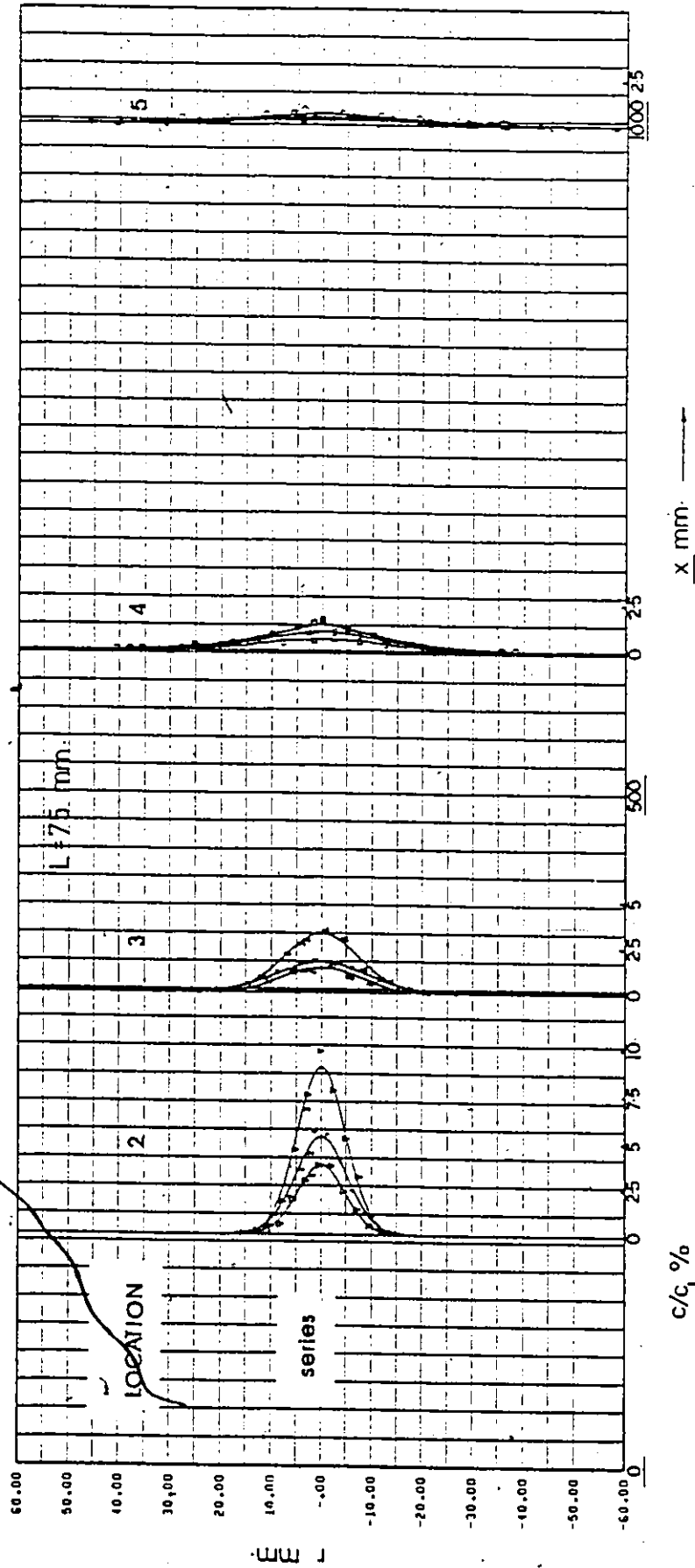


Figure 93. Concentration Profiles (Point Source Injection - Uniform Flow - Water Injection).

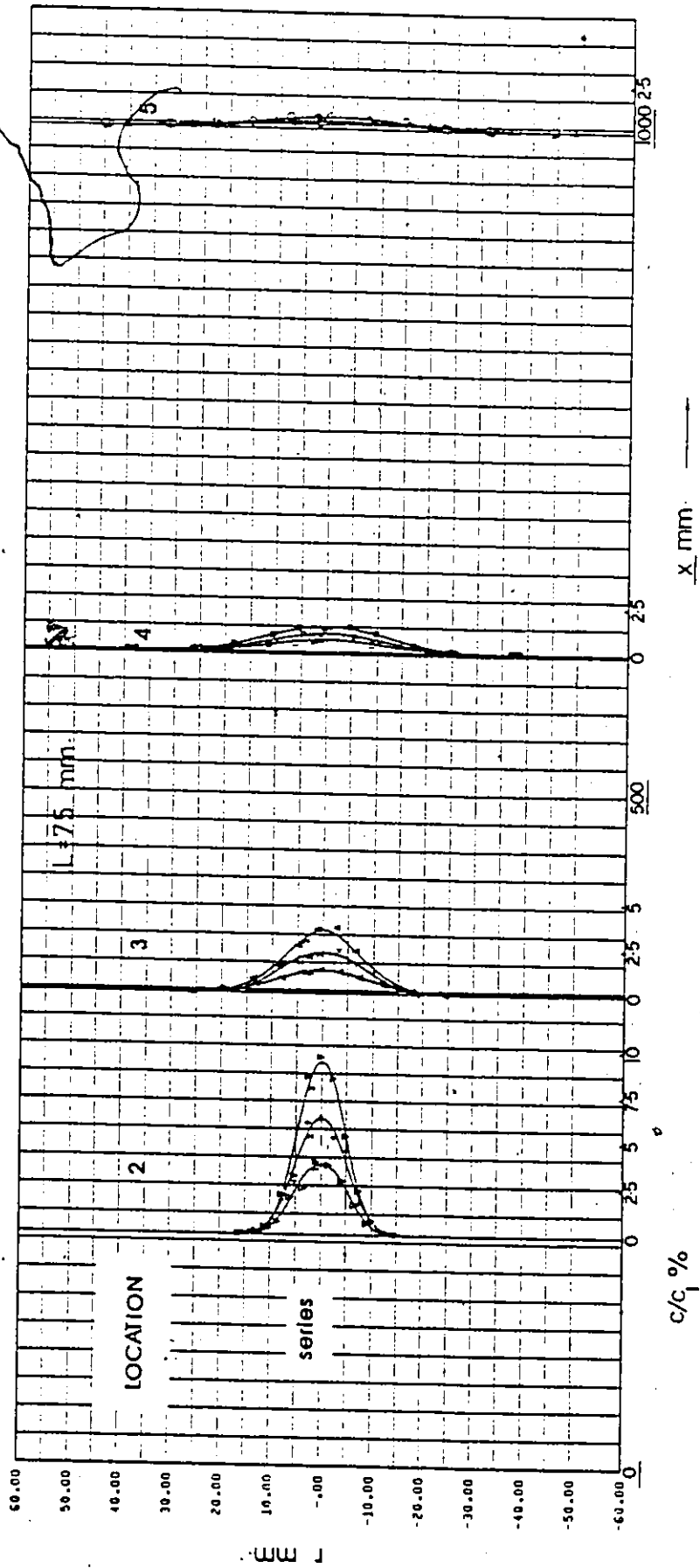


Figure 94. Concentration Profiles (Point Source Injection - Uniform Flow - $C_i = 100$ w.p.p.m.).

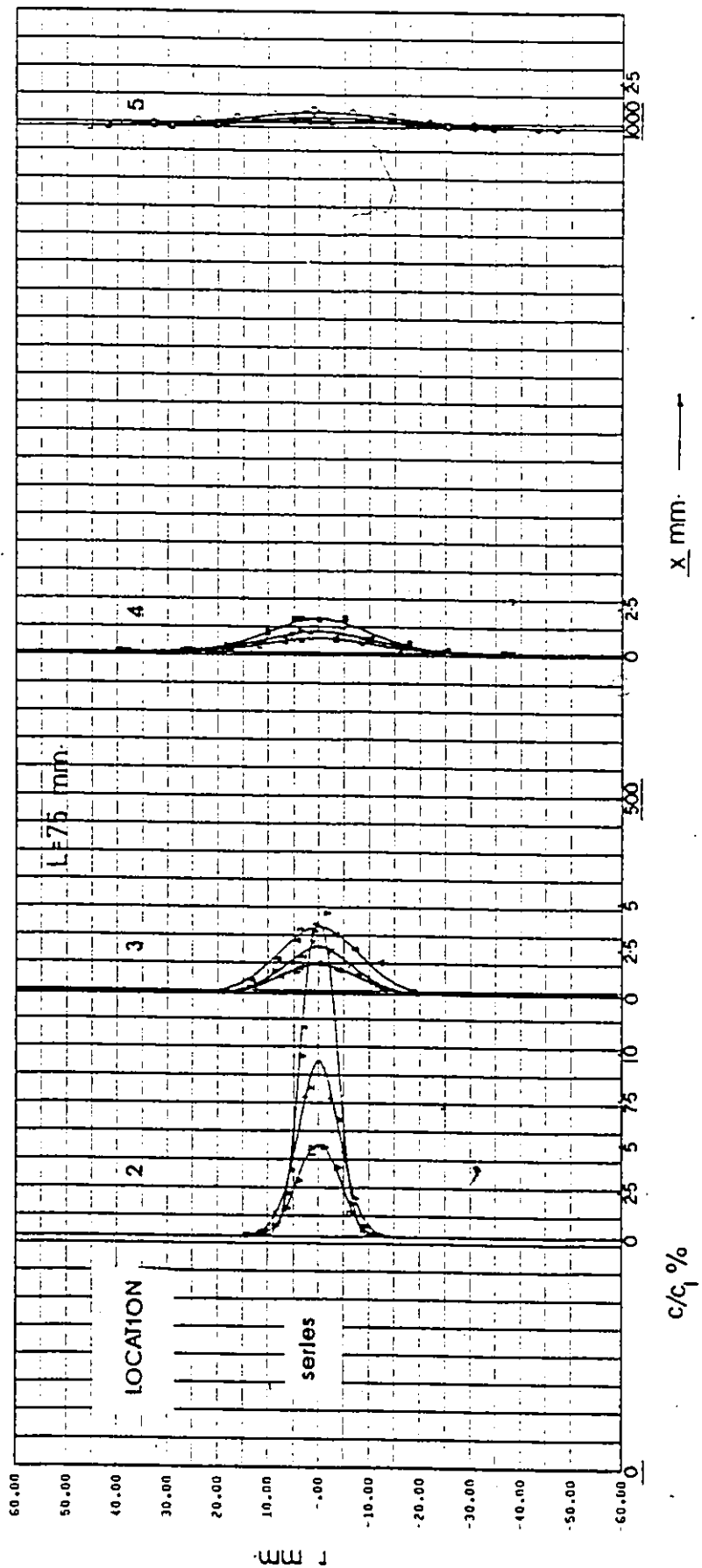


Figure 95. Concentration Profiles (Point Source Injection - Uniform Flow - $C_i = 500$ w.p.p.m.).

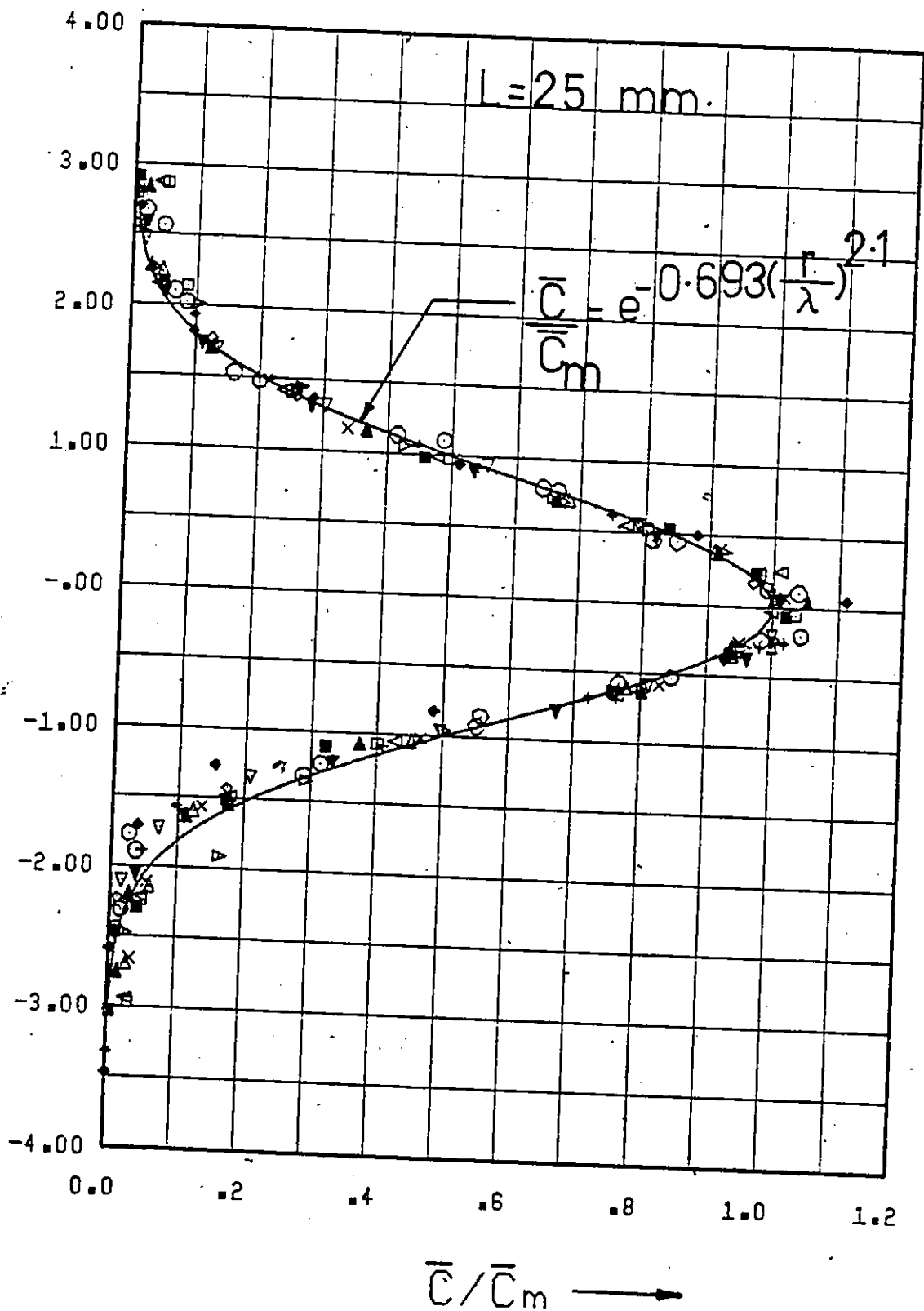


Figure 96. Universal Concentration Profile (Point Source Injection - Fully Developed Flow - Water Injection).

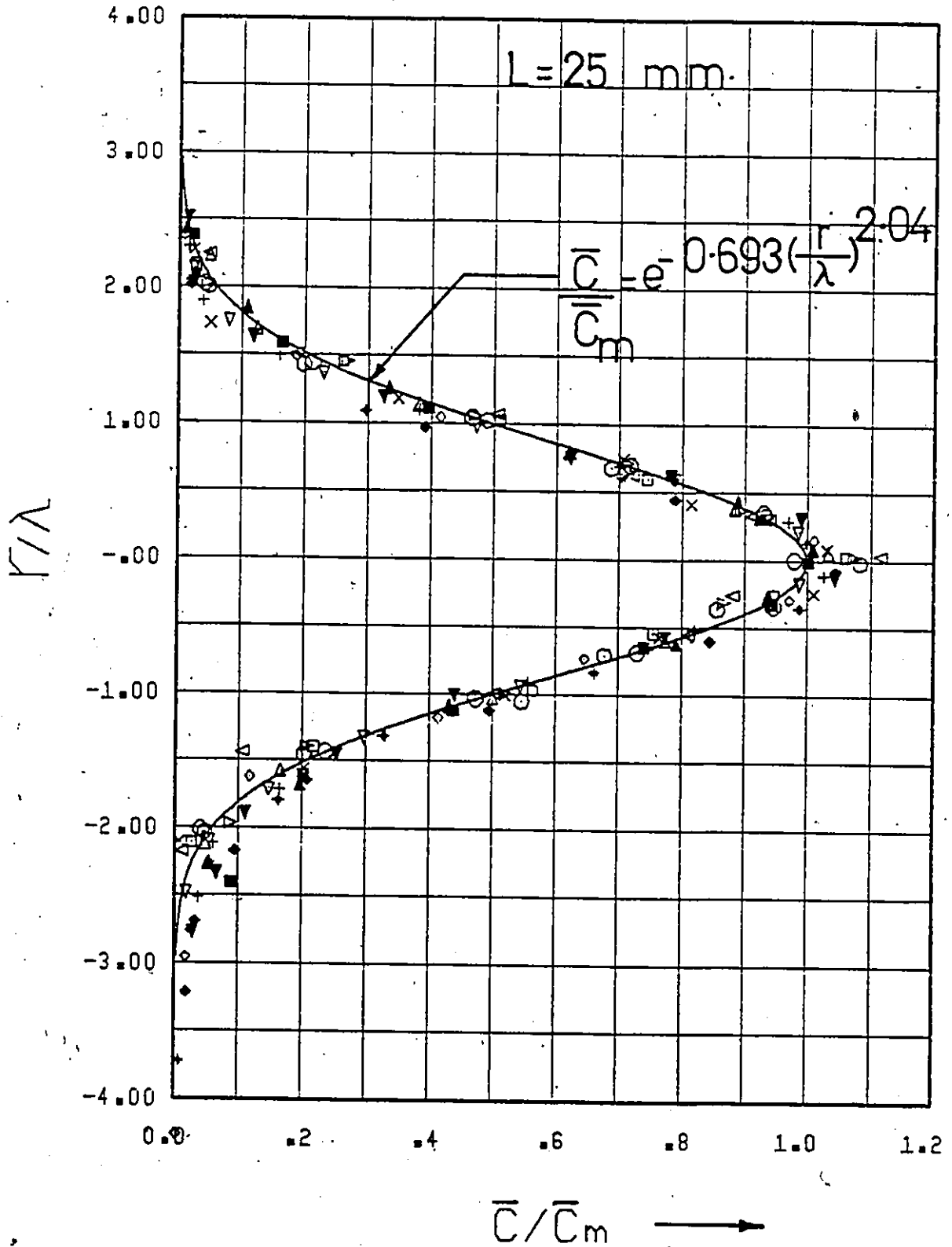


Figure 97. Universal Concentration Profile (Point Source Injection - Fully Developed Flow - $C_i = 100 \text{ w.p.p.m.}$).

IF

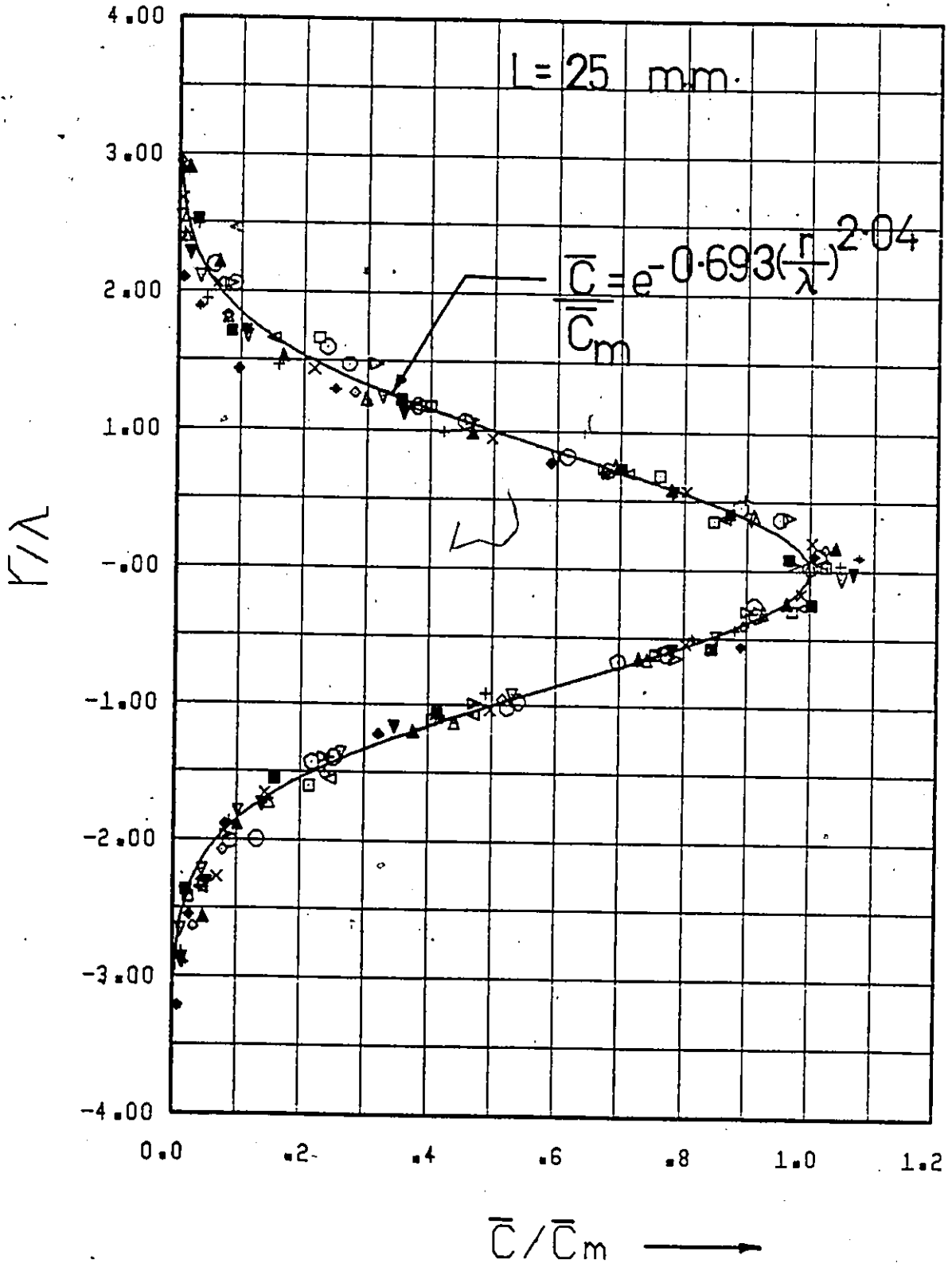


Figure 98. Universal Concentration Profile (Point Source Injection - Fully Developed Flow - $C_i = 500$ w.p.p.m.).

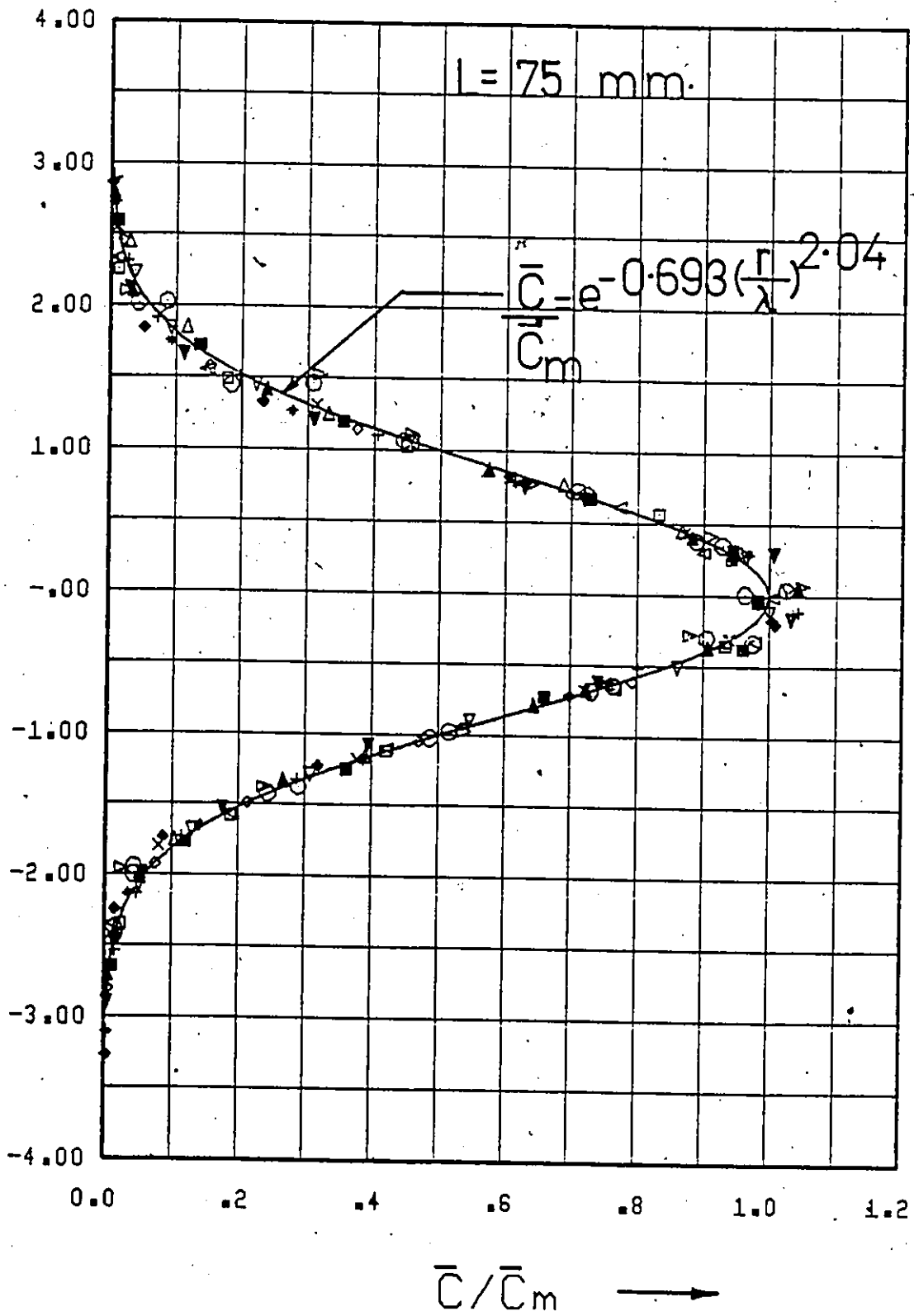


Figure 99. Universal Concentration Profile (Point Source Injection - Fully Developed Flow - Water Injection).

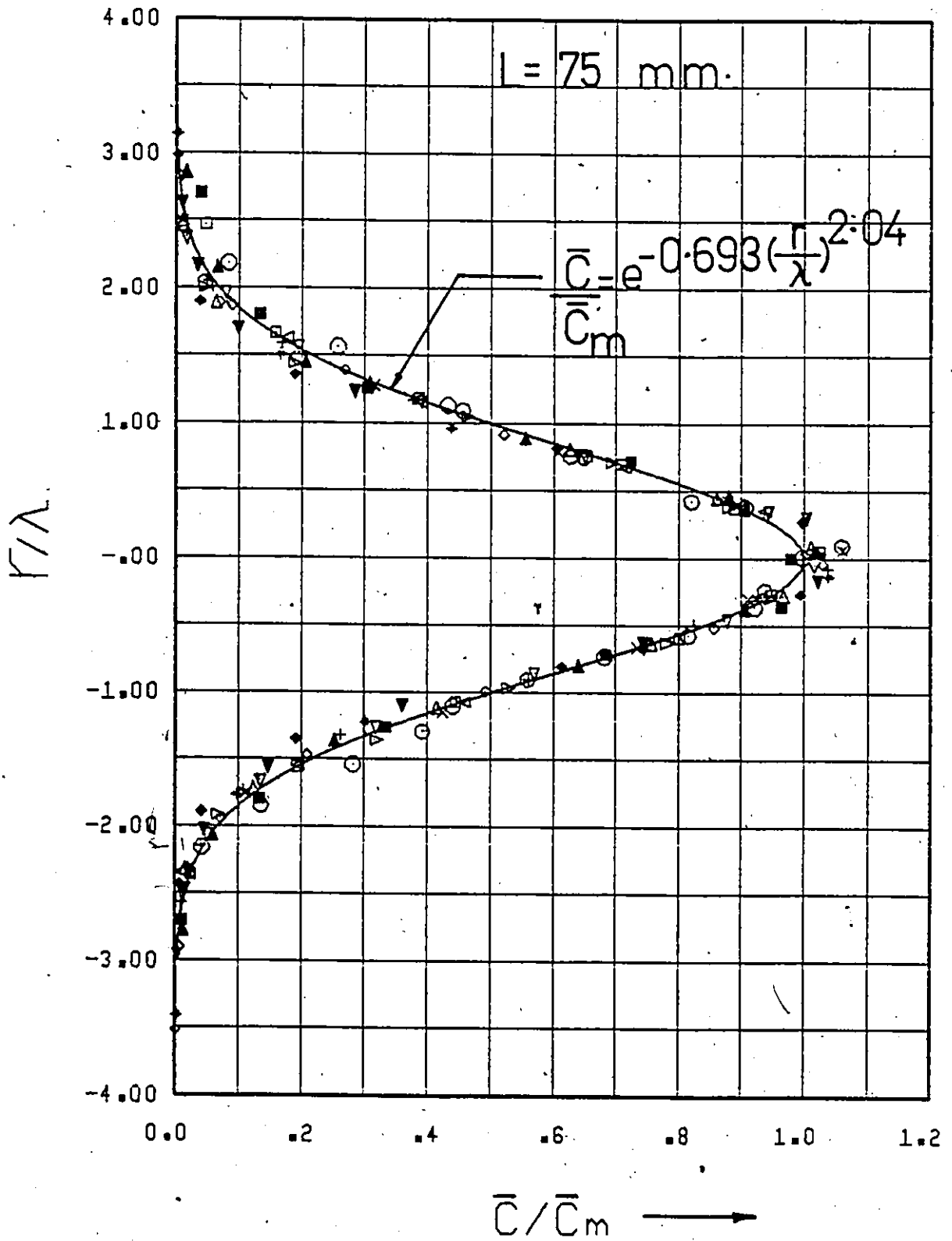


Figure 100. Universal Concentration Profile (Point Source Injection - Fully Developed Flow - $C_i = 100$ w.p.p.m.).

5

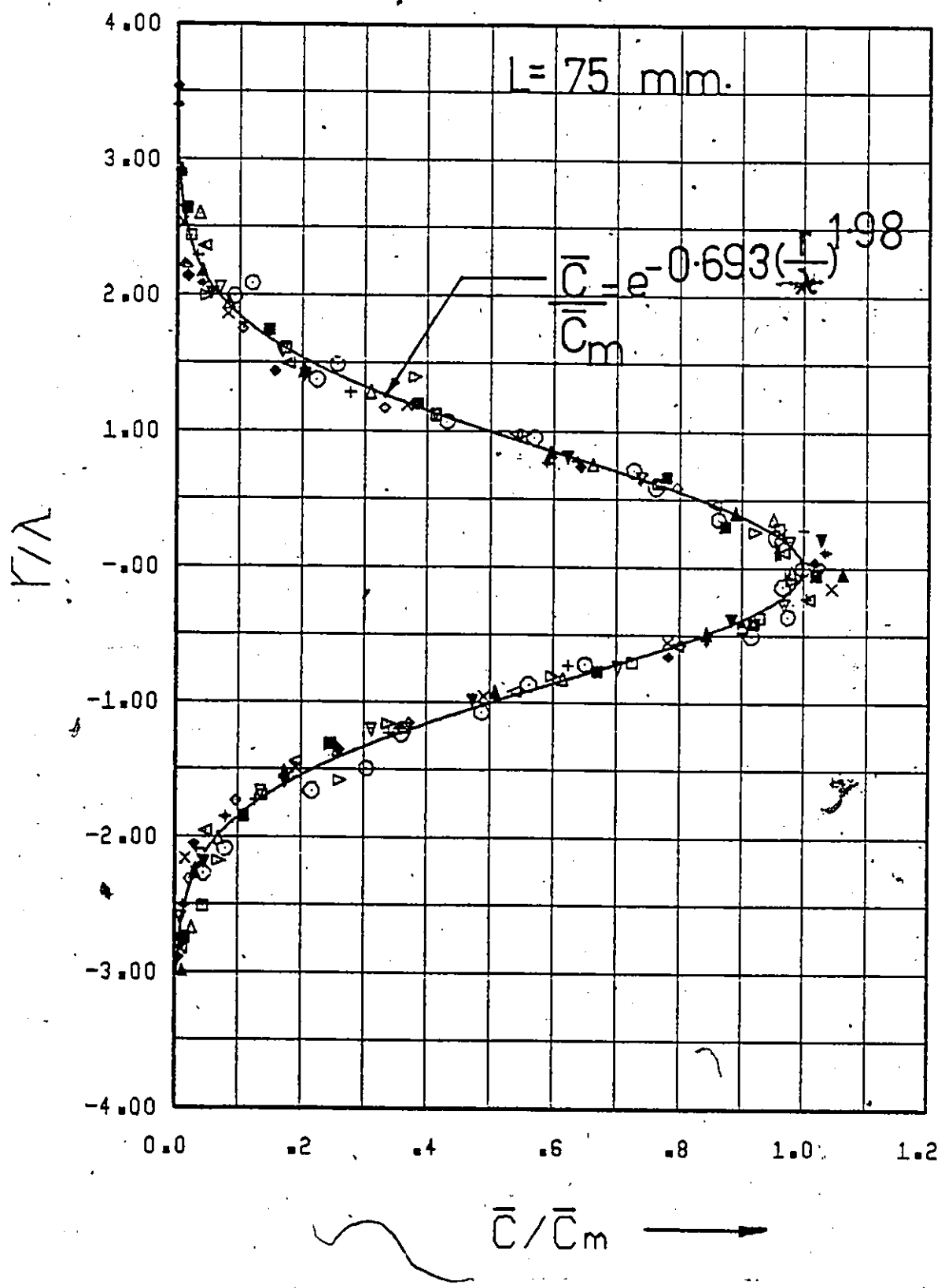


Figure 101. Universal Concentration Profile (Point Source Injection - Fully Developed Flow - $C_i = 500 \text{ w.p.p.m.}$).

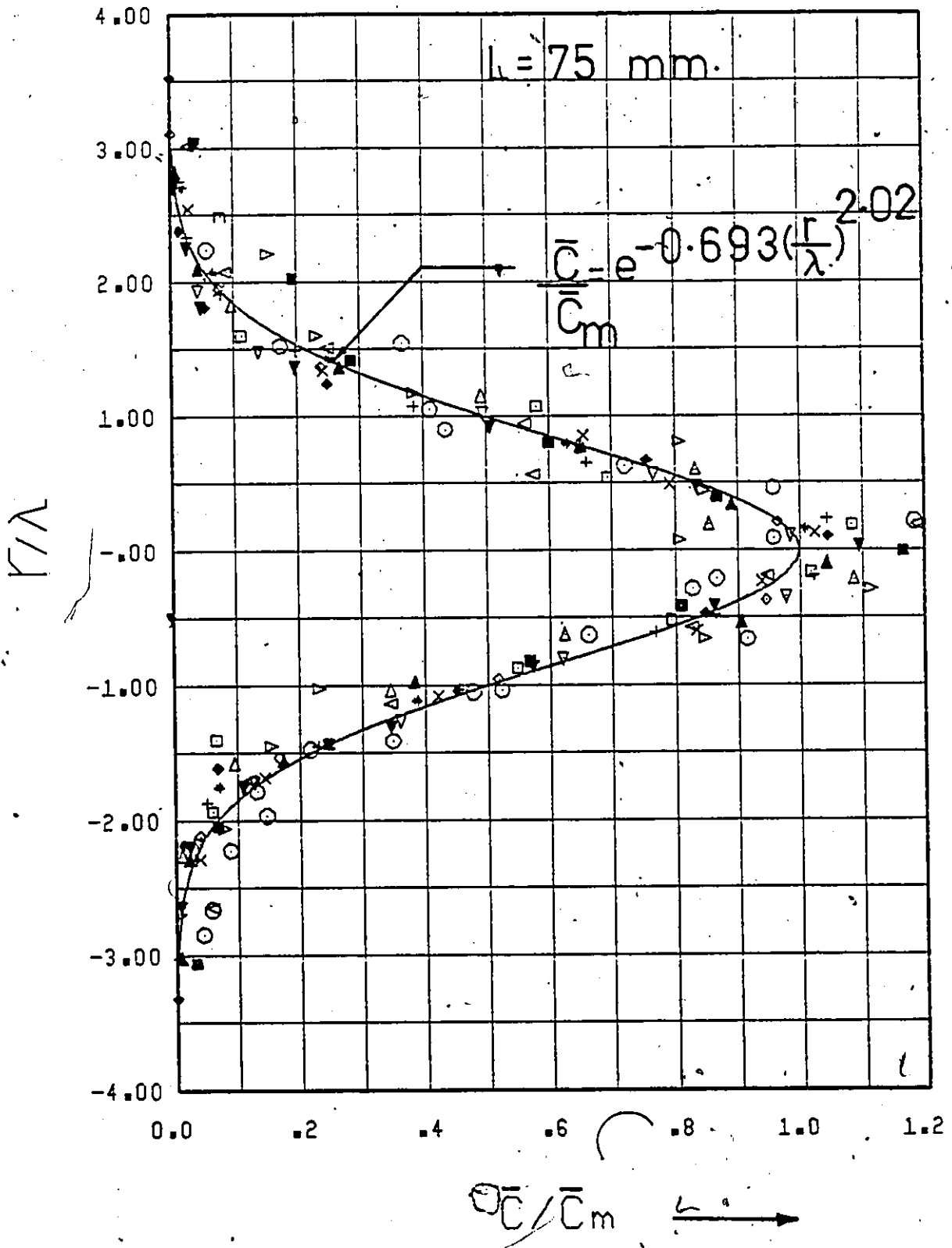


Figure 102. Universal Concentration Profile (Point Source Injection - Uniform Flow - Water Injection).

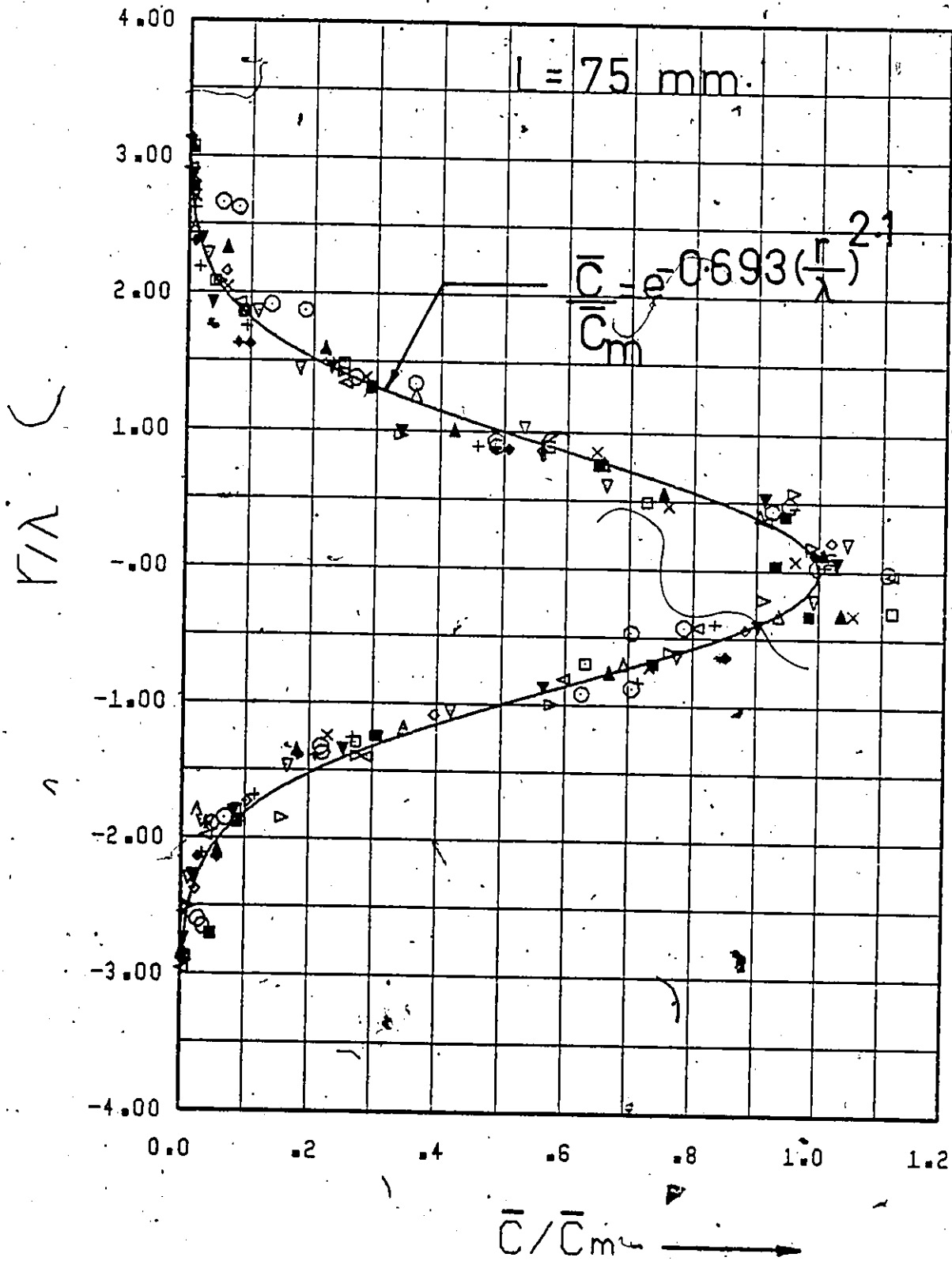


Figure 103. Universal Concentration Profile (Point Source Injection - Uniform Flow - $C_i = 100 \text{ w.p.p.m.}$).

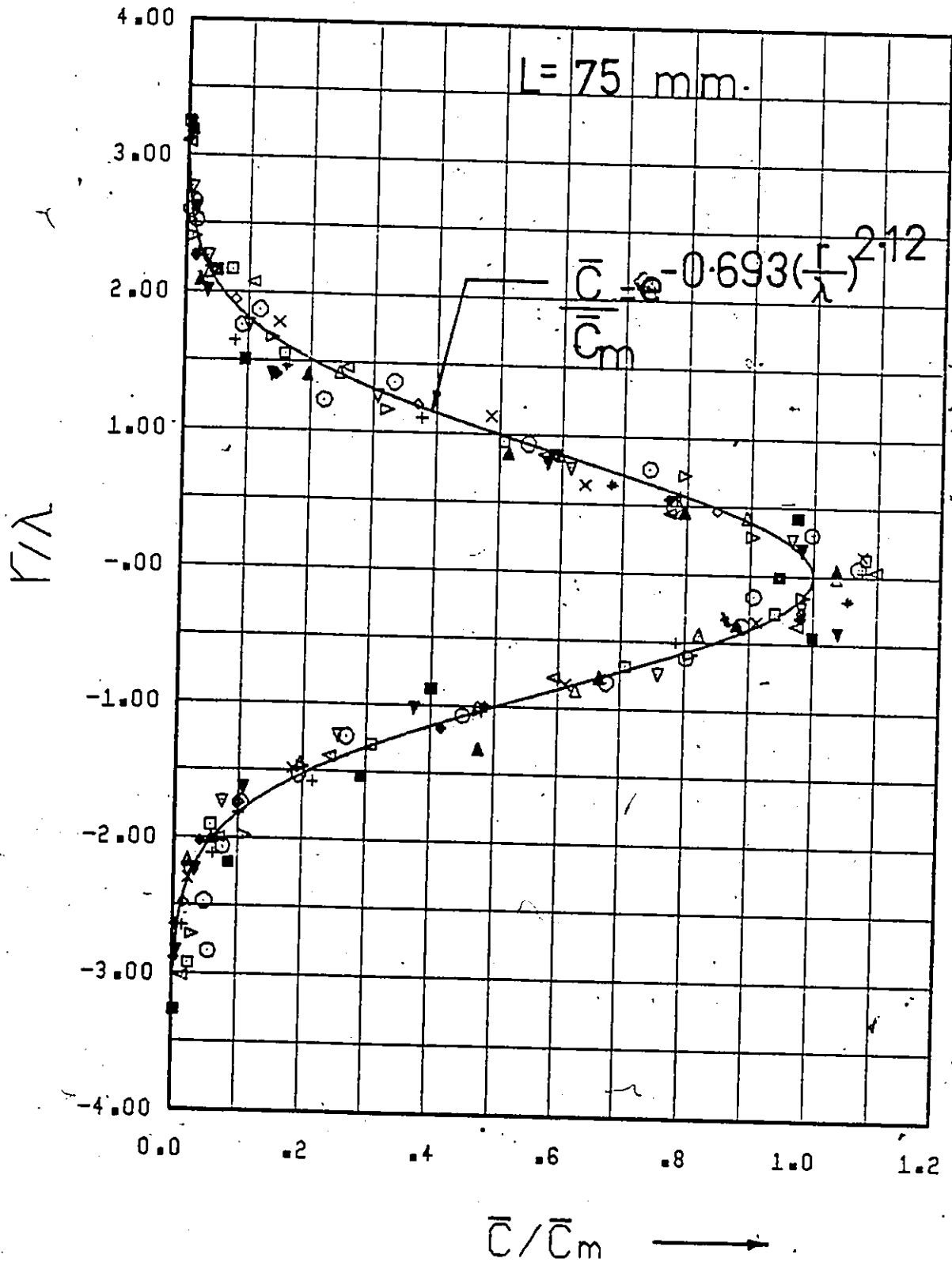


Figure 104. Universal Concentration Profile (Point Source Injection - Uniform Flow - $C_i = 500 \text{ w.p.p.m.}$).

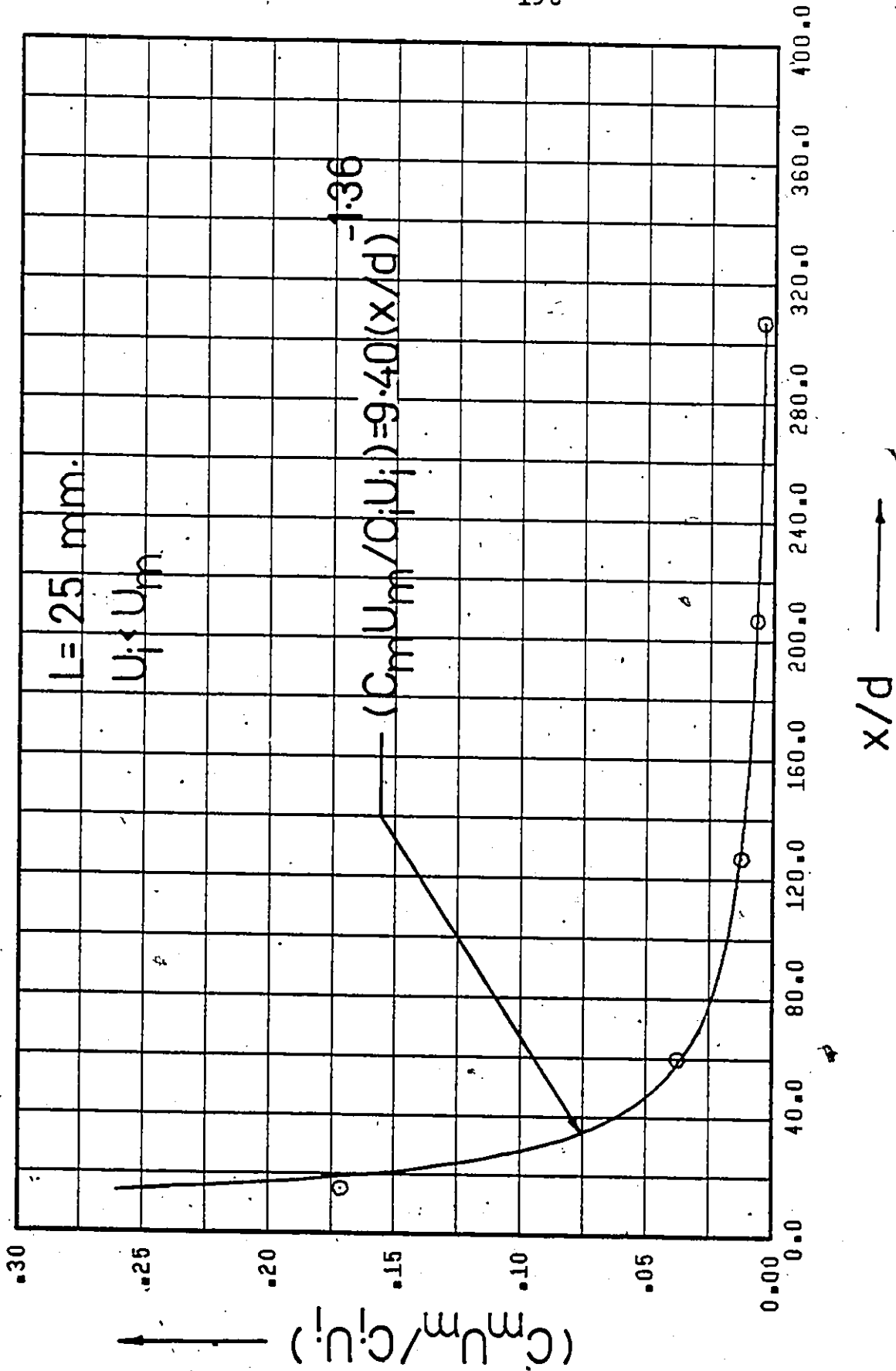


Figure 105. $(C_m U_m / C_i U_i)$ vs. x/d (Point Source Injection - Fully Developed Flow - Water Injection).

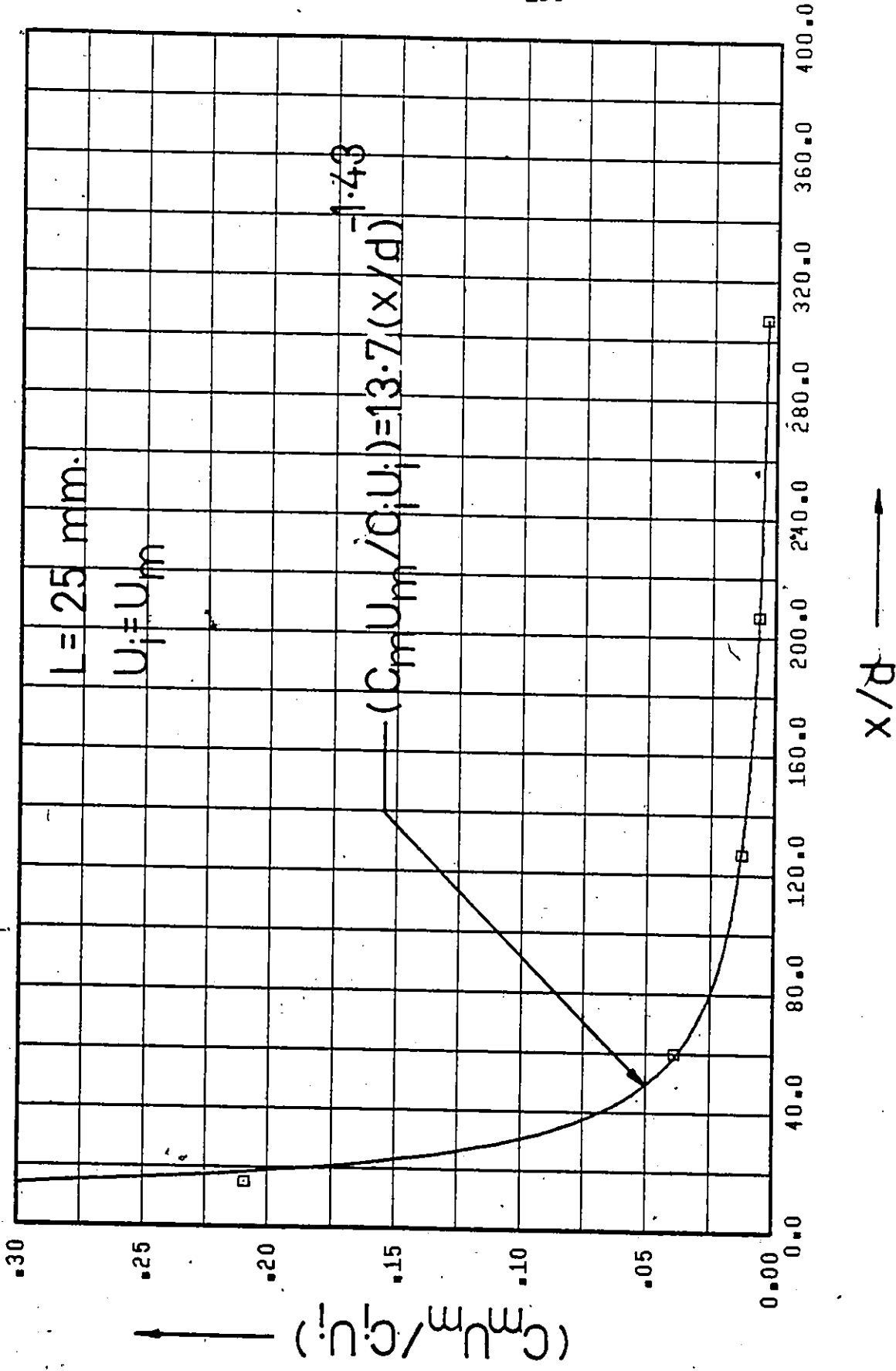


Figure 106. $(C_m U_m / C_i U_i)$ vs. x/d (Point Source Injection - Fully Developed Flow - Water Injection).

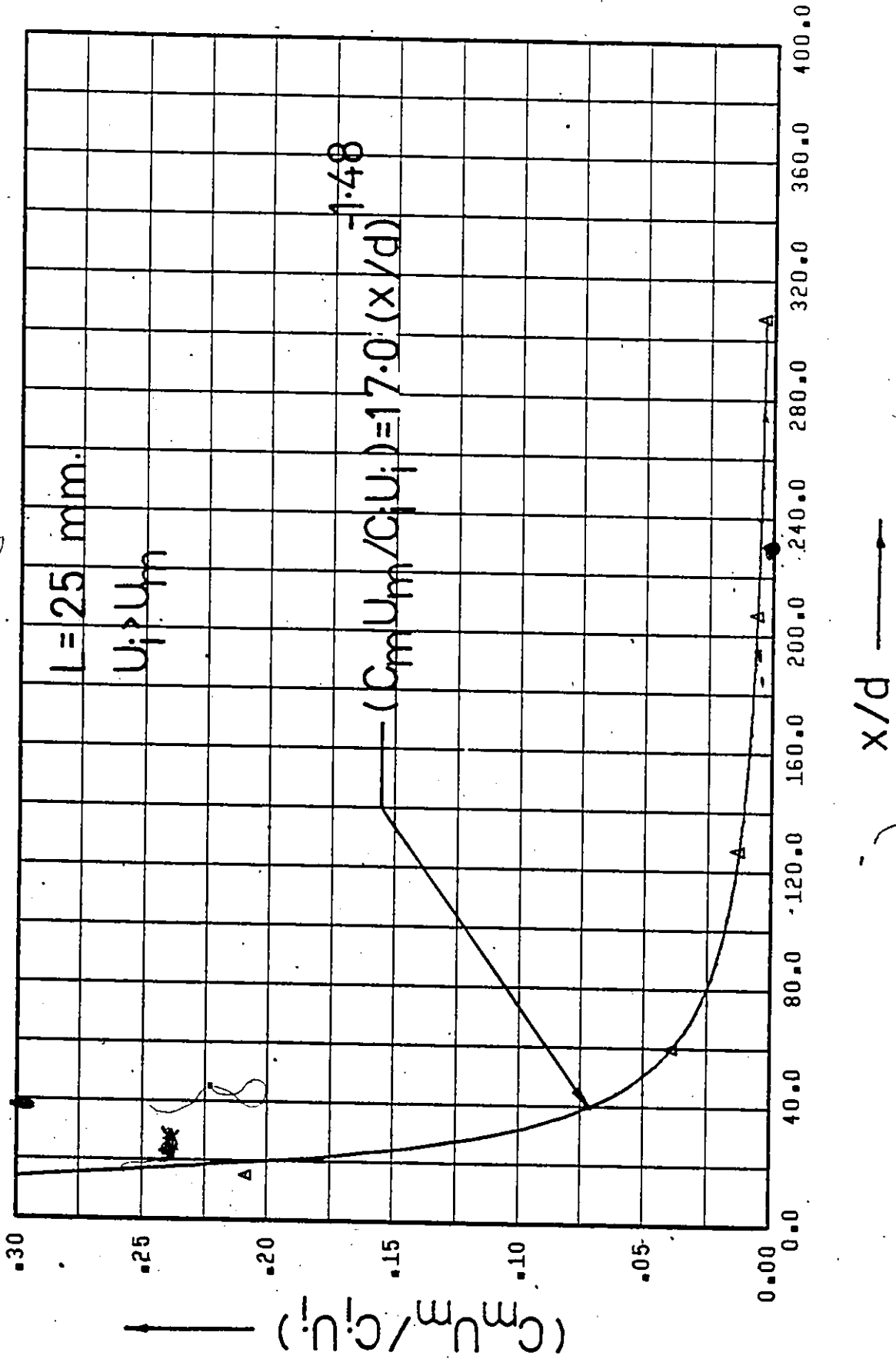


Figure 107. $(C_m U_m / C_i U_i)$ vs. x/d (Point Source Injection - Fully Developed Flow - Water Injection).

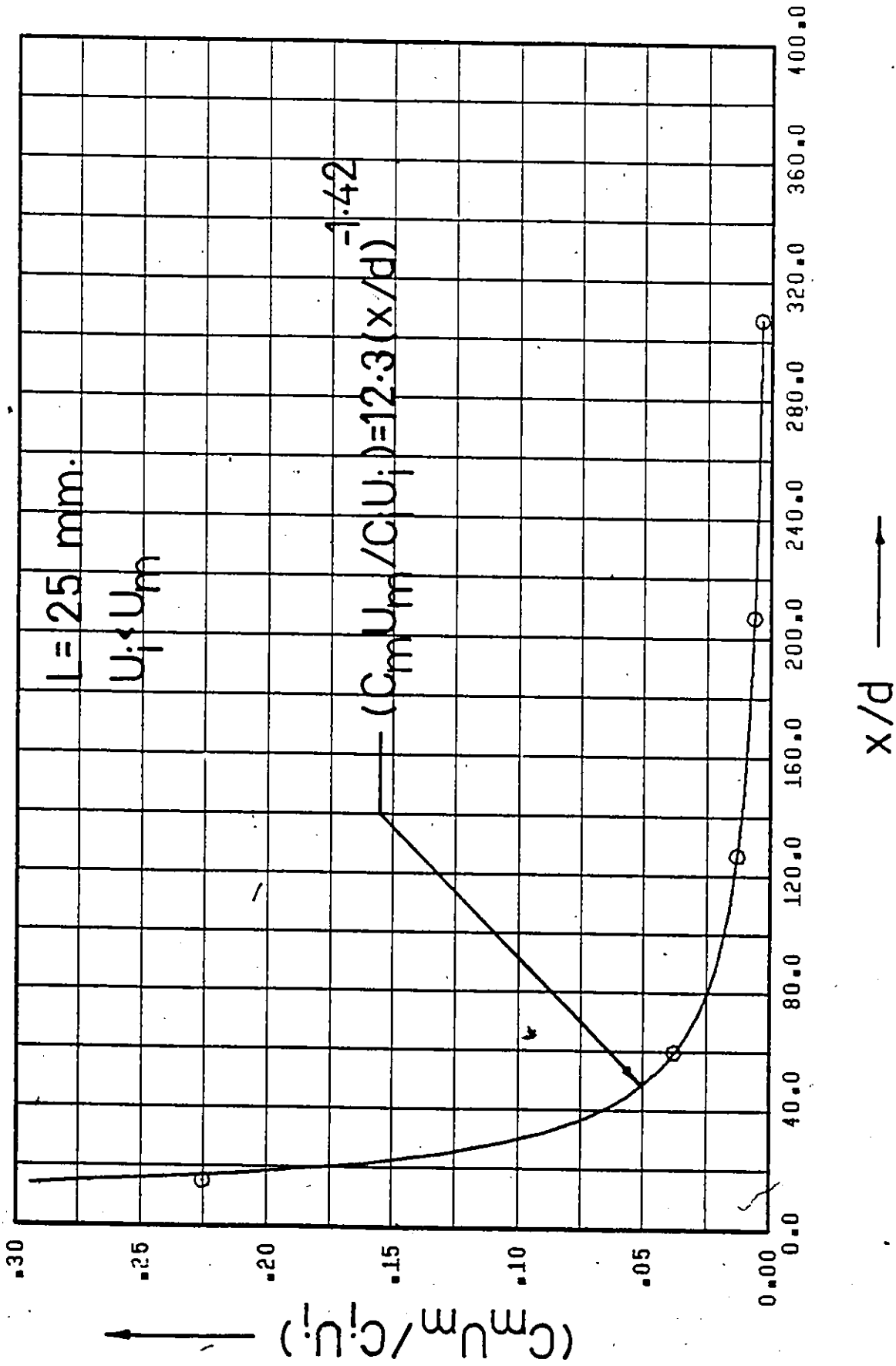


Figure 108 $(C_m U_m / C_i U_i)$ vs. x/d (Point Source Injection - Fully Developed Flow - $C_i = 50 \text{ w.p.p.m.}$).

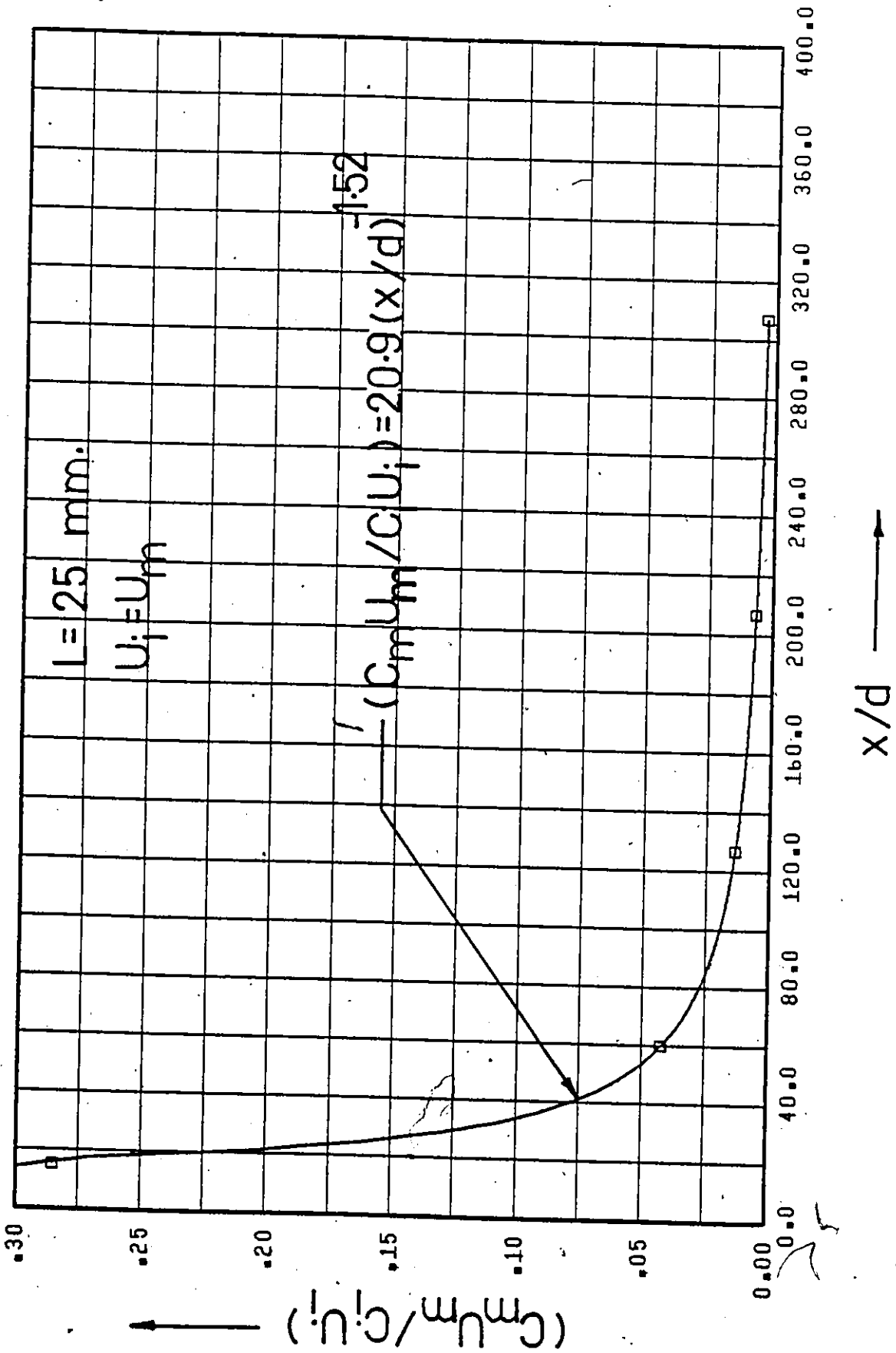


Figure 109. $(C_m U_m / C_i U_i)$ vs. x/d (Point Source Injection - Fully Developed Flow - $C_i = 50 \text{ w.p.p.m.}$).

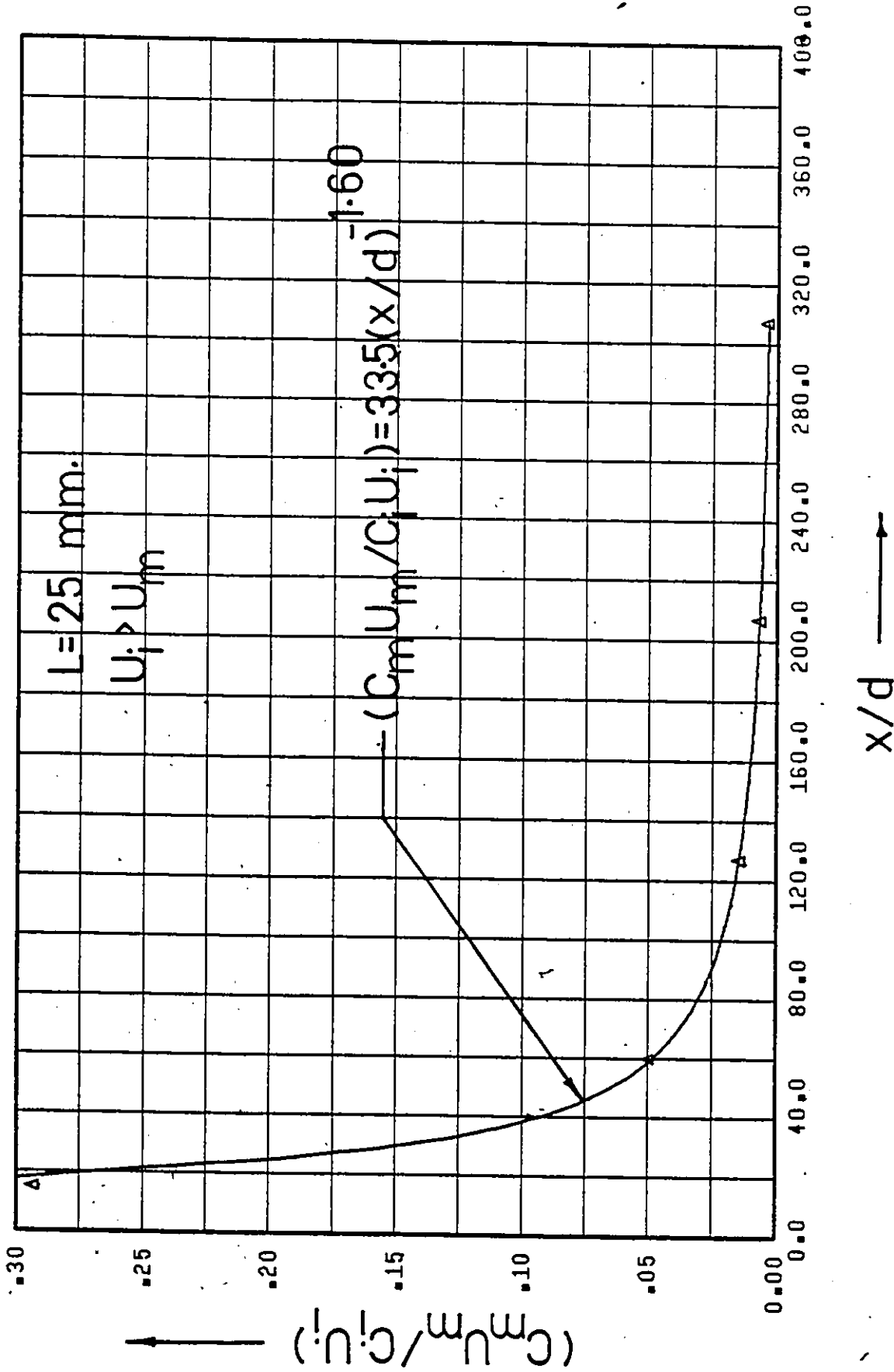


Figure 110. $(C_m U_m / C_i U_i)$ vs. x/d (Point Source Injection - Fully Developed Flow - $C_i = 50$ w.p.p.m.).

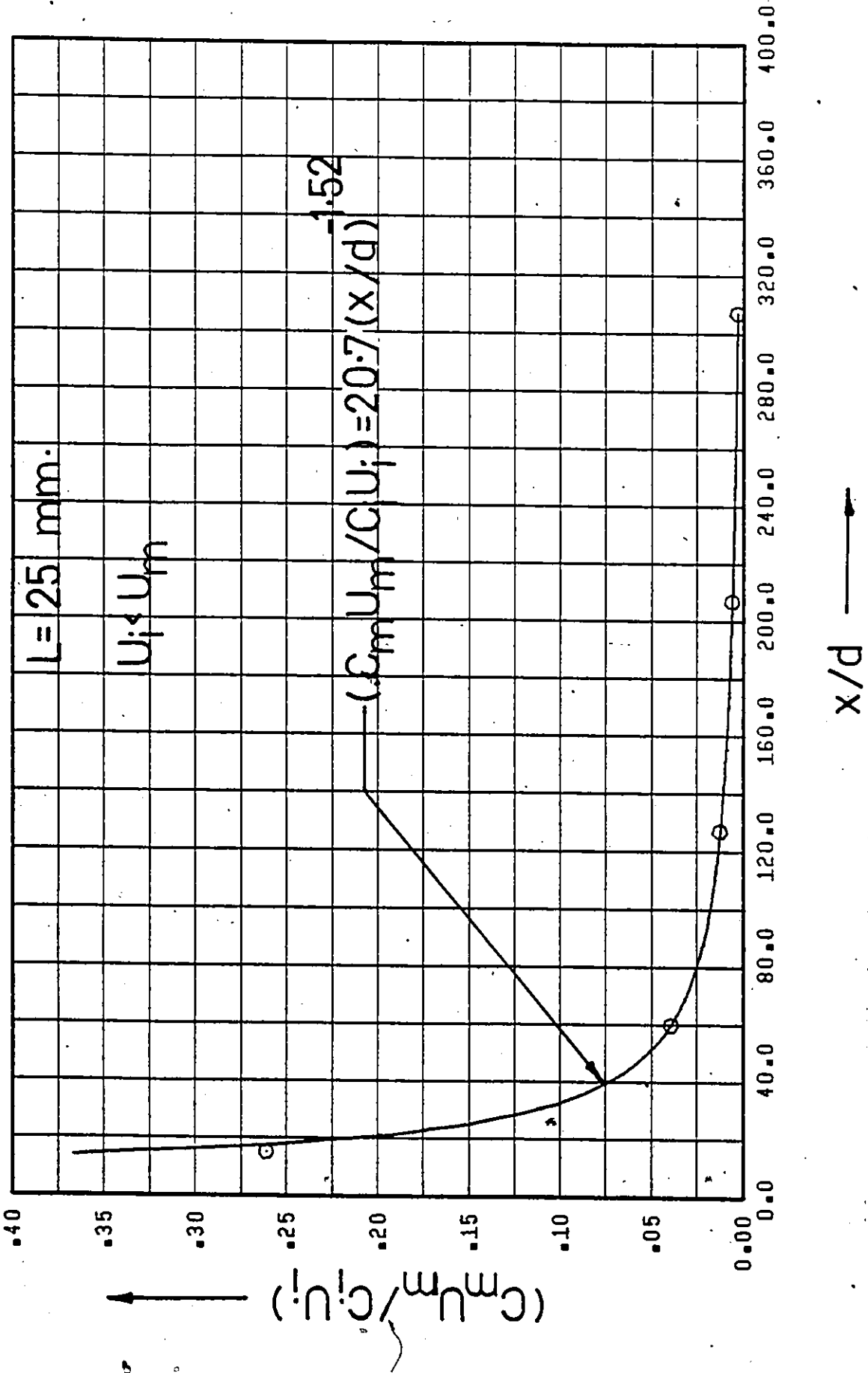


Figure 111. $(C_m U_m / C_i U_i)$ vs. x/d (Point Source Injection - Fully Developed Flow - $C_i = 100 \text{ w.p.p.m.}$).

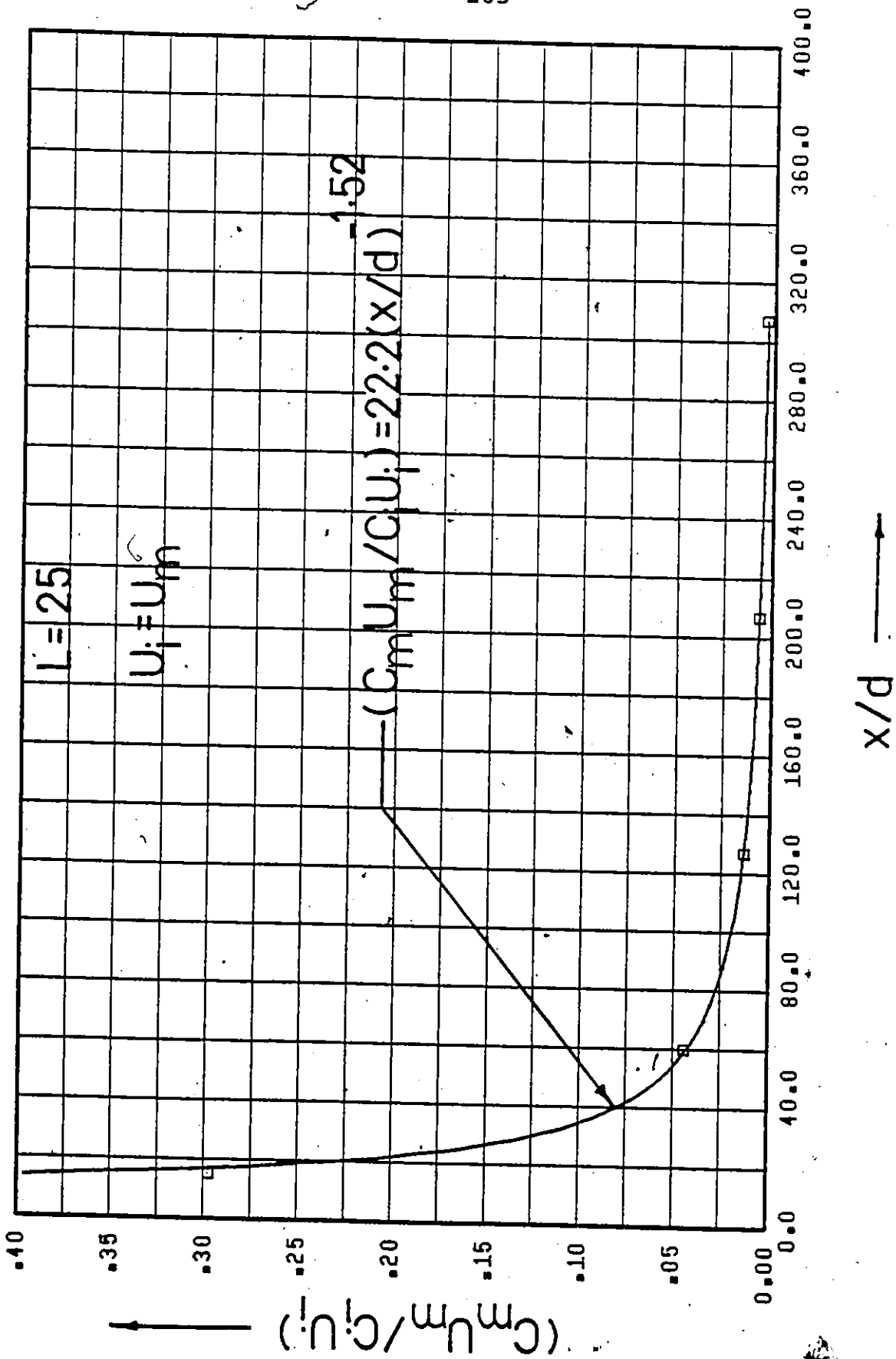


Figure 112. $(C_m U_m / C_i U_i)$ vs. x/d (Point Source Injection - Fully Developed Flow - $C_i = 100$ w.p.p.m.).

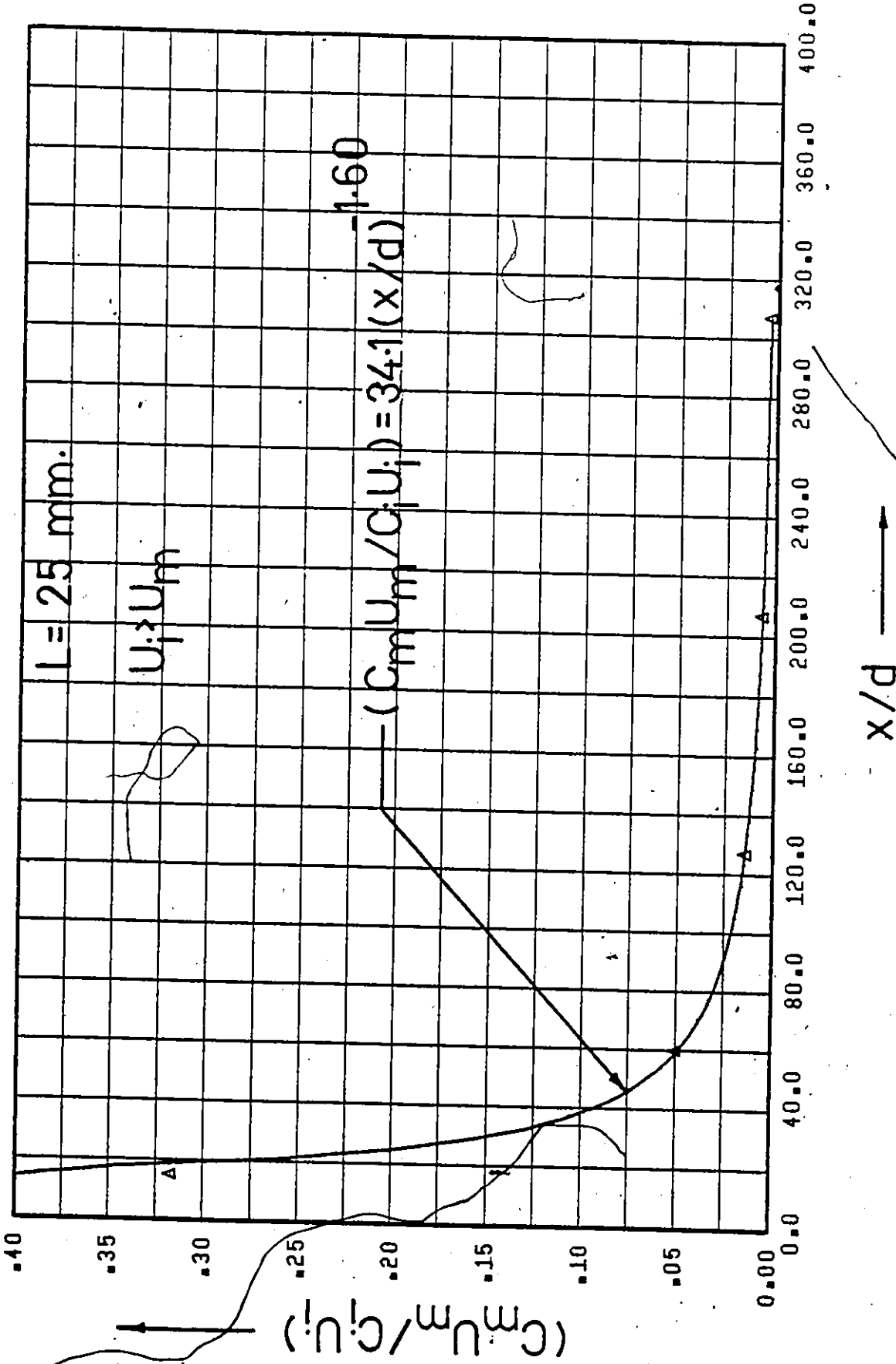


Figure 113. $(C_m U_m / C_i U_i)$ vs. x/d (Point Source Injection - Fully Developed Flow - $C_i = 100 \text{ w.p.p.m.}$).

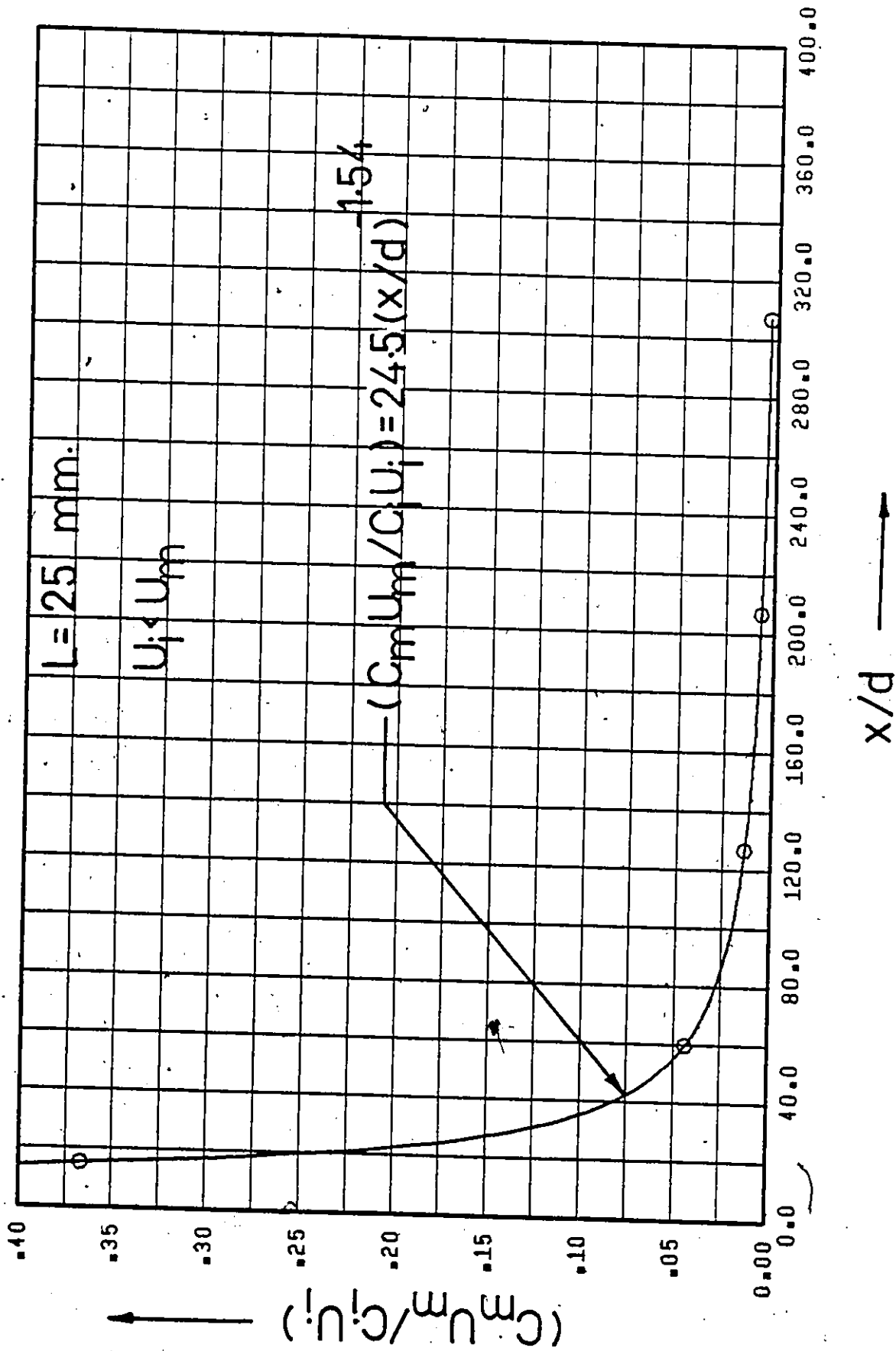


Figure 114. $(C_m U_m / C_i U_i)$ vs. x/d (Point Source Injection Fully Developed Flow - $C_i = 250 \text{ w.p.p.m.}$).

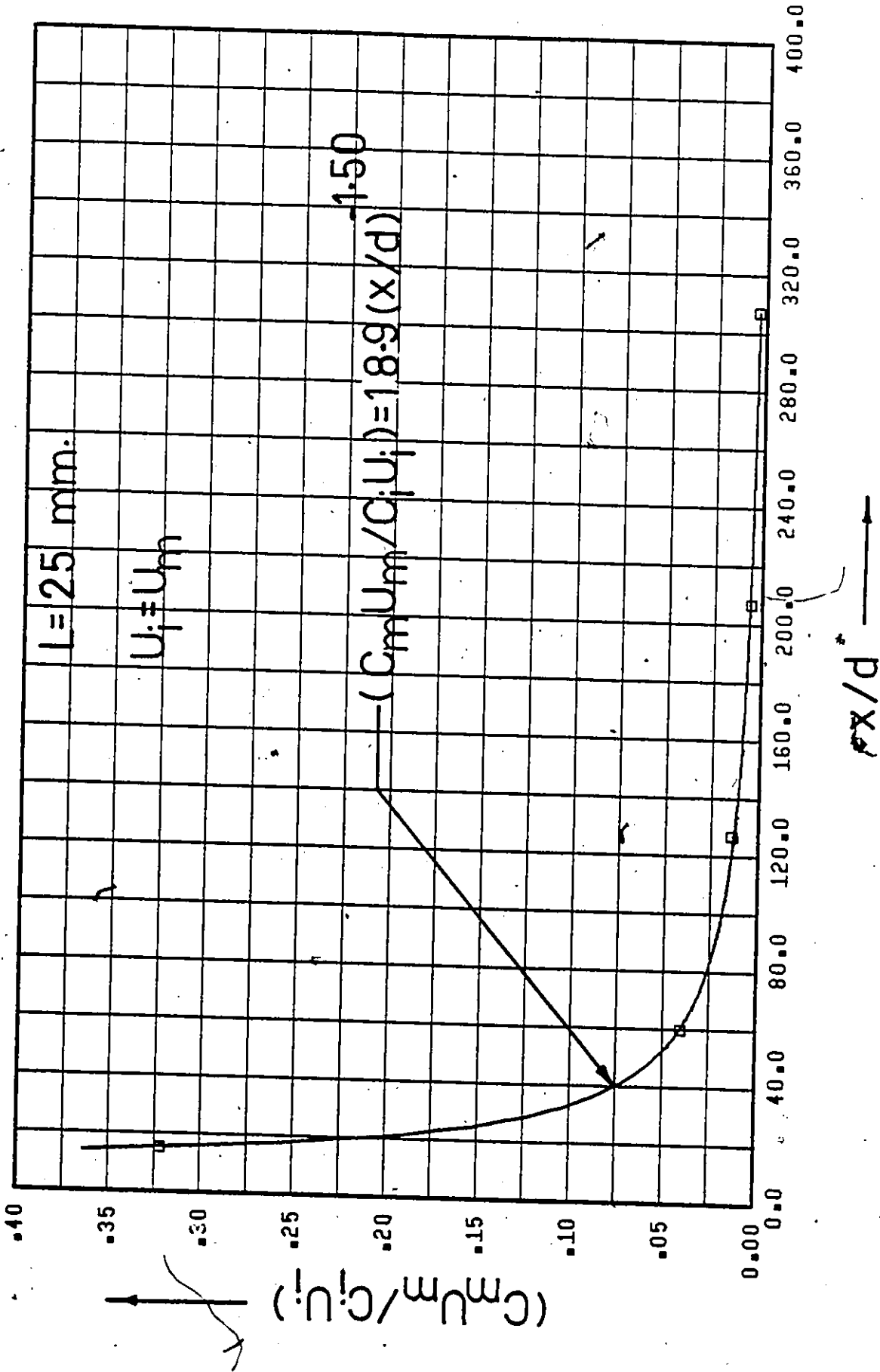


Figure 115. $(C_m U_m / C_i U_i)$ vs. x/d (Point Source Injection - Fully Developed Flow - $C_i = 250 \text{ w.p.p.m.}$).

2

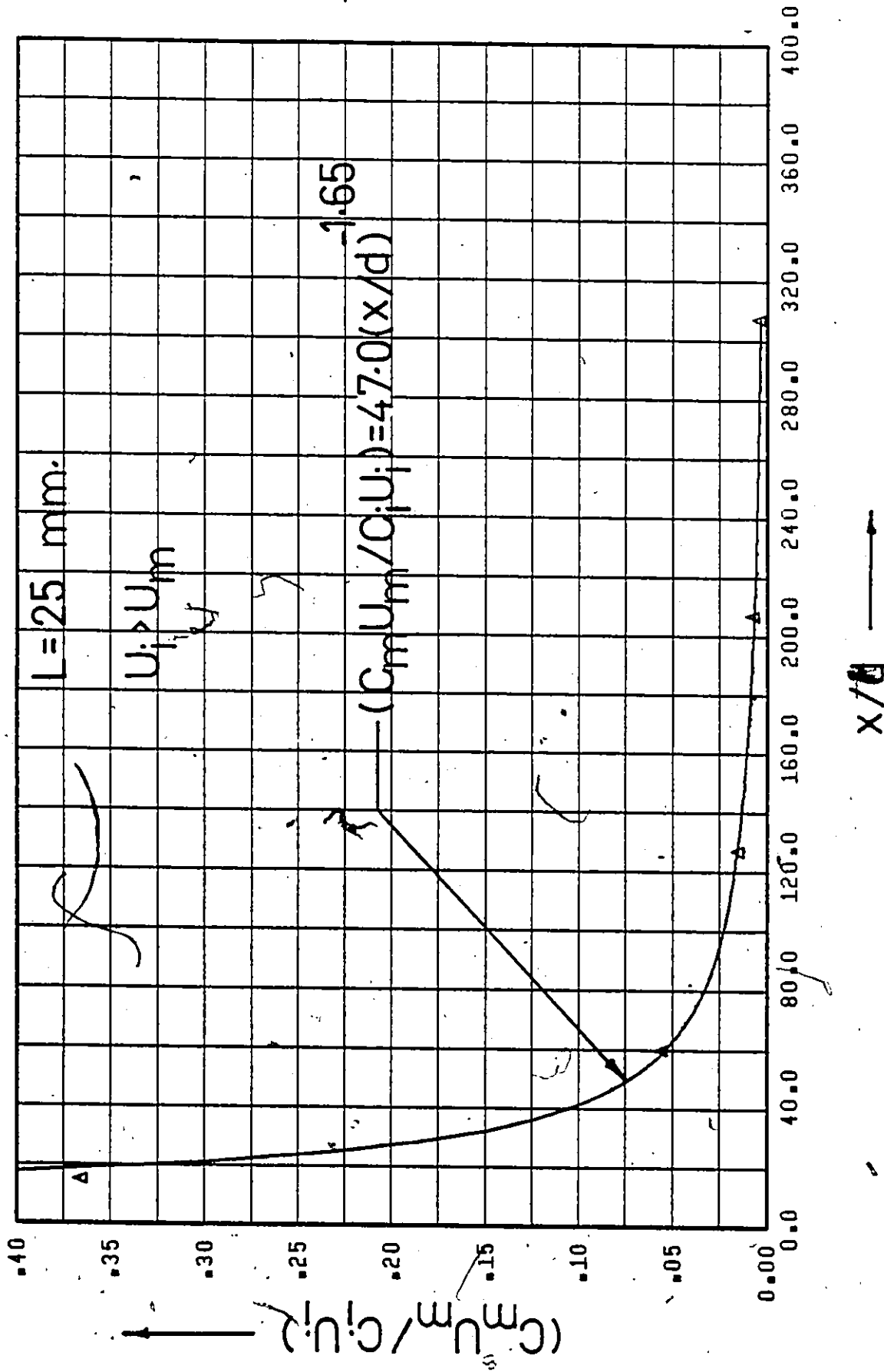


Figure 116. $(C_m U_m / C_i U_i)$ vs. x/d (Point Source Injection - Fully Developed Flow - $C_i = 250 \text{ w.p.m.}$).

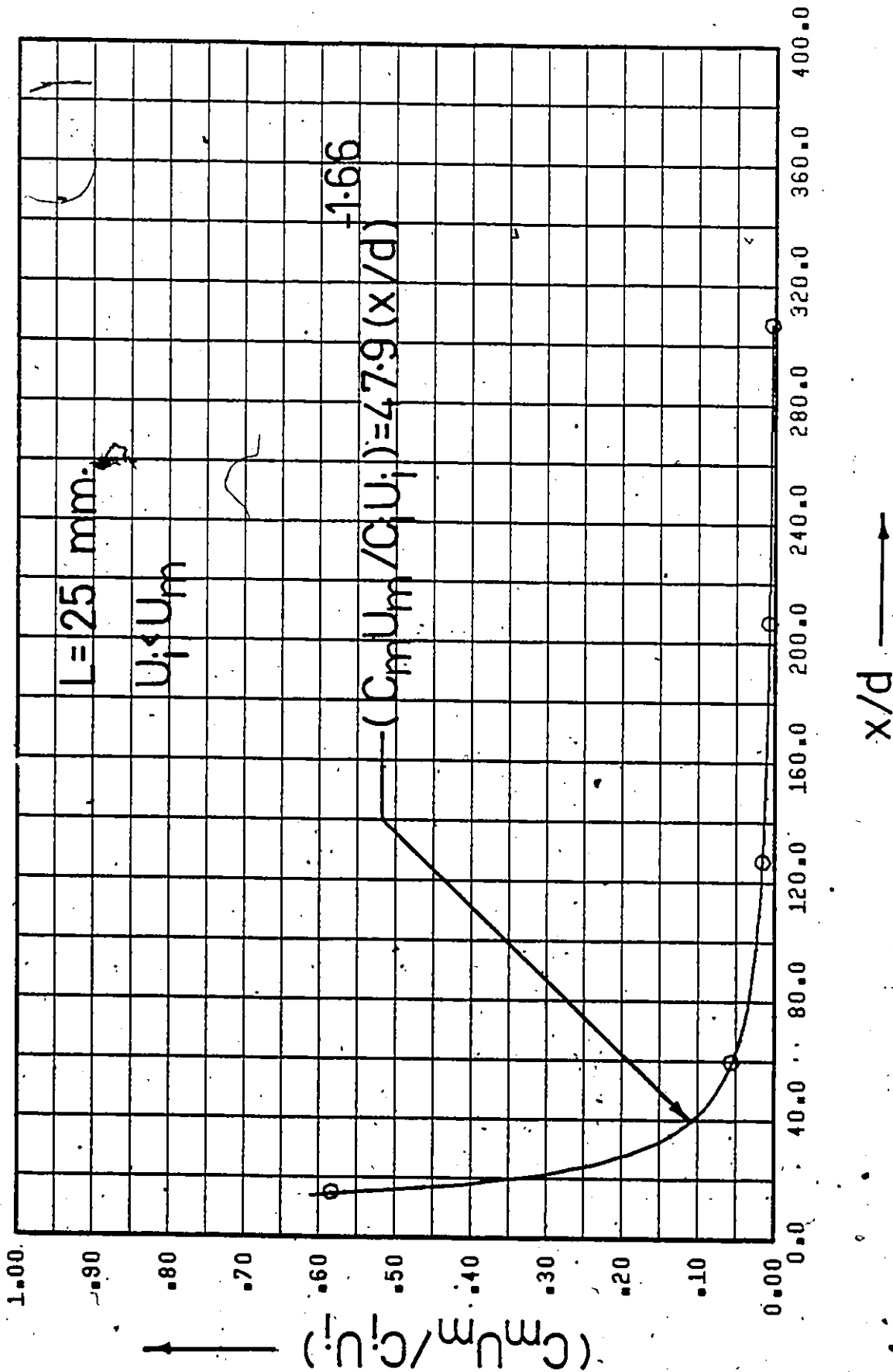


Figure 117. $(C_m U_m / C_i U_i)$ vs. x/d (Point Source Injection - Fully Developed Flow - $C_i = 500 \text{ w.p.p.m.}$).

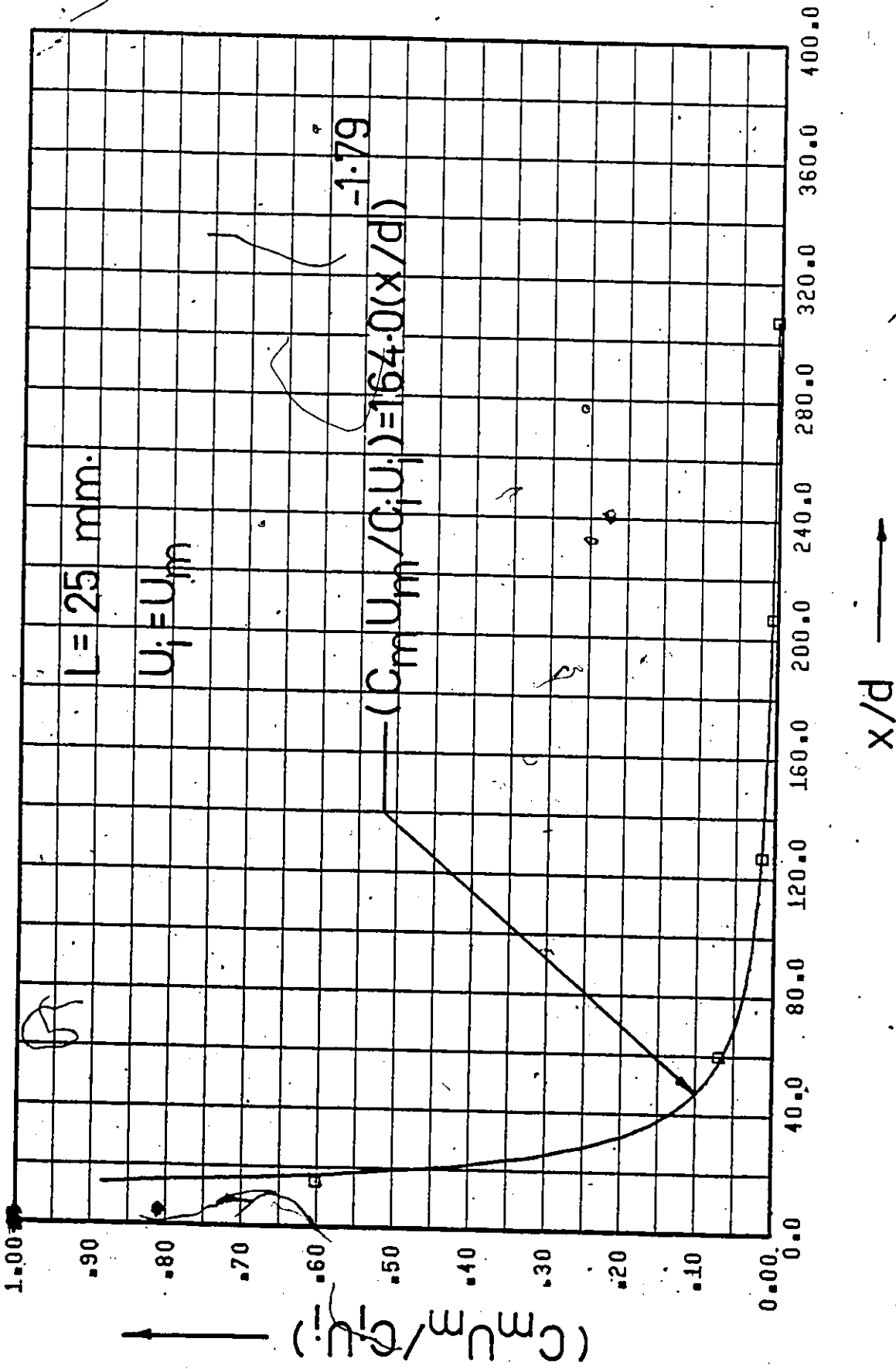


Figure 118. $(C_m U_m / C_i U_i)$ vs. x/d (Point Source Injection - Fully Developed Flow - $C_i = 500 \text{ w.p.p.m.}$).

C

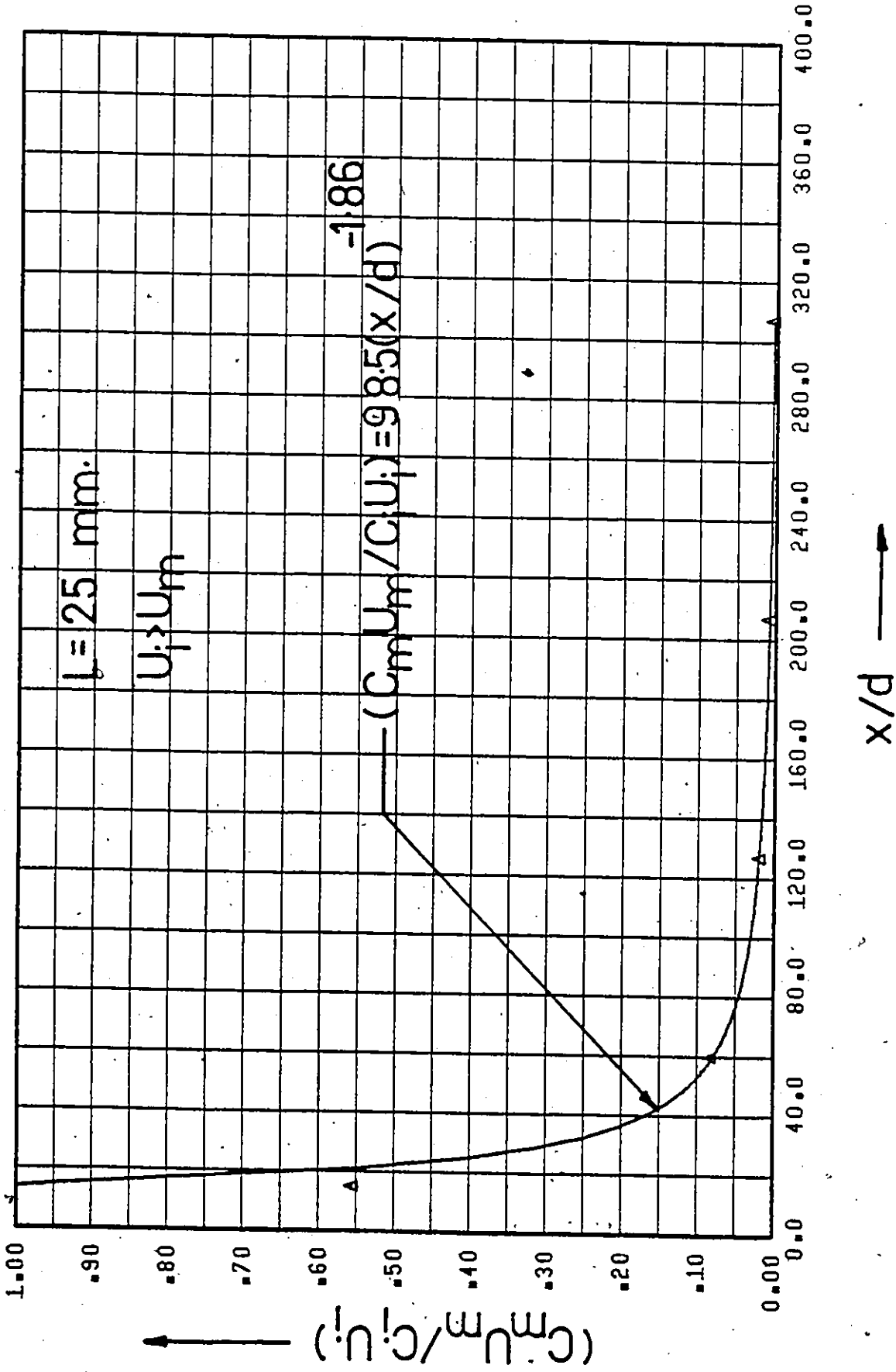


Figure 119. $(C_m U_m / C_i U_i)$ vs. x/d (Point Source Injection - Fully Developed Flow - $C_i = 500 \text{ w.p.p.m.}$).

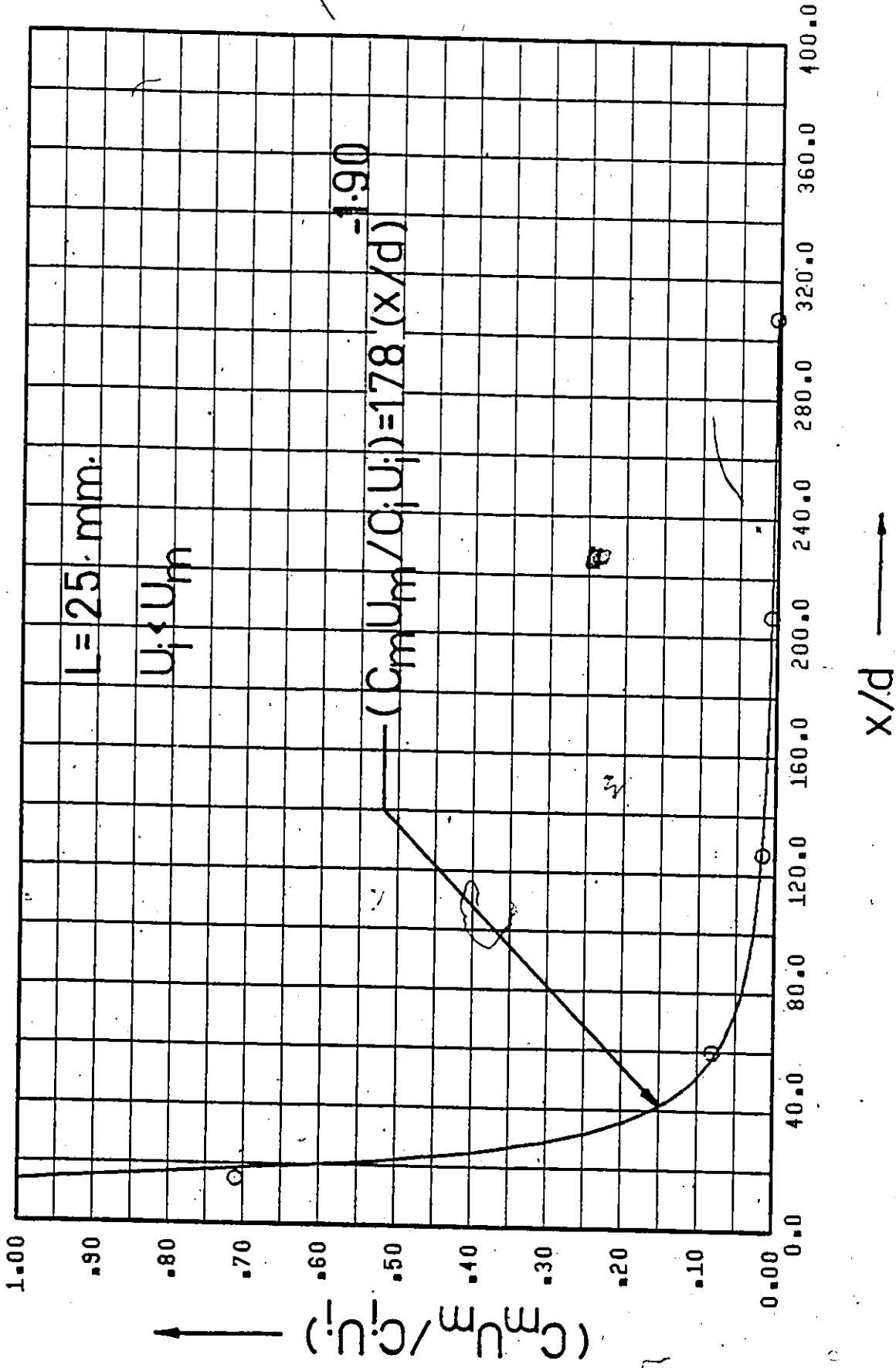


Figure 120. $(C_m U_m / C_i U_i)$ vs. x/d (point Source
 Injection - Fully Developed Flow -
 $C_i = 1000 \text{ w.p.p.m.}$).

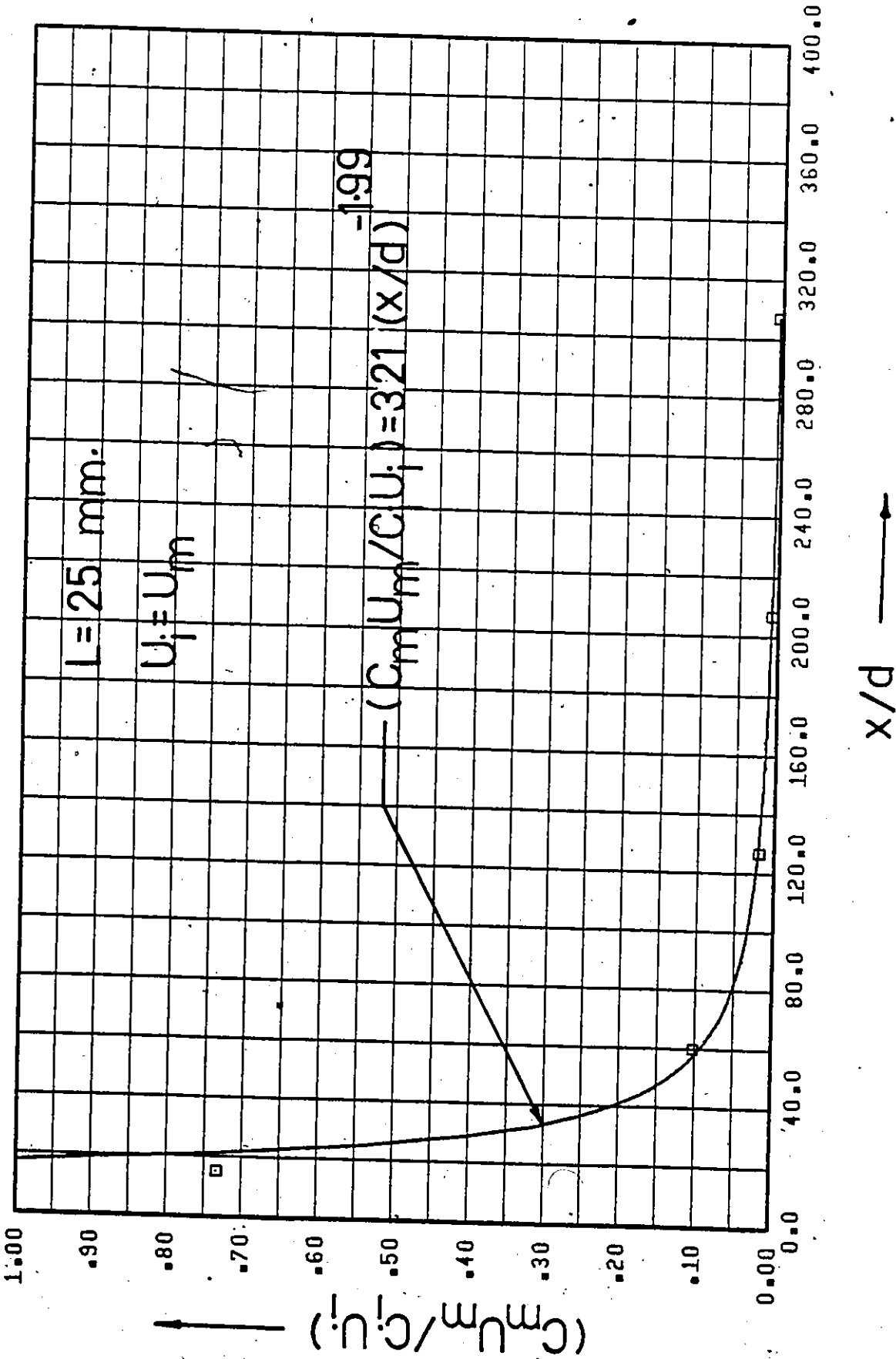


Figure 121. $(C_m U_m / C_i U_i)$ vs. x/d (Point Source Injection - Fully Developed Flow - $C_i = 1000 \text{ w.p.p.m.}$).

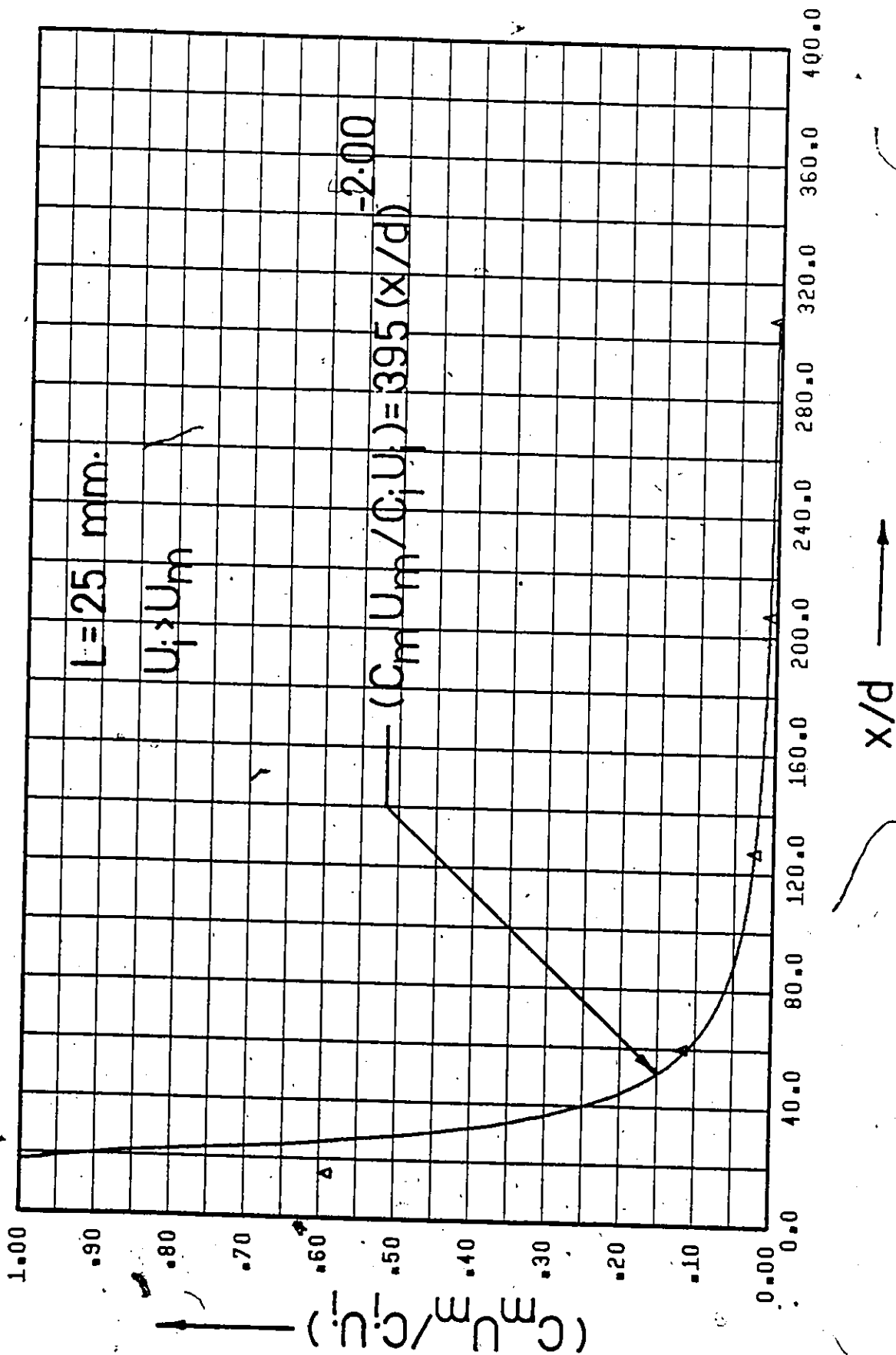


Figure 122. $(C_m U_m / C_i U_i)$ vs. x/d (Point Source Injection - Fully Developed Flow - $C_i = 1000 \text{ w.p.p.m.}$).

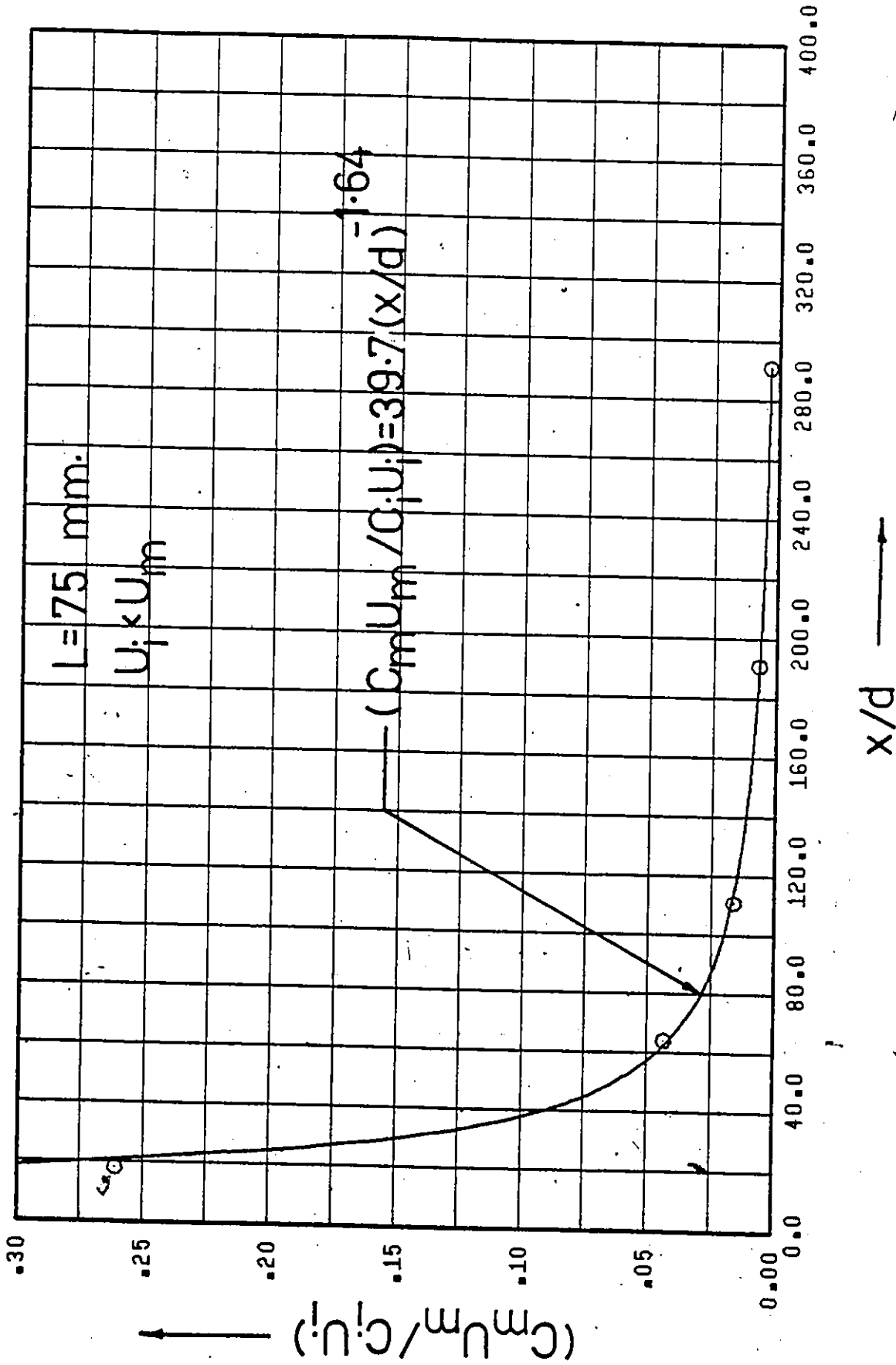


Figure 123. $(C_m U_m / C_i U_i)$ vs. x/d (Point Source Injection - Fully Developed Flow - Water Injection).

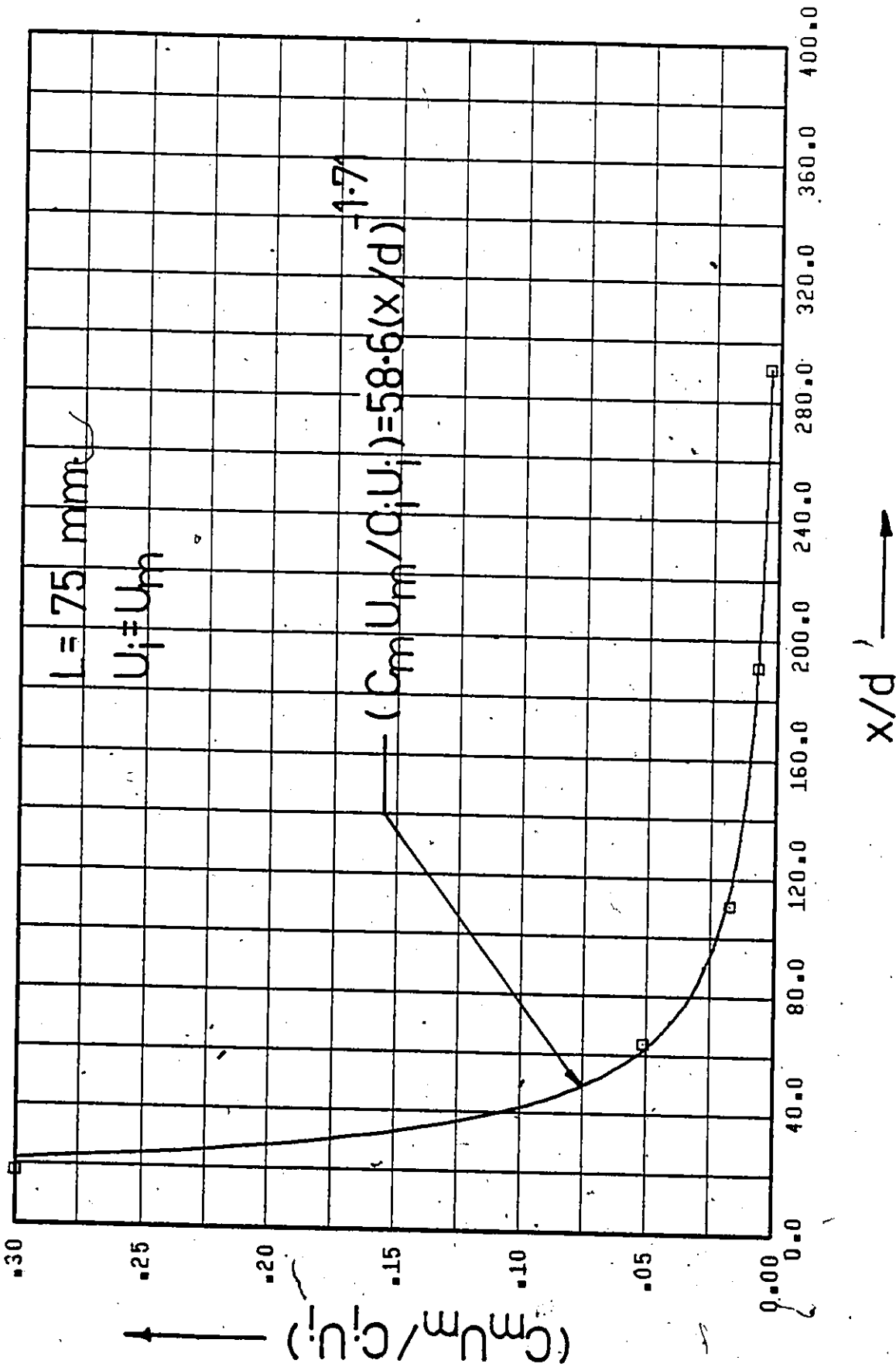


Figure 124. $(C_m U_m / C_i U_i)$ vs. x/d (Point Source Injection - Fully Developed Flow - Water Injection).

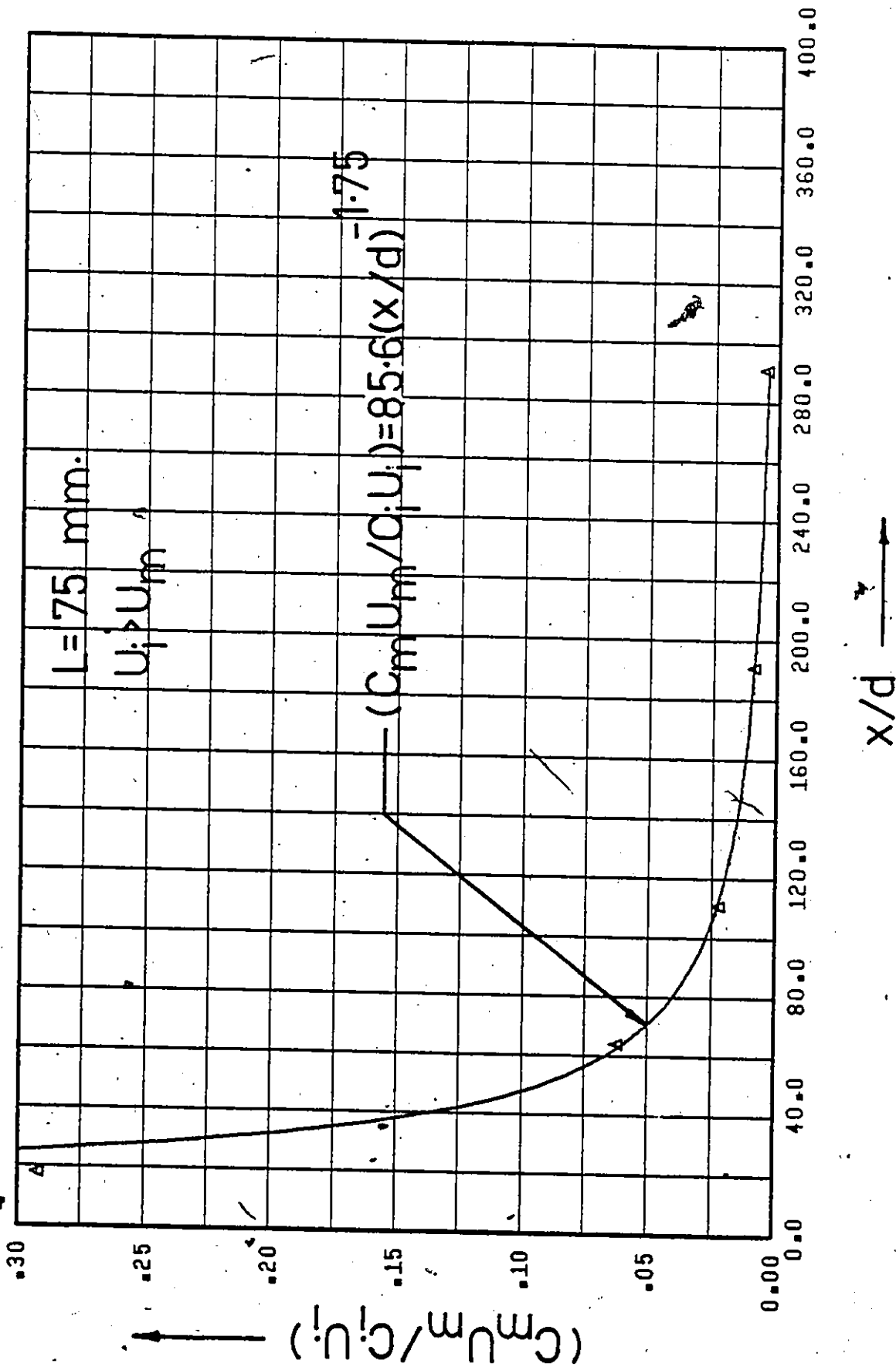


Figure 125. $(C_m U_m / C_i U_i)$ vs. x/d (Point Source Injection - Fully Developed Flow - Water Injection).

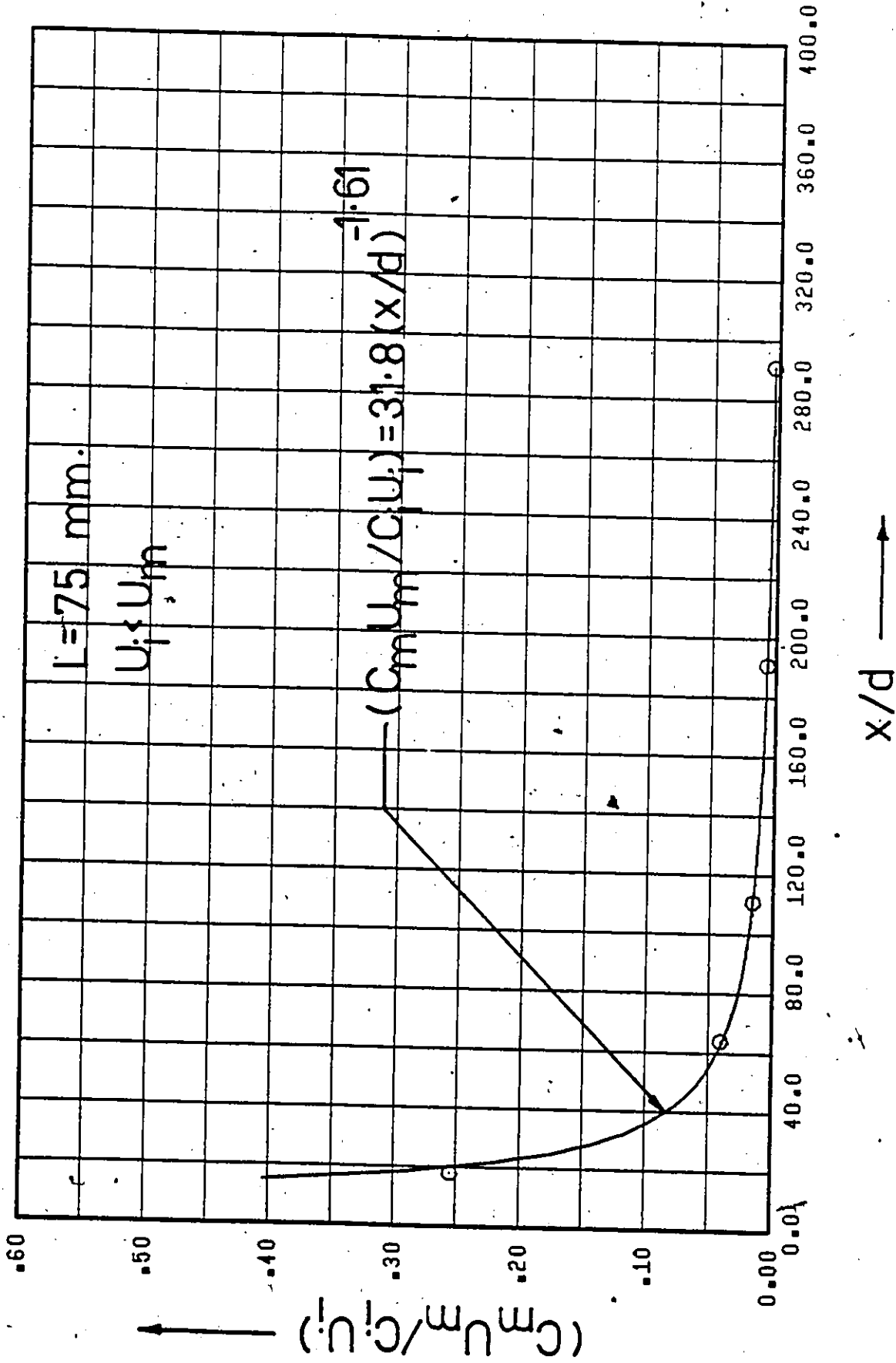


Figure 126. $(C_m U_m / C_i U_i)$ vs. x/d (Point Source Injection - Fully Developed Flow - $C_i = 50 \text{ w.p.p.m.}$).

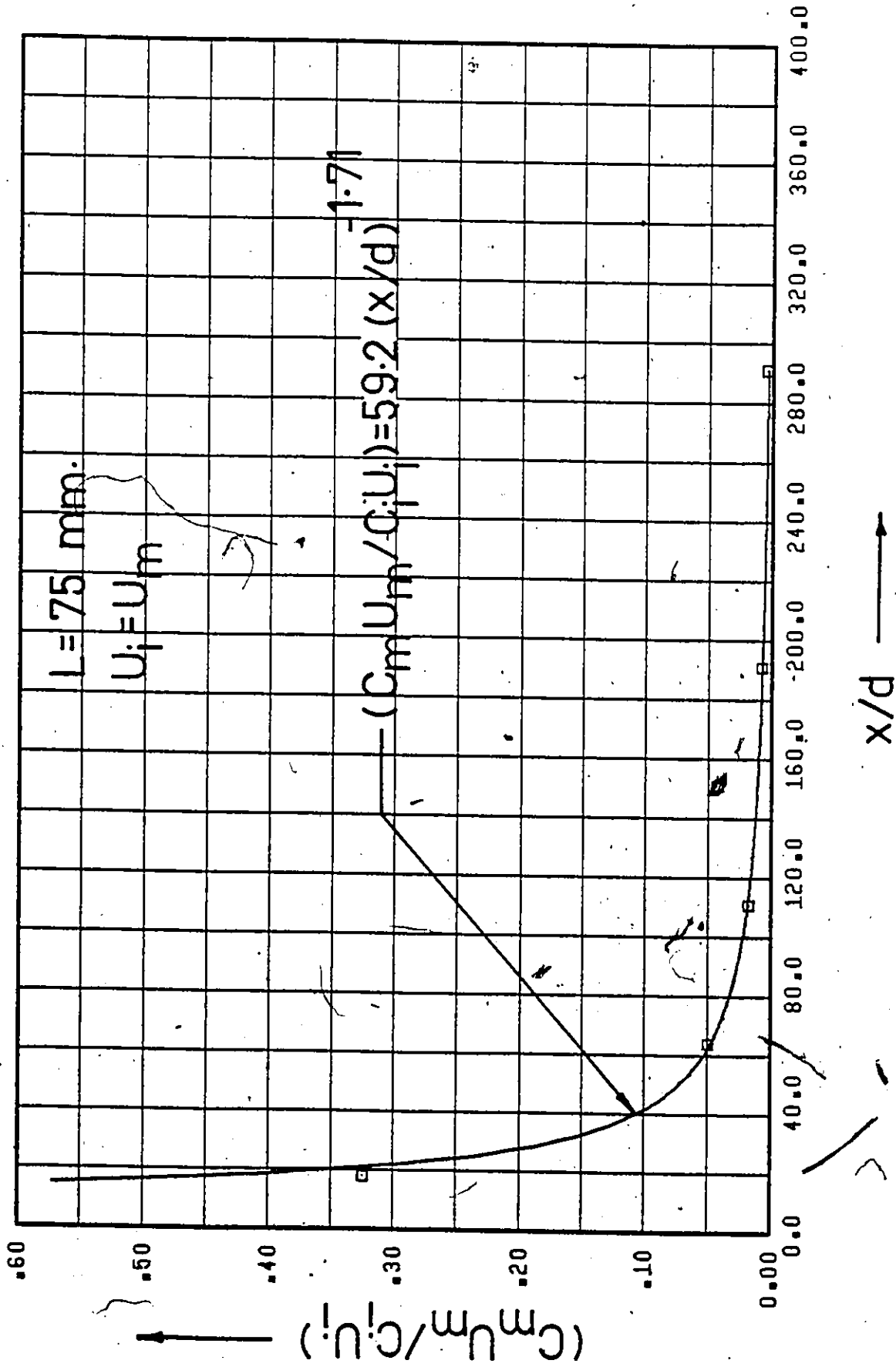


Figure 127. $(C_m U_m / C_i U_i)$ vs. x/d (Point Source Injection - Fully Developed Flow - $C_i = 50 \text{ w.p.p.m.}$).

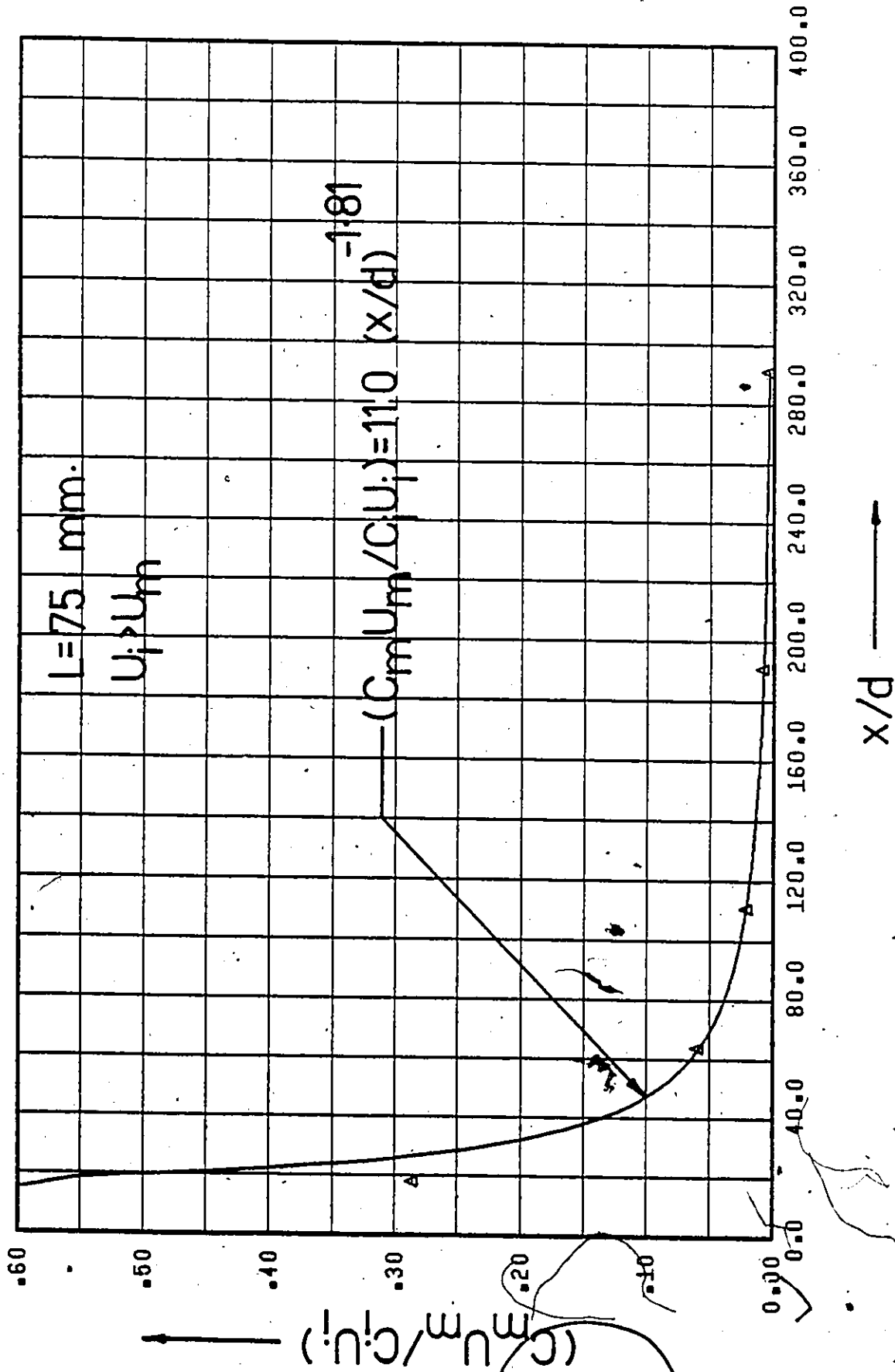


Figure 128. $(C_m U_m / C_i U_i)$ vs. x/d (Point Source Injection - Fully Developed Flow - $C_i = 50 \text{ w.p.p.m.}$).

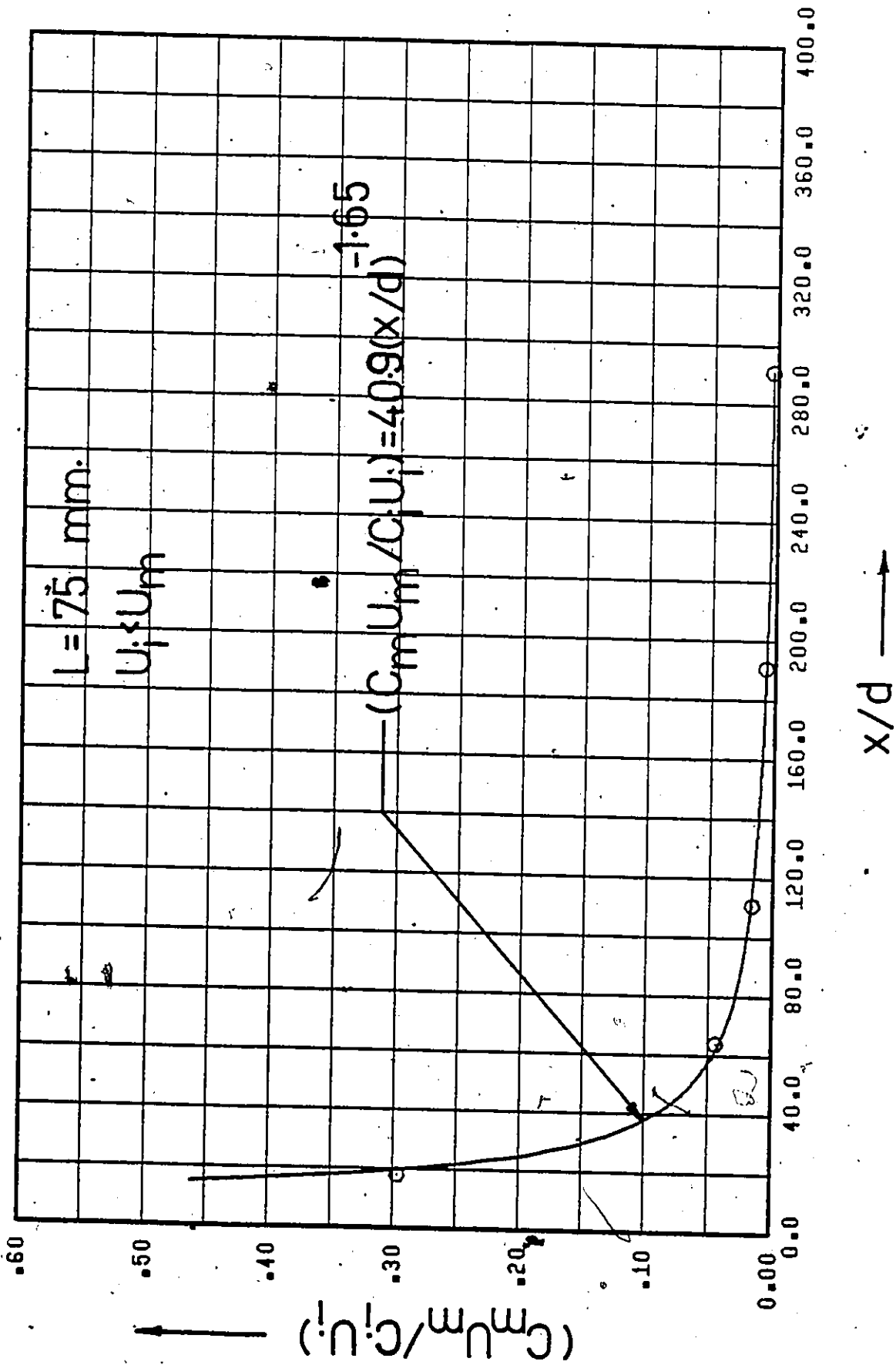


Figure 129. $(C_m U_m / C_i U_i)$ vs. x/d (Point Source Injection - Fully Developed Flow - $C_i = 100 \text{ w.p.p.m.}$).

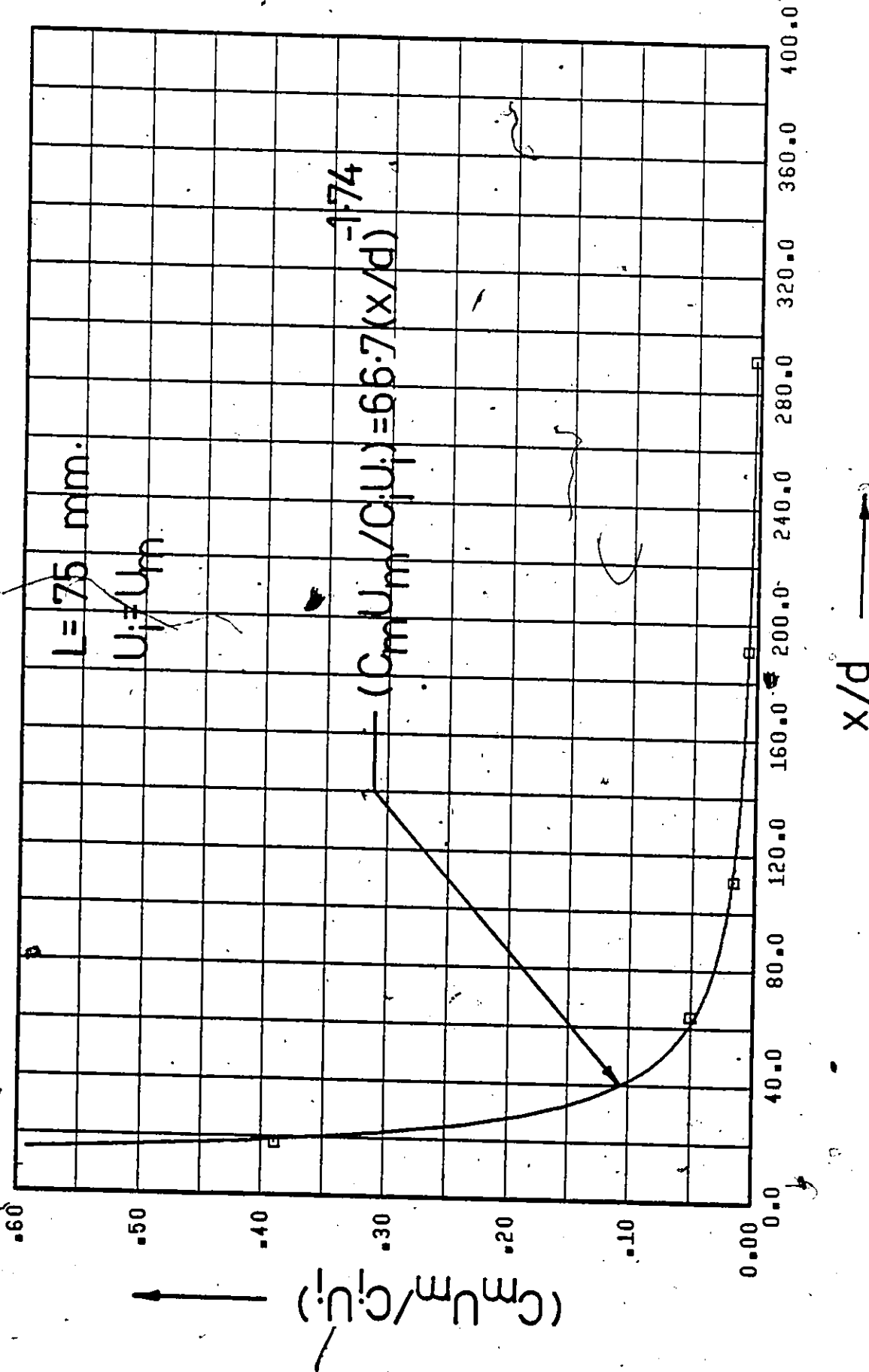


Figure 130. $(C_m U_m / C_i U_i)$ vs. x/d (Point Source Injection - Fully Developed Flow - $C_i = 100 \text{ w.p.p.m.}$).

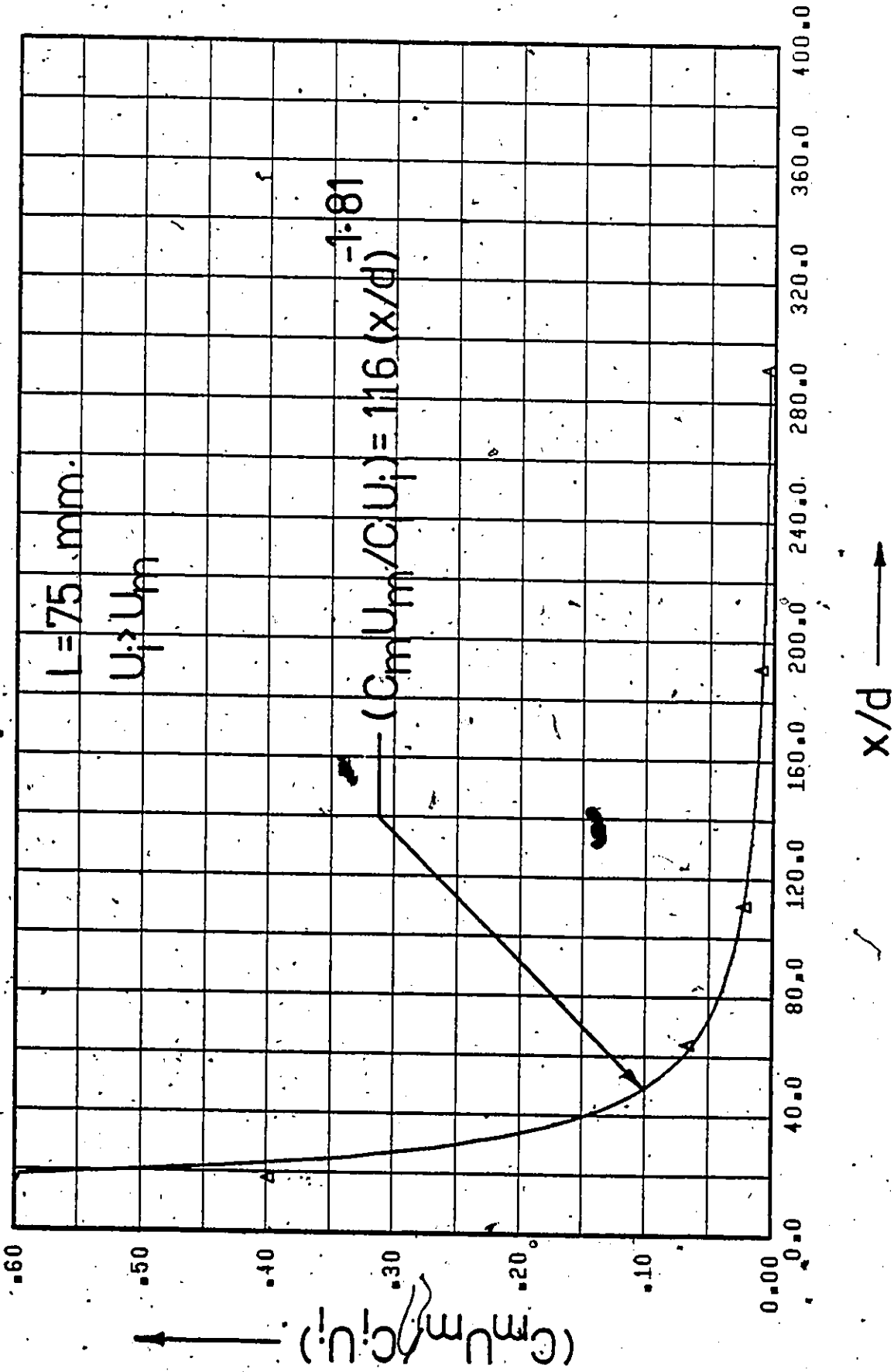


Figure 131. $(C_m U_m / C_i U_i)$ vs. x/d (Point Source Injection - Fully Developed Flow $C_i = 100 \text{ w.p.p.m.}$).

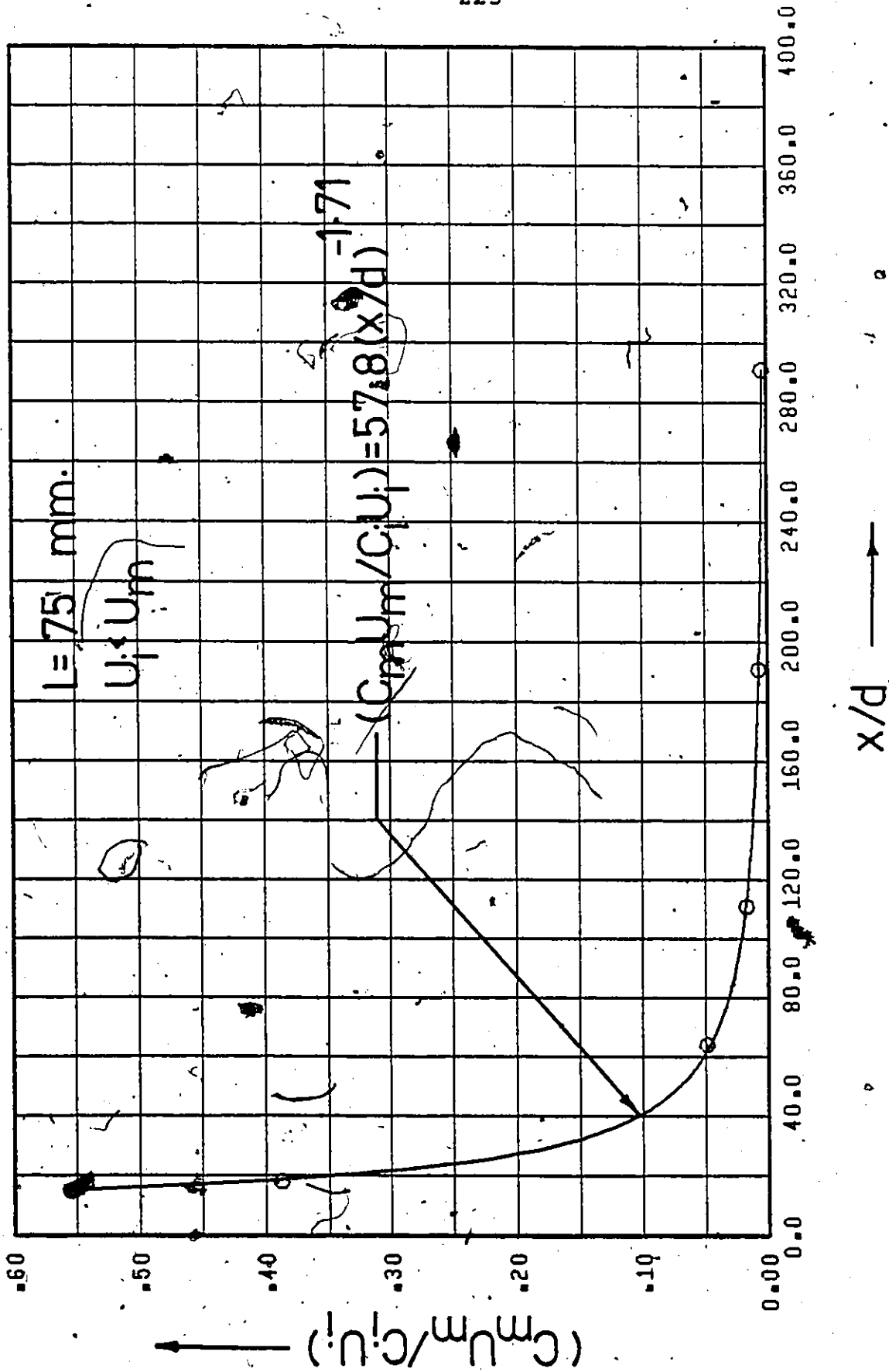


Figure 132. $(C_m U_m / C_i U_i)$ vs. x/d (Point Source Injection - Fully Developed Flow - $C_i = 250 \text{ w.p.p.m.}$).

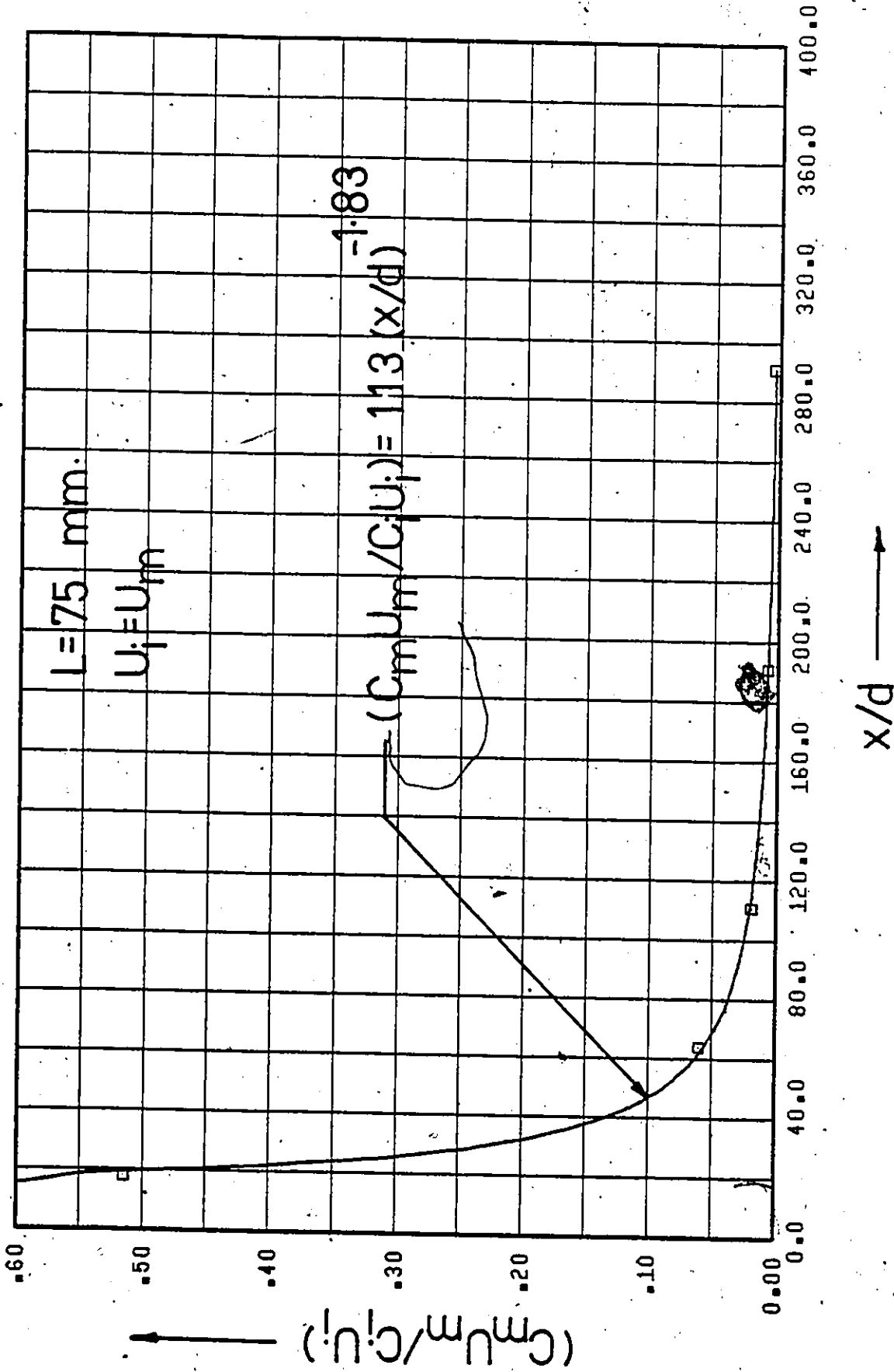


Figure 133. $(C_m U_m / C_i U_i)$ vs. x/d (Point Source Injection - Fully Developed Flow - $C_i = 250 \text{ w.p.p.m.}$).

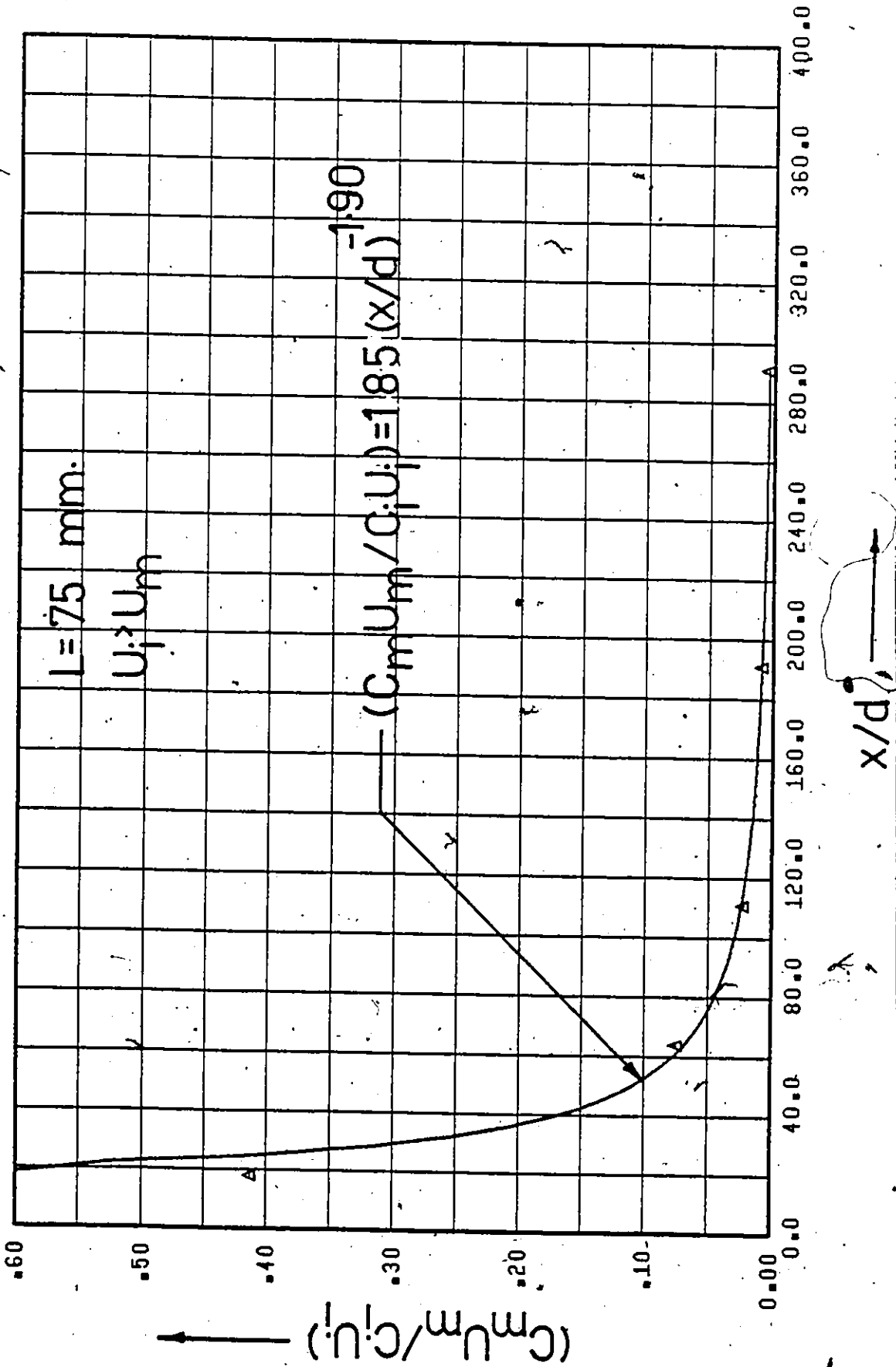


Figure 134. $(C_m U_m / C_i U_i)$ vs. x/d (Point Source Injection - Fully Developed Flow - $C_i = 250 \text{ w.p.p.m.}$).

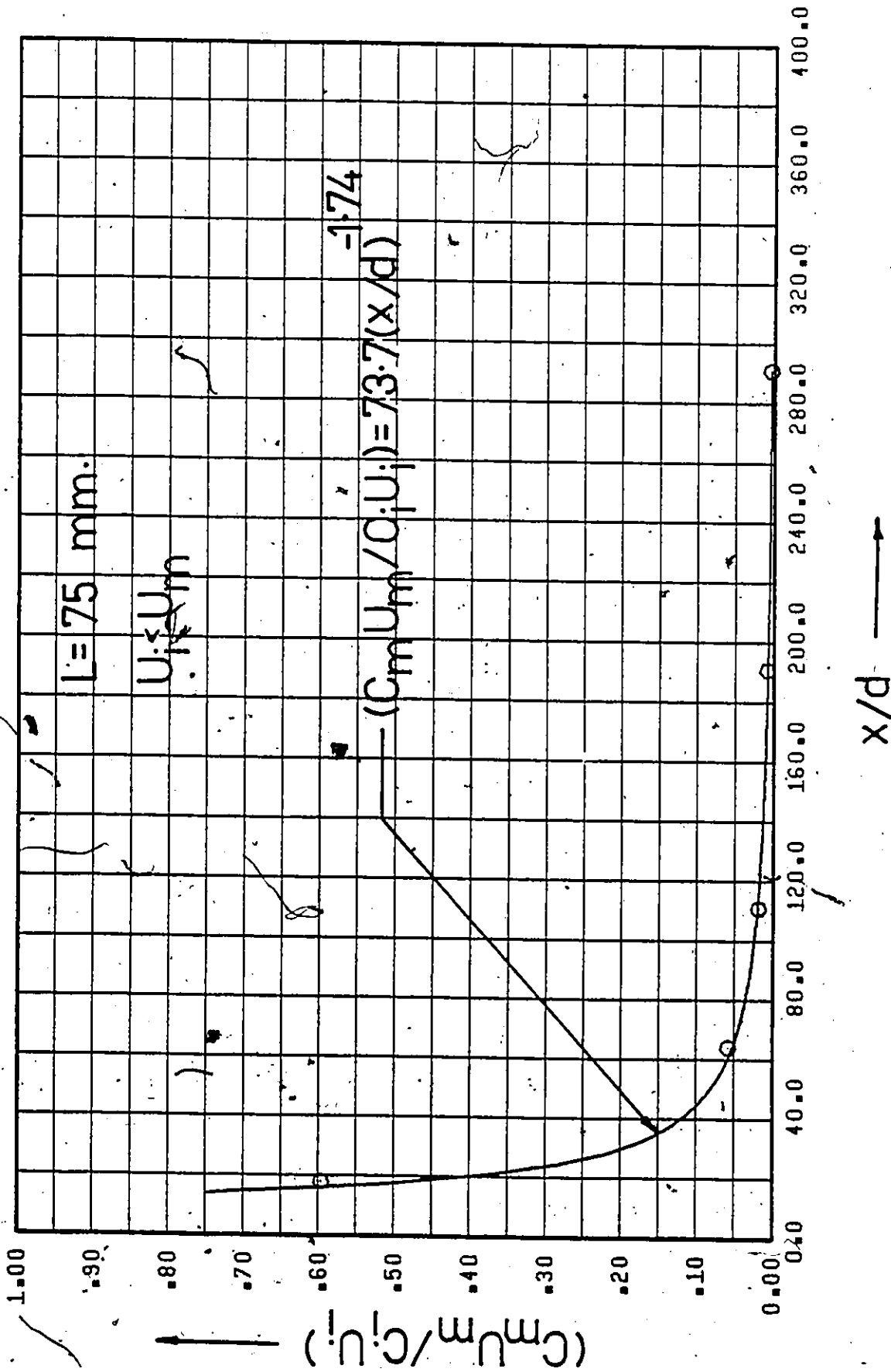


Figure 135. $(C_m U_m / C_i U_i)$ vs. x/d (Point Source Injection - Fully Developed Flow - $C_i = 500 \text{ w.p.p.m.}$).

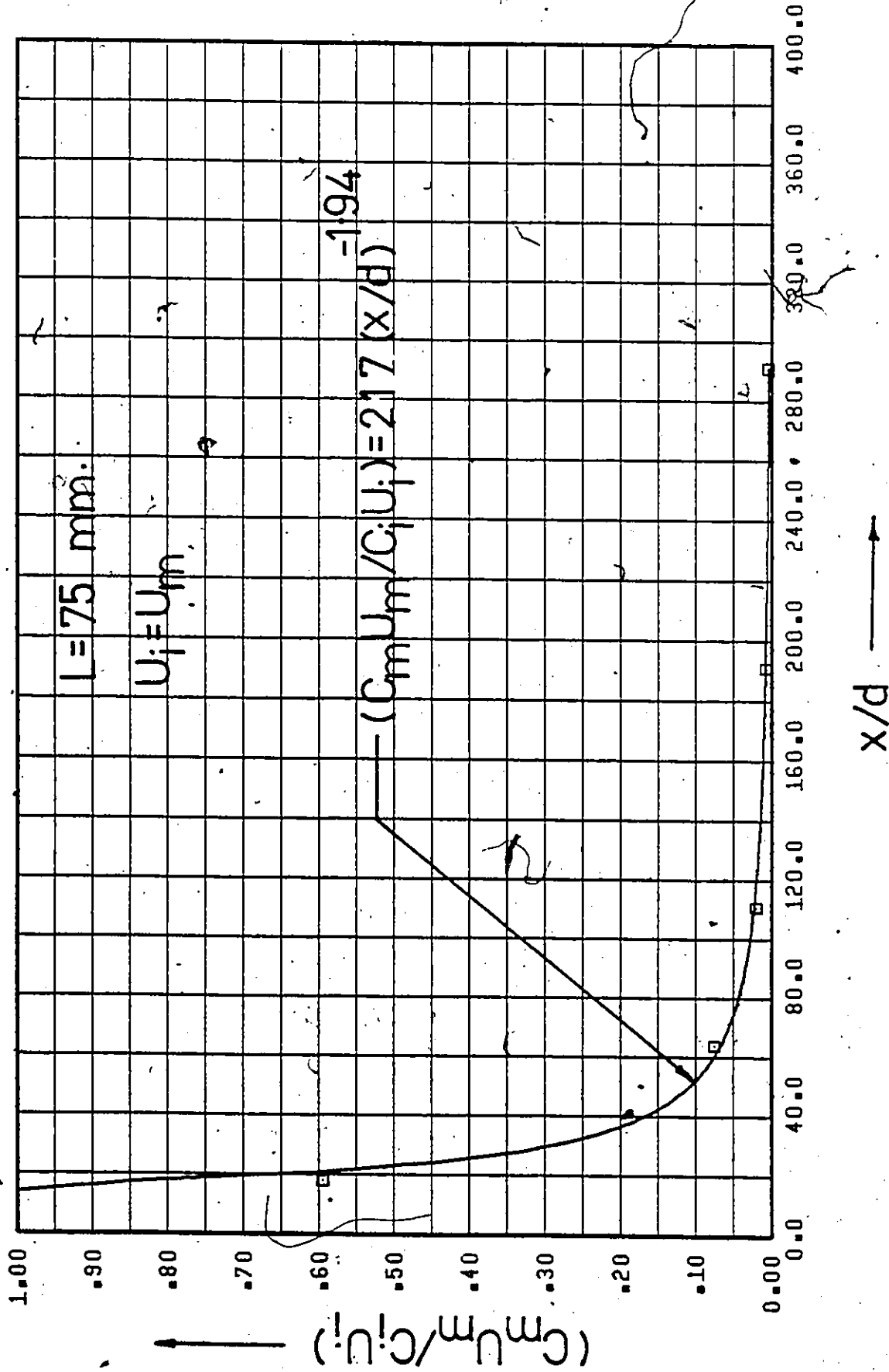


Figure 136. $(C_m U_m / C_i U_i)$ vs. x/d (Point Source Injection - Fully Developed Flow - $C_i = 500 \text{ w.p.p.m.}$).

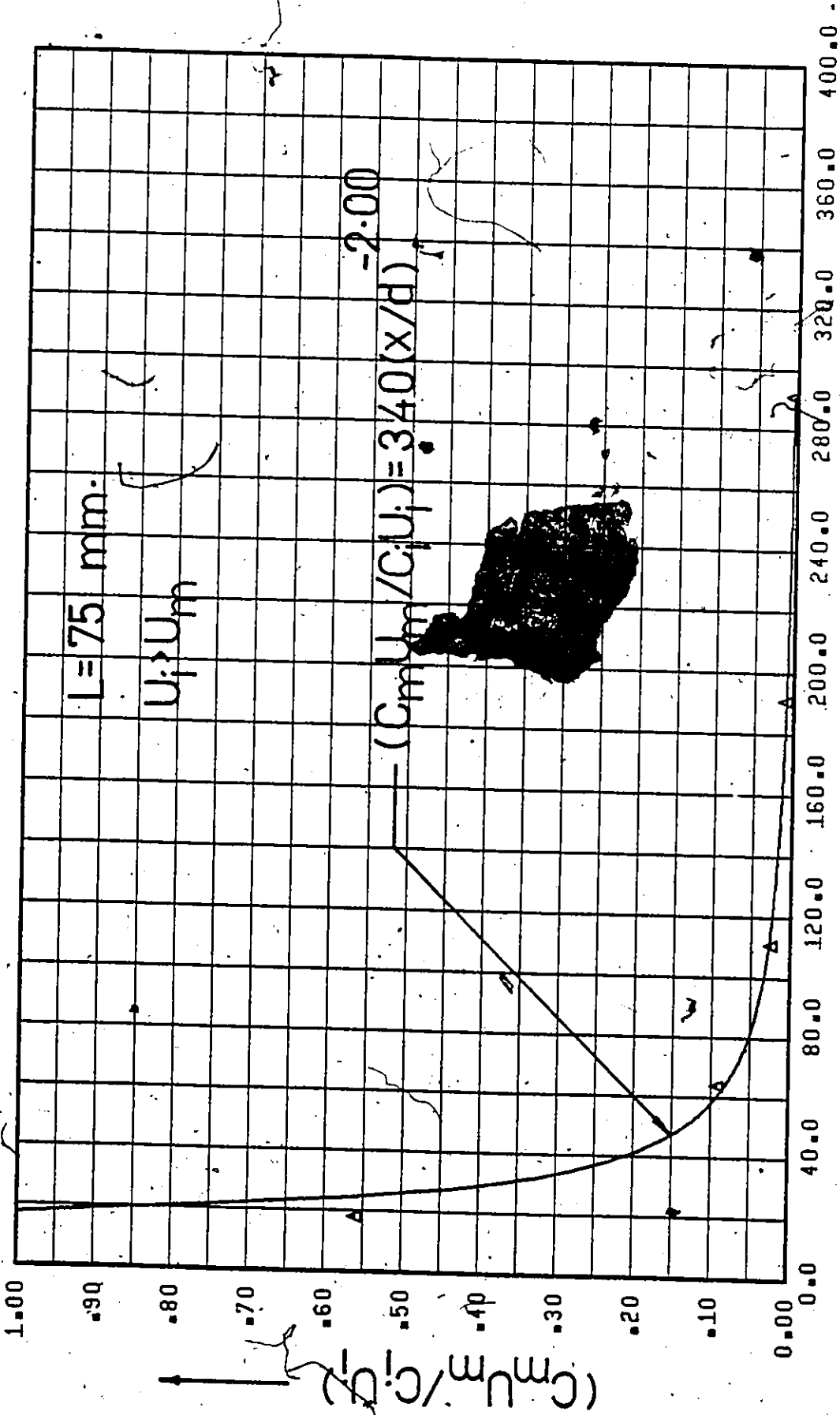
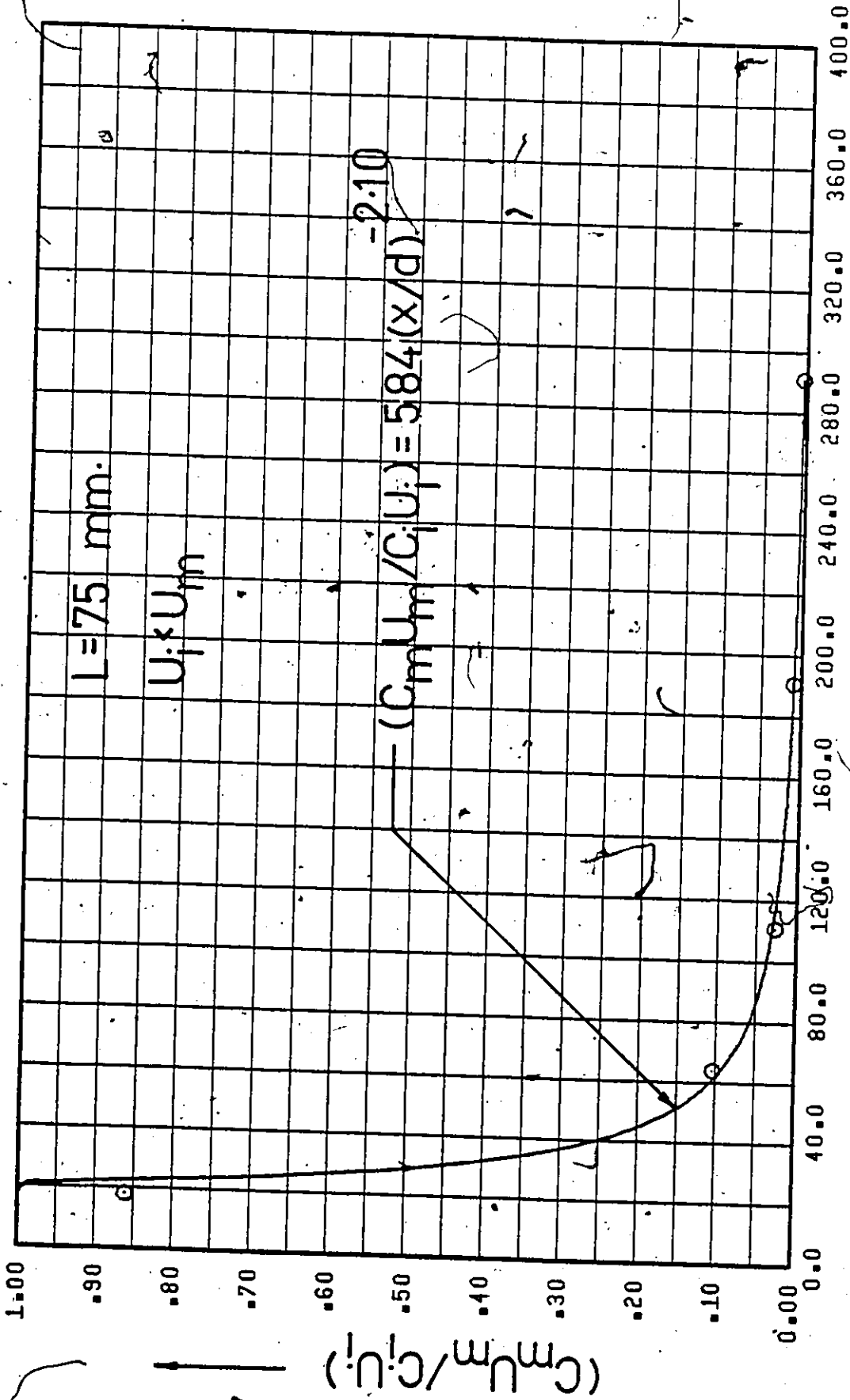


Figure 137. $(C_m U_m / C_i U_i)$ vs. x/d (Point Source Injection - Fully Developed Flow - $C_i = 500 \text{ w.p.p.m.}$).



x/d →

Figure 138. $(C_m U_m / C_i U_i)$ vs. x/d (Point Source Injection - Fully Developed Flow - $C_i = 1000 \text{ w.p.p.m.}$).

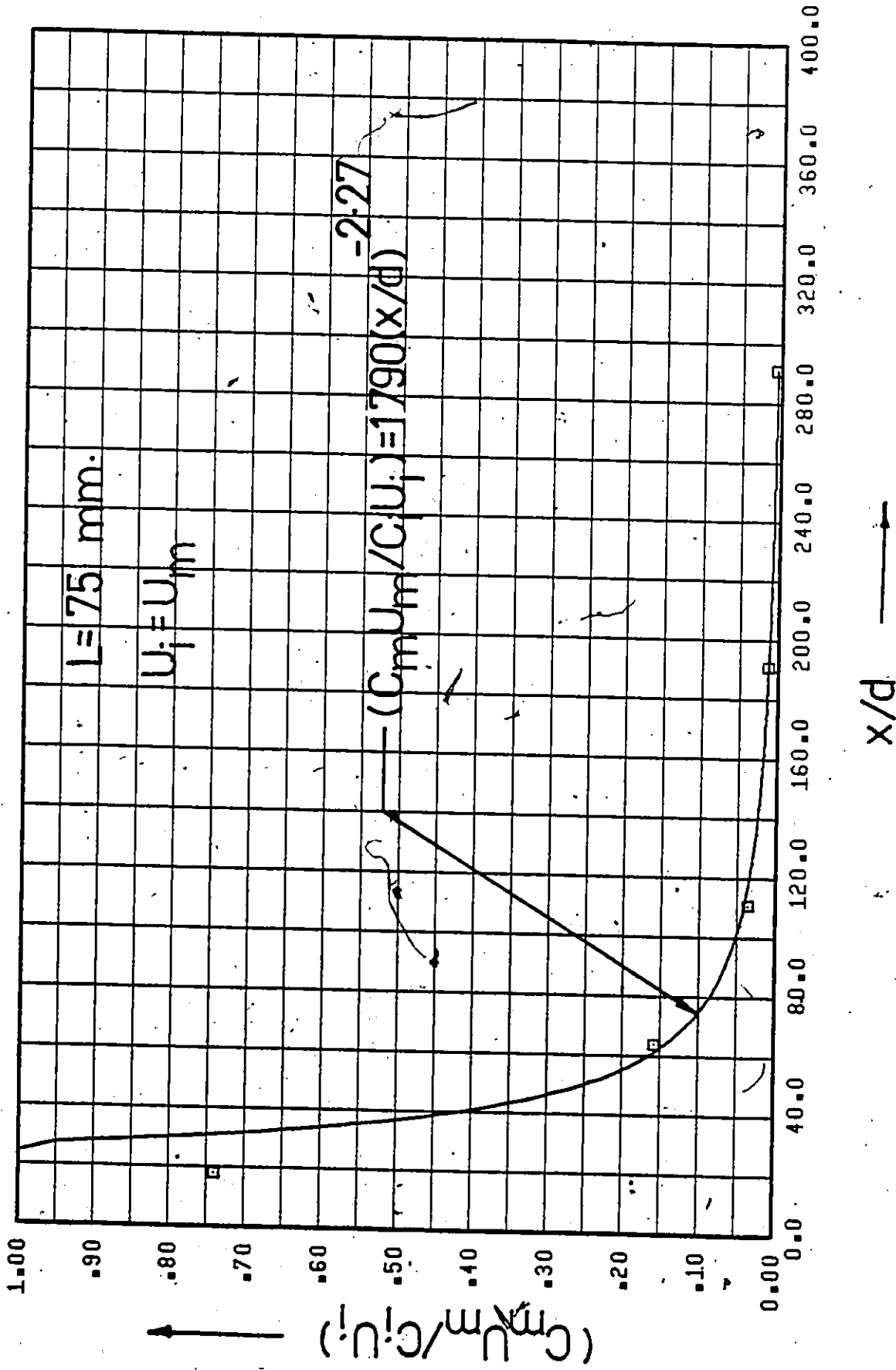


Figure 139. $(C_m U_m / C_i U_i)$ vs. x/d (Point Source Injection - Fully Developed Flow - $C_i = 1000 \text{ w.p.p.m.}$).

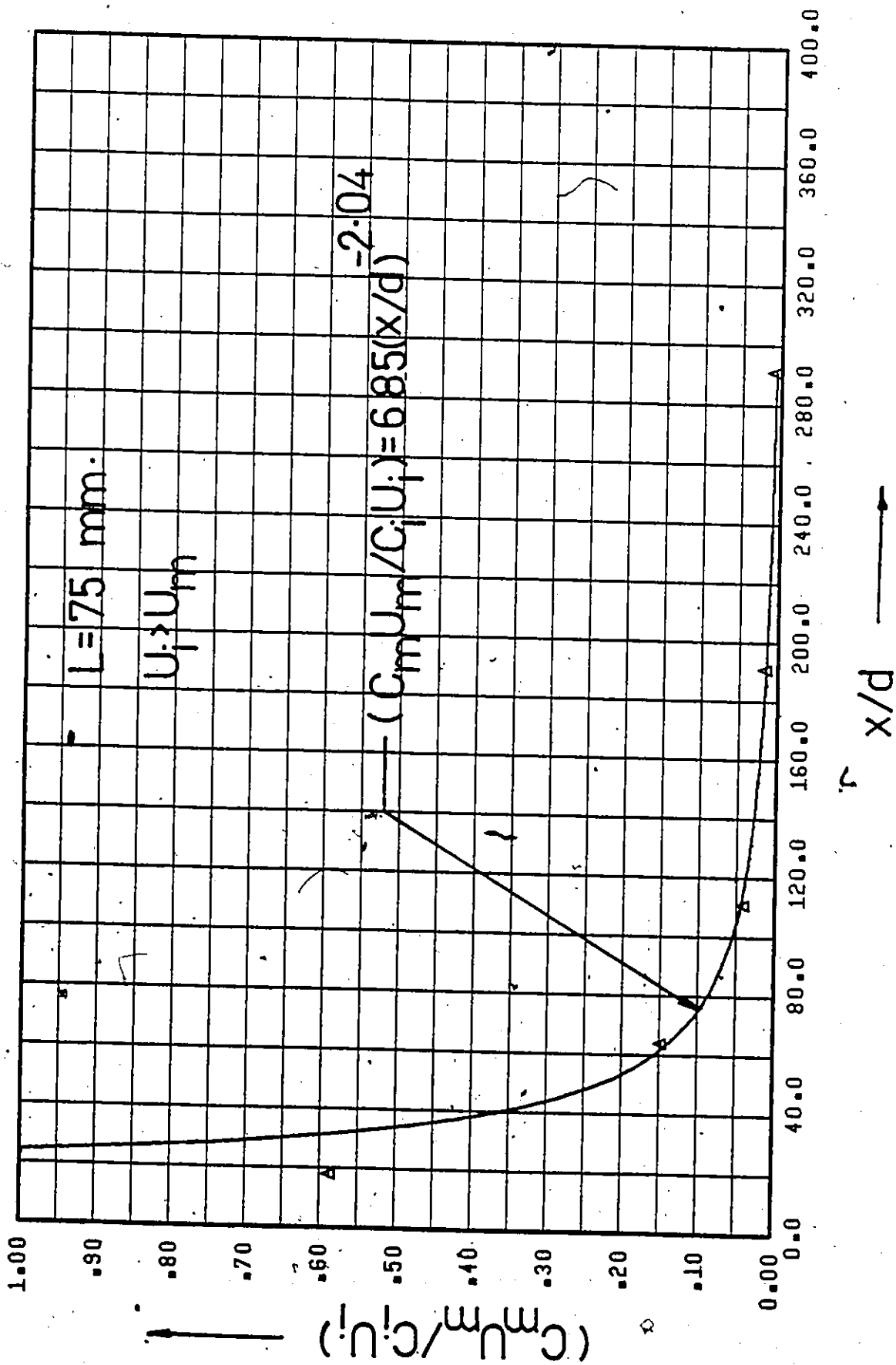


Figure 140. $(C_m U_m / C_i U_i)$ vs. x/d (Point Source Injection - Fully Developed Flow - $C_i = 1000 \text{ w.p.p.m.}$).

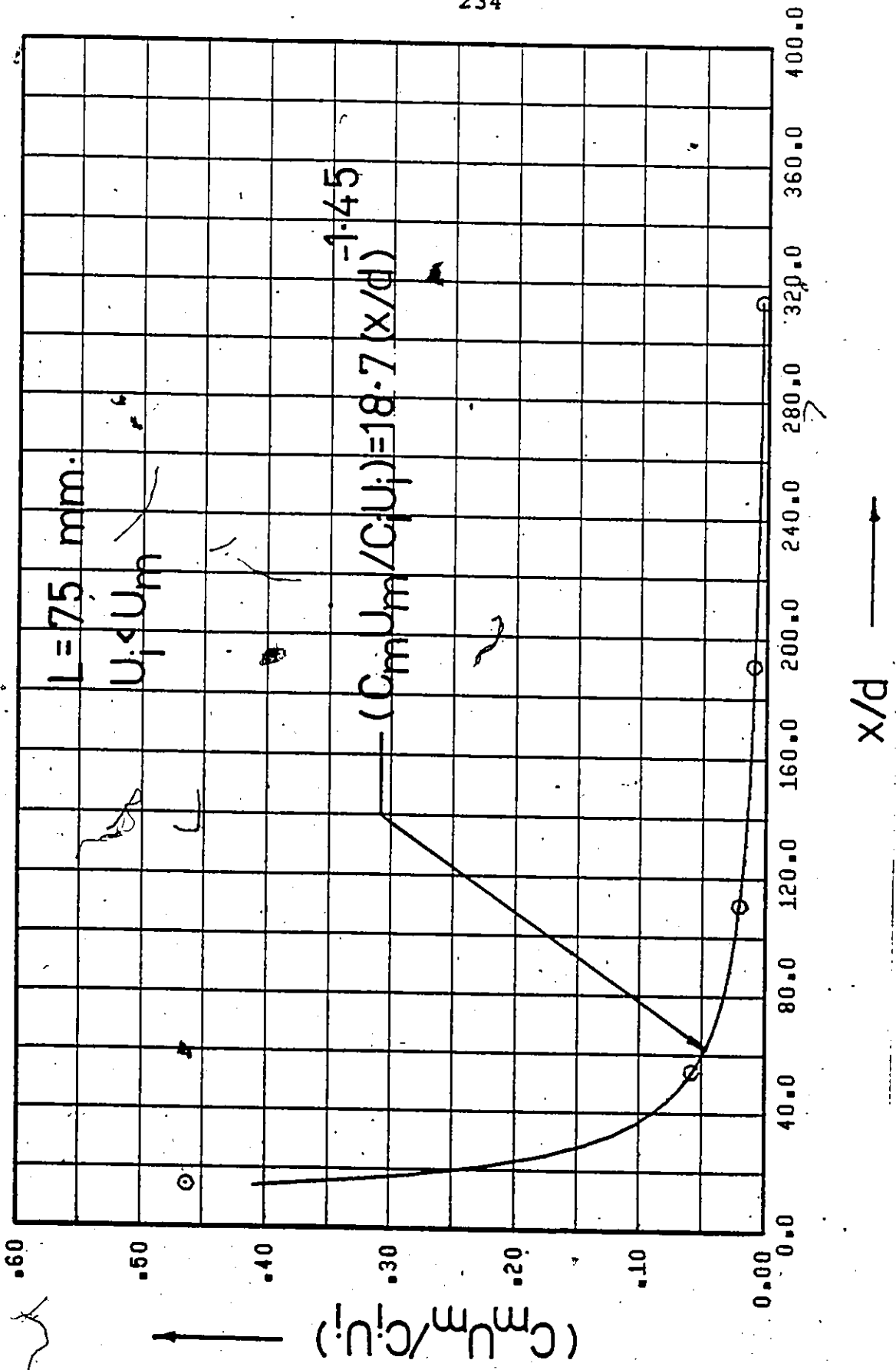


Figure 141. $(C_m U_m / C_i U_i)$ vs. x/d (Point Source Injection - Uniform Flow - Water Injection).

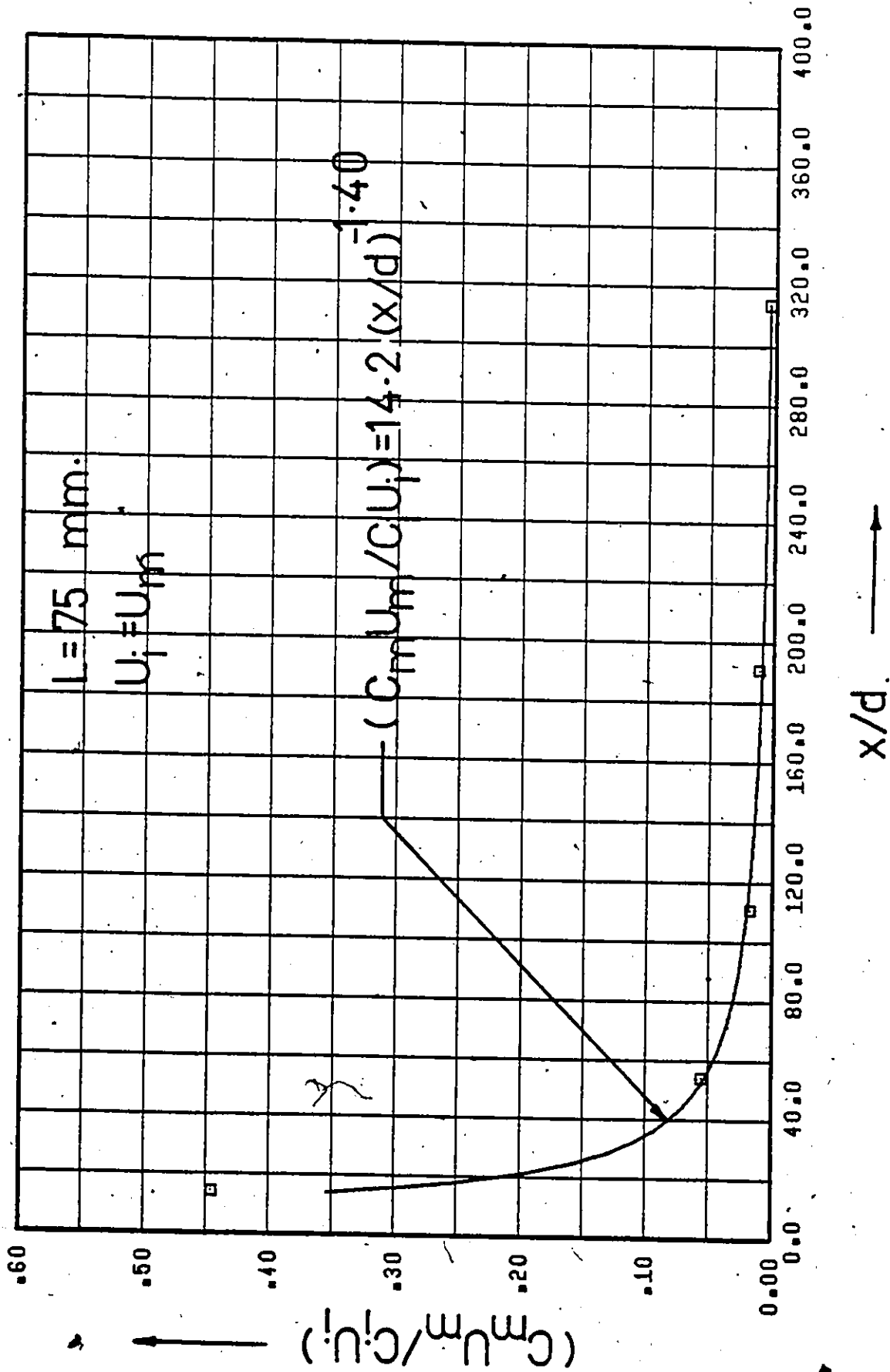


Figure 142. $(C_m U_m / C_i U_i)$ vs. x/d (Point Source Injection - Uniform Flow - Water Injection).

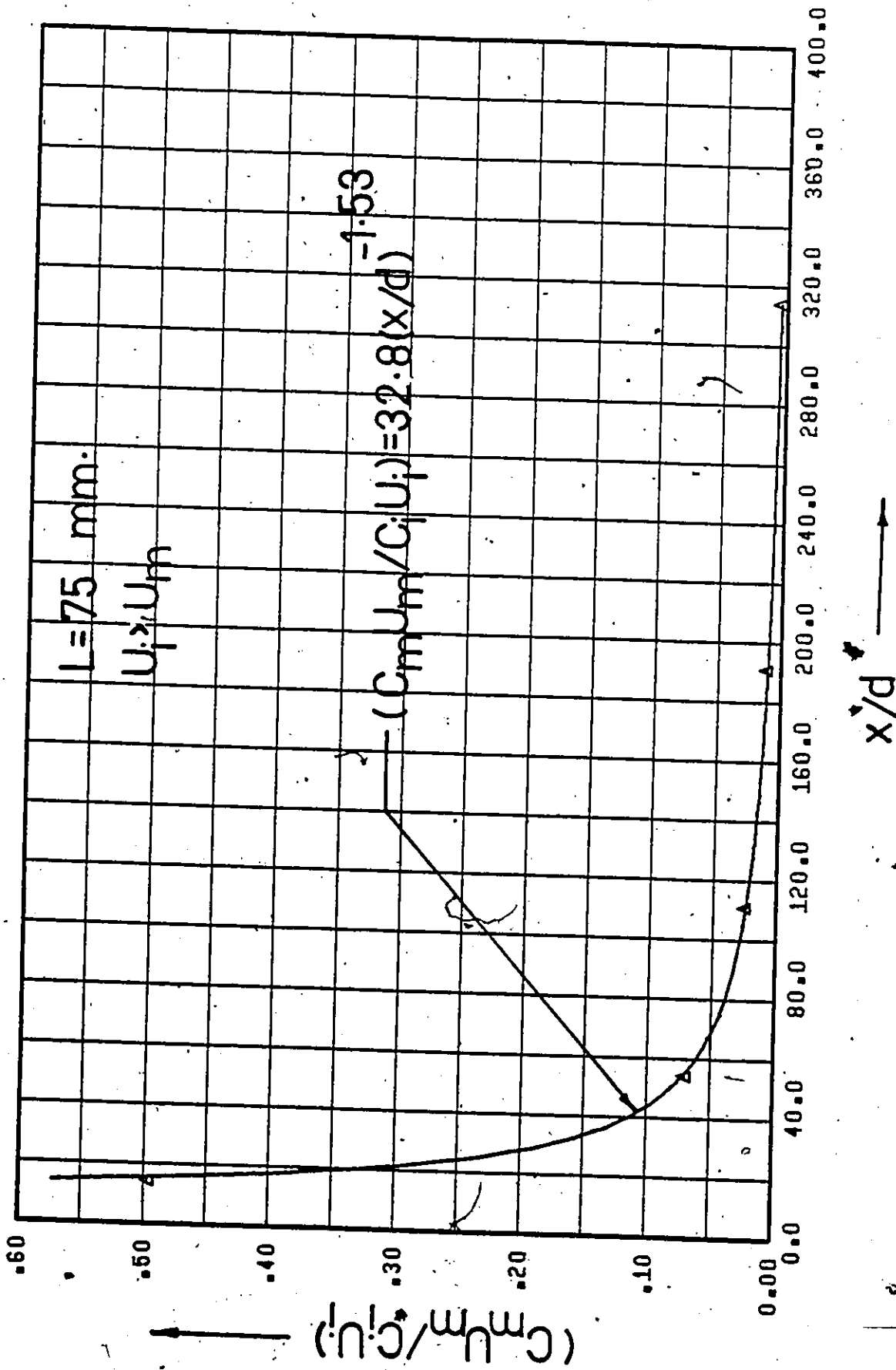


Figure 143. $(C_m U_m / C_i U_i)$ vs. x/d (Point Source Injection - Uniform Flow - Water Injection).

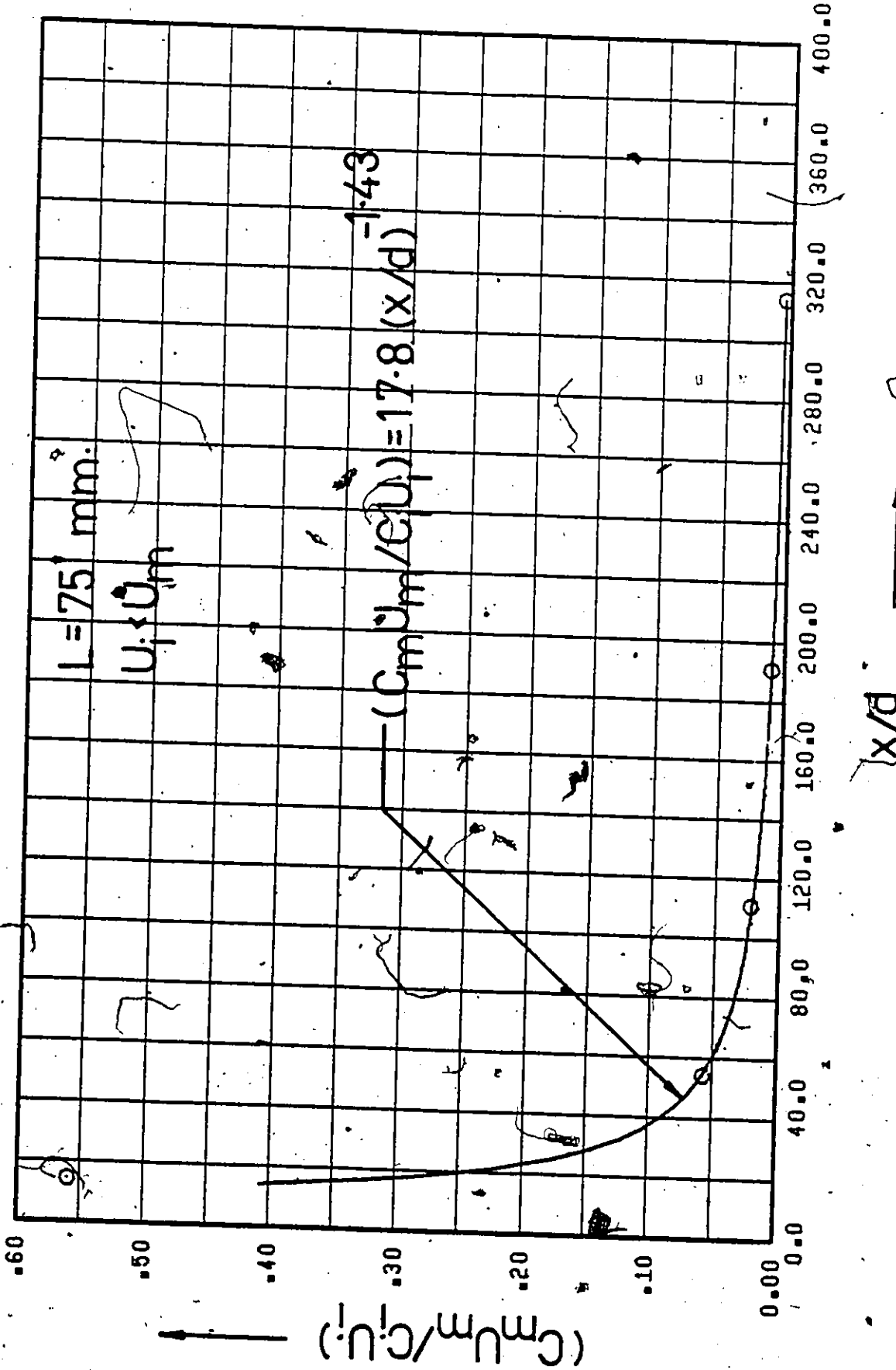


Figure 144. $(C_m U_m / C_i U_i)$ vs. x/d (Point-Source Injection - Uniform Flow - $C_i = 50$ w.p.p.m.).

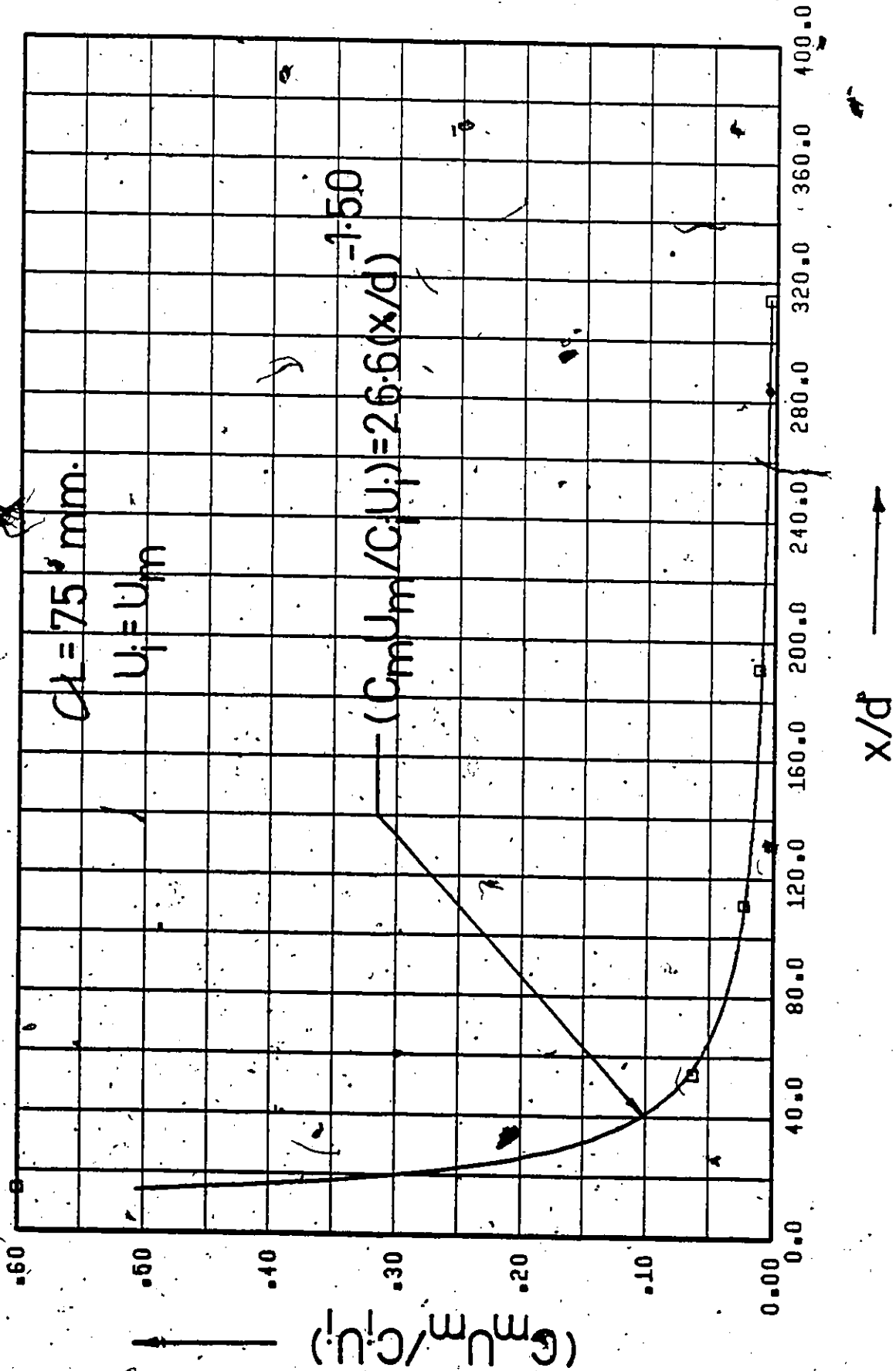


Figure 145. $(C_m U_m / C_i U_i)$ vs. x/d (Point Source Injection - Uniform Flow - $C_i = 50$ w.p.p.m.).

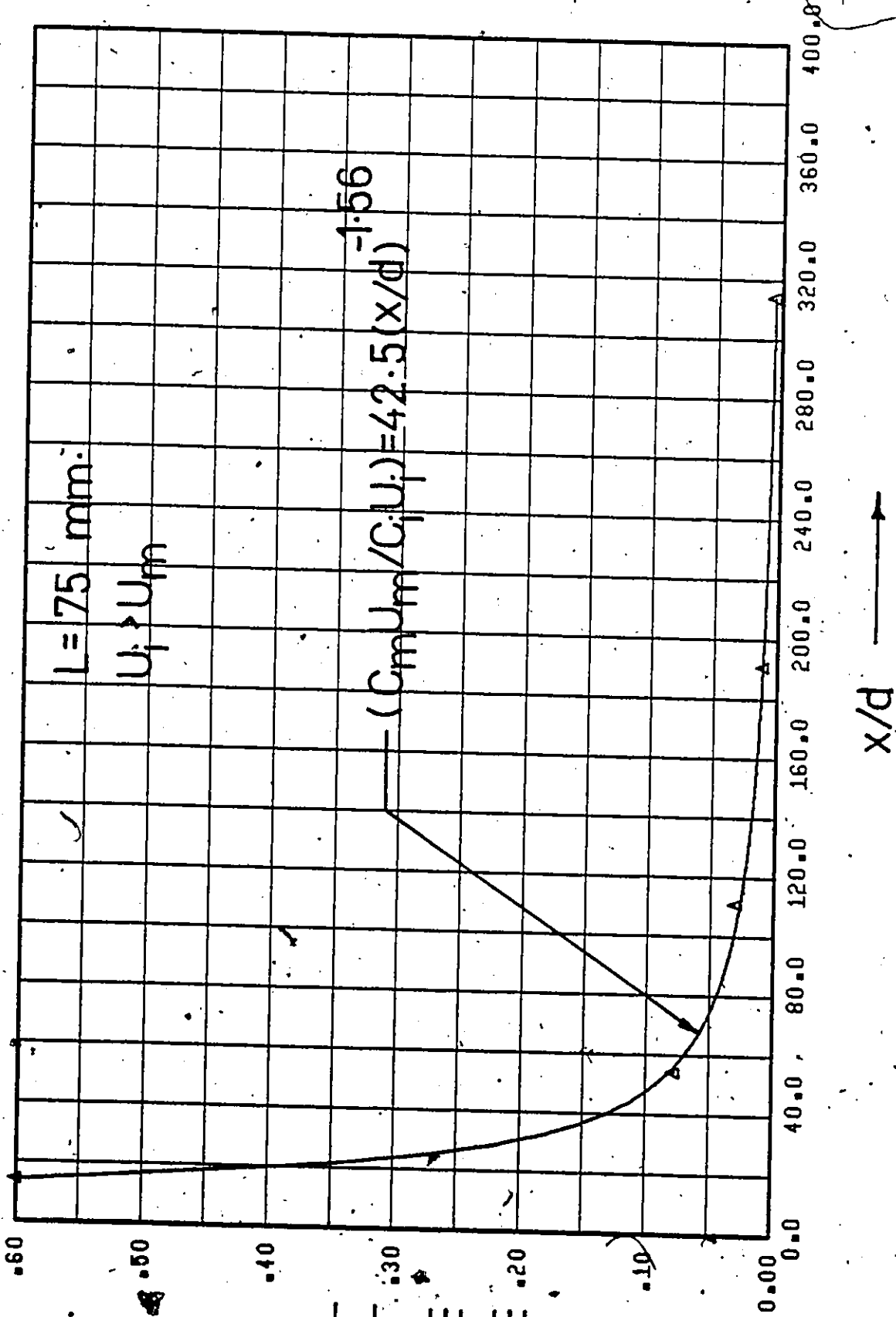


Figure 146. $(C_m U_m / C_i U_i)$ vs. x/d (Point Source Injection - Uniform Flow - $C_i = 50$ w.p.p.m.).

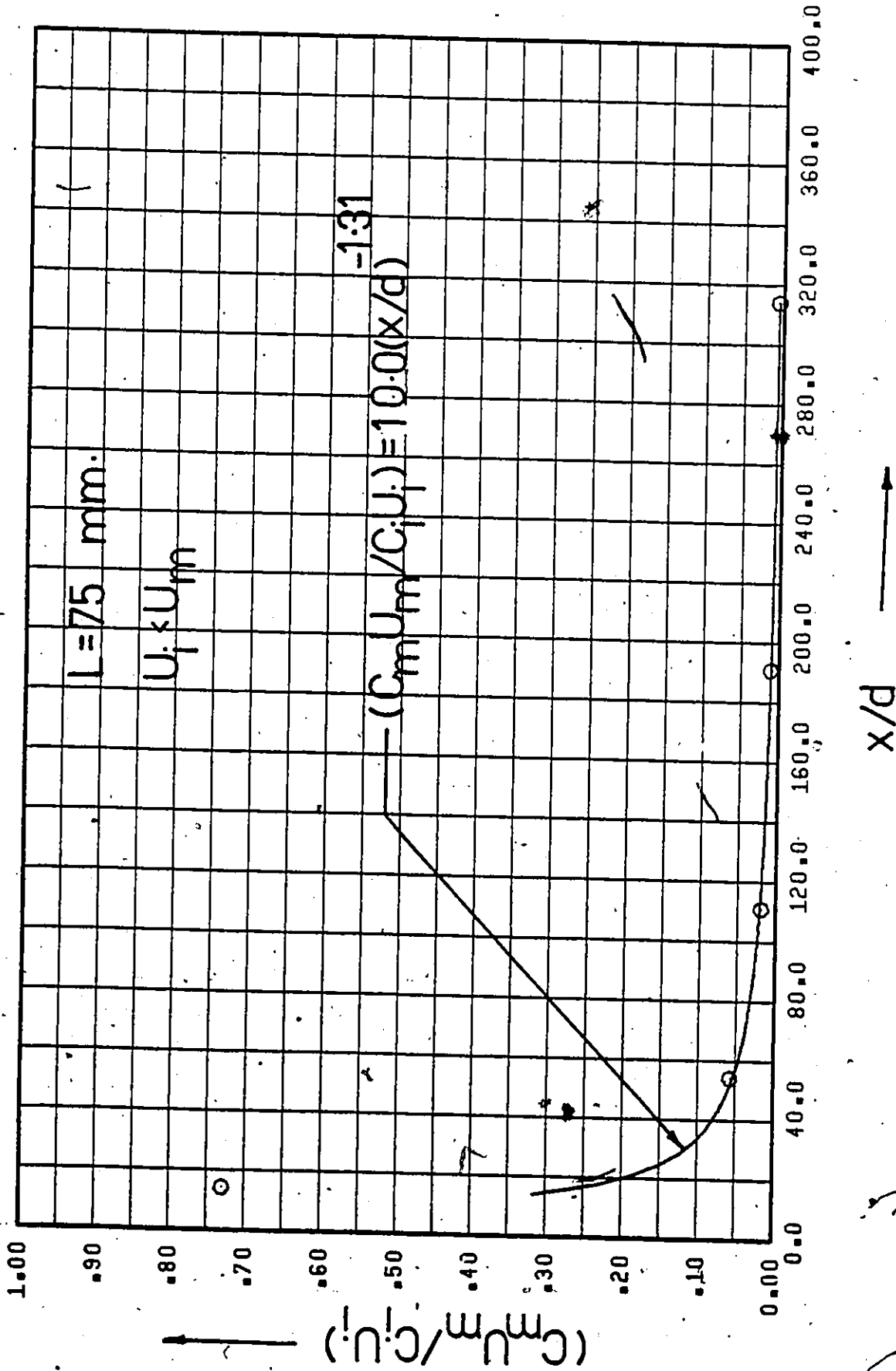


Figure 147. $(C_m U_m / C_i U_i)$ vs. x/d (Point Source Injection - Uniform Flow - $C_i = 100$ w.p.p.m.).

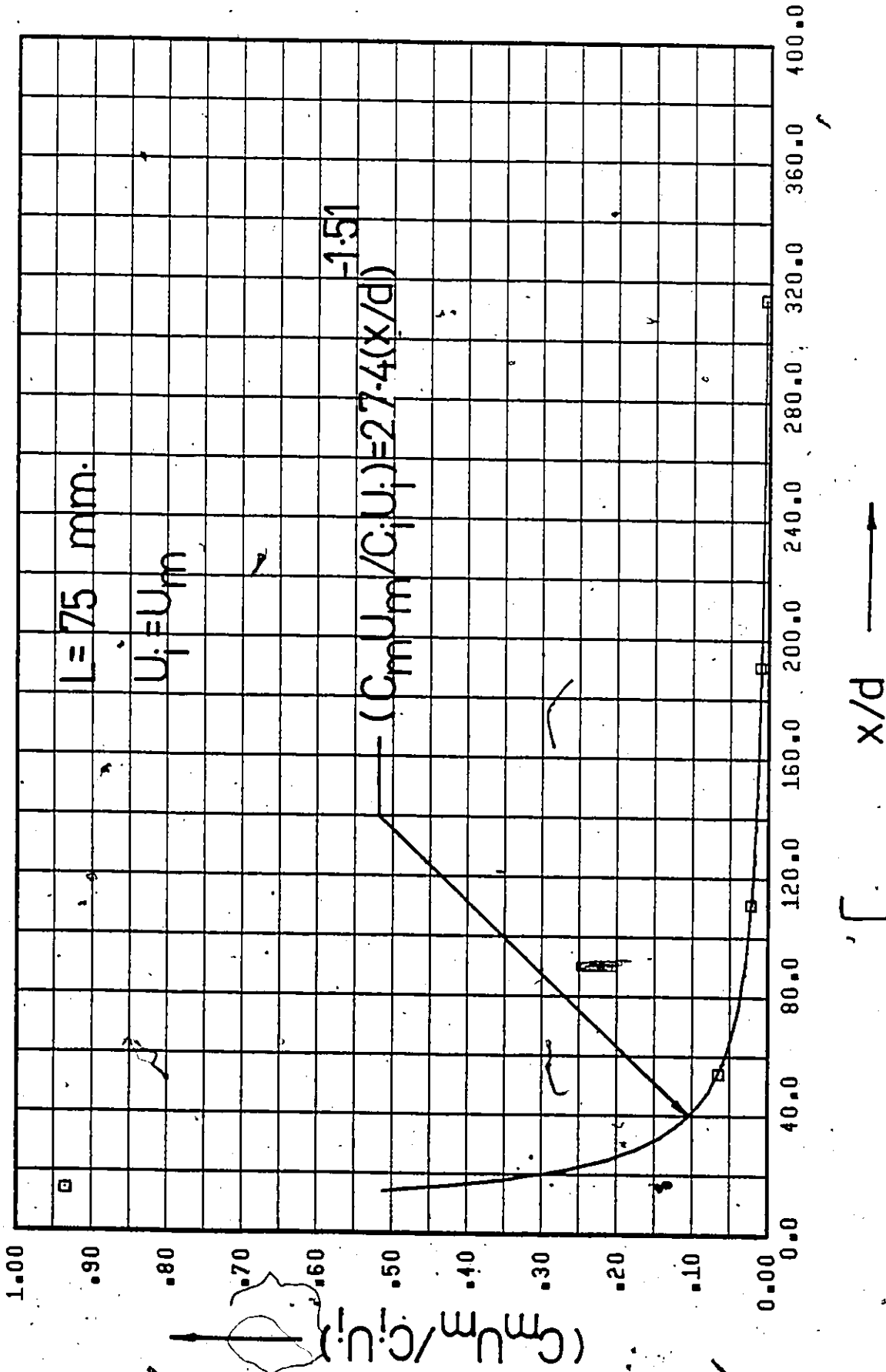


Figure 148. $(C_m U_m / C_i U_i)$ vs. x/d (Point Source Injection - Uniform Flow - $C_i = 100$ w.p.p.m.).

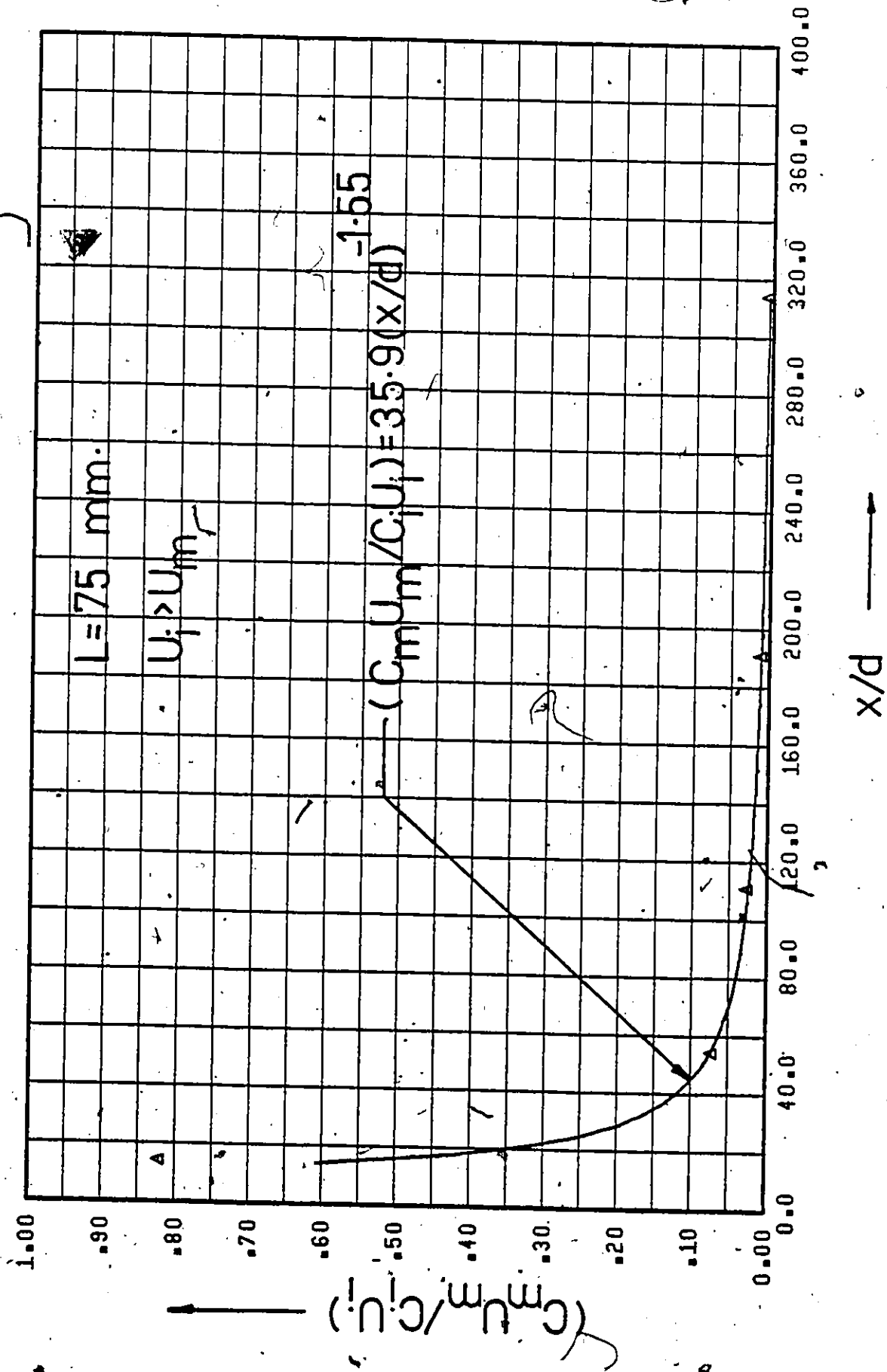


Figure 149. $(C_m U_m / C_i U_i)$ vs. x/d (Point Source Injection - Uniform Flow - $C_i = 100$ w.p.p.m.)

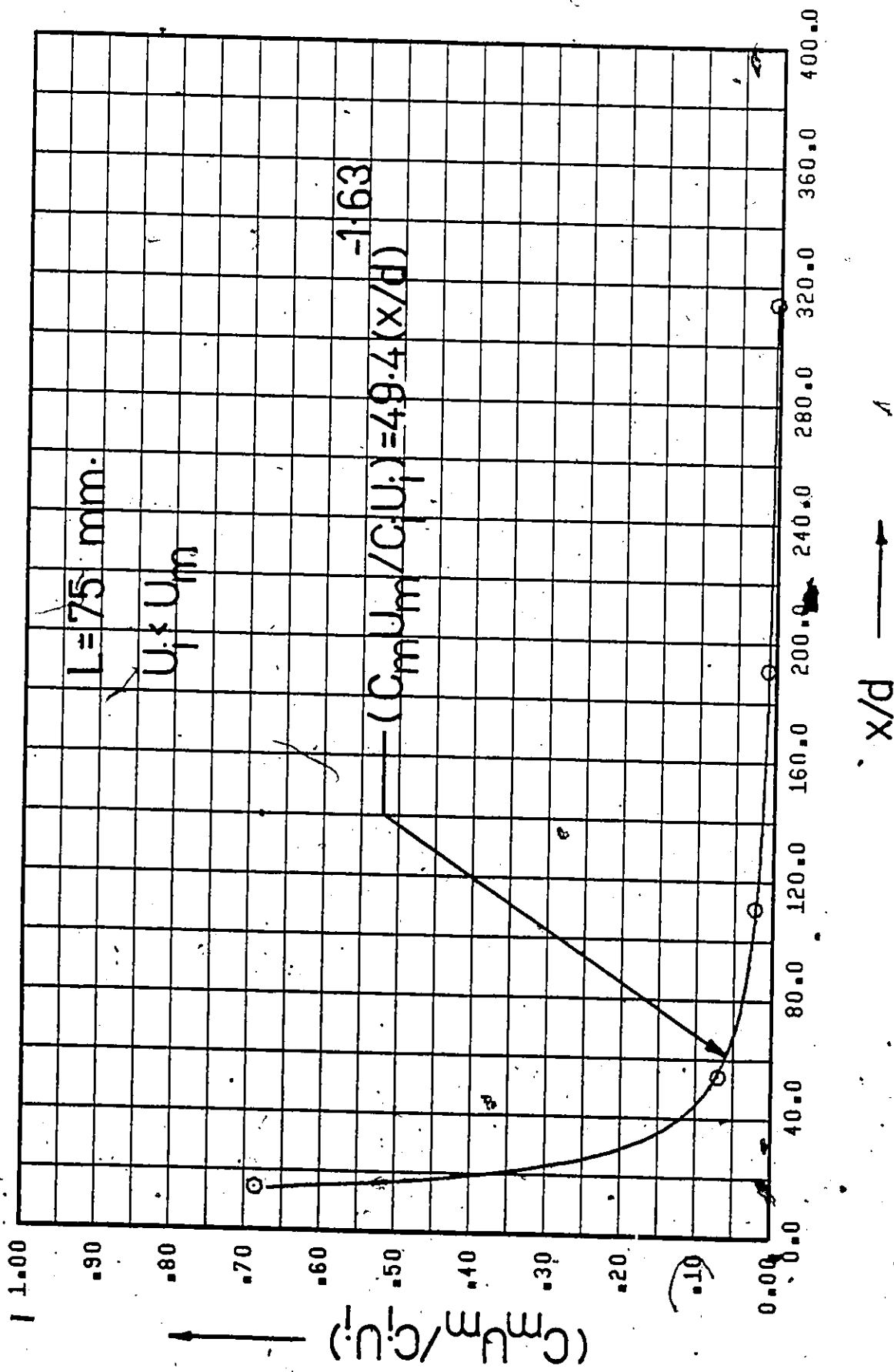


Figure 150. $(C_m U_m / C_i U_i)$ vs. x/d (Point Source Injection - Uniform Flow - $C_i = 250$ W.P.P.M.).

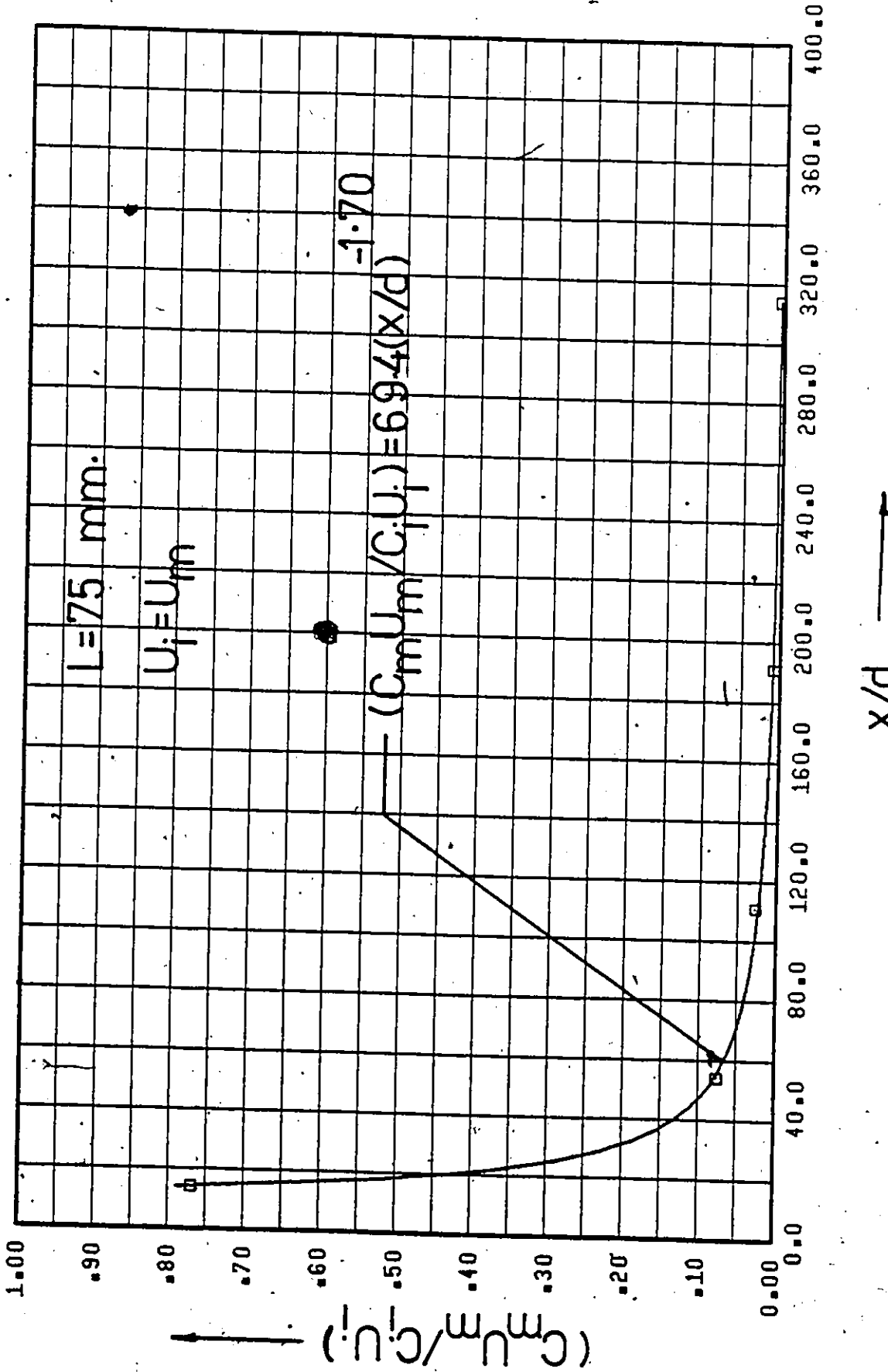


Figure 151. $(C_m U_m / C_i U_i)$ vs. x/d (Point Source Injection - Uniform Flow - $C_i = 250$ w.p.p.m.).

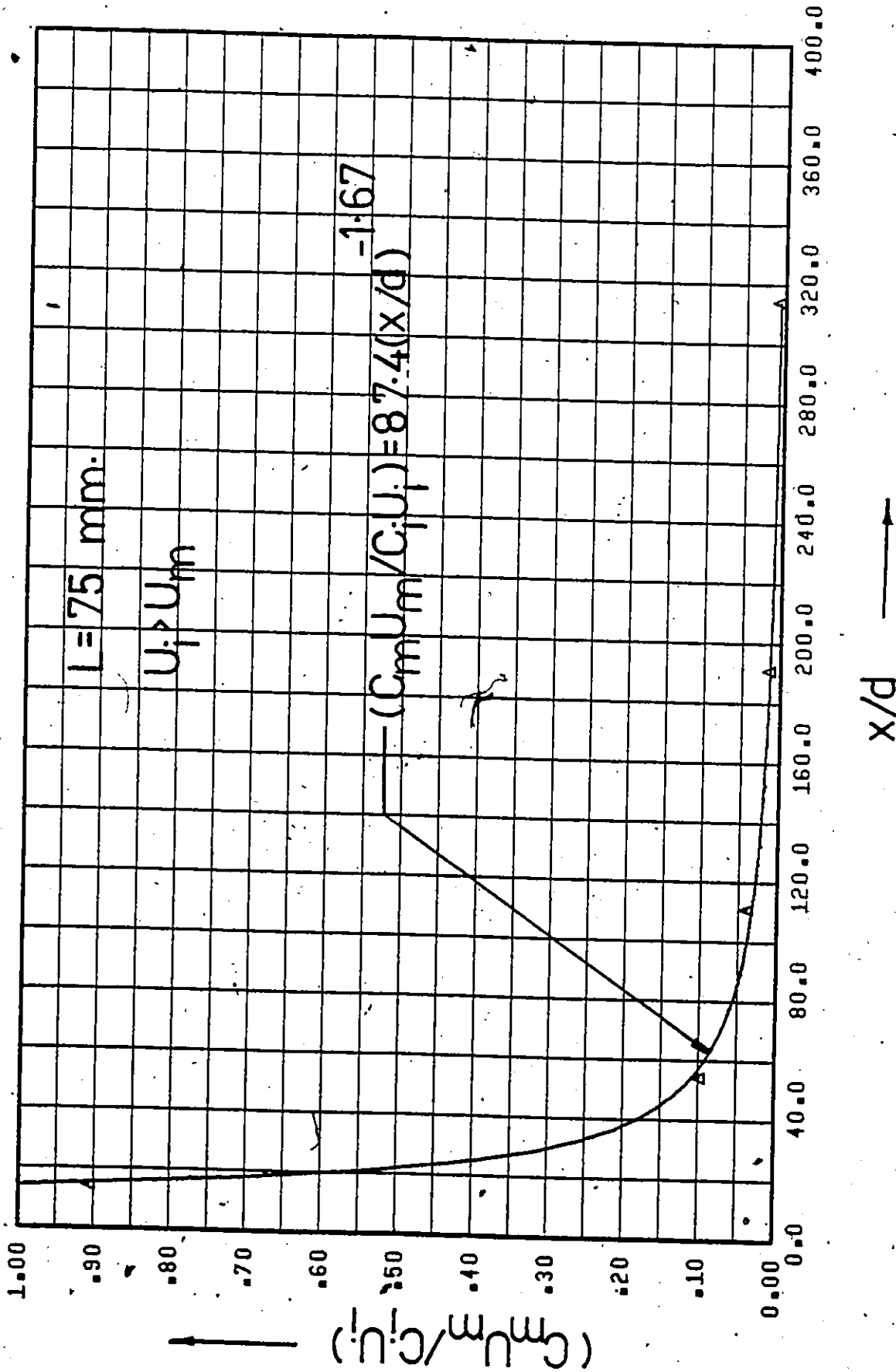


Figure 152. $(C_m U_m / C_i U_i)$ vs. x/d (Point Source Injection - Uniform Flow - $C_i = 250$ w.p.p.m.).

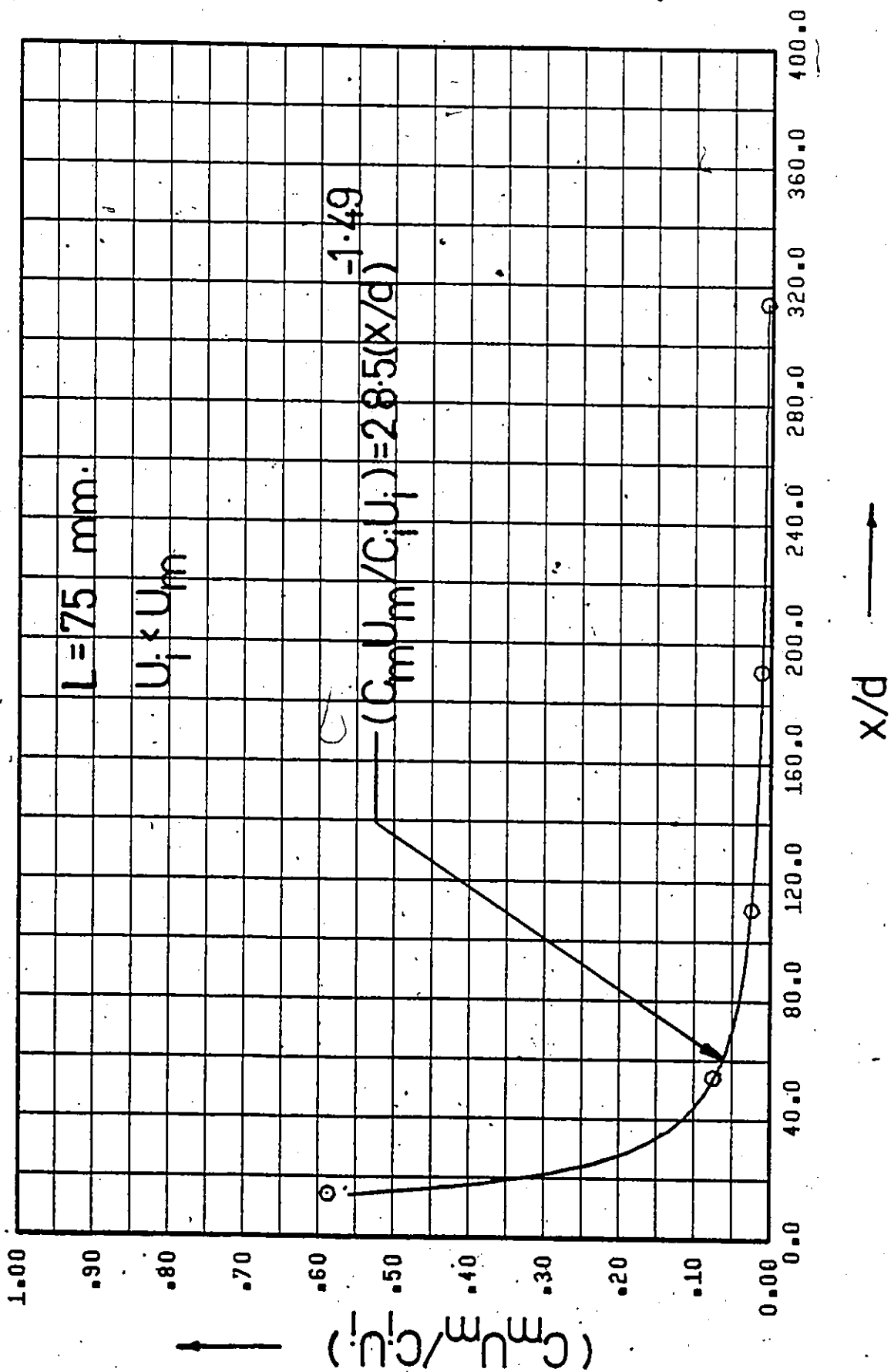


Figure 153. $(C_m U_m / C_i U_i)$ vs. x/d (Point Source Injection - Uniform Flow - $C_i = 500$ w.p.p.m.).

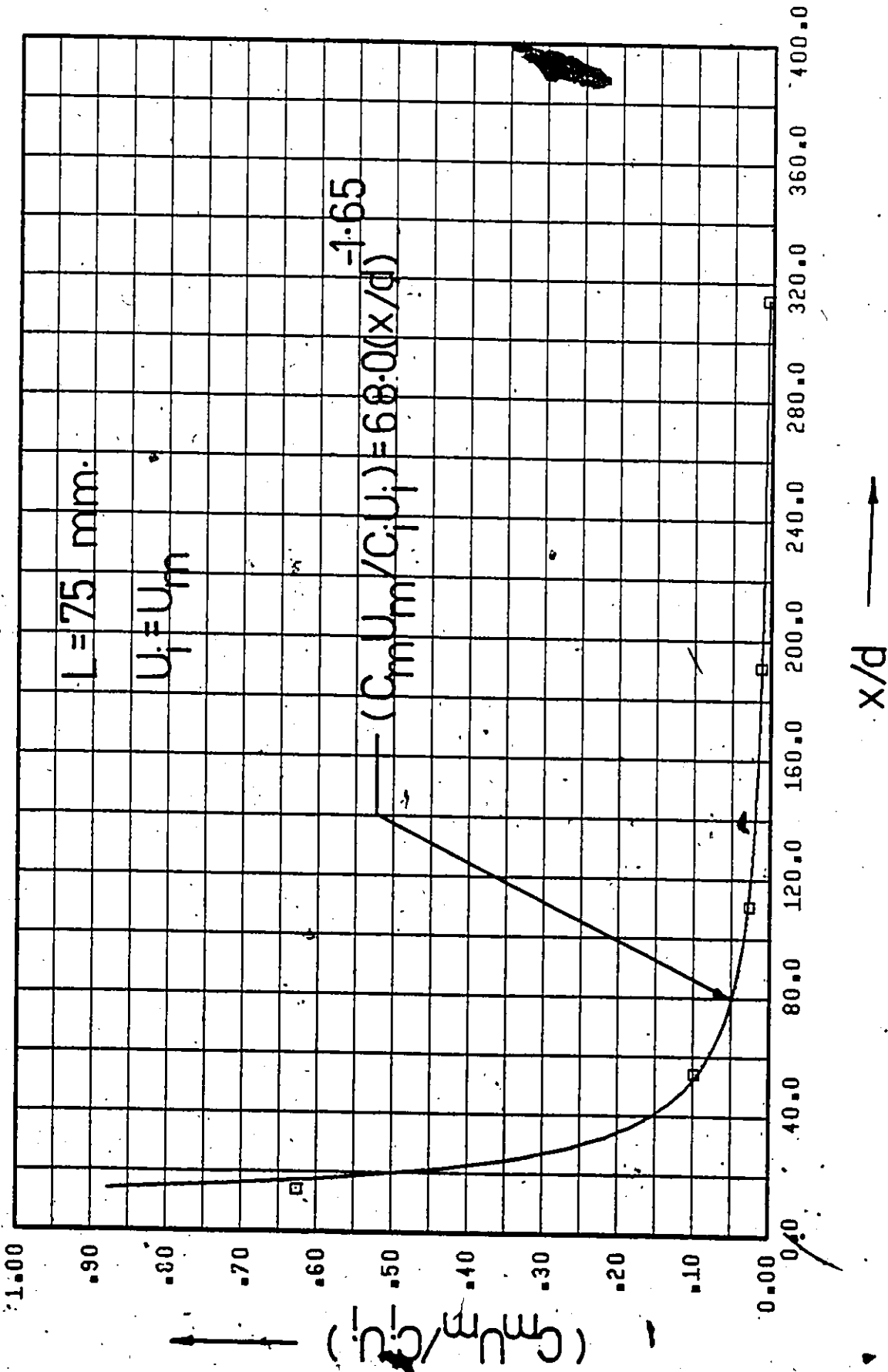


Figure 154. $(C_m U_m / C_i U_i)$ vs. x/d (Point Source Injection - Uniform Flow - $C_i = 500$ w.p.p.m.).

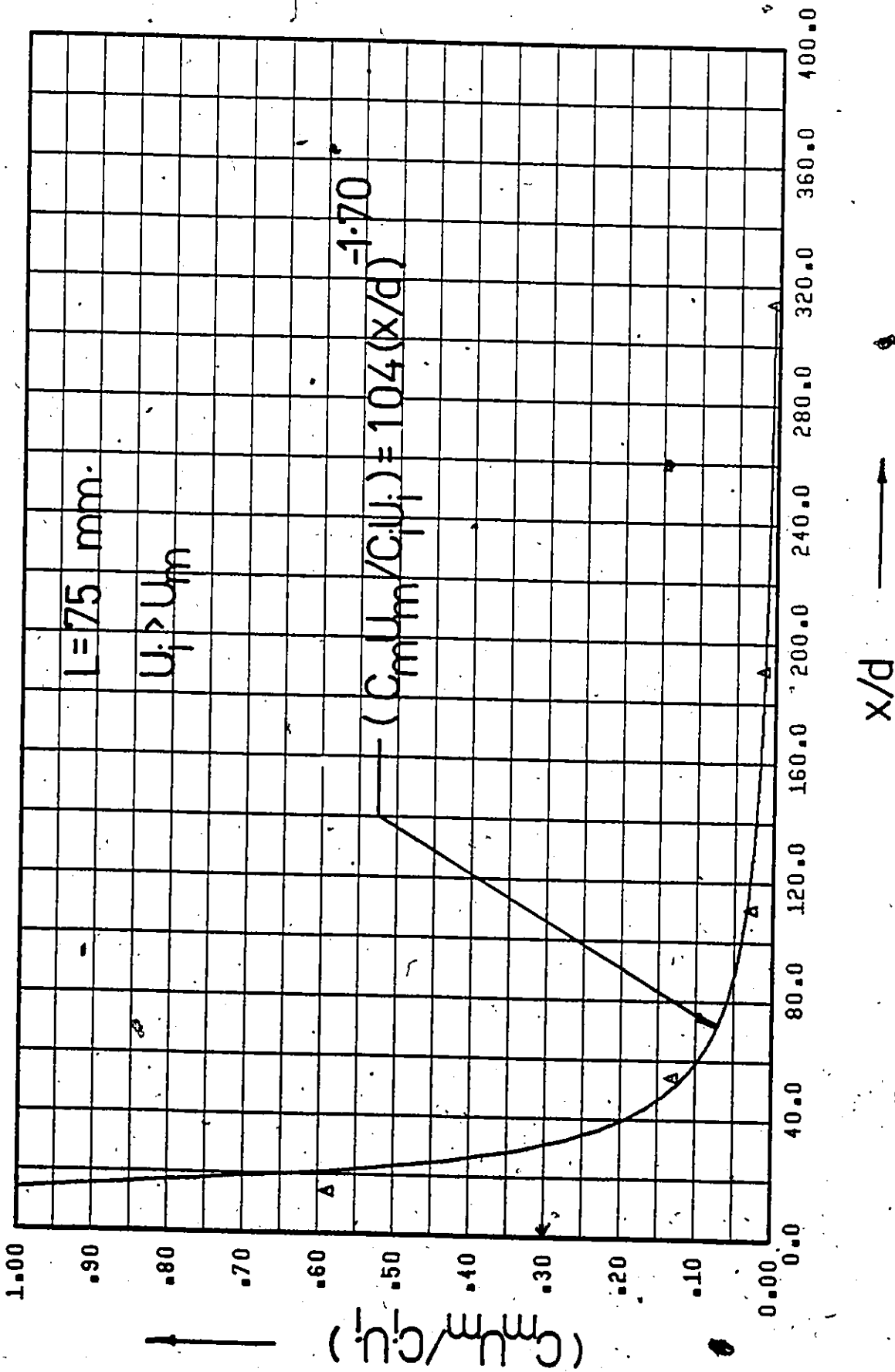


Figure 155. $(C_m U_m / C_i U_i)$ vs. x/d (Point Source Injection - Uniform Flow - $C_i = 500$ w.p.p.m.).

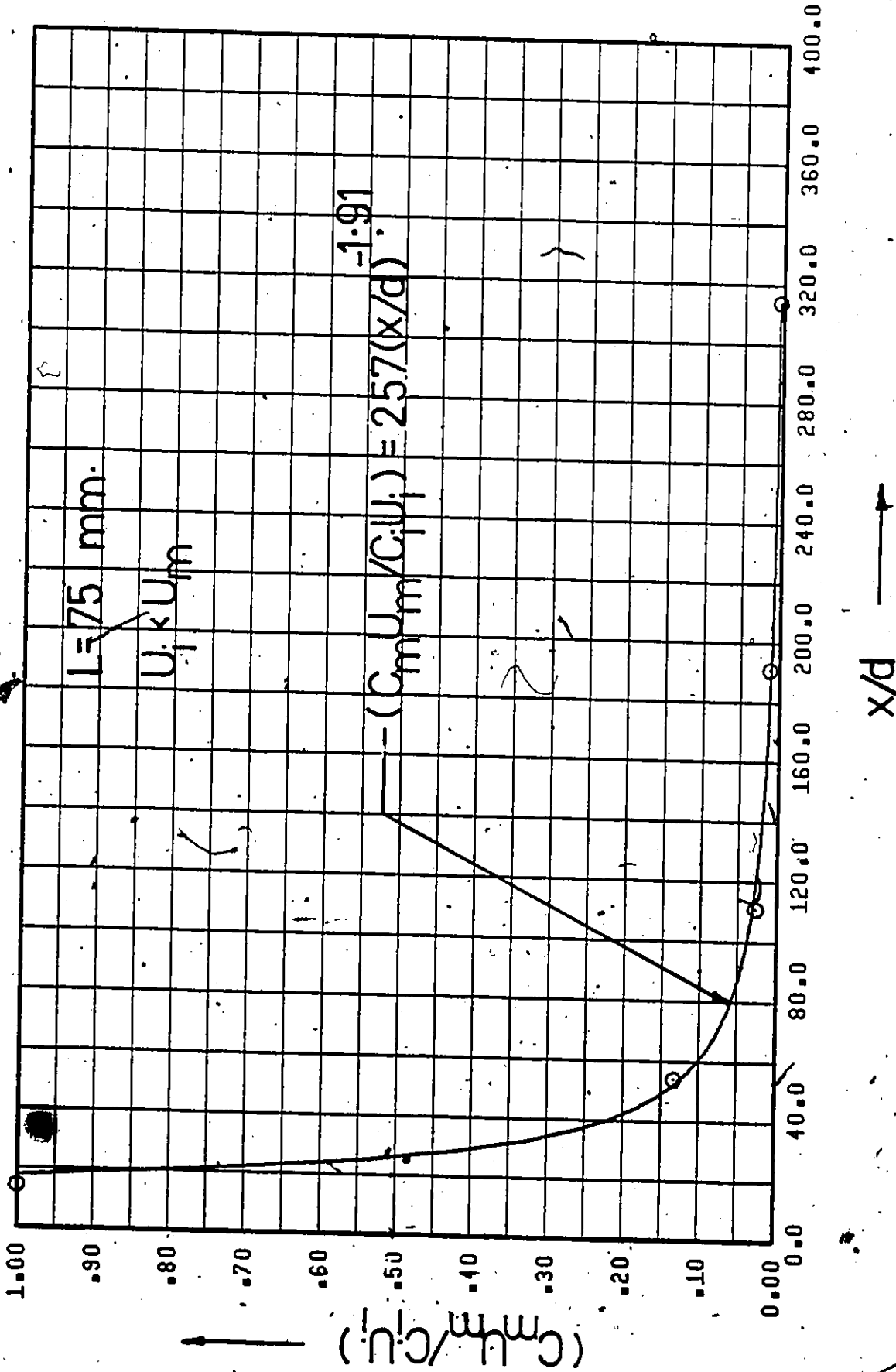


Figure 156. $(C_m U_m / C_i U_i)$ vs. x/d (Point Source Injection ~ Uniform Flow - $C_i = 1000 \text{ w.p.p.m.}$).

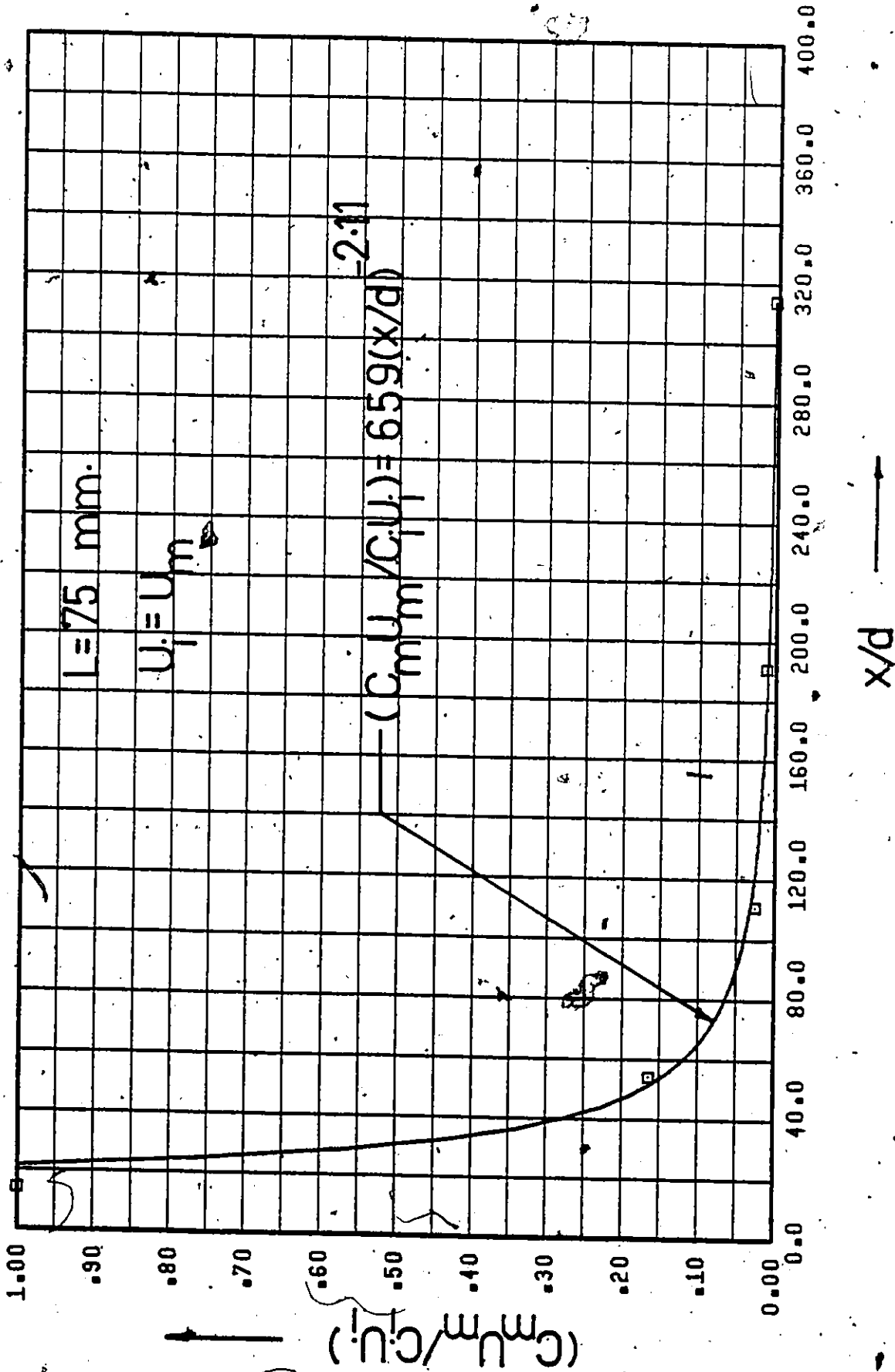


Figure 157. (C_m/C_i) vs. x/d (Point Source Injection - Uniform Flow - $C_i = 1000 \text{ w.p.p.m.}$).

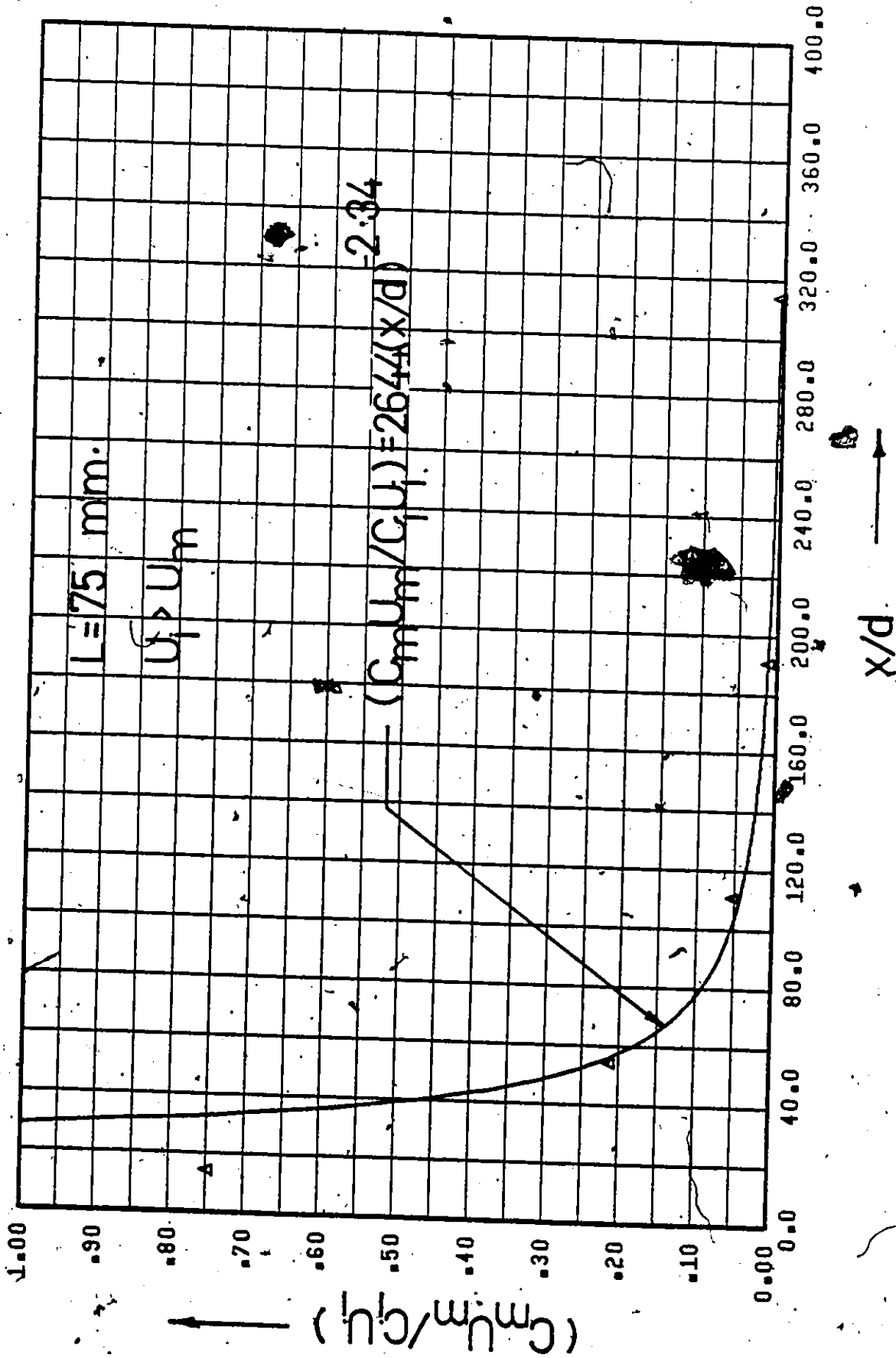


Figure 158. $(C_m U_m / C_i U_i)$ vs. x/d (Point Source Injection - Uniform Flow - $C_i = 1000$ w.p.p.m.).

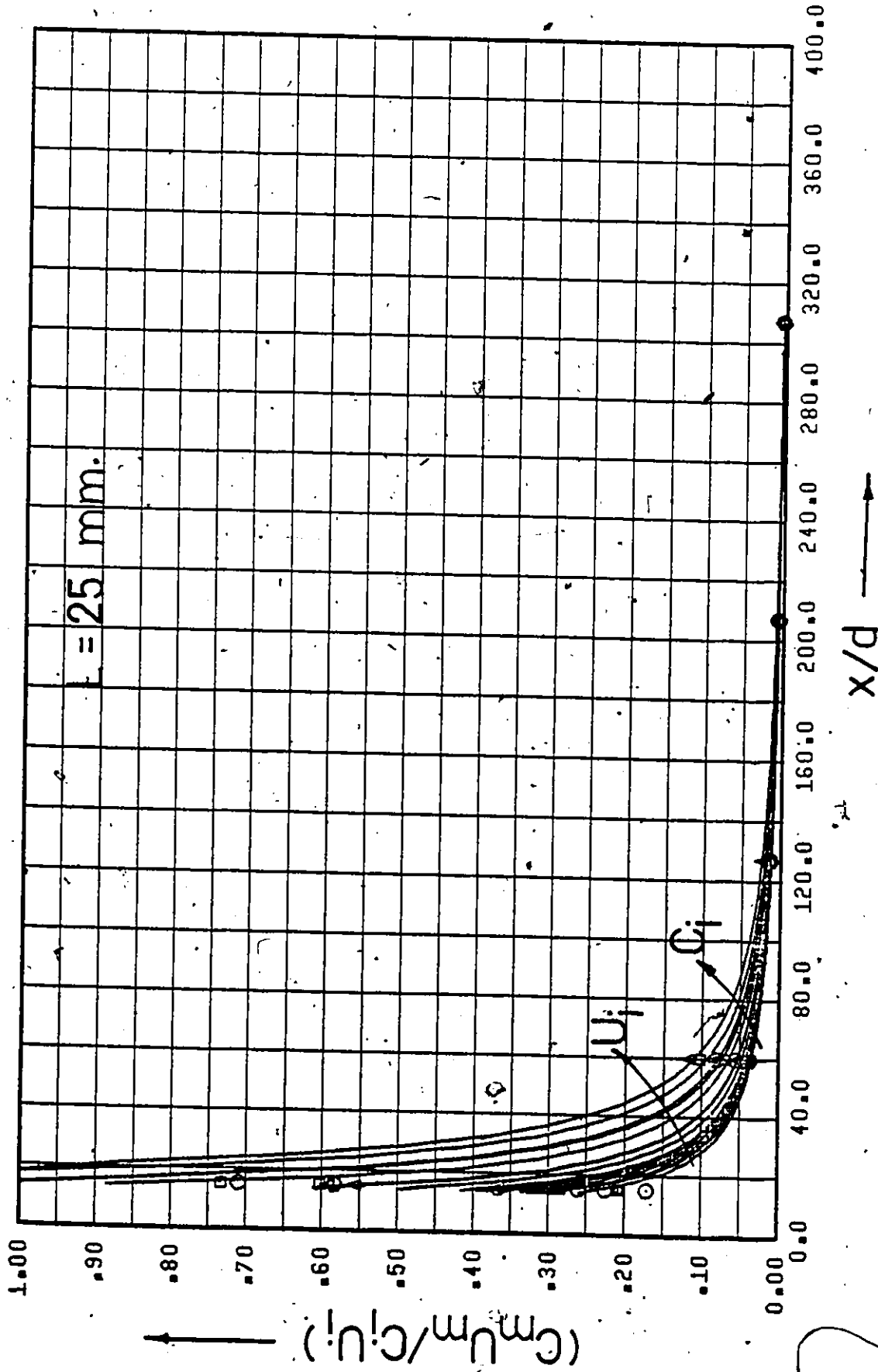


Figure 159. Wall Concentration Profiles (Point Source Injection - Fully Developed Flow).

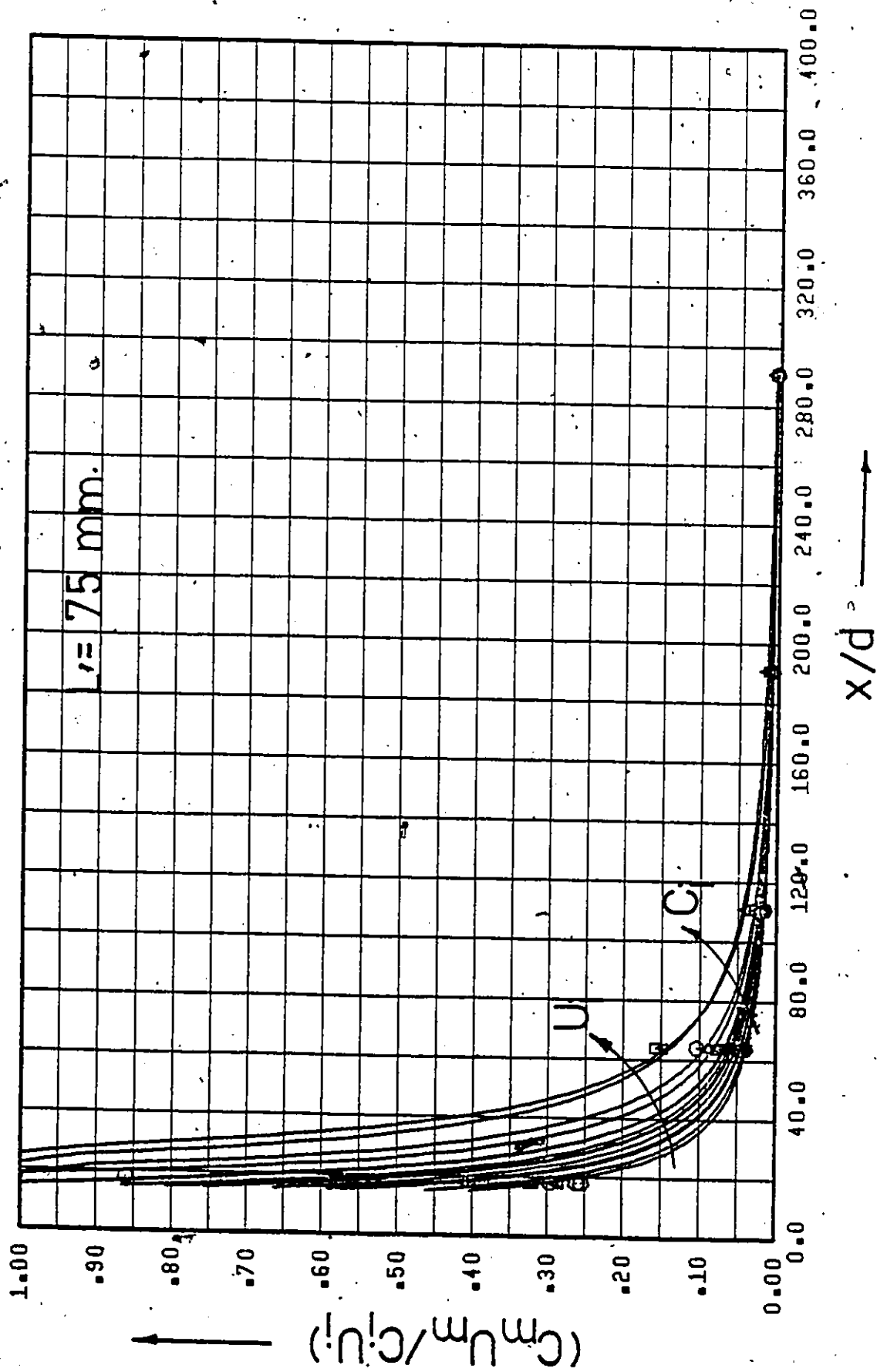


Figure 160. Wall Concentration Profiles (Point Source Injection - Fully Developed Flow).

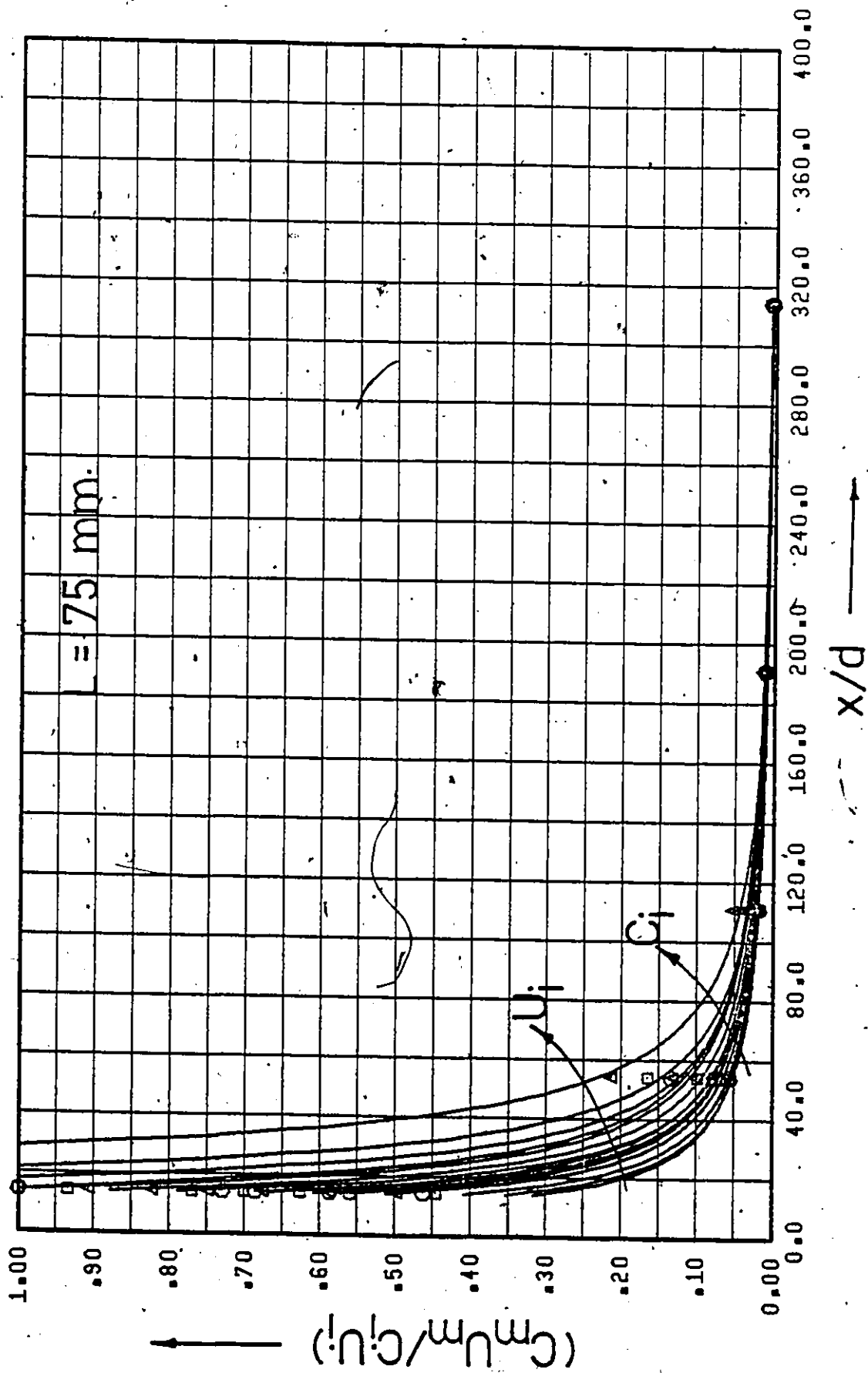


Figure 161. Wall Concentration Profiles (Point Source Injection - Uniform Flow).

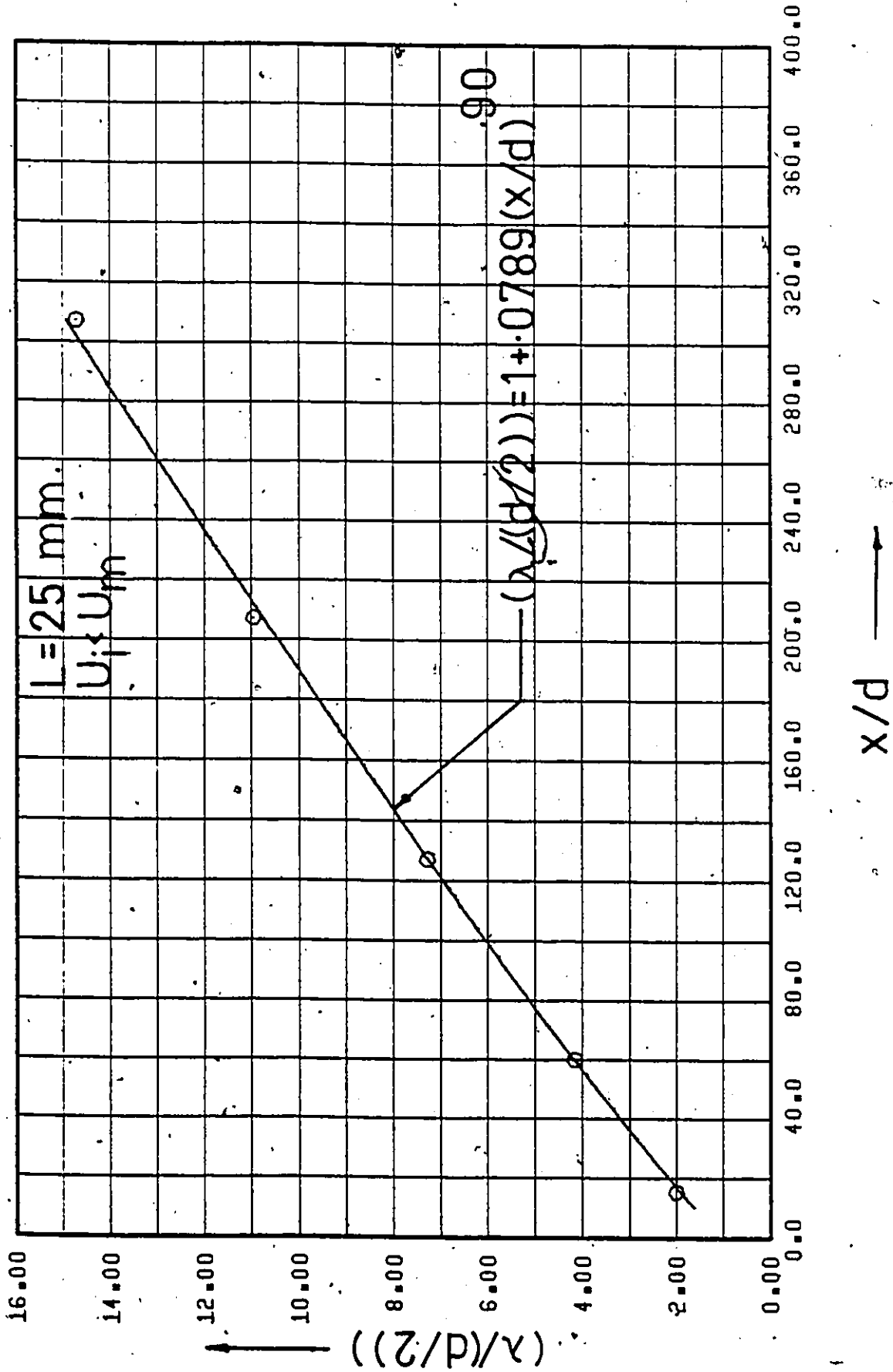


Figure 162. $(\lambda/(d/2))$ vs. x/d (Point Source Injection - Fully Developed Flow - Water Injection).

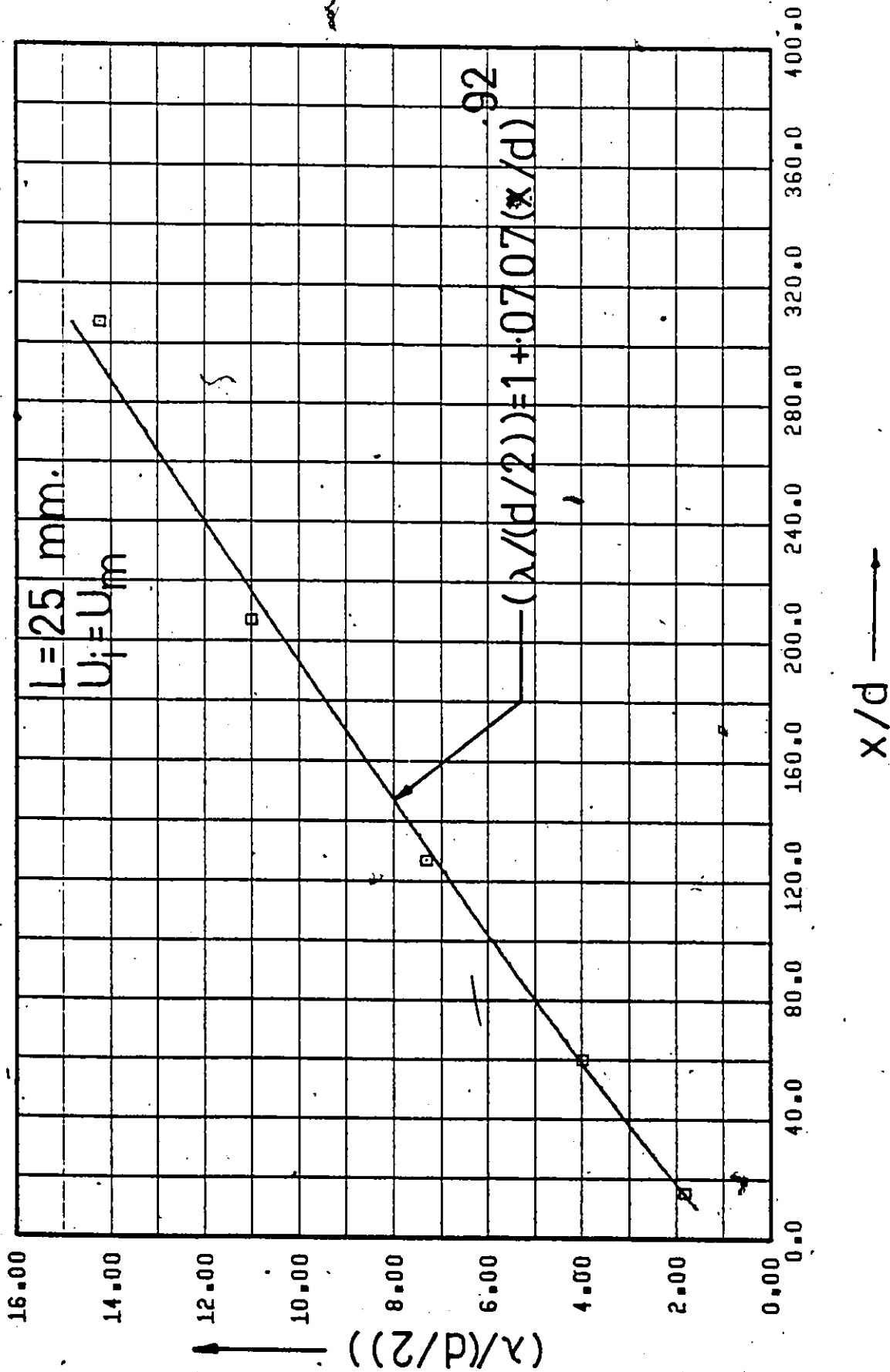


Figure 163. $(\lambda/(d/2))$ vs. x/d (Point Source Injection - Fully Developed Flow - Water Injection).

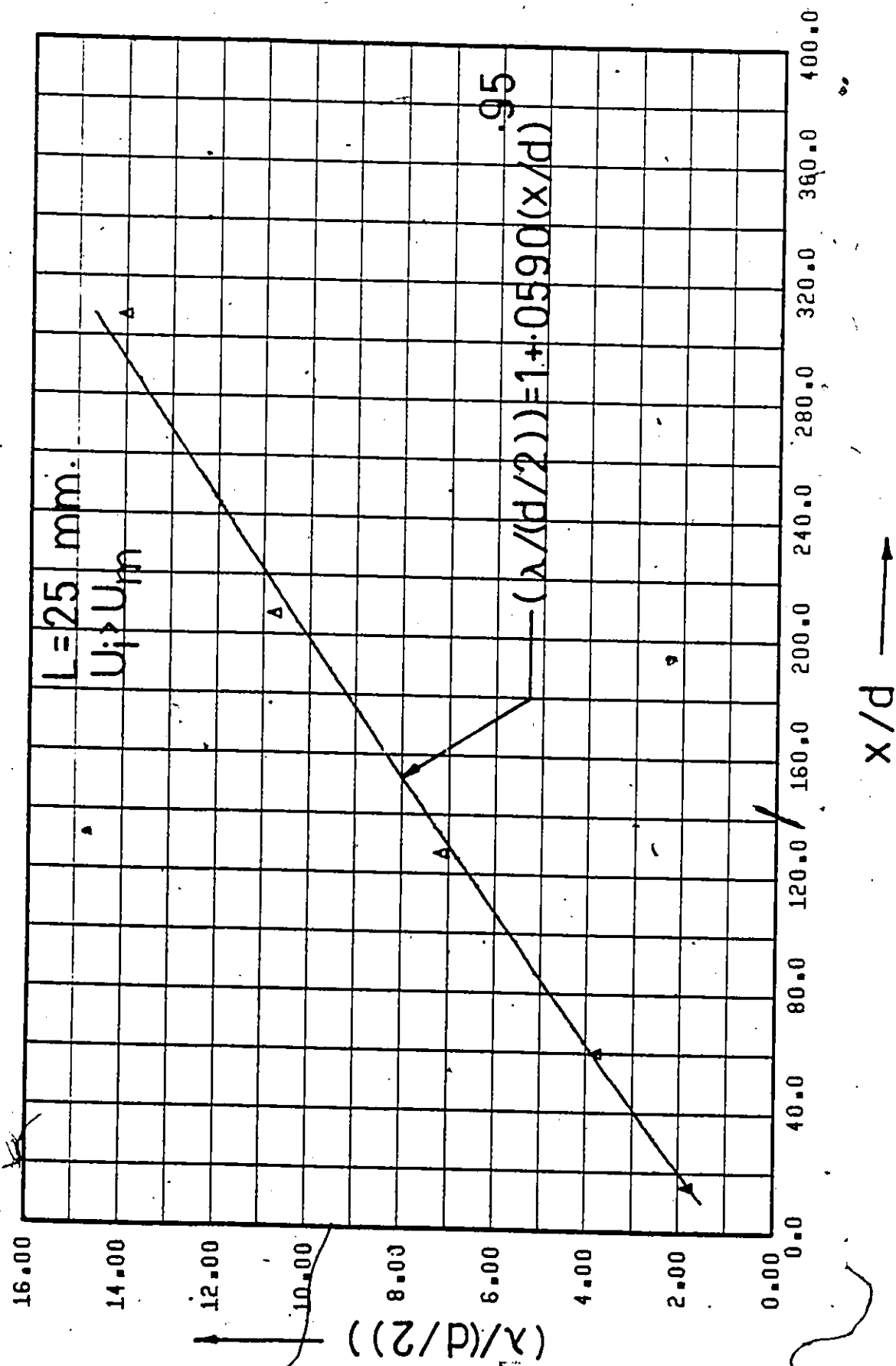


Figure 164. $(\lambda/(d/2))$ vs. x/d (Point Source Injection - Fully Developed Flow - Water Injection).

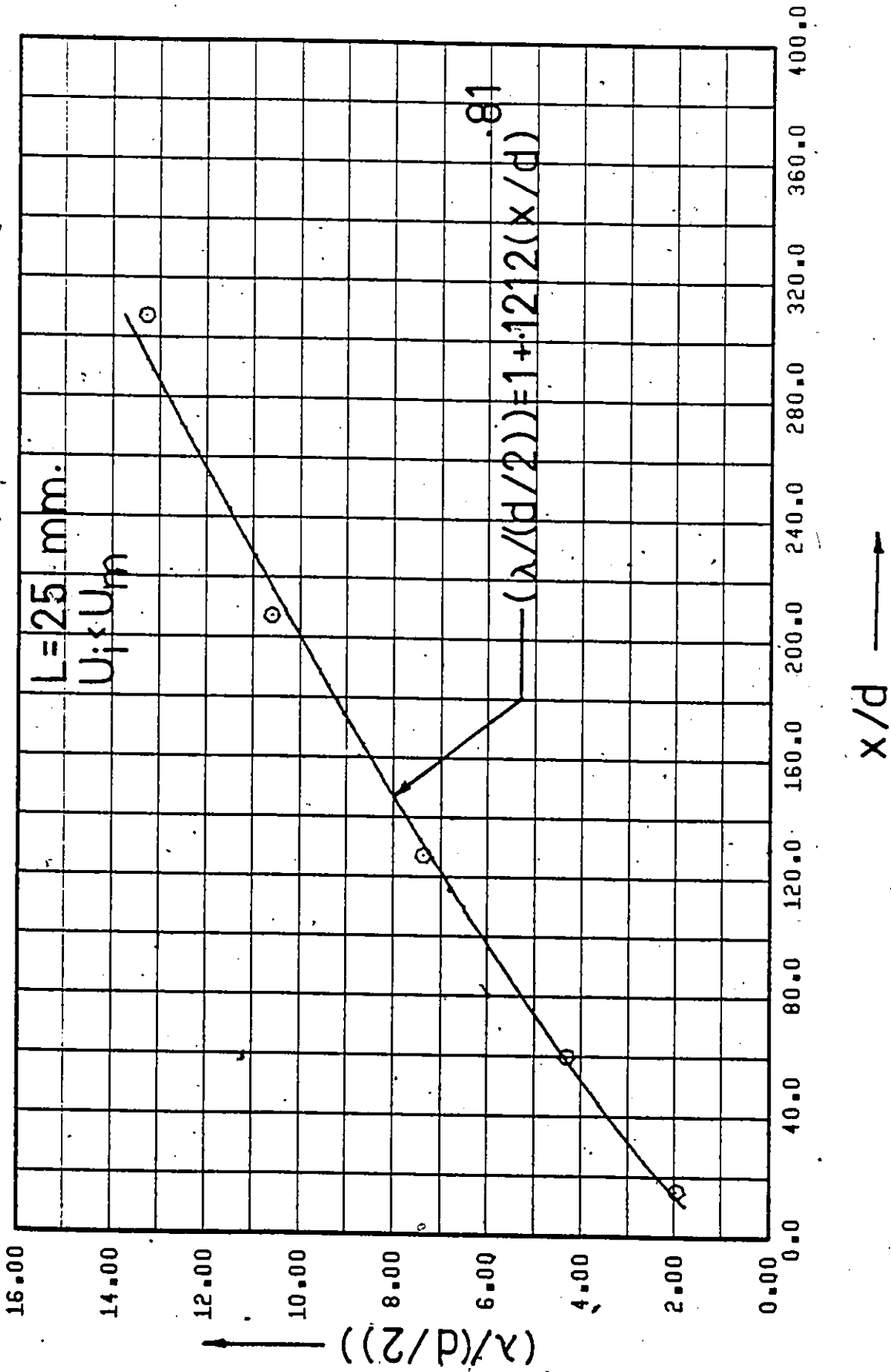


Figure 165. $(\lambda/(d/2))$ vs. x/d (Point Source Injection - Fully Developed Flow - $C_i = 50 \text{ w.p.p.m.}$).

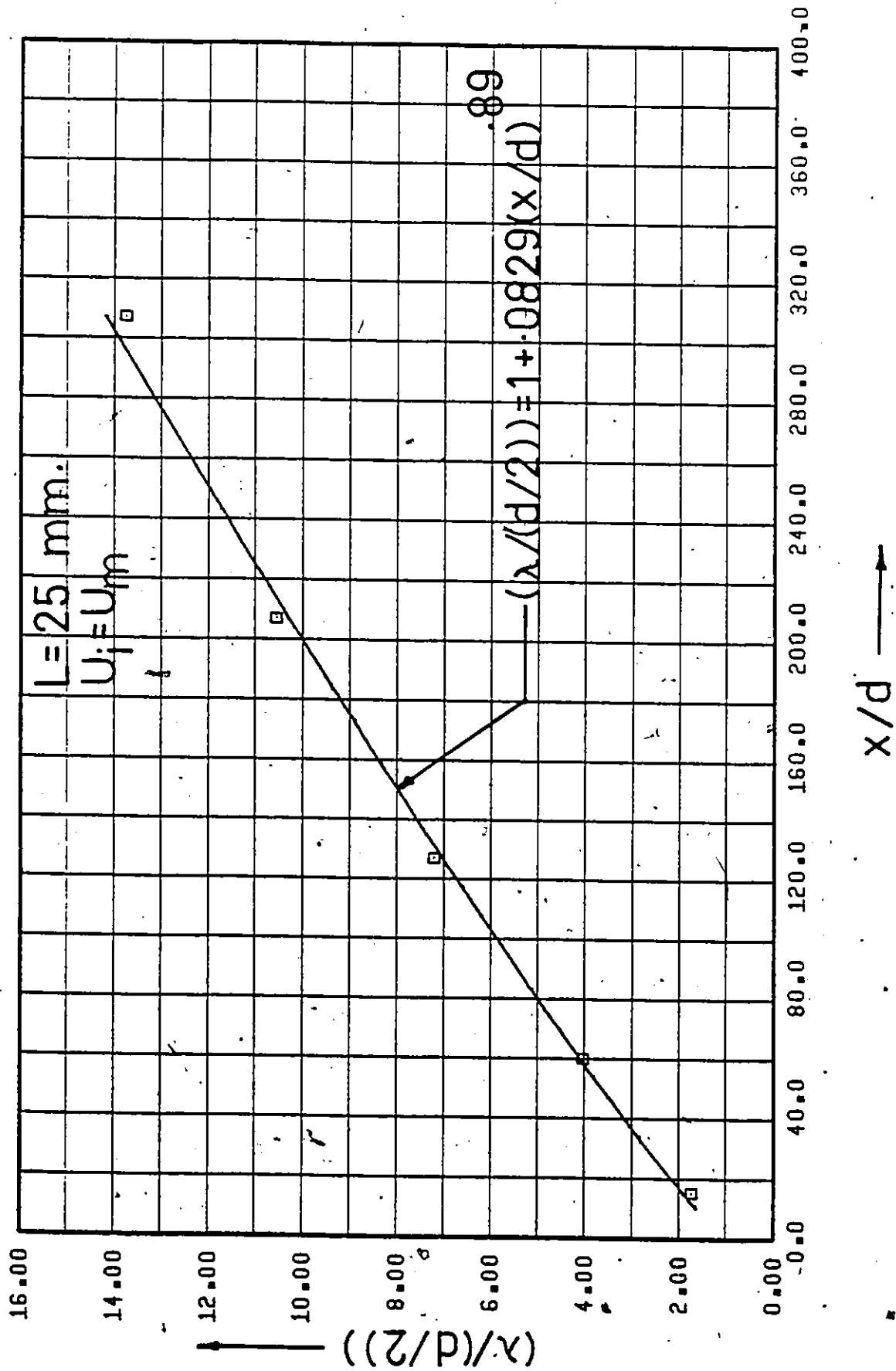


Figure 166. $(\lambda/(d/2))$ vs. x/d (Point Source Injection - Fully Developed Flow - $C_i = 50 \text{ w.p.p.m.}$).

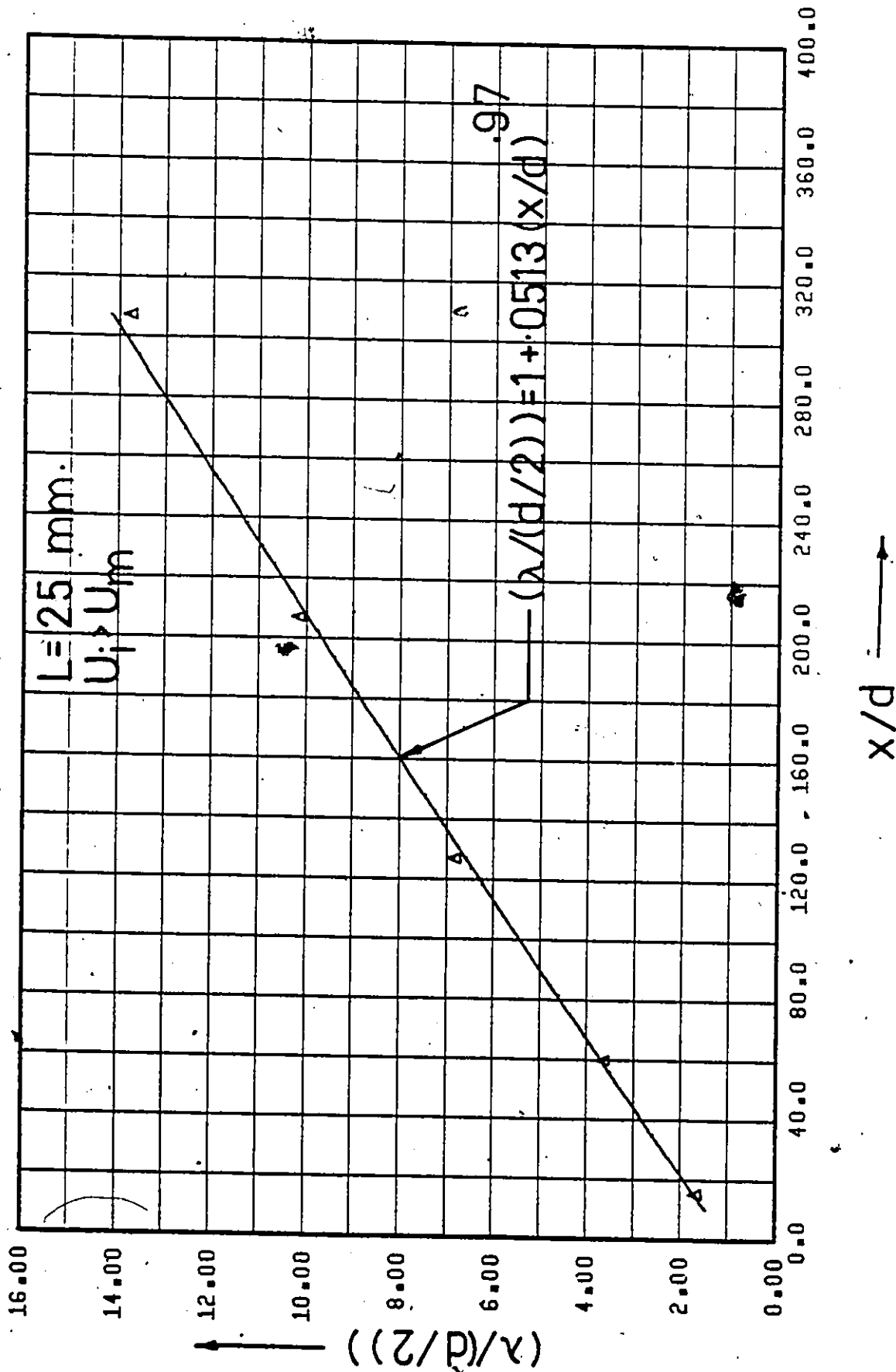


Figure 167. $(\lambda/(d/2))$ vs. x/d (Point Source Injection - Fully Developed Flow - $C_i = 50 \text{ w.p.p.m.}$).

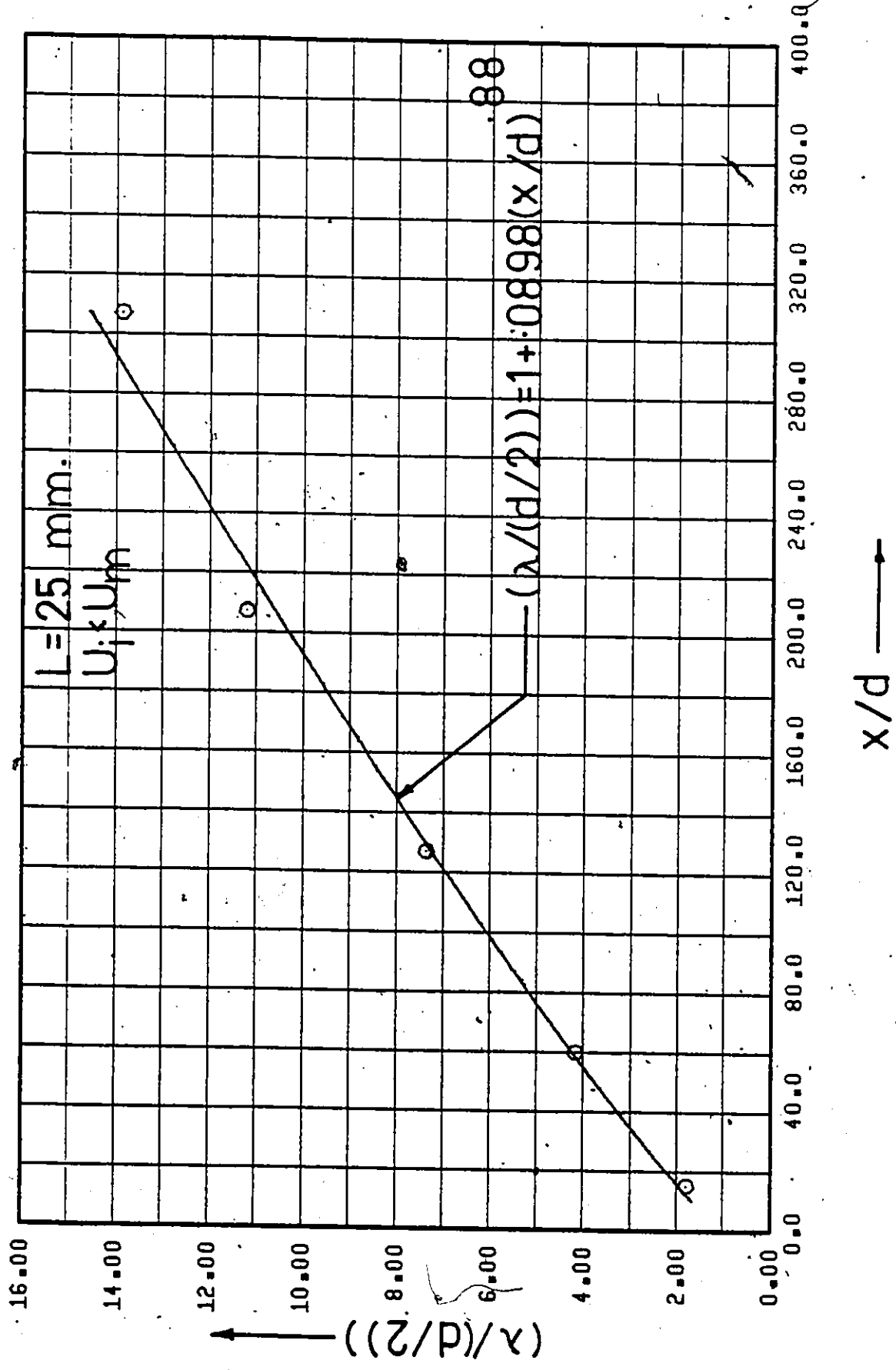


Figure 168. $(\lambda/(d/2))$ vs. x/d (Point Source Injection - Fully Developed Flow - $C_i = 100$ w.p.p.m.).

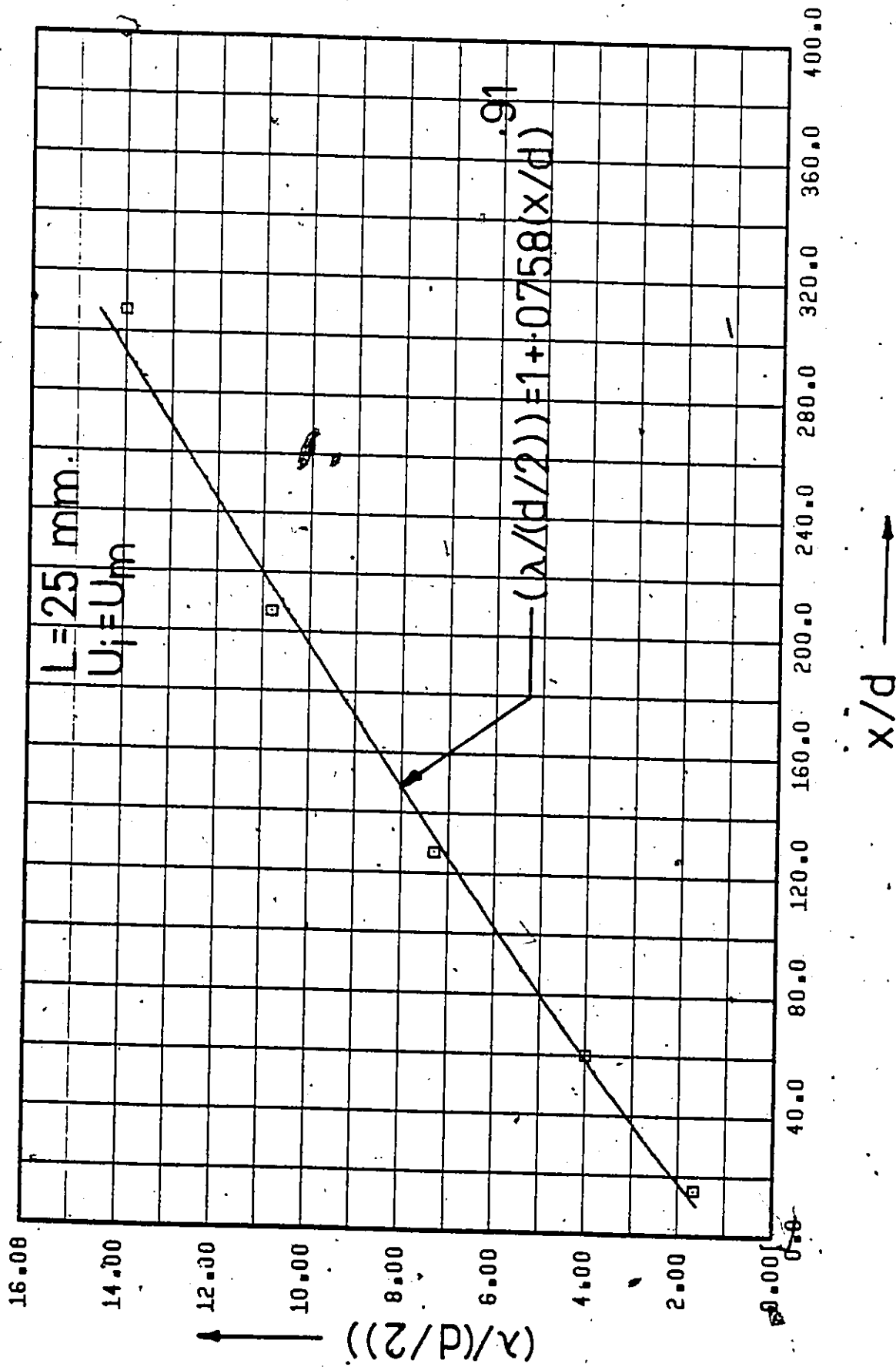


Figure 169. $(\lambda/(d/2))$ vs. x/d (Point Source Injection - Fully Developed Flow - $C_i = 100$ w.p.p.m.).

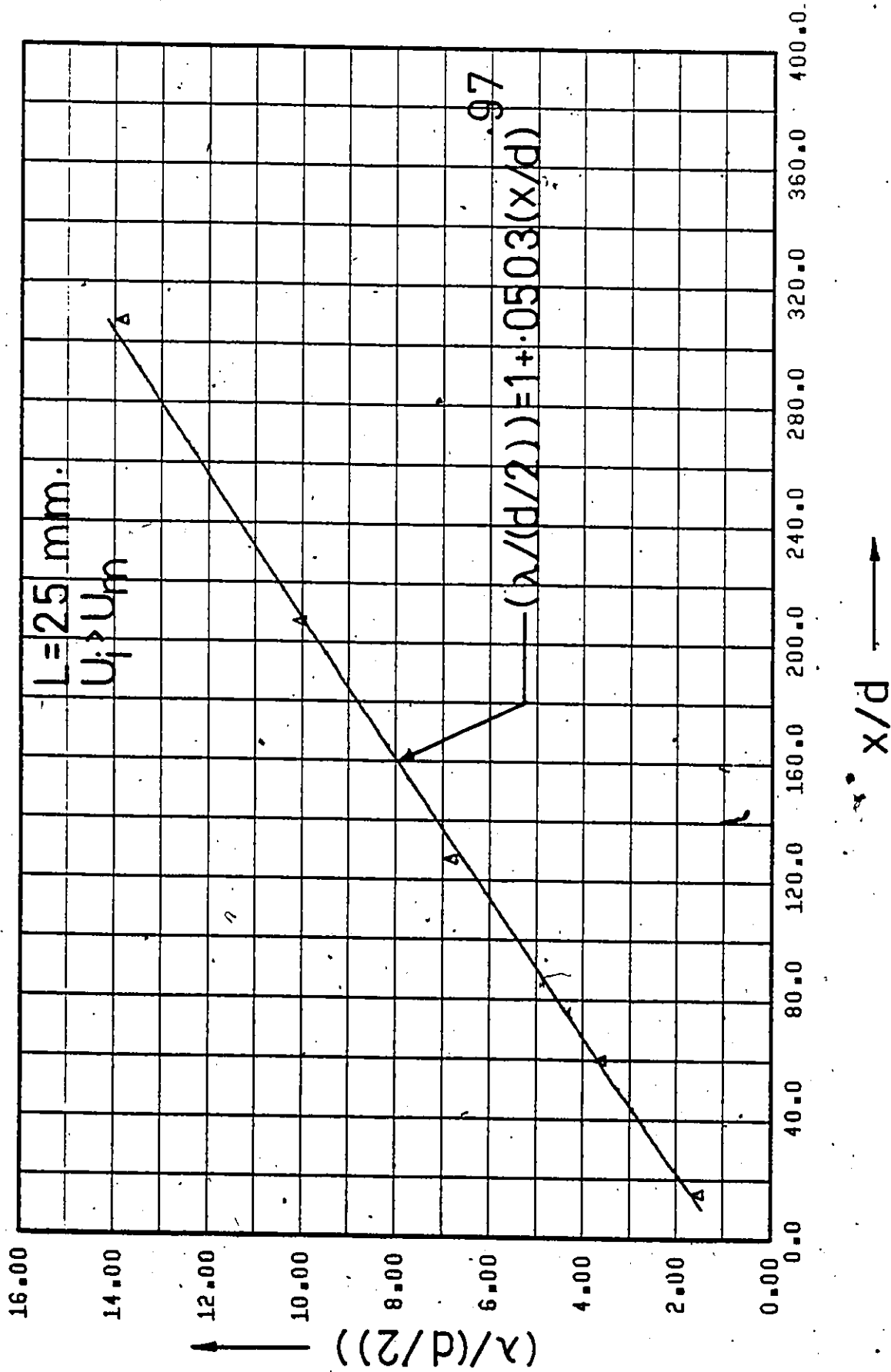


Figure 170. $(\lambda/(d/2))$ vs. x/d (Point Source Injection - Fully Developed Flow - $C_i = 100$ w.p.p.m.).

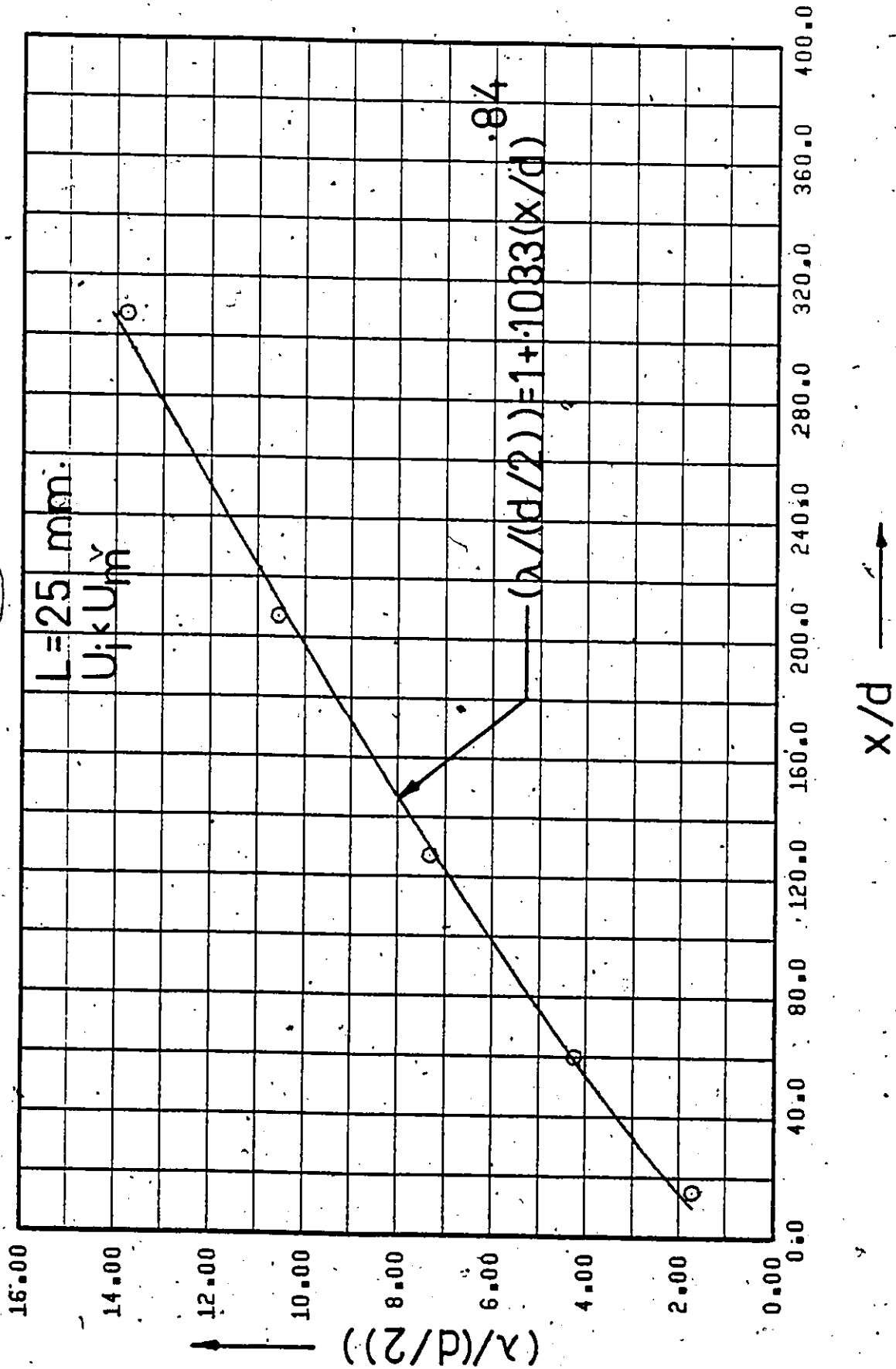


Figure 171. $(\lambda/(d/2))$ vs. x/d (Point Source Injection - Fully Developed Flow - $C_i = 250 \text{ w.p.p.m.}$).

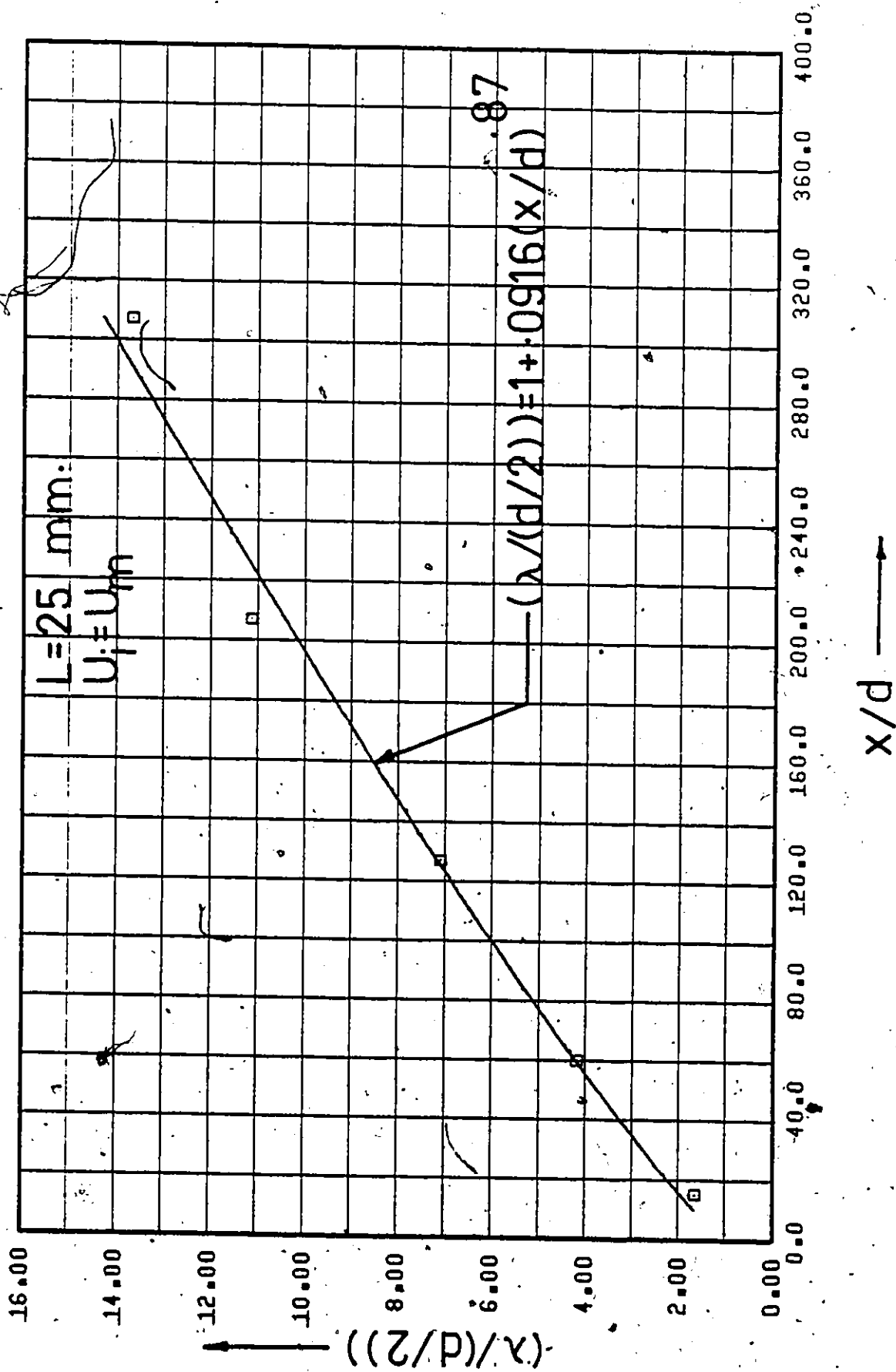


Figure 172. $(\lambda/(d/2))$ vs. x/d (Point Source Injection - Fully Developed Flow - $C_i = 250 \text{ w.p.p.m.}$).

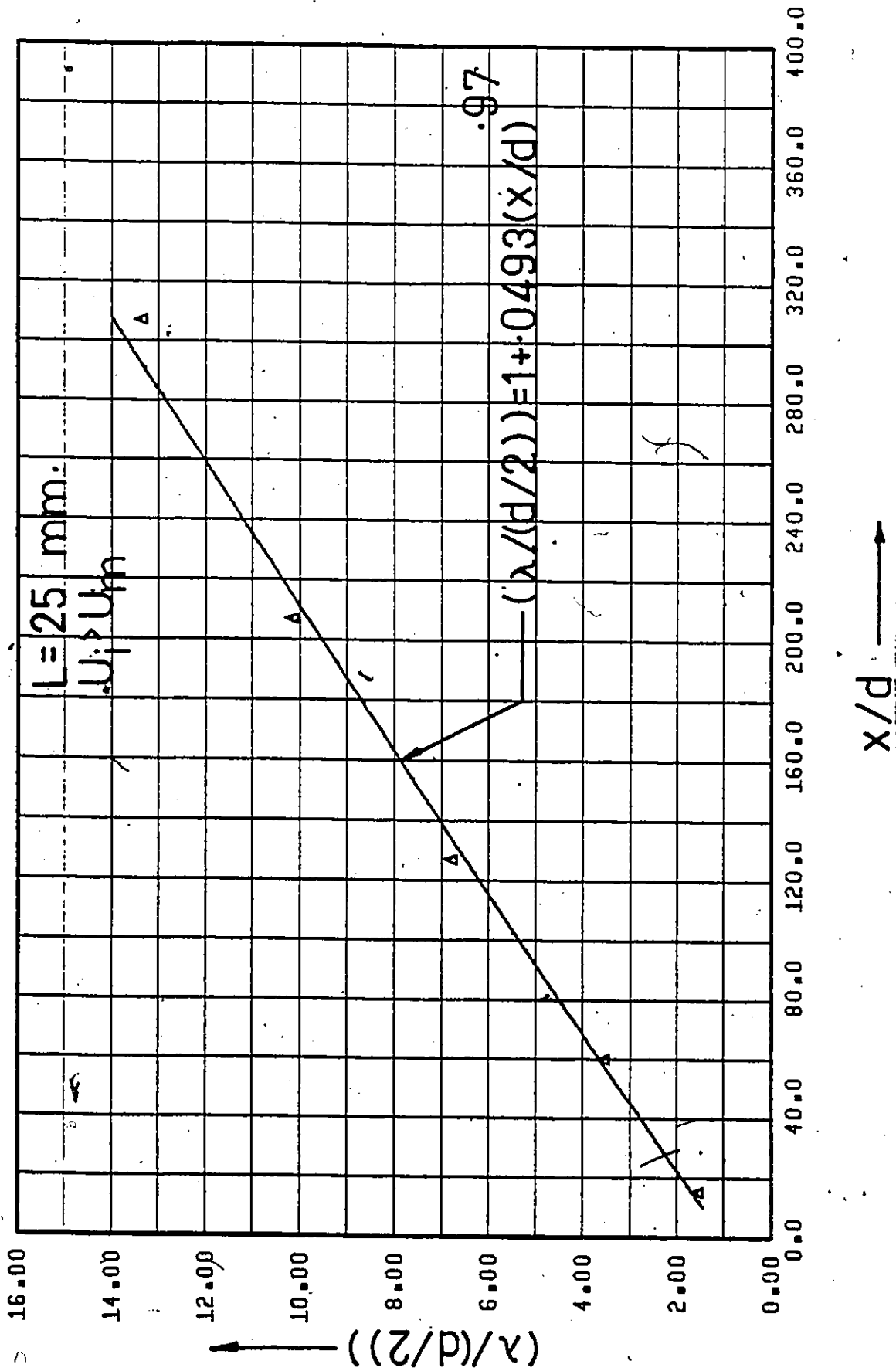


Figure 173. $(\lambda/(d/2))$ vs. x/d (Point Source Injection - Fully Developed Flow - $C_i = 250 \text{ w.p.p.m.}$).

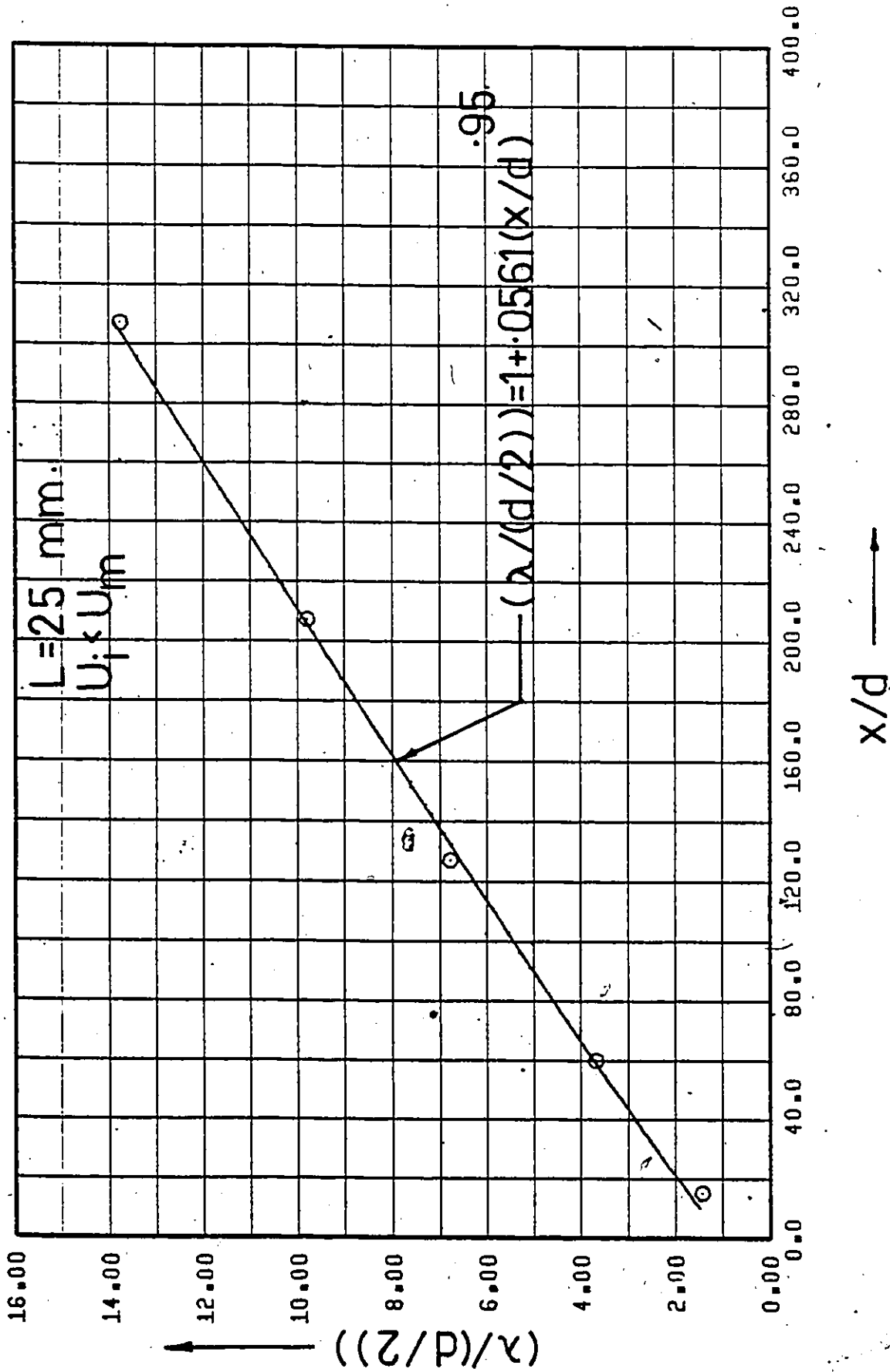


Figure 174. $(\lambda/(d/2))$ vs. x/d (Point Source Injection - Fully Developed Flow - $C_i = 500$ w.p.p.m.).

5

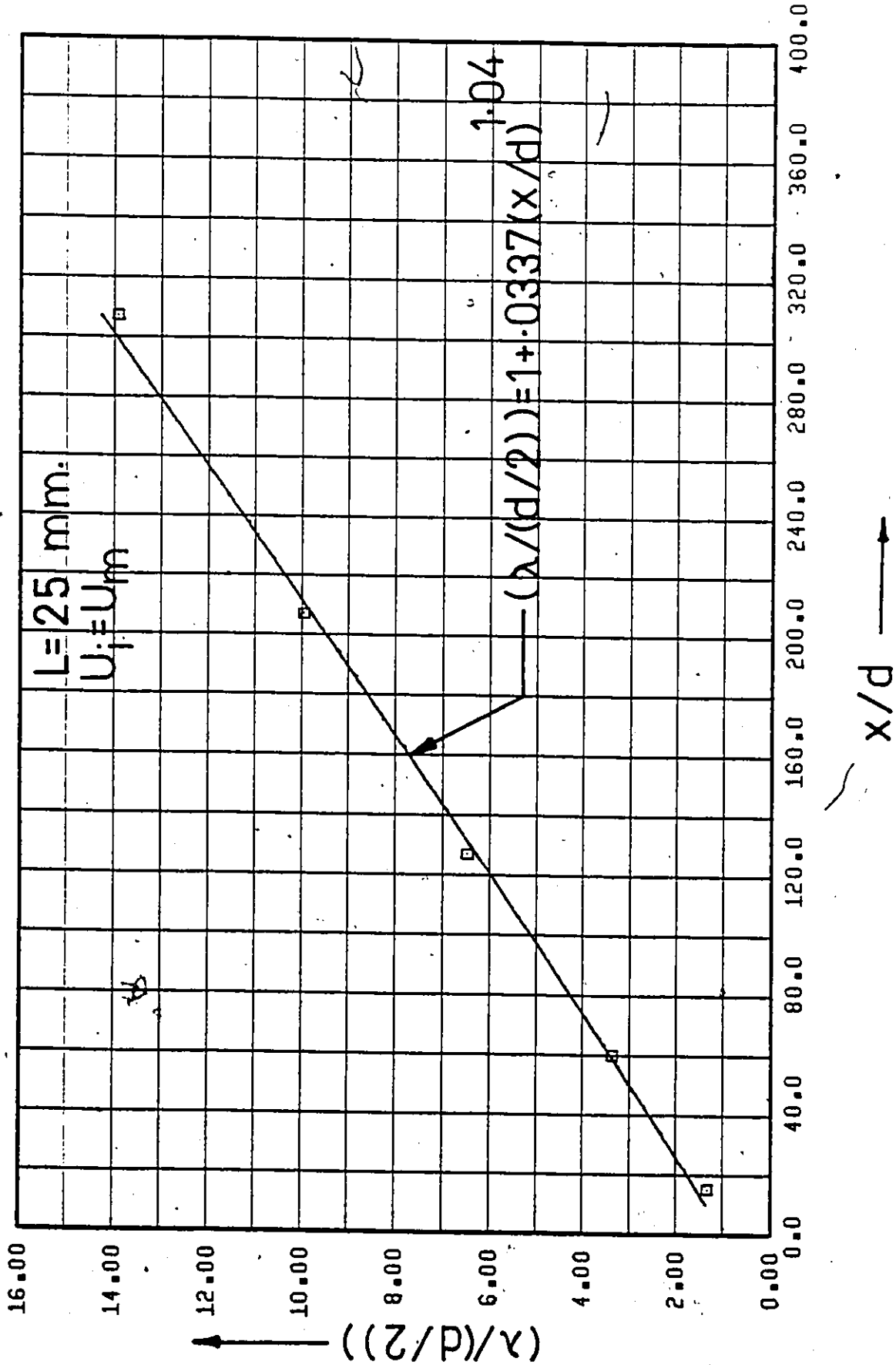


Figure 175. $(\lambda/(d/2))$ vs. x/d (Point Source Injection - Fully Developed Flow - $C_i = 500$ w.p.p.m.).

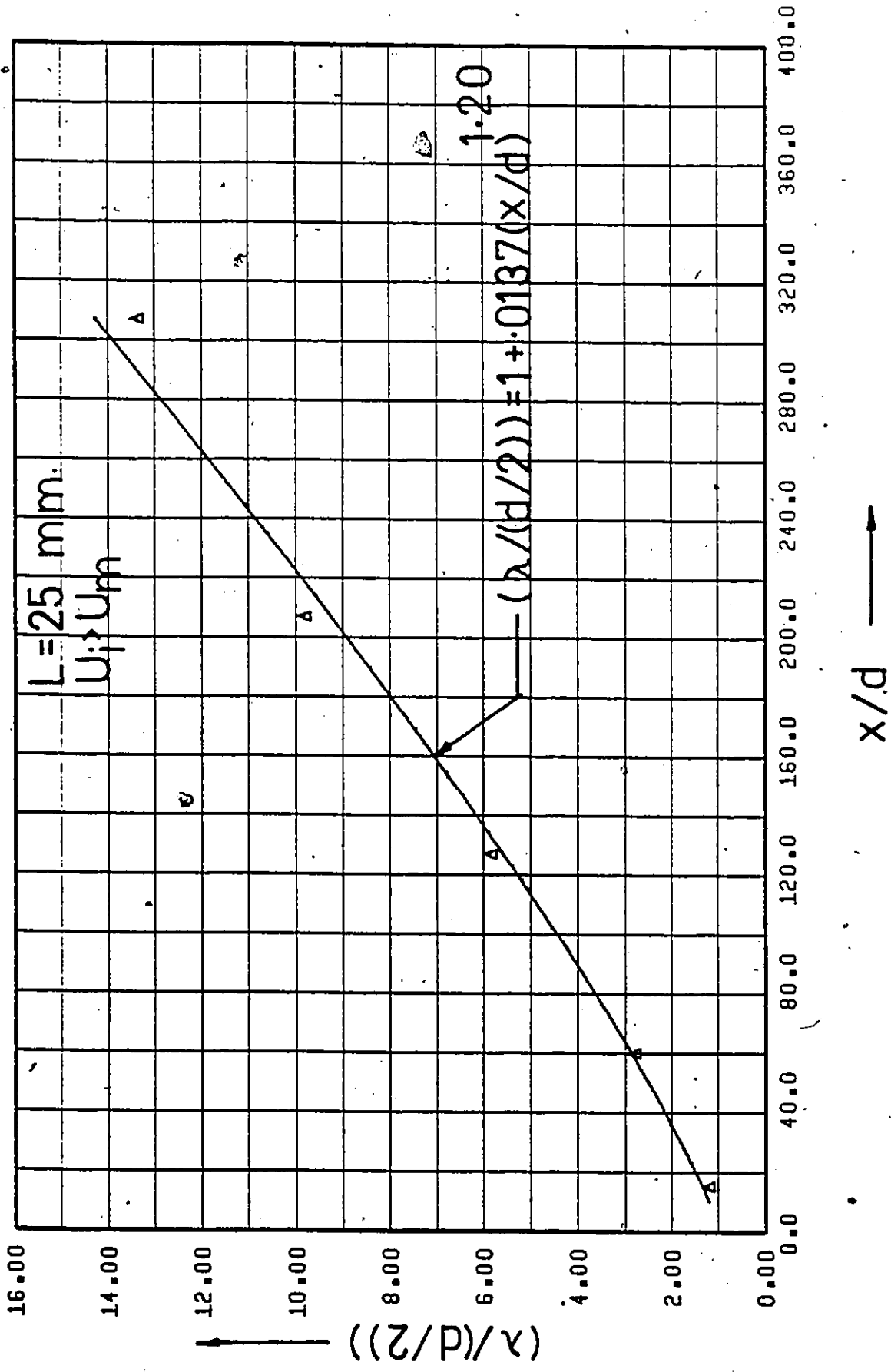


Figure 176. $(\lambda/(d/2))$ vs. x/d (Point Source Injection - Fully Developed Flow - $C_i = 500$ w.p.p.m.).

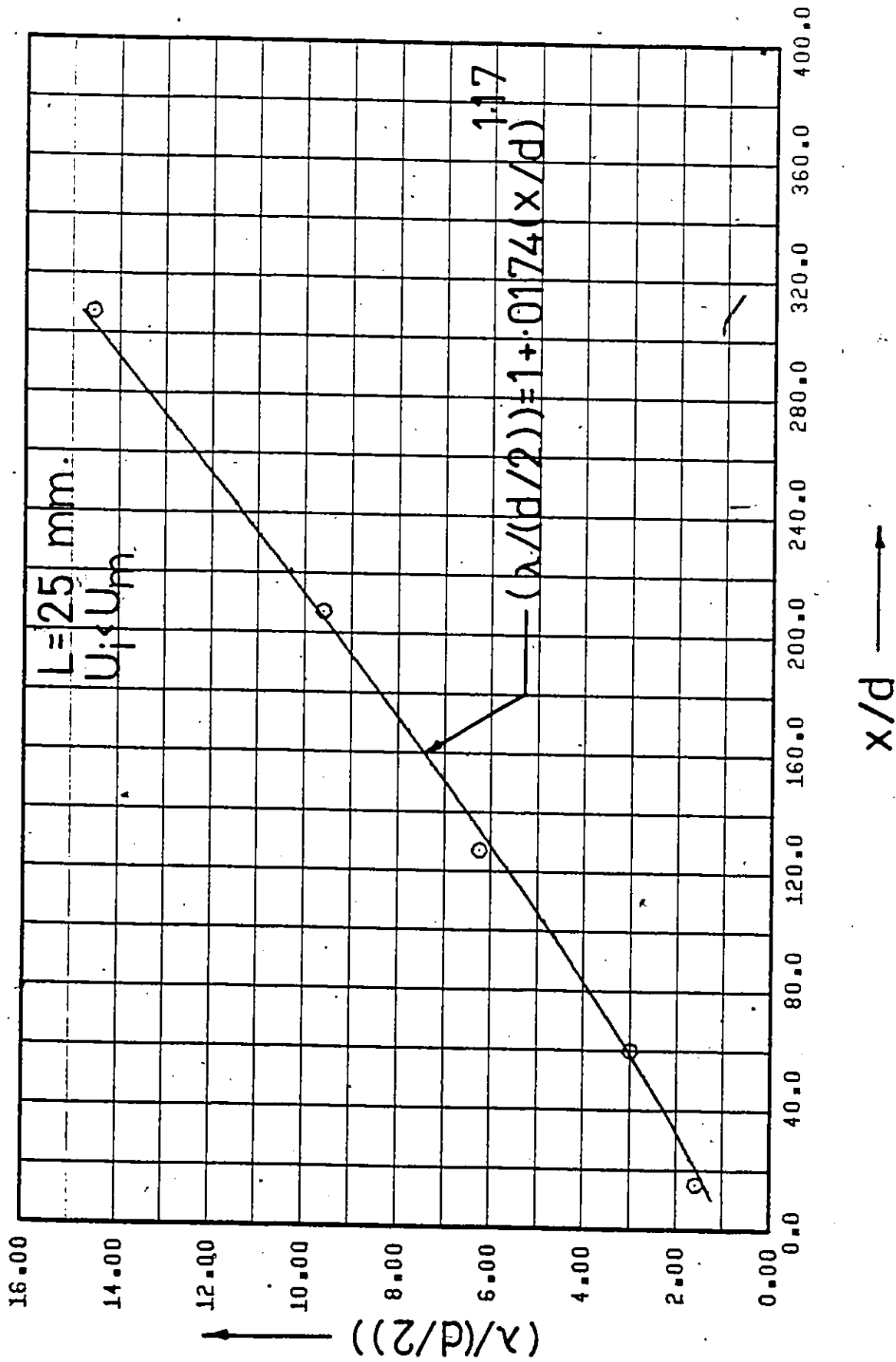


Figure 177. $(\lambda/(d/2))$ vs. x/d (Point Source Injection - Fully Developed Flow - $C_i = 1000 \text{ w.p.p.m.}$).

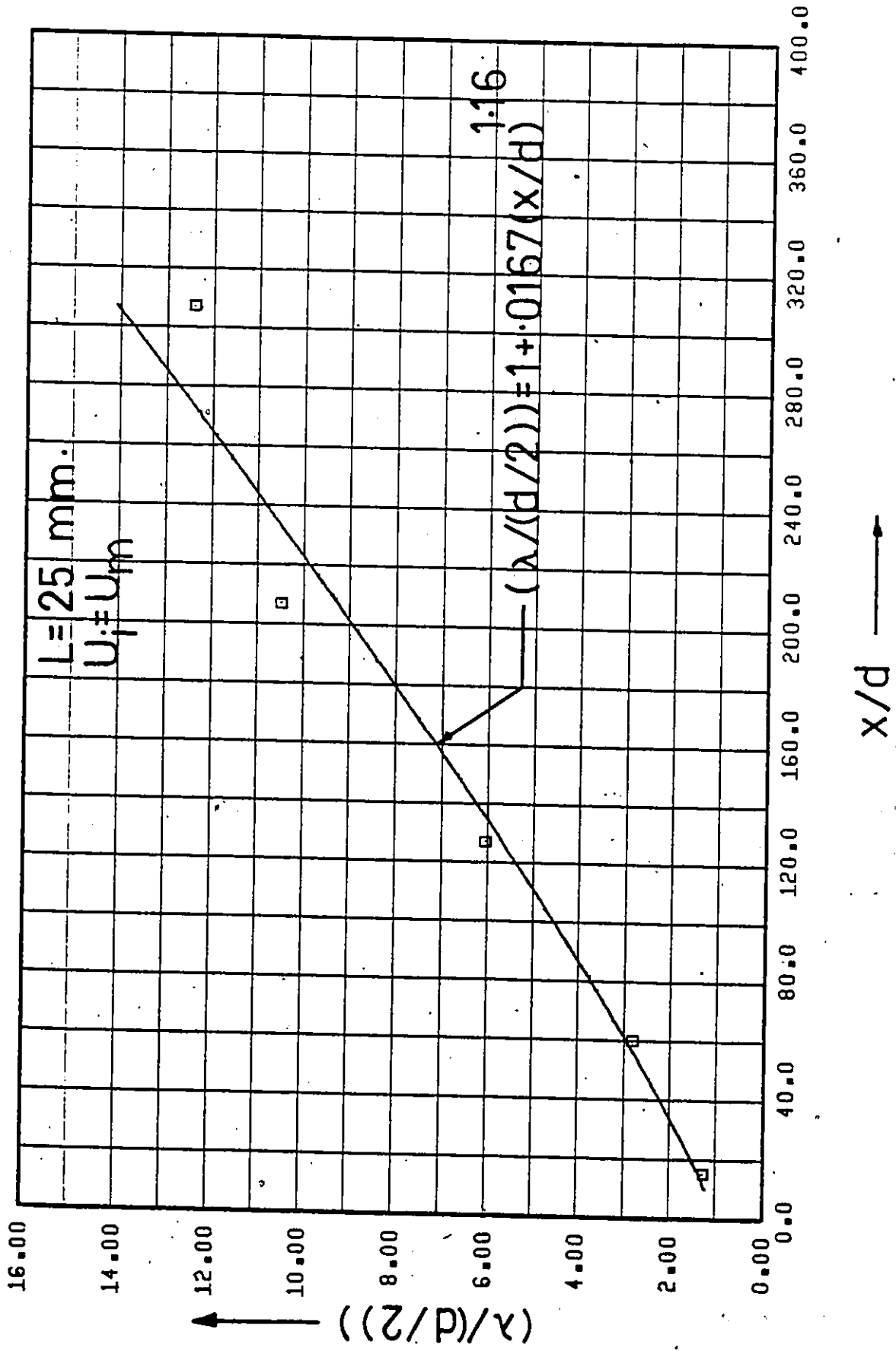


Figure 178. $(\lambda/(d/2))$ vs. x/d (Point Source Injection - Fully Developed Flow - $C_i = 1000 \text{ w.p.p.m.}$).

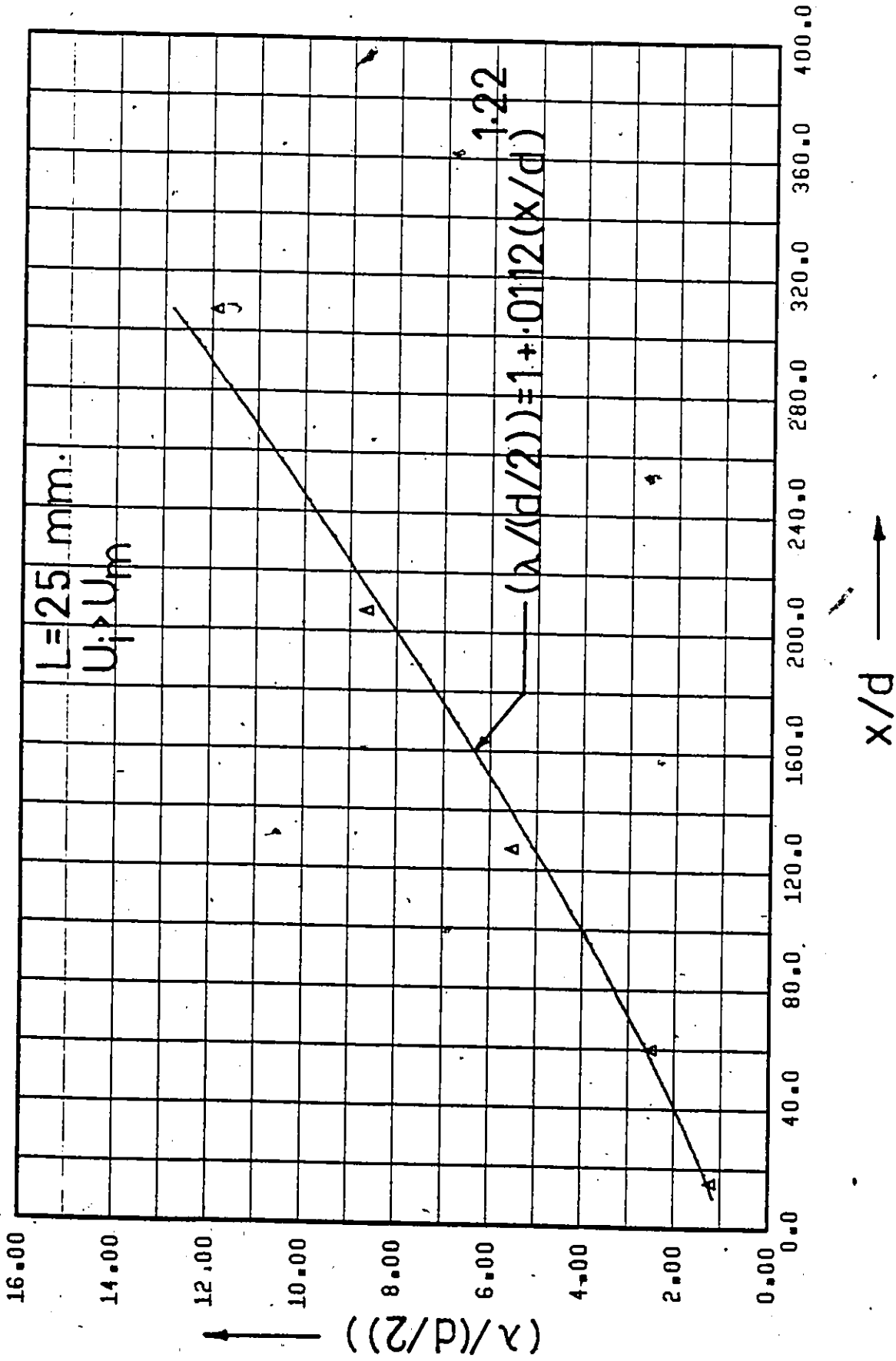


Figure 179. $(\lambda/(d/2))$ vs. x/d (Point Source Injection - Fully Developed Flow - $C_i = 1000 \text{ w.p.p.m.}$).

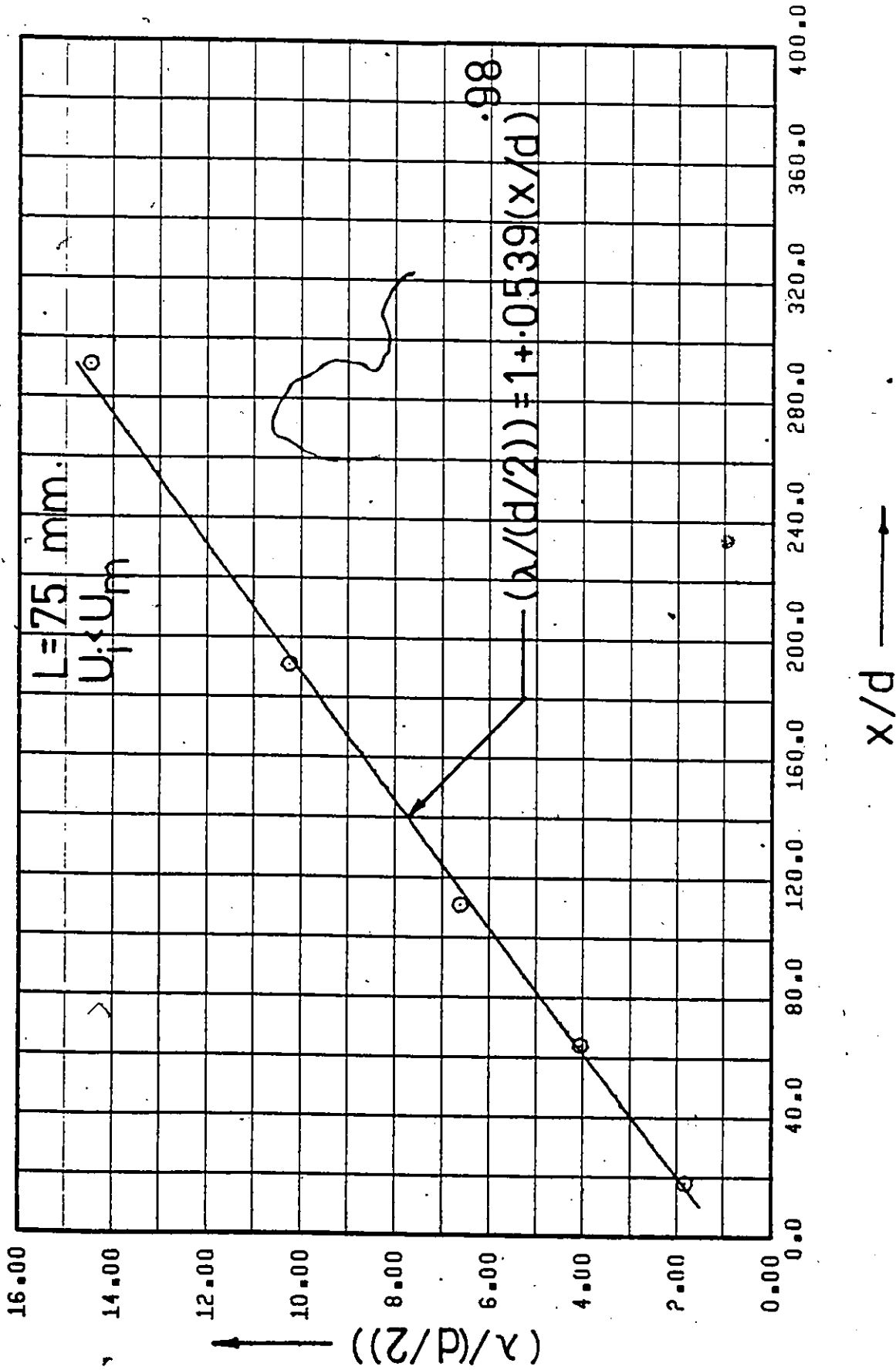


Figure 180. $(\lambda/(d/2))$ vs. x/d (Point Source Injection - Fully Developed Flow - Water Injection).

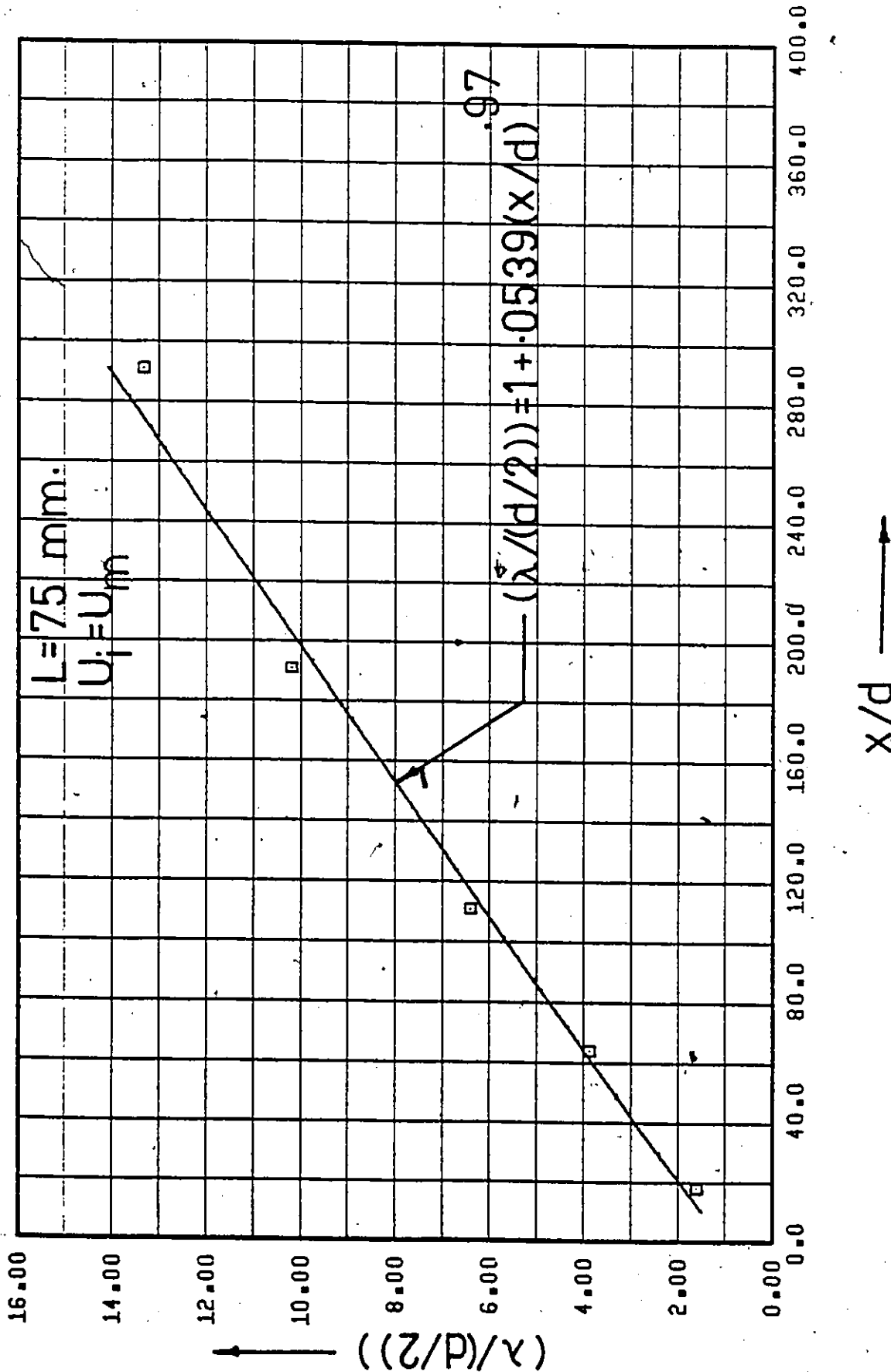


Figure 181. $(\lambda/(d/2))$ vs. x/d (Point Source Injection - Fully Developed Flow - Water Injection).

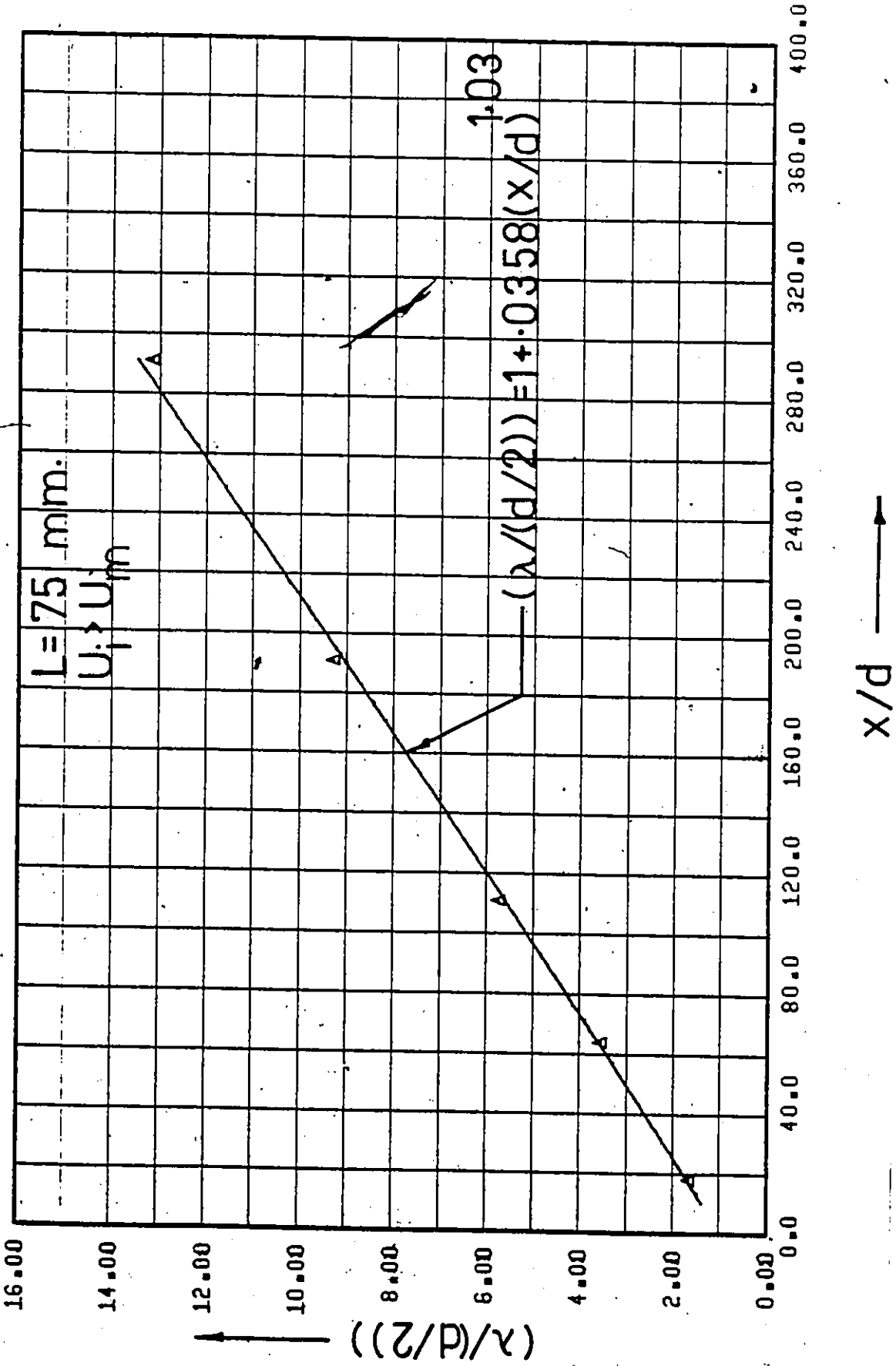


Figure 182. - $(\lambda/(d/2))$ vs. x/d (Point Source Injection - Fully Developed Flow - Water Injection).

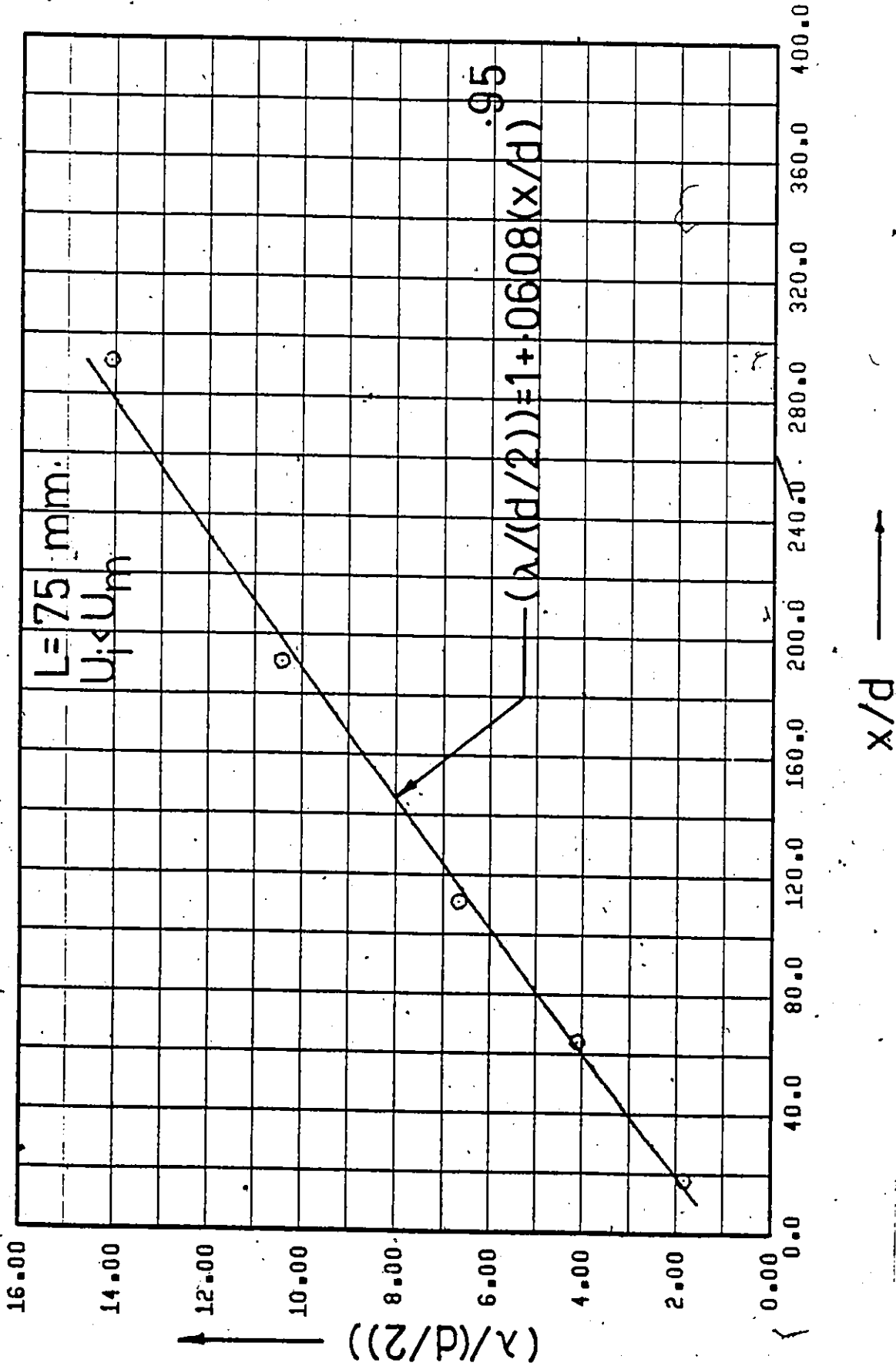


Figure 183. $(\lambda/(d/2))$ vs. x/d (Point Source Injection - Fully Developed Flow - $C_i = 50 \text{ v.p.p.m.}$).

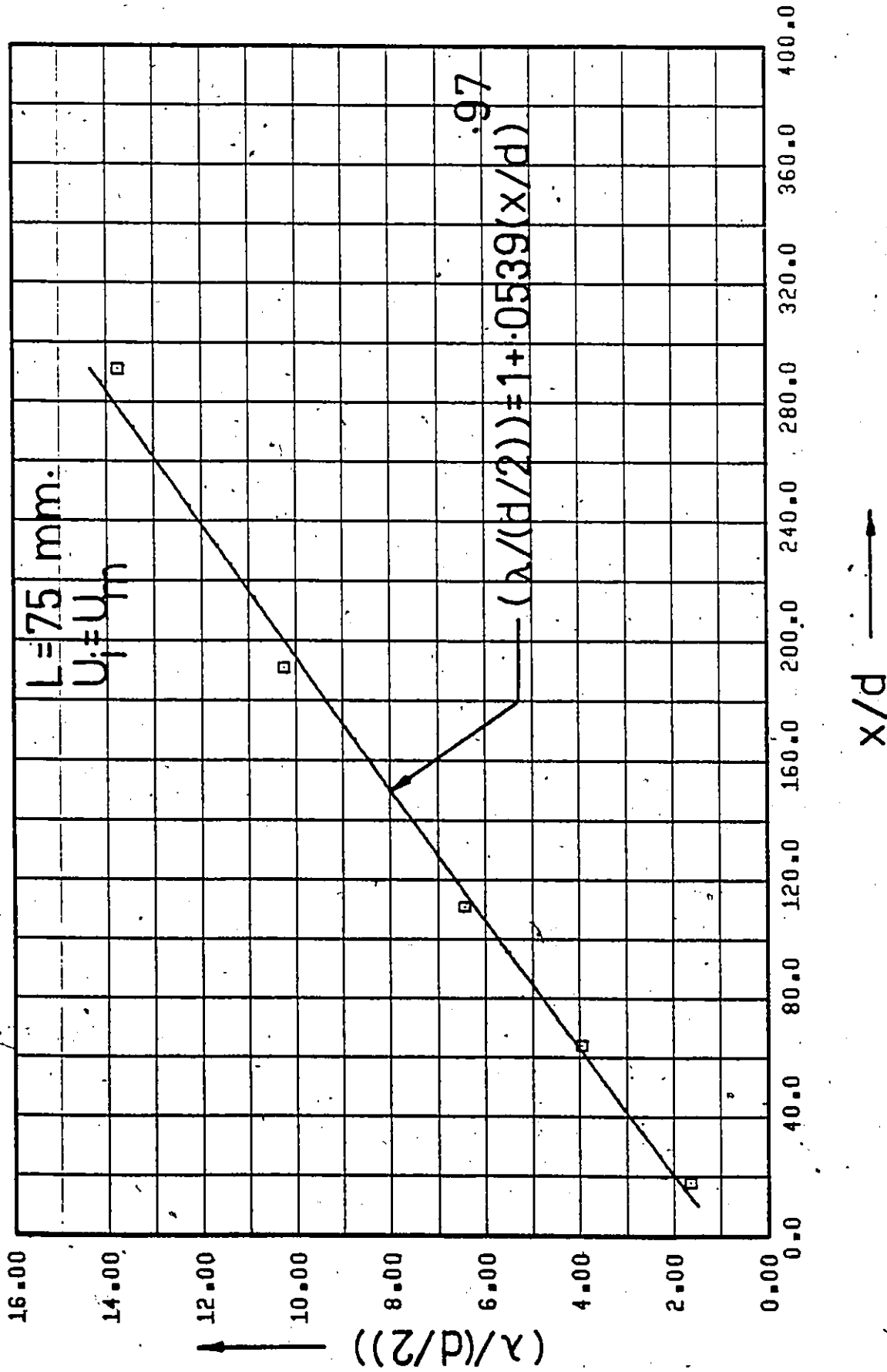


Figure 184. $\left(\frac{\lambda}{(d/2)}\right)$ vs. x/d (Point Source Injection - Fully Developed Flow - $C_i = 50 \text{ w.p.p.m.}$).

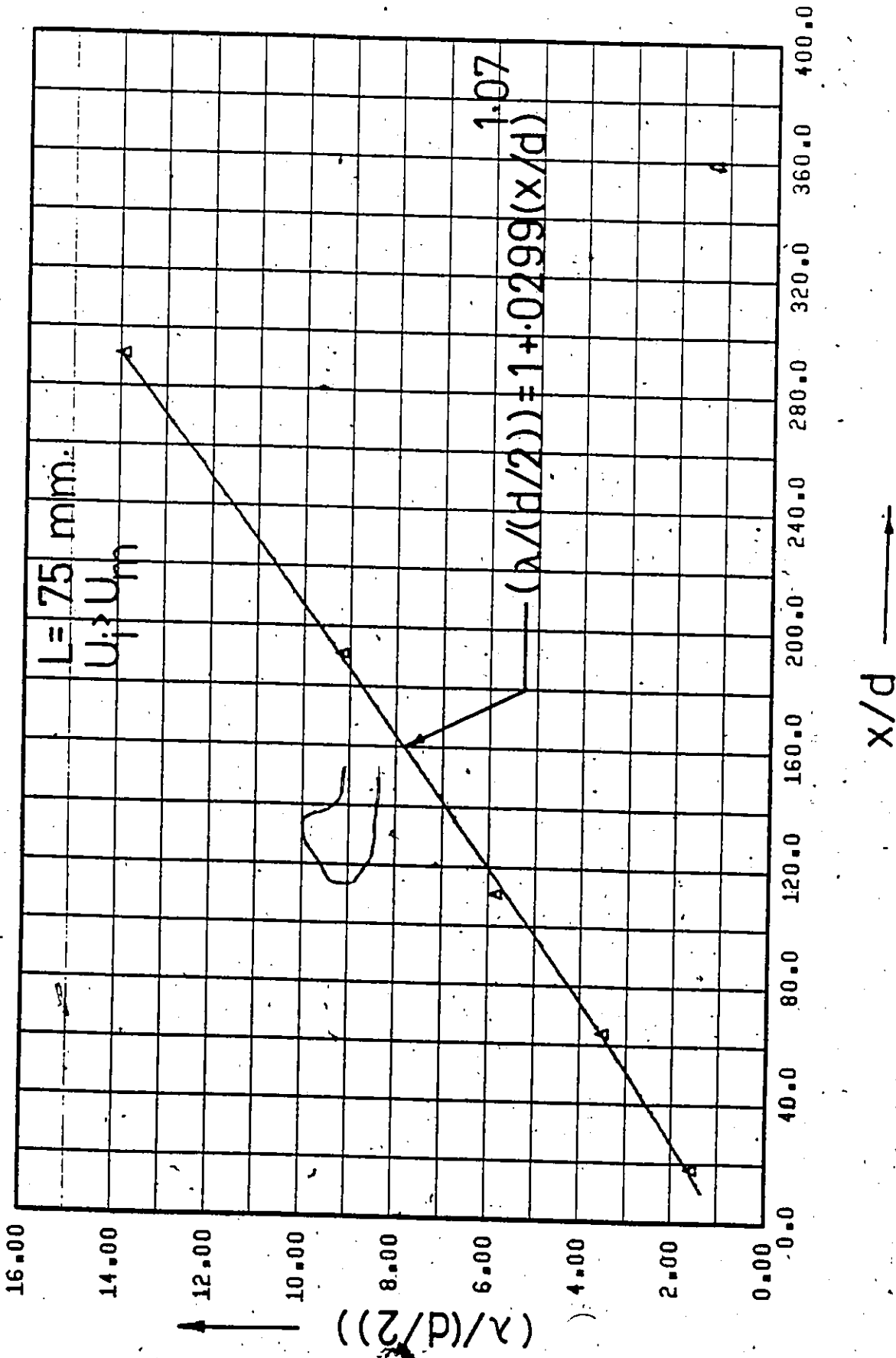


Figure 185. $(\lambda/(d/2))$ vs. x/d (Point Source Injection - Fully Developed Flow - $C_i = 50$ w.p.p.m.).

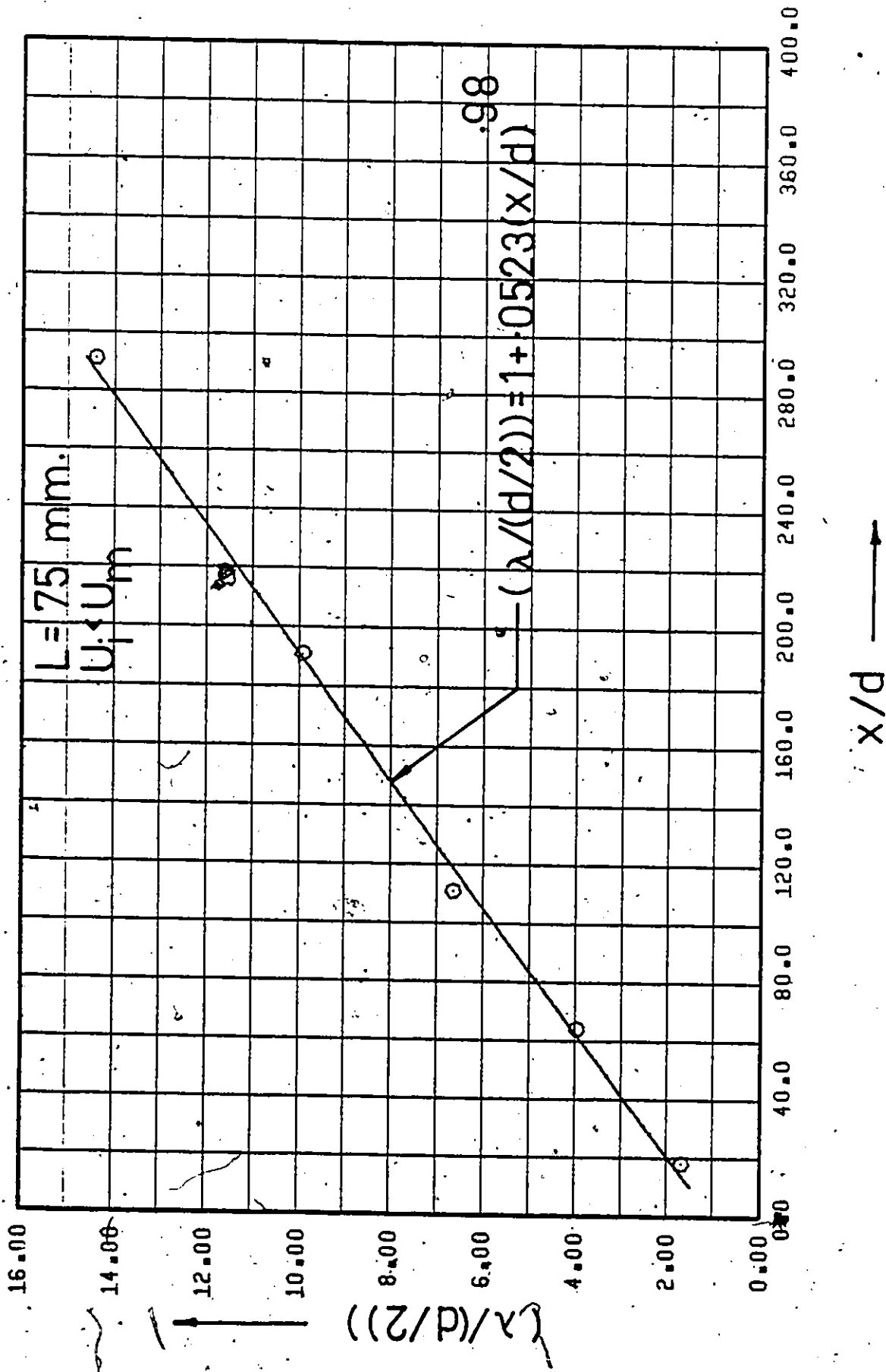


Figure 186. $(\lambda/(d/2))$ vs. x/d (Point Source Injection - Fully Developed Flow - $C_i = 100 \text{ w.p.p.m.}$).

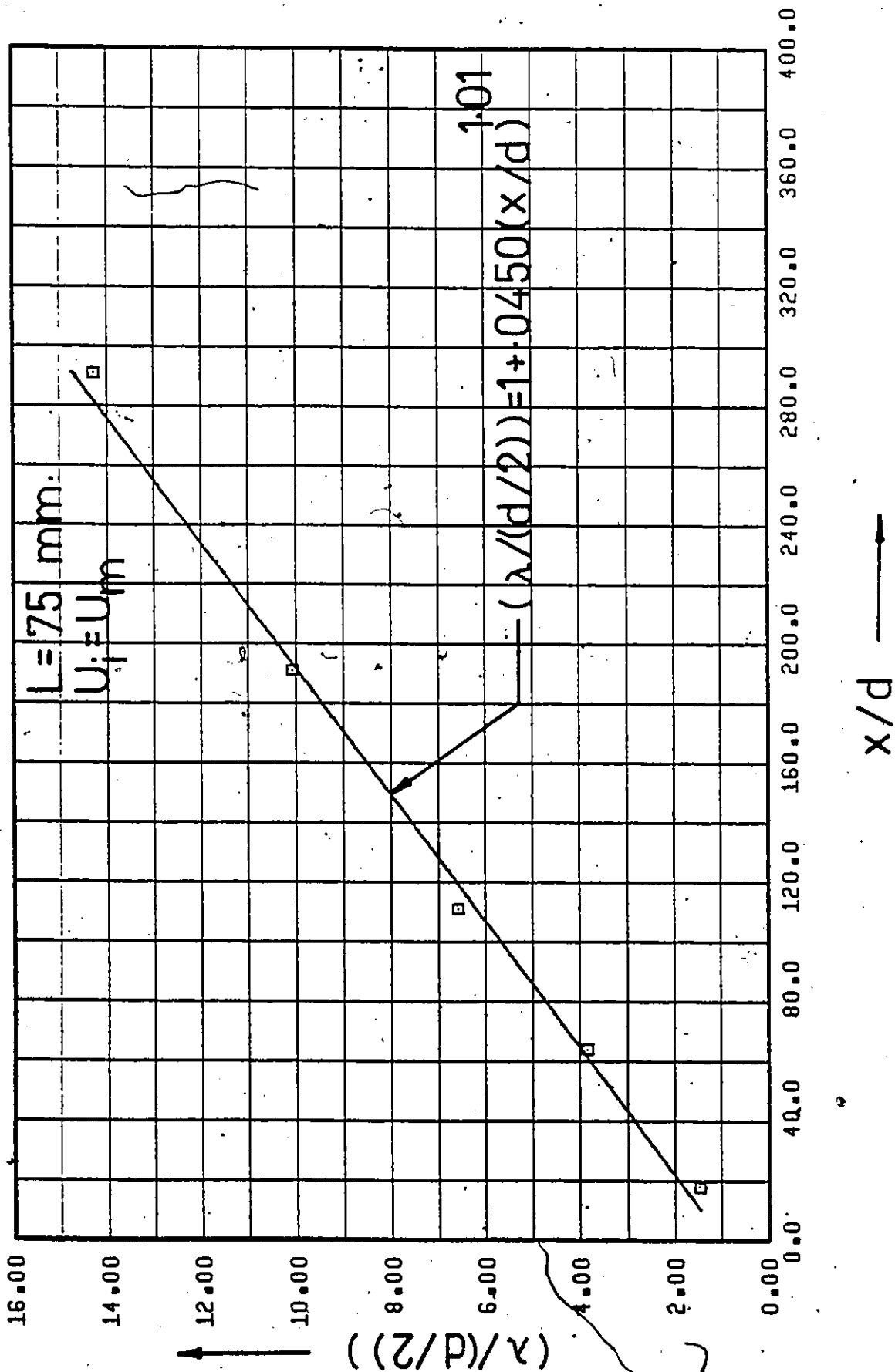


Figure 187. $(\lambda/(d/2))$ vs. x/d (Point Source Injection - Fully Developed Flow - $C_i = 100$ w.p.p.m.).

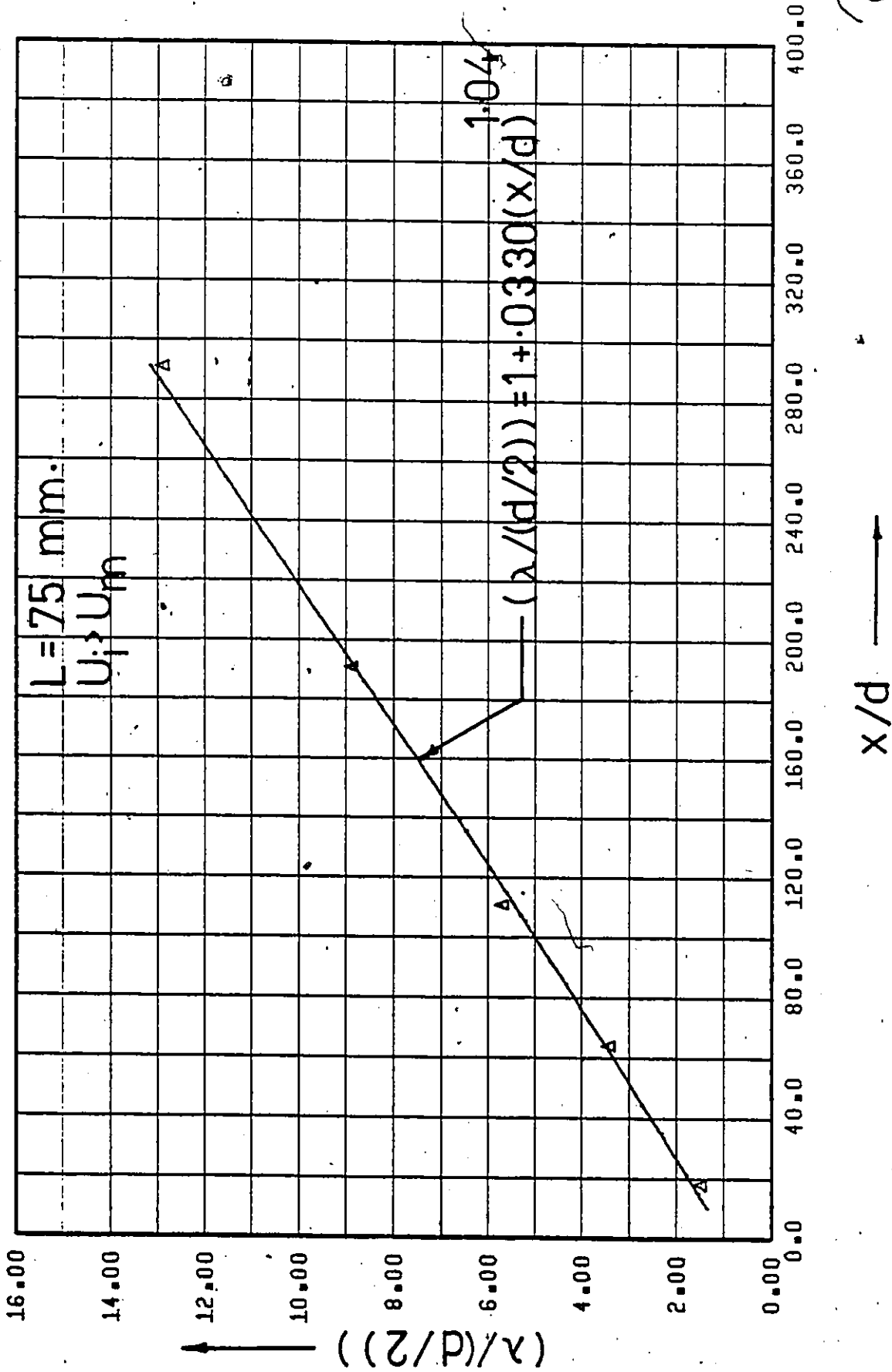


Figure 188. $(\lambda/(d/2))$ vs. x/d (Point Source Injection - Fully Developed Flow - $C_i = 100$ w.p.p.m.).

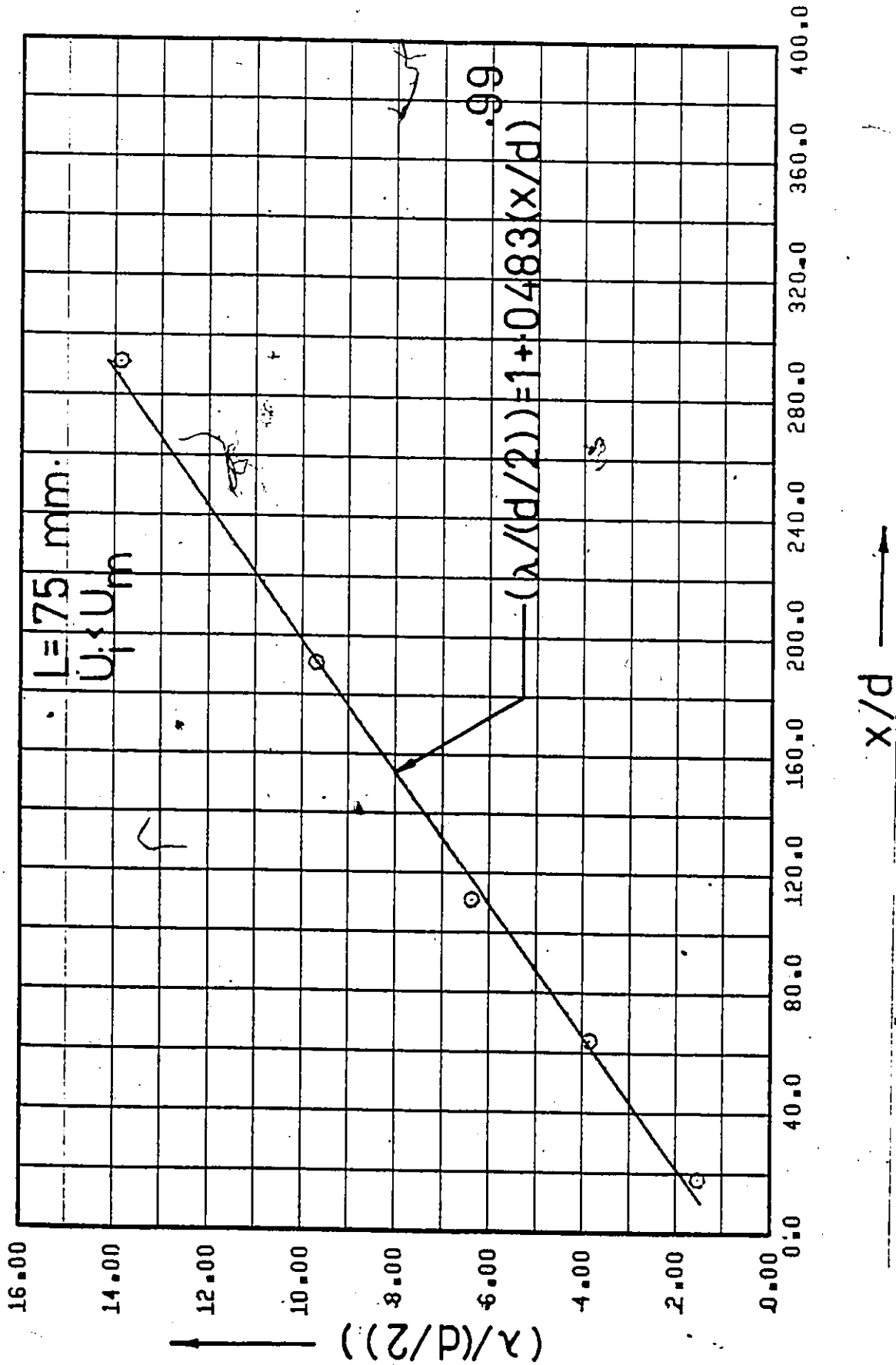


Figure 189. $(\lambda/(d/2))$ vs. x/d (Point Source Injection - Fully Developed Flow - $C_i = 250 \text{ w.p.p.m.}$).

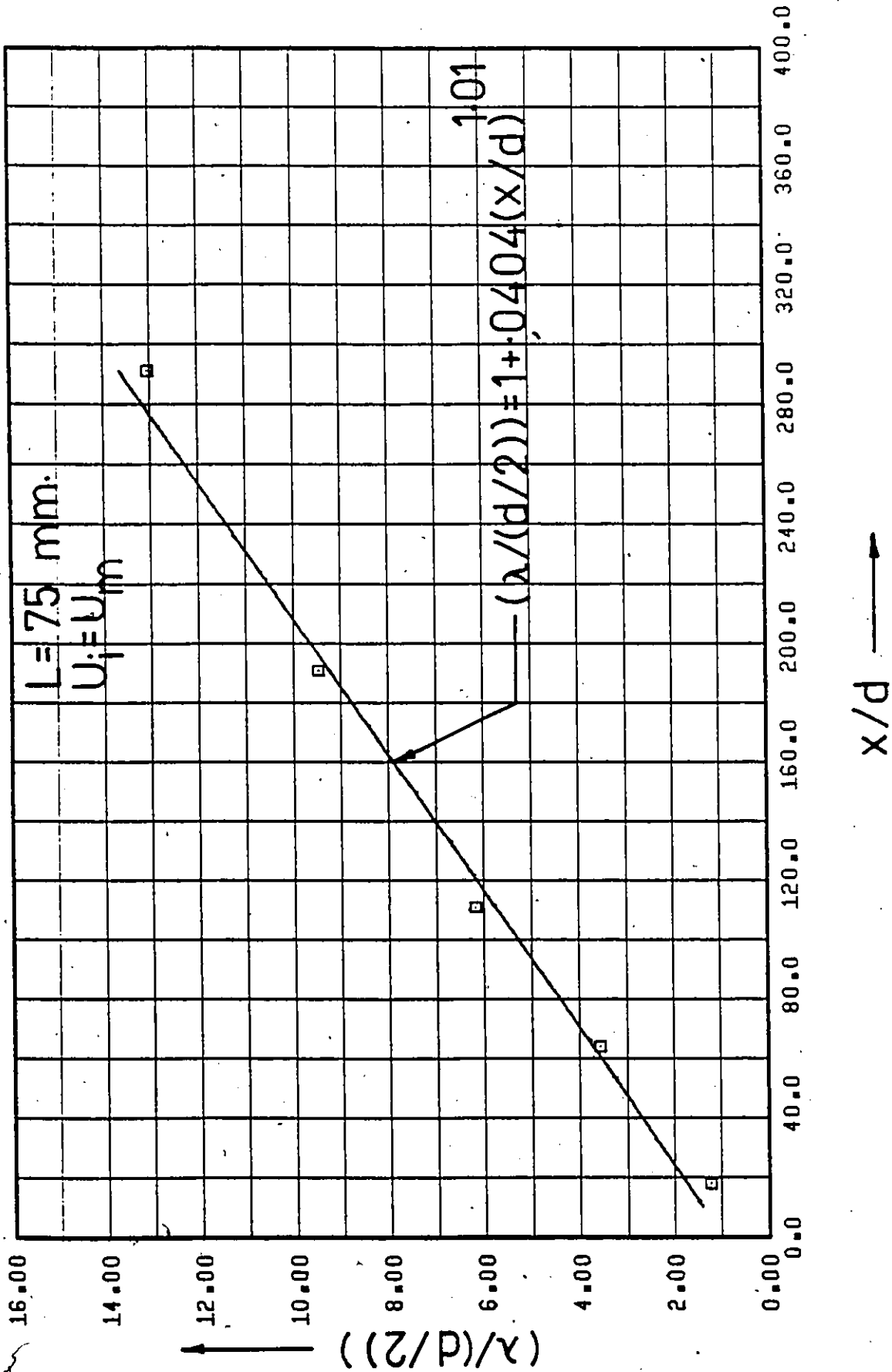


Figure 190. $(\lambda/(d/2))$ vs. x/d (Point Source Injection - Fully Developed Flow - $C_i = 250 \text{ w.p.p.m.}$).

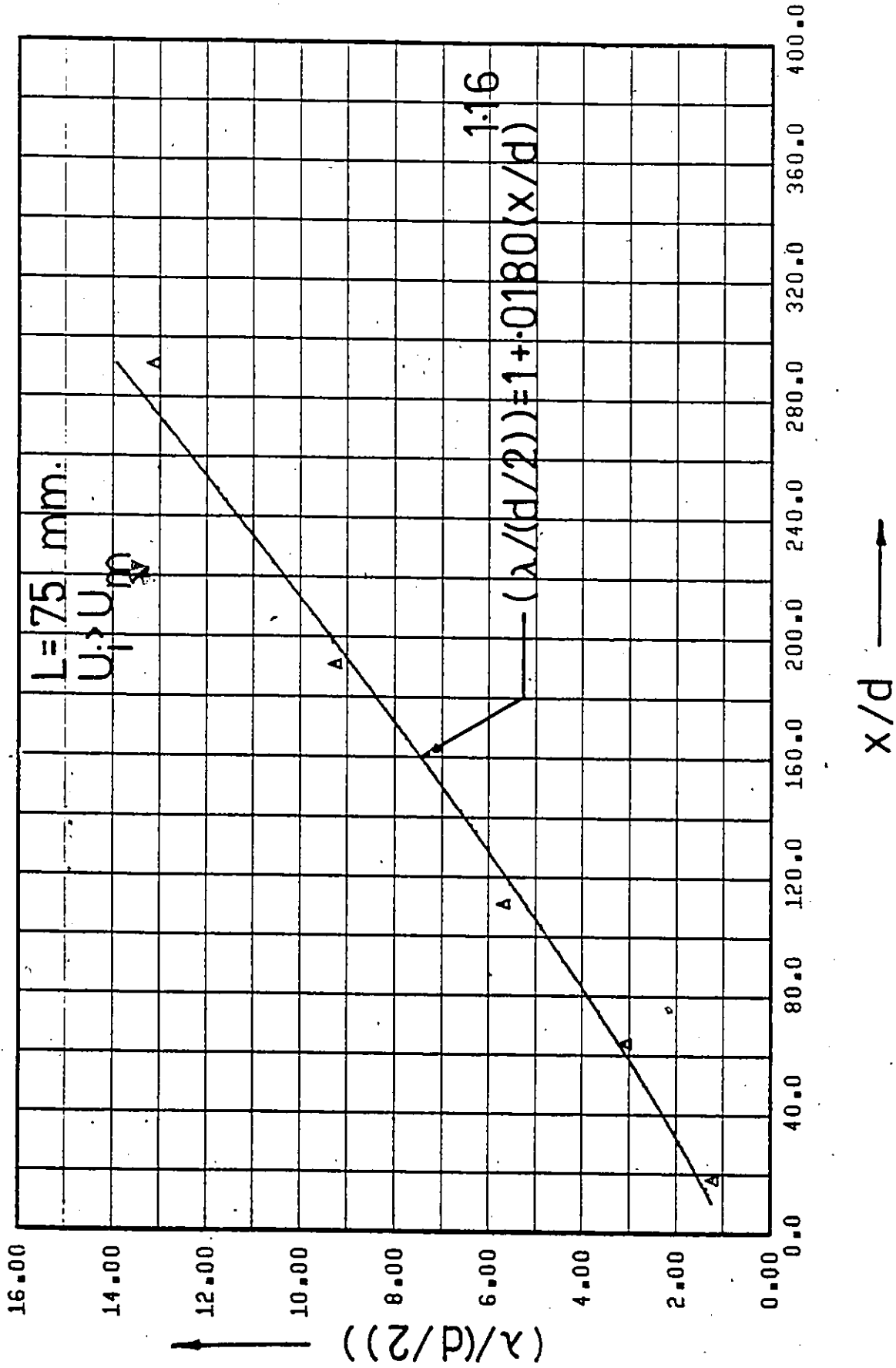


Figure 191. $(\lambda/(d/2))$ vs. x/d (Point Source Injection - Fully Developed Flow - $C_i = 250$ w.p.p.m.).

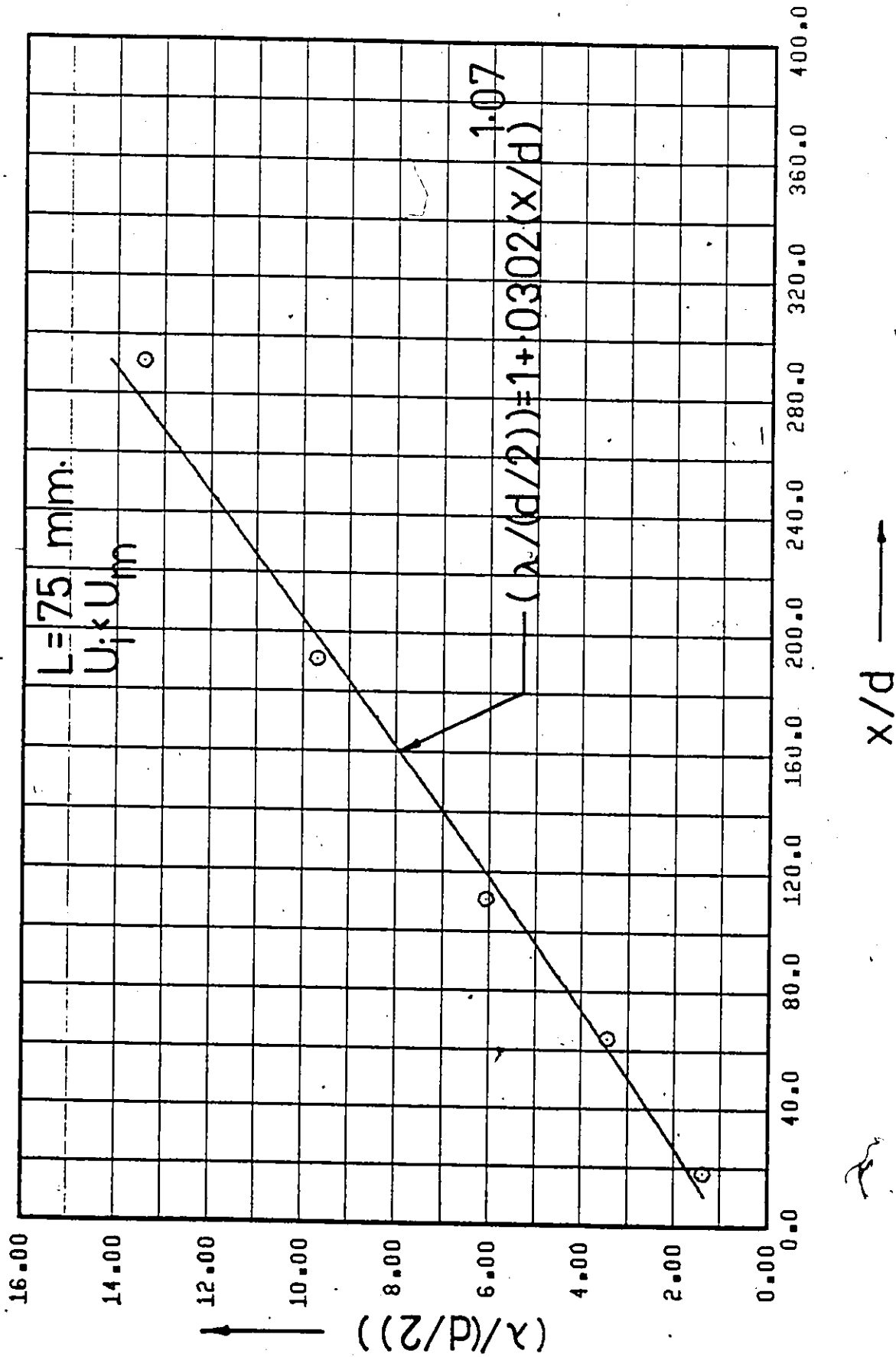


Figure 192. $(\lambda/(d/2))$ vs. x/d (Point Source Injection - Fully Developed Flow - $C_i = 500$ w.p.p.m.).

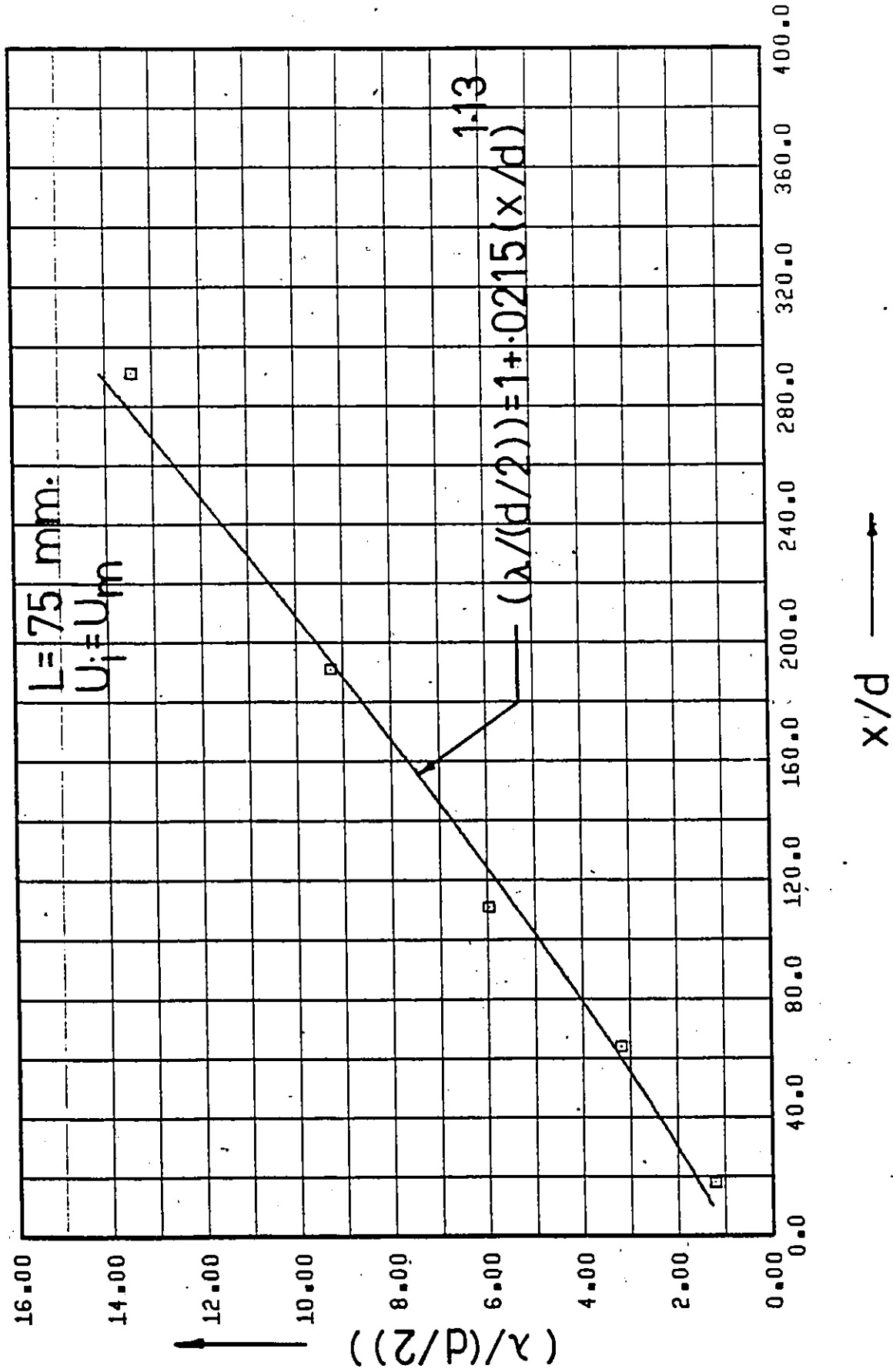


Figure 193. $(\lambda/(d/2))$ vs. x/d (Point Source Injection - Fully Developed Flow - $C_i = 500 \text{ w.p.p.m.}$).

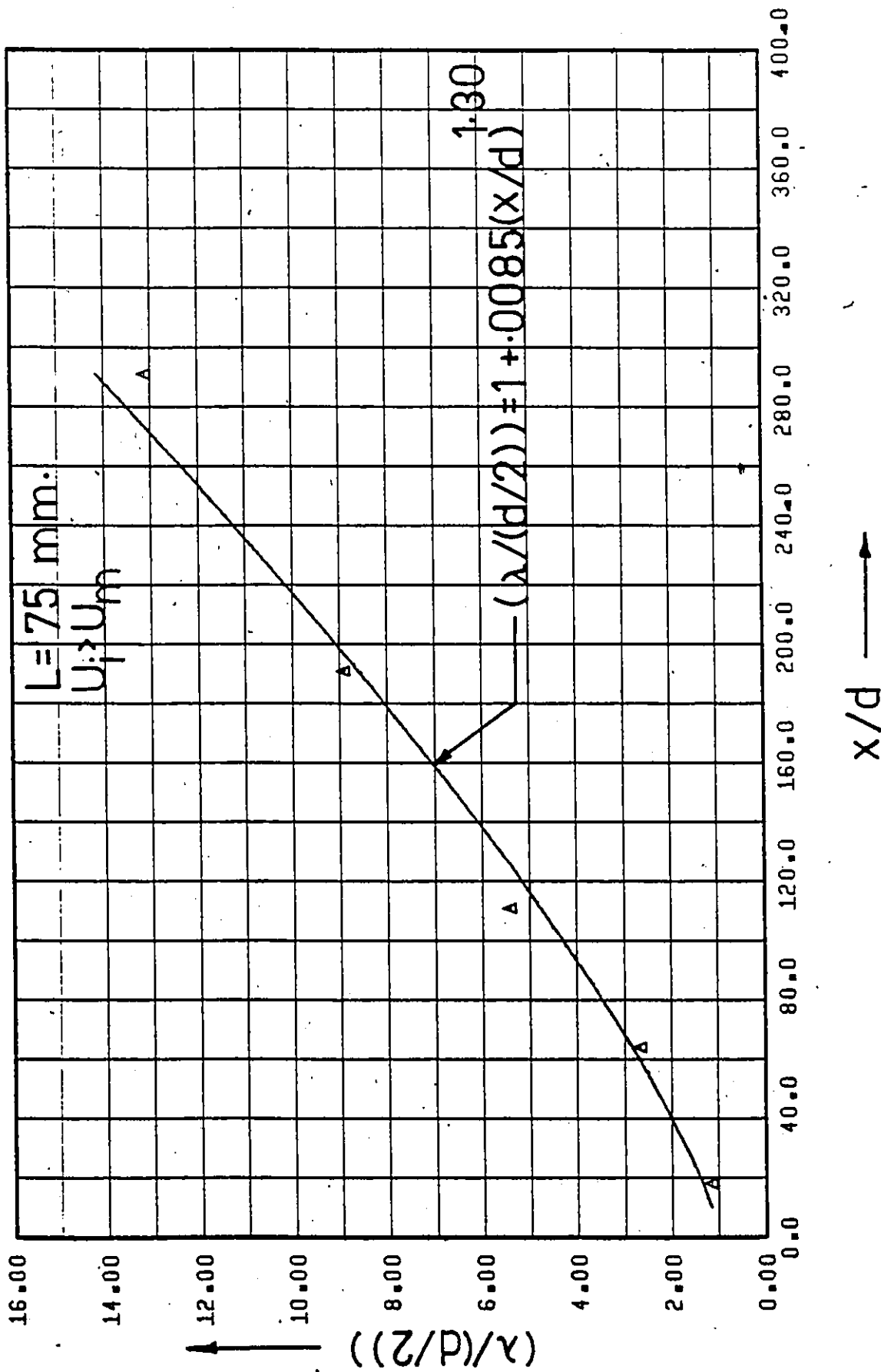


Figure 194. $(\lambda/(d/2))$ vs. x/d (Point Source Injection - Fully Developed Flow - $C_i = 500$ w.p.p.m.).

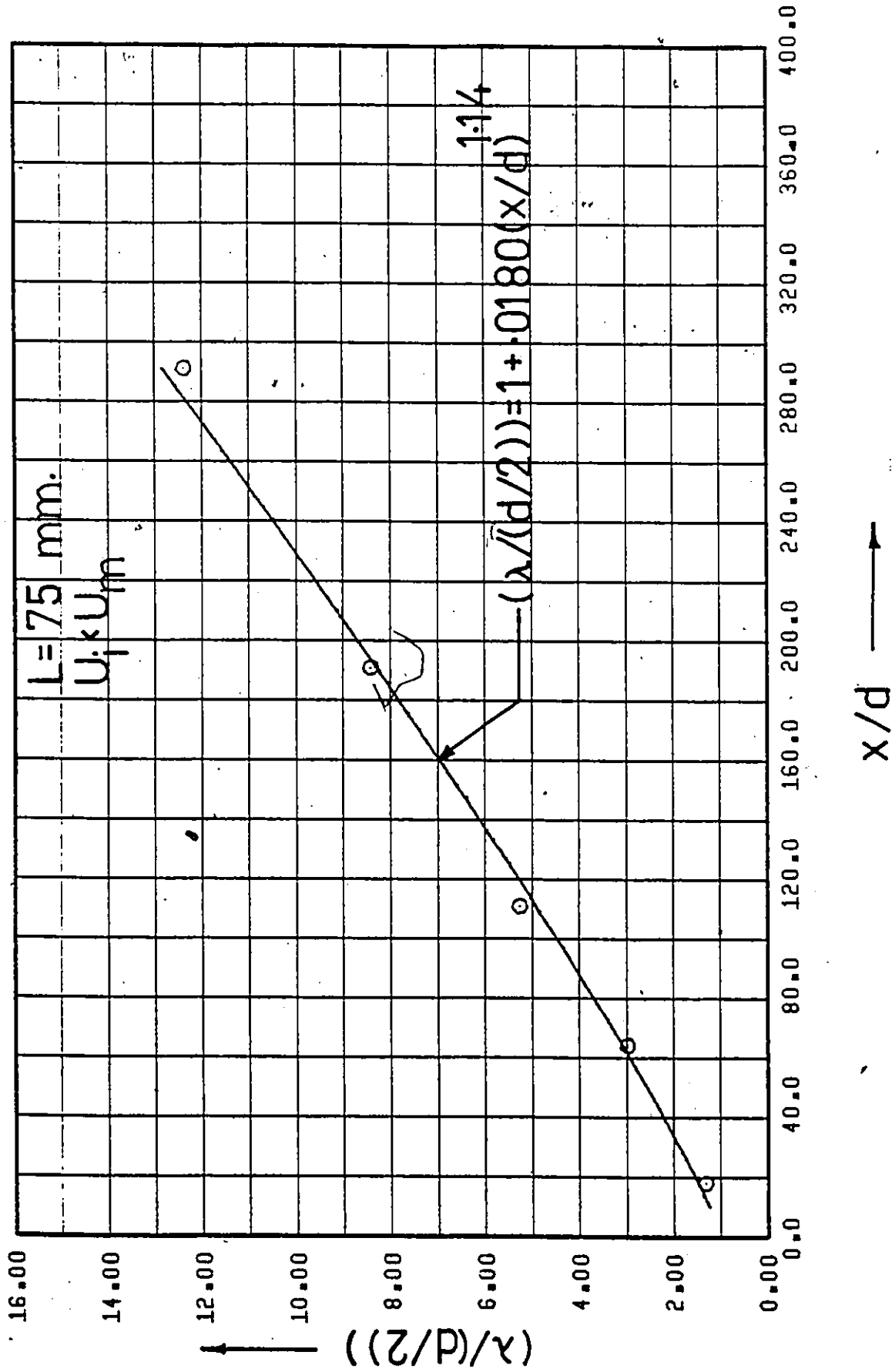


Figure 195. $(\lambda/(d/2))$ vs. x/d (Point Source Injection - Fully Developed Flow - $C_i = 1000 \text{ w.p.p.m.}$).

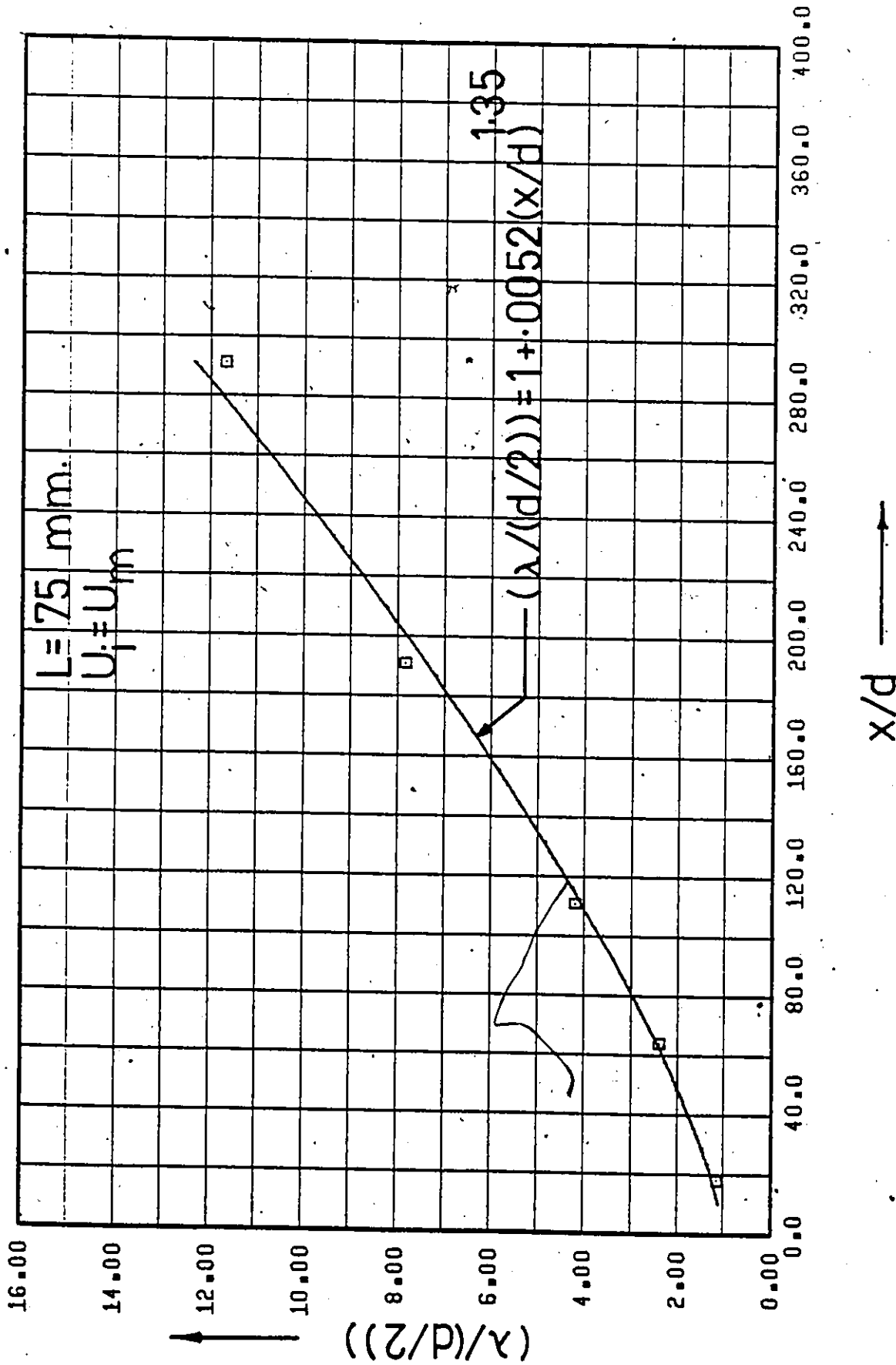


Figure 196. $(\lambda/(d/2))$ vs. x/d (Point Source Injection - Fully Developed Flow - $C_i = 1000$ w.p.p.m.).

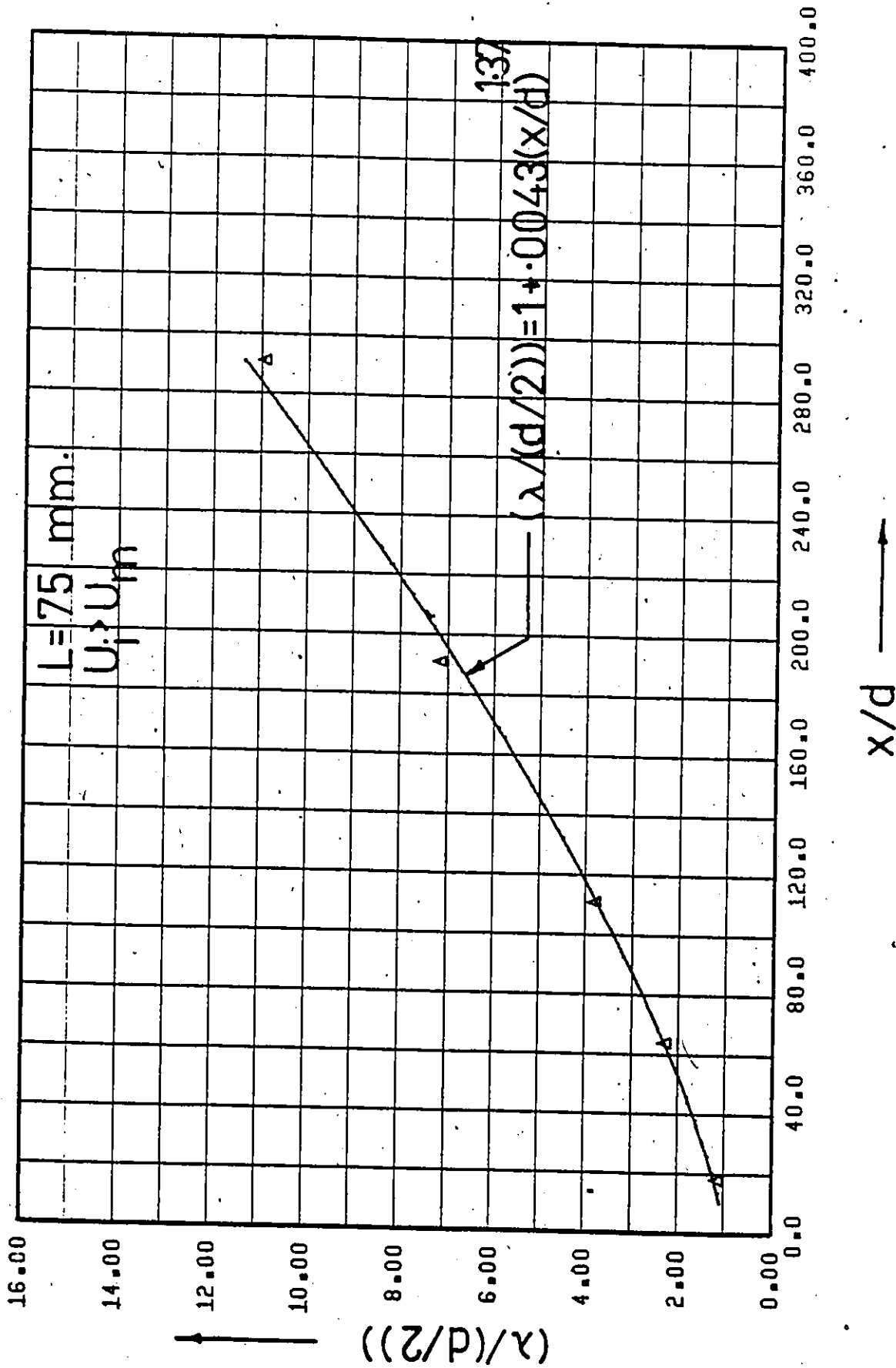


Figure 197. $(\lambda/(d/2))$ vs. x/d (Point Source Injection - Fully Developed Flow - $C_i = 1000 \text{ w.p.p.m.}$).

25

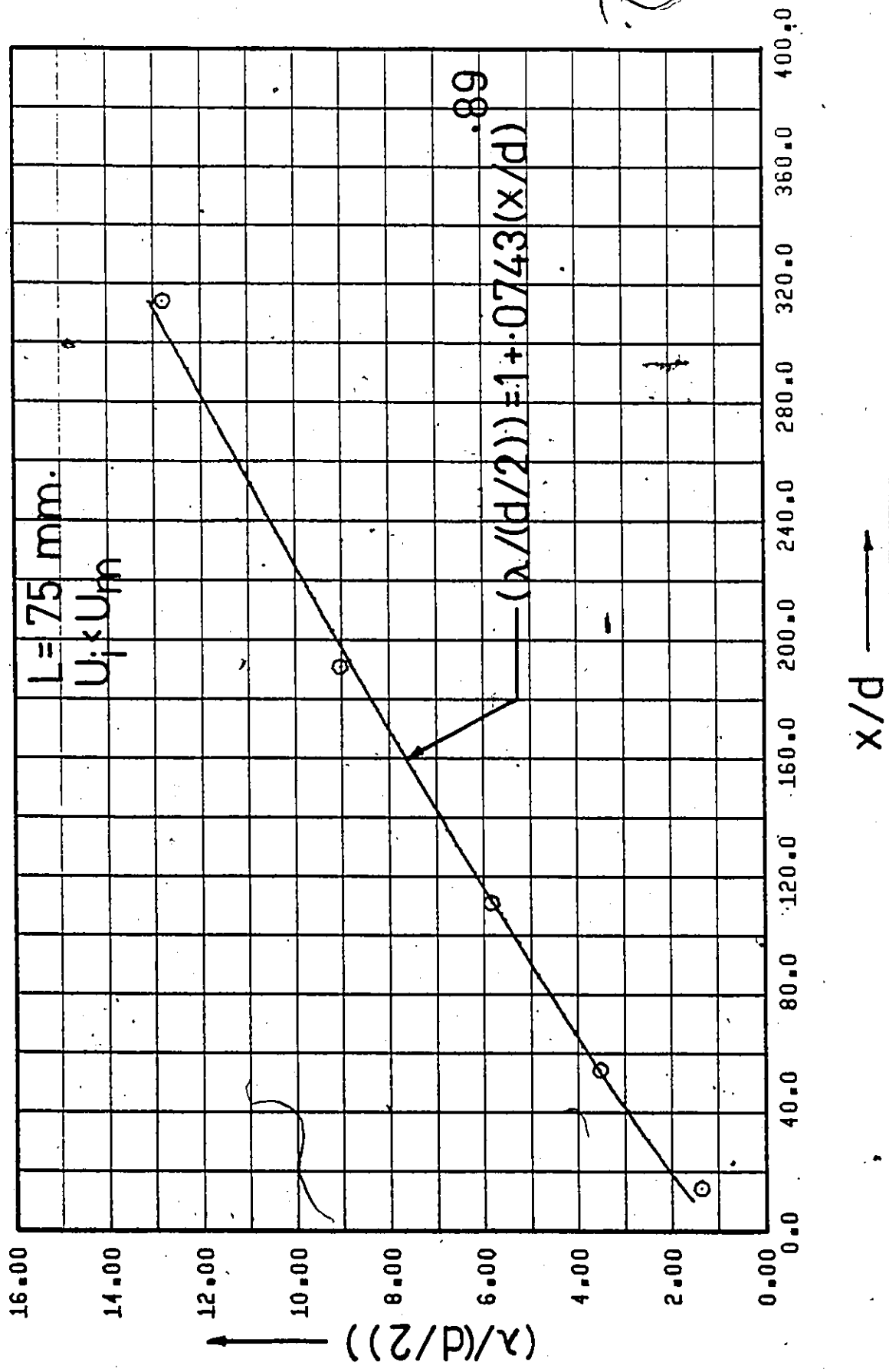


Figure 198. $(\lambda/(d/2))$ vs. x/d (Point Source Injection - Uniform Flow - Water Injection).

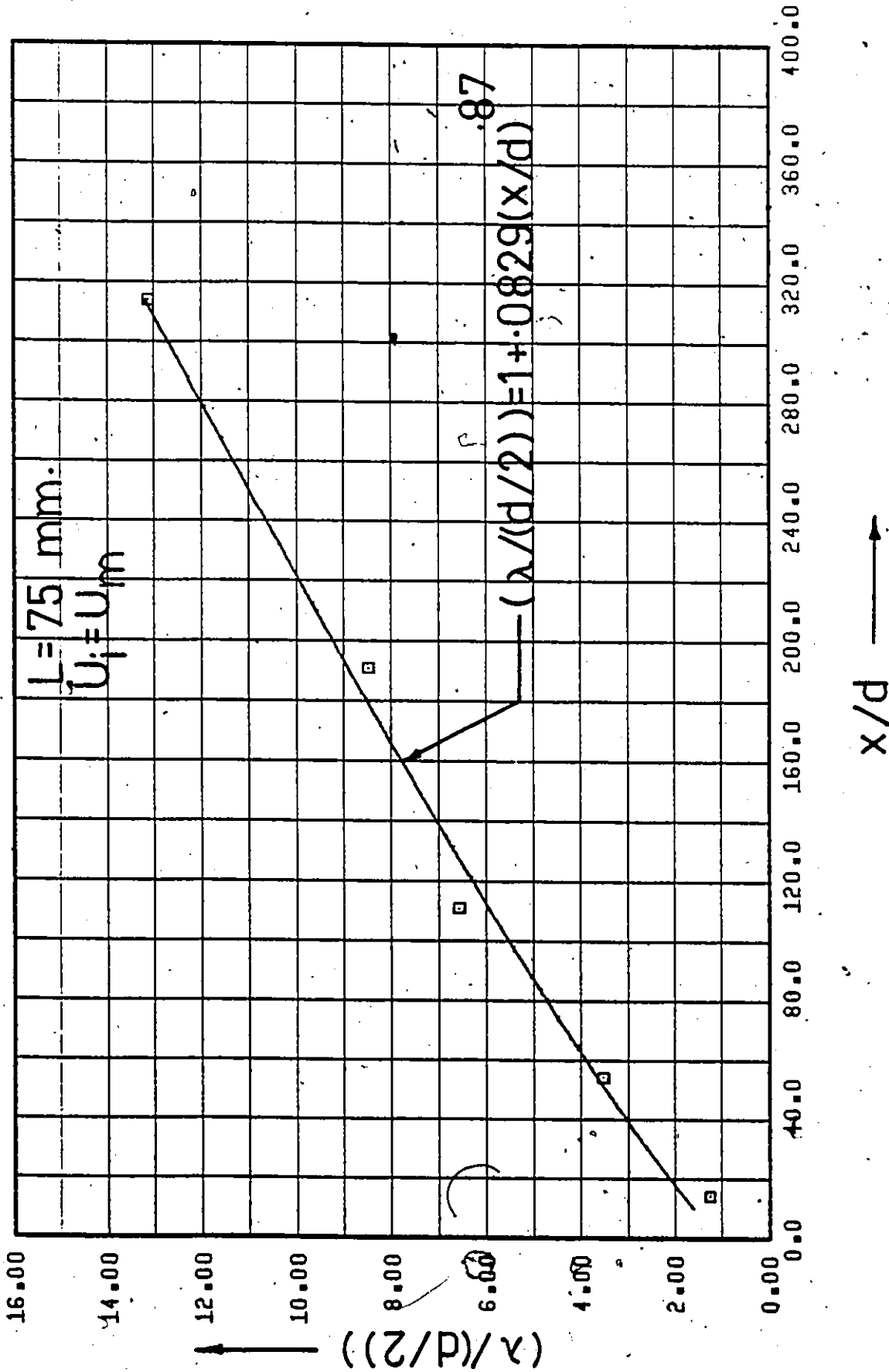


Figure 199. $(\lambda/(d/2))$ vs. x/d (Point Source Injection - Uniform Flow - Water Injection).

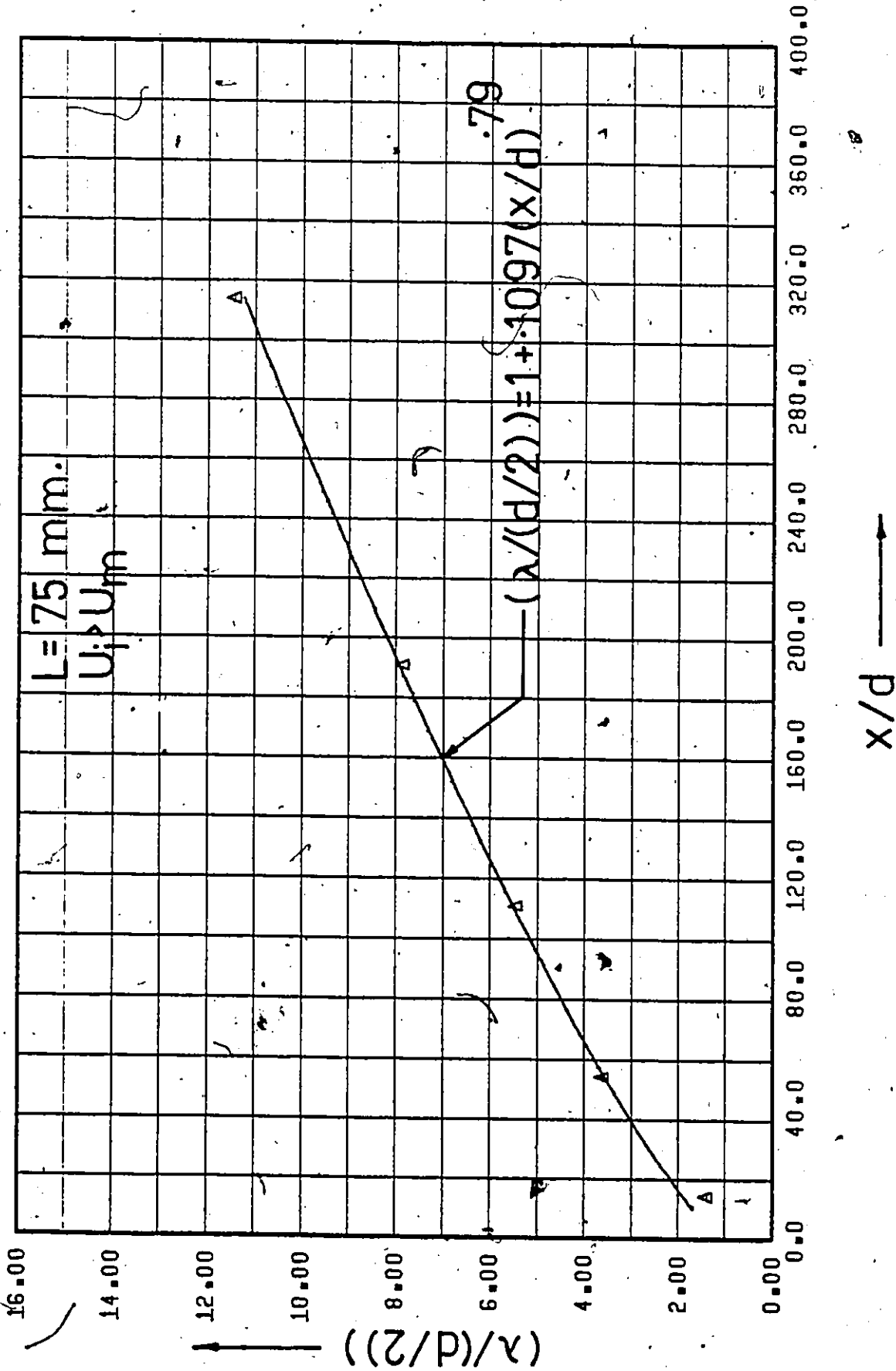


Figure 200. $(\lambda/(d/2))$ vs. x/d (Point Source Injection - Uniform Flow Water Injection).

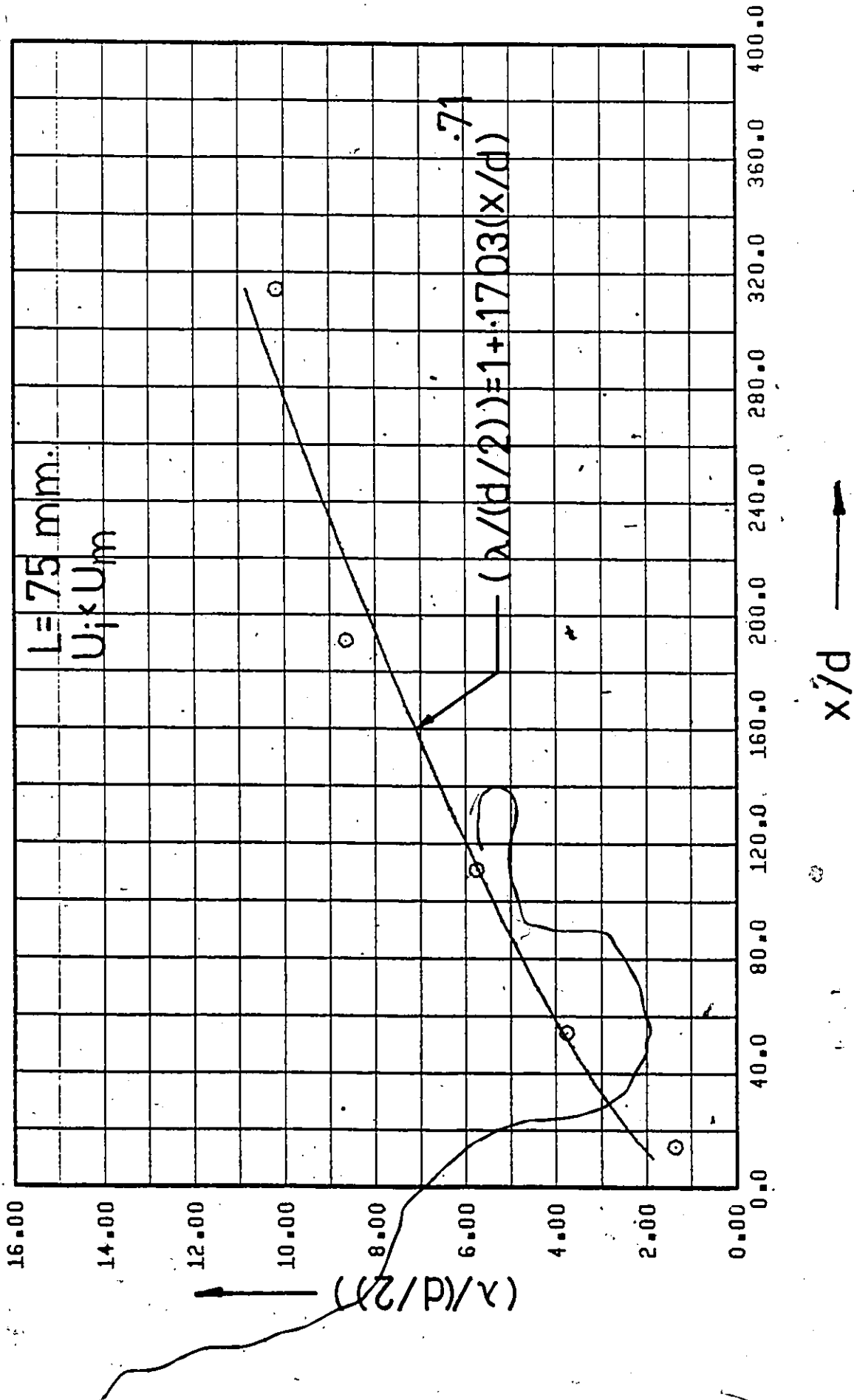


Figure 201. $(\lambda/(d/2))$ vs. x/d (Point Source Injection - Uniform Flow - $C_i = 50$ w.p.p.m.).

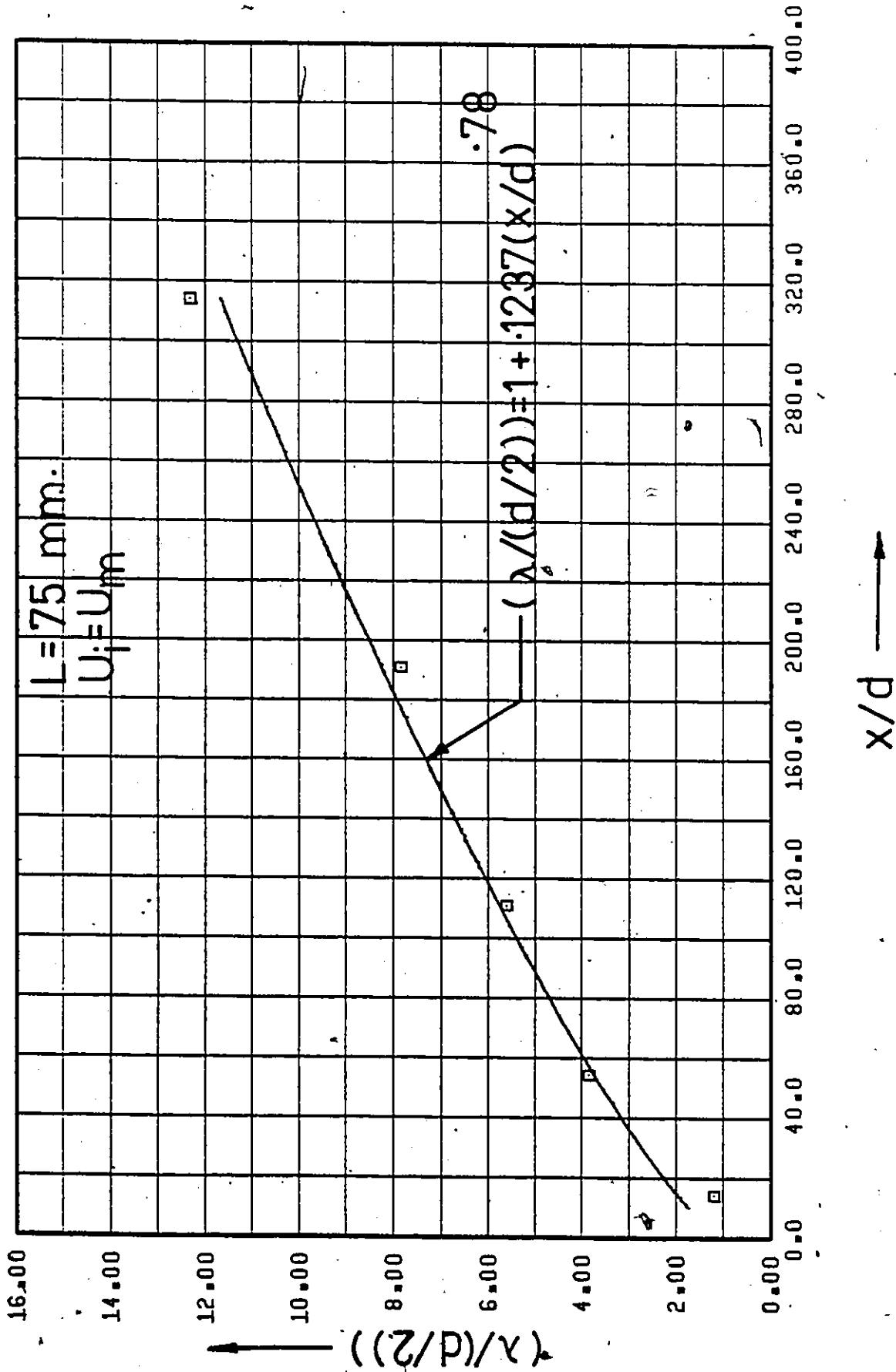


Figure 202. $(\lambda/(d/2))$ vs. x/d (Point Source Injection - Uniform Flow - $C_i = 50 \text{ w.p.p.m.}$).

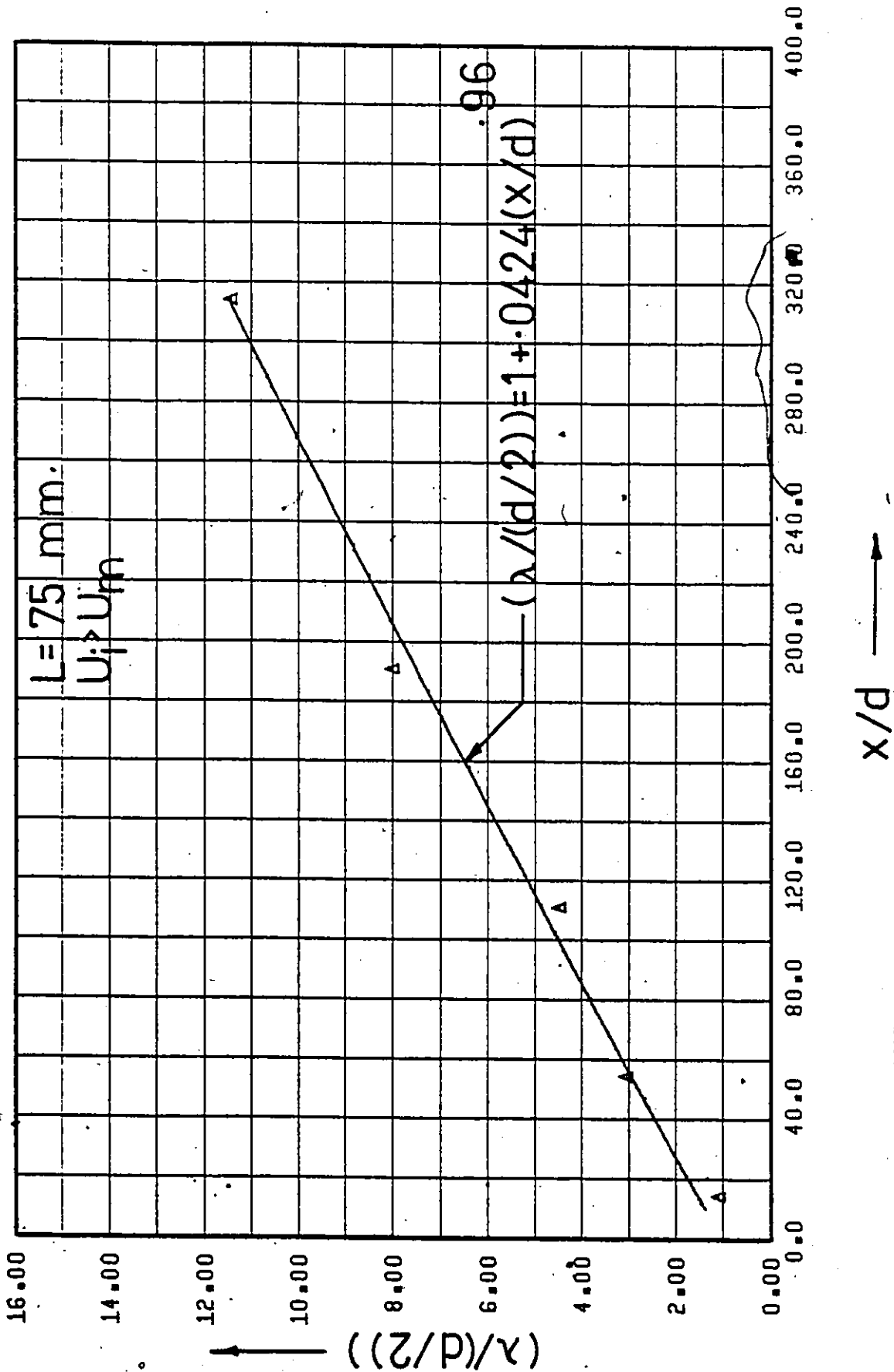


Figure 203. $(\lambda/(d/2))$ vs. x/d (Point Source Injection - Uniform Flow - $C_i = 50 \text{ w.p.p.m.}$).

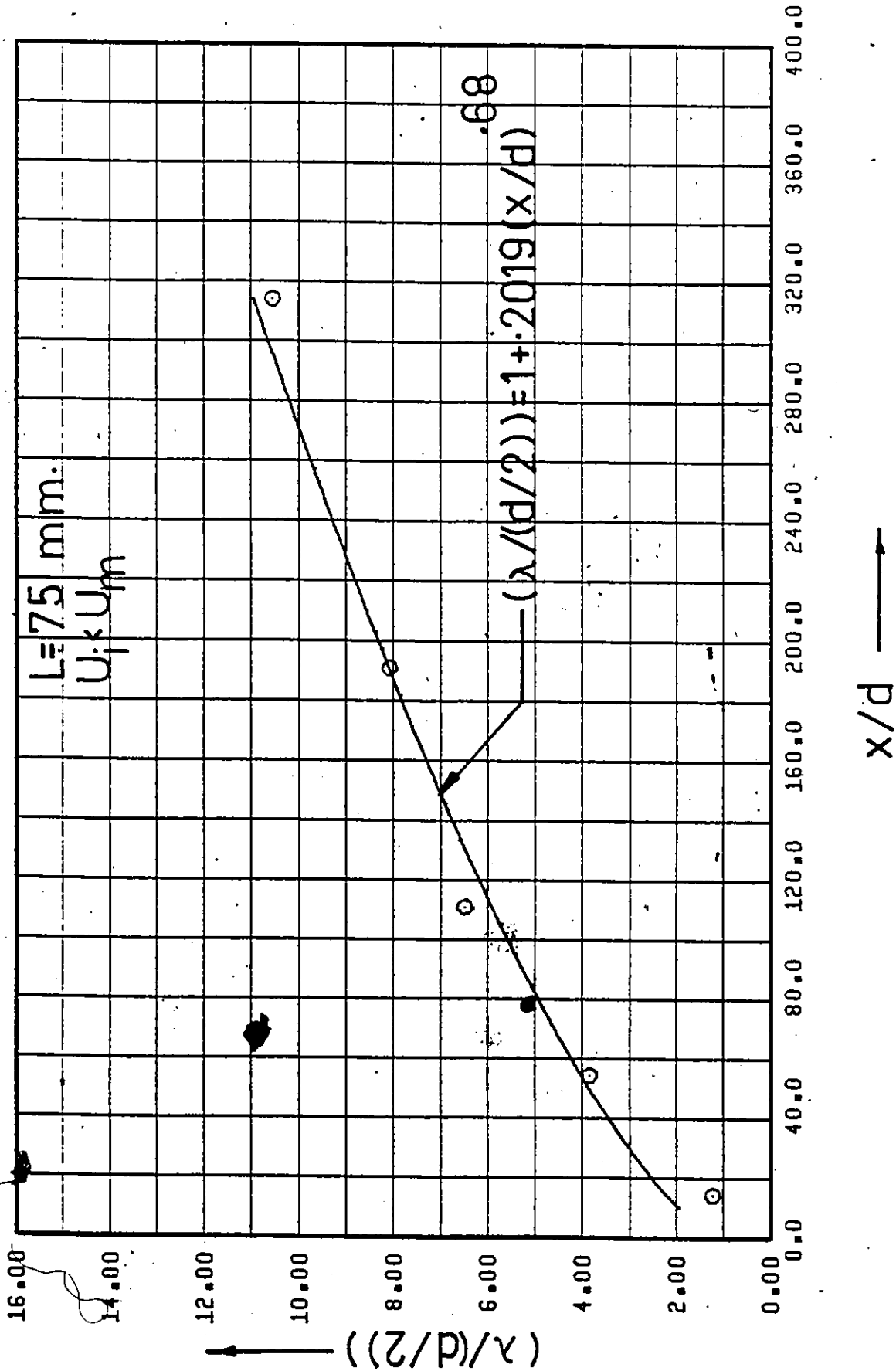


Figure 204. $(\lambda/d/2)$ vs. x/d (Point Source Injection - Uniform Flow - $C_i = 100 \text{ w.p.p.m.}$).

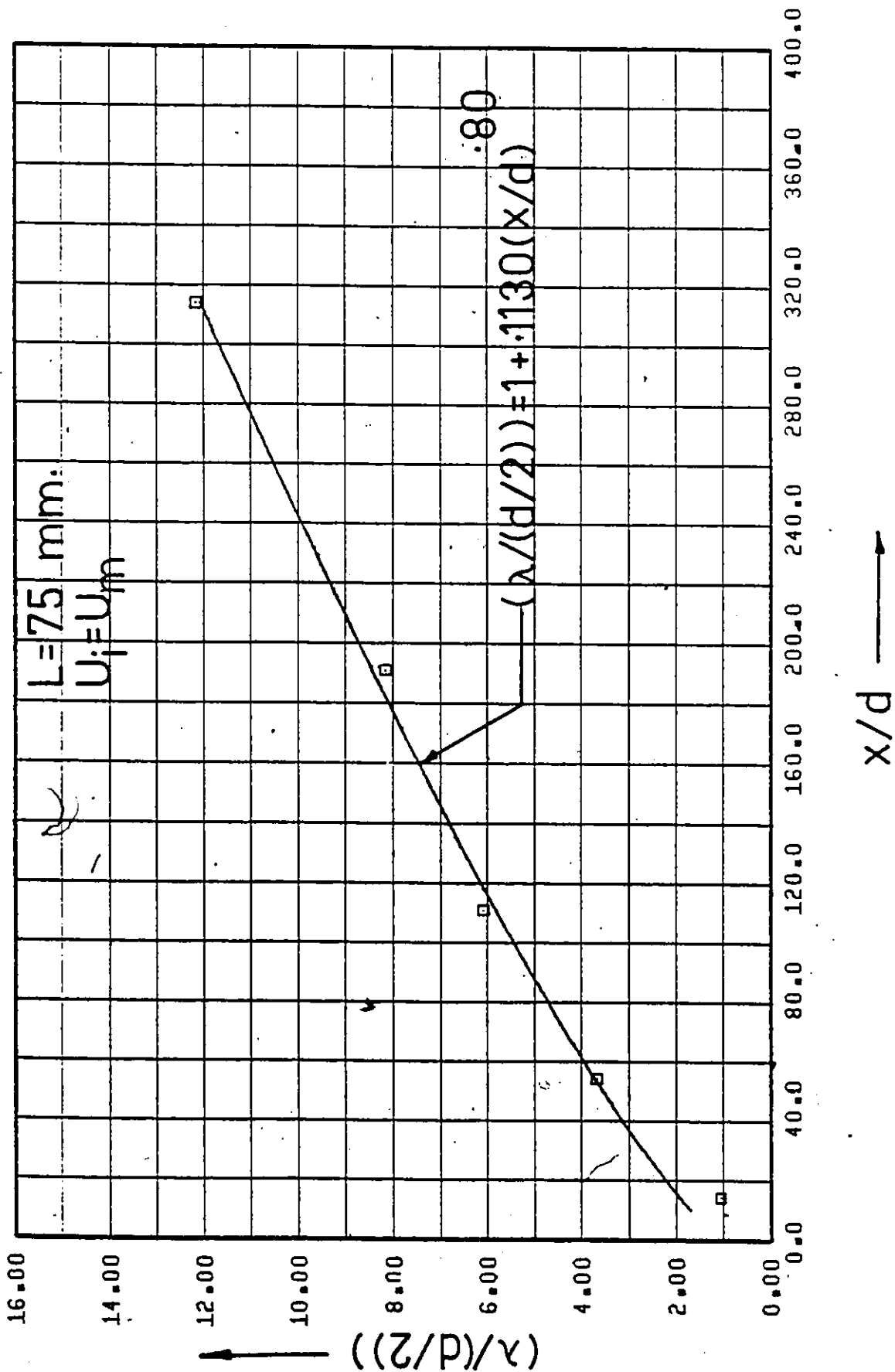


Figure 205. $(\lambda/(d/2))$ vs. x/d (Point Source Injection - Uniform Flow - $C_i = 100$ w.p.p.m.).

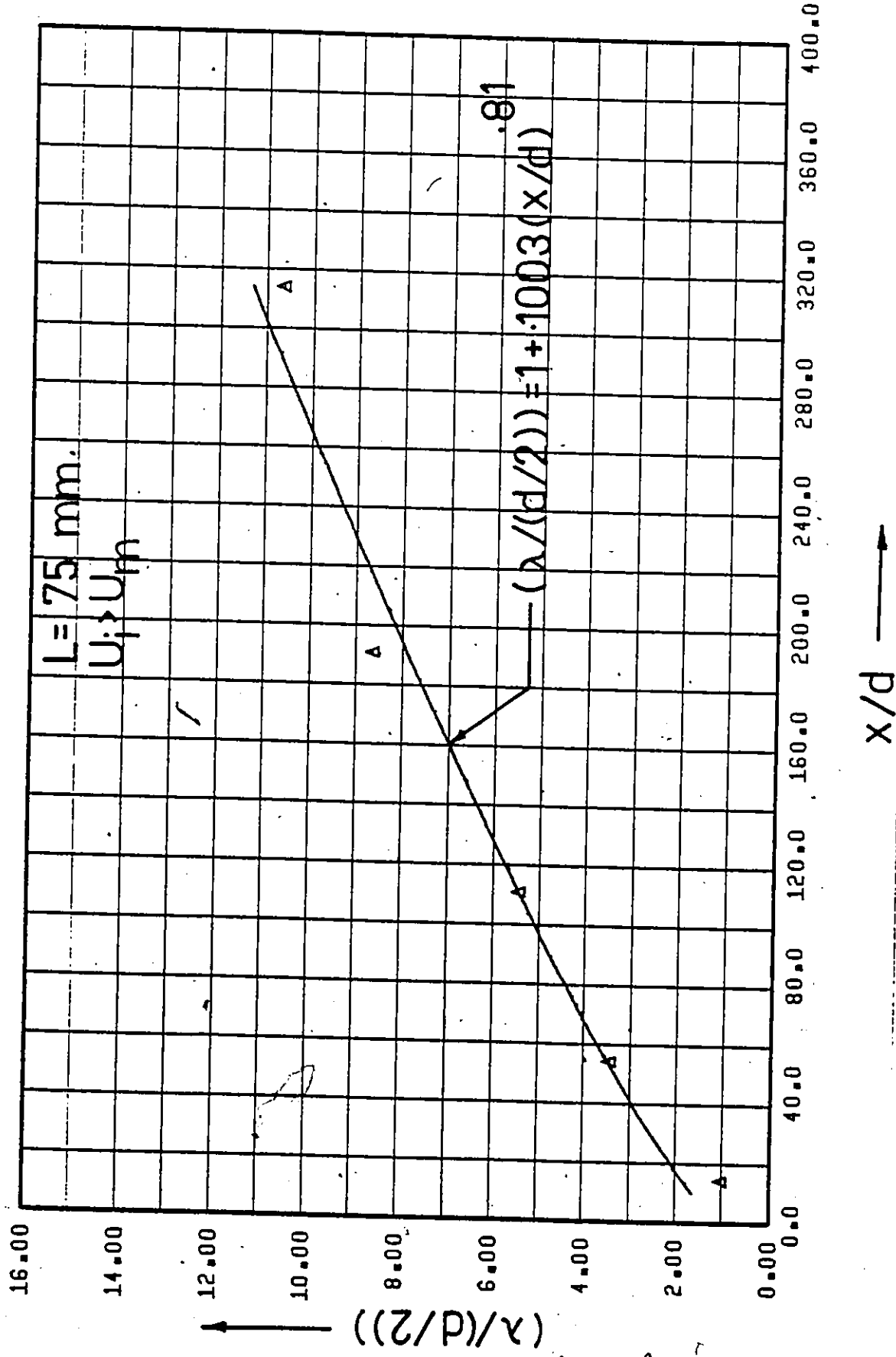


Figure 206. $(\lambda/(d/2))$ vs. x/d (Point Source Injection - Uniform Flow - $C_i = 100$ w.p.p.m.).

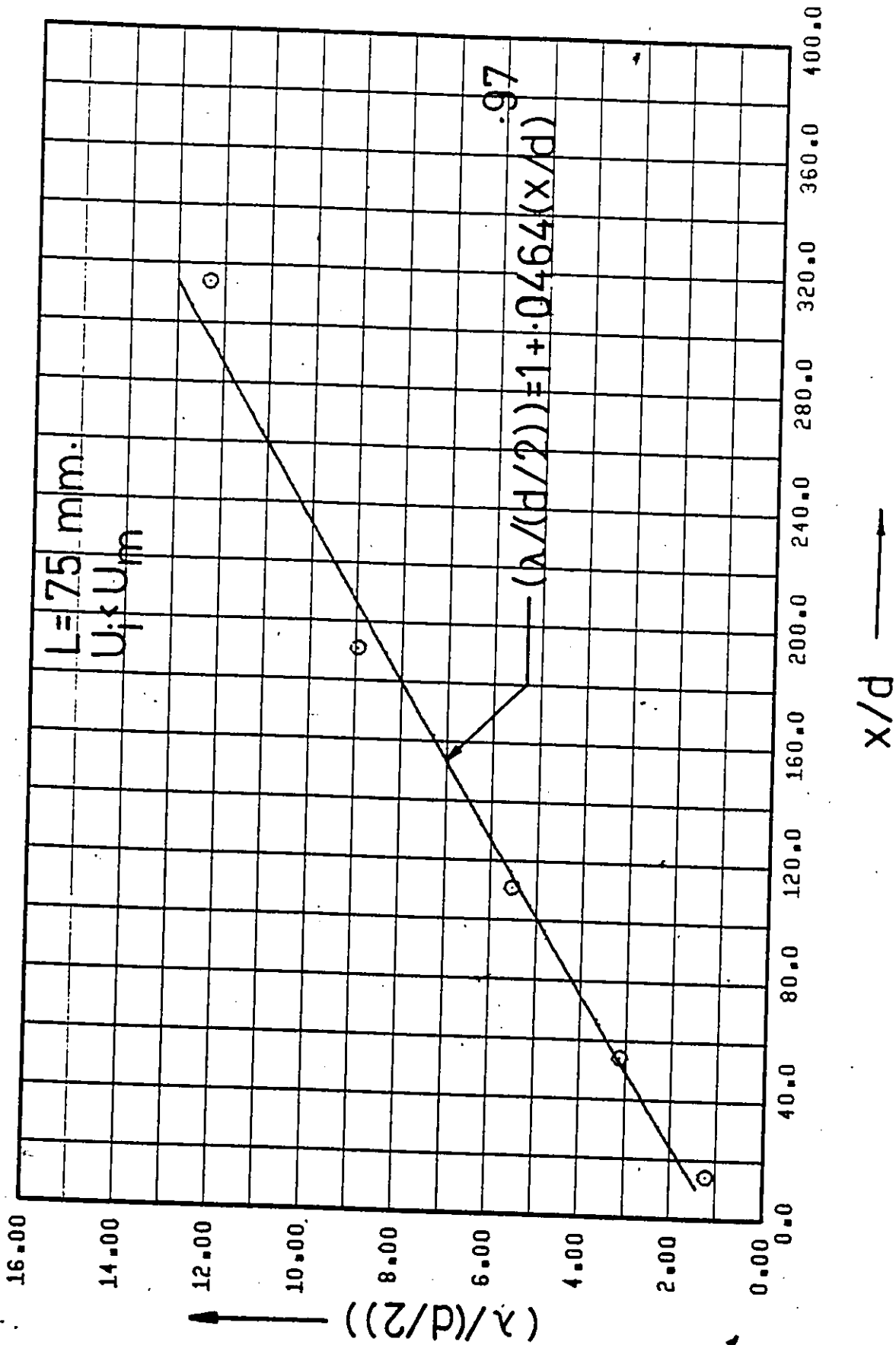


Figure 207. $(\lambda/(d/2))$ vs. x/d (Point Source Injection - Uniform Flow - $C_1 = 250 \text{ w.p.p.m.}$).

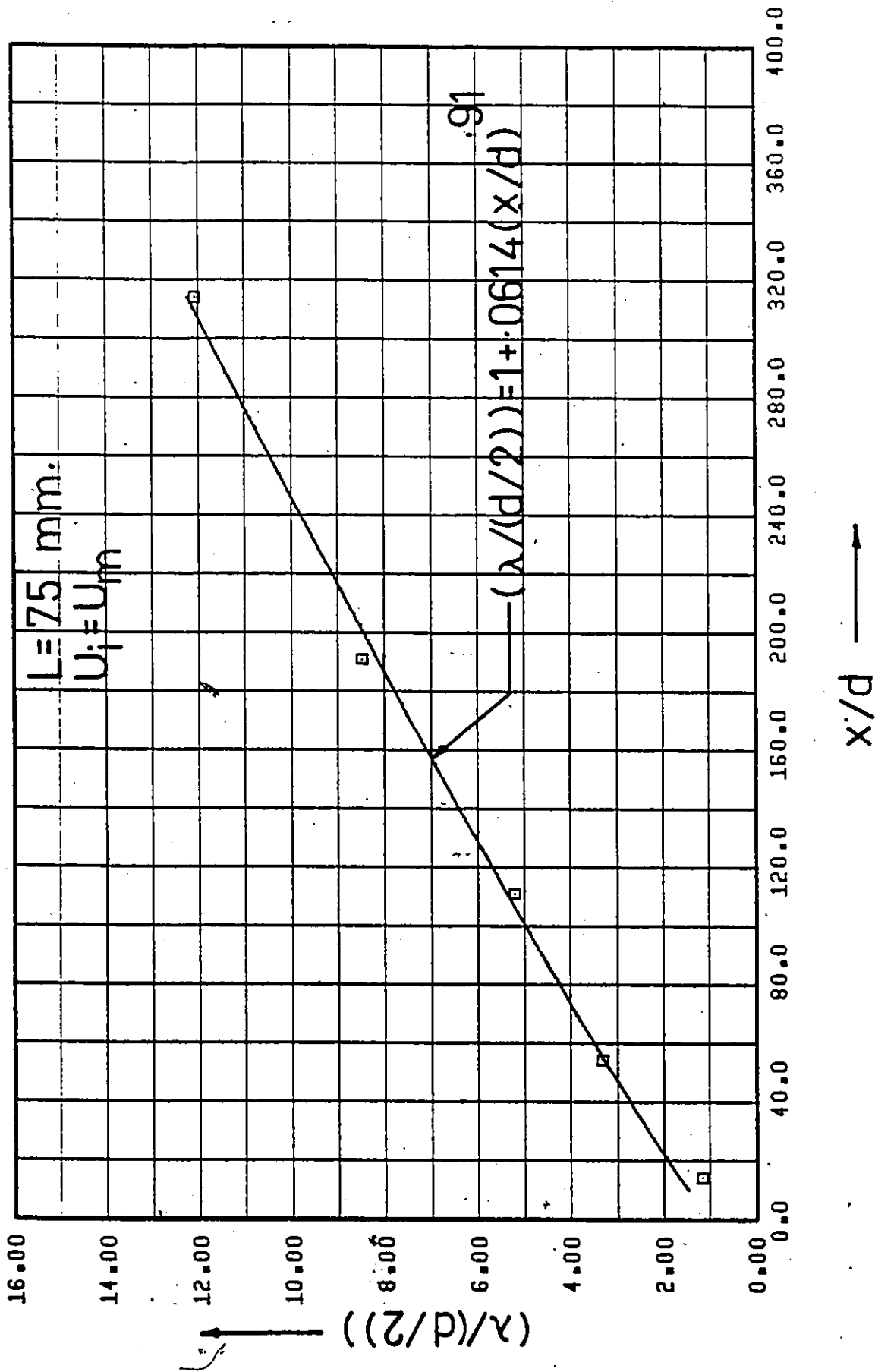


Figure 208. $(\lambda/(d/2))$ vs. x/d (Point Source Injection - Uniform Flow - $C_i = 250$ w.p.p.m.).

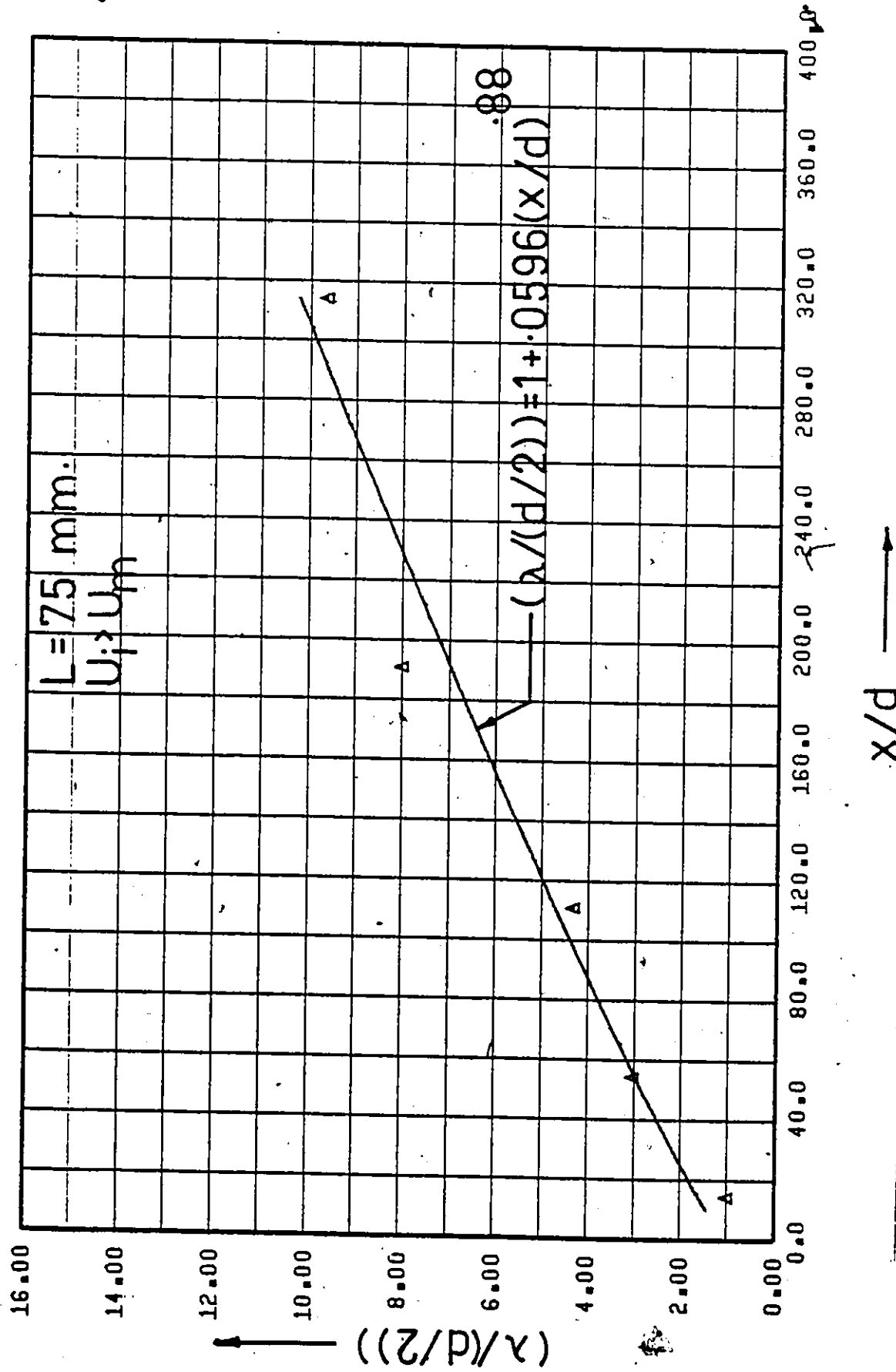


Figure 209 $(\lambda/(d/2))$ vs. x/d (Point Source Injection - Uniform Flow - $C_i = 250 \text{ w.p.p.m.}$).

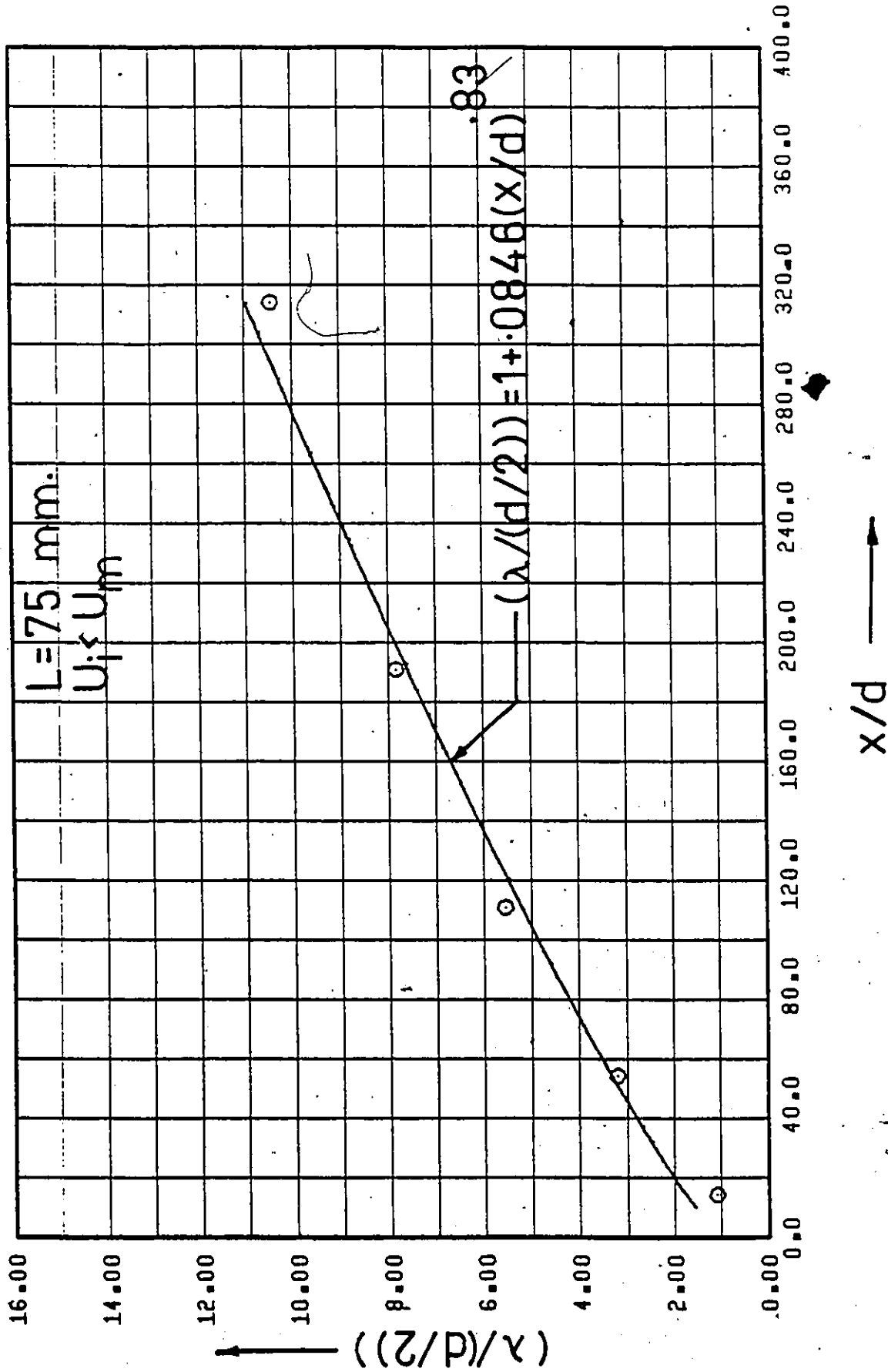


Figure 210. $(\lambda/(d/2))$ vs. x/d (Point Source Injection - Uniform Flow - $C_i = 500$ w.p.p.m.).

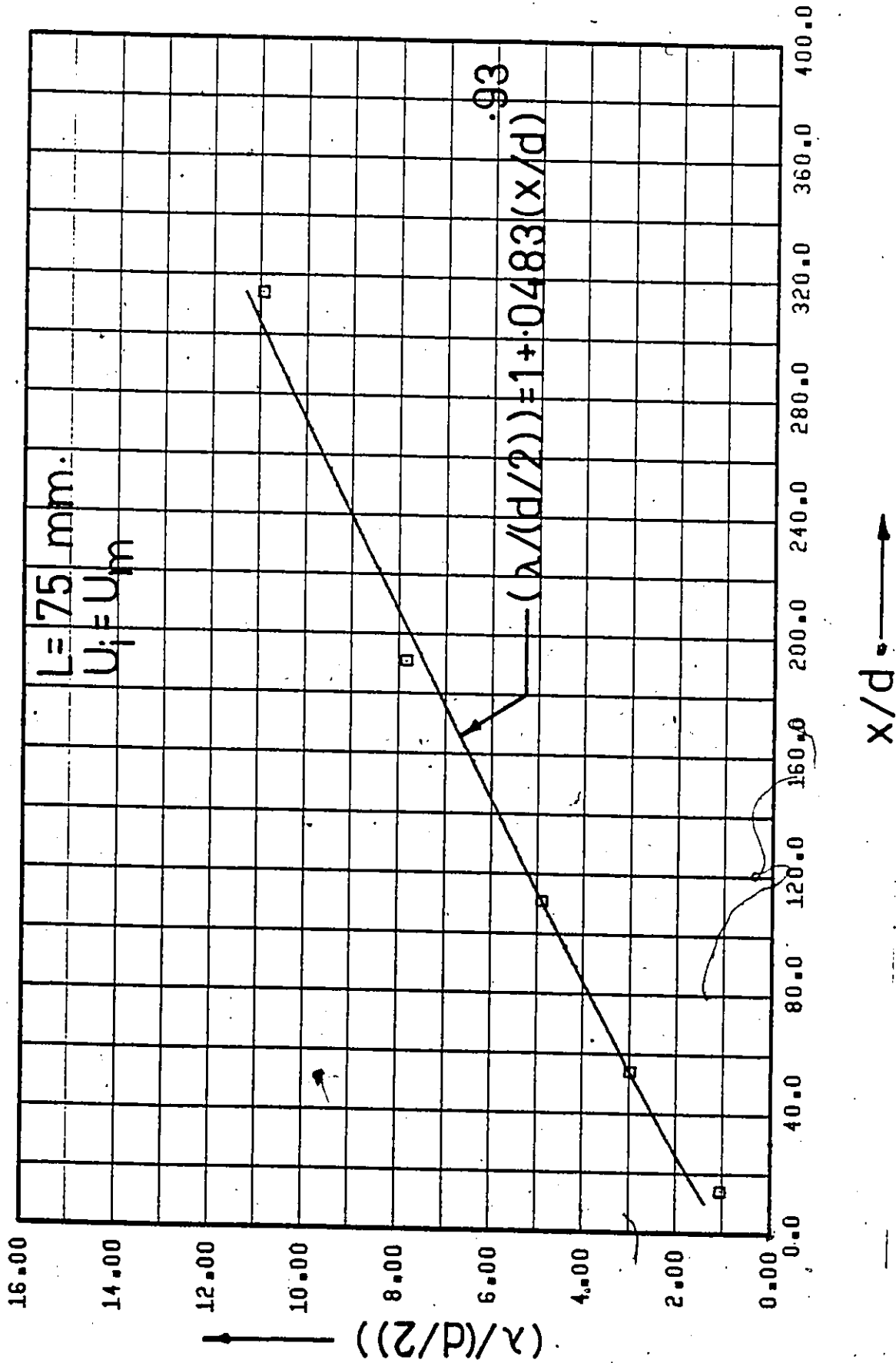
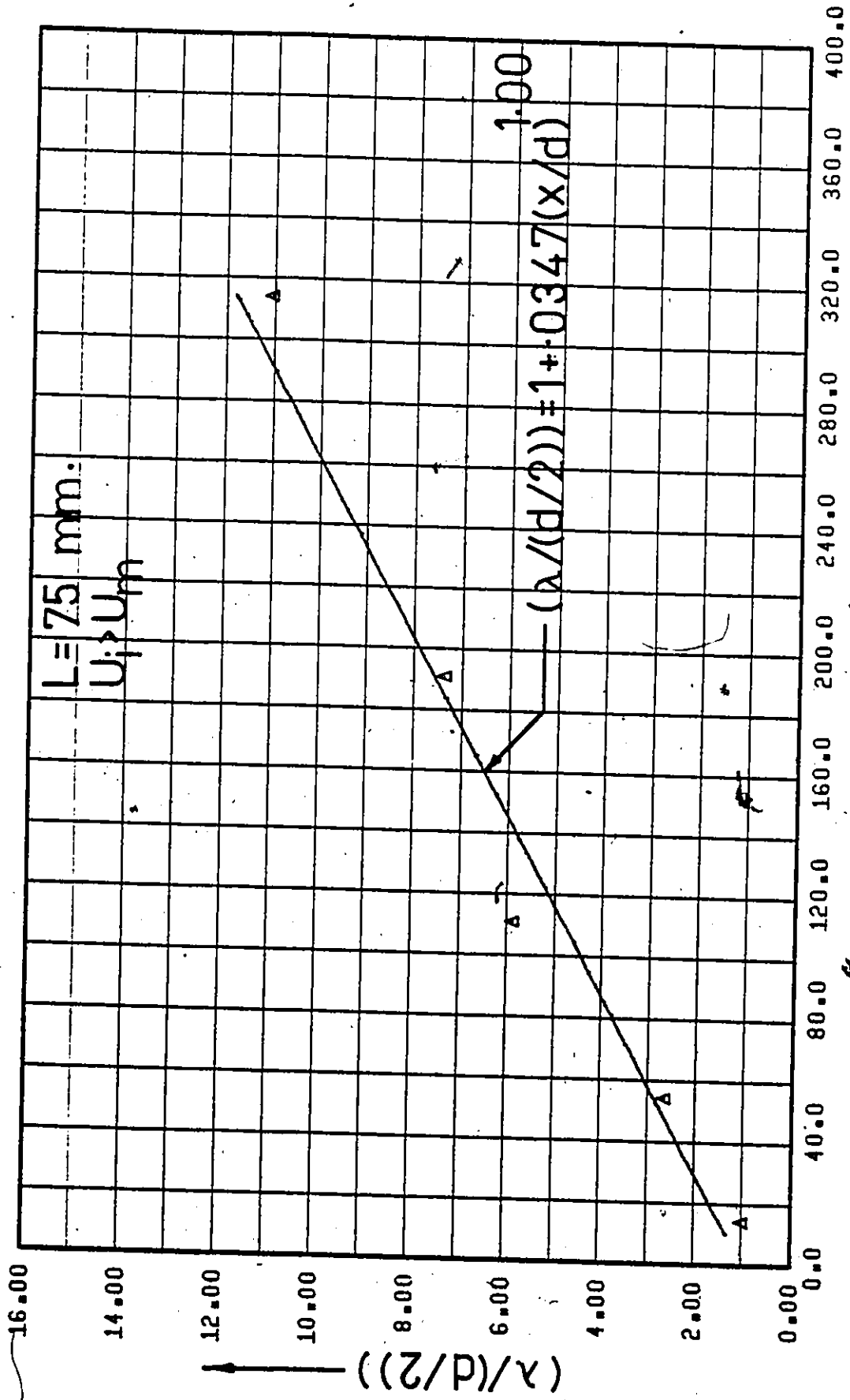


Figure 211. $(\lambda/(d/2))$ vs. x/d (Point Source Injection - Uniform Flow; $C_i = 500 \text{ w.p.p.m.}$).



x/d →

Figure 212. $(\lambda/(d/2))$ vs. x/d (Point Source Injection - Uniform Flow - $C_i = 500 \text{ w.p.p.m.}$).

2

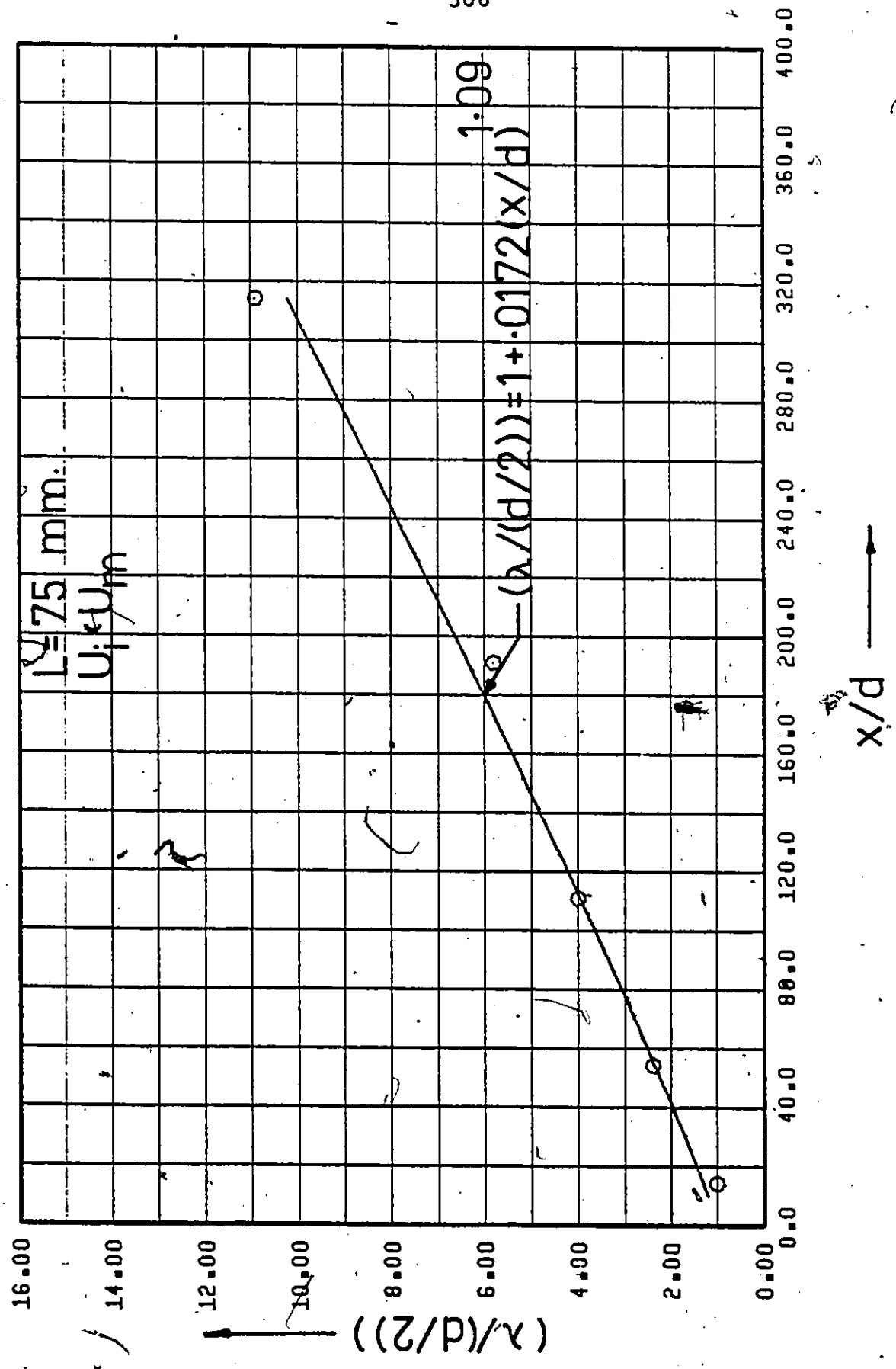


Figure 213. $(\lambda/(d/2))$ vs. x/d (Point Source Injection - Uniform Flow - $C_i = 1000$ w.p.p.m.).

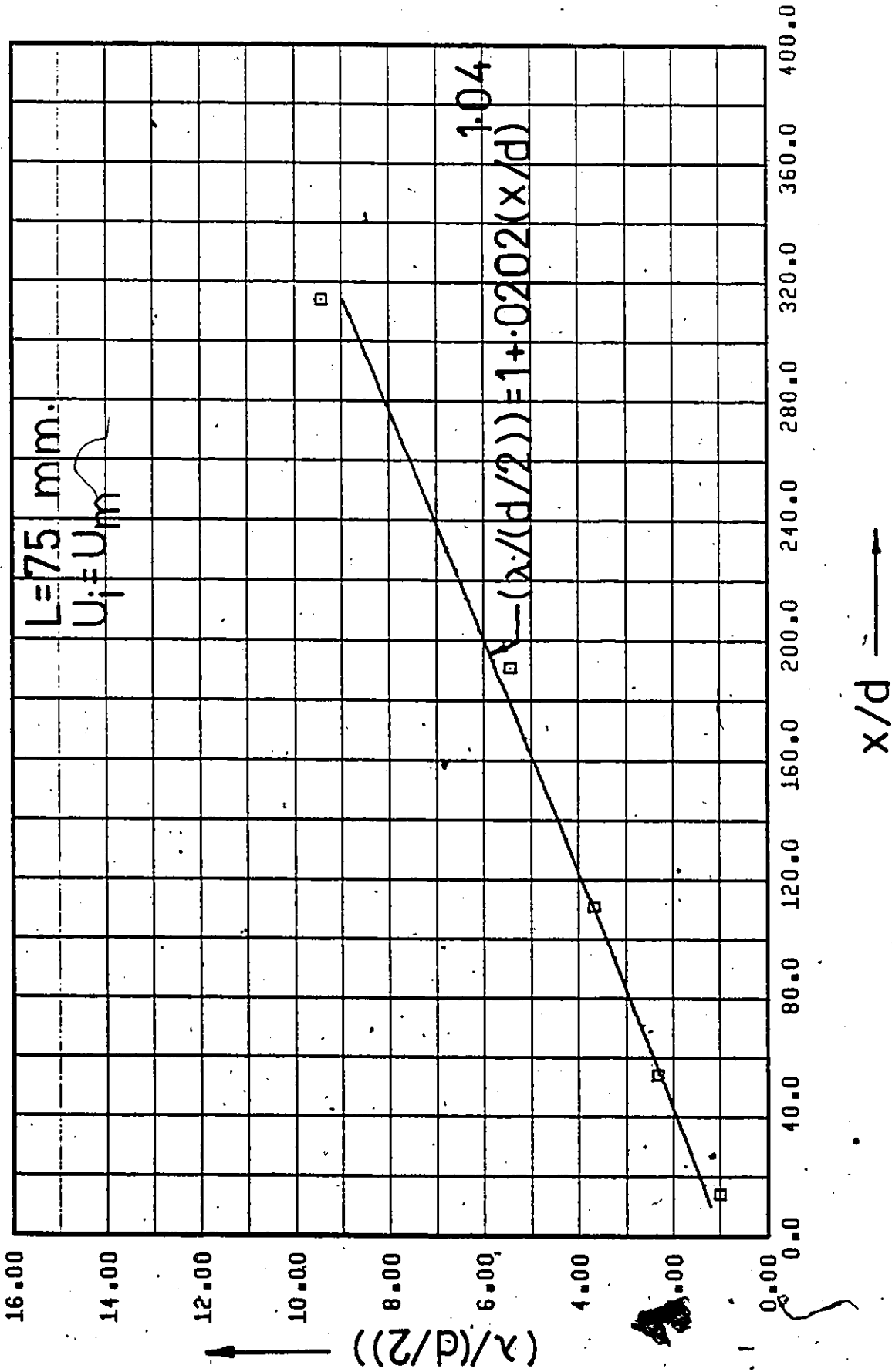
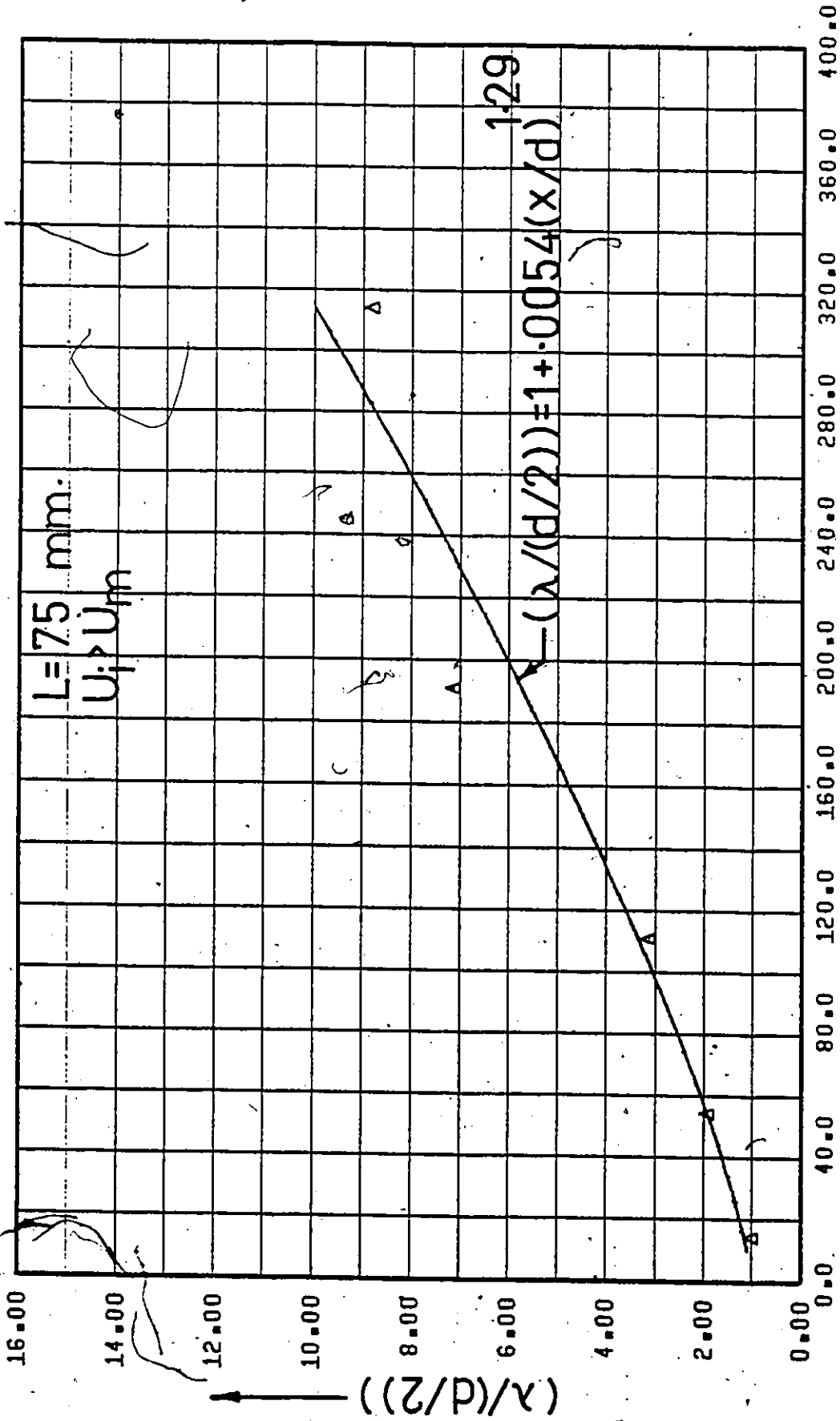


Figure 214. $(\lambda/(d/2))$ vs. x/d (Point Source Injection - Uniform Flow - $C_i = 1000 \text{ w.p.p.m.}$).



x/d →

Figure 215. $(\lambda/(d/2))$ vs. x/d (Point Source Injection - Uniform Flow - $C_i = 1000$ w.p.p.m.).

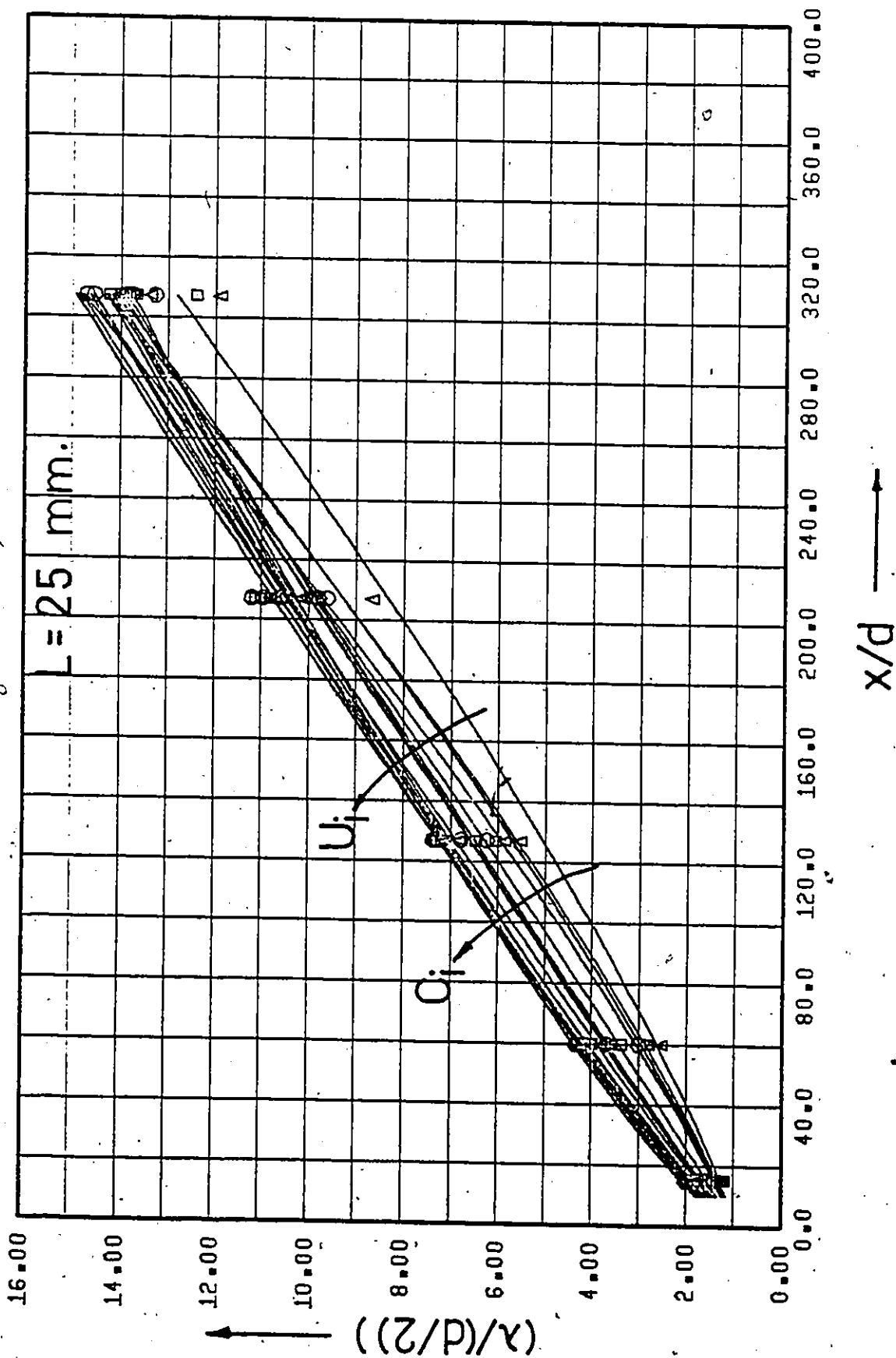


Figure 216. Non-dimensional Diffusion Boundary Layer Thickness Profiles (Point Source Injection - Fully Developed Flow).

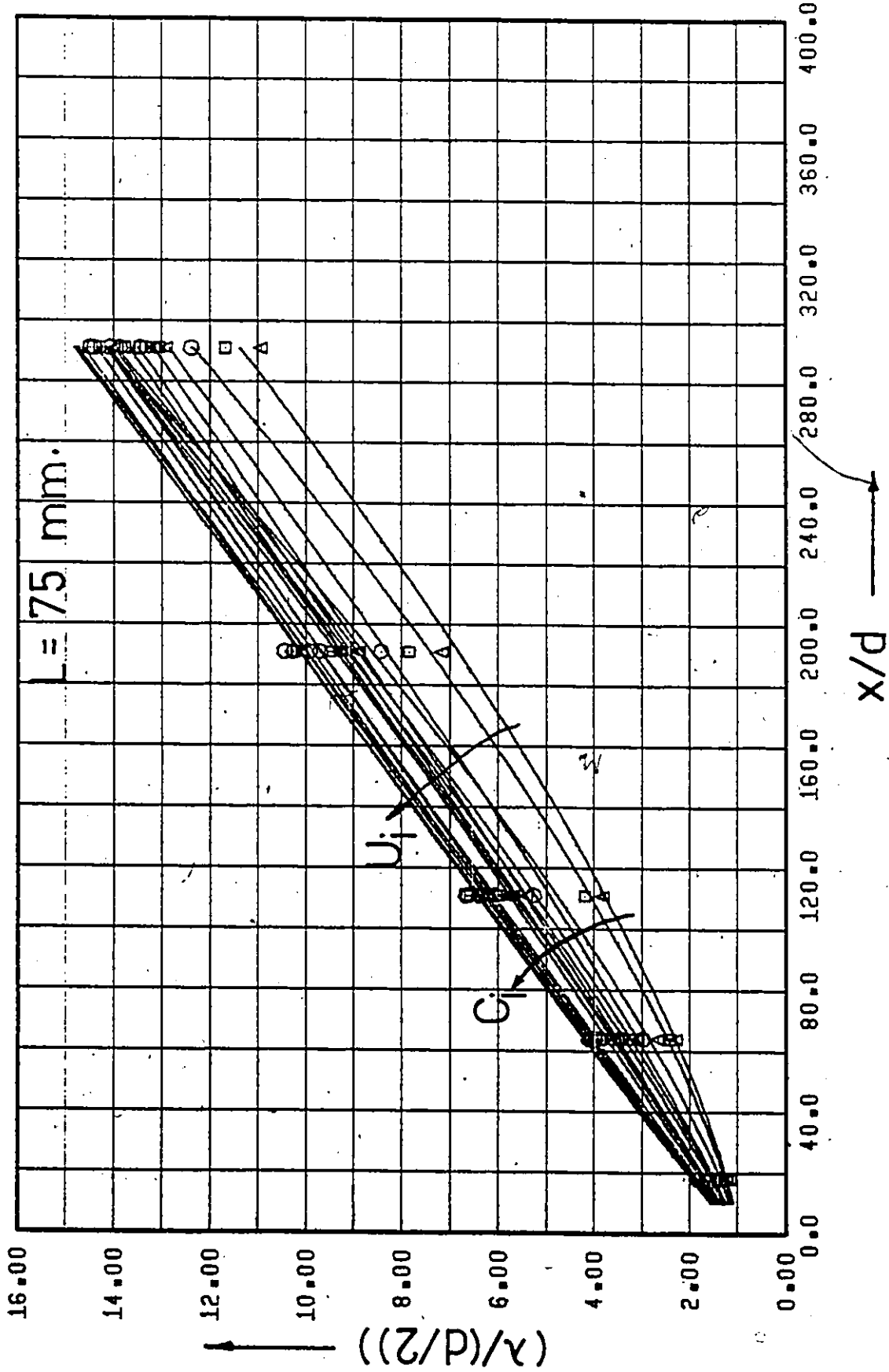


Figure 217. Non-dimensional Diffusion Boundary Layer Thickness Profiles (Point Source Injection - Fully Developed Flow).

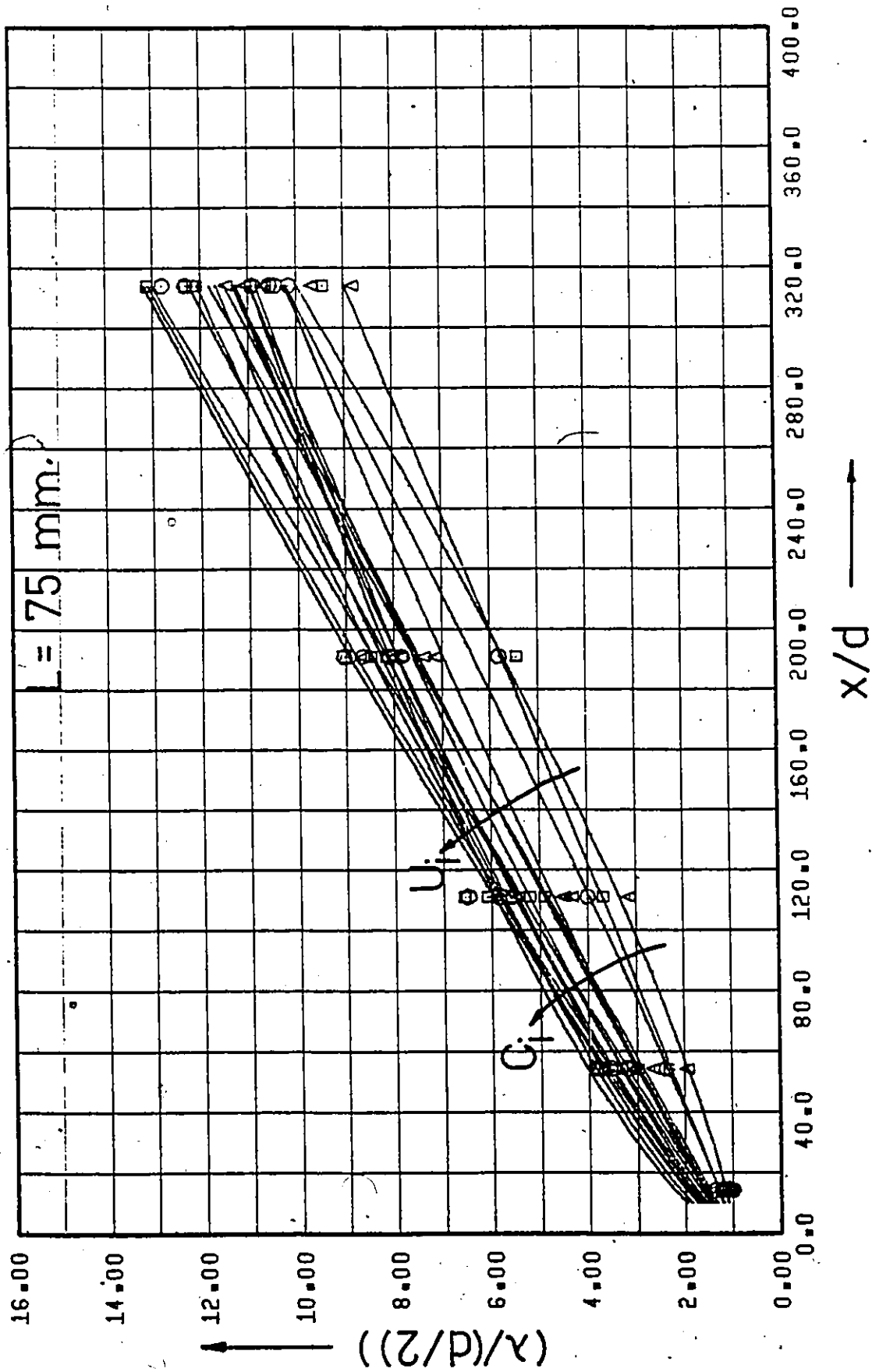


Figure 218. Non-dimensional Diffusion Boundary Layer Thickness Profiles (Point Source Injection - Uniform Flow).

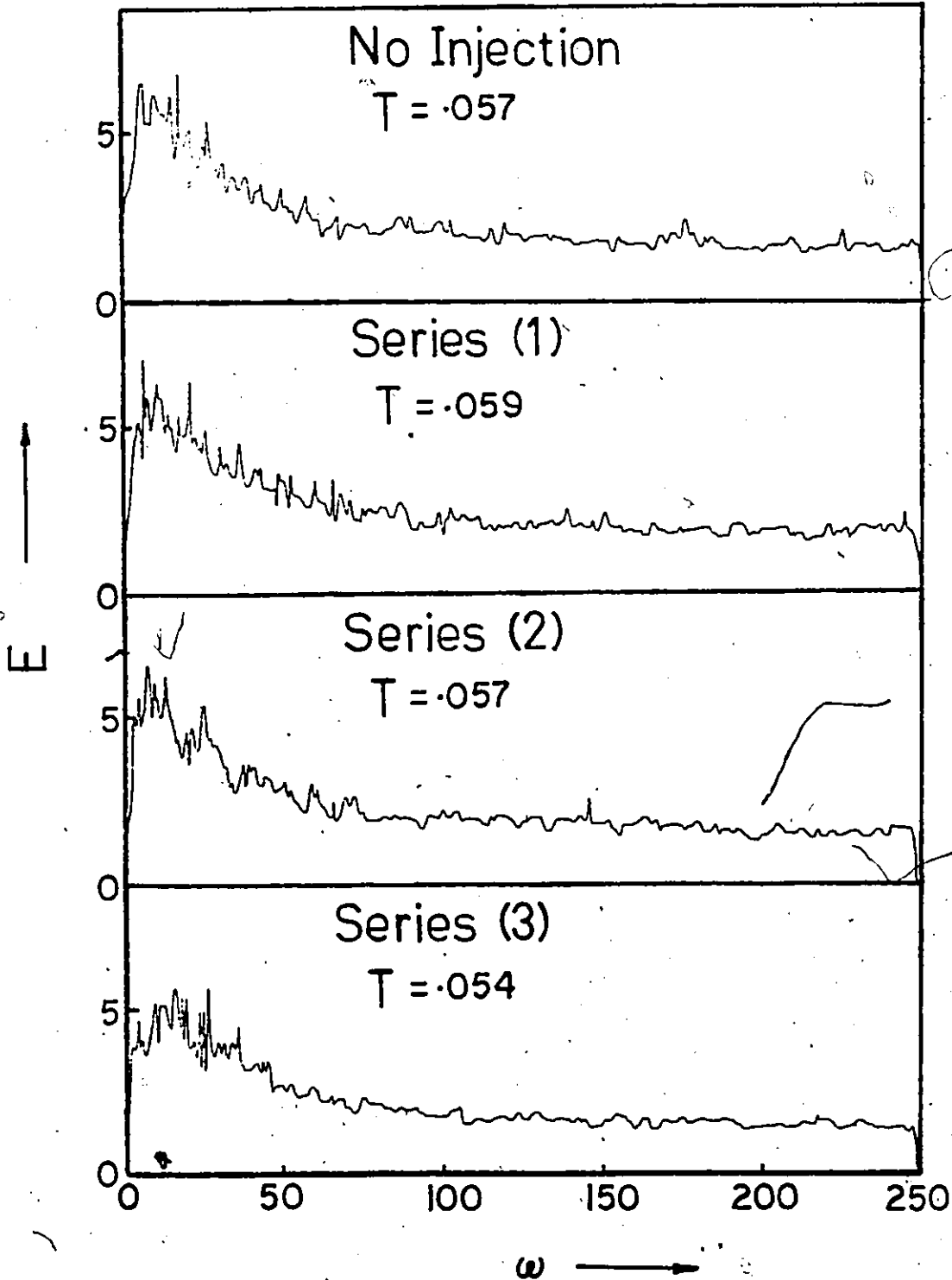


Figure 219. Energy Spectra (Point Source Injection - Fully Developed Flow - Water Injection).

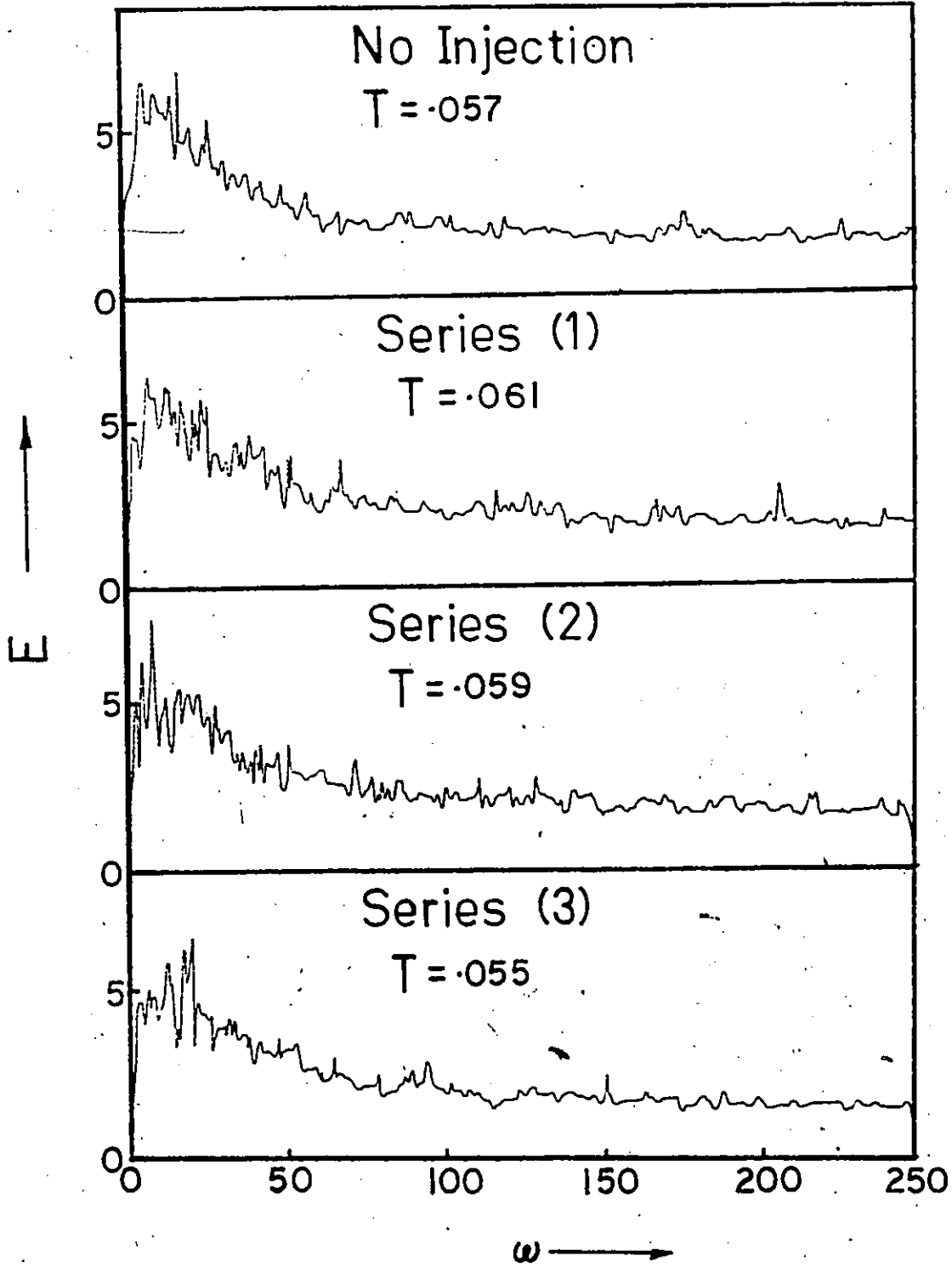


Figure 220. Energy Spectra (Point Source Injection - Fully Developed Flow - $C_i = 50$ w.p.p.m.).

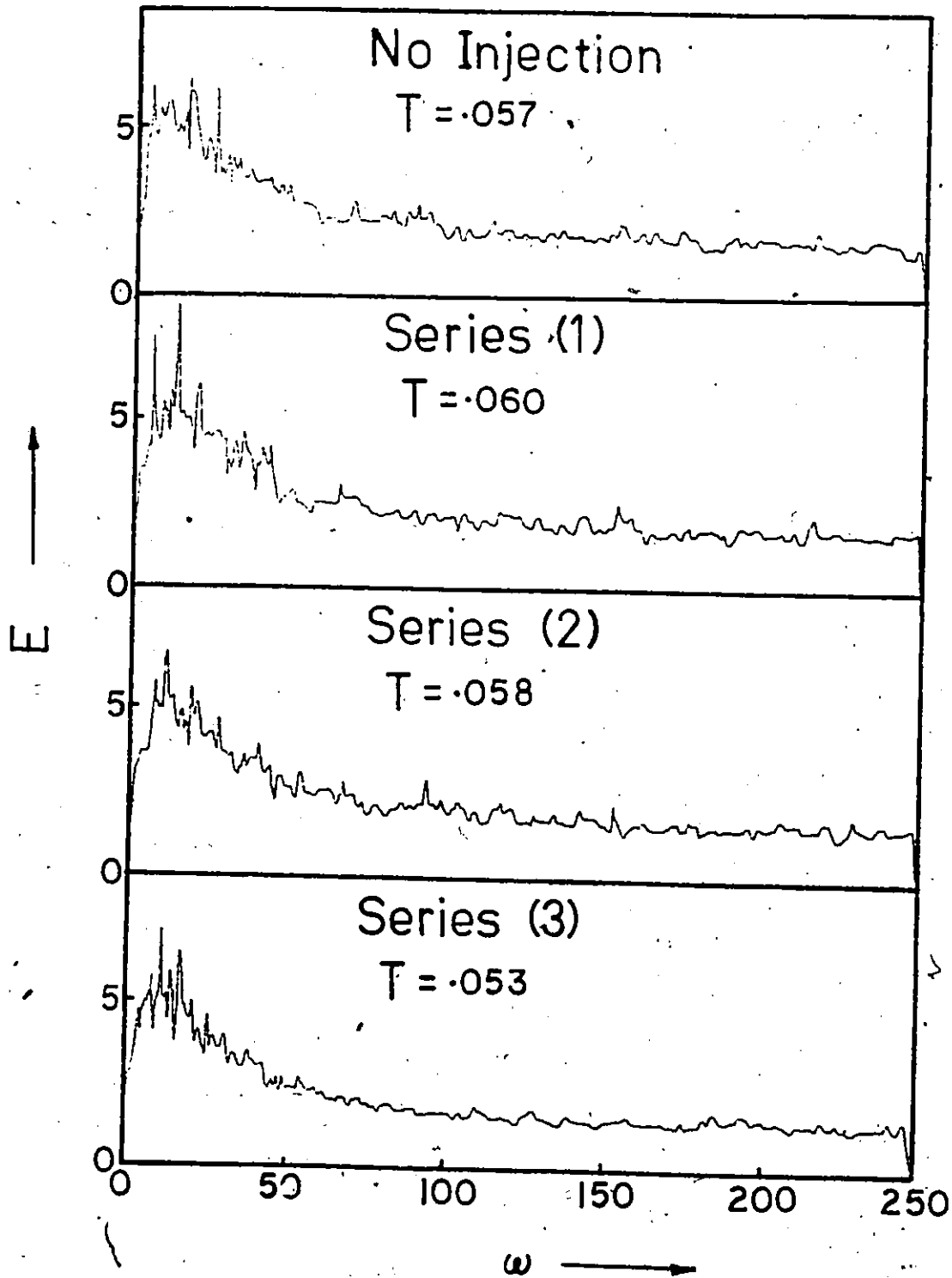


Figure 221. Energy Spectra (Point Source Injection - Fully Developed Flow - $C_i = 100$ w.p.p.m.).

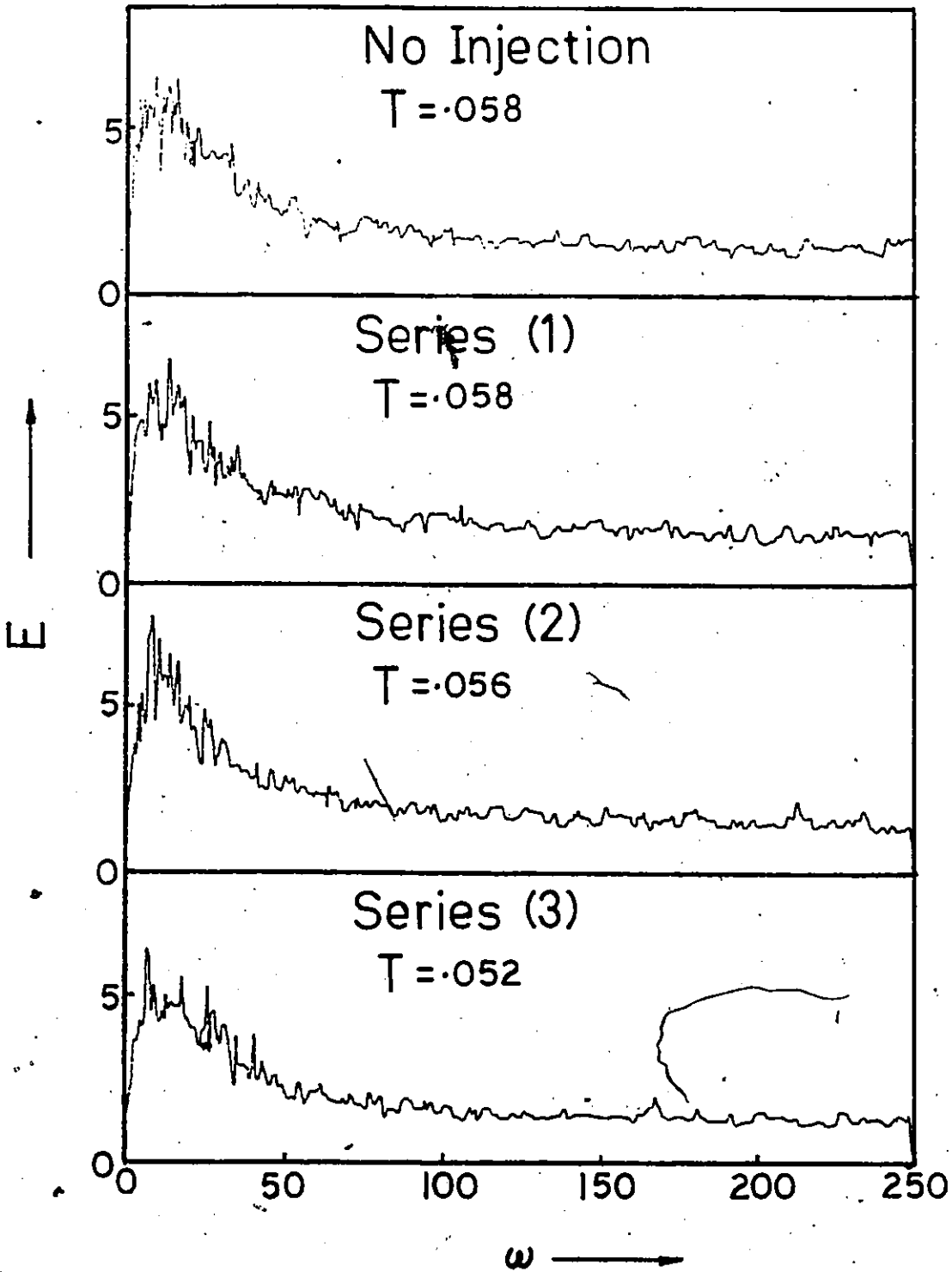


Figure 22. Energy Spectra (Point Source
 Injection - Fully Developed Flow -
 $C_i = 250$ w.p.p.m.).

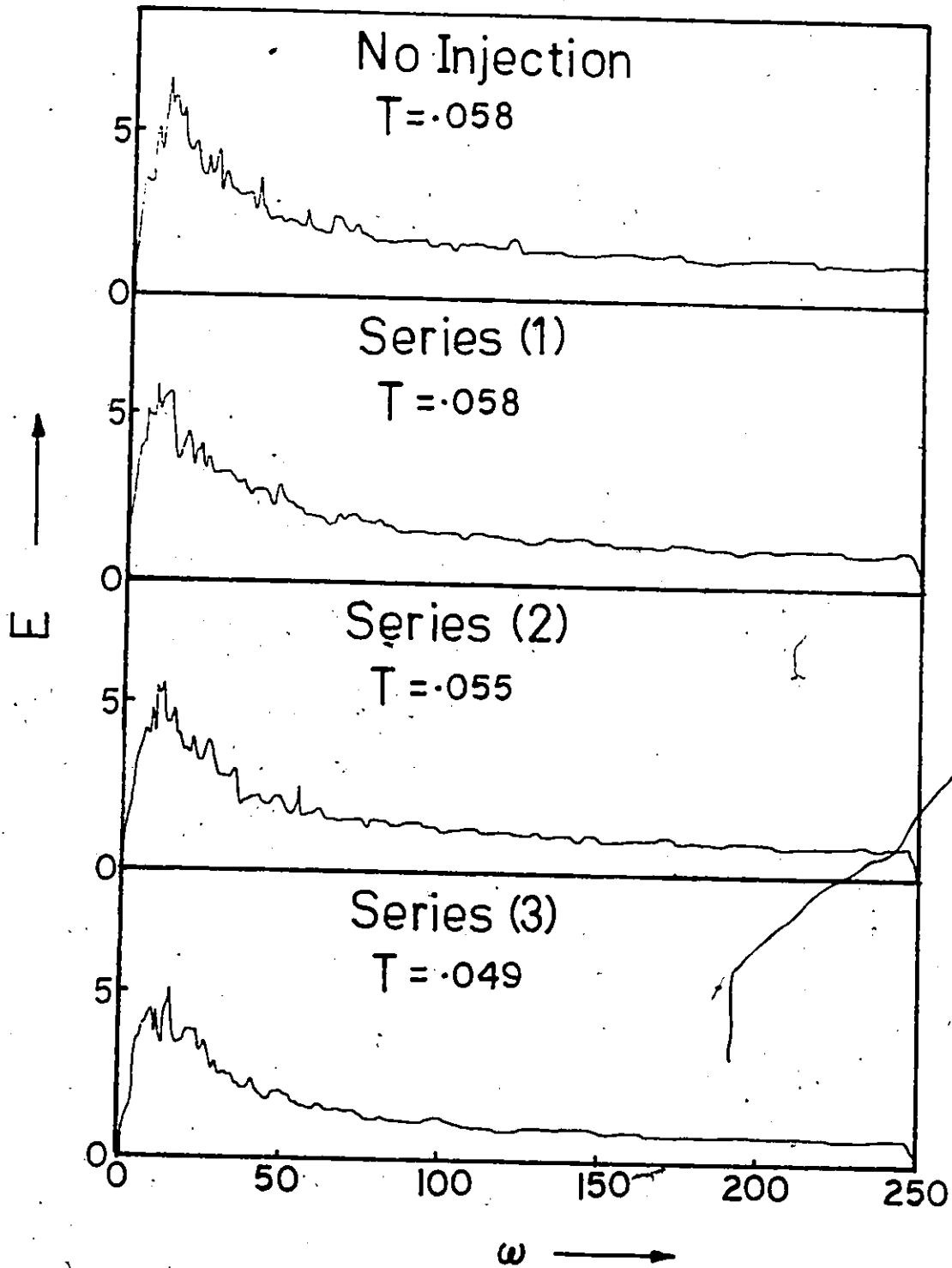


Figure 223. Energy Spectra (Point Source Injection - Fully Developed Flow - $C_i = 500$ w.p.p.m.).

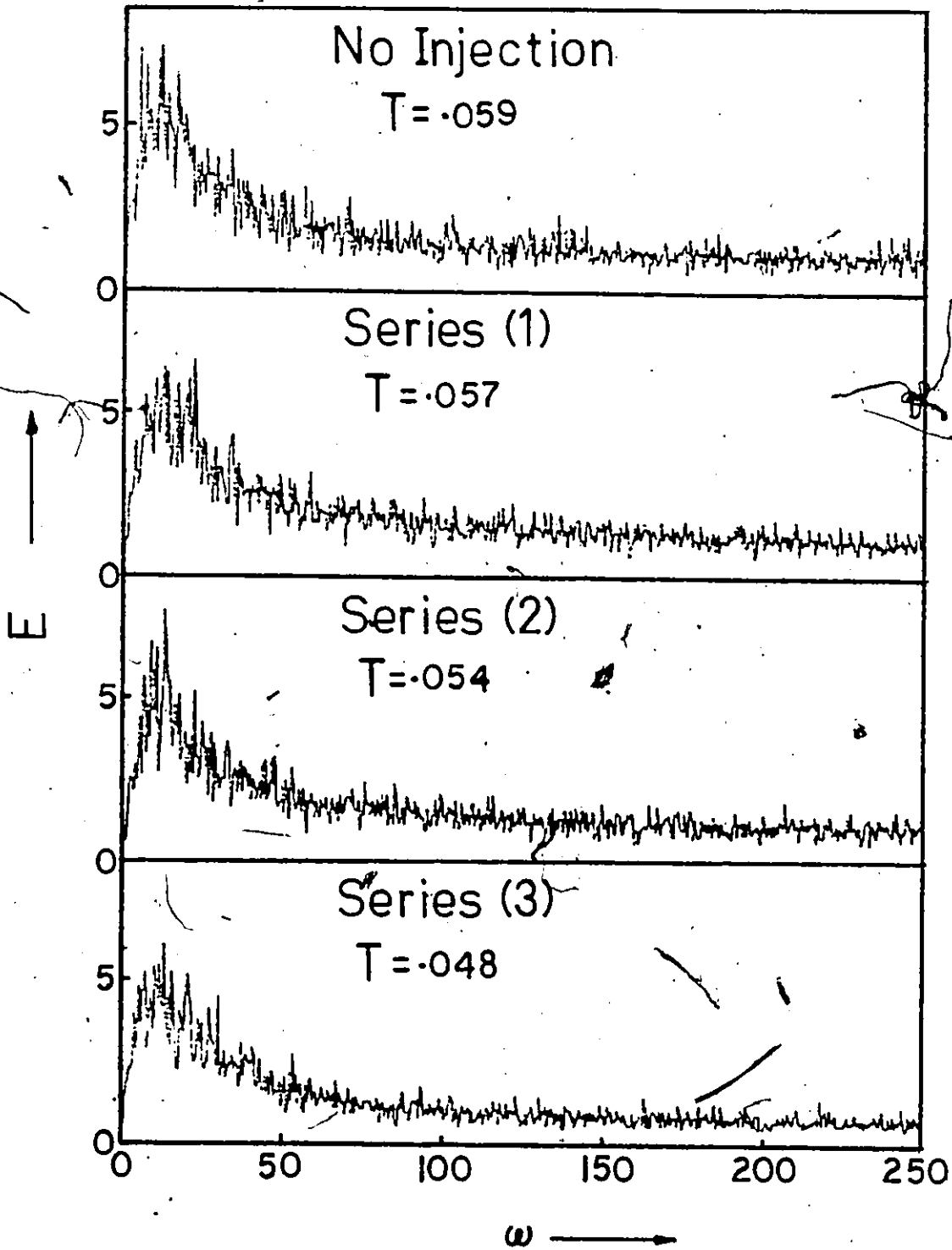


Figure 224. Energy Spectra (Point Source Injection - Fully Developed Flow - $C_i = 1000$ w.p.p.m.).

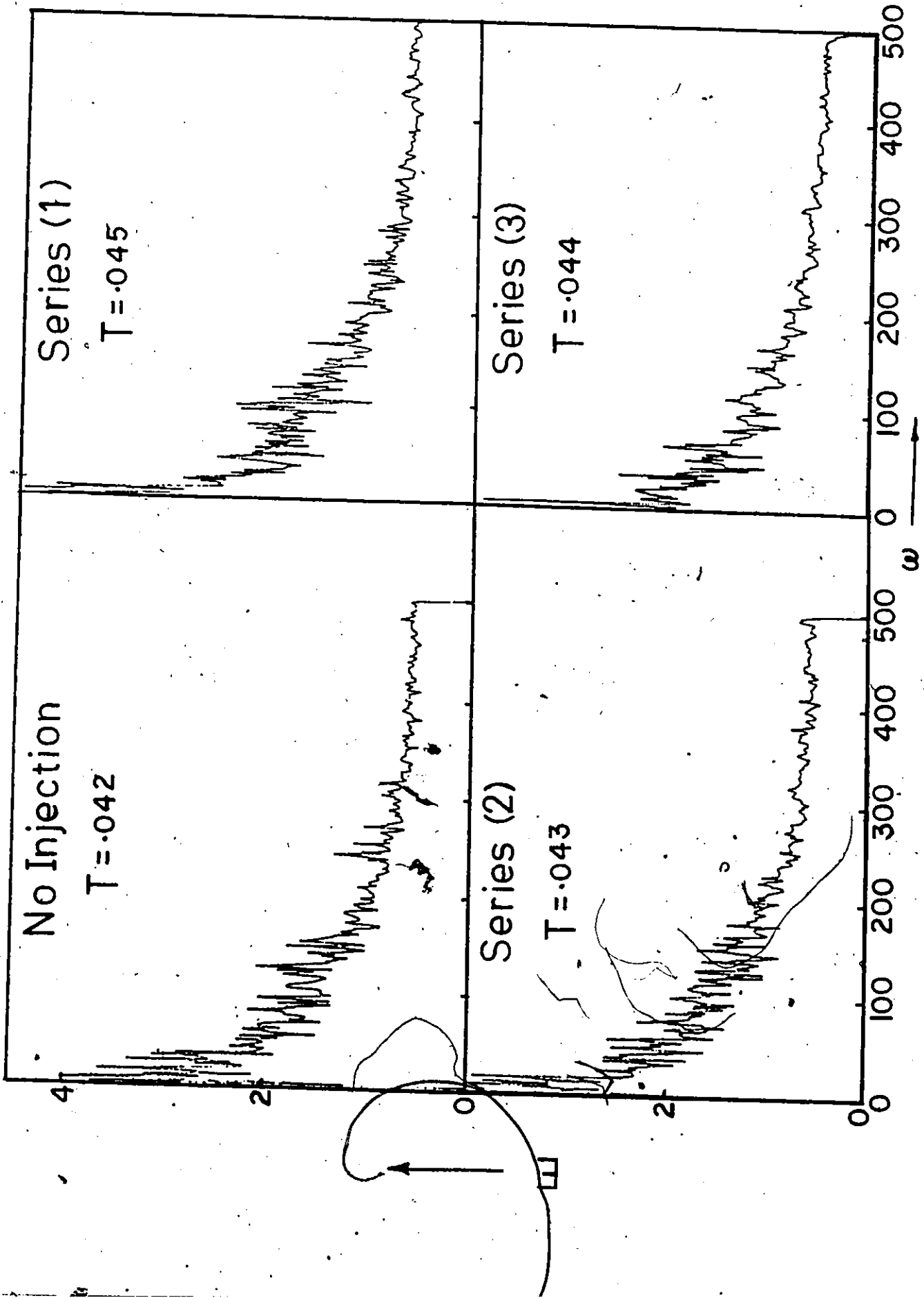


Figure 225. Energy Spectra (Point Source Injection - Uniform Flow - Water Injection).

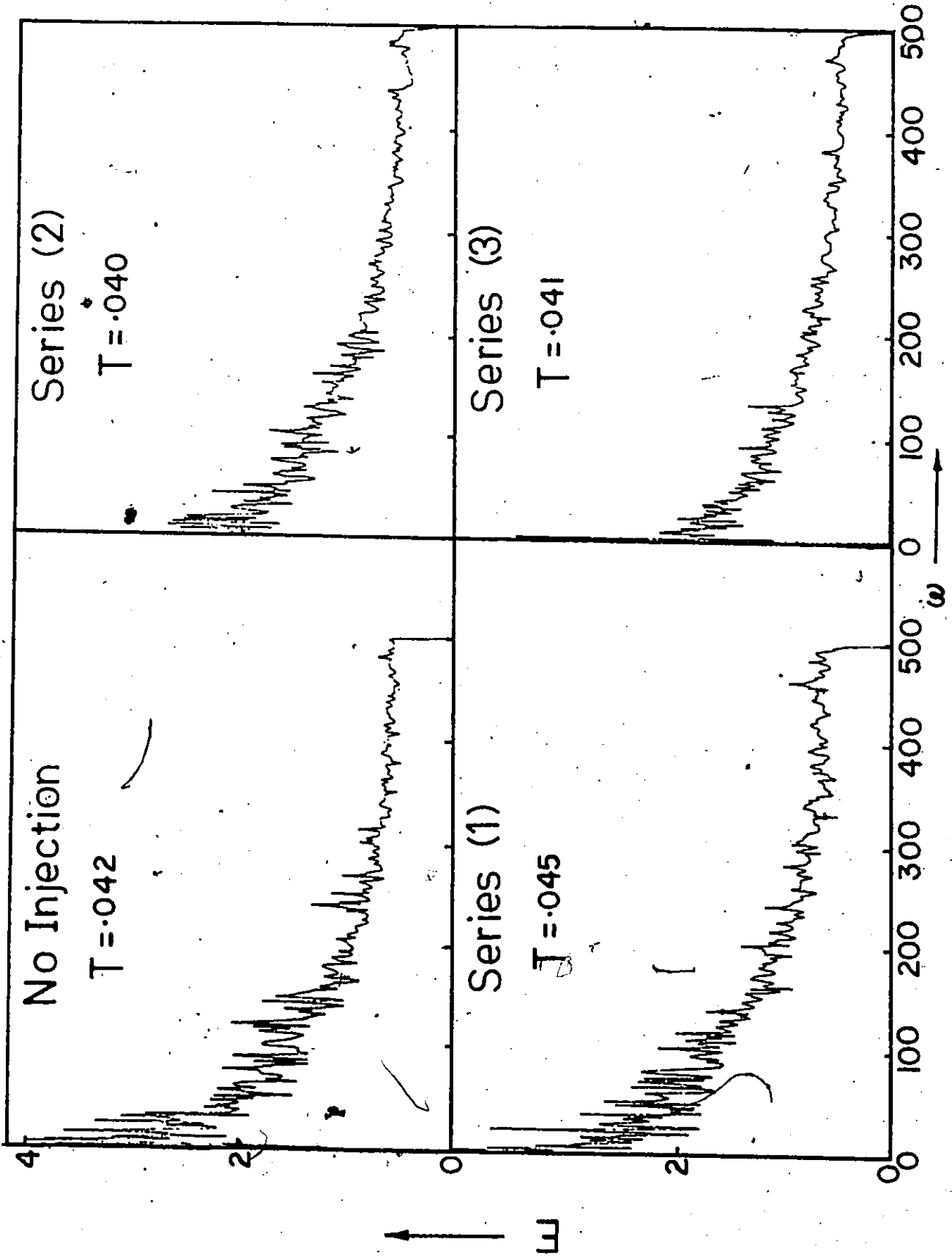


Figure 226. Energy Spectra (Point Source Injection - Uniform Flow - Water Injection - $C_i = 50$ w.p.p.m.).

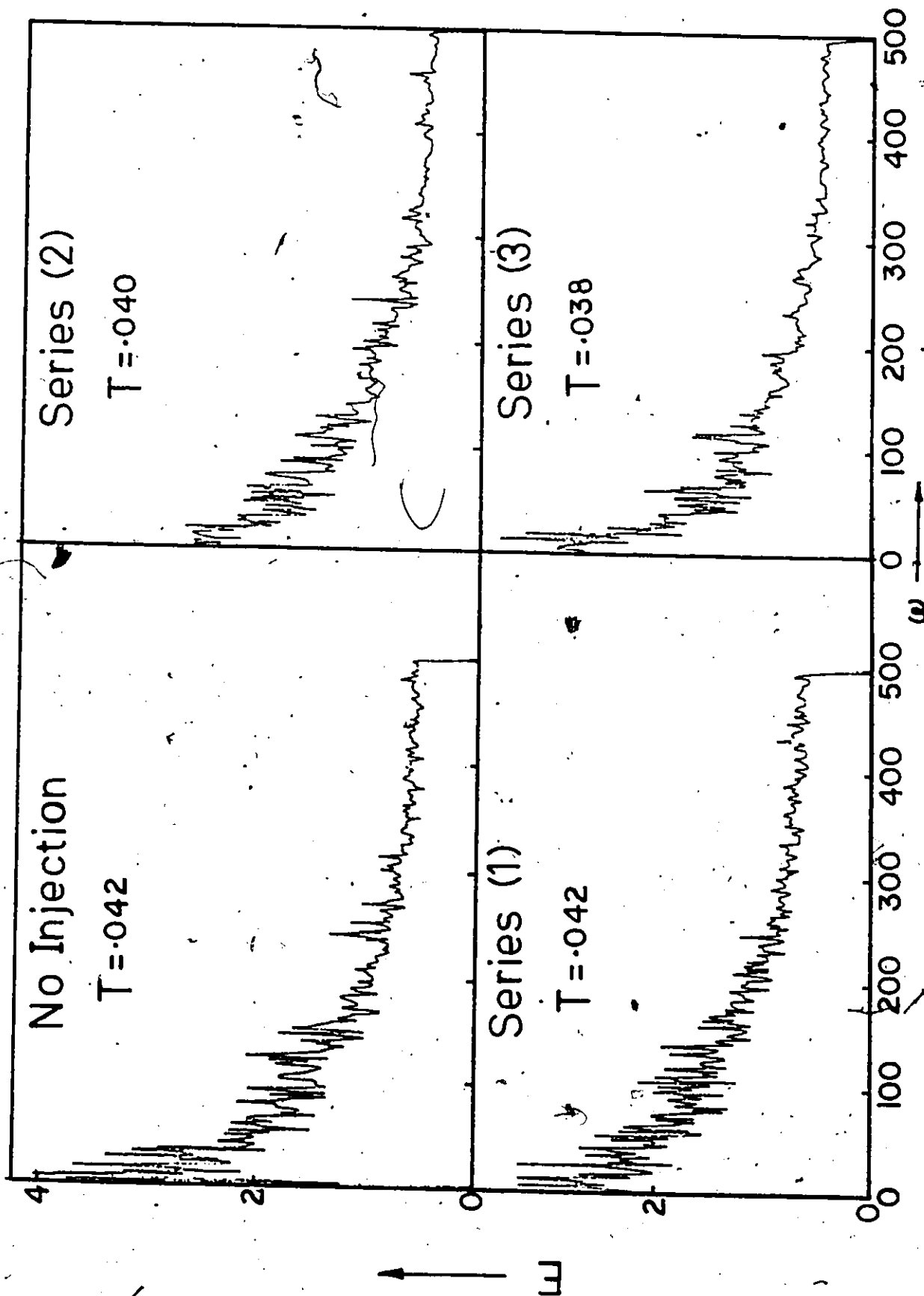


Figure 227. Energy Spectra (Point Source Injection - Uniform Flow - Water Injection - $C_i = 100$ w.p.p.m.).

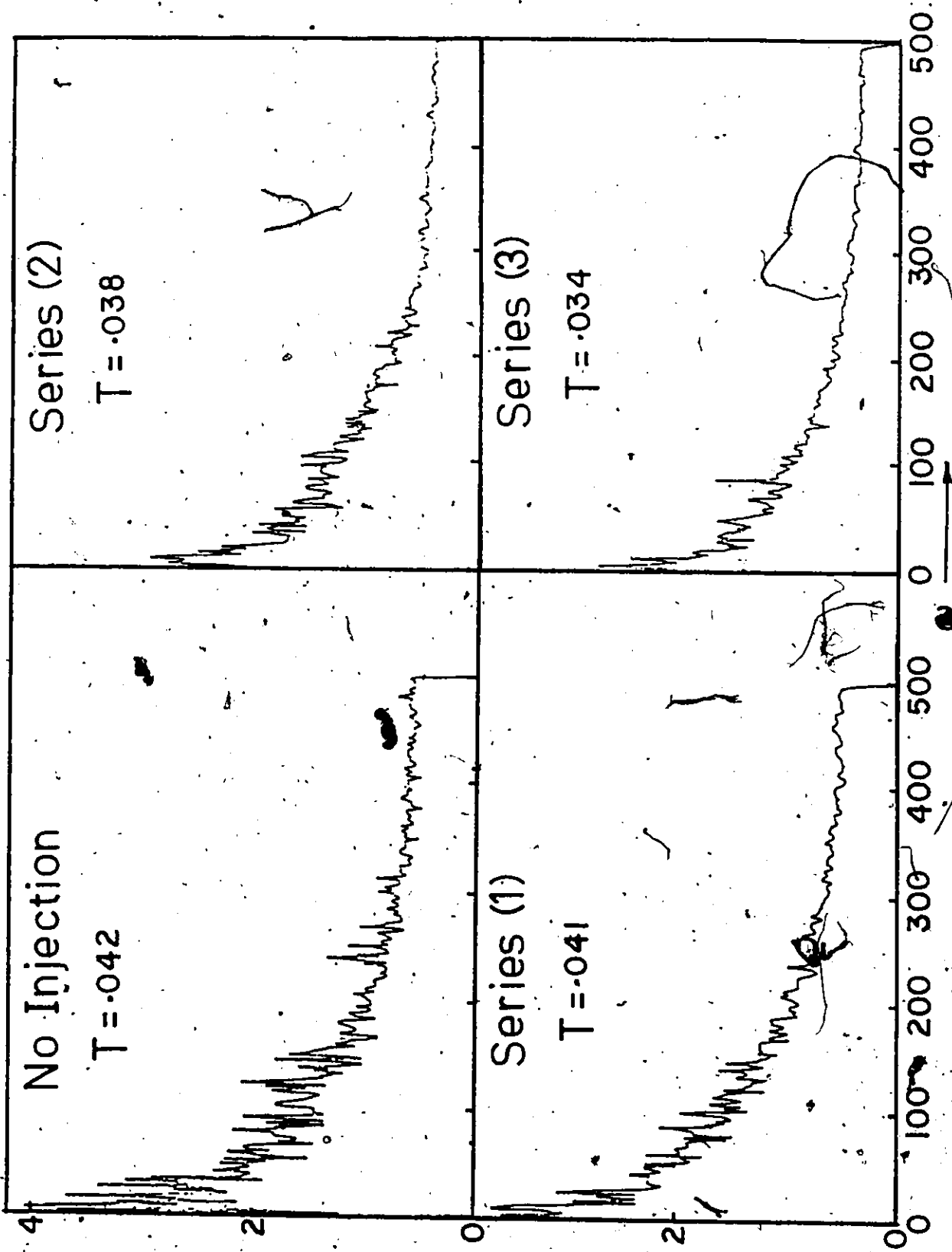


Figure 228. Energy Spectra (Point Source Injection - Uniform Flow - Water Injection - $C_i = 250$ w.p.p.m.).

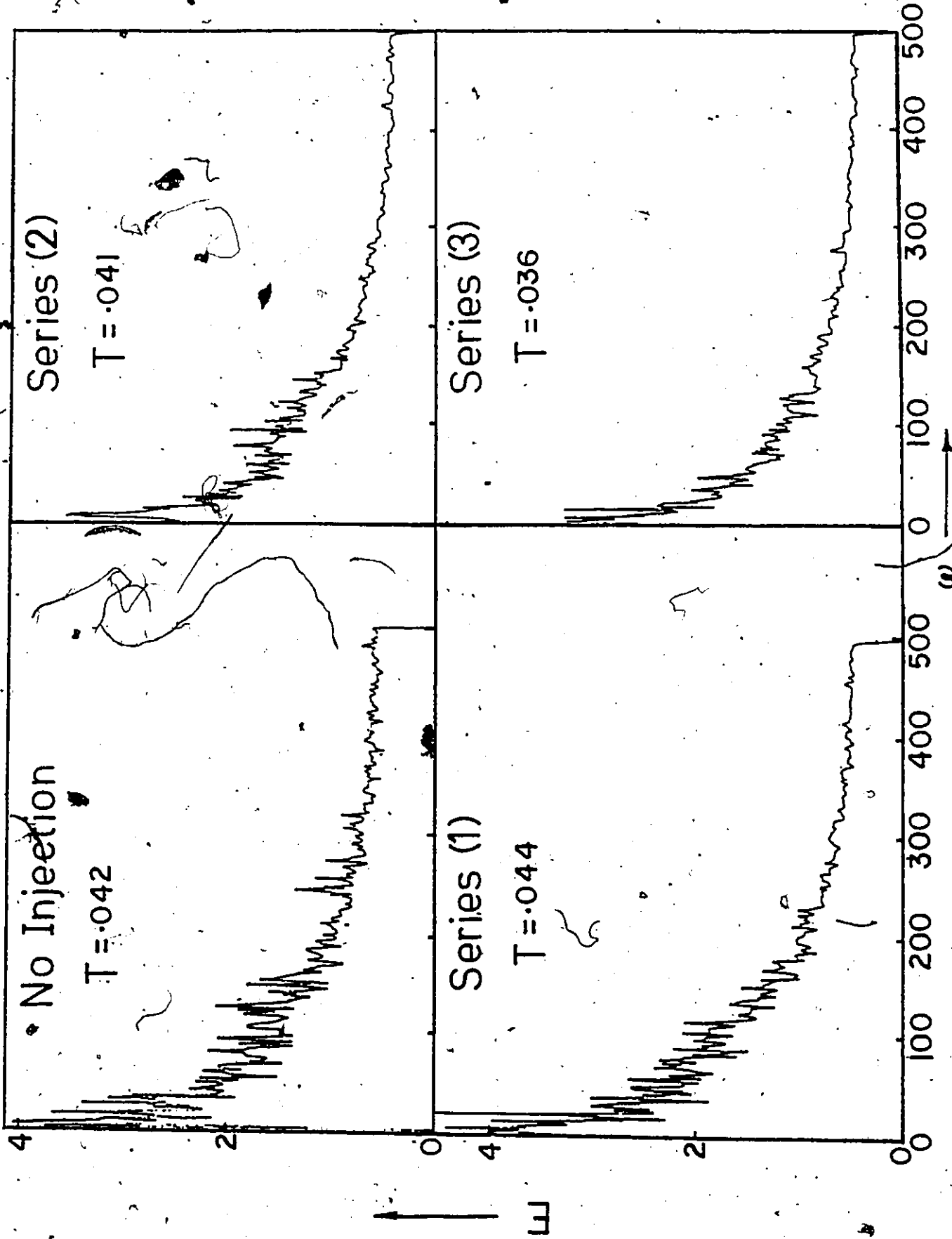


Figure 229. Energy Spectra (Point Source Injection - Uniform Flow - Water Injection - $C_i = 500$ w.p.p.m.).

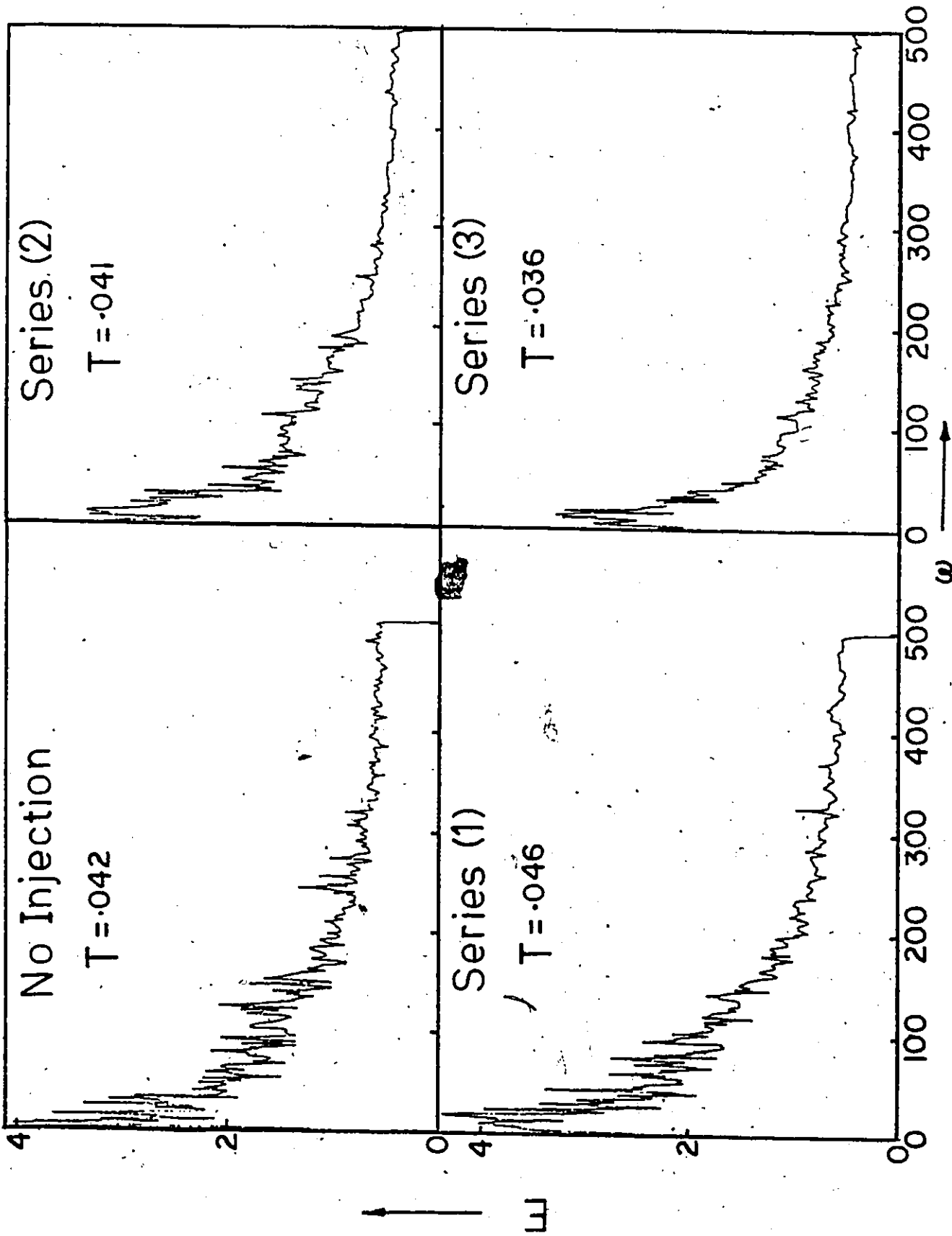


Figure 230. Energy Spectra (Point Source Injection - Uniform Flow - Water Injection - $C_i = 1000$ w.p.p.m.).

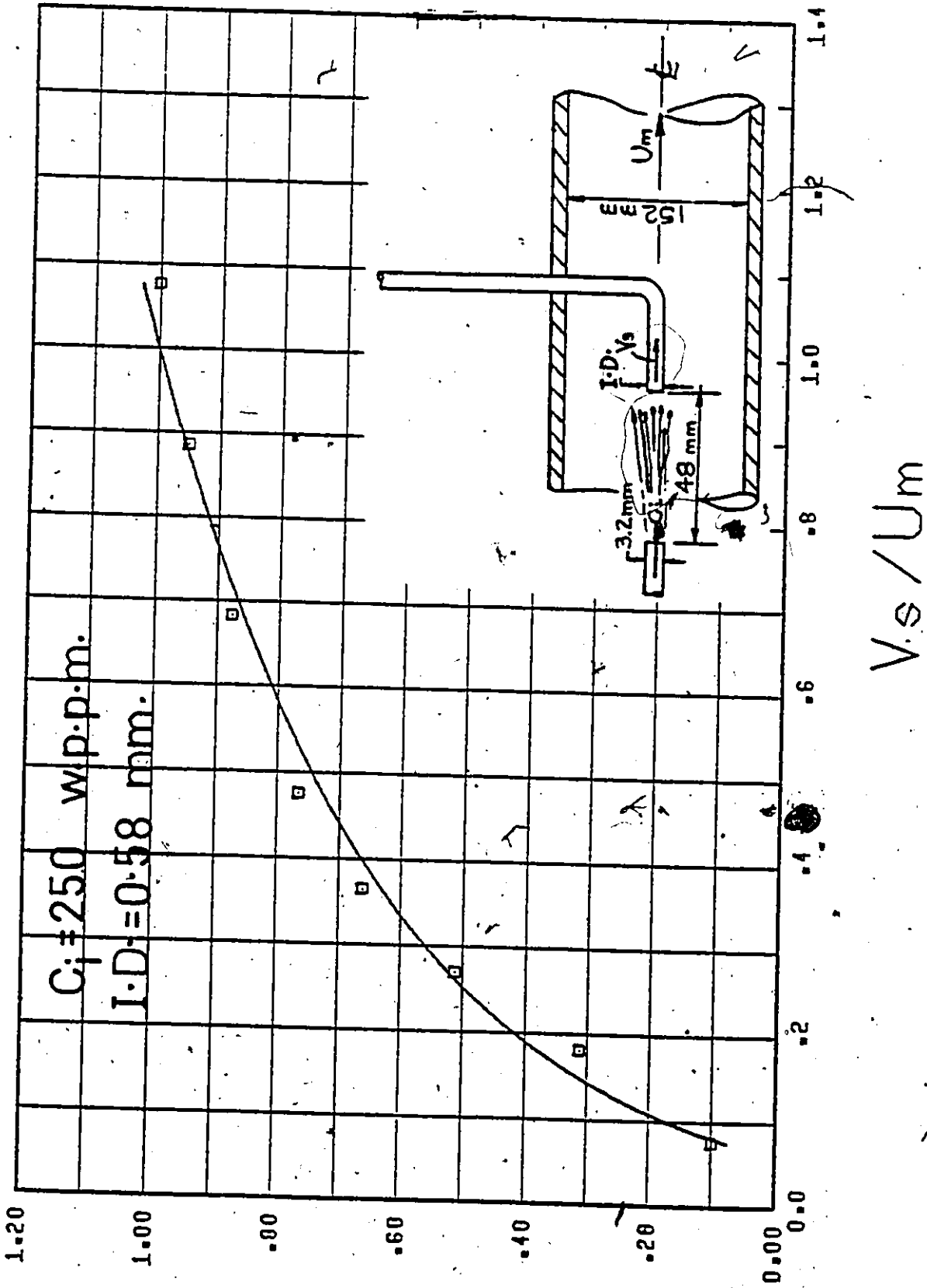
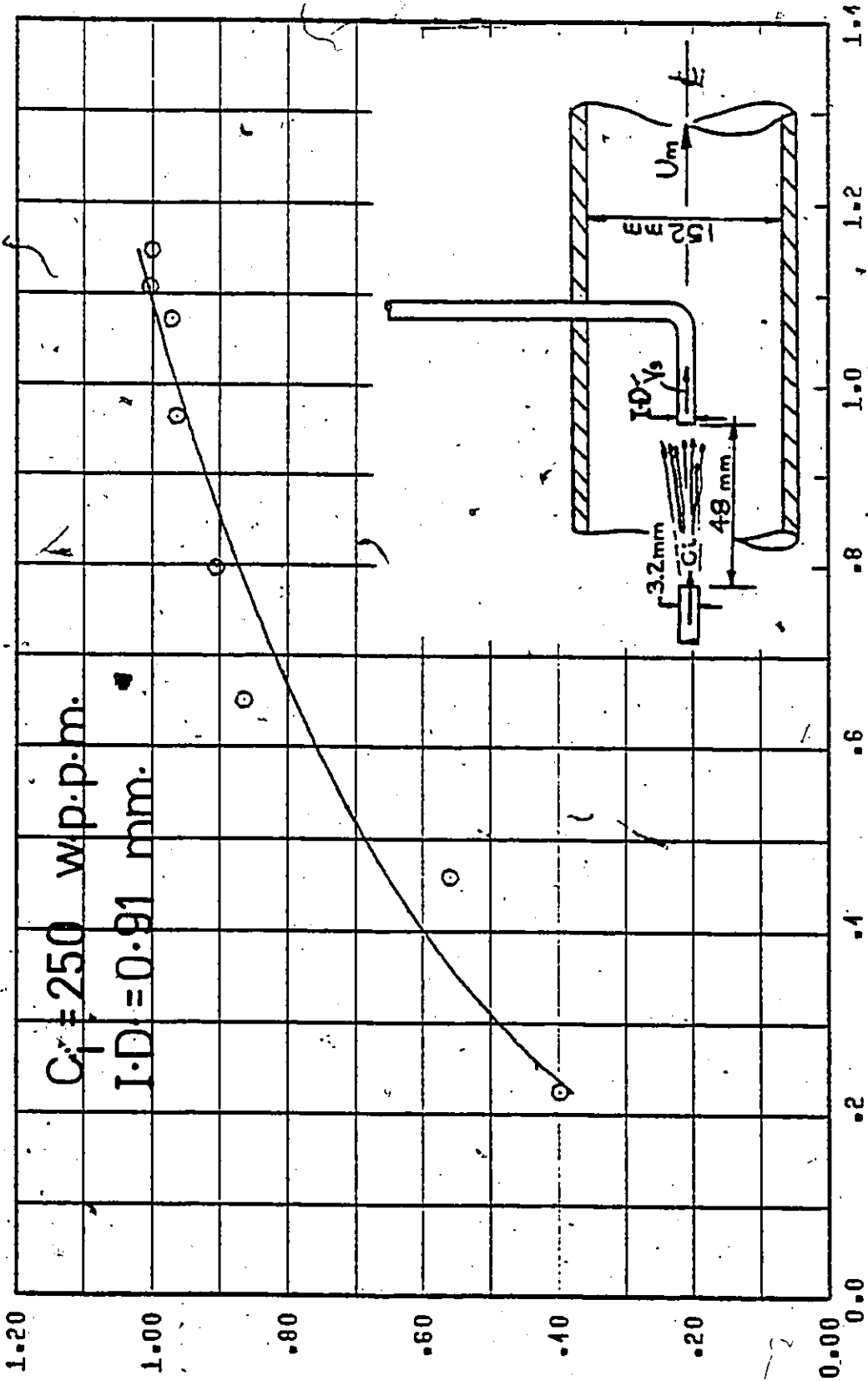


Figure 231. Sampling Rate Effect.



V_s / U_m

Figure 232. Sampling Rate Effect.

C/C₀

APPENDIX I
SAMPLING RATE EFFECT

As mentioned previously in Chapter 5, a series of tests for which the sampling rate was varied at various concentrations and probe diameters were performed. Plots of \bar{C}/\bar{C}_m versus V_s/U_m for both the point source and the line source injection experiments, for all injection concentrations and probe diameters are shown in Figures (A1-A16).

The sampling rate had apparently no effect on the measured concentration, for water, and the data have not been included in the figures. This indicates that the sampling rate is only important for polymer solutions. It can be deduced from Figures (A1-A16) that the measured concentration will gradually increase with sampling rate until it reaches a constant value at which condition the sampling velocity approaches the main stream velocity which is an isokinetic condition.

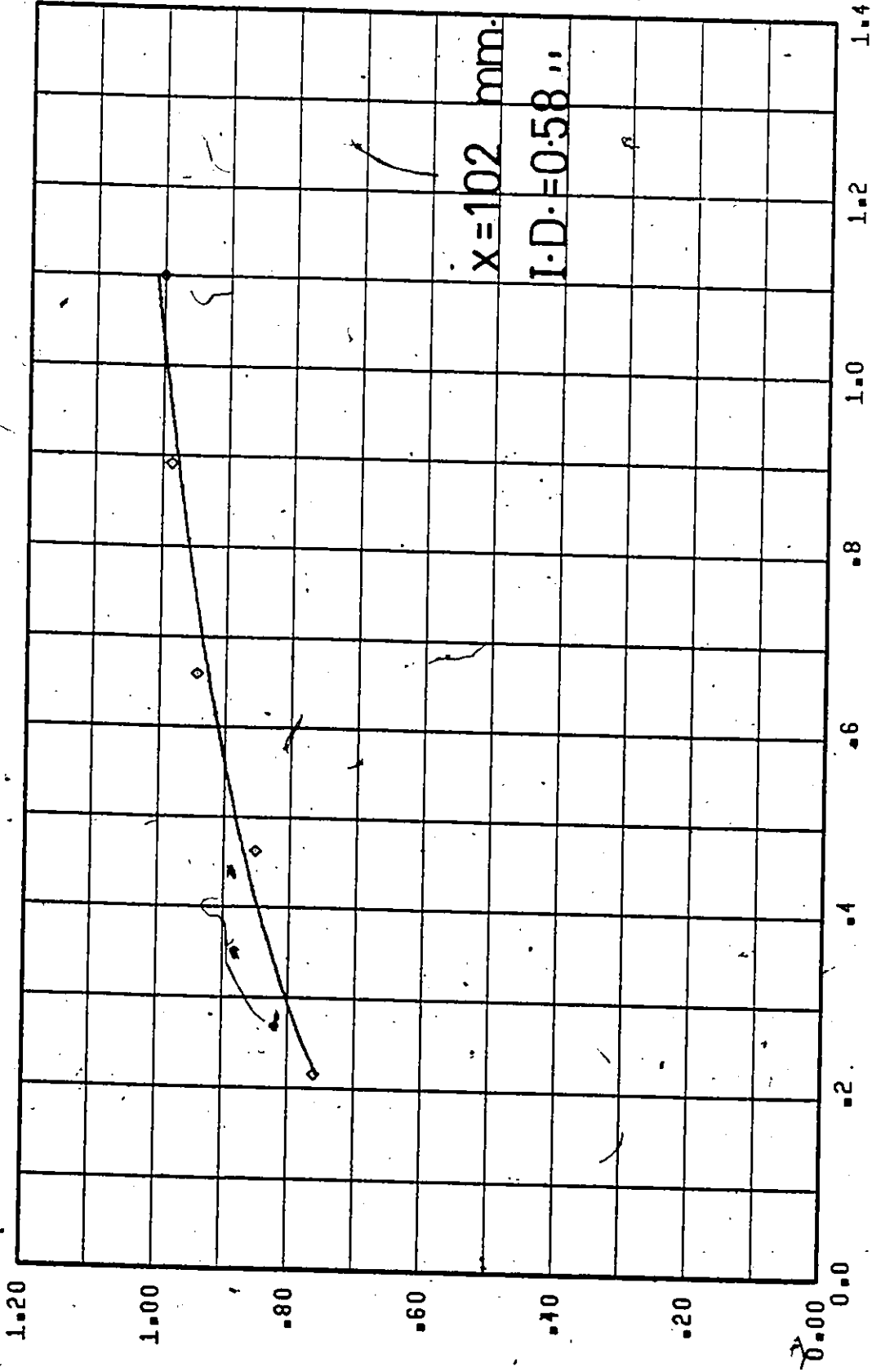
This phenomenon can be attributed to the fact that a polymer solution has an extensional or compressional viscosity which is much higher than that of the solvent. In fact the extensional or compressional viscosity is reckoned to be as much as 4×10^3 to 8×10^3 times the magnitude of the solvent viscosity, as indicated by Balakrishnan and Gordon [43]. This high compressional viscosity would require a relatively

high suction, which increases with the solution concentration, at the probe inlet in order to collect samples of the polymer solution. This lead to tunnelling or sucking of the low concentration solution from the sides rather than drawing in the higher concentration solution, which is normally on the probe center line, when the concentration in the flow field is heterogeneous, and would be a reason for discrepancies between observed experimental data. The effect of increasing the probe on this phenomenon, is to reduce the suction needed the samples. This very interesting phenomenon apparently not been discussed before.

Uebler [44] also observed a similar phenomena (Uebler effect) to that described above. He performed a series of tests for the flow of water and polymer solution in a sudden contraction in a tube. He used photographs of a bubble, introduced into water along the center of a tube having a sudden contraction, to show the forward motion and acceleration of the bubble as it moved into the smaller duct. When using macromolecular fluids if the bubbles were too big, of the order of $1/6$ to $1/8$ of the small tube diameter, those moving along the center line came to a sudden stop at the entrance to the small tube. A stationary bubble could remain in that position for a minute or more before proceeding down the tube. This was called the Uebler effect. Away from the center line the bubbles were not held back and would move past the stationary bubble.

The Uebler effect indicates that the polymer solution will affect the flow pattern in a sudden contraction in a tube, which substantiates the argument given for the phenomenon of the sampling rate effect.

This phenomenon is of interest and should be taken into consideration, for example, when using sampling techniques to obtain concentration profiles in heterogeneous polymer solutions.



V_s/U_m

Figure (A.1) Sampling Rate Effect (Line Source Injection - $C_i = 250 \text{ w.p.p.m.}$).

C/C_m

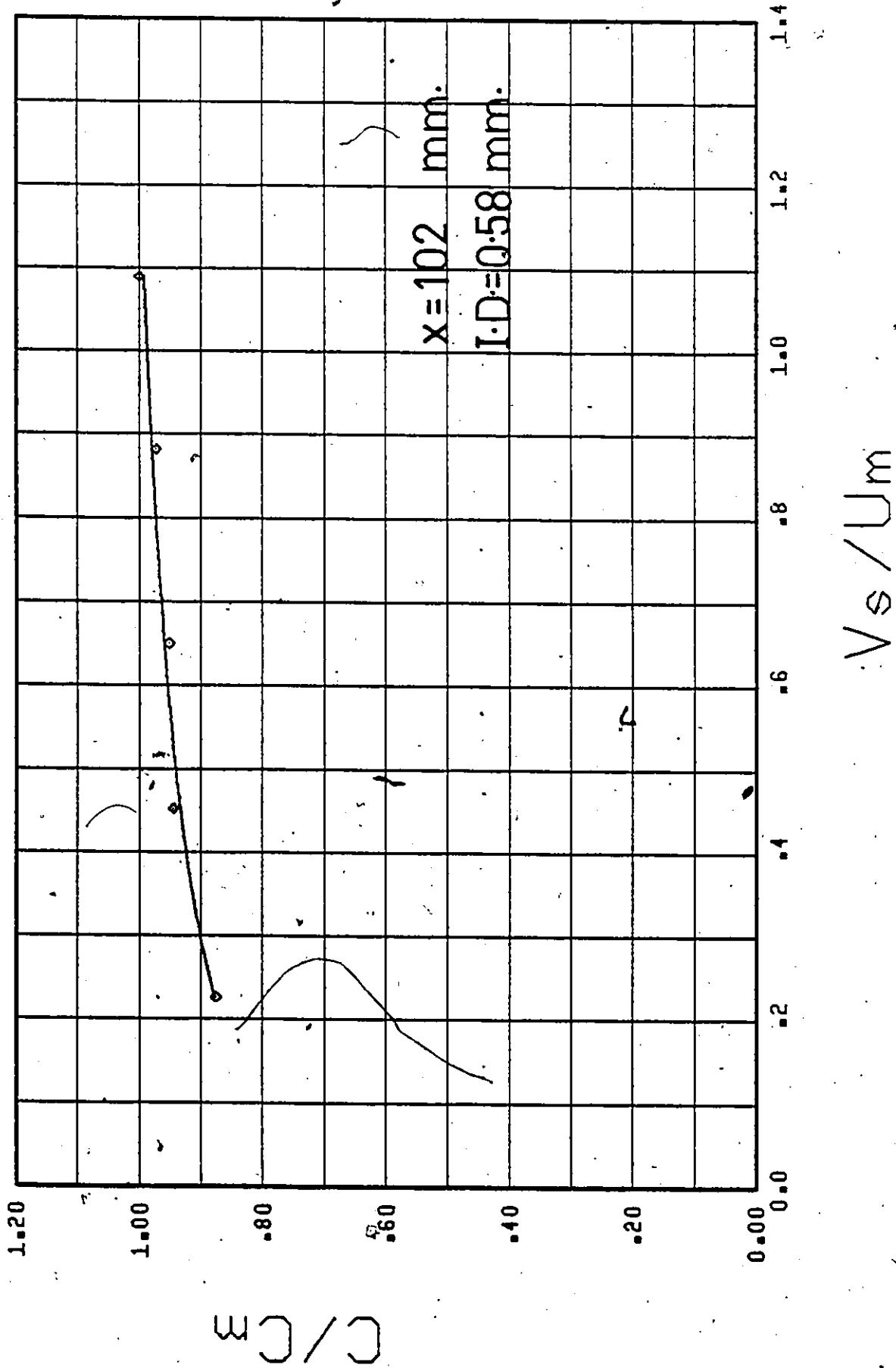
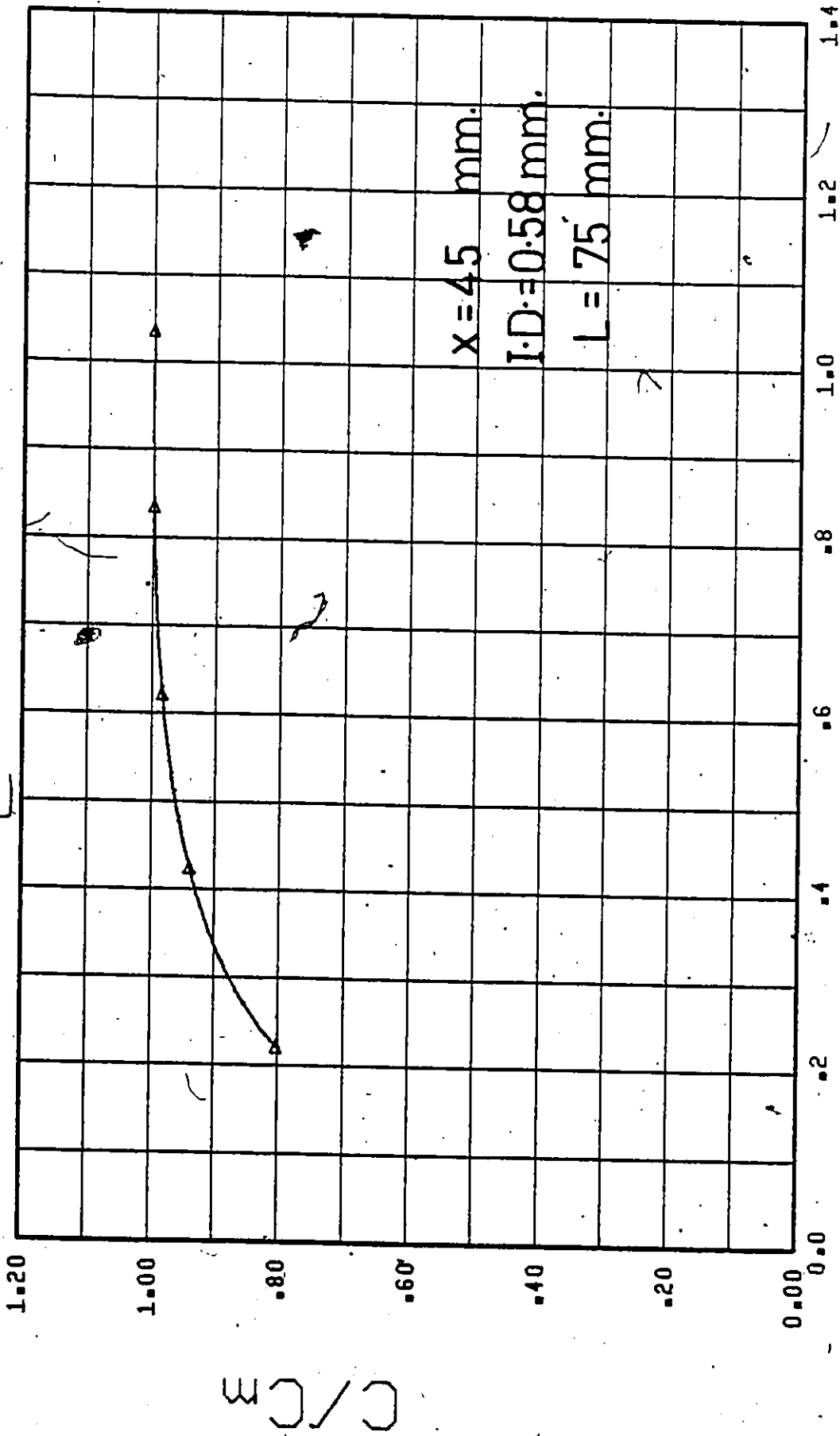


Figure (A.2) Sampling Rate Effect (Line Source Injection - $C_i = 100 \text{ w.p.p.m.}$).



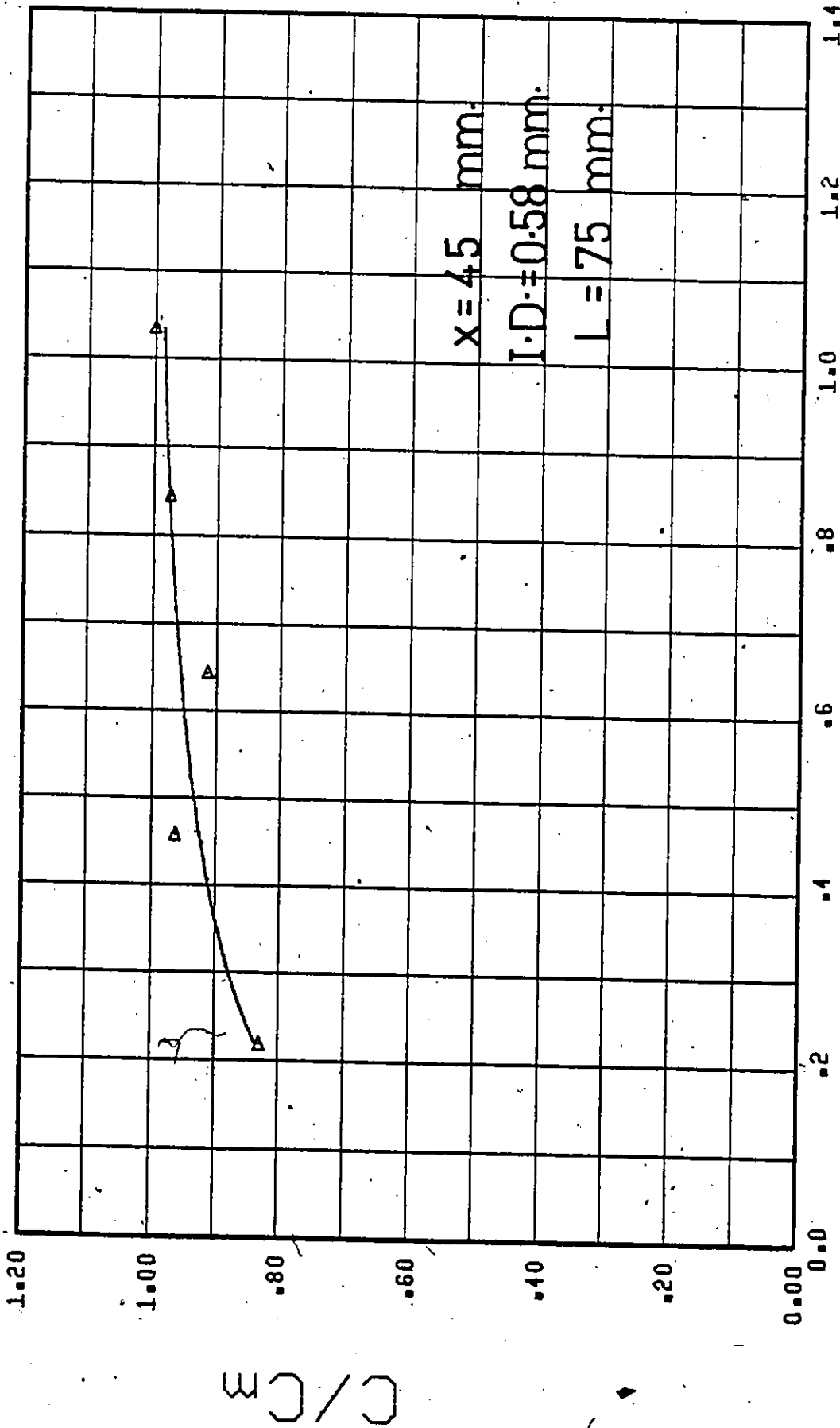
$X = 45 \text{ mm.}$

$I.D. = 0.58 \text{ mm.}$

$L = 75 \text{ mm.}$

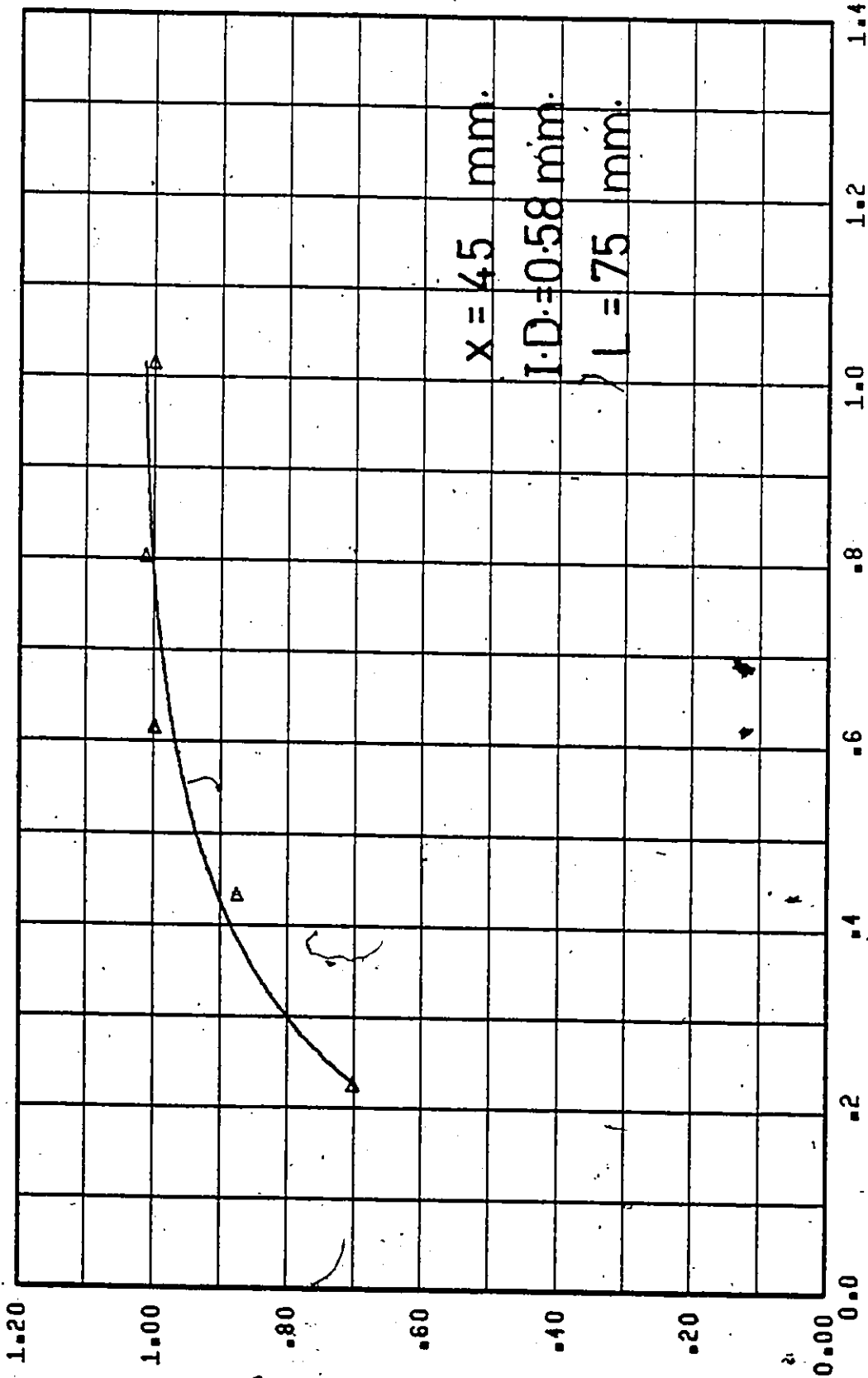
V_s/U_m

Figure (A.3) Sampling Rate Effect (Point Source Injection - Uniform Flow - $C_i = 50 \text{ w.p.p.m.}$).



V_s / U_m

Figure (A.4) Sampling Rate Effect (Point Source Injection - Uniform Flow - $C_i = 100 \text{ w.p.p.m.}$).



V_s / U_m

Figure (A.5) Sampling Rate Effect (Point Source Injection - Uniform Flow - $C_i = 250 \text{ w.p.p.m.}$).

C/C0

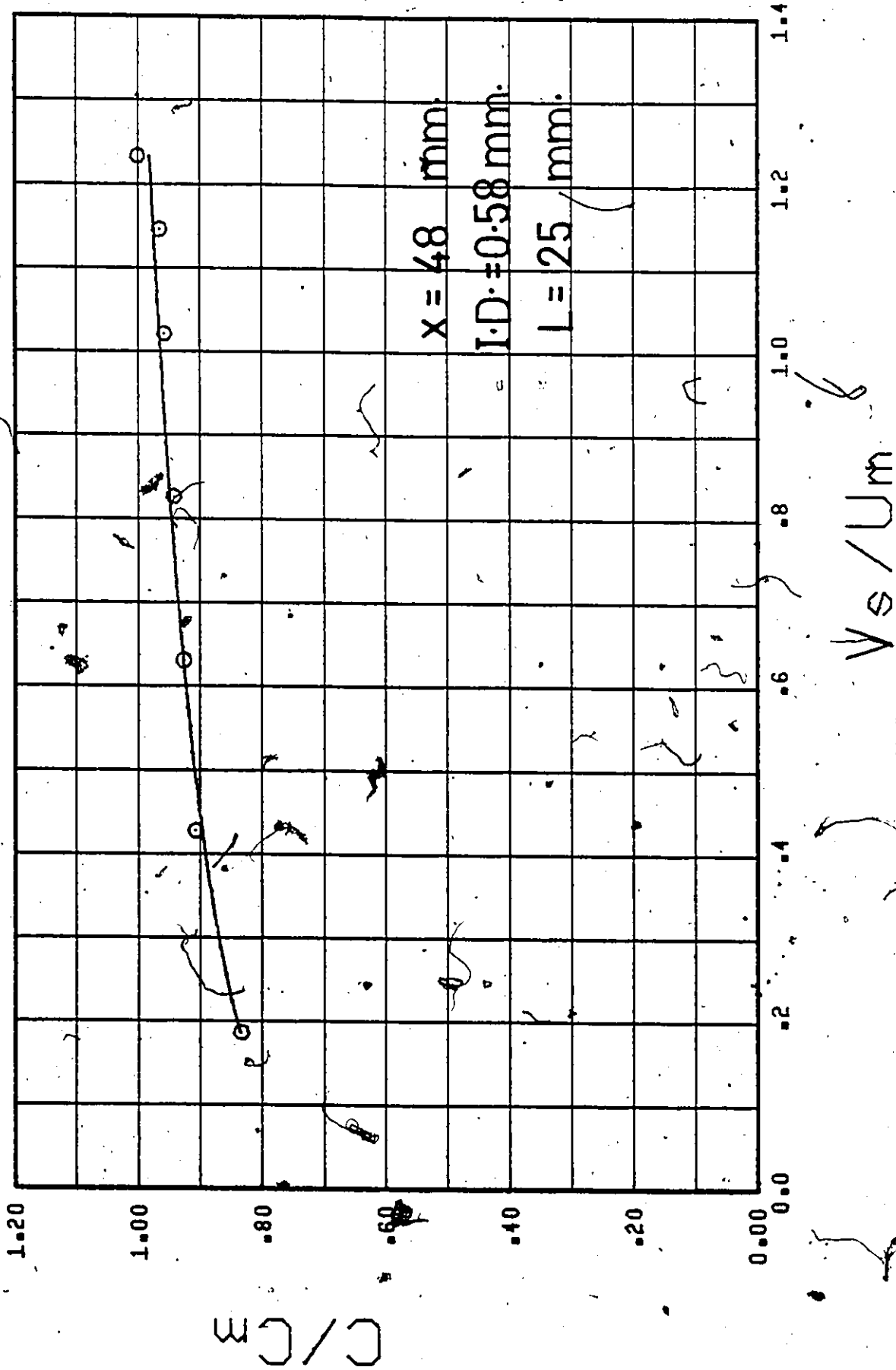
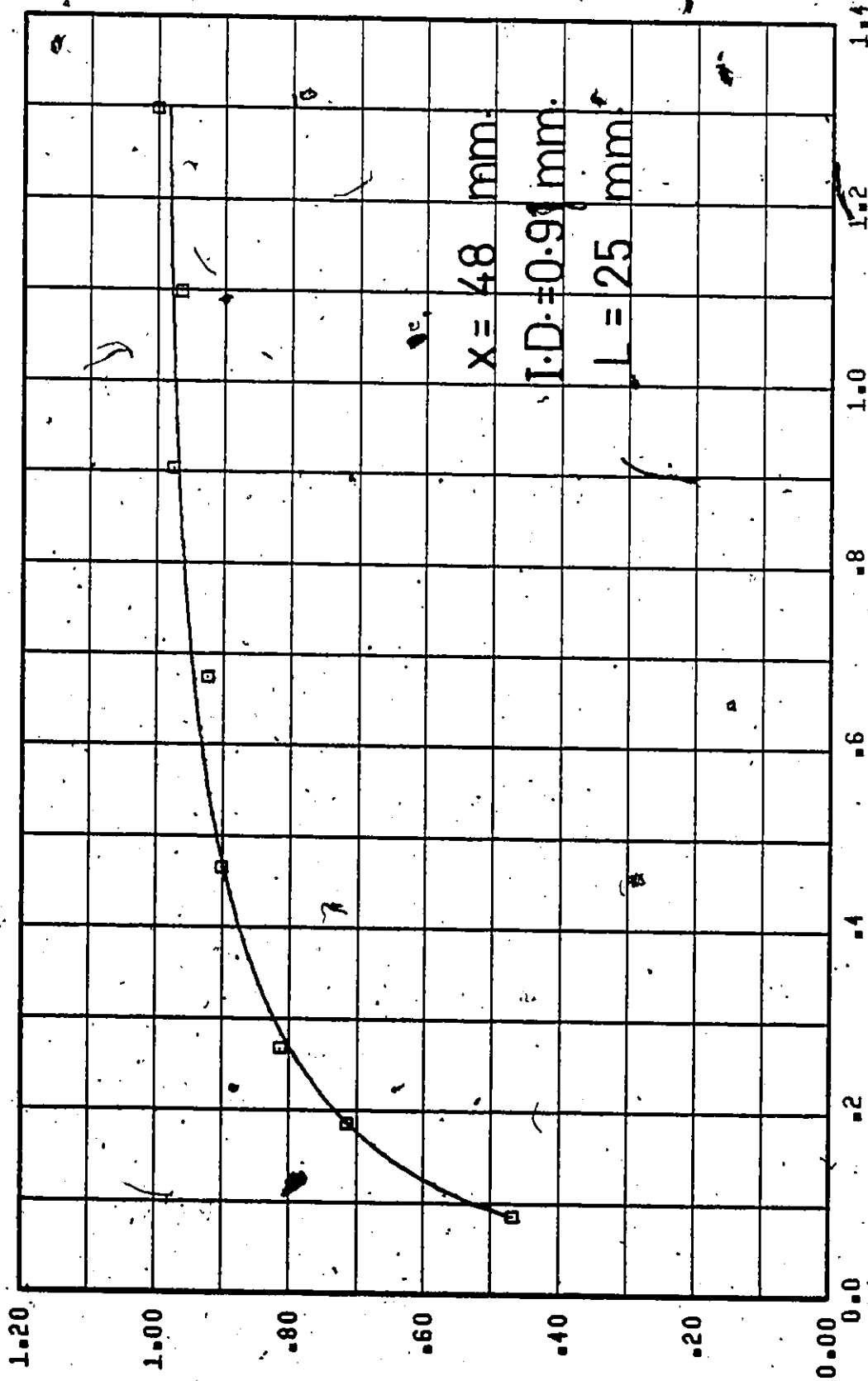


Figure (A.6) Sampling Rate Effect (Point Source Injection - Fully Developed Flow - $C_i = 50 \text{ w.p.p.m.}$).



V_s/U_m

Figure (A.7) Sampling Rate Effect (Point Source Injection - Fully Developed Flow - $C_i = 50 \text{ w.p.p.m.}$).

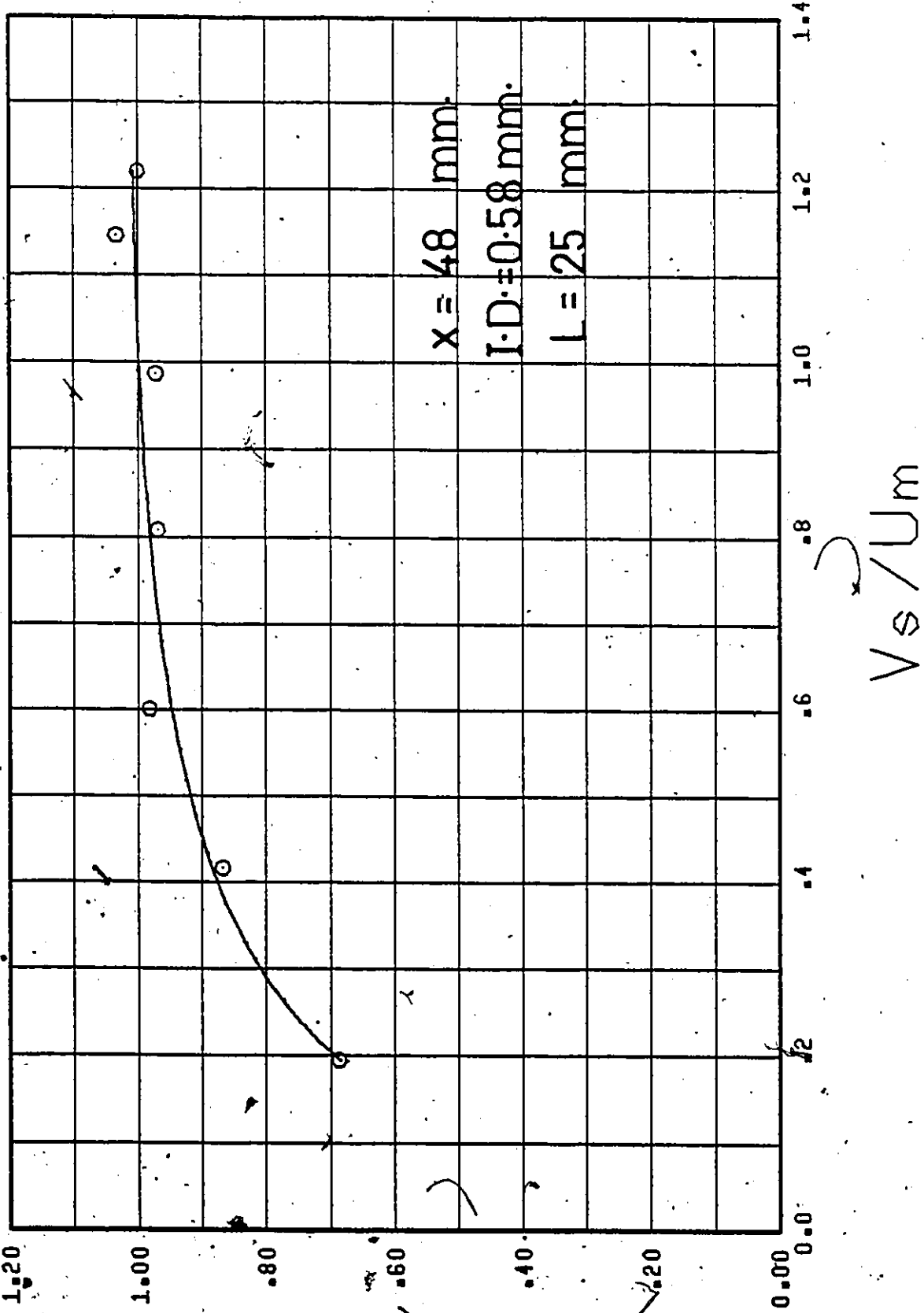


Figure (A.8) Sampling Rate Effect (Point Source Injection - Fully Developed Flow - $C_i = 100 \text{ w.p.p.m.}$).

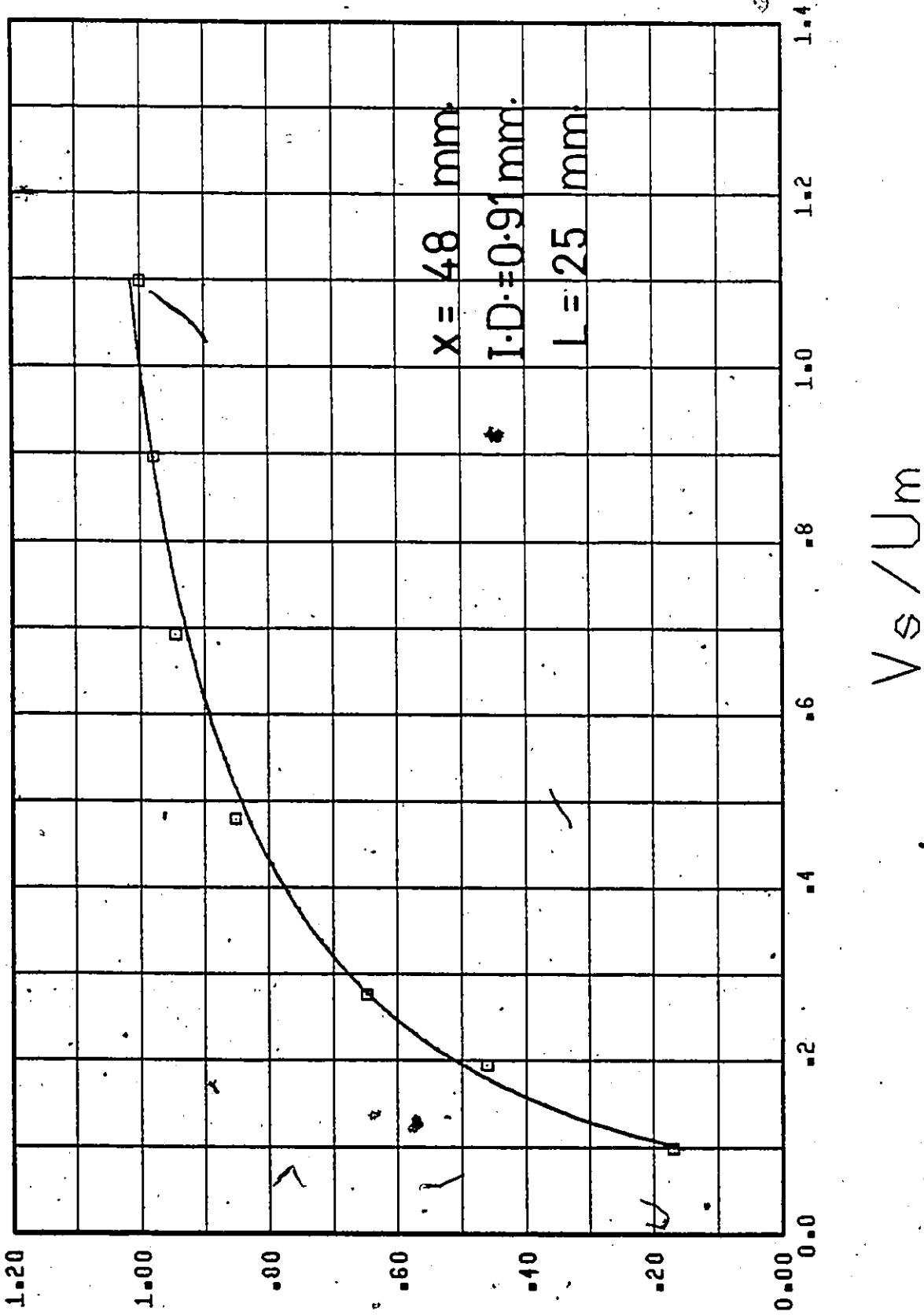


Figure (A.9) Sampling Rate Effect (Point Source Injection - Fully Developed Flow - $C_i = 100$ w.p.p.m.).

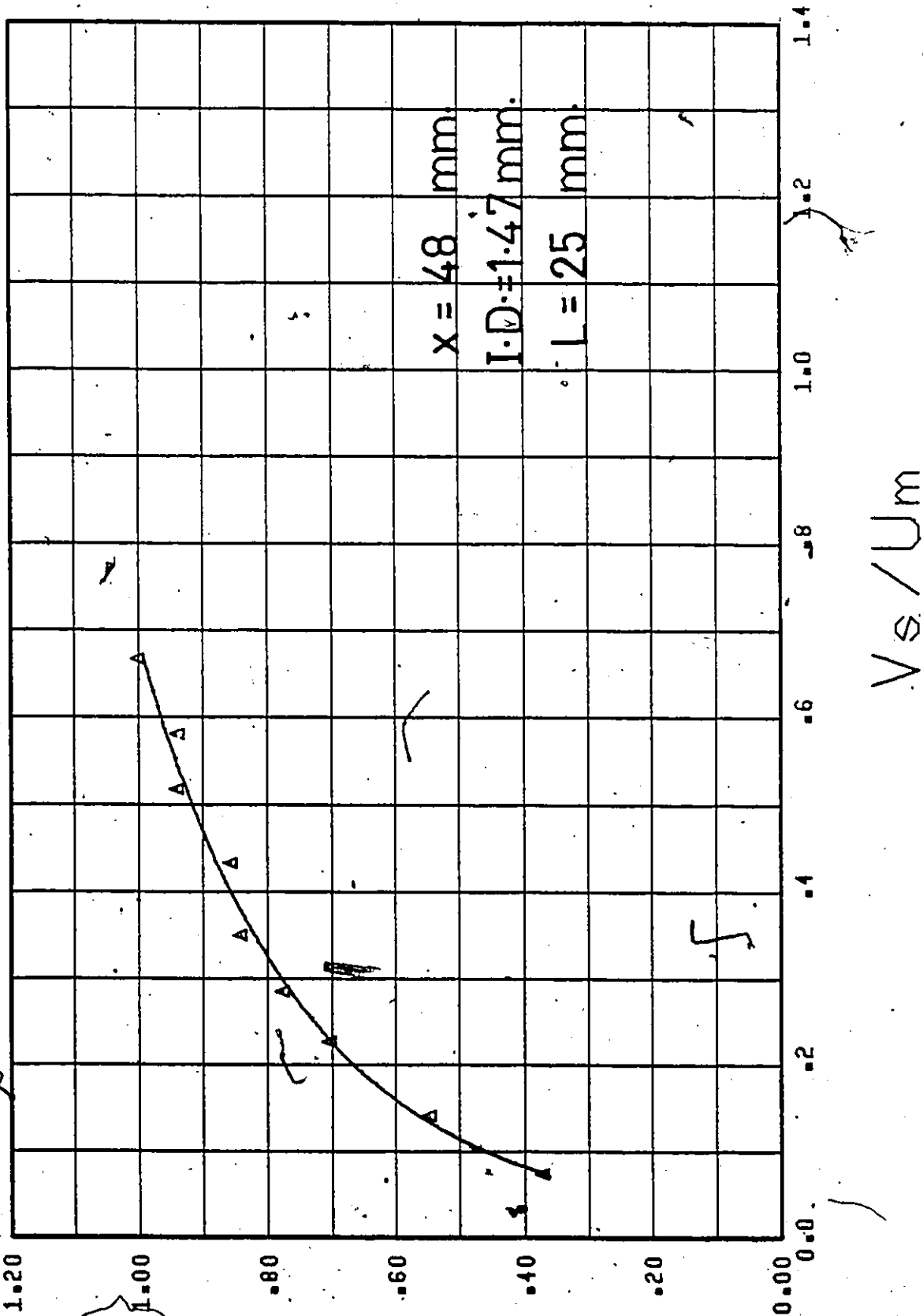
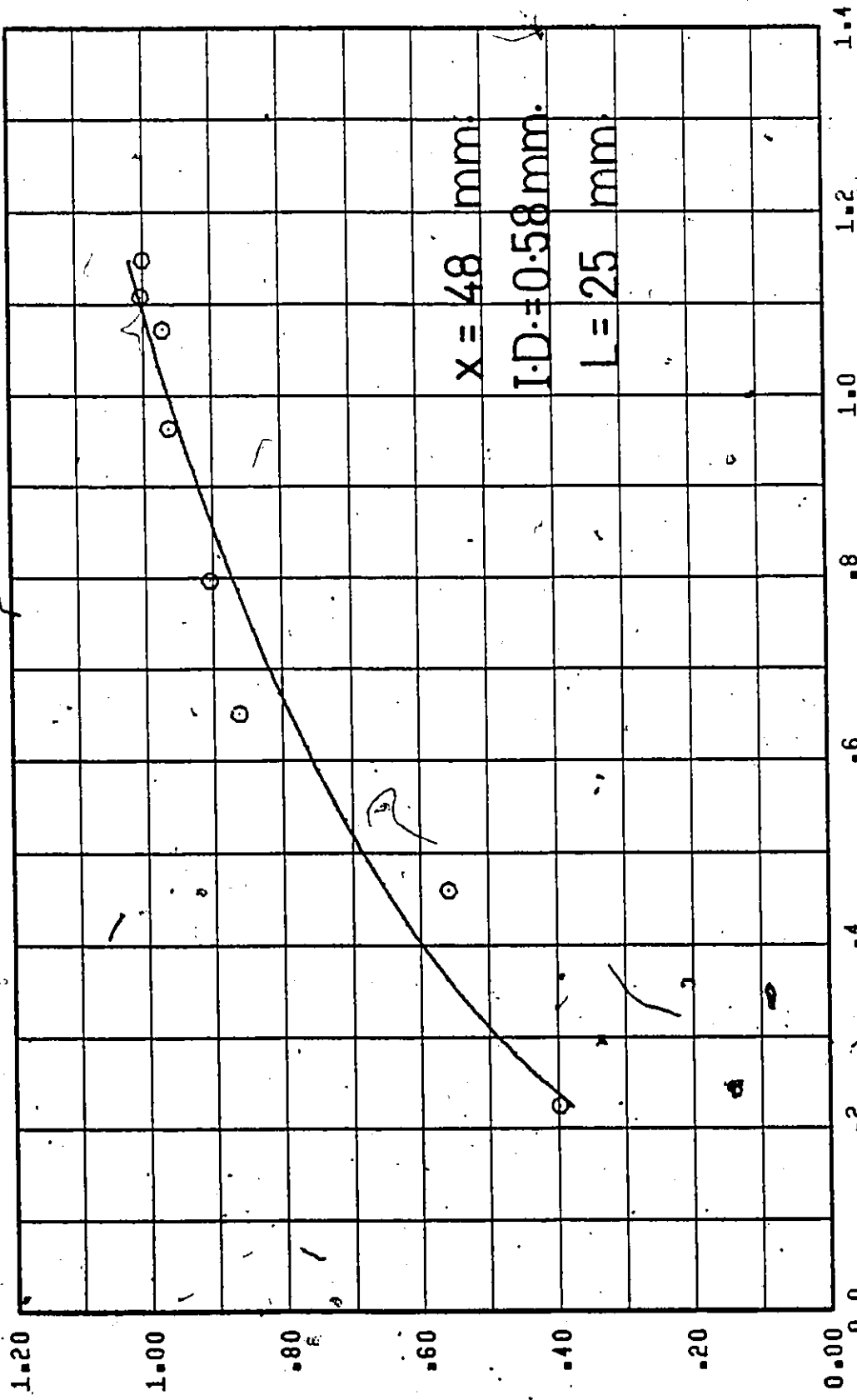


Figure (A.10) Sampling Rate Effect (Point Source Injection - Fully Developed Flow - $C_i = 100 \text{ w.p.p.m.}$).



C/C_i

6



V_s / U_m

Figure (A.11) Sampling Rate Effect (Point Source Injection - Fully Developed Flow - $C_i = 250 \text{ w.p.p.m.}$).

C / C_i

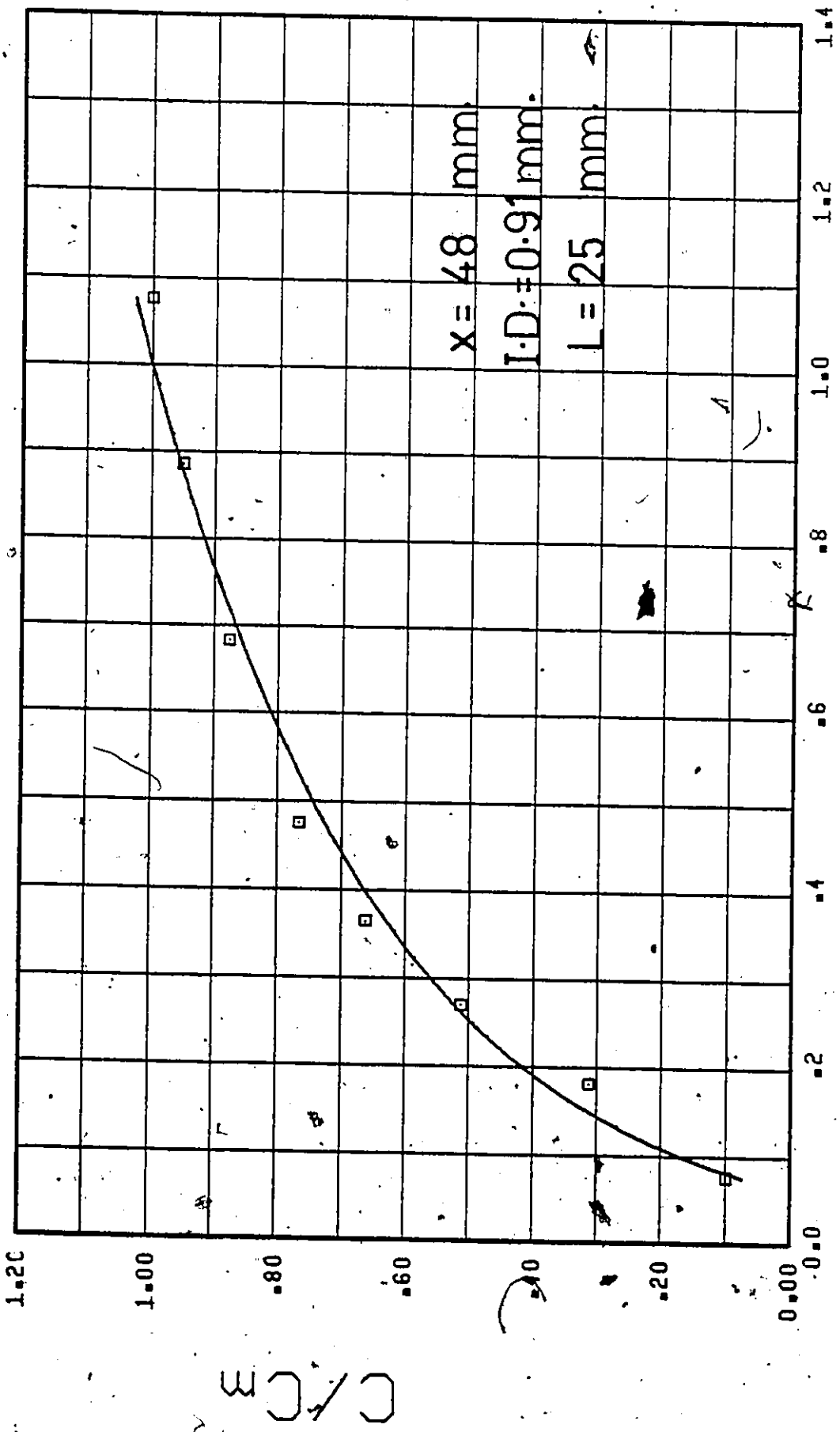
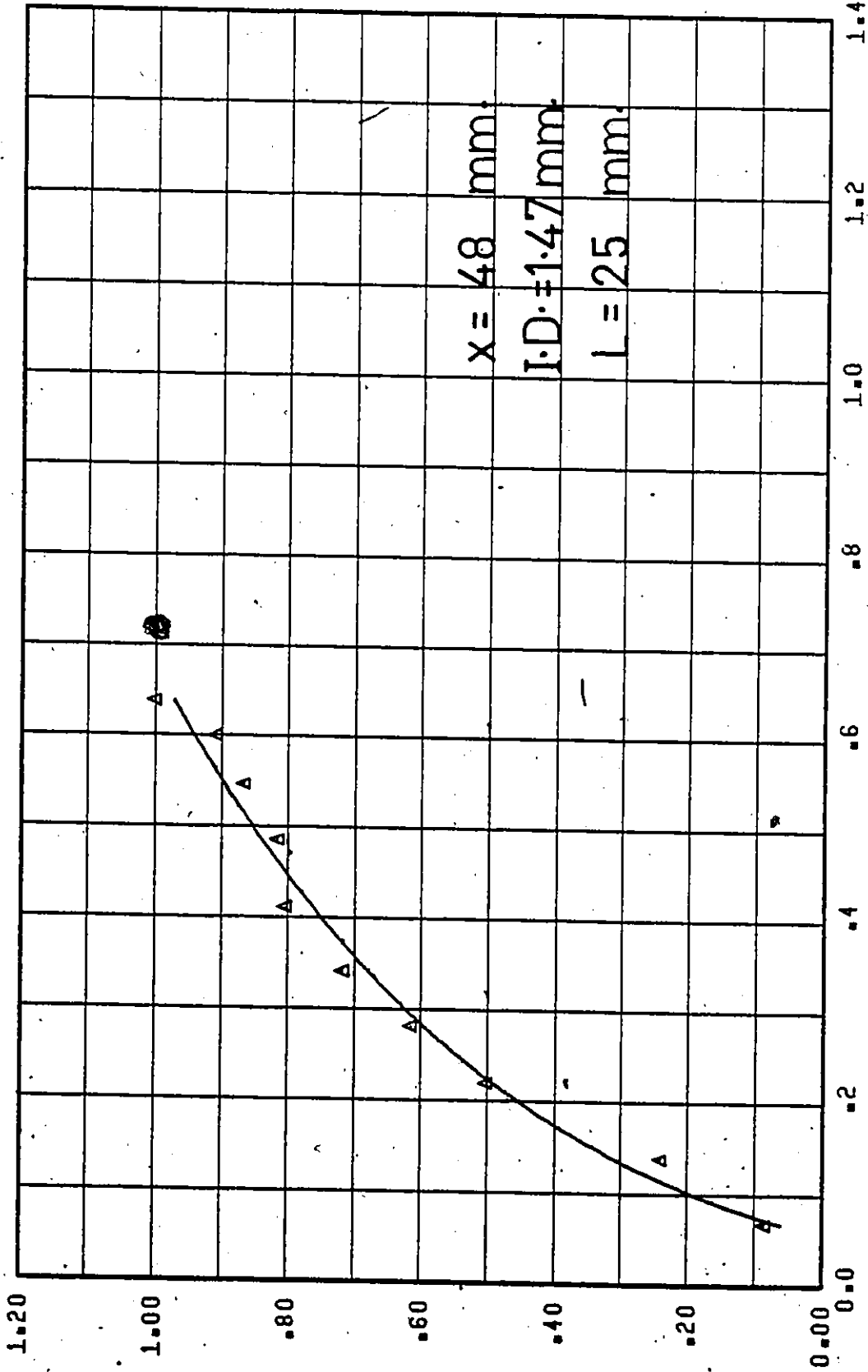


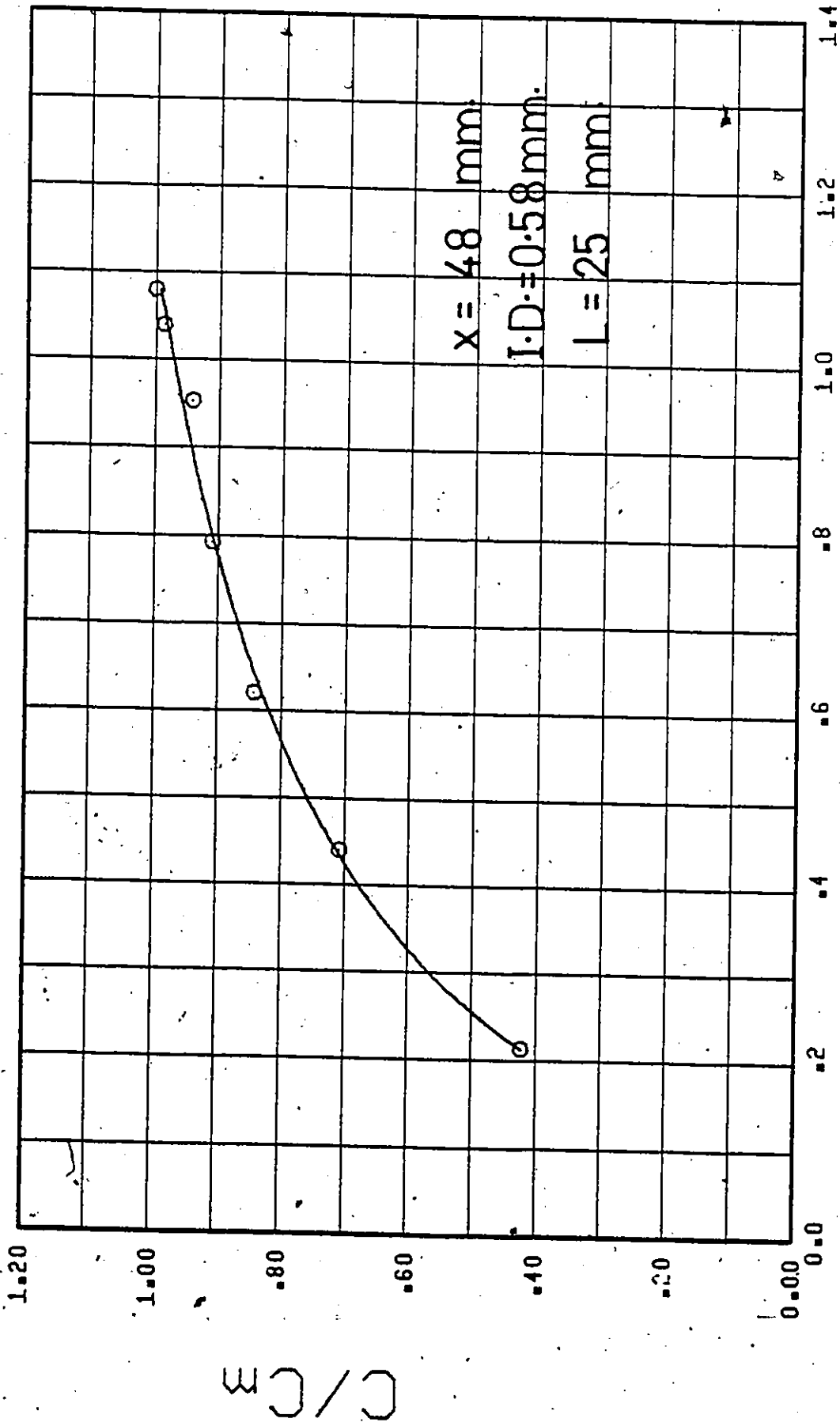
Figure (A.12) Sampling Rate Effect (Point Source Injection - Fully Developed Flow - $C_i = 250 \text{ w.p.p.m.}$).



V_s / U_m

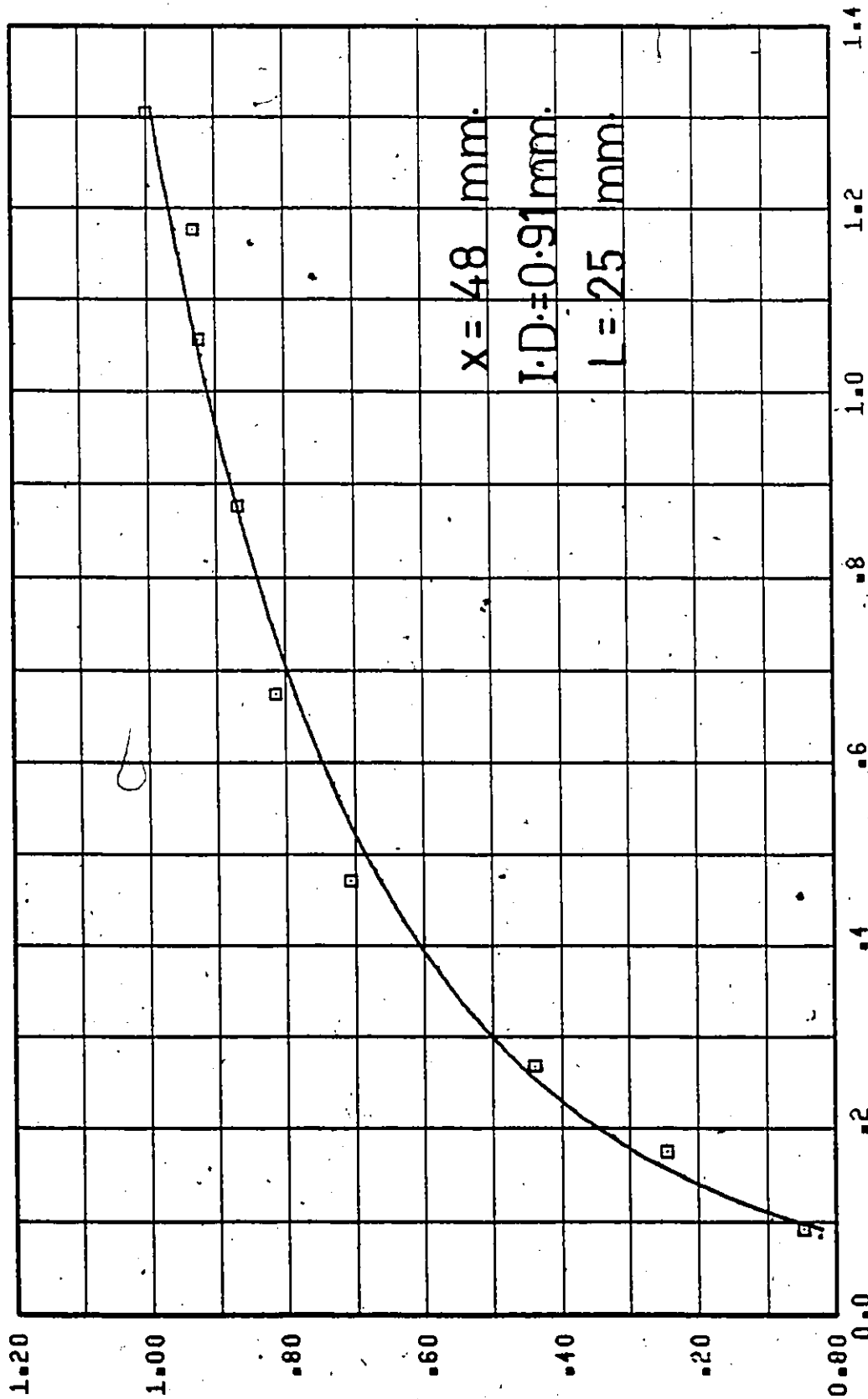
Figure (A.13) Sampling Rate Effect (Point Source Injection - Fully Developed Flow - $C_i = (250 \text{ w.p.p.m.})$).

C/C_i



V_s / U_m

Figure (A.14) Sampling Rate Effect (Point Source Injection - Fully Developed Flow - $C_i = 500$ w.p.p.m.).



V_s / U_m

Figure (A.15) Sampling Rate Effect (Point Source Injection - Fully Developed Flow - $C_i = 500 \text{ w.p.p.m.}$).

C/Ci

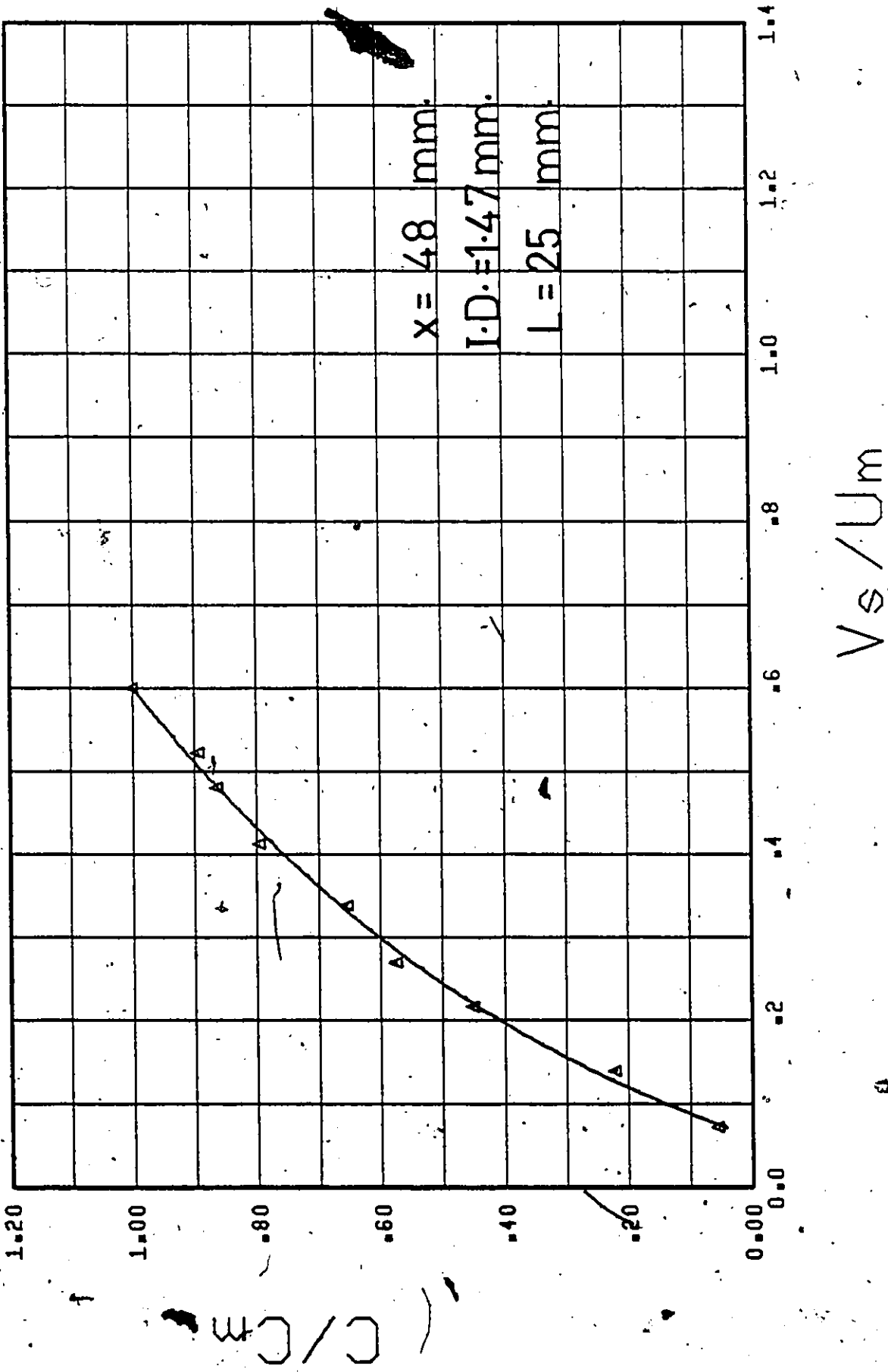


Figure (A.16) Sampling Rate Effect (Point Source
 Injection - Fully Developed Flow -
 $C_i = 500 \text{ w.p.p.m.}$)

APPENDIX II
CALIBRATION CURVES

Calibration curves of the rotameter reading versus injection flow rate for various polymer concentrations are shown in Figure (A17). These data for the curves were obtained by passing a known concentration of polymer solution through the rotometer and volumetrically measuring the flow rate by timing given values of fluid to pass through the meter.

The calibration curve for determining the optimum exciting wave length for Rhodamine WT is shown in Figure (A18). The data for this curve were obtained by applying various exciting wave lengths for the same concentration. The calibration curve for the relation between the concentration and the optical density is shown in Figure (A19) and was obtained by applying the optimum exciting wave length for the known concentration.

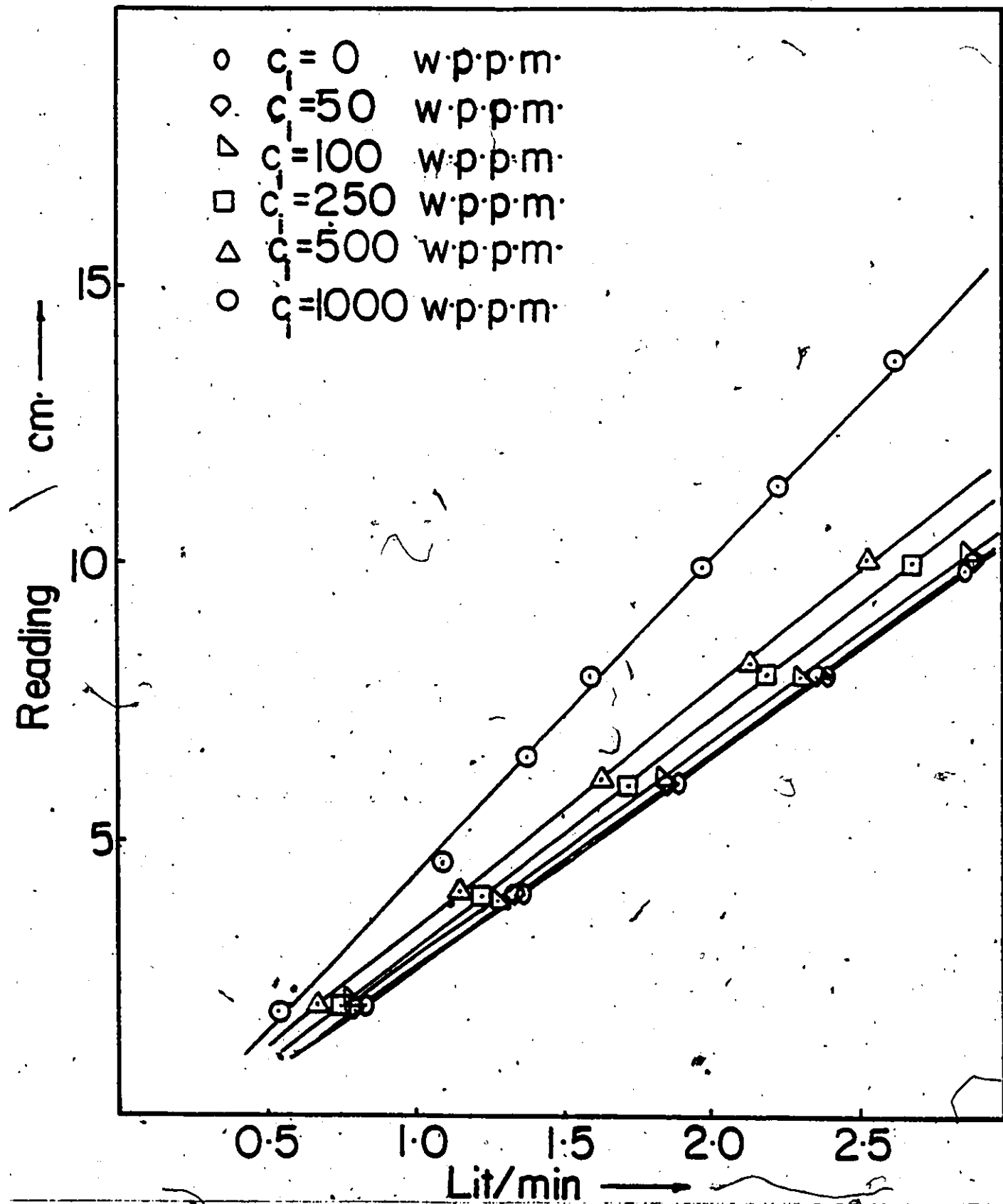


Figure (A.17) Calibration Curve for the Rotometer.

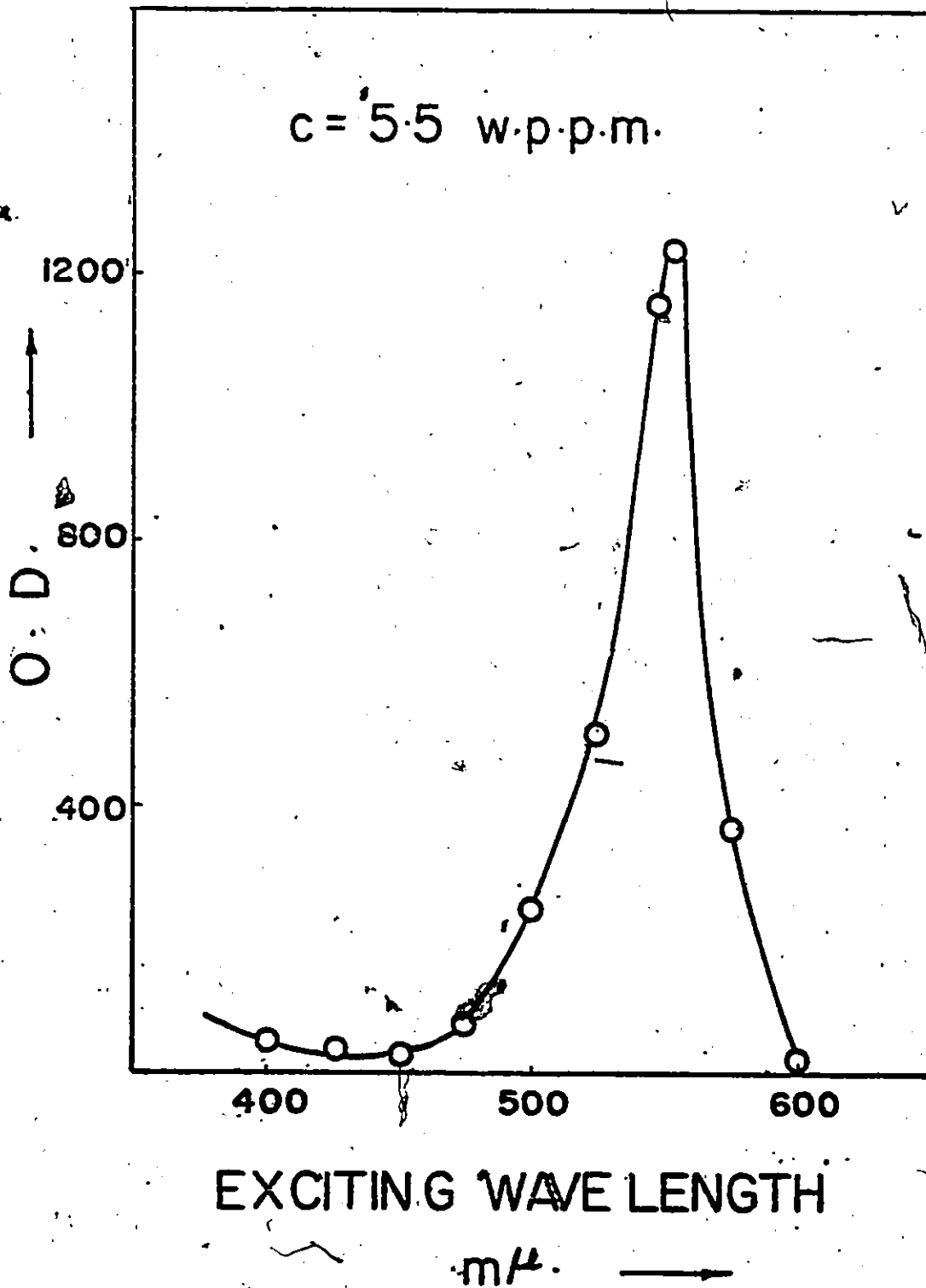


Figure (A.18) Optical Density (O.D.) vs. Exciting Wave Length.

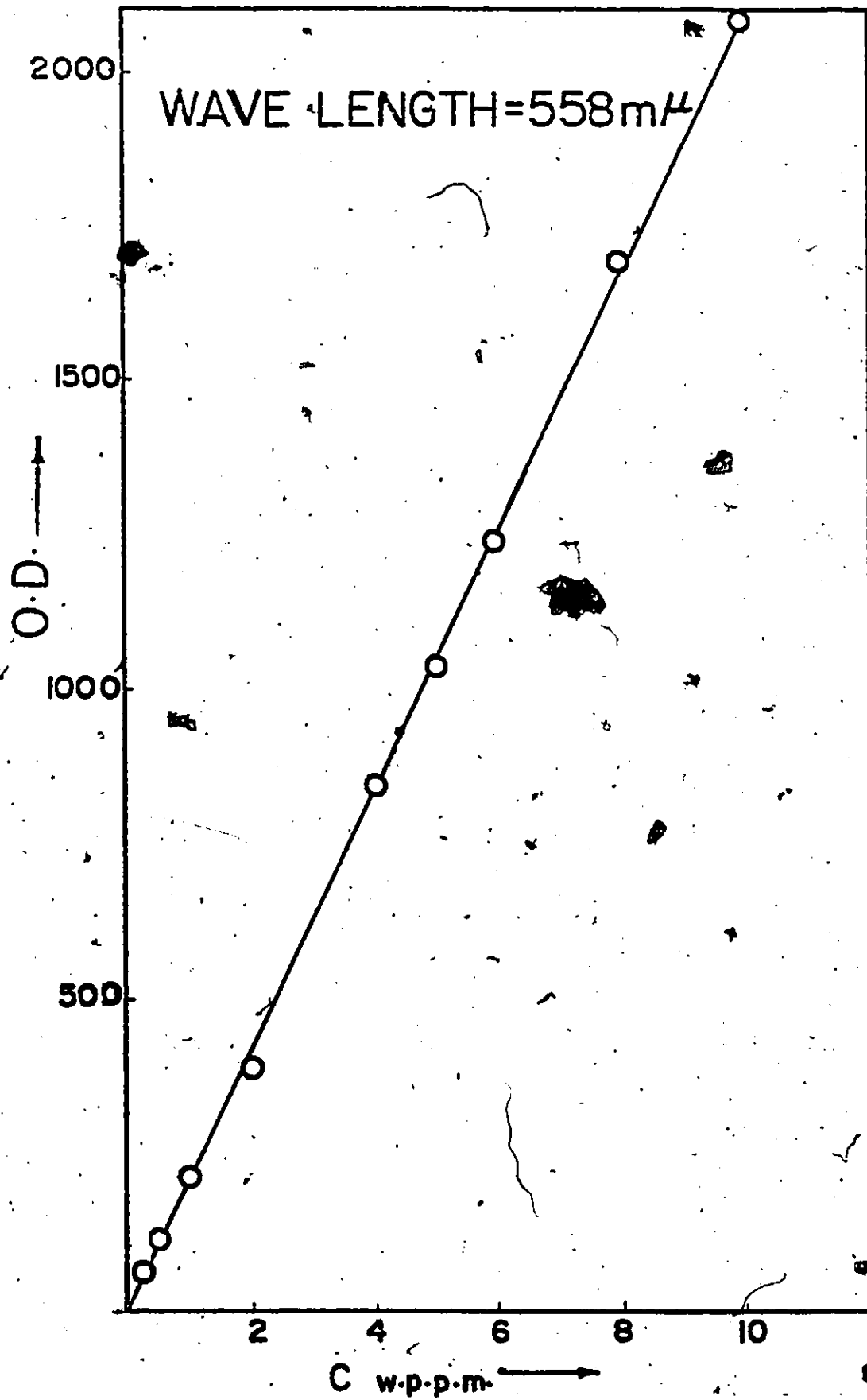


Figure (A.19) Calibration Curve for the Spectrophotometer.

APPENDIX III

DATA TABLES

All the measured experimental data that were obtained, together with the calculated parameters λ , (a) and C_m , are presented in the following tables.

Tables 3 through 71 are for the concentration at various longitudinal (cm) and radial (inches) locations, in terms of optical density (which is directly proportional to the actual concentration) and the parameters λ (inches), (a) and C_m (optical density).

Tables 72 through 77 are for the mean local velocity \bar{U} in volts (which is directly proportional to the actual velocity in m/s.) and the fluctuating velocity component U' (volt) at various radial locations (inches).

Tables 78 through 90 are for the data on sampling rate on the basis of volume (cm^3) collected in a given time (s) for the various injection concentration C_i (optical density) and sampling probe diameters (small diameter (0.58 mm), medium diameter (0.91 mm) and large diameter (1.47 mm)).

(a) Concentration Data

Tables 3 through 71 are for point source injection for both fully developed and uniform flow and also for line source injection for developing flow.

The first four lines present the value of (a) , x , λ

and C_m . The rest of the table presents the concentration versus radius (point source injection) or the concentration versus the height from the wall (line source injection).

(b) Velocity data

Table 72 gives the velocity measurement data obtained using a pitot tube, for the line source injection experiment at three longitudinal locations. The first line in this table present longitudinal location x (cm) and in the rest of the table the first column is the vertical height (inches), the second column is the pressure drop in the manometer (cm) in mercury. The remaining columns present the same parameters for various longitudinal location.

Tables 73 through 77 present the velocity measurements using the laser doppler anemometer at the second sampling locations. In these tables, the first line presents the momentum thickness (inches), the first column presents the vertical height from the wall (inches), the second column presents \bar{U} (volts) and the third column presents U' (volts).

(c) Sampling Rate Effect

Tables 78 through 82 presents sampling rate effect for the fully developed flow experiment with the injection source length $L = 25$ mm. Tables 83 through 87 presents the sampling rate effect for the uniform flow experiment for $L = 75$ mm. Tables 88 through present sampling rate effect for the line source injection experiment. In these tables the first column presents the collected volume (cm^3), second column presents the time (s) required to collect that volume and the third column presents the optical density. The remaining three columns

present the same parameters for the various sampling probe diameters.

 *
 * CONCENTRATION DATA *
 *

POINT SOURCE INJECTION
 FULLY DEVELOPED FLOW
 L = 25.0 MM.

TABLE(3)

INJECTION CONCENTRATION = 0 W.P.P.M.
 INJECTION VELOCITY / MAIN STREAM VELOCITY = .67
 INJECTION OPTICAL DENSITY = 20250
 UPSTREAM CONCENTRATION = 2.0

	2.14		2.02		2.08		2.12		1.98
	97.5		65.7		40.3		19.0		4.8
	0.920		0.685		0.455		0.26		0.125
	64.0		99.0		191.0		581.0		2654
-2.25	3.0	2.0	12.0	-1.25	19.0	0.6	35.0	-0.40	40.0
-1.75	4.0	1.5	16.0	-1.00	26.0	0.5	55.0	-0.3	61.0
-1.25	23.0	1.0	33.0	-0.75	39.0	0.4	104.0	-0.2	496.0
-0.90	39.0	0.7	58.0	-0.5	103.0	0.3	203.0	-0.15	1267.0
-0.60	58.0	0.4	89.0	-0.3	166.0	0.2	350.0	-0.10	2077.0
-0.30	71.0	0.2	107.0	-0.15	209.0	0.1	486.0	-0.05	2700.0
0.00	68.0	0.0	113.0	0.00	210.0	0.00	598.0	-0.00	2610.0
0.30	57.0	-0.2	104.0	0.15	193.0	-0.1	610.0	0.05	2151.0
0.60	48.0	-0.4	87.0	0.30	151.0	-0.2	502.0	0.10	1397.0
0.90	37.0	-0.7	52.0	0.50	92.0	-0.3	320.0	0.15	799.0
1.25	19.0	-1.0	30.0	0.75	46.0	-0.4	153.0	0.20	377.0
1.75	12.0	-1.5	18.0	1.00	32.0	-0.5	74.0	0.30	83.0
2.25	10.0	-2.0	17.0	1.25	25.0	-0.6	43.0		
2.9	7.0	2.9	14.0	2.9	24.0	2.9	34.0	2.9	44.0

TABLE(4)

INJECTION CONCENTRATION = 0 W.P.P.M.
 INJECTION VELOCITY / MAIN STREAM VELOCITY = 1.00
 INJECTION OPTICAL DENSITY = 20250
 UPSTREAM CONCENTRATION = 0.0

	2.02		1.87		2.06		2.02		2.36
	4.8		97.5		65.7		40.3		19.0
	0.114		0.89		0.688		0.457		0.249
	4781.0		86.0		143.0		288.0		892.0
-0.40	3.0	-2.25	16.0	2.0	31.0	-1.25	44.0	0.6	66.0
-0.30	20.0	-1.75	29.0	1.5	32.0	-1.00	52.0	0.5	99.0
-0.20	472.0	-1.25	41.0	1.0	61.0	-0.75	77.0	0.4	162.0
-0.15	1544.	-0.90	60.0	0.7	96.0	-0.50	174.0	0.3	311.0
-0.10	3452.	-0.60	87.0	0.4	139.0	-0.30	280.0	0.2	541.0
-0.05	4870.	-0.30	101.0	0.2	174.0	-0.15	316.0	0.1	770.0
0.00	4696.	0.00	106.0	0.00	173.0	0.00	337.0	0.00	949.0
0.05	3591.	0.30	100.0	-0.2	166.0	0.15	310.0	-0.1	937.0
0.10	2155.	0.60	78.0	-0.4	145.0	0.30	241.0	-0.2	744.0
0.15	1064.	0.90	59.0	-0.7	94.0	0.50	146.0	-0.3	430.0
0.20	482.0	1.25	46.0	-1.0	59.0	0.75	87.0	-0.4	218.0
0.30	74.0	1.75	33.0	-1.5	41.0	1.00	63.0	-0.5	108.0
		2.25	25.0	-2.0	39.0	1.25	56.0	-0.60	74.0
2.9	14.0	2.9	24.0	2.9	35.0	2.9	53.0	2.9	69.0

TABLE(5)

INJECTION CONCENTRATION = 0 W.P.P.M.
 INJECTION VELOCITY / MAIN STREAM VELOCITY = 1.34
 INJECTION OPTICAL DENSITY = 20250
 UPSTREAM CONCENTRATION = 4.0

	2.10		2.10		2.08		2.14		2.35
	97.5		65.7		40.3		19.0		4.8
	0.876		0.672		0.447		0.237		0.113
	106.5		185.0		396.0		1192.0		6382.0
2.25	6.0	-2.0	16.0	1.25	34.5	-0.6	46.5	0.30	114.0
1.75	12.0	-1.5	23.0	1.00	38.0	-0.5	80.0	0.20	675.0
1.25	23.0	-1.0	49.0	0.75	79.0	-0.4	168.0	0.15	1699.0
0.90	51.0	-0.75	77.0	0.50	174.0	-0.3	436.0	0.10	3322.0
0.60	76.0	-0.4	160.0	0.30	292.0	-0.2	842.0	0.05	5670.0
0.30	99.0	-0.2	193.0	0.15	392.0	-0.1	1187.0	0.00	7143.0
0.00	120.0	0.0	209.0	0.00	447.0	0.0	1249.0	-0.05	5980.0
-0.30	115.0	0.2	201.0	-0.15	403.0	0.1	1017.0	-0.10	3157.0
-0.60	93.0	0.4	177.0	-0.30	350.0	0.2	681.0	-0.15	1044.0
-0.90	71.0	0.7	108.0	-0.50	181.0	0.3	381.0	-0.20	311.0
-1.25	44.0	1.0	72.0	-0.75	78.0	0.4	178.0	-0.30	69.0
-1.75	18.0	1.5	34.0	-1.00	45.0	0.5	96.0	-0.40	67.0
-2.25	16.0	2.0	27.0	-1.25	40.0	0.6	73.0		
2.9	15.0	2.9	26.0	2.9	35.0	2.9	48.0	2.9	66.0

TABLE(6)

INJECTION CONCENTRATION = 50 W.P.P.M.

INJECTION VELOCITY / MAIN STREAM-VELOCITY = .67

INJECTION OPTICAL DENSITY = 9333

UPSTREAM CONCENTRATION = 1.0

	1.75		1.81		1.86		2.1		1.97
	0.83		0.663		0.46		0.269		0.122
	23.7		39.8		80.8		237.5		1413.0
	97.5		65.7		40.3		19.0		4.8
-1.75	3.0	1.5	5.3	-1.00	12.0	0.6	14.0	-0.30	35.0
-1.25	7.5	1.0	13.0	-0.75	23.5	0.5	25.0	-0.2	167.0
-0.90	12.0	0.7	21.0	-0.50	49.0	0.4	58.0	-0.15	321.0
-0.60	19.0	0.4	35.0	-0.30	69.5	0.3	111.0	-0.10	624.0
-0.30	24.0	0.2	41.0	-0.15	85.0	0.2	181.0	-0.05	1001.0
0.00	24.5	0.0	45.0	0.00	87.0	0.1	231.0	0.00	1384.0
0.30	24.0	-0.2	42.0	0.15	80.0	0.0	249.0	0.05	1418.0
0.60	19.0	-0.40	36.0	0.30	65.0	-0.1	226.0	0.10	1205.0
0.90	12.0	-0.7	25.0	0.50	36.0	-0.2	164.0	0.15	757.0
1.25	10.5	-1.0	16.0	0.75	18.0	-0.3	108.0	0.20	334.0
1.75	6.0	-1.5	8.0	1.00	12.0	-0.4	59.0	0.30	31.0
						-0.5	33.0		
						-0.6	22.0		
2.9	3.0	2.9	6.0	2.9	8.0	2.9	13.0	2.9	17.0

TABLE(7)

INJECTION CONCENTRATION = 50 W.P.P.M.

INJECTION VELOCITY / MAIN STREAM VELOCITY = 1.00

INJECTION OPTICAL DENSITY = 6519

UPSTREAM CONCENTRATION \leq 2.0

	1.80		2.13		1.92		1.93		2.13
	0.86		0.66		0.45		0.252		0.108
	23.8		43.7		90.4		285.0		1908.0
	97.5		65.7		40.3		19.0		4.8
-1.75	4.0	1.5	6.0	-1.0	13.0	0.6	14.0	-0.30	28.0
-1.25	9.0	1.0	13.0	-0.75	25.0	0.5	27.0	-0.20	84.0
-0.90	14.0	0.7	24.0	-0.50	51.0	0.4	64.0	-0.15	202.0
-0.60	20.0	0.4	41.0	-0.30	77.0	0.3	117.0	-0.10	456.0
-0.30	24.0	0.2	46.0	-0.15	95.0	0.2	207.0	-0.05	965.0
0.00	27.0	0.0	48.0	0.00	97.0	0.1	284.0	0.00	1696.0
0.30	26.0	-0.2	46.0	0.15	88.0	0.0	301.0	0.05	2042.0
0.60	19.0	-0.4	39.0	0.30	72.0	-0.1	254.0	0.10	1690.0
0.90	15.0	-0.7	25.0	0.50	40.0	-0.2	175.0	0.15	944.0
1.25	9.5	-1.0	16.0	0.75	21.0	-0.3	110.0	0.20	384.0
1.75	4.5	-1.5	8.0	1.00	12.0	-0.4	64.0	0.30	42.0
						-0.5	34.0		
						-0.6	20.5		
2.9	4.0	2.9	6.0	2.9	9.0	2.9	18.0	2.9	16.0

TABLE(8)

INJECTION CONCENTRATION = 50 W.P.P.M.

INJECTION VELOCITY / MAIN STREAM VELOCITY = 1.34

INJECTION OPTICAL DENSITY = 5032

UPSTREAM CONCENTRATION = 2.0

	1.76	1.94	1.98	2.08	2.33	
	0.86	0.635	0.426	0.227	0.104	
	25.7	45.2	99.2	345.0	2030.0	
	97.5	65.7	48.3	19.0	4.8	
-1.75	4.5	1.5	6.5	-1.00 14.0	0.6 13.0	-0.30 27.0
-1.25	11.0	1.0	14.0	-0.75 26.0	0.5 21.0	-0.20 74.0
-0.90	14.0	0.7	26.0	-0.50 57.5	0.4 44.0	-0.15 164.0
-0.60	21.0	0.4	40.0	-0.30 88.0	0.3 106.0	-0.10 422.0
-0.30	27.0	0.2	51.0	-0.15 108.0	0.2 210.0	-0.05 1034.0
0.00	28.5	0.0	53.0	0.00 107.0	0.1 325.0	0.00 1839.0
0.30	28.0	-0.2	48.0	0.15 94.0	0.0 370.0	0.05 2152.0
0.60	23.5	-0.4	41.0	0.30 68.0	-0.1 311.0	0.10 1752.0
0.90	17.0	-0.7	28.0	0.50 38.0	-0.2 197.0	0.15 877.0
1.25	12.5	-1.0	17.0	0.75 16.0	-0.3 106.0	0.20 284.0
1.75	8.0	-1.5	9.5	1.00 11.5	-0.4 55.0	0.30 27.0
					-0.5 34.0	
					-0.6 21.5	
2.9	5.5	2.9	8.5	2.9 10.0	2.9 14.0	2.9 17.0

TABLE(9)

INJECTION CONCENTRATION = 100 W.P.P.M.

INJECTION VELOCITY / MAIN STREAM VELOCITY = .67

INJECTION OPTICAL DENSITY = 9333

UPSTREAM CONCENTRATION = 2.0

	2.09		2.04		1.98		2.12		2.21
	97.5		65.7		40.3		19.0		4.8
	0.867		0.70		0.46		0.26		0.112
	21.2		38.7		82.8		257.5		1696.0
-1.75	3.0	1.5	5.0	-1.00	12.0	0.6	17.0	-0.30	46.0
-1.25	6.5	1.0	14.5	-0.75	22.0	0.5	32.0	-0.20	96.0
-0.90	14.0	0.7	24.5	-0.50	50.0	0.4	71.0	-0.15	218.0
-0.60	17.0	0.4	34.0	-0.30	73.0	0.3	134.0	-0.10	721.0
-0.30	21.0	0.2	42.0	-0.15	87.0	0.2	216.0	-0.05	1115.0
0.00	26.0	0.0	47.0	0.00	95.0	0.1	267.0	0.00	1667.0
0.30	23.0	-0.2	43.0	0.15	83.0	0.0	268.0	0.05	1733.0
0.60	18.0	-0.4	36.0	0.30	70.0	-0.1	225.0	0.10	1355.0
0.90	14.0	-0.7	29.0	0.50	42.0	-0.2	155.0	0.15	725.0
1.25	8.0	-1.0	16.0	0.75	21.0	-0.3	92.0	0.20	340.0
1.75	5.0	-1.5	9.0	1.00	15.0	-0.4	54.0	0.30	35.0
						-0.50	30.5		
						-0.6	21.5		
2.9	4.0	2.9	8.0	2.9	11.0	2.9	17.0	2.9	23.0

TABLE(10)

INJECTION CONCENTRATION = 100 W.P.P.M.

INJECTION VELOCITY / MAIN STREAM VELOCITY = 1.00

INJECTION OPTICAL DENSITY = 6154

UPSTREAM CONCENTRATION = 0.0

	1.88		2.03		2.33		1.87		1.72
	97.5		65.7		40.3		19.0		4.8
	0.875		0.675		0.456		0.25		0.104
	23.3		40.1		84.7		278.5		1878.0
-1.75	2.0	1.5	4.0	-1.00	6.0	0.6	12.0	-0.30	21.0
-1.25	5.0	1.0	10.0	-0.75	23.0	0.5	19.0	-0.20	60.0
-0.90	12.5	0.7	23.0	-0.50	50.0	0.4	53.0	-0.15	121.0
-0.60	18.0	0.4	32.0	-0.30	71.0	0.3	114.5	-0.10	318.0
-0.30	21.0	0.2	40.0	-0.15	92.0	0.2	204.0	-0.05	631.0
0.00	26.0	0.0	48.5	0.00	94.0	0.1	279.0	0.00	1256.0
0.30	22.0	-0.2	39.5	0.15	76.0	0.0	295.0	0.05	1868.0
0.60	18.0	-0.4	37.0	0.30	67.0	-0.1	238.0	0.10	1889.0
0.90	12.5	-0.7	25.0	0.50	37.0	-0.2	164.5	0.15	1335.0
1.25	8.0	-1.0	9.5	0.75	12.0	-0.3	101.0	0.20	571.0
1.75	3.0	-1.5	6.0	1.00	10.0	-0.4	56.0	0.30	49.0
						-0.5	27.0		
						-0.6	21.0		
2.9	2.0	2.9	5.5	2.9	8.0	2.9	10.5	2.9	14.0

TABLE(11)

INJECTION CONCENTRATION = 100 W.P.P.M.
 INJECTION VELOCITY / MAIN STREAM VELOCITY = 1.34
 INJECTION OPTICAL DENSITY = 4850
 UPSTREAM CONCENTRATION = 0.0

	2.17		1.96		1.91		1.86		1.62
	97.5		65.7		40.3		19.0		4.8
	0.865		0.627		0.426		0.226		0.0956
	24.5		45.0		94.8		335.0		2113.0
-1.75	1.0	1.5	3.0	-1.00	8.0	0.6	11.0	-0.30	13.0
-1.25	6.0	1.0	9.5	-0.75	22.0	0.5	15.0	-0.20	46.0
-0.90	12.0	0.7	20.0	-0.50	44.5	0.4	46.0	-0.15	76.0
-0.60	18.5	0.4	37.5	-0.30	79.0	0.3	115.0	-0.10	208.0
-0.30	24.0	0.2	44.0	-0.15	93.0	0.2	215.0	-0.05	448.0
0.00	24.0	0.0	47.5	0.00	100.0	0.1	338.0	0.00	1056.0
0.30	24.0	-0.2	45.0	0.15	89.0	0.0	356.0	0.05	1797.0
0.60	19.0	-0.4	36.0	0.30	64.0	-0.1	266.0	0.10	2218.0
0.90	13.0	-0.7	22.5	0.50	37.0	-0.2	154.0	0.15	1678.0
1.25	7.0	-1.0	12.0	0.75	16.0	-0.3	92.0	0.20	836.0
1.75	3.0	-1.5	7.0	1.00	7.0	-0.4	44.0	0.30	51.0
						-0.5	29.0		
						-0.6	16.5		
2.9	2.0	2.9	3.0	2.9	6.0	2.9	7.0	2.9	10.0

TABLE(12)

INJECTION CONCENTRATION = 250 W.P.P.M.

INJECTION VELOCITY / MAIN STREAM VELOCITY = .67

INJECTION OPTICAL DENSITY = 8800

UPSTREAM CONCENTRATION = 2.0

	2.03		1.94		1.99		2.18		2.04
	97.5		65.7		40.3		19.0		4.8
	0.862		0.66		0.458		0.265		0.107
	21.5		40.2		84.6		270.0		2248.0
-1.75	3.0	1.5	4.5	-1.00	10.0	0.6	12.0	-0.30	24.0
-1.25	8.0	1.00	12.0	-0.75	19.0	0.5	21.0	-0.20	123.0
-0.90	12.0	0.7	25.5	-0.50	44.0	0.4	57.0	-0.15	284.0
-0.60	17.0	0.4	36.0	-0.30	75.0	0.3	124.0	-0.10	626.0
-0.30	23.0	0.2	44.0	-0.15	87.0	0.2	212.0	-0.05	1257.0
0.00	24.0	0.0	48.0	0.00	92.0	0.1	272.0	0.00	2086.0
0.30	23.0	-0.2	39.5	0.15	83.0	0.0	273.0	0.05	2420.0
0.60	20.0	-0.4	35.0	0.30	68.0	-0.1	245.0	0.10	1822.0
0.90	14.0	-0.7	23.0	0.50	43.0	-0.2	181.0	-0.15	944.0
1.25	9.0	-1.0	13.0	0.75	20.0	-0.3	110.0	0.20	351.0
1.75	5.0	-1.5	10.5	1.00	9.0	-0.4	60.5	0.30	34.0
						-0.5	32.0		
						-0.6	19.0		
2.9	4.0	2.9	6.0	2.9	8.0	2.9	12.0	2.9	15.0

TABLE(13)

INJECTION CONCENTRATION = 250 W.P.P.M.

INJECTION VELOCITY / MAIN STREAM VELOCITY = 1.00

INJECTION OPTICAL DENSITY = 6500

UPSTREAM CONCENTRATION = 1.0

	2.09		2.13		1.94		2.17		2.10
	97.5		65.7		40.3		19.0		4.8
	0.835		0.696		0.443		0.261		0.103
	23.7		37.2		91.6		259.0		2048.0
-1.75	3.0	1.5	10.0	-1.00	12.0	0.6	12.0	-0.30	25.0
-1.25	8.0	1.00	14.0	-0.75	23.0	0.5	22.0	-0.20	111.0
-0.90	14.5	0.7	28.0	-0.50	48.0	0.4	57.0	-0.15	272.0
-0.60	21.0	0.4	35.5	-0.30	85.0	0.3	121.0	-0.10	563.0
-0.30	24.0	0.2	40.0	-0.15	91.0	0.2	210.0	-0.05	1157.0
0.00	28.0	0.0	45.0	0.00	100.0	0.1	263.0	0.00	1899.0
0.30	26.0	-0.2	41.0	0.15	93.0	0.0	267.0	0.05	2226.0
0.60	19.5	-0.4	35.0	0.30	67.0	-0.1	227.0	0.10	1604.0
0.90	15.0	-0.7	22.0	0.50	42.0	-0.2	165.0	0.15	675.0
1.25	8.5	-1.0	14.0	0.75	16.0	-0.3	103.0	0.20	190.0
1.75	6.0	-1.5	8.0	1.00	12.0	-0.4	50.0	0.30	21.0
						-0.5	28.0		
						-0.6	16.0		
2.9	5.0	2.9	7.0	2.9	9.0	2.9	12.0	2.9	14.0

TABLE(14)

INJECTION CONCENTRATION = 250 W.P.P.M.
 INJECTION VELOCITY / MAIN STREAM VELOCITY = 1.34
 INJECTION OPTICAL DENSITY = 5000
 UPSTREAM CONCENTRATION = 3.0

	1.76		2.05		1.99		2.06		2.29
	97.5		65.7		40.3		19.0		4.8
	0.835		0.635		0.424		0.222		0.0973
	25.1		47.2		100.8		376.0		2462.0
-1.75	4.0	1.5	5.0	-1.00	10.0	0.6	9.0	-0.30	16.0
-1.25	8.0	1.0	12.0	-0.75	23.0	0.5	15.5	-0.20	61.0
-0.90	14.0	0.7	24.5	-0.50	53.0	0.4	35.0	-0.15	146.0
-0.60	20.0	0.4	40.0	-0.30	86.0	0.3	105.0	-0.10	447.0
-0.30	26.0	0.2	49.0	-0.15	102.0	0.2	228.0	-0.05	1118.0
0.00	28.5	0.0	51.0	0.00	109.0	0.1	382.0	0.00	2223.0
0.30	24.0	-0.2	48.0	0.15	94.0	0.0	386.0	0.05	2728.0
0.90	20.0	-0.4	40.0	0.30	67.0	-0.1	313.0	0.10	1974.0
0.90	14.0	-0.7	24.0	0.50	38.0	-0.2	196.0	0.15	720.0
1.25	9.0	-1.0	12.0	0.75	16.5	-0.3	99.0	0.20	128.0
1.75	5.0	-1.5	6.0	1.00	9.0	-0.4	49.0	0.30	18.0
						-0.5	26.0		
						-0.6	15.0		
2.9	3.0	2.9	5.0	2.9	8.0	2.9	11.0	2.9	16.0

TABLE(15)

INJECTION CONCENTRATION = 500 W.P.P.M.

INJECTION VELOCITY / MAIN STREAM VELOCITY = .67

INJECTION OPTICAL DENSITY = 8812

UPSTREAM CONCENTRATION = 2.0

	1.79		1.86		2.14		2.07		1.80
	97.5		65.7		40.3		19.0		4.8
	0.86		0.612		0.424		0.23		0.0896
	22.5		43.5		92.0		341.0		3535.0
-1.75	4.0	1.5	4.0	-1.00	10.0	0.6	9.0	-0.30	24.0
-1.25	7.0	1.0	13.0	-0.75	20.0	0.5	20.0	-0.20	123.0
-0.90	14.0	0.7	21.0	-0.50	47.0	0.4	46.0	-0.15	284.0
-0.60	18.0	0.4	37.0	-0.30	75.0	0.3	119.0	-0.10	851.0
-0.30	23.0	0.2	41.0	-0.15	92.0	0.2	213.0	-0.05	1838.0
0.00	25.0	0.0	49.0	0.00	99.0	0.1	318.0	0.00	3177.0
0.30	24.0	-0.2	47.0	0.15	91.0	0.0	367.0	0.05	3629.0
0.60	18.0	-0.4	38.0	0.30	71.0	-0.1	300.0	0.10	2407.0
0.90	13.0	-0.7	23.0	0.50	35.0	-0.2	191.0	0.15	1004.0
1.25	9.0	-1.0	15.0	0.75	15.0	-0.3	100.0	0.20	289.0
1.75	5.0	-1.5	7.0	1.00	9.0	-0.4	45.0	0.30	24.0
						-0.5	26.0		
						-0.6	15.0		
2.9	3.0	2.9	6.0	2.9	8.0	2.9	11.0	2.9	13.0

TABLE (16)

INJECTION CONCENTRATION = 500 W.P.P.M.

INJECTION VELOCITY / MAIN STREAM VELOCITY = 1.00

INJECTION OPTICAL DENSITY = 6250

UPSTREAM CONCENTRATION = 2.0

1.80		1.78		2.06		2.15		1.91	
97.5		65.7		40.3		19.0		4.8	
0.87		0.622		0.404		0.21		0.0835	
24.7		43.6		102.3		448.0		3862.0	
-1.75	4.0	1.5	8.0	-1.00	14.0	0.5	14.0	-0.30	23.0
-1.25	8.0	1.0	11.0	-0.75	22.0	0.4	31.0	-0.20	78.0
-0.90	14.0	0.7	21.0	-0.50	58.5	0.3	83.0	-0.15	187.0
-0.60	22.0	0.4	36.0	-0.30	90.0	0.2	201.0	-0.10	588.0
-0.30	25.0	0.2	43.0	-0.15	109.0	0.1	414.0	-0.05	1648.0
0.00	27.0	0.0	50.0	0.00	111.0	0.0	482.0	0.00	3160.0
0.30	27.0	-0.2	49.0	0.15	91.0	-0.1	408.0	0.05	4176.0
0.60	20.0	-0.4	39.5	0.30	60.0	-0.2	234.0	0.10	2616.0
0.90	15.0	-0.7	27.0	0.50	31.5	-0.3	124.0	0.15	983.0
1.25	11.5	-1.0	17.5	0.75	16.0	-0.4	54.0	0.20	152.0
1.75	6.0	-1.5	9.0	1.00	10.5	-0.5	34.0	0.30	20.0
2.9	4.0	2.9	7.0	2.9	10.0	2.9	16.0	2.9	20.0

TABLE(17)

INJECTION CONCENTRATION = 500 W.P.P.M.

INJECTION VELOCITY / MAIN STREAM VELOCITY = 1.34

INJECTION OPTICAL DENSITY = 4875

UPSTREAM CONCENTRATION = 2.5

	1.81		2.24		1.87		1.92		2.62
	97.5		65.7		48.3		19.0		4.8
	0.835		0.613		0.365		0.174		0.075
	26.6		51.5		128.0		551.0		3724.0
-1.75	6.0	1.5	7.0	-1.00	13.0	0.5	15.0	-0.30	14.0
-1.25	9.5	1.0	10.0	-0.75	20.0	0.4	19.0	-0.20	41.0
-0.90	17.5	0.7	24.0	-0.50	55.5	0.30	69.0	-0.15	107.0
-0.60	24.0	0.4	42.0	-0.30	101.0	0.2	207.0	-0.10	316.0
-0.30	28.0	0.2	51.0	-0.15	131.0	0.1	441.0	-0.05	1213.0
0.00	31.0	0.0	56.0	0.00	141.0	0.0	599.0	0.00	3333.0
0.30	28.0	-0.2	58.0	0.15	108.0	-0.1	442.0	0.05	3761.0
0.60	21.0	-0.4	50.0	0.30	68.0	-0.2	203.0	0.10	2213.0
0.90	15.0	-0.7	28.0	0.50	30.0	-0.3	89.0	0.15	375.0
1.25	11.5	-1.0	15.0	0.75	17.0	-0.4	42.0	0.20	46.0
1.75	7.0	-1.5	8.0	1.00	11.0	-0.5	21.0	0.30	19.0
2.9	5.5	2.9	7.0	2.9	9.0	2.9	14.0	2.9	17.0

TABLE(18)

INJECTION CONCENTRATION = 1000 W.P.P.M.

INJECTION VELOCITY / MAIN STREAM VELOCITY = .67

INJECTION OPTICAL DENSITY = 9900

UPSTREAM CONCENTRATION = 2.0

	2.31		1.86		2.08		1.93		2.14
	97.5		65.7		40.3		19.0		4.8
	0.91		0.60		0.39		0.187		0.099
	25.1		48.0		110.9		557.0		4896.0
-1.75	3.0	1.5	6.0	-1.00	10.0	0.50	16.5	-0.30	26.0
-1.25	8.0	1.0	13.0	-0.75	18.0	0.4	47.0	-0.20	168.0
-0.90	17.0	0.7	28.0	-0.50	46.0	0.3	132.0	-0.15	394.0
-0.60	23.0	0.40	41.0	-0.30	81.0	0.2	279.0	-0.10	1433.0
-0.30	24.0	0.20	54.5	-0.15	112.0	0.1	495.0	-0.05	2800.0
0.00	30.0	0.0	57.5	0.00	122.0	0.0	605.0	0.00	4670.0
0.30	29.5	-0.2	48.0	0.15	109.0	-0.1	418.0	0.05	5200.0
0.60	22.0	-0.4	40.0	0.30	79.0	-0.2	200.0	0.10	3480.0
0.90	17.0	-0.7	26.0	0.50	42.0	-0.3	92.0	0.15	1277.0
1.25	14.0	-1.0	16.0	0.75	16.0	-0.4	44.0	0.20	212.0
1.75	7.0	-1.5	8.0	1.00	10.0	-0.5	23.0	0.30	21.0
2.9	6.0	2.9	8.0	2.9	10.0	2.9	11.0	2.9	18.0

TABLE(19)

INJECTION CONCENTRATION = 1000 W.P.P.M.

INJECTION VELOCITY / MAIN STREAM VELOCITY = 1.00

INJECTION OPTICAL DENSITY = 5625

UPSTREAM CONCENTRATION = 2.5

	1.96		2.35		1.96		2.12		2.53
	97.5		65.7		48.3		19.0		4.8
	0.776		0.655		0.378		0.176		0.0797
	27.9		48.3		127.6		685.0		4893.0
-1.75	4.0	1.5	5.0	-1.00	10.0	0.5	12.0	-0.30	13.0
-1.25	8.0	1.0	9.0	-0.75	22.0	0.4	19.0	-0.20	51.0
-0.90	16.0	0.7	24.0	-0.50	58.0	0.3	77.0	-0.15	143.0
-0.60	22.0	0.4	43.0	-0.30	98.0	0.2	198.0	-0.10	445.0
-0.30	29.0	0.2	52.0	-0.15	134.0	0.1	511.0	-0.05	2041.0
0.00	32.0	0.0	56.0	0.00	137.0	0.0	740.0	0.00	4286.0
0.30	27.0	-0.2	47.0	0.15	113.0	-0.1	594.0	0.05	4849.0
0.60	21.0	-0.4	45.0	0.30	74.0	-0.2	291.0	0.10	3319.0
0.90	13.0	-0.7	30.0	0.50	34.0	-0.3	126.0	0.15	713.0
1.25	8.0	-1.0	14.0	0.75	14.0	-0.4	53.0	0.20	92.0
1.75	5.0	-1.5	8.0	1.00	11.0	-0.5	28.0	0.30	21.0
2.9	4.0	2.9	7.0	2.9	9.0	2.9	11.0	2.9	16.0

TABLE(20)

INJECTION CONCENTRATION = 1000 W.P.P.M.

INJECTION VELOCITY / MAIN STREAM VELOCITY = 1.34

INJECTION OPTICAL DENSITY = 4667

UPSTREAM CONCENTRATION = 1.0

	1.70	1.85	2.00	2.08	2.35				
	97.5	65.7	40.3	19.0	4.8				
	0.743	0.54	0.344	0.157	0.0762				
	30.3	51.4	150.4	744.0	3737.0				
-1.75	3.0	1.5	4.0	-1.00	11.0	0.5	10.0	-0.30	13.0
-1.25	7.0	1.0	8.0	-0.75	17.0	0.4	14.0	-0.20	21.0
-0.90	11.0	0.7	15.5	-0.50	51.0	0.3	47.0	-0.15	58.0
-0.60	23.0	0.4	28.0	-0.30	110.0	0.2	162.0	-0.10	296.0
-0.30	29.0	0.2	37.0	-0.15	165.0	0.1	517.0	-0.05	1470.0
0.00	30.0	0.0	40.0	0.00	159.0	0.0	820.0	0.00	3334.0
0.30	31.0	-0.2	38.0	0.15	114.0	-0.1	590.0	0.05	3809.0
0.60	22.5	-0.4	31.0	0.30	71.0	-0.2	226.0	0.10	2097.0
0.90	12.0	-0.7	21.5	0.50	26.0	-0.3	78.0	0.15	394.0
1.25	8.5	-1.0	13.0	0.75	12.0	-0.4	31.0	0.20	52.0
1.75	5.0	-1.5	7.0	1.00	9.0	-0.5	18.0	0.30	18.0
2.9	3.0	2.9	6.0	2.9	9.0	2.9	11.0	2.9	16.0

POINT SOURCE INJECTION

FULLY DEVELOPED FLOW

L = 75.0 MM.

TABLE(21)

INJECTION CONCENTRATION = 0 W.P.P.M.

INJECTION VELOCITY / MAIN STREAM VELOCITY = .67

INJECTION OPTICAL DENSITY = 9900

UPSTREAM CONCENTRATION = 2.0

	1.95		2.06		2.03		2.06		2.23
	92.4		60.6		35.2		20.3		5.7
	0.905		0.64		0.413		0.253		0.114
	24.3		47.4		110.1		299.2		1799.0
-1.75	3.0	1.5	6.0	-1.00	10.0	0.5	41.0	-0.30	16.5
-1.25	9.0	1.0	13.0	-0.75	20.0	0.4	79.0	-0.2	45.5
-0.90	14.0	0.7	27.0	-0.50	50.0	0.3	148.0	-0.15	127.5
-0.60	20.0	0.4	44.0	-0.30	89.0	0.2	238.0	-0.10	342.0
-0.30	26.0	0.2	50.0	-0.15	112.0	0.1	309.0	-0.05	860.0
0.00	27.0	0.0	54.0	0.00	121.0	0.0	312.0	0.00	1436.0
0.30	25.0	-0.2	50.0	0.15	107.0	-0.1	253.0	0.05	1823.0
0.60	22.0	-0.4	41.0	0.30	85.0	-0.2	172.0	0.10	1776.0
0.90	16.0	-0.7	26.5	0.50	46.0	-0.3	98.0	0.15	1251.0
1.25	12.0	-1.0	17.0	0.75	21.0	-0.4	51.0	0.20	664.0
1.75	6.0	-1.5	9.0	1.00	14.0	-0.5	28.5	0.30	96.0
2.9	4.0	2.9	8.0	2.9	11.0	2.9	15.0	2.9	23.0

TABLE(22)

INJECTION CONCENTRATION = 0 W.P.P.M.
 INJECTION VELOCITY / MAIN STREAM VELOCITY = 1.00
 INJECTION OPTICAL DENSITY = 6095
 UPSTREAM CONCENTRATION = 4.0

	1.83		1.99		2.02		2.03		2.12
	92.4		60.6		35.2		20.3		5.7
	0.833		0.637		0.40		0.242		0.10
	24.0		45.6		109.9		321.0		1999.0
-1.75	5.0	1.5	6.0	-1.00	9.0	0.5	30.0	-0.30	18.0
-1.25	11.0	1.0	14.0	-0.75	16.0	0.4	77.0	-0.20	81.0
-0.90	14.0	0.7	24.0	-0.50	44.0	0.3	141.0	-0.15	251.0
-0.60	20.0	0.4	39.0	-0.30	81.0	0.2	250.0	-0.10	694.0
-0.30	27.0	0.2	48.0	-0.15	111.0	0.1	321.0	-0.05	1427.0
0.00	28.0	0.0	52.0	0.00	117.0	0.0	332.0	0.00	2021.0
0.30	26.0	-0.2	48.0	0.15	109.0	-0.1	272.0	0.05	1960.0
0.60	23.0	-0.4	41.0	0.30	77.5	-0.2	155.0	0.10	1210.0
0.90	16.0	-0.7	27.0	0.50	45.0	-0.3	89.0	0.15	556.0
1.25	11.0	-1.0	14.0	0.75	18.0	-0.4	42.0	0.20	199.0
1.75	7.0	-1.5	7.0	1.00	10.0	-0.5	24.0	0.30	32.0
2.9	5.0	2.9	6.0	2.9	9.0	2.9	11.0	2.9	15.0

TABLE(23)

INJECTION CONCENTRATION = 0 W.P.P.M.
 INJECTION VELOCITY / MAIN STREAM VELOCITY = 1.34
 INJECTION OPTICAL DENSITY = 4875
 UPSTREAM CONCENTRATION = 1.0

	2.11		2.02		1.98		2.08		2.29
	92.4		60.6		35.2		20.3		5.7
	0.822		0.58		0.358		0.222		0.103
	29.7		57.1		149.1		415.3		1956.0
-1.75	2.0	1.5	4.0	-1.00	6.0	0.5	26.0	-0.30	12.0
-1.25	8.0	1.0	11.0	-0.75	14.0	0.4	59.0	-0.20	54.0
-0.90	15.0	0.7	26.0	-0.50	42.0	0.30	147.0	-0.15	176.0
-0.60	22.0	0.4	45.0	-0.30	101.5	0.2	286.0	-0.10	590.0
-0.30	30.0	0.2	58.0	-0.15	144.0	0.1	427.0	-0.05	1345.0
0.00	32.0	0.0	62.0	0.00	159.0	0.0	435.0	0.00	1908.0
0.30	28.0	-0.2	56.0	0.15	135.0	-0.1	310.0	0.05	1948.0
0.60	23.0	-0.4	44.0	0.30	88.0	-0.2	171.0	0.10	1401.0
0.90	15.0	-0.7	24.0	0.50	42.0	-0.3	78.0	0.15	653.0
1.25	8.0	-1.0	12.0	0.75	14.0	-0.4	34.0	0.20	200.0
1.75	5.0	-1.5	7.0	1.00	8.0	-0.5	16.0	0.30	25.0
2.9	3.0	2.9	5.0	2.9	7.0	2.9	10.0	2.9	15.0

TABLE(24)

INJECTION CONCENTRATION = 50 W.P.P.M.
 INJECTION VELOCITY / MAIN STREAM VELOCITY = .67
 INJECTION OPTICAL DENSITY = 9578
 UPSTREAM CONCENTRATION = 2.0

	1.83		2.29		2.03		2.06		2.02
	92.4		60.6		35.2		20.3		5.7
	0.88		0.652		0.416		0.256		0.114
	23.4		43.7		104.1		268.2		1700.0
-1.75	3.0	1.5	4.0	-1.00	8.0	0.5	33.0	-0.30	20.5
-1.25	9.0	1.0	12.0	-0.75	17.0	0.4	68.0	-0.20	139.0
-0.90	14.5	0.7	24.0	-0.50	47.0	0.3	132.0	-0.15	376.0
-0.60	20.5	0.4	41.0	-0.30	82.0	0.2	202.0	-0.10	612.0
-0.30	24.0	0.2	46.0	-0.15	104.0	0.1	268.0	-0.05	1361.0
0.00	27.0	0.0	48.0	0.00	113.0	0.0	278.0	0.00	1718.0
0.30	24.0	-0.2	46.0	0.15	99.0	-0.1	241.0	0.05	1616.0
0.60	20.0	-0.4	39.0	0.30	79.0	-0.2	157.0	0.10	1200.0
0.90	14.0	-0.7	24.0	0.50	42.0	-0.3	93.0	0.15	649.0
1.25	11.0	-1.0	14.0	0.75	20.0	-0.4	46.0	0.20	272.0
1.75	6.0	-1.5	7.0	1.00	11.0	-0.5	25.0	0.30	46.0
2.9	4.0	2.9	6.0	2.9	8.0	2.9	11.5	2.9	15.0

TABLE(25)

INJECTION CONCENTRATION = 50 W.P.P.M.

INJECTION VELOCITY / MAIN STREAM VELOCITY = 1.00

INJECTION OPTICAL DENSITY = 6065

UPSTREAM CONCENTRATION = 2.5

	2.21		2.06		2.01		2.07		2.08
	92.4		60.6		35.2		20.3		5.7
	0.86		641		0.402		0.247		0.103
	22.7		45.7		110.0		308.0		2017.0
-1.75	3.0	1.5	4.0	-1.00	7.0	0.5	30.0	-0.30	16.0
-1.25	8.0	1.0	11.0	-0.75	15.0	0.4	69.0	-0.20	81.0
-0.90	15.0	0.7	25.0	-0.50	48.0	0.3	133.0	-0.15	299.0
-0.60	20.0	0.4	40.0	-0.30	86.0	0.2	230.0	-0.10	794.0
-0.30	23.0	0.2	46.0	-0.15	110.0	0.1	300.0	-0.05	1472.0
0.00	27.0	0.0	51.0	0.00	121.0	0.0	330.0	0.00	2044.0
0.30	24.0	-0.2	50.0	0.15	103.0	-0.1	256.0	0.05	1964.0
0.60	18.0	-0.4	40.0	0.30	74.0	-0.2	176.0	0.10	1254.0
0.90	14.0	-0.7	25.0	0.50	42.0	-0.3	98.0	0.15	571.0
1.25	11.0	-1.0	14.5	0.75	16.0	-0.4	45.0	0.20	201.0
1.75	4.0	-1.5	6.0	1.00	9.0	-0.5	24.5	0.30	28.0
2.9	4.0	2.9	6.0	2.9	8.0	2.9	10.0	2.9	16.0

TABLE(26)

INJECTION CONCENTRATION = 50 W.P.P.M.

INJECTION VELOCITY / MAIN STREAM VELOCITY = 1.84

INJECTION OPTICAL DENSITY = 4556

UPSTREAM CONCENTRATION = 2.0

	2.16		1.95		2.06		2.19		2.32
	92.4		60.6		35.2		20.3		5.7
	0.87		0.573		0.364		0.219		0.098
	23.4		50.4		128.9		372.0		1790.0
-1.75	3.0	1.5	5.0	-1.00	6.0	0.5	20.0	-0.30	13.0
-1.25	8.0	1.0	12.0	-0.75	13.0	0.4	51.0	-0.20	36.5
-0.90	14.0	0.7	23.0	-0.50	41.0	0.3	124.0	-0.15	164.0
-0.60	20.0	0.4	42.0	-0.30	90.0	0.2	243.0	-0.10	582.0
-0.30	26.0	0.2	53.0	-0.15	124.0	0.1	383.0	-0.05	1262.0
0.00	26.0	0.0	55.0	0.00	142.0	0.0	393.0	0.00	1816.0
0.30	25.5	-0.2	54.0	0.15	119.5	-0.1	285.0	0.05	1722.0
0.60	21.0	-0.4	39.0	0.30	82.0	-0.2	156.0	0.10	1094.0
0.90	15.0	-0.7	24.0	0.50	39.0	-0.3	75.0	0.15	428.0
1.25	9.0	-1.0	11.0	0.75	13.0	-0.4	30.0	0.20	105.0
1.75	6.0	-1.5	6.0	1.00	9.0	-0.5	17.0	0.30	16.0
2.9	5.0	2.9	6.0	2.9	9.0	2.9	10.0	2.9	14.0

TABLE(27)

INJECTION CONCENTRATION = 100 W.P.P.M.

INJECTION VELOCITY / MAIN STREAM VELOCITY = .67

INJECTION OPTICAL DENSITY = 9000

UPSTREAM CONCENTRATION = 1.0

	1.73		1.95		2.06		2.02		2.01
	92.4		60.6		35.2		20.3		5.7
	0.90		0.62		0.415		0.248		0.105
	22.2		42.7		98.7		276.3		1859.0
-1.75	4.0	1.5	6.0	-1.00	8.0	0.5	31.0	-0.30	21.0
-1.25	10.0	1.0	11.0	-0.75	19.0	0.4	63.0	-0.20	144.0
-0.90	14.0	0.7	21.0	-0.50	48.0	0.3	117.0	-0.15	400.0
-0.60	20.0	0.4	35.0	-0.30	82.0	0.2	189.0	-0.10	926.0
-0.30	23.0	0.2	43.0	-0.15	103.0	0.1	270.0	-0.05	1605.0
0.00	26.0	0.0	49.0	0.00	107.5	0.0	290.0	0.00	1925.0
0.30	21.0	-0.2	46.0	0.15	93.0	-0.1	232.0	0.05	1615.0
0.60	17.0	-0.4	40.0	0.30	70.0	-0.2	167.0	0.10	981.0
0.90	13.5	-0.7	25.0	0.50	39.0	-0.3	98.0	0.15	512.0
1.25	8.0	-1.0	14.5	0.75	15.0	-0.4	47.0	0.20	179.0
1.75	5.0	-1.5	7.5	1.00	10.0	-0.5	24.0	0.30	28.0
2.9	4.0	2.9	6.5	2.9	9.0	2.9	10.0	2.9	14.0

TABLE (28)

INJECTION CONCENTRATION = 100 W.P.P.M.

INJECTION VELOCITY / MAIN STREAM VELOCITY = 1.00

INJECTION OPTICAL DENSITY = 6300

UPSTREAM CONCENTRATION = 1.5

	2.10		1.95		1.99		2.05		2.17
	92.4		60.6		35.2		20.3		5.7
	0.893		0.63		0.411		0.24		0.0916
	22.8		44.1		105.9		326.0		2516.0
-1.75	3.0	1.5	4.0	-1.00	8.0	0.5	27.0	-0.30	15.0
-1.25	9.0	1.0	12.0	-0.75	17.5	0.4	63.0	-0.20	61.0
-0.90	14.0	0.7	21.5	-0.50	51.0	0.3	131.0	-0.15	254.0
-0.60	20.0	0.4	36.0	-0.30	84.0	0.2	224.0	-0.10	770.0
-0.30	24.0	0.2	46.0	-0.15	103.0	0.1	314.0	-0.05	1885.0
0.00	26.0	0.0	49.0	0.00	119.0	0.0	347.0	0.00	2625.0
0.30	23.0	-0.2	46.0	0.15	100.0	-0.1	278.0	0.05	2290.0
0.60	19.0	-0.4	40.0	0.30	71.5	-0.2	192.0	0.10	1112.0
0.90	14.0	-0.7	25.5	0.50	41.0	-0.3	95.0	0.15	430.0
1.25	8.0	-1.0	14.0	0.75	16.0	-0.4	45.0	0.20	138.0
1.75	5.0	-1.5	6.0	1.00	9.0	-0.5	23.0	0.30	19.0
2.9	4.0	2.9	5.0	2.9	8.0	2.9	10.0	2.9	13.0

TABLE(29)

INJECTION CONCENTRATION = 100 W.P.P.M.
 INJECTION VELOCITY / MAIN STREAM VELOCITY = 1.34
 INJECTION OPTICAL DENSITY = 4200
 UPSTREAM CONCENTRATION = 1.0

	1.68	1.90	2.05	2.26	2.87				
	92.4	60.6	35.2	20.3	5.7				
	0.806	0.555	0.356	0.214	0.0923				
	24.1	30.8	125.2	381.0	2299.0				
-1.75	2.0	1.5	5.0	-1.00	7.0	0.5	20.0	-0.30	11.0
-1.25	8.0	1.0	10.0	-0.75	13.0	0.4	45.0	-0.20	26.0
-0.90	12.0	0.7	19.0	-0.50	37.5	0.3	116.0	-0.15	104.0
-0.60	18.0	0.4	40.5	-0.30	86.0	0.2	251.0	-0.10	450.0
-0.30	24.0	0.2	50.0	-0.15	119.5	0.1	390.0	-0.05	1420.0
0.00	26.0	0.0	54.0	0.00	134.0	0.0	397.0	0.00	2294.0
0.30	24.0	-0.2	53.5	0.15	116.5	-0.1	292.0	0.05	2302.0
0.60	18.0	-0.4	39.5	0.30	76.0	-0.2	146.0	0.10	1402.0
0.90	13.0	-0.7	22.0	0.50	32.5	-0.3	65.0	0.15	446.0
1.25	9.0	-1.0	12.0	0.75	15.0	-0.4	26.5	0.20	98.0
1.75	5.0	-1.5	6.0	1.00	9.0	-0.5	14.0	0.30	16.0
2.9	3.0	2.9	5.5	2.9	7.0	2.9	10.0	-2.9	12.5

TABLE(30)

INJECTION CONCENTRATION = 250 W.P.P.M.

INJECTION VELOCITY / MAIN STREAM VELOCITY = .67

INJECTION OPTICAL DENSITY = 8800

UPSTREAM CONCENTRATION = 0.0

	1.78		1.94		2.91		2.09		2.84
	92.4		60.6		35.2		20.3		5.7
	0.867		0.606		0.398		0.24		0.0953
	22.1		42.7		105.5		298.0		2378.0
-1.75	1.0	1.5	4.0	-1.00	7.0	0.5	30.0	-0.30	13.0
-1.25	6.5	1.0	13.0	-0.75	13.5	0.4	64.0	-0.20	80.0
-0.90	10.0	0.7	21.5	-0.50	37.0	0.3	138.0	-0.15	322.0
-0.60	16.0	0.4	40.0	-0.30	75.5	0.2	239.0	-0.10	857.0
-0.30	22.0	0.2	43.0	-0.15	102.0	0.1	313.0	-0.05	1732.0
0.00	23.0	0.0	45.0	0.00	113.0	0.0	299.0	0.00	2518.0
0.30	22.0	-0.2	42.0	0.15	97.0	-0.1	230.0	0.05	2190.0
0.60	19.0	-0.4	34.0	0.30	80.0	-0.2	137.0	0.10	1144.0
0.90	13.5	-0.7	17.0	0.50	40.0	-0.3	71.0	0.15	492.0
1.25	9.0	-1.0	11.0	0.75	15.0	-0.4	37.0	0.20	171.0
1.75	6.0	-1.5	6.0	1.00	9.0	-0.5	16.0	0.30	18.0
2.9	3.0	2.9	4.0	2.9	6.0	2.9	10.0	2.9	12.0

TABLE(31)

INJECTION CONCENTRATION = 250 W.P.P.M.
 INJECTION VELOCITY / MAIN STREAM VELOCITY = 1.00
 INJECTION OPTICAL DENSITY = 5700
 UPSTREAM CONCENTRATION = 1.0

	1.78		2.07		2.04		2.27		2.01
	92.4		60.6		35.2		20.3		5.7
	0.816		0.593		0.386		0.223		0.077
	21.8		44.3		111.9		353.0		3013.0
-1.75	2.0	1.5	3.0	-1.00	6.0	0.5	21.0	-0.30	11.0
-1.25	6.5	1.0	9.0	-0.75	13.0	0.4	53.0	-0.20	38.0
-0.90	11.0	0.7	21.0	-0.50	36.0	0.3	135.0	-0.15	153.0
-0.60	14.5	0.4	39.0	-0.30	77.5	0.2	247.0	-0.10	749.0
-0.30	21.0	0.2	43.0	-0.15	103.5	0.1	356.0	-0.05	1957.0
0.00	23.5	0.0	48.5	0.00	117.0	0.0	364.0	0.00	3029.0
0.30	23.5	-0.2	45.0	0.15	109.0	-0.1	272.0	0.05	2570.0
0.60	18.0	-0.4	34.0	0.30	79.0	-0.2	148.0	0.10	1028.0
0.90	13.0	-0.7	19.0	0.50	39.0	-0.3	56.0	0.15	248.0
1.25	8.5	-1.0	11.0	0.75	13.0	-0.4	24.0	0.20	72.0
1.75	4.0	-1.5	6.0	1.00	7.0	-0.5	13.0	0.30	14.0
2.9	3.0	2.9	4.0	2.9	5.0	2.9	8.0	2.9	12.0

TABLE(32)

INJECTION CONCENTRATION = 250 W.P.P.M.

INJECTION VELOCITY / MAIN STREAM VELOCITY = 1.34

INJECTION OPTICAL DENSITY = 4300

UPSTREAM CONCENTRATION = 0.0

	1.61		1.88		2.04		2.06		2.09
	92.4		60.6		35.2		20.3		5.7
	0.821		0.578		0.354		0.192		0.0763
	25.0		48.7		132.0		442.0		2442.0
-1.75	2.0	1.5	2.0	-1.00	8.0	0.5	12.0	-0.30	10.5
-1.25	5.0	1.0	7.0	-0.75	14.5	0.4	36.0	-0.20	32.0
-0.90	11.0	0.7	18.0	-0.50	35.5	0.3	100.0	-0.15	149.0
-0.60	17.0	0.4	41.0	-0.30	91.0	0.2	249.0	-0.10	603.0
-0.30	24.0	0.2	48.0	-0.15	127.0	0.1	406.0	-0.05	1750.0
0.00	26.0	0.0	52.0	0.00	142.0	0.0	463.0	0.00	2507.0
0.30	22.0	-0.2	48.0	0.15	118.0	-0.1	331.0	0.05	1863.0
0.60	19.0	-0.4	35.0	0.30	76.0	-0.2	163.0	0.10	828.0
0.90	12.0	-0.7	23.0	0.50	36.0	-0.3	67.0	0.15	193.0
1.25	8.0	-1.0	13.0	0.75	11.0	-0.4	25.0	0.20	35.0
1.75	4.0	-1.5	6.0	1.00	7.0	-0.5	14.0	0.30	15.0
2.9	1.0	2.9	5.0	2.9	6.0	2.9	9.0	2.9	13.0

TABLE(33)

INJECTION CONCENTRATION = 500 W.P.P.M.
 INJECTION VELOCITY / MAIN STREAM VELOCITY = .67
 INJECTION OPTICAL DENSITY = 8700
 UPSTREAM CONCENTRATION = 1.0

	1.53		2.01		1.94		2.03		2.10
	92.4		60.6		35.2		20.3		5.7
	0.84		0.606		0.379		0.215		0.0861
	25.0		45.0		111.2		350.0		3612.0
-1.75	3.0	1.5	6.0	-1.00	10.0	0.5	33.0	-0.30	13.0
-1.25	9.0	1.0	13.0	-0.75	15.0	0.4	68.0	-0.20	29.0
-0.90	14.0	0.7	24.0	-0.50	36.0	0.3	154.0	-0.15	92.0
-0.60	18.5	0.4	40.0	-0.30	76.0	0.2	268.0	-0.10	361.0
-0.30	27.0	0.2	49.0	-0.15	108.0	0.1	352.0	-0.05	1354.0
0.00	28.0	0.0	50.0	0.00	117.0	0.0	349.0	0.00	2909.0
0.30	25.0	-0.2	48.0	0.15	114.0	-0.1	256.0	0.05	3727.0
0.60	22.0	-0.4	39.0	0.30	82.0	-0.2	120.0	0.10	2888.0
0.90	15.0	-0.7	23.0	0.50	43.0	-0.3	59.0	0.15	1211.0
1.25	11.0	-1.0	13.0	0.75	18.0	-0.4	26.0	0.20	395.0
1.75	8.0	-1.5	9.0	1.00	13.0	-0.5	14.0	0.30	33.0
2.9	5.0	2.9	7.0	2.9	9.0	2.9	12.0	2.9	15.0

TABLE(34)

INJECTION CONCENTRATION = 500 W.P.P.M.
 INJECTION VELOCITY / MAIN STREAM VELOCITY = 1.00
 INJECTION OPTICAL DENSITY = 5500
 UPSTREAM CONCENTRATION = 1.0

	1.75		2.18		2.07		1.99		2.10
	92.4		60.6		35.2		20.3		5.7
	0.84		0.579		0.373		0.199		0.076
	22.0		43.6		112.9		426.0		3357.0
-1.75	2.5	1.5	6.0	-1.00	7.0	0.5	22.0	-0.30	12.0
-1.25	7.0	1.0	12.0	-0.75	8.0	0.4	53.5	-0.20	17.0
-0.90	9.0	0.7	28.0	-0.50	28.0	0.3	126.0	-0.15	56.0
-0.60	15.0	0.4	42.0	-0.30	62.0	0.2	280.0	-0.10	280.0
-0.30	22.0	0.2	47.0	-0.15	95.0	0.1	435.0	-0.05	1202.0
0.00	24.0	0.0	49.0	0.00	125.0	0.0	437.0	0.00	2844.0
0.30	23.0	-0.2	40.0	0.15	116.0	-0.1	275.0	0.05	3486.0
0.60	20.0	-0.4	29.0	0.30	91.0	-0.2	154.0	0.10	1992.0
0.90	15.5	-0.7	14.0	0.50	49.0	-0.3	64.0	0.15	702.0
1.25	12.0	-1.00	8.0	0.75	17.0	-0.4	24.0	0.20	150.0
1.75	5.0	-1.5	6.0	1.00	9.0	-0.5	14.0	0.30	18.0
2.9	4.0	2.9	6.0	2.9	8.0	2.9	10.0	2.9	15.0

TABLE(35)

INJECTION CONCENTRATION = 500 W.P.P.M.
 INJECTION VELOCITY / MAIN STREAM VELOCITY = 1.34
 INJECTION OPTICAL DENSITY = 5500
 UPSTREAM CONCENTRATION = 2.5

	1.81		1.90		1.97		2.03		2.33
	92.4		60.6		35.2		20.3		5.7
	0.82		0.557		0.338		0.166		0.0716
	32.9		66.7		181.2		694.0		4232.0
-1.75	4.0	1.5	7.0	-1.00	10.0	0.5	19.0	-0.30	23.0
-1.25	10.0	1.0	16.0	-0.75	14.0	0.4	49.0	-0.20	29.0
-0.90	15.0	0.7	32.0	-0.50	40.0	0.3	153.0	-0.15	37.0
-0.60	22.0	0.4	58.5	-0.30	101.0	0.2	443.0	-0.10	130.0
-0.30	34.0	0.2	65.0	-0.15	162.0	0.1	725.0	-0.05	736.0
0.00	36.0	0.0	75.0	0.00	202.0	0.0	625.0	0.00	3324.0
0.30	36.0	-0.2	68.5	0.15	171.0	-0.1	340.0	0.05	4320.0
0.60	30.0	-0.4	52.0	0.30	118.0	-0.2	133.0	0.10	2786.0
0.90	24.0	-0.7	24.0	0.50	47.0	-0.3	45.0	0.15	520.0
1.25	13.0	-1.0	15.0	0.75	18.0	-0.4	21.5	0.20	87.0
1.75	9.0	-1.5	9.0	1.00	12.0	-0.5	14.5	0.30	25.0
2.9	6.0	2.9	8.0	2.9	11.0	2.9	13.0	2.9	23.0

TABLE(36)

INJECTION CONCENTRATION = 1000 W.P.P.M.

INJECTION VELOCITY / MAIN STREAM VELOCITY = .67

INJECTION OPTICAL DENSITY = 7800

UPSTREAM CONCENTRATION = 1.5

	1.63		1.74		2.13		2.29		2.07
	92.4		60.6		35.2		20.3		5.7
	0.774		0.526		0.329		0.186		0.083
	22.7		50.9		141.7		563.0		4675.0
-1.75	3.0	1.5	5.0	-1.00	7.0	0.5	15.5	-0.30	12.0
-1.25	7.0	1.0	11.0	-0.75	11.0	0.4	46.0	-0.20	52.0
-0.90	11.0	0.7	20.5	-0.50	30.0	0.3	130.0	-0.15	396.0
-0.60	16.0	0.4	38.5	-0.30	74.5	0.2	321.0	-0.10	1678.0
-0.30	23.0	0.2	55.0	-0.15	135.0	0.1	554.0	-0.05	3464.0
0.00	26.0	0.0	56.0	0.00	157.0	0.0	575.0	0.00	4818.0
0.30	23.0	-0.2	50.0	0.15	129.0	-0.1	379.0	0.05	3727.0
0.60	19.0	-0.4	36.0	0.30	82.5	-0.2	172.0	0.10	1780.0
0.90	13.0	-0.7	20.0	0.50	34.5	-0.3	49.0	0.15	508.0
1.25	8.0	-1.0	12.0	0.75	13.0	-0.4	19.0	0.20	78.0
1.75	6.0	-1.5	7.0	1.00	11.0	-0.5	16.0	0.30	17.0
2.9	4.0	2.9	6.0	2.9	8.0	2.9	11.0	2.9	14.0

TABLE(37)

INJECTION CONCENTRATION = 1000 W.P.P.M.

INJECTION VELOCITY / MAIN STREAM VELOCITY = 1.00

INJECTION OPTICAL DENSITY = 5400

UPSTREAM CONCENTRATION = 3.0

	1.86		1.98		1.77		1.99		2.25
	92.4		60.6		35.2		20.3		5.7
	0.73		0.49		0.262		0.15		0.072
	27.3		66.1		199.3		877.0		4099.0
-1.75	3.0	1.5	4.0	-1.00	6.0	0.5	12.0	-0.30	13.0
-1.25	7.0	1.0	8.0	-0.75	7.0	0.4	22.0	-0.20	23.0
-0.90	13.0	0.7	22.0	-0.50	37.0	0.3	68.0	-0.15	171.0
-0.60	19.0	0.4	38.0	-0.30	101.0	0.2	287.0	-0.10	1010.0
-0.30	29.0	0.2	67.0	-0.15	172.0	0.1	750.0	-0.05	2940.0
0.00	29.0	0.0	70.0	0.00	210.0	0.0	910.0	0.00	4212.0
0.30	26.0	-0.2	68.0	0.15	154.0	-0.1	512.0	0.05	2970.0
0.60	20.0	-0.4	42.0	0.30	72.0	-0.2	209.0	0.10	908.0
0.90	11.0	-0.7	20.0	0.50	27.0	-0.3	46.0	0.15	105.0
1.25	7.0	-1.0	9.0	0.75	13.0	-0.4	17.0	0.20	23.0
1.75	3.0	-1.5	5.0	1.00	9.0	-0.5	13.0	0.30	16.0
2.9	3.0	2.9	5.0	2.9	8.0	2.9	12.0	2.9	14.0

TABLE(38)

INJECTION CONCENTRATION = 1000 W.P.P.M.

INJECTION VELOCITY / MAIN STREAM VELOCITY = 1.34

INJECTION OPTICAL DENSITY = 4200

UPSTREAM CONCENTRATION = 1.0

	2.12		2.08		1.90		2.50		2.40
	92.4		60.6		35.2		20.3		5.7
	0.683		0.447		0.237		0.142		0.0718
	37.8		85.2		236.2		857.0		3387.0
-1.75	2.0	1.5	4.0	-1.00	7.0	0.5	10.0	-0.30	11.0
-1.25	5.0	1.0	7.0	-0.75	9.0	0.4	14.0	-0.20	12.0
-0.90	10.0	0.7	17.0	-0.50	20.0	0.3	50.0	-0.15	44.0
-0.60	28.0	0.4	54.0	0					
-0.60	28.0	0.4	54.0	-0.30	85.0	0.2	284.0	-0.10	481.0
-0.30	36.5	0.2	91.0	-0.15	176.0	0.1	822.0	-0.05	2145.0
0.00	41.0	0.0	94.0	0.00	257.0	0.0	872.0	0.00	3363.0
0.30	31.0	-0.2	69.0	0.15	182.0	-0.1	337.0	0.05	2800.0
0.60	24.0	-0.4	43.0	0.30	78.0	-0.2	88.0	0.10	1001.0
0.90	13.0	-0.7	17.0	0.50	17.0	-0.3	21.0	0.15	90.0
1.25	5.0	-1.0	9.0	0.75	10.0	-0.4	13.0	0.20	18.0
1.75	4.0	-1.5	7.0	1.00	9.0	-0.5	11.0	0.30	14.0
2.9	3.0	2.9	6.0	2.9	8.0	2.0	11.0	2.9	14.0

POINT SOURCE INJECTION

UNIFORM FLOW

L = 75.0 MM.

TABLE(39)

INJECTION CONCENTRATION = 0 W.P.P.M.
 INJECTION VELOCITY / MAIN STREAM VELOCITY = .67
 INJECTION OPTICAL DENSITY = 8000
 UPSTREAM CONCENTRATION = 2.0

	1.86		2.13		2.33		2.63		2.07
	99.7		60.6		35.2		17.2		4.5
	0.80		0.565		0.365		0.22		0.086
	28.0		50.5		103.5		300.0		2400.0
-1.75	3.0	1.5	6.0	-1.00	6.0	0.5	19.0	-0.30	7.0
-1.25	4.0	1.0	8.0	-0.75	6.0	0.4	48.0	-0.20	21.0
-0.90	5.0	0.7	32.0	-0.50	15.0	0.3	155.0	-0.15	101.0
-0.60	10.0	0.4	38.0	-0.30	41.0	0.2	236.0	-0.10	408.0
-0.30	14.0	0.2	58.0	-0.15	70.0	0.1	302.0	-0.05	1248.0
0.00	23.0	0.0	55.0	0.00	118.0	0.0	300.0	0.00	2275.0
0.30	21.0	-0.2	44.0	0.15	94.0	-0.1	193.0	0.05	2320.0
0.60	24.0	-0.4	32.0	0.30	92.0	-0.2	115.0	0.10	1567.0
0.90	24.0	-0.7	8.0	0.50	57.0	-0.3	45.0	0.15	581.0
1.25	12.0	-1.00	8.0	0.75	16.0	-0.4	18.0	0.20	191.0
1.75	6.0	-1.5	5.0	1.00	6.0	-0.5	8.0	0.30	10.0
2.9	2.0	2.9	5.0	2.9	6.0	2.9	7.0	2.9	9.0

TABLE(40)

INJECTION CONCENTRATION = 0 W.P.P.M.
 INJECTION VELOCITY / MAIN STREAM VELOCITY = 1.00
 INJECTION OPTICAL DENSITY = 6400
 UPSTREAM CONCENTRATION = 2.0

	1.81		1.72		1.98		2.03		1.93
	99.7		60.6		35.2		17.2		4.5
	0.82		0.53		0.41		0.22		0.0785
	26.0		67.0		104.0		337.0		2724.0
-1.75	4.0	1.5	4.0	-1.00	7.0	0.5	13.0	-0.30	12.0
-1.25	6.0	1.0	8.0	-0.75	18.0	0.4	31.0	-0.20	197.0
-0.90	8.0	0.7	19.0	-0.50	47.0	0.3	71.0	-0.15	1060.0
-0.60	24.0	0.4	40.0	-0.30	90.0	0.2	134.0	-0.10	2355.0
-0.30	31.0	0.2	41.0	-0.15	101.0	0.1	227.0	-0.05	2752.0
0.00	23.0	0.0	82.0	0.00	110.0	0.0	356.0	0.00	1721.0
0.30	24.0	-0.2	66.0	0.15	86.0	-0.1	349.0	0.05	688.0
0.60	23.0	-0.4	58.0	0.30	72.0	-0.2	263.0	0.10	190.0
0.90	12.0	-0.7	26.0	0.50	29.0	-0.3	158.0	0.15	55.0
1.25	8.0	-1.0	11.0	0.75	12.0	-0.4	82.0	0.20	40.0
1.75	6.0	-1.5	7.0	1.00	7.0	-0.5	22.0	0.30	10.0
2.9	2.0	2.9	3.0	2.9	4.0	2.9	5.0	2.9	6.0

TABLE(41)

INJECTION CONCENTRATION = 0 W.P.P.M.
 INJECTION VELOCITY / MAIN STREAM VELOCITY = 1.34
 INJECTION OPTICAL DENSITY = 4400.0
 UPSTREAM CONCENTRATION = 0.0

	1.51		1.44		2.07		2.05		2.41
	99.7		60.6		35.2		17.2		4.5
	0.715		0.49		0.34		0.225		0.087
	26.0		63.0		138.0		394.0		2797.0
-1.75	1.5	1.5	4.0	-1.00	5.0	0.5	14.0	-0.30	5.0
-1.25	4.0	1.0	14.0	-0.75	7.0	0.4	23.0	-0.20	42.0
-0.90	6.0	0.7	20.0	-0.50	28.0	0.3	82.0	-0.15	196.0
-0.60	13.0	0.4	40.0	-0.30	57.0	0.2	204.0	-0.10	1268.0
-0.30	18.0	0.2	57.0	-0.15	129.0	0.1	333.0	-0.05	2374.0
0.00	23.5	0.0	76.0	0.00	148.0	0.0	436.0	0.00	2926.0
0.30	32.0	-0.2	54.0	0.15	127.0	-0.1	344.0	0.05	2116.0
0.60	20.0	-0.4	39.0	0.30	94.0	-0.2	231.0	0.10	702.0
0.90	16.0	-0.7	19.0	0.50	41.0	-0.3	141.0	0.15	158.0
1.25	11.0	-1.0	8.0	0.75	10.0	-0.4	48.0	0.20	44.0
1.75	3.0	-1.5	6.0	1.00	5.0	-0.5	14.0	0.30	7.0
2.9	1.5	2.9	4.0	2.9	4.0	2.9	5.0	2.9	6.0

TABLE(42)

INJECTION CONCENTRATION = 50 W.P.P.M.
 INJECTION VELOCITY / MAIN STREAM VELOCITY = .67
 INJECTION OPTICAL DENSITY = 24000
 UPSTREAM CONCENTRATION = 5.0

	1.72		1.93		2.17		2.25		2.06
	99.7		60.6		35.2		17.2		4.5
	0.635		0.54		0.36		0.235		0.085
	72.5		151.5		342.5		891.0		8707.0
2.9	5.0	2.9	19.0	2.9	5.0	2.9	19.0	2.9	0.0
-1.75	6.0	1.5	20.0	-1.00	7.0	0.5	45.0	-0.30	13.0
-1.25	11.0	1.0	37.0	-0.75	13.0	0.4	80.0	-0.20	405.0
-0.90	19.0	0.7	76.0	-0.50	85.0	0.3	213.0	-0.15	1699.0
-0.60	37.0	0.4	124.0	-0.30	194.0	0.2	524.0	-0.10	4707.0
-0.30	45.0	0.2	165.0	-0.15	313.0	0.1	740.0	-0.05	8429.0
0.00	86.0	0.0	160.0	0.00	378.0	0.0	924.0	0.00	8496.0
0.30	78.0	-0.2	172.0	0.15	286.0	-0.1	862.0	0.05	4882.0
0.60	52.0	-0.4	100.0	0.30	240.0	-0.2	619.0	0.10	2023.0
0.90	29.5	-0.7	58.0	0.50	89.0	-0.3	354.0	0.15	674.0
1.25	24.0	-1.0	32.5	0.75	21.0	-0.4	141.0	0.20	229.0
1.75	7.0	-1.5	19.0	1.00	11.0	-0.5	52.0	0.30	27.0
2.9	6.0	2.9	18.0	2.9	9.0	2.9	19.0	2.9	0.0

TABLE(43)

INJECTION CONCENTRATION = 50 W.P.P.M.

INJECTION VELOCITY / MAIN STREAM VELOCITY = 1.00

INJECTION OPTICAL DENSITY = 24000

UPSTREAM CONCENTRATION = 14.0

	1.89		1.86		2.07		2.17		2.14
	99.7		60.6		35.2		17.2		4.5
	0.77		0.49		0.35		0.24		0.0745
	97.0		264.0		528.0		1440.0		16064.0
2.9	14.0	2.9	21.0	2.9	16.0	2.9	21.0	2.9	27.0
-1.75	17.0	1.5	27.0	-1.00	24.0	0.5	86.0	-0.30	40.0
-1.25	20.0	1.0	42.0	-0.75	32.0	0.4	242.0	-0.20	526.0
-0.90	40.0	0.7	77.0	-0.50	137.0	0.3	474.0	-0.15	1915.0
-0.60	75.0	0.4	192.0	-0.30	338.0	0.2	865.0	-0.10	6136.0
-0.30	92.0	0.2	267.0	-0.15	421.0	0.1	1324.0	-0.05	14174.0
0.00	92.0	0.0	285.0	0.00	596.0	0.0	1493.0	0.00	16197.0
0.30	120.0	-0.2	263.0	0.15	506.0	-0.1	1314.0	0.05	8645.0
0.60	71.0	-0.4	150.0	0.30	289.0	-0.2	898.0	0.10	2522.0
0.90	51.0	-0.7	85.0	0.50	138.0	-0.3	484.0	0.15	482.0
1.25	28.0	-1.0	40.0	0.75	39.0	-0.4	194.0	0.20	121.0
1.75	12.0	-1.5	22.5	1.00	17.0	-0.5	59.0	0.30	2.0
2.9	6.0	2.9	18.0	2.9	9.0	2.9	19.0	2.9	0.0

TABLE(44)

INJECTION CONCENTRATION = 50 W.P.P.M.

INJECTION VELOCITY / MAIN STREAM VELOCITY = 1.34

INJECTION OPTICAL DENSITY = 24000

UPSTREAM CONCENTRATION = 14.0

2.16	2.01	1.72	2.00	2.84					
99.7	60.6	35.2	17.2	4.5					
0.715	0.50	0.28	0.19	0.068					
158.0	339.0	914.0	2386.0	20751.0					
2.9	14.0	2.9	21.0	2.9	16.0	2.9	21.0	2.9	27.0
-1.75	25.0	1.5	24.0	-1.00	17.0	0.5	75.0	-0.30	30.0
-1.25	27.0	1.0	32.0	-0.75	39.0	0.4	216.0	-0.20	67.0
-0.90	49.0	0.7	114.0	-0.50	164.0	0.3	469.0	-0.15	674.0
-0.60	101.0	0.4	227.0	-0.30	522.0	0.2	954.0	-0.10	5934.0
-0.30	145.0	0.2	349.0	-0.15	717.0	0.1	1658.0	-0.05	18935.0
0.00	153.0	0.0	386.0	0.00	949.0	0.0	2550.0	0.00	20944.0
0.30	178.0	-0.2	308.0	0.15	801.0	-0.1	2236.0	0.05	7930.0
0.60	152.0	-0.4	219.0	0.30	345.0	-0.2	1123.0	0.10	2104.0
0.90	61.0	-0.7	107.0	0.50	141.0	-0.3	475.0	0.15	378.0
1.25	56.0	-1.0	43.0	0.75	49.0	-0.4	142.0	0.20	54.0
1.75	26.0	-1.5	29.0	1.00	24.0	-0.5	52.0	0.30	27.0
2.9	19.0	2.9	25.0	2.9	19.0	2.9	24.0	2.9	25.0

TABLE(45)

INJECTION CONCENTRATION = 100 W.P.P.M.
 INJECTION VELOCITY / MAIN STREAM VELOCITY = .67
 INJECTION OPTICAL DENSITY = 24000
 UPSTREAM CONCENTRATION = 1.0

	1.53		1.99		2.09		2.44		1.98
	99.7		60.6		35.2		17.2		4.5
	0.66		0.505		0.405		0.24		0.077
	88.0		161.5		296.0		894.0		11350.0
2.9	1.0	2.9	21.0	2.9	5.0	2.9	15.0	2.9	0.0
-1.75	4.0	1.5	23.0	-1.00	7.0	0.5	43.0	-0.30	2.0
-1.25	5.5	1.0	28.0	-0.75	12.0	0.4	115.0	-0.20	244.0
-0.90	21.0	0.7	61.0	-0.50	100.0	0.3	175.0	-0.15	1167.0
-0.60	57.0	0.4	113.0	-0.30	210.0	0.2	492.0	-0.10	4492.0
-0.30	64.0	0.2	138.0	-0.15	282.0	0.1	608.0	-0.05	10016.0
0.00	100.0	0.0	185.0	0.00	308.0	0.0	950.0	0.00	11563.0
0.30	84.0	-0.2	201.0	0.15	273.0	-0.1	903.0	0.05	6352.0
0.60	46.0	-0.4	123.0	0.30	200.0	-0.2	710.0	0.10	2551.0
0.90	35.0	-0.7	65.0	0.50	112.0	-0.3	393.0	0.15	692.0
1.25	20.0	-1.0	35.0	0.75	32.0	-0.4	165.0	0.20	95.0
1.75	11.0	-1.5	22.0	1.00	8.0	-0.5	45.0	0.30	2.0
2.9	4.0	2.9	21.0	2.9	5.0	2.9	17.0	2.9	0.0

TABLE(46)

INJECTION CONCENTRATION = 100 W.P.P.M.

INJECTION VELOCITY / MAIN STREAM VELOCITY = 1.00

INJECTION OPTICAL DENSITY = 24000

UPSTREAM CONCENTRATION = 13.0

	1.98		1.95		2.35		2.18		2.64
	99.7		60.6		35.2		17.2		4.5
	0.76		0.51		0.38		0.23		0.0664
	102.0		243.0		521.0		1487.0		21409.0
2.9	13.0	2.9	22.0	2.9	10.0	2.9	20.0	2.9	0.0
-1.75	14.0	1.5	23.0	-1.00	13.0	0.5	47.0	-0.30	2.0
-1.25	28.0	1.0	42.0	-0.75	32.0	0.4	158.0	-0.20	163.0
-0.90	39.0	0.7	83.0	-0.50	128.0	0.3	453.0	-0.15	1208.0
-0.60	69.0	0.4	181.0	-0.30	390.0	0.2	702.0	-0.10	4492.0
-0.30	87.0	0.2	244.0	-0.15	557.0	0.1	1443.0	-0.05	18050.0
0.00	101.0	0.0	293.0	0.00	508.0	0.0	1518.0	0.00	21457.0
0.30	108.0	-0.2	218.0	0.15	403.0	-0.1	1258.0	0.05	10410.0
0.60	104.0	-0.4	167.0	0.30	343.0	-0.2	1078.0	0.10	1724.0
0.90	40.0	-0.7	92.0	0.50	153.0	-0.3	413.0	0.15	299.0
1.25	30.0	-1.0	31.0	0.75	38.0	-0.4	185.0	0.20	41.0
1.75	9.0	-1.5	22.0	1.00	10.0	-0.5	62.0	0.30	2.0
2.9	4.0	2.9	21.0	2.9	5.0	2.9	13.0	2.9	0.0

TABLE(47)

INJECTION CONCENTRATION = 100 W.P.M.

INJECTION VELOCITY / MAIN STREAM VELOCITY = 1.34

INJECTION OPTICAL DENSITY = 27000

UPSTREAM CONCENTRATION = 13.0

	1.98		2.18		1.92		2.18		2.74
	99.7		60.6		35.2		17.2		4.5
	0.665		0.54		0.34		0.215		0.064
	149.0		329.0		817.0		2220.0		25236.0
2.9	13.0	2.9	21.0	2.9	10.0	2.9	20.0	2.9	0.0
-1.75	17.0	1.5	22.0	-1.00	12.0	0.5	67.0	-0.30	2.0
-1.25	24.0	1.0	50.0	-0.75	57.0	0.4	107.0	-0.20	14.0
-0.90	47.0	0.7	117.0	-0.50	158.0	0.3	528.0	-0.15	651.0
-0.60	120.0	0.4	235.0	-0.30	358.0	0.2	773.0	-0.10	4614.0
-0.30	133.0	0.2	332.0	-0.15	857.0	0.1	2047.0	-0.05	21511.0
0.00	165.0	0.0	327.0	0.00	835.0	0.0	2303.0	0.00	25022.0
0.30	159.0	-0.2	345.0	0.15	627.0	-0.1	2027.0	0.05	12798.0
0.60	91.0	-0.4	264.0	0.30	358.0	-0.2	1280.0	0.10	2497.0
0.90	59.0	-0.7	122.0	0.50	192.0	-0.3	585.0	0.15	285.0
1.25	40.0	-1.0	50.0	0.75	65.0	-0.4	205.0	0.20	41.0
1.75	29.0	-1.5	37.0	1.00	20.0	-0.5	63.0	0.30	2.0
2.9	21.0	2.9	22.0	2.9	15.0	2.9	25.0	2.9	0.0

TABLE(48)

INJECTION CONCENTRATION = 250 W.P.P.M.

INJECTION VELOCITY / MAIN STREAM VELOCITY = .67

INJECTION OPTICAL DENSITY = 24000

UPSTREAM CONCENTRATION = 2.0

	2.13		1.97	<i>Q</i>	1.93		2.09		2.21
	99.7		60.6		35.2		17.2		4.5
	0.77		0.56		0.345		0.195		0.076
	60.0		162.0		369.0		1091.0		10668.0
2.9	2.0	2.9	16.0	2.9	0.0	2.9	15.0	2.9	14.0
-1.75	2.5	1.5	17.0	-1.00	2.0	0.5	32.0	-0.30	28.0
-1.25	12.0	1.0	24.0	-0.75	27.0	0.4	95.0	-0.20	247.0
-0.90	15.0	0.7	74.0	-0.50	90.0	0.3	169.0	-0.15	1620.0
-0.60	35.0	0.4	120.0	-0.30	232.0	0.2	461.0	-0.10	5547.0
-0.30	50.0	0.2	144.0	-0.15	335.0	0.1	840.0	-0.05	11052.0
0.00	59.0	0.0	187.0	0.00	400.0	0.0	1147.0	0.00	9542.0
0.30	62.0	-0.2	186.0	0.15	304.0	-0.1	982.0	0.05	3940.0
0.60	56.0	-0.4	141.0	0.30	191.0	-0.2	619.0	0.10	947.0
0.90	35.0	-0.7	71.0	0.50	80.0	-0.3	274.0	0.15	206.0
1.25	22.0	-1.0	28.0	0.75	35.0	-0.4	86.0	0.20	69.0
1.75	7.0	-1.5	22.0	1.00	5.				
1.75	7.0	-1.5	22.0	1.00	8.0	-0.5	45.0	0.30	15.0
2.9	5.0	2.9	19.0	2.9	5.0	2.9	18.0	2.9	14.0

TABLE(49)

INJECTION CONCENTRATION = 250 W.P.P.M.
 INJECTION VELOCITY / MAIN STREAM VELOCITY = 1.00
 INJECTION OPTICAL DENSITY = 24000
 UPSTREAM CONCENTRATION = 12.0

2.22		2.03		2.64		2.17		2.38	
99.7		60.6		35.2		17.2		4.5	
0.755		0.53		0.325		0.207		0.073	
96.0		187.0		615.0		1746.0		17634.0	
2.9	12.0	2.9	21.0	2.9	8.0	2.9	18.0	2.9	14.0
-1.75	17.0	1.5	22.0	-1.00	10.0	0.5	40.0	-0.30	28.0
-1.25	18.0	1.0	33.0	-0.75	15.0	0.4	111.0	-0.20	206.0
-0.90	38.0	0.7	85.0	-0.50	93.0	0.3	295.0	-0.15	1634.0
-0.60	49.0	0.4	147.0	-0.30	395.0	0.2	938.0	-0.10	10764.0
-0.30	103.0	0.2	222.0	-0.15	649.0	0.1	1220.0	-0.05	18920.0
0.00	87.0	0.0	206.0	0.00	556.0	0.0	1721.0	0.00	13977.0
0.30	99.0	-0.2	180.0	0.15	508.0	-0.1	1800.0	0.05	4270.0
0.60	92.0	-0.4	110.0	0.30	290.0	-0.2	1030.0	0.10	810.0
0.90	51.0	-0.7	80.0	0.50	95.0	-0.3	350.0	0.15	82.0
1.25	24.0	-1.0	38.0	0.75	13.0	-0.4	100.0	0.20	41.0
1.75	7.0	-1.5	23.0	1.00	8.0	-0.5	37.0	0.30	28.0
2.9	5.0	2.9	19.0	2.9	5.0	2.9	18.0	2.9	14.0

TABLE(50)

INJECTION CONCENTRATION = 250 W.P.P.M.
 INJECTION VELOCITY / MAIN STREAM VELOCITY = 1.34
 INJECTION OPTICAL DENSITY = 26000
 UPSTREAM CONCENTRATION = 11.0

	1.80		2.25		1.96		2.02		2.30
	99.7		60.6		35.2		17.2		4.5
	0.603		0.50		0.27		0.189		0.0625
	144.0		359.0		1051.0		2653.0		24356.0
2.9	11.0	2.9	21.0	2.9	10.0	2.9	18.0	2.9	14.0
-1.75	12.0	1.5	22.0	-1.00	13.0	0.5	32.0	-0.30	28.0
-1.25	29.0	1.0	52.0	-0.75	40.0	0.4	96.0	-0.20	55.0
-0.90	35.0	0.7	100.0	-0.50	128.0	0.3	254.0	-0.15	892.0
-0.60	61.0	0.4	244.0	-0.30	533.0	0.2	546.0	-0.10	10476.0
-0.30	141.0	0.2	361.0	-0.15	918.0	0.1	1706.0	-0.05	22695.0
0.00	154.0	0.0	339.0	0.00	1084.0	0.0	2818.0	0.00	21116.0
0.30	151.0	-0.2	392.0	0.15	772.0	-0.1	2414.0	0.05	6230.0
0.60	91.0	-0.4	257.0	0.30	383.0	-0.2	1505.0	0.10	453.0
0.90	67.0	-0.7	104.0	0.50	189.0	-0.3	480.0	0.15	69.0
1.25	47.0	-1.0	60.0	0.75	22.0	-0.4	181.0	0.20	56.0
1.75	21.0	-1.5	33.0	1.00	18.0	-0.5	61.0	0.30	42.0
2.9	20.0	2.9	25.0	2.9	17.0	2.9	28.0	2.9	27.0

TABLE(51)

INJECTION CONCENTRATION = 500 W.P.P.M.

INJECTION VELOCITY / MAIN STREAM VELOCITY = .67

INJECTION OPTICAL DENSITY = 21000

UPSTREAM CONCENTRATION = 1.0

2.21		1.88		2.06		2.25		1.95	
99.7		60.6		35.2		17.2		4.5	
0.653		0.49		0.347		0.200		0.0678	
72.0		163.0		329.0		1023.0		7985.0	
2.9	1.0	2.9	17.0	2.9	2.0	2.9	17.0	2.9	23.0
-1.75	5.0	1.5	18.0	-1.00	3.0	0.5	26.0	-0.30	25.0
-1.25	7.0	1.0	29.0	-0.75	9.0	0.4	53.0	-0.20	152.0
-0.90	16.0	0.7	43.0	-0.50	67.0	0.3	120.0	-0.15	832.0
-0.60	35.0	0.4	100.0	-0.30	210.0	0.2	330.0	-0.10	3810.0
-0.30	61.0	0.2	144.0	-0.15	274.0	0.1	646.0	-0.05	7854.0
0.00	69.0	0.0	194.0	0.00	345.0	0.0	1005.0	0.00	6787.0
0.30	76.0	-0.2	171.0	0.15	299.0	-0.1	1021.0	0.05	2977.0
0.60	58.0	-0.4	133.0	0.30	202.0	-0.2	793.0	0.10	656.0
0.90	21.0	-0.7	68.0	0.50	87.0	-0.3	277.0	0.15	140.0
1.25	12.0	-1.0	27.0	0.75	19.0	-0.4	92.0	0.20	36.0
1.75	7.0	-1.5	23.0	1.00	8.0	-0.5	39.0	0.30	25.0
2.9	6.0	2.9	18.0	2.9	7.0	2.9	17.0	2.9	23.0

TABLE(52)

INJECTION CONCENTRATION = 500 W.P.P.M.

INJECTION VELOCITY / MAIN STREAM VELOCITY = 1.00

INJECTION OPTICAL DENSITY = 21000

UPSTREAM CONCENTRATION = 11.0

2.21		1.75		1.86		1.91		2.13	
99.7		60.6		35.2		17.2		4.5	
0.684		0.49		0.306		0.186		0.0659	
106.5		241.0		535.0		1975.0		12559.0	
2.9	11.0	2.9	20.0	2.9	10.0	2.9	17.0	2.9	23.0
-1.75	14.0	1.5	21.0	-1.00	17.0	0.5	27.0	-0.30	25.0
-1.25	22.0	1.0	46.0	-0.75	22.0	0.4	91.0	-0.20	70.0
-0.90	31.0	0.7	82.0	-0.50	108.0	0.3	173.0	-0.15	1278.0
-0.60	60.0	0.4	158.0	-0.30	337.0	0.2	761.0	-0.10	6131.0
-0.30	95.0	0.2	206.0	-0.15	497.0	0.1	1574.0	-0.05	13293.0
0.00	113.0	0.0	284.0	0.00	585.0	0.0	2144.0	0.00	8592.0
0.30	104.0	-0.2	254.0	0.15	350.0	-0.1	1596.0	0.05	2051.0
0.60	92.0	-0.4	162.0	0.30	268.0	-0.2	966.0	0.10	246.0
0.90	41.0	-0.7	77.0	0.50	87.0	-0.3	443.0	0.15	35.0
1.25	21.0	-1.0	35.0	0.75	14.0	-0.4	135.0	0.20	25.0
1.75	7.0	-1.5	22.0	1.00	8.0	-0.5	46.0	0.30	23.0
2.9	6.0	2.9	18.0	2.9	7.0	2.9	17.0	2.9	23.0

TABLE(53)

INJECTION CONCENTRATION = 500 W.P.P.M.
 INJECTION VELOCITY / MAIN STREAM VELOCITY = 1.34
 INJECTION OPTICAL DENSITY = 21000
 UPSTREAM CONCENTRATION = 11.0

	1.79		1.92		2.05		2.44		2.17
	99.7		60.6		35.2		17.2		4.5
	0.691		0.46		0.367		0.165		0.058
	167.0		385.0		757.0		3499.0		15783.0
2.9	11.0	2.9	19.0	2.9	10.0	2.9	17.0	2.9	23.0
-1.75	19.0	1.5	20.0	-1.00	12.0	0.5	32.0	-0.30	25.0
-1.25	29.0	1.0	38.0	-0.75	53.0	0.4	70.0	-0.20	47.0
-0.90	57.0	0.7	57.0	-0.50	371.0	0.8	137.0	-0.15	656.0
-0.60	126.0	0.4	247.0	-0.30	516.0	0.2	504.0	-0.10	6588.0
-0.30	162.0	0.2	396.0	-0.15	680.0	0.1	2041.0	-0.05	15479.0
0.00	193.0	0.0	386.0	0.00	798.0	0.0	3453.0	0.00	12202.0
0.30	145.0	-0.2	407.0	0.15	617.0	-0.1	3658.0	0.05	2321.0
0.60	107.0	-0.4	177.0	0.30	405.0	-0.2	1332.0	0.10	258.0
0.90	72.0	-0.7	136.0	0.50	164.0	-0.3	397.0	0.15	47.0
1.25	37.0	-1.0	57.0	0.75	34.0	-0.4	140.0	0.20	36.0
1.75	19.0	-1.5	27.0	1.00	22.0	-0.5	44.0	0.30	23.0
2.9	18.0	2.9	25.0	2.9	17.0	2.9	27.0	2.9	23.0

TABLE(54)

INJECTION CONCENTRATION = 1000 W.P.P.M.
 INJECTION VELOCITY / MAIN STREAM VELOCITY = .67
 INJECTION OPTICAL DENSITY = 21000
 UPSTREAM CONCENTRATION = 2.0

1.92		1.94		2.52		2.73		1.98	
99.7		60.6		35.2		17.2		4.5	
0.682		0.363		0.25		0.149		0.0617	
58.0		171.0		367.0		1816.0		16876.0	
2.9	2.0	2.9	17.0	2.9	3.0	2.9	9.0	2.9	13.0
-1.75	6.0	1.5	18.0	-1.00	8.0	0.5	21.0	-0.38	39.0
-1.25	8.0	1.0	19.0	-0.75	17.0	0.2	34.0	-0.20	76.0
-0.90	12.0	0.7	27.0	-0.50	59.0	0.3	129.0	-0.15	835.0
-0.60	43.0	0.4	59.0	-0.30	134.0	0.2	244.0	-0.10	5428.0
-0.30	58.0	0.2	156.0	-0.15	313.0	0.1	1130.0	-0.05	15183.0
0.00	62.0	0.0	162.0	0.00	370.0	0.0	1512.0	0.00	15272.0
0.30	45.0	-0.2	192.0	0.15	299.0	-0.1	1954.0	0.05	6010.0
0.60	41.0	-0.4	105.0	0.30	86.0	-0.2	575.0	0.10	974.0
0.90	20.0	-0.7	46.0	0.50	25.0	-0.3	86.0	0.15	127.0
1.25	9.0	-1.0	25.0	0.75	10.0	-0.4	46.0	0.20	39.0
1.75	8.0	-1.5	23.0	1.00	8.0	-0.5	24.0	0.30	15.0
2.9	4.0	2.9	18.0	2.9	3.0	2.9	17.0	2.9	13.0

TABLE(55)

INJECTION CONCENTRATION = 1000 W.P.P.M.

INJECTION VELOCITY / MAIN STREAM VELOCITY = 1.00

INJECTION OPTICAL DENSITY = 21000

UPSTREAM CONCENTRATION = 10.0

	1.67		1.62		2.43		2.49		2.43
	99.7		60.6		35.2		17.2		4.5
	0.59		0.34		0.23		0.145		0.0593
	74.0		238.0		518.0		3302.0		20964.0
2.9	10.0	2.9	20.0	2.9	7.0	2.9	17.0	2.9	26.0
-1.75	14.0	1.5	21.0	-1.00	17.0	0.5	20.0	-0.30	30.0
-1.25	19.0	1.0	25.0	-0.75	22.0	0.4	34.0	-0.20	51.0
-0.90	23.0	0.7	50.0	-0.50	41.0	0.3	201.0	-0.15	329.0
-0.60	39.0	0.4	78.0	-0.30	151.0	0.2	431.0	-0.10	5023.0
-0.30	51.0	0.2	158.0	-0.15	545.0	0.1	2254.0	-0.05	18486.0
0.00	85.0	0.0	265.0	0.00	453.0	0.0	3233.0	0.00	19005.0
0.30	70.0	-0.2	232.0	0.15	338.0	-0.1	2685.0	0.05	7491.0
0.60	49.0	-0.4	143.0	0.30	98.0	-0.2	1069.0	0.10	367.0
0.90	22.0	-0.7	54.0	0.50	30.0	-0.3	98.0	0.15	26.0
1.25	13.0	-1.0	27.0	0.75	12.0	-0.4	39.0	0.20	20.0
1.75	7.0	-1.5	23.0	1.00	10.0	-0.5	28.0	0.30	15.0
2.9	4.0	2.9	18.0	2.9	3.0	2.9	17.0	2.9	13.0

TABLE(56)

INJECTION CONCENTRATION = 1000 W.P.P.M.

INJECTION VELOCITY / MAIN STREAM VELOCITY = 1.34

INJECTION OPTICAL DENSITY = 21000

UPSTREAM CONCENTRATION = 10.0

	1.68		2.75		2.48		2.23		2.19
	99.7		60.6		35.2		17.2		4.5
	0.55		0.445		0.195		0.12		0.0458
	101.0		296.0		1405.0		5727.0		20135.0
2.9	10.0	2.9	20.0	2.9	7.0	2.9	17.0	2.9	26.0
-1.75	18.0	1.5	21.0	-1.00	13.0	0.5	21.0	-0.30	30.0
-1.25	19.0	1.0	22.0	-0.75	20.0	0.4	42.0	-0.20	52.0
-0.90	31.0	0.7	25.0	-0.50	46.0	0.3	49.0	-0.15	63.0
-0.60	53.0	0.4	95.0	-0.30	250.0	0.2	400.0	-0.10	3176.0
-0.30	120.0	0.2	225.0	-0.15	986.0	0.1	2939.0	-0.05	12476.0
0.00	113.0	0.0	303.0	0.00	1615.0	0.0	6510.0	0.00	19587.0
0.30	70.0	-0.2	317.0	0.15	622.0	-0.1	3108.0	0.05	4036.0
0.60	66.0	-0.4	279.0	0.30	118.0	-0.2	791.0	0.10	291.0
0.90	31.0	-0.7	62.0	0.50	52.0	-0.8	120.0	0.15	38.0
1.25	28.0	-1.0	42.0	0.75	24.0	-0.4	39.0	0.20	29.0
1.75	25.0	-1.5	31.0	1.00	21.0	-0.5	29.0	0.30	26.0
2.9	17.0	2.9	24.0	2.9	15.0	2.9	24.0	2.9	26.0

LINE SOURCE INJECTION

TABLE(57)

INJECTION CONCENTRATION = 0 W.P.P.M.

INJECTION VELOCITY / MAIN STREAM VELOCITY = 0.118

INJECTION OPTICAL DENSITY = 24300

UPSTREAM CONCENTRATION = 2.0

	2.67		2.24		1.93		1.74		1.48
	105.9		67.8		42.5		23.5		10.2
	0.623		0.472		0.396		0.292		0.151
	101.6		122.2		149.9		215.6		394.0
5.5	2.0	5.5	12.0	5.5	14.0	5.5	22.0	5.5	24.0
0.02	100.0	0.02	131.0	0.02	164.0	0.02	229.0	0.02	405.0
0.32	84.0	0.22	120.0	0.17	147.0	0.12	199.0	0.10	295.0
0.62	50.0	0.42	89.0	0.32	112.0	0.22	158.0	0.14	232.0
0.82	25.0	0.62	46.0	0.47	71.0	0.32	117.0	0.18	192.0
1.02	9.0	0.82	29.0	0.62	45.0	0.42	78.0	0.22	144.0
1.27	7.0	1.02	20.0	0.77	28.0	0.52	52.0	0.27	96.0
0.00	102.0	0.00	132.0	0.00	164.0	0.00	235.0	0.00	421.0
5.5	1.0	5.5	13.0	5.5	16.0	5.5	19.0	5.5	27.0

TABLE(58)

INJECTION CONCENTRATION = 0 W.P.P.M.

INJECTION VELOCITY / MAIN STREAM VELOCITY = 0.175

INJECTION OPTICAL DENSITY = 24300

UPSTREAM CONCENTRATION = 1.0

	2.15		1.99		1.95		1.81		1.70
	105.9		67.8		42.5		23.5		10.2
	0.589		0.487		0.398		0.292		0.156
	157.0		188.6		235.4		333.4		615.1
5.5	1.0	5.5	13.0	5.5	16.0	5.5	19.0	5.5	27.0
0.02	156.0	0.02	199.0	0.02	252.0	0.02	339.0	0.02	599.0
0.32	132.0	0.22	171.0	0.17	220.0	0.12	299.0	0.10	460.0
0.62	78.0	0.42	121.0	0.32	164.0	0.22	231.0	0.14	367.0
0.82	41.0	0.62	75.0	0.47	108.0	0.32	171.0	0.18	286.0
1.02	22.0	0.82	36.0	0.62	62.0	0.42	109.0	0.22	195.0
1.27	9.0	1.02	23.0	0.77	35.0	0.52	67.0	0.27	133.0
0.00	160.0	0.00	201.0	0.00	251.0	0.00	356.0	0.00	641.0
5.5	6.0	5.5	14.0	5.5	17.0	5.5	23.0	5.5	26.0

TABLE(59)

INJECTION CONCENTRATION = 0 W.P.P.M.

INJECTION VELOCITY / MAIN STREAM VELOCITY = 0.234

INJECTION OPTICAL DENSITY = 24300

UPSTREAM CONCENTRATION = 6.0

2.04		1.91		1.98		1.77		1.64	
105.9		67.8		42.5		23.5		10.2	
0.581		0.466		0.40		0.294		0.161	
221.1		263.8		326.3		454.1		827.6	
5.5	6.0	5.5	14.0	5.5	17.0	5.5	23.0	5.5	26.0
0.02	214.0	0.02	275.0	0.02	342.0	0.02	470.0	0.02	821.0
0.32	189.0	0.22	240.0	0.17	299.0	0.12	417.0	0.10	630.0
0.62	111.0	0.42	165.0	0.32	224.0	0.22	320.0	0.14	504.0
0.82	66.0	0.62	94.0	0.47	147.0	0.32	227.0	0.18	389.0
1.02	35.0	0.82	50.0	0.62	83.0	0.42	152.0	0.22	278.0
1.27	14.0	1.02	26.0	0.77	44.0	0.52	91.0	0.27	195.0
0.00	221.0	0.00	279.0	0.00	348.0	0.00	478.0	0.00	854.0
5.5	12.0	5.5	14.0	5.5	22.0	5.5	24.0	5.5	27.0

TABLE(60)

INJECTION CONCENTRATION = 100 W.P.P.M.

INJECTION VELOCITY / MAIN STREAM VELOCITY = 0.118

INJECTION OPTICAL DENSITY = 23800

UPSTREAM CONCENTRATION = 4.0

2.28		2.16		1.97		1.55		1.37	
105.9		67.8		42.5		23.5		10.2	
0.619		0.507		0.402		0.273		0.127	
95.6		131.2		173.3		250.7		527.5	
5.5	4.0	5.5	14.0	5.5	13.0	5.5	18.0	5.5	19.0
0.02	99.5	0.02	137.0	0.02	185.0	0.02	253.0	0.02	503.0
0.32	83.0	0.22	124.0	0.17	155.0	0.12	225.0	0.10	324.0
0.62	53.0	0.42	90.0	0.32	121.0	0.22	165.0	0.14	268.0
0.82	28.0	0.62	56.0	0.47	82.0	0.32	126.0	0.18	195.0
1.02	15.0	0.82	26.0	0.62	47.0	0.42	87.0	0.22	128.5
1.27	8.0	1.02	13.0	0.77	26.0	0.52	55.0	0.27	94.0
0.00	99.0	0.00	142.0	0.00	185.0	0.00	280.0	0.00	540.0
5.5	4.0	5.5	6.0	5.5	13.0	5.5	21.0	5.5	19.0

TABLE(61)

INJECTION CONCENTRATION = 100 W.P.P.M.

INJECTION VELOCITY / MAIN STREAM VELOCITY = 0.173

INJECTION OPTICAL DENSITY = 23800

UPSTREAM CONCENTRATION = 4.0

2.21		2.14		2.00		1.58		1.00	
105.9		67.8		42.5		23.5		10.2	
0.619		0.515		0.415		0.264		0.101	
154.3		204.5		256.8		402.4		891.6	
5.5	4.0	5.5	6.0	5.5	13.0	5.5	21.0	5.5	19.0
0.02	154.0	0.02	202.0	0.02	265.0	0.02	386.0	0.02	728.0
0.32	129.0	0.22	191.0	0.17	242.0	0.12	318.0	0.10	493.0
0.62	86.0	0.42	139.0	0.32	180.0	0.22	244.0	0.14	391.0
0.82	47.0	0.62	83.0	0.47	123.0	0.32	184.0	0.18	281.0
1.02	22.0	0.82	42.0	0.62	71.0	0.42	114.0	0.22	220.0
1.27	13.0	1.02	18.0	0.77	33.0	0.52	71.0	0.27	153.0
0.00	160.0	0.00	216.0	0.00	275.0	0.00	432.0	0.00	951.0
5.5	5.0	5.5	13.0	5.5	18.0	5.5	17.0	5.5	21.0

TABLE(62)

INJECTION CONCENTRATION = 100 W.P.P.M.

INJECTION VELOCITY / MAIN STREAM VELOCITY = 0.234

INJECTION OPTICAL DENSITY = 23800

UPSTREAM CONCENTRATION = 5.0

1.91		2.27		1.86		1.61		0.986	
105.9		67.8		42.5		23.5		10.2	
0.571		0.541		0.411		0.294		0.101	
213.4		269.3		346.1		565.7		1342.1	
5.5	5.0	5.5	13.0	5.5	18.0	5.5	17.0	5.5	21.0
0.02	210.0	0.02	275.0	0.02	353.0	0.02	539.0	0.02	1074.0
0.32	176.0	0.22	260.0	0.17	324.0	0.12	464.0	0.10	736.0
0.62	108.0	0.42	195.0	0.32	237.0	0.22	364.0	0.14	562.0
0.82	62.0	0.62	118.0	0.47	162.0	0.32	277.0	0.18	418.0
1.02	37.0	0.82	60.0	0.62	96.0	0.42	184.0	0.22	297.0
1.27	15.0	1.02	26.0	0.77	46.0	0.52	109.0	0.27	209.0
0.00	167.0	0.00	284.0	0.00	371.0	0.00	603.0	0.00	1428.0
5.5	12.0	5.5	13.0	5.5	18.0	5.5	98.0	5.5	27.0

TABLE(63)

INJECTION CONCENTRATION = 250 W.P.P.M.
 INJECTION VELOCITY / MAIN STREAM VELOCITY = 0.118
 INJECTION OPTICAL DENSITY = 23900
 UPSTREAM CONCENTRATION = 3.0

2.19		1.78		1.73		1.59		0.916
105.9		67.8		42.5		23.5		10.2
0.59		0.44		0.386		0.251		0.072
115.3		146.1		179.7		264.4		609.0
5.5	3.0	5.5	7.0	5.5	12.0	5.5	23.0	5.5 18.0
0.02	120.0	0.02	151.0	0.02	186.0	0.02	272.0	0.02 506.0
0.32	92.0	0.17	140.0	0.12	174.0	0.12	230.0	0.09 278.0
0.62	54.0	0.32	106.0	0.22	147.0	0.22	165.0	0.14 208.0
0.82	32.0	0.52	68.0	0.32	122.0	0.32	120.0	0.18 152.0
1.02	13.0	0.72	38.0	0.47	80.0	0.42	73.0	0.22 93.0
1.27	5.0	0.92	20.0	0.62	50.0	0.52	48.0	0.27 64.0
0.00	114.0	0.00	159.0	0.00	195.0	0.00	287.0	0.00 632.0
5.5	2.0	5.5	12.0	5.5	13.0	5.5	18.0	5.5 15.0

TABLE(64)

INJECTION CONCENTRATION = 250 W.P.P.M.
 INJECTION VELOCITY / MAIN STREAM VELOCITY = 0.175
 INJECTION OPTICAL DENSITY = 23900
 UPSTREAM CONCENTRATION = 2.0

2.39		1.83		1.52		1.31		0.702
105.9		67.8		42.5		23.5		10.2
0.607		0.446		0.36		0.206		0.041
168.0		214.2		286.3		468.6		1302.0
5.5	2.0	5.5	12.0	5.5	13.0	5.5	18.0	5.5 15.0
0.02	171.0	0.02	220.0	0.02	297.0	0.02	420.0	0.02 920.0
0.32	145.0	0.17	205.0	0.12	263.0	0.12	338.0	0.09 418.0
0.62	85.0	0.32	160.0	0.22	221.0	0.22	235.0	0.14 288.0
0.82	44.0	0.52	97.0	0.32	173.0	0.32	167.0	0.18 206.0
1.02	18.0	0.72	55.0	0.47	118.0	0.42	100.0	0.22 134.0
1.27	6.0	0.92	27.0	0.62	65.0	0.52	58.0	0.27 82.0
0.00	169.0	0.00	229.0	0.00	305.0	0.00	520.0	0.00 1379.0
5.5	5.0	5.5	11.0	5.5	18.0	5.5	21.0	5.5 28.0

TABLE(65)

INJECTION CONCENTRATION = 250 W.P.P.M.

INJECTION VELOCITY / MAIN STREAM VELOCITY = 0.234

INJECTION OPTICAL DENSITY = 23900

UPSTREAM CONCENTRATION = 5.0

2.37	1.96	1.33	0.751	0.682					
105.9	67.8	42.5	23.5	10.2					
0.623	0.471	0.298	0.121	0.031					
231.9	303.6	431.0	768.4	2117.0					
5.5	5.0	5.5	11.0	5.5	18.0	5.5	21.0	5.5	28.0
0.02	235.0	0.02	309.0	0.02	441.0	0.02	633.0	0.02	1359.0
0.32	193.0	0.17	280.0	0.12	360.0	0.12	426.0	0.09	506.0
0.62	118.0	0.32	230.0	0.22	285.0	0.22	280.0	0.14	360.0
0.82	70.0	0.52	141.0	0.32	229.0	0.32	202.0	0.18	247.0
1.02	29.0	0.72	70.0	0.47	142.0	0.42	131.0	0.22	185.0
1.27	12.0	0.92	35.0	0.62	86.0	0.52	71.0	0.27	111.0
0.00	237.0	0.00	318.0	0.00	455.0	0.00	837.0	0.00	2298.0
5.5	7.0	5.5	12.0	5.5	23.0	5.5	18.0	5.5	31.0

TABLE(66)

INJECTION CONCENTRATION = 500 W.P.P.M.

INJECTION VELOCITY / MAIN STREAM VELOCITY = 0.118

INJECTION OPTICAL DENSITY = 24550

UPSTREAM CONCENTRATION = 1.0

2.06	1.60	1.12	0.633						
105.9	67.8	42.5	23.5						
0.58	0.386	0.245	0.06						
123.1	170.0	240.9	532.0						
5.5	1.0	5.5	12.0	5.5	15.0	5.5	18.0	5.5	5.0
0.02	124.0	0.02	181.0	0.02	246.0	0.02	398.0	0.02	1066.0
0.22	111.0	0.17	154.0	0.12	197.0	0.07	278.0	0.05	396.0
0.42	85.0	0.32	110.0	0.22	146.0	0.12	219.0	0.09	233.0
0.62	59.0	0.47	82.0	0.32	115.0	0.17	185.0	0.13	170.0
0.82	38.0	0.62	53.0	0.42	94.0	0.27	110.0	0.18	94.0
1.02	14.0	0.77	31.0	0.52	65.0	0.37	79.0	0.23	53.0
0.00	127.0	0.00	183.0	0.00	263.0	0.00	605.0	0.00	2058.0
5.5	4.0	5.5	13.0	5.5	18.0	5.5	23.0	5.5	8.0

TABLE(69)

INJECTION CONCENTRATION = 1000 W.P.P.M.

INJECTION VELOCITY / MAIN STREAM VELOCITY = 0.118

INJECTION OPTICAL DENSITY = 100

UPSTREAM CONCENTRATION = 0.025

1.48		0.928		0.639					
105.9		67.8		42.5		23.5		10.2	
0.344		0.162		0.0557		0.0138			
0.82		1.186		2.01		6.21		100.0	
5.5	0.025	5.5	0.041	5.5	0.066	5.5	0.103	5.5	0.079
0.02	0.839	0.02	1.091	0.02	1.583	0.02	2.240	0.02	19.200
0.22	0.566	0.12	0.764	0.07	0.963	0.045	1.157	0.045	5.970
0.42	0.343	0.22	0.504	0.12	0.653	0.07	0.921	0.07	1.140
0.57	0.211	0.32	0.409	0.17	0.562	0.12	0.649	0.095	0.810
0.72	0.120	0.42	0.277	0.22	0.500	0.17	0.438	0.12	0.510
0.82	0.099	0.52	0.202	0.32	0.335	0.22	0.360	0.17	0.340
0.00	0.818	0.00	1.285	0.00	2.200	0.00	8.050	0.00	100.00
5.5	0.017	5.5	0.062	5.5	0.083	5.5	0.079	5.5	0.042

TABLE(70)

INJECTION CONCENTRATION = 1000 W.P.P.M.

INJECTION VELOCITY / MAIN STREAM VELOCITY = 0.175

INJECTION OPTICAL DENSITY = 100

UPSTREAM CONCENTRATION = 0.017

0.875		0.676							
105.9		67.8		42.5		23.5		10.2	
0.181		0.0637		0.0323					
2.1		3.55		6.07		100.0		100.0	
5.5	0.017	5.5	0.062	5.5	0.083	5.5	0.079	5.5	0.042
0.02	1.789	0.02	2.591	0.02	4.674	0.02	11.250	0.02	44.500
0.22	0.967	0.12	1.306	0.07	1.455	0.045	2.471	0.045	2.640
0.42	0.537	0.22	0.769	0.12	0.975	0.07	1.471	0.07	1.470
0.57	0.343	0.32	0.545	0.17	0.760	0.12	0.872	0.095	1.100
0.72	0.194	0.42	0.368	0.22	0.563	0.17	0.628	0.12	0.610
0.82	0.112	0.52	0.256	0.32	0.388	0.22	0.442	0.17	0.440
0.00	2.322	0.00	4.041	0.00	6.120	0.00	100.00	0.00	100.00
5.5	0.037	5.5	0.074	5.5	0.095	5.5	0.099	5.5	0.094

TABLE(71)

INJECTION CONCENTRATION = 1000 W.P.P.M.

INJECTION VELOCITY / MAIN STREAM VELOCITY = 0.234

INJECTION OPTICAL DENSITY = 100

UPSTREAM CONCENTRATION = 0.037

0.813		0.652							
105.9		67.8		42.5		23.5		10.2	
0.118		0.0378		0.023					
4.067		7.98		100.0		100.0		100.0	
5.5	0.037	5.5	0.074	5.5	0.095	5.5	0.099	5.5	0.094
0.02	3.335	0.02	6.210	0.02	16.000	0.02	64.000	0.02	100.0
0.22	1.397	0.12	1.579	0.07	2.037	0.045	4.281	0.045	62.000
0.42	0.624	0.22	0.975	0.12	1.124	0.07	1.744	0.07	4.900
0.57	0.397	0.32	0.686	0.17	0.818	0.12	1.066	0.095	1.560
0.72	0.198	0.42	0.380	0.22	0.686	0.17	0.628	0.12	0.950
0.82	0.136	0.52	0.273	0.32	0.442	0.22	0.492	0.17	0.645
0.00	4.483	0.00	7.900	0.00	100.0	0.00	100.0	0.00	100.0
5.5	0.041	5.5	0.066	5.5	0.103	5.5	0.079	5.5	0.177

* *
 * VELOCITY DATA *
 * *

TABLE(72)

23.5		67.8		105.9	
0.027		0.041		0.056	
0.02	3.00	0.02	2.00	0.02	1.70
0.07	4.00	0.12	3.70	0.12	3.20
0.12	4.30	0.22	4.50	0.22	4.00
0.22	5.00	0.32	5.10	0.42	5.10
0.32	5.30	0.42	5.30	0.62	5.40
0.42	5.50	0.52	5.50	0.82	5.50
0.52	5.50	0.62	5.50	1.02	5.50

TABLE(73)

NO INJECTION

0.0362		
0.015	0.76	0.12
0.020	0.86	0.12
0.025	0.90	0.117
0.040	0.98	0.110
0.060	1.05	0.105
0.080	1.10	0.104
0.100	1.13	0.102
0.150	1.18	0.096
0.20	1.21	0.092
0.30	1.27	0.081
0.400	1.31	0.066
0.500	1.34	0.047
0.600	1.34	0.035

TABLE(74)

INJECTION CONCENTRATION = 100 W.P.P.M.

HEIGHT	NO INJECTION		SERIES(1)		SERIES(2)		SERIES(3)	
	0.0362	0.0357	0.0348	0.0325				
0.015	0.75	0.14	0.75	0.145	0.75	0.142	0.79	0.118
0.020	0.84	0.128	0.89	0.123	0.90	0.125	0.93	0.110
0.025	0.91	0.117	0.93	0.117	0.943	0.117	0.96	0.103
0.040	0.99	0.110	0.99	0.107	1.01	0.107	1.02	0.100
0.060	1.05	0.110	1.05	0.107	1.06	0.103	1.06	0.097
0.080	1.08	0.107	1.09	0.103	1.10	0.100	1.10	0.094
0.100	1.10	0.103	1.11	0.100	1.12	0.098	1.13	0.092
0.150	1.15	0.097	1.15	0.095	1.16	0.093	1.16	0.087
0.200	1.19	0.092	1.19	0.090	1.19	0.089	1.20	0.084
0.300	1.24	0.082	1.24	0.082	1.24	0.080	1.25	0.078
0.400	1.28	0.068	1.28	0.068	1.28	0.068	1.29	0.064
0.500	1.30	0.052	1.30	0.052	1.30	0.052	1.30	0.051
0.600	1.30	0.042	1.30	0.042	1.30	0.042	1.30	0.042

TABLE(75)

INJECTION CONCENTRATION = 500 W.P.P.M.

HEIGHT	NO INJECTION		SERIES (1)	
	0.0305	0.0263		
0.015	0.85	0.12	0.82	0.145
0.020	0.90	0.116	0.90	0.137
0.025	0.93	0.113	0.95	0.134
0.040	1.00	0.107	1.06	0.107
0.060	1.05	0.104	1.10	0.096
0.080	1.10	0.101	1.14	0.090
0.100	1.13	0.097	1.17	0.087
0.150	1.17	0.090	1.20	0.082
0.200	1.21	0.085	1.23	0.078
0.300	1.26	0.070	1.26	0.066
0.400	1.30	0.053	1.30	0.053
0.500	1.30	0.042	1.30	0.042

TABLE(76)

INJECTION CONCENTRATION = 500 W.P.P.M.				
HEIGHT	NO INJECTION		SERIES (2)	
	0.0307		0.0242	
0.015	0.78	0.115	0.60	0.125
0.020	0.86	0.113	0.80	0.142
0.025	0.90	0.111	0.90	0.138
0.040	0.98	0.103	1.05	0.117
0.060	1.05	0.100	1.11	0.105
0.080	1.09	0.098	1.15	0.095
0.100	1.13	0.095	1.17	0.088
0.150	1.18	0.091	1.21	0.080
0.200	1.21	0.084	1.24	0.073
0.300	1.26	0.072	1.28	0.067
0.400	1.30	0.053	1.30	0.054
0.500	1.30	0.042	1.30	0.042
0.600	1.30	0.036	1.30	0.036

TABLE(77)

INJECTION CONCENTRATION = 1000 W.P.P.M.				
HEIGHT	NO INJECTION		SERIES (1)	
	0.0256		0.0196	
0.015	0.78	0.110		
0.020	0.86	0.107	0.75	0.137
0.025	0.92	0.102	0.85	0.135
0.040	1.00	0.099	1.05	0.118
0.060	1.05	0.097	1.12	0.097
0.080	1.10	0.095	1.16	0.084
0.100	1.15	0.093	1.20	0.079
0.150	1.20	0.080	1.23	0.070
0.200	1.24	0.075	1.26	0.068
0.300	1.29	0.064	1.30	0.056
0.400	1.30	0.048	1.30	0.048
0.500	1.30	0.040	1.30	0.040
0.600	1.30	0.036	1.30	0.036

 * *
 * SAMPLING RATE DATA *
 * *

TABLE(78)
 SERIES (2)

INJECTION CONCENTRATION = 50 W.P.P.M.

SMALL DIAMETER			MEDIUM DIAMETER			LARGE DIAMETER		
10.0	50.5	1426.0	10.0	45.0	743.0	20.0	39.0	1001.0
20.0	44.0	1552.0	20.0	41.3	1115.0	40.0	41.0	1285.0
30.0	44.8	1584.0	30.0	43.0	1264.0	70.0	45.5	1461.0
40.0	45.6	1611.0	50.0	41.3	1397.0	70.0	35.9	1534.0
50.0	46.1	1637.0	60.0	34.2	1430.0	90.0	38.0	1594.0
60.0	49.3	1650.0	80.0	34.0	1508.0	100.0	34.1	1507.0
60.0	45.8	1710.0	90.0	31.5	1492.0			
			90.0	26.65	1545.0			

TABLE(79)
 SERIES (1)

INJECTION CONCENTRATION = 100 W.P.P.M.

SMALL DIAMETER			MEDIUM DIAMETER			LARGE DIAMETER		
15.0	72.4	1276.0	10.0	48.0	180.0	20.0	40.4	747.0
20.0	45.2	1613.0	20.0	42.0	474.0	40.0	42.0	1098.0
30.0	47.0	1825.0	30.0	41.8	663.0	60.0	39.1	1411.0
40.0	46.6	1800.0	40.0	32.1	870.0	70.0	36.3	1558.0
50.0	47.7	1806.0	60.0	33.3	964.0	100.0	42.3	1690.0
50.0	41.1	1920.0	80.0	34.3	997.0	100.0	34.2	1720.0
50.0	38.6	1858.0	90.0	31.5	1019.0	100.0	28.6	1886.0
						100.0	25.5	1884.0

TABLE(80)

SERIES (1)

INJECTION CONCENTRATION = 250 W.P.P.M.

SMALL DIAMETER			MEDIUM DIAMETER			LARGE DIAMETER		
15.0	62.7	1143.0	15.0	76.5	206.0	20.0	87.3	120.0
20.0	41.0	1595.0	20.0	42.4	597.0	20.0	40.0	220.0
30.0	43.4	2446.0	30.0	42.7	963.0	30.0	41.8	376.0
40.0	47.3	2560.0	40.0	42.1	1236.0	40.0	40.6	576.0
50.0	48.8	2724.0	50.0	40.4	1427.0	50.0	39.9	883.0
50.0	43.9	2746.0	70.0	39.4	1630.0	70.0	37.8	1305.0
50.0	42.5	2835.0	100.0	43.4	1765.0	80.0	33.3	1680.0
50.0	41.0	2826.0	100.0	35.7	1793.0	80.0	27.0	1919.0
			120.0	36.1	1820.0	80.0	22.8	2034.0

TABLE(81)

SERIES (1)

INJECTION CONCENTRATION = 500 W.P.P.M.

SMALL DIAMETER			MEDIUM DIAMETER			LARGE DIAMETER		
10.0	44.1	671.0	10.0	42.0	107.0	20.0	41.3	156.0
20.0	42.75	1104.0	20.0	43.9	451.0	40.0	42.6	548.0
30.0	45.5	1308.0	30.0	43.0	783.0	60.0	41.0	1086.0
40.0	47.5	1410.0	50.0	40.8	1243.0	70.0	38.4	1380.0
50.0	49.4	1460.0	60.0	34.2	1429.0	90.0	39.4	1565.0
50.0	45.3	1528.0	70.0	30.7	1522.0	100.0	30.9	1898.0
60.0	52.3	1548.0	80.0	29.1	1618.0	100.0	30.8	2059.0
			90.0	29.4	1680.0	150.0	42.5	2130.0
			90.0	26.5	1747.0	150.0	37.0	2380.0

TABLE(82)

SERIES (1)

INJECTION CONCENTRATION = 1000 W.P.P.M.

10.0	36.7	975.0	10.0	44.8	208.0	20.0	38.7	144.0
20.0	45.6	1942.0	10.0	21.5	766.0	20.0	27.5	257.0
20.0	37.5	2211.0	20.0	27.7	1268.0	30.0	24.4	674.0
30.0	50.1	2358.0	30.0	26.3	1817.0	50.0	27.8	1025.0
30.0	49.8	2467.0	40.0	25.9	2103.0	60.0	26.4	1266.0
			50.0	26.5	2367.0	70.0	26.2	1633.0
			60.0	30.2	2411.0	80.0	26.4	1679.0
						90.0	27.9	1818.0
						100.0	28.9	1803.0

TABLE(83)

SERIES (2)

INJECTION CONCENTRATION = 50 W.P.P.M.

SMALL DIAMETER			LARGE DIAMETER		
15.0	57.4	984.0	15.0	51.6	1114.0
25.0	49.9	1151.0	15.0	28.1	1192.0
25.0	34.0	1205.0	25.0	33.4	1283.0
25.0	25.3	1223.0	25.0	24.4	1423.0
25.0	20.4	1225.0	25.0	19.1	1387.0

TABLE(84)

SERIES (2)

INJECTION CONCENTRATION = 100 W.P.P.M.

SMALL DIAMETER			LARGE DIAMETER		
15.0	57.9	1382.0	15.0	52.5	834.0
25.0	46.2	1601.0	25.0	46.8	1064.0
25.0	32.8	1521.0	25.0	31.8	1338.0
25.0	25.0	1619.0	25.0	23.9	1249.0
25.0	20.4	1663.0	25.0	18.8	1434.0
			60.0	32.0	1487.0
			80.0	32.4	1500.0
			80.0	26.3	1525.0

TABLE(85)

SERIES (2)

INJECTION CONCENTRATION = 250 W.P.P.M.

	SMALL DIAMETER	LARGE DIAMETER
15.0	56.4	940.0
25.0	48.8	1171.0
25.0	34.3	1335.0
25.0	26.3	1353.0
25.0	20.8	1337.0

TABLE(86)

SERIES (2)

INJECTION CONCENTRATION = 500 W.P.P.M.

	SMALL DIAMETER	LARGE DIAMETER
15.0	55.6	767.0
25.0	48.4	1061.0
25.0	35.2	1183.0
25.0	27.6	1339.0
25.0	23.6	1344.0

TABLE(87)

SERIES (2)

INJECTION CONCENTRATION = 1000 W.P.P.M.

	SMALL DIAMETER	LARGE DIAMETER
15.0	59.5	708.0
20.0	47.4	1253.0
25.0	44.8	1402.0
25.0	39.4	1497.0
25.0	39.3	1618.0

TABLE(88)
SERIES (2)

INJECTION CONCENTRATION = 100 W.P.P.M.

SMALL DIAMETER

15.0	62.3	254.0
20.0	41.6	274.0
25.0	36.2	276.0
25.0	26.7	282.0
25.0	21.6	290.0

TABLE(89)
SERIES (2)

INJECTION CONCENTRATION = 250 W.P.P.M.

SMALL DIAMETER

15.0	65.4	282.0
20.0	40.7	316.0
25.0	35.7	350.0
25.0	26.4	366.0
25.0	21.4	371.0

TABLE(90)
SERIES (2)

INJECTION CONCENTRATION = 500 W.P.P.M.

SMALL DIAMETER

15.0	59.6	321.0
20.0	39.5	488.0
25.0	36.1	638.0
25.0	26.9	742.0
25.0	22.3	843.0

APPENDIX IV ERROR ANALYSIS

The error analysis presented here is not intended to show the magnitude of all the errors but attempts to indicate the relative significance of each of the errors.

Velocity Measurements

The maximum error occurred when the minimum velocity was being measured. This minimum value was equivalent to a reading of 0.7 volts by the anemometer. The assessed accuracy of the reading is ± 0.01 V therefore the maximum error is $\pm 0.01/0.7$ or equal to $\pm 1.5\%$ decreasing as the velocity is increased.

Concentration Measurements

The spectrophotometer had an excellent sensitivity, of the order of 0.005 w.p.p.m. The maximum error occurred when the measurements were taken at the 5th location where the concentration was minimum. For concentrations of about 50% of the maximum concentration, (i.e., relatively distant downstream from the injection source), the optimal density obtained from the spectrophotometer was 12 ± 1 or the maximum error was equal to $\pm 8\%$, decreasing as the concentration increased and almost negligible for concentration measurements upstream from the 5th location.

Sampling Location

The error in determining the longitudinal location is maximum for the first location and gradually decreases as the distance was increased. The first location was at 45 ± 1 mm. downstream from the injection source, then the maximum error was $\pm 1/45$ or equal to about $\pm 2\%$.

For the vertical location a micrometer with assessed accuracy of the reading of 0.001" was used. The minimum vertical movement of the probe was 0.025" which incurred a maximum error of $\pm 0.001/0.025$ or equal to about 4%.

Injection Velocity Flow Rate

The injection flow rate is measured using a standard rotameter. The minimum reading of the rotameter, which produced the maximum error, was 40 ± 0.5 mm. Therefore the maximum error was equal to about $\pm 1.25\%$ decreasing as the injection flow rate was increased.

Injection Concentration

The injection concentration was based on weighing a given amount of polymer and then adding it to the water. This produced maximum error for the minimum injection concentration used. The minimum amount of polymer to be mixed with water was about 2.00 ± 0.01 g. Therefore the assessed maximum error was about $\pm 0.5\%$ decreasing as the injection concentration was increased.

In conclusion, based on the above analysis and assuming that the errors are interacting, the combined

maximum error may be expressed as

$$\sqrt{(1.5)^2 + (8)^2 + (2)^2 + (4)^2 + (1.25)^2 + (0.5)^2}$$

or equal to about $\pm 9.4\%$, which is larger than the experimental scatter or precision for the majority of the fitted curves.